



**LIBRARY**  
New Delhi

Call No. \_\_\_\_\_

Acc. No. 19391

**Indian Agricultural Research Institute (Pusa)**  
**LIBRARY, NEW DELHI-110012**

This book can be issued on or after \_\_\_\_\_

Return Date	Return Date



**PROCEEDINGS**  
**OF THE**  
**NATIONAL INSTITUTE OF SCIENCES OF INDIA**

**VOL. VIII**

**1942**

**CALCUTTA :**  
**PUBLISHED BY THE NATIONAL INSTITUTE OF SCIENCES OF INDIA**





## CONTENTS

No. 1—March, 1942.

	PAGE
Seventeenth Ordinary General Meeting .. .. .	1
Seventh Annual General Meeting .. .. .	5
Annual Report .. .. .	9
Annual Address. <i>By</i> DR. BAINI PRASHAD .. .. .	27
Radio-activity of Rubidium. <i>By</i> P. K. SEN-CHOWDHURY .. .. .	45
On the Existence of an Isotope of Cobalt, Co <sup>57</sup> . <i>By</i> P. K. SEN-CHOWDHURY .. .. .	55
Development of Embryo-sac and Endosperm-haustoria in <i>Tetranema mexicana</i> Benth. and <i>Verbascum thapsus</i> Linn. <i>By</i> C. V. KRISHNA IYENGAR .. .. .	59
Studies in Floral Anatomy. II. Floral Anatomy of the Moringaceae with special reference to Gynaecium constitution. <i>By</i> V. PURI .. .. .	71
The Relation of Gas Pressure to Radiation Pressure in a Bose-Einstein Gas. <i>By</i> B. N. SINGH and A. G. CHOWDRI .. .. .	89
Properties of a Confluent Hyper-geometric Function. <i>By</i> B. MOHAN .. .. .	93
On a Physical Theory of the Solar Corona. <i>By</i> M. N. SAHA .. .. .	99
X-ray Studies in Indian Coals. Part I. <i>By</i> J. DHAR and B. B. NIYOGI .. .. .	127
Induced Reactions with Ascorbic Acid as Inductor. <i>By</i> G. GOPALA RAO and T. V. SUBBA RAO .. .. .	137

No. 2—August, 1942.

White Dwarf and Harmonic Oscillator. <i>By</i> F. C. AULUCK .. .. .	147
Degenerate Gas and the Motion of a Particle in a Uniform Field. <i>By</i> D. S. KOTHARI and F. C. AULUCK .. .. .	157
Fermi-Dirac and Bose-Einstein Gas in a Uniform Field of Force. <i>By</i> D. S. KOTHARI and F. C. AULUCK .. .. .	165
The Instability of Radial Oscillations of a Variable Star and the Origin of the Solar System. <i>By</i> A. C. BANERJI .. .. .	173
On the Collision between Meson and Electron. <i>By</i> S. GUPTA and R. C. MAJUMDAR .. .. .	199
On the Origin of Extra Spots in Laue Photographs. <i>By</i> S. C. SIRKAR and B. M. BISHUI .. .. .	217
On the Production of Mesons by Non-ionising Agents in Cosmic Rays. <i>By</i> S. C. SIRKAR and S. K. GHOSH .. .. .	233
Development of Seed and its Nutritional Mechanism in Scrophulariaceae. <i>By</i> C. V. KRISHNA IYENGAR .. .. .	249

# CONTENTS

	PAGE
East-West Asymmetry of Cosmic Rays at Calcutta and Darjeeling. By P. C. BHATTACHARYA .. .. .	263
Fine Structure in the Directional Intensity of Cosmic Rays at Calcutta ( $\lambda = 12^\circ \text{N.}$ , $h = 80 \text{ ft.}$ ). By P. C. BHATTACHARYA .. .. .	273
Studies on Helium-filled Geiger-Müller Counters. By H. R. SARNA, P. L. KAPUR and CHARANJIT .. .. .	277
The Ultra-violet Band Spectrum of Mercury Iodide. By M. G. SASTRY	289
On Integration of Stellar Equations for Bethe's Law of Energy Gene- ration. By U. R. BURMAN .. .. .	301
On Stellar Models based on Bethe's Law of Energy Generation. By N. R. SEN .. .. .	317

## No. 3—December, 1942.

Accurate Calculations on the Cascade Theory of Electronic Showers without Collision Loss. By S. K. CHAKRABARTY .. .. .	331
Contribution to the Theory of Stellar Models. By N. R. SEN .. .. .	339
Fermi-Dirac and Bose-Einstein Gas in a Gravitational Field. By BRIJ NATH and P. L. BHATNAGAR .. .. .	361
On the Elastic Scattering of the Fast Mesons. By S. GUPTA .. .. .	369
Pressure Ionisation and Maximum Radius for a Cold Body. By P. L. BHATNAGAR and D. S. KOTHARI .. .. .	377
Photochemical Analysis. By G. GOPALA RAO and P. T. RAMACHARLU	383
On the Extra Spots in Laue Photographs of Metadinitrobenzene. By M. GANGULY .. .. .	389
Obituary Notice: Rai Bahadur Gouripati Chatterjee .. .. .	397
Eighteenth Ordinary General Meeting .. .. .	399

## Seventeenth Ordinary General Meeting.

The Seventeenth Ordinary General Meeting of the National Institute of Sciences of India was held at 11 A.M. on Friday, the 29th August, 1941, in the hall of the Royal Asiatic Society of Bengal, 1 Park Street, Calcutta.

*Present:—*

Dr. B. Prashad, *President*, in the Chair.  
Prof. J. N. Mukherjee, *Vice-President*.  
Dr. B. S. Guha, *Honorary Treasurer*.  
Dr. K. N. Bagehi.  
Prof. S. R. Bose.  
Dr. H. Chaudhuri.  
Sir R. N. Chopra.  
Prof. J. Ghosh.  
Dr. S. L. Hora.  
Dr. R. B. Lal.  
Prof. S. K. Mitra.  
Dr. F. G. Percival.  
Prof. M. N. Saha.  
Dr. N. K. Sur.  
Prof. S. P. Agharkar, *Honorary Secretary*.

Besides the Fellows there were also some visitors present.

1. The minutes of the Sixteenth Ordinary General Meeting held at Delhi on the 19th April, 1941, were read and confirmed.

2. The following Ordinary Fellows were admitted as per provisions of Rule 13:

Dr. F. G. Percival.  
Dr. N. K. Sur.

3. Proposals for changes in Rules in connection with the procedure for the election of the Council, previously circulated, were considered.

Dr. H. Chaudhuri proposed that in Rule 43, line 1 'three' should be replaced by 'nine' instead of by 'six' as proposed by the Council.

The motion was seconded by Dr. S. R. Bose.

The Honorary Secretary pointed out that the result of Dr. Chaudhuri's proposal would be to prescribe that the entire Council (apart from the President, Vice-Presidents, Treasurer and the Secretaries) would be changed every two years, whereas the Council's proposal made such change obligatory every three years.

It was resolved after discussion to accept the Council's proposal.

It was also resolved to authorise the Honorary Secretary to take necessary steps to place the alterations to the Rules before the Annual General Meeting in accordance with the Rules.

## 4. The following papers were read:—

- (1) P. C. Bhattacharya: A search for the Double Proton. (Communicated by Prof. M. N. Saha.)
- (2) T. J. Job: Efficiency of the Killifish *Aplocheilus panchax* (Hamilton) in the control of Mosquitoes. (Communicated by Dr. S. L. Hora.)
- (3) S. Parthasarathy, S. C. Sircar and K. C. Niyogi: On the Polarisation of Light Scattered by Optical Glasses. (Communicated by Prof. M. N. Saha.)

## 5. The following papers were read by title only owing to the absence of the authors:—

- (1) N. R. Dhar, E. V. Seshacharyulu and N. N. Biswas: New aspects of nitrogen fixation and loss in soils.
- (2) F. C. Auluck: Energy levels of an artificially bounded Linear Oscillator. (Communicated by Dr. D. S. Kothari.)
- (3) B. Mohan: A confluent Hyper-geometric function. (Communicated by Prof. V. V. Narlikar.)
- (4) N. R. Sen: On the inversion of density gradient and convection in Stellar bodies.
- (5) R. M. Chaudhri and A. W. Khan: Secondary electron emission from Tungsten. (Communicated by Prof. M. N. Saha.)
- (6) Miss B. S. Alamela and B. B. Dey: Studies in the Isoquinoline series. Parts IX and X.
- (7) M. R. Siddiqi: On the field of operators in the theory of quaternions.
- (8) V. V. Narlikar: The Two-Body Problem in Einstein's New Relativity.
- (9) B. B. Ray and B. Bhowmik: On the K-spectra of Elements (11Na-15P) and Conduction Electrons. Part I.
- (10) B. B. Ray and S. S. Sen: Secondary K-absorption edges of iron and its compounds in the solid state and in solution.
- (11) A. M. Subba Rao: Studies in the Malpighiaceae. 2. Structure and development of the ovules and embryo-sacs of *Malpighia coccifera* Linn. and *Tristellatia australis* Linn. (Communicated by Dr. P. Maheshwari.)
- (12) S. B. Kausik: Studies in the Proteaceae. V. Vascular Anatomy of the Flower of *Grevillea robusta* Cunn. (Communicated by Dr. P. Maheshwari.)
- (13) B. N. Srivastava: Thermal Transpiration in presence of Dissociation. (Communicated by Prof. M. N. Saha.)
- (14) M. G. Sastry: Ultra-violet Band Spectrum of Mercuric Chloride. (Communicated by Prof. M. N. Saha.)
- (15) M. G. Sastry: The Ultra-violet Band Spectrum of Mercury Bromide. (Communicated by Prof. M. N. Saha.)

- (16) J. Gupta and M. P. Guha: On the Constitution of some Oxyacids of Sulphur. (Communicated by Prof. M. N. Saha.)
- (17) H. K. Sen: Polytropic Transformations for a Fermi-Dirac Gas. (Communicated by Dr. D. S. Kothari.)
- (18) F. C. Auluck: The artificially bounded relativistic Linear Oscillator. (Communicated by Dr. D. S. Kothari.)
- (19) K. Banerjee and A. K. Ray: The Structure of Jute Fibre by X-ray Diffraction Method.
- (20) Vishwa Nath: The Decapod Sperm.

The meeting terminated with a vote of thanks to the Chair.



## Seventh Annual General Meeting.

The Seventh Annual General Meeting of the National Institute of Sciences of India was held at 3 p.m. on Thursday, the 1st January, 1942, in the Central Hall of the Baroda College, Baroda.

The following Fellows were present:—

Dr. C. W. B. Normand, *Vice-President, in the Chair.*

Mr. W. D. West, *Additional Vice-President.*

Prof. S. P. Agharkar, *Honorary Secretary.*

Prof. Y. Bharadwaja.

Prof. F. R. Bharucha.

Dr. N. L. Bor.

Dr. H. Chaudhuri.

Dr. K. A. Chowdhury.

Dr. B. B. Dikshit.

Dr. J. A. Dunn.

Prof. G. S. Ghurye.

Prof. B. C. Guha.

Prof. K. B. Madhava.

Principal G. R. Paranjpe.

Principal P. Parija.

Prof. R. C. Shah.

Dr. H. K. Sen.

Prof. B. N. Singh.

Prof. V. Subrahmanyam.

The meeting was also attended by visitors.

In the unavoidable absence of the President, Dr. Bains Prasad, Dr. C. W. B. Normand, Vice-President, took the Chair.

The following Ordinary Fellows signed the duplicate obligation and were admitted as Fellows as per Rule 13.

Dr. N. L. Bor.

Dr. K. A. Chowdhury.

Dr. B. B. Dikshit.

Prof. G. S. Ghurye.

Prof. B. C. Guha.

Prof. R. C. Shah.

Prof. B. N. Singh.

1. The minutes of the Seventeenth Ordinary General Meeting of the Institute were read and confirmed.

2. The Chairman appointed Principal G. R. Paranjpe and Mr. W. D. West to act as scrutineers of the ballot papers received for the election of officers and other members of Council for the year 1942.

The following were declared elected officers and other members of Council for the year 1942:—

*President:* Dr. B. Prasad.

*Vice-Presidents:* Prof. J. N. Mukherjee and Dr. C. W. B. Normand.

*Treasurer:* Dr. B. S. Guha.

*Foreign Secretary:* Prof. J. C. Ghosh.

*Secretaries:* Prof. S. P. Agharkar and Dr. C. S. Fox.

*Members of Council:* Dr. K. N. Bagchi, Sir S. S. Bhatnagar, Dr. F. H. Gravely, Dr. S. L. Hora, Dr. M. Ishaq, Dr. D. S. Kothari, Dr. M. S. Krishnan, Prof. G. Matthai, Prof. V. V. Narlikar, Principal G. R. Paranjpe, Principal P. Parija, Dr. F. G. Percival, Prof. M. Qureshi,



Dr. K. R. Ramanathan, Rao Bahadur G. N. Rangaswami Ayyanger, Prof. M. R. Siddiqi, Prof. N. K. Sur, Mr. F. Ware.

3. The Chairman appointed Dr. H. Chaudhuri and Principal P. Parija to act as scrutineers of the ballot papers received in connection with the modifications to Rules 41 and 43.

Of the 46 votes received, the scrutineers declared 42 for and 1 against any change in the Rules and 3 invalid. The Chairman accordingly declared as passed the following modifications to Rules 41 and 43.

**RULE 41.**—In place of the words 'The Council shall prepare a list . . . . . before the date fixed for the Annual Meeting' insert:

'The Council shall prepare, in accordance with the following procedure, a list of the names of those persons whom it recommends for election as President, Vice-Presidents, Secretaries, Foreign Secretary, Treasurer, Additional Secretaries and other members of the Council for the ensuing year.

(i) The Council shall determine, at its meeting to be held in August, the vacancies that will occur among the officers and other members of the Council during the ensuing year taking into consideration the length of service on the Council, the number of meetings attended, interest in the work of the Council as evidenced by communications on matters under discussion and other relevant matters.

(ii) A list of the Council of the current and two preceding years, indicating the vacancies that will be occurring in the ensuing year, shall be circulated to all Ordinary Fellows in good standing in September, inviting suggestions regarding vacancies, so as to reach the office by the middle of October.

(iii) The suggestions shall be circulated to the members of the Council by the 1st of November for expression of their views, and considered at the meeting of the Council to be held in November when final nominations shall be made.

The list of nominations shall be printed, and a copy sent by post to each resident Fellow of the Institute at least one month before the date selected for the Annual General Meeting of the Institute. These voting lists shall have a blank column for such alterations as any Fellow may wish to make. These voting papers shall be returned to the Secretaries at least a week before the date fixed for an Annual General Meeting.'

**RULE 43.**—In line 1 replace 'three' by 'six'.

4. Dr. H. Chaudhuri moved an amendment that in Rule 43, line 1, replace 'six' by 'nine'.

The amendment was supported by the following:—

Prof. Y. Bharadwaja.

Dr. N. L. Bor.

Prof. F. R. Bharucha.

Dr. K. A. Chowdhury.

Prof. B. C. Guha.

Prof. K. B. Madhava.

Principal G. R. Paranjpe.

Principal P. Parija.

Dr. H. K. Sen.

Prof. B. N. Singh.

Prof. V. Subrahmanyam.

It was resolved that the amendment having been formally moved it should be circulated to all Resident Ordinary Fellows in accordance with the Rules.

5. The Annual Report for the year 1941, prepared by the Council, and the budget estimates of income and expenditure for the year 1942 were considered and approved.

6. The following papers were read:—

- (1) Development of Embryo-sac and Endosperm-haustoria in *Tetranema mexicana* Benth. and *Verbascum thapsus* Linn. By C. V. Krishna Iyengar. (Communicated by Dr. P. Maheshwari.)
- (2) Radio-activity of Rubidium. By P. K. Sen-Chowdhury. (Communicated by Prof. M. N. Saha.)
- (3) On the existence of an isotope of Cobalt, Co<sup>57</sup>. By P. K. Sen-Chowdhury. (Communicated by Prof. M. N. Saha.)
- (4) X-Ray studies in Indian Coals. Part I. By J. Dhar and B. B. Niyogi. (Communicated by Dr. K. Banerjee.)
- (5) Studies in Floral Anatomy. II. Floral anatomy of the Morinaceae with special reference to Gynaeceum constitution. By V. Puri. (Communicated by Dr. P. Maheshwari.)
- (6) The relation of gas pressure to Radiation pressure in a Bose-Einstein Gas. By B. N. Singh and A. G. Chowdri. (Communicated by Dr. D. S. Kothari.)
- (7) Properties of a confluent Hyper-geometric Function. By B. Mohan. (Communicated by Prof. V. V. Narlikar.)
- (8) Degenerate gas and the motion of a particle in a uniform field. By D. S. Kothari and F. C. Auluck.
- (9) Fermi-Dirac and Bose-Einstein Gas in a uniform field of Force. By D. S. Kothari and F. C. Auluck.
- (10) White Dwarf and Harmonic Oscillator. By F. C. Auluck. (Communicated by Dr. D. S. Kothari.)
- (11) Studies on Helium-filled Geiger-Müller Counters. By H. R. Sarna, P. L. Kapur and Charanjit. (Communicated by Prof. M. N. Saha.)

7. In the absence of the President his Annual Address was read by Dr. C. W. B. Normand. The Address will be printed in the *Proceedings*.

With a vote of thanks to the Chair the meeting terminated.



# National Institute of Sciences of India.

## ANNUAL REPORT.

The Council of the National Institute of Sciences of India have pleasure in submitting the following report on the general concerns of the Institute for the year 1941, as required by the provisions of Rule 48(f).

### *Membership.*

The number of Fellows on the roll of the Institute at the beginning of the year was 170 Ordinary Fellows and 21 Honorary Fellows. Fourteen Ordinary Fellows and four Honorary Fellows were elected during the year in accordance with the procedure laid down in the Regulations. Two Ordinary Fellows resigned, and three Ordinary Fellows and two Honorary Fellows died during the year. The total number of Fellows on the roll at the end of the year is 179 Ordinary Fellows and 23 Honorary Fellows. Of the 179 Ordinary Fellows 8 are non-resident.

### *Meetings.*

The sixth Annual Meeting was held in the Institute of Agricultural Research, Benares Hindu University, on the 2nd January, 1941. An account of the meeting was published in the *Proceedings*, Vol. VII, No. 1, pp. 3-5.

Two Ordinary General Meetings were held during the year. The first was held in the Physics Lecture Theatre of the University of Delhi on the 19th April, 1941. The meeting was followed by a Symposium on 'Heavy Chemical Industries in India' at which a number of interesting papers were read and discussed. The second meeting was held in the rooms of the Royal Asiatic Society of Bengal, Calcutta, on the 29th August, 1941. The papers read at these meetings will be published in the *Proceedings*.

### *The Council.*

The officers and members of Council for the year 1941 were elected at the Sixth Annual Meeting held on the 2nd January, 1941. The Council, together with the representatives of the co-operating Academies, the Indian Science Congress Association and the Government of India, was constituted as follows:—

<i>President</i>	..	..	Dr. Bains Prashad.
<i>Vice-Presidents</i>	..	..	Prof. J. N. Mukherjee. Dr. C. W. B. Normand.

<i>Additional Vice-Presidents</i>	..	Prof. A. C. Banerji. Khan Bahadur M. Afzal Hussain. Prof. K. S. Krishnan. Mr. W. D. West.
<i>Treasurer</i>	..	Dr. B. S. Guha.
<i>Foreign Secretary</i>	..	Dr. J. O. Ghosh.
<i>Secretaries</i>	..	Prof. S. P. Agharkar. Dr. C. S. Fox.
<i>Members of Council</i>	..	Sir S. S. Bhatnagar. Rai Bahadur Dr. S. L. Hora. Dr. M. S. Krishnan. Dr. R. B. Lal. Prof. G. Matthai. Principal G. R. Paranjpe. Principal P. Parija. Dr. F. G. Percival. Prof. M. Qureshi. Rao Bahadur G. N. Rangaswami Ayyangar. Prof. M. N. Saha. Prof. N. R. Sen. Prof. M. R. Siddiqi. Dr. N. K. Sur. Col. J. Taylor. Rao Bahadur B. Venkatesachar. Mr. F. Ware. Brevet-Col. Sir R. N. Chopra } <i>Ex-officio</i> . Sir Lewis Fermor
<i>Additional Members of Council</i>		Prof. P. C. Mahalanobis. Prof. S. K. Mitra. Major C. L. Pasricha. Prof. B. K. Singh.

The Council held seven ordinary and two emergency meetings during the year.

#### *Committees.*

The Sectional Committees are given in Appendix II.

#### *Publications.*

Three numbers of the *Proceedings*, one number of the *Transactions* and one number of *Indian Science Abstracts* were published during the year.

#### *Exchanges.*

One additional Institution was placed on the exchange list for the publications of the Institute, bringing the total number on the list to ninety-five (*vide* Appendix III).

#### *Library.*

Three hundred and ninety-seven books, parts of periodicals and reprints were added to the library during the year (*vide* Appendix IV). A noteworthy addition was a number of publications on Botany received from the University of California.

*Presents and Donations.*

The following grants-in-aid were made to the Institute during the year.

- (1) Rs.500 from the Calcutta University.
- (2) Rs.300 from the Osmania University.
- (3) Rs.200 from the Dacca University.

The Government of India increased their annual grant to the Institute from Rs.6,000 to Rs.7,000 from the current official year.

*Finance.*

An audited statement of accounts of the Institute for the period from 1st December, 1940, to 30th November, 1941, is submitted (*vide* Appendix V). The total ordinary receipts for this period are Rs.15,468-15-0 (inclusive of the Government of India grant of Rs.7,000) and the ordinary payments are Rs.12,014-5-3, leaving a balance of Rs.3,454-9-9\*. A sum of Rs.320-0-0 was realised on account of admission fees and Rs.130-14-0 as compounding fee.

At the beginning of the year the cash position of the Institute was as follows:—

			Rs.	A.	P.
In Savings Bank account	..	..	3,688	1	0
„ Government paper	..	..	40,000	0	0
„ Current account	..	..	2,948	3	0
„ hand	..	..	4	13	0
TOTAL			46,641	1	0

At the end of the year, however, the cash position was as shown below:—

			Rs.	A.	P.
In Savings Bank account	..	..	5,713	9	0
„ Government paper	..	..	40,000	0	0
„ Current account	..	..	4,818	12	9
„ hand	..	..	14	3	0
TOTAL			50,546	8	9

## APPENDICES.

- I. List of Fellows.
- II. Committees, 1942.
- III. List of Institutions on the exchange list.
- IV. Periodicals received for the library.
- V. Audited statement of accounts, Dec. 1940–Nov. 1941.
- VI. Budget Estimates, Dec. 1941–Nov. 1942.

---

\* The small surplus of Rs.3,454-9-9 as shown above in the current year's accounts is really due to outstanding bills on account of printing.

## APPENDIX I.

### LIST OF FELLOWS.

#### ORDINARY FELLOWS.

1. ABRAHAM, LT.-COL. W. E. V., A.R.C.S. (I.), F.G.S., M.Inst.P.T., Senior Geologist, Burmah Oil Co., Ltd., Burma, Khodaung, Magwe, Burma. (1936).
2. AGHARKAR, S. P., M.A., Ph.D., F.L.S., Ghose Professor of Botany, Calcutta University, 35, Ballygunge Circular Road, Calcutta.
3. AHMAD, NAZIR, O.B.E., M.Sc., Ph.D., Director, Indian Central Cotton Committee's Technological Laboratory, Matunga, Bombay.
4. AIYAR, R. GOPALA, M.A., L.T., M.Sc., University Professor of Zoology and Director, University Zoological Laboratory, Madras. (1938).
5. AJREKAR, S. L., B.A., I.E.S. (Retd.), Bhandarkar Institute Road, Poona 4.
6. ANANDA RAO, K., Rao Bahadur, M.A., I.E.S., Professor of Mathematics, Presidency College, Madras.
7. ASH, W. C., B.Sc., M.Inst.C.E., A.M.I.Mech.E., Bengal Club, Calcutta.
8. AUDEN, J. B., M.A. (Cantab.), Geologist, Geological Survey of India, Indian Museum, Calcutta. (1938).
9. AWATI, P. R., B.A., D.I.C., I.E.S., Professor of Zoology, Royal Institute of Science, Mayo Road, Bombay 1.
10. BAGOHEE, K. D., D.Sc., D.I.C., Mycologist, Imperial Forest Research Institute, Dehra Dun, U.P.
11. BAGCHI, K. N., Rai Bahadur, B.Sc., M.B., D.T.M., F.I.C., Chemical Examiner to the Government of Bengal and Professor of Chemistry, Calcutta Medical College, Calcutta. (1940).
12. BAHL, K. N., D.Sc., D.Phil., Professor of Zoology, Lucknow University, Lucknow.
13. BANERJEE, K., D.Sc., Reader in Physics, Dacca University, Ramna, Dacca. (1939).
14. BANERJI, A. C., M.Sc., M.A., F.R.A.S., I.E.S., Professor of Mathematics, Allahabad University, Allahabad.
15. BANERJI, S. K., D.Sc., Superintending Meteorologist, Meteorological Office, Thube Park, Ganeshkhind Road, Poona 5.
16. BASU, J. K., M.Sc., Ph.D., Soil Physicist, Sugarcane Research Institute, Padegaon, P.O. Nira R. S., Dt. Poona. (1941).
17. BEESON, C. F. C., C.I.E., D.Sc., Thames House, near Eynsham, Oxford.
18. BEHARI, RAM, M.A., Ph.D., Reader in Mathematics, Delhi University and Professor, St. Stephen's College, Delhi. (1941).
19. BHABHA, H. J., Ph.D., F.R.S., Visiting Professor, Indian Institute of Science, Bangalore, Mehrangir, Little Gibbs Road, Malabar Hill, Bombay. (1941).
20. BHARADWAJA, Y., M.Sc., Ph.D. (Lond.), F.L.S., Professor of Botany and Head of the Department, Benares Hindu University, Benares. (1937).
21. BHARUCHA, F. R., B.A., B.Sc., M.Sc., D.Sc., Professor of Botany and Head of the Department, Royal Institute of Science, Bombay. (1939).
22. BHASKARA SHASTRI, T. P., M.A., F.R.A.S., Director, Nizamiah Observatory, Hyderabad (Deccan).
23. BHATNAGAR, SIR S. S., Kt. O.B.E., D.Sc., Director of Scientific and Industrial Research, 1B, Judges Court Road, Calcutta.
24. BHATTACHARYA, D. R., M.Sc., Ph.D., Dr. ès Sciences (Paris), Professor of Zoology, Allahabad University, 7, Malaviya Road, Allahabad.
25. BOMFORD, MAJOR GUY, R.E., Survey of India, 13, Wood Street, Calcutta. (1935).
26. BOR, N. L., M.A., D.Sc., F.L.S., Forest Botanist, Forest Research Institute, Dehra Dun. (1941).

27. BOSE, D. M., M.A., B.Sc., Ph.D., Director, Bose Institute, 93, Upper Circular Road, Calcutta.
28. BOSE, G. S., D.Sc., M.B., Head of the Department of Experimental Psychology, Calcutta University, 92, Upper Circular Road, Calcutta.
29. BOSE, N. K., M.Sc., Ph.D., Mathematical Officer, Punjab Irrigation Research Institute, Lahore. (1938).
30. BOSE, S. N., M.Sc., Professor of Physics and Head of the Department, Dacca University, Ramna, Dacca.
31. BOSE, S. R., M.A., Ph.D., F.R.S.E., Professor of Botany, Carmichael Medical College, Calcutta. (1935).
32. BRAHMACHARI, SIR U. N., Kt., Rai Bahadur, M.A., M.D., Ph.D., F.R.A.S.B., K.I.H., Physician, Medical College Hospitals, Calcutta (Retired), 19, Loudon Street, Calcutta.
33. BURRIDGE, W., D.M., M.A. (Oxon), Professor of Physiology, Lucknow University, Lucknow.
34. BURT, SIR BRYCE C., Kt., C.I.E., M.B.E., B.Sc., I.A.S. (Retd.), Bryn Dano, Allanson Road, Rhos-on-ss, Denbighshire, Great Britain.
35. CALDER, C. C., B.Sc. (Agr.), F.L.S., 18, Gladstone Place, Aberdeen, Scotland.
36. CHAKRAVARTI, S. N., D.Sc., D.Phil., F.C.S., F.I.C., Chemical Examiner to the Governments of U.P. and C.P., 45, Taj Road, Agra. (1935).
37. CHATTERJEE, G., M.Sc., Meteorologist-in-charge, Upper Air Observatory, Agra. (1935).
38. CHAUDHURI, H., D.Sc., Ph.D., D.I.C., Head of the Department of University Teaching in Botany and Director, Kashyap Research Laboratory, Panjab University, Lahore.
39. CHOPRA, B. N., D.Sc., F.L.S., Assistant Superintendent, Zoological Survey of India, Indian Museum, Calcutta. (1935).
40. CHOPRA, BREVET-COL. SIR R. N., Kt., C.I.E., M.D., Sc.D., F.R.A.S.B., F.R.C.P., I.M.S. (Retd.), Director, Drug Research Laboratory, Jammu-Tawi, Jammu and Kashmir State.
41. CHOWDHURY, J. K., M.Sc., Dr.Phil. (Berlin), Reader in Chemistry, Dacca University, Ramna, Dacca. (1938).
42. CHOWDHURY, K. AHMAD, B.A., B.Sc., M.S., D.Sc., Wood Technologist, Forest Research Institute, New Forest, Dehra Dun. (1940).
43. COULSON, A. L., D.Sc., D.I.C., F.G.S., Superintending Geologist, Geological Survey of India, Indian Museum, Calcutta. (1935).
44. CROOKSHANK, H., B.S., D.Sc., B.A.I., Capt., A.I.R.O., Superintending Geologist, Geological Survey of India, c/o Garrison Engineer, Razmak. (1938).
45. DASTUR, R. H., M.Sc., Cotton Physiologist, Agricultural College, Lyallpur, Punjab.
46. DATTA, S., M.Sc., D.Sc., D.I.C., Principal, Rajshahi College, Rajshahi. (1935).
47. DATTA, CAPTAIN S. C. A., D.Sc., F.R.S.E., M.R.C.V.S., D.T.V.M., Officer-in-charge, Section of Veterinary Zoology, Imperial Veterinary Research Institute, Izatnagar, U.P. (1938).
48. DEY, B. B., D.Sc., F.I.C., I.E.S., Professor of Chemistry, Presidency College, Madras.
49. DEB, N. R., D.Sc., F.I.C., I.E.S., Deputy Director of Public Instruction, U. P., Allahabad.
50. DEB, S. C., M.Sc., D.Sc. (Cal., Edin.), F.R.S.E., Professor and Head of the Department of Mathematics, Nagpur University, Nagpur. (1938).
51. DIXHIT, B. B., Ph.D. (Edin.), M.R.C.P. (Edin.), D.P.H. (Calcutta), M.B.B.S. (Bombay), Officer-in-charge, Pharmacology Department, Haffkine Institute, Bombay. (1941).
52. DUNN, J. A., D.Sc., D.I.C., F.G.S., Superintending Geologist, Geological Survey of India, Indian Museum, Calcutta. (1935).
53. DUNNICLIFF, H. B., M.A., Sc.D., F.I.C., I.E.S., Chief Chemist, Central Revenues, and Director, Control Laboratory, New Delhi.
54. DUTT, S. B., D.Sc., D.I.C., Reader in Organic Chemistry, Allahabad University, Allahabad. (1935).



55. EVANS, P., B.A., F.G.S., c/o Messrs. Burmah Oil Co., Ltd., Britannic House, Finsbury Circus, London, E.C.2.
56. FERMOR, SIR LEWIS L., Kt., O.B.E., D.Sc., A.R.S.M., M.Inst.M.M., F.G.S., F.R.A.S.B., F.R.S., 24, Durdham Park, Bristol 6.
57. FOWLER, GILBERT J., D.Sc., F.I.C., Consulting Chemist, Mackay's Gardens Annexe, Graimes Road, Cathedral P.O., Madras.
58. FOX, C. S., D.Sc., M.I.Min.E., F.G.S., F.R.A.S.B., Director, Geological Survey of India, Indian Museum, Calcutta.
59. GEE, E. R., M.A., F.G.S., Geologist, Geological Survey of India, Indian Museum, Calcutta. (1935).
60. GHOSE, S. L., M.Sc., Ph.D., Professor of Botany, Government College, Lahore.
61. GHOSH, J., M.A., Ph.D., Professor of Mathematics, Presidency College, Calcutta. (1936).
62. GHOSH, J. C., D.Sc., Director, Indian Institute of Science, Hebbal, Bangalore.
63. GHOSH, P. K., M.Sc., D.I.C., D.Sc. (Lond.), Geologist, Geological Survey of India, Calcutta. (1941).
64. GHOSH, P. N., M.A., Ph.D., Sc.D. (Hon.), F.Inst.P., Ghosh Professor of Applied Physics, Calcutta University, 92, Upper Circular Road, Calcutta.
65. GHOSH, R. N., D.Sc., Reader in Physics, Allahabad University, Allahabad. (1939).
66. GHURYE, G. S., M.A., Ph.D., Professor of Sociology in the University of Bombay. (1941).
67. GLENNIE, LT.-COL. E. A., D.S.O., R.E., Survey of India, Dehra Dun.
68. GRAVELY, F. H., D.Sc., F.R.A.S.B., Superintendent, Government Museum, Museum House, Egmore, Madras.
69. GUHA, B. C., D.Sc., Ghosh Professor of Applied Chemistry, Calcutta University. (1941).
70. GUHA, B. S., M.A., Ph.D., F.R.A.S.B., Assistant Superintendent, Zoological Survey of India, Indian Museum, Calcutta.
71. GUHA, P. C., D.Sc., Acting Professor of Organic Chemistry, Indian Institute of Science, Hebbal, Bangalore. (1935).
72. HADDOW, J. R., B.Sc., M.R.C.V.S., D.V.S.M., I.V.S., Deputy Director and Officer-in-charge, Pathology and Bacteriology, Imperial Veterinary Research Institute, Muktesar-Kumaun, U.P.
73. HENDRY, D., M.C., B.Sc., N.D.A., Director, Imperial Chemical Industries, India, Calcutta. (1938).
74. HERON, A. M., D.Sc., F.G.S., F.R.G.S., F.R.S.E., F.R.A.S.B., Mines and Geology Office, Hyderabad (Deccan).
75. HORA, S. L., Rai Bahadur, D.Sc., F.R.S.E., F.L.S., F.Z.S., F.R.A.S.B., Assistant Superintendent, Zoological Survey of India, Indian Museum, Calcutta.
76. HUSAIN, M. AFZAL, Khan Bahadur, M.A., M.Sc., I.A.S., Vice-Chancellor, Panjab University, Lahore.
77. ISHAQ, MOHAMMED, M.Sc., Ph.D., Head of the Department of Physics, Muslim University, Aligarh. (1940).
78. IYENGAR, M. O. P., M.A., Ph.D., F.L.S., University Professor of Botany, Madras University, Triplicane, Madras.
79. JOSHI, A. C., D.Sc., Assistant Professor of Botany, Benares Hindu University, Benares. (1938).
80. KAPUR, S. N., Ph.D., c/o Gun Carriage Factory, Jubbulpore.
81. KIOHLU, P. K., D.Sc., Professor of Physics, Government College, Lahore. (1935).
82. KOTHARI, D. S., M.Sc., Ph.D., Reader and Head of the Department of Physics, Delhi University, Delhi. (1936).
83. KRISHNA, S., Ph.D., D.Sc., F.I.C., Forest Biochemist, Forest Research Institute, New Forest, Dehra Dun (U.P.).
84. KRISHNAN, K. S., D.Sc., F.R.S., Mahendra Lal Sircar Professor of Physics, Indian Association for the Cultivation of Science, 210, Bow Bazar Street, Calcutta.
85. KRISHNAN, K. V., M.B.B.S., L.R.C.P., D.B., D.Sc., Professor of Malariology and Rural Hygiene, All-India Institute of Hygiene and Public Health, Calcutta.

86. KRISHNAN, M. S., A.R.C.S., Ph.D., D.I.C., Geologist, Geological Survey of India, Indian Museum, Calcutta. (1935).
87. LAL, R. B., M.B.B.S., D.P.H., D.T.M. & H., D.B., Professor of Vital Statistics and Epidemiology, All-India Institute of Hygiene and Public Health, Calcutta. (1935).
88. LAW, S. C., M.A., B.L., Ph.D., M.B.O.U., 50, Kailas Bose Street, Calcutta. (1936).
89. MACMAHON, P. S., M.Sc., B.Sc. (Oxon), F.I.C., I.E.S., Professor of Chemistry, Lucknow University, Lucknow.
90. MADHAVA, K. B., M.A., A.I.A. (Lond.), Professor of Mathematical Economics and Statistics, Mysore University, Lakshmipuram, Mysore. (1940).
91. MAHAJANI, G. S., M.A., Ph.D., Principal and Professor of Mathematics, Fergusson College, Poona 4.
92. MAHALANOBIS, P. C., M.A., B.Sc., I.E.S., Professor of Physics, Presidency College, Calcutta.
93. MAHESHWARI, P., D.Sc., Head of the Department of Biology, Dacca University, Rainna, Dacca. (1935).
94. MAJUMDAR, D. N., M.A., Ph.D., F.R.A.I., Lecturer in Anthropology, Lucknow University, Lucknow. (1940).
95. MAJUMDAR, R. C., Dr. Phil. Nat. (Jena), Research Fellow, Bose Institute, Calcutta. (1941).
96. MATTHAI, GEORGE, M.A., Sc.D., F.L.S., F.Z.S., F.R.S.E., Professor of Zoology, Government College, Lahore.
97. MEHRA, H. R., M.Sc., Ph.D., Reader in Zoology, Allahabad University, Allahabad.
98. MEHTA, K. C., Rai Bahadur, M.Sc., Ph.D., Professor of Botany, Agra College, Agra.
99. MILLS, J. P., M.A., I.C.S., Secretary to H.E. the Governor of Assam, Government House, Shillong, Assam. (1936).
100. MITRA, S. C., M.A., D.Phil. (Leip.), Lecturer in Psychology, Calcutta University. (1941).
101. MITRA, S. K., M.B.E., D.Sc., Ghose Professor of Physics, Calcutta University, 92, Upper Circular Road, Calcutta.
102. MITTER, P. C., M.A., Ph.D., Palit Professor of Chemistry, Calcutta University, 92, Upper Circular Road, Calcutta.
103. MOOKERJEE, H. K., D.Sc., D.I.C., University Professor of Zoology and Head of the Department, Calcutta University, 35, Ballygunge Circular Road, Calcutta. (1939).
104. MOWDAWALLA, F. N., M.A., M.I.E.E., Mem.A.I.E.E., M.I.E., 301, Frere Road, Fort, Bombay.
105. MUKHERJEE, J. N., D.Sc., F.C.S., F.R.A.S.B., Ghose Professor of Chemistry, Calcutta University, 92, Upper Circular Road, Calcutta.
106. NAIK, K. G., D.Sc., F.I.C., Professor of Chemistry, Baroda College, Baroda.
107. NARAYANAMURTI, D., B.Sc., Dr.Ing., Officer-in-charge, Wood Preservation Section, Forest Research Institute, New Forest, Dehra Dun. (1940).
108. NARLIKAR, V. V., B.Sc. (Bom.), B.A. (Cantab.), F.R.A.S., Professor of Mathematics and Head of the Department, Benares Hindu University, Benares. (1939).
109. NATH, VISHWA, M.Sc., Ph.D., F.R.M.S., Lecturer in Zoology, Government College, Lahore. (1940).
110. NEOGL, P., M.A., Ph.D., I.E.S. (Retd.), 44A, New Shambazar Street, Calcutta. (1936).
111. NORMAND, C. W. B., M.A., D.Sc., Director-General of Observatories, Meteorological Office, Poona 5.
112. OLYER, COL. SIR ARTHUR, C.B., C.M.G., F.R.C.V.S., Principal, Royal Veterinary College, Edinburgh.
113. PANDIT, C. G., M.B.B.S., Ph.D., D.P.H., D.T.M., Director, King Institute of Preventive Medicine, Guindy, Madras. (1939).
114. PARANJPE, G. R., M.Sc., A.I.I.Sc., I.E.S., Principal and Professor of Physics, Royal Institute of Science, Bombay. (1937).
115. PARANJPE, R. P., D.Sc., Purushottam Ashram, Poona 4.

116. PARIJA, P. K., M.A., B.Sc., I.E.S., Principal and Professor of Botany, Ravenshaw College, Cuttack.
117. PASSICHA, MAJOR C. L., M.A., M.B., B.Chir., M.R.C.S., L.R.C.P., I.M.S., Combined Indian Military Hospital, Dehra Dun. (1939).
118. PERCIVAL, F. G., Ph.D., F.G.S., Superintendent of Mines and Quarries, Tata Iron & Steel Co., Ltd., 3, Beldih Lake Road, Jamshedpur. (1936).
119. PHILPOT, H. P., B.Sc. (Eng.), M.Inst.C.E., M.I.Mech.E., M.I.A.E., M.I.M., Principal and Jodhpur Hardinge Professor of Technology, Engineering College, Benares Hindu University, Benares.
120. PINFOLD, E. S., M.A., F.G.S., Geologist, The Attock Oil Co., Ltd., Rawalpindi.
121. PRASAD, B. N., M.Sc., D.Sc., Ph.D., Mathematics Department, Allahabad University, Allahabad. (1936).
122. PRASAD, MATA, D.Sc., F.I.C., Professor of Inorganic and Physical Chemistry, Royal Institute of Science, Bombay. (1935).
123. PRASHAD, BAINI, D.Sc., F.R.S.E., F.L.S., F.Z.S., F.R.A.S.B., Director, Zoological Survey of India, Indian Museum, Calcutta.
124. PRUTHI, H. S., M.Sc., Ph.D., Imperial Entomologist, Imperial Institute of Agricultural Research, New Delhi.
125. QURESHI, MUZAFARUDDIN, Ph.D., Professor of Chemistry, Osmania University, Hyderabad (Deccan).
126. RAJ, B. SUNDARA, Diwan Bahadur, M.A., Ph.D., Director of Fisheries, Madras. (1935).
127. RAMANATHAN, K. R., M.A., D.Sc., Superintending Meteorologist, Meteorological Office, Poona 5.
128. RAMDAS, L. A., M.A., Ph.D., Agricultural Meteorologist, Meteorological Office, Poona 5. (1935).
129. RANGASWAMI AYYANGAR, G. N., Rao Bahadur, B.A., I.A.S., Millets Specialist and Geneticist, and Principal, Agricultural College and Research Institute, P.O. Lawley Road, Coimbatore, S.I.
130. RAO, B. RAMA, M.A., D.I.C., F.G.S., Director, Geological Survey Department, Mysore State, Bangalore.
131. RAO, C. V. HANUMANTHA, M.A., Professor of Mathematics, Panjab University, Lahore.
132. RAO, H. SRINIVASA, M.A., D.Sc., Assistant Superintendent, Zoological Survey of India, Indian Museum, Calcutta. (1937).
133. RAO, K. RANGADHAMA, D.Sc. (Madras and London), Reader in Physics, Andhra University, Waltair. (1937).
134. RAO, L. RAMA, M.A., F.G.S., Professor of Geology, Central College, Bangalore. (1939).
135. RAY, B. B., D.Sc., Khaira Professor of Physics, Calcutta University, 92, Upper Circular Road, Calcutta. (1935).
136. RAY, J. N., D.Sc., Ph.D., F.I.C., Professor of Organic Chemistry, University Chemical Laboratories, Panjab University, Lahore. (1935).
137. RAY, SIR P. C., Kt., M.A., Ph.D., D.Sc., F.R.A.S.B., Emeritus Professor of Chemistry, Calcutta University, 92, Upper Circular Road, Calcutta.
138. RAY, P. R., M.A., Khaira Professor of Chemistry, Calcutta University, 92, Upper Circular Road, Calcutta.
139. ROW, LT.-COL. R., M.D., D.Sc., I.M.S. (Hon.), 27, New Marine Lines, Bombay 1.
140. ROY, S. C., M.Sc., D.Sc., F.R.Met.Soc. (Lond.), Director of the Burma Meteorological Service, Rangoon. (1940).
141. ROY, S. K., Ph.D., Professor of Geology, Indian School of Mines, Dhanbad. (1940).
142. SAHA, M. N., D.Sc., F.R.S., F.R.A.S.B., Palit Professor of Physics, Calcutta University, 92, Upper Circular Road, Calcutta.
143. SARKAR, P. B., Dr. és Sc., A.I.C., Lecturer in Chemistry, Calcutta University, 92, Upper Circular Road, Calcutta. (1935).
144. SAYUR, S. R., M.A., L.T., Ph.D., Director, The Observatory, Colaba, Bombay. (1941).
145. SEN, B. M., M.A., M.Sc., I.E.S., Principal, Presidency College, Calcutta.

146. SEN, H. K., M.A., D.Sc., D.I.C., Director, Indian Lac Research Institute, Namkum, Ranchi.
147. SEN, J. M., B.Sc., M.Ed. (Leeds), Dip.Ed. (Oxford), T.D. (London), F.R.G.S., Principal, Krishnagar College, Krishnagar. (1935).
148. SEN, N. R., D.Sc., Ph.D., Ghose Professor of Applied Mathematics, Calcutta University, 92, Upper Circular Road, Calcutta.
149. SENGUPTA, N. N., Ph.D., Professor of Psychology, Lucknow University, Lucknow.
150. SEYMOUR SEWELL, LT.-COL. R. B., C.I.E., M.A., Sc.D., F.R.S., M.R.C.S., L.R.C.P., F.Z.S., F.L.S., Zoological Laboratory, Cambridge University, Cambridge. (1936).
151. SHAH, R. C., M.Sc., Ph.D. (Lond.), Professor of Organic Chemistry, Royal Institute of Science, Bombay. (1941).
152. SHARIF, M., D.Sc., Ph.D., Entomologist, Haffkine Institute, Parel, Bombay. (1939).
153. SHORTT, LT.-COL. H. E., C.I.E., M.D., Ch.B., D.T.M. & H., D.Sc., I.M.S., Inspector-General of Civil Hospitals, Assam, Shillong. (1936).
154. SIDDIQI, M. R., M.A., Ph.D., Professor of Mathematics, Osmania University, Hyderabad (Deccan). (1937).
155. SINGH, B. K., M.A., Sc.D., F.I.C., I.E.S., Professor of Chemistry, Allahabad University, Allahabad.
156. SINGH, B. N., M.Sc., D.Sc., Irwin Professor of Agriculture, University Professor of Plant Physiology and Head of the Institute of Agricultural Research, Benares Hindu University. (1941).
157. SINTON, LT.-COL. J. A., V.C., O.B.E., M.D., D.Sc., D.P.H., D.T.M., I.M.S., Malaria Laboratory, Horton Hospital, Epsom, Surrey, England.
158. SIRCAR, A. C., M.A., Ph.D., Professor of Chemistry, Presidency College, Calcutta. (1937).
159. SOKHEY, LT.-COL. S. S., M.A., M.D., D.T.M. & H., I.M.S., Director, Haffkine Institute, Parel, Bombay.
160. SONDI, V. P., M.B.E., M.Sc., F.G.S., Geologist, Geological Survey of India, Calcutta. (1941).
161. SOPARKAR, M. B., M.D., B.Hy., 117 Khar, Bombay 21. (1937).
162. SPENCER, E., D.Sc., Ph.D., F.I.C., A.R.S.M., M.I.M.M., F.G.S., Consulting Chemist, Bird & Co., Chartered Bank Buildings, Clive Street, Calcutta.
163. SRIVASTAVA, P. L., Raj Sahib, M.A., D.Phil., Reader in Mathematics, Allahabad University, Allahabad. (1935).
164. SUBRAHMANYAN, V., D.Sc., F.I.C., Professor of Biochemistry, Indian Institute of Science, Bangalore.
165. SUR, N. K., D.Sc., Meteorologist, Alipore Observatory, Calcutta. (1938).
166. TAYLOR, MAJOR-GENERAL J., C.I.E., D.S.O., M.D., D.P.H., I.M.S., Director, Central Research Institute, Kasauli (Simla Hills).
167. TEMPLE, F. C., (Hony. Col.) A.F. (I.), C.I.E., V.D., A.D.C., 28, Victoria Street London, S.W.1. (1937).
168. TIRUMURTI, T. S., Rao Bahadur, B.A., M.B. & C.M., D.T.M. & H., Retired Civil Surgeon, 1, Krishnamachari Road, Nungumbakam, Madras.
169. UKIL, A. C., M.B., M.S.P.E., Tuberculosis Research Officer, All-India Institute of Hygiene and Public Health, Calcutta. (1935).
170. VENKATARAMAN, K., M.S.Tech., Ph.D., D.Sc., Director, Bombay University Laboratories of Chemical Technology and Textile Chemistry, Bombay. (1939).
171. VENKATARAMAN, T. S., Diwan Bahadur, B.A., I.A.S., Imperial Sugar Cane Specialist, P.O. Lawley Road, Coimbatore.
172. VENKATESACHAR, B., Rao Bahadur, M.A., F.Inst.P., Ambika Bilas, Bull Temple Road, Basavangudi, Bangalore.
173. VIJAYARAGHAVAN, T., Ph.D. (Oxon), Reader in Mathematics, Dacca University, Ramna, Dacca.
174. VISWANATH, B., Rao Bahadur, F.I.C., F.C.S., Director, Imperial Agricultural Research Institute, New Delhi.
175. WADIA, D. N., M.A., B.Sc., F.G.S., F.R.G.S., F.R.A.S.B., Mineralogist to the Ceylon Government, Torrington Square, Colombo.

176. WARR, F., C.I.E., F.R.C.V.S., I.V.S., Animal Husbandry Commissioner with the Government of India, New Delhi.
177. WEST, W. D., M.A. (Cantab.), Geologist, Geological Survey of India, Indian Museum, Calcutta.
178. WHEELER, T. S., D.Sc., Ph.D., F.R.C.Sc.I., F.I.C., F.Inst.P., M.I.Chem.E., State Chemist, State Laboratory, Upper Merrion St., Dublin, Eire.
179. YAJNIK, N. A., M.A., D.Sc., A.I.C., Professor of Chemistry, Punjab University, Lahore. (1940).

## HONORARY FELLOWS.

1. DR. E. V. APPLETON, M.A., D.Sc., F.R.S., Secretary, Department of Scientific and Industrial Research of Great Britain, London.
2. DR. E. B. BAILEY, F.R.S., Director-General, Geological Survey of Great Britain, London.
3. PROF. NIELS BOHR, N. L., 15, Belgdamsvej, Copenhagen.
4. PROF. F. O. BOWER, Sc.D. (Cantab.), LL.D., F.R.S., Emeritus Professor of Botany, Glasgow University, 2, The Crescent, Ripon, Yorks.
5. SIR RICKARD CHRISTOPHERS, Kt., C.I.E., O.B.E., M.B., Brevet-Colonel, I.M.S. (Retd.), 186, Huntingdon Road, Cambridge.
6. PROF. LUDWIG DIELS, Director-General of the Botanical Garden and Museum, 7, Konigin Luise Strasse, Berlin-Dahlem, Germany.
7. PROF. F. G. DONNAN, F.R.S., Formerly Director, Sir William Ramsay Laboratory, University College, 23, Woburn Square, London, W.C. 1.
8. SIR ARTHUR EDDINGTON, D.Sc., LL.D., F.R.S., Plumian Professor of Astronomy and Experimental Philosophy, Cambridge University, Cambridge.
9. PROF. CHARLES W. EDMUNDS, A.B., M.D., Professor of Pharmacology and Therapeutics, University of Michigan Medical School, Ann Arbor, Michigan, U.S.A.
10. PROF. ALBERT EINSTEIN, N.L., Princeton University, New Jersey, U.S.A.
11. PROF. R. A. FISHER, Sc.D., F.R.S., Galton Professor in the University of London.
12. PROF. E. S. GOODRICH, M.A., D.Sc., F.R.S., Linacre Professor of Zoology and Comparative Anatomy, University of Oxford.
13. MAJOR M. GREENWOOD, D.Sc., F.R.C.P., F.R.S., Professor of Epidemiology and Vital Statistics, London School of Tropical Medicine and Hygiene.
14. SIR THOMAS H. HOLLAND, K.C.S.I., K.C.I.E., D.Sc., F.R.S., Principal of the University of Edinburgh.
15. SIR FREDERICK GOWLAND HOPKINS, Kt., M.A., D.Sc., N.L., F.R.S., Sir William Dunn Professor of Biochemistry in the University of Cambridge.
16. SIR ARTHUR B. KEITH, M.D., F.R.C.S., LL.D., F.R.S., Buckston Browne Farm, Downe, Farnborough, Kent, England.
17. PROF. E. O. LAWRENCE, Radiation Laboratory, California University, Berkeley, U.S.A.
18. SIR GUY A. K. MARSHALL, C.M.G., F.R.S., Director, Imperial Institute of Entomology, London.
19. PROF. J. PERRIN, N.L., Sorbonne, Paris.
20. SIR ROBERT ROBINSON, D.Sc., F.R.S., Waynflete Professor of Organic Chemistry in the Dyson Perrins Laboratory, Oxford University.
21. SIR E. JOHN RUSSELL, D.Sc., F.R.S., Director, Rothamsted Agricultural Experimental Station, Harpenden, Herts, England.
22. SIR CHARLES S. SHERRINGTON, O.M., G.B.E., N.L., F.R.S., Formerly Waynflete Professor of Physiology in the University of Oxford, Broomside, Valley Road, Ipswich, England.
23. DR. C. M. WENYON, C.M.G., C.B.E., F.R.S., Director-in-chief, Wellcome Bureau of Scientific Research, 183, Euston Road, London, N.W. 1.

## APPENDIX II.

## COMMITTEES, 1942.

## SECTIONAL COMMITTEES.

## (1) 'Mathematics' Committee for Mathematics, Astronomy and Geodesy:—

	To serve until Dec. 31.
Mr. T. P. Bhaskara Shastri .. .. .	1942.
Lt.-Col. E. A. Glennie .. .. .	1942.
Dr. S. K. Banerji (Secretary and Convener) .. .. .	1943.
Prof. V. V. Narlikar .. .. .	1943.
Principal B. M. Sen .. .. .	1944.
Prof. P. C. Mahalanobis .. .. .	1944.

## (2) 'Physics' Committee for Physics and Meteorology:—

Prof. K. S. Krishnan (Secretary and Convener) .. .. .	1942.
Prof. S. N. Bose .. .. .	1942.
Prof. P. K. Kichlu .. .. .	1943.
Prof. B. B. Ray .. .. .	1943.
Dr. N. K. Sur .. .. .	1944.
Dr. D. S. Kothari .. .. .	1944.

## (3) 'Chemistry' Committee for Pure and Applied Chemistry:—

Prof. P. C. Mitter (Secretary and Convener) .. .. .	1942.
Sir S. S. Bhatnagar .. .. .	1942.
Dr. K. Venkataraman .. .. .	1943.
Prof. M. Qureshi .. .. .	1943.
Dr. J. K. Basu .. .. .	1944.
Dr. B. C. Guha .. .. .	1944.

## (4) 'Engineering Sciences' Committee for Engineering, Metallurgy, Electro-technics and kindred subjects:—

Mr. F. N. Mowdawalla .. .. .	1942.
Prof. P. N. Ghosh .. .. .	1942.
Dr. F. G. Percival (Secretary and Convener) .. .. .	1943.
Mr. W. C. Ash .. .. .	1943.
Dr. Gilbert Fowler .. .. .	1944.

## (5) 'Geology' Committee for Geology, Palaeontology, Mineralogy and Geography:—

Prof. L. Rama Rao .. .. .	1942.
Mr. W. D. West (Secretary and Convener) .. .. .	1942.
Mr. D. N. Wadia .. .. .	1943.
Mr. E. S. Pinfold .. .. .	1943.
Dr. M. S. Krishnan .. .. .	1944.
Mr. J. B. Auden .. .. .	1944.

## (6) 'Botany' Committee for Pure and Applied Botany, Forestry and Agronomy:—

Dr. K. Bagchee .. .. .	1942.
Dr. P. Maheshwari .. .. .	1942.
Principal P. Parija (Secretary and Convener) .. .. .	1943.
Prof. S. R. Bose .. .. .	1943.
Prof. S. P. Agharkar .. .. .	1944.
Rao Bahadur G. N. Rangaswami Ayyangar .. .. .	1944.

## (7) 'Zoology' Committee for Pure and Applied Zoology and Anthropology including Ethnology:—

	To serve until Dec. 31.
Mr. J. P. Mills .. .. .	.. 1942.
Dr. B. Prashad (Secretary and Convener) .. .. .	.. 1942.
Dr. B. S. Guha .. .. .	.. 1943.
Dr. H. S. Pruthi .. .. .	.. 1943.
Khan Bahadur M. Afzal Hussain .. .. .	.. 1944.
Prof. R. Gopala Aiyar .. .. .	.. 1944.

## (8) 'Physiology' Committee for Animal Physiology, Pathology, Bacteriology, Psychology and other Medical and Veterinary subjects:—

Bt.-Col. Sir R. N. Chopra .. .. .	.. 1942.
Dr. C. G. Pandit .. .. .	.. 1942.
Major C. L. Pasricha (Secretary and Convener) .. .. .	.. 1942.
Sir U. N. Brahmachari .. .. .	.. 1943.
Major-General J. Taylor .. .. .	.. 1943.
Dr. K. N. Bagchi .. .. .	.. 1943.
Mr. F. Ware .. .. .	.. 1944.
Lt.-Col. S. S. Sokhey .. .. .	.. 1944.
Prof. N. N. Sen Gupta .. .. .	.. 1944.

## APPENDIX III.

## LIST OF INSTITUTIONS ON THE EXCHANGE LIST.

*Indian.**Allahabad.*

1. Allahabad University.
2. National Academy of Sciences, India.

*Bangalore.*

3. Department of Agriculture, Mysore State.
4. Electrical Engineering Society.
5. Geological Survey Department, Mysore State.
6. Indian Academy of Sciences.
7. Indian Institute of Science.
8. Meteorological Department, Mysore State.
9. Mysore University.
10. Society of Biological Chemists, India.

*Benares.*

11. Indian Botanical Society.

*Bombay.*

12. Anthropological Society of Bombay.
13. Bombay Natural History Society.
14. Indian Central Cotton Committee.
15. Royal Institute of Science.

*Calcutta.*

16. Anthropological Society of India.
17. Biochemical Society of India.
18. Botanical Survey of India.
19. Calcutta Mathematical Society.
20. Calcutta Medical Club.
21. Calcutta School of Tropical Medicine.
22. Calcutta University.
23. Carmichael Medical College.
24. Geological, Mining and Metallurgical Society of India.
25. Geological Survey of India.
26. Indian Association for the Cultivation of Science.
27. Indian Chemical Society.
28. Indian Medical Gazette (Thacker, Spink & Co. (1933) Ltd.)
29. Indian Physical Society.
30. Indian Psychological Association.
31. Indian Statistical Institute.
32. Indian Tea Association.
33. Institution of Chemists, India.
34. Mining, Geological and Metallurgical Institute of India.
35. Physiological Society of India.
36. Royal Agri-Horticultural Society of India.
37. Royal Asiatic Society of Bengal.
38. Science and Culture.
39. Survey of India Department.
40. Zoological Survey of India.

*Coochpur.*

41. Pasteur Institute of Southern India.

*Dacca.*

42. Dacca University.

*Dehra Dun.*

43. Board of Management, Indian Forester.
44. Imperial Forest Research Institute.

*Hyderabad (Deccan).*

45. Department of Mines and Geological Survey, H.E.H. Nizam's Government.
46. Osmania University.

*Indore.*

47. Institute of Plant Industry.

*Kasauli.*

48. Central Research Institute.
49. Indian Journal of Medical Research.
50. Malaria Institute of India.

*Lahore.*

51. Punjab University.

*Lucknow.*

52. Indian Zoological Memoirs.
53. Lucknow University.



*Madras.*

- 54. King Institute of Preventive Medicine.
- 55. Madras Fisheries Department.
- 56. Madras Government Museum.

*Muktesar.*

- 57. Imperial Veterinary Research Institute.

*Naggar (Punjab).*

- 58. Himalayan Research Institute, Roerich Museum.

*New Delhi.*

- 59. Imperial Council of Agricultural Research.

*Poona.*

- 60. Indian Mathematical Society.
- 61. India Meteorological Department.

*Ranchi*

- 62. Indian Lac Research Institute.

*Simla.*

- 63. Himalayan Club.

*Foreign.**Canada.*

- 64. Department of Mines, Ottawa.
- 65. Geological Survey of Canada, Ottawa.

*Cape Colony.*

- 66. South African Library, Cape Town.

*China.*

- 67. Chinese Physical Society, Kunming.
- 68. National Agricultural Research Bureau, Nanking.

*France.*

- 69. Museum d'Histoire Naturelle, Paris.

*Germany.*

- 70. Chemisches Zentralblatt, Berlin.

*Great Britain.*

- 71. British Museum, Natural History Section, London.
- 72. Imperial Bureau of Plant Genetics (for crops other than Herbage), Cambridge.
- 73. Imperial Bureau of Plant Genetics (Herbage plants), Aberystwyth.
- 74. Nature, London.
- 75. Patent Office, London.

- 76. Royal Botanic Gardens, Edinburgh.
- 77. Royal Society of Edinburgh.
- 78. Science Museum, London.

*Italy.*

- 79. Institute International d'Agriculture, Rome.

*Java.*

- 80. Department van Economische Zaken, Batavia.

*Palestine.*

- 81. Jewish National University, Rehovoth.

*Philippines.*

- 82. Scientific Library, Bureau of Science, Manila.

*Russia.*

- 83. All-Union Lenin Library, Moscow.

*Uganda.*

- 84. Geological Survey of Uganda.

*U.S.A.*

- 85. American Chemical Society, Columbus.
- 86. American Museum of Natural History, New York.
- 87. California University, Berkeley.
- 88. Marine Biological Laboratory, Woods Hole, Mass.
- 89. Missouri Academy of Science, Columbia.
- 90. Scripta Mathematica, New York.
- 91. Smithsonian Institution, Washington.
- 92. Treasury Department, U.S. Public Health Service, Washington.
- 93. U.S. Department of Agriculture, Washington.
- 94. U.S. National Bureau of Standards, Washington.
- 95. U.S. National Museum, Washington.

## APPENDIX IV.

## LIST OF PERIODICALS RECEIVED IN EXCHANGE OR AS PRESENTATION.

*Indian.*

Annual Report Haffkine Institute.  
 Annual Report of the Imperial Veterinary Research Institute.  
 Annual Report of the Indian Central Cotton Committee.  
 Annual Report of the Department of Agriculture, Mysore.  
 Annual Report of the Indian Association for the Cultivation of Science.  
 Annual Return of Statistics relating to Forest Administration in British India.  
 Annual Review of Biochemical and Allied Research in India.  
 Bulletin Madras Fisheries.  
 Bulletin of the Indian Central Cotton Committee.  
 Bulletin of the Calcutta Mathematical Society.  
 Calcutta Medical Journal,

Forest Bulletin.  
 Forest Research in India and Burma.  
 General Report of the Survey of India.  
 Indian Farming.  
 Indian Forester.  
 Indian Forest Records.  
 Indian Journal of Agricultural Science.  
 Indian Journal of Medical Research.  
 Indian Journal of Physics.  
 Indian Journal of Veterinary Science and Animal Husbandry.  
 Indian Medical Gazette.  
 Indian Zoological Memoirs.  
 Industrial and News Edition, Indian Chemical Society.  
 Journal of the Indian Chemical Society.  
 Journal of the Indian Mathematical Society.  
 Journal of the Indian Medical Association.  
 Journal of the Malaria Institute, India.  
 Journal of the University of Bombay.  
 Journal of the University of Mysore.  
 Journal of the Osmania University.  
 Mysore Agricultural Calendar.  
 Popular Studies, Mysore Geological Department.  
 Proceedings of the Indian Academy of Sciences.  
 Proceedings of the Institute of Chemists (India).  
 Quarterly Journal of the Geological, Mining and Metallurgical Society of India.  
 Rasayanam.  
 Records of the Botanical Survey of India.  
 Records of the Mysore Geological Department.  
 Report Bio-Chemical Standard Laboratory.  
 Report of the Botanical Survey of India.  
 Report of the King Institute of Preventive Medicine, Madras.  
 Science and Culture.  
 Scientific Monograph, Imperial Council of Agricultural Research.  
 Scientific Notes of the India Meteorological Department.  
 Seismological Bulletin of the India Meteorological Department.  
 Statistical Leaflets of the Indian Central Cotton Committee.  
 Summary Proceedings of the Meetings of the Indian Central Cotton Committee.  
 The Mathematics Student.  
 Transactions of the Mining, Geological and Metallurgical Institute of India.

### *Foreign.*

American Museum Novitates, New York.  
 Annales du Jardin Botanique de Buitenzorg.  
 Biological Bulletin of the Marine Biological Laboratory, Woods Hole, Mass., U.S.A.  
 Bulletin, Jardin Botanique, Buitenzorg.  
 Bulletin of the Agricultural Experiment Station, Rehovoth, Palestine.  
 Bulletin of the Scripps Institute of Oceanography, California University.  
 Bulletin of the American Museum of Natural History, New York.  
 Bulletin (Herbage Publication Series), Imperial Bureau of Plant Genetics, Aberystwyth.  
 Bulletin of the U.S. National Museum, Washington.  
 Contributions from the U.S. Herbarium, Washington.  
 Crop Reports, National Agricultural Research Institute, Szechuan.  
 Experiment Station Record, U.S. Department of Agriculture, Washington.  
 Geological Survey Paper, Canada Department of Mines.  
 Journal of the American Chemical Society.  
 Memoirs of the Canada Department of Mines.  
 Proceedings of the Royal Society of Edinburgh.  
 Proceedings of the U.S. National Museum.  
 Papers in Physical Oceanography and Meteorology, Woods Hole Oceanographic Institute.  
 Publications in Botany, University of California.  
 Report of the Canada Department of Mines.  
 Scripta Mathematica, New York.  
 Technical News Bulletin, National Bureau of Standards, Washington.  
 Transactions and Proceedings of the Botanical Society of Edinburgh.  
 Treubia.

## APPENDIX V.

## THE NATIONAL INSTITUTE OF SCIENCES OF INDIA.

*Receipts and Payments Account for the year ended 30th November, 1941.*

RECEIPTS.				PAYMENTS			
	Rs.	A.	P.		Rs.	A.	P.
To Balance brought forward	..	..	47,427 14 10	By Salaries of Staff	..	..	3,171 5 6
" Members' Admission Fees	..	..	320 0 0	" Printing Circulars, Notices, etc.	..	..	65 7 0
" Subscriptions	..	..	5,504 1 0	" Publications, Reports, etc.	..	..	3,565 0 6
" Contributions towards publication of	..	..	..	" 'Indian Science Abstracts'	..	..	2,169 8 0
" 'Indian Science Abstracts'	..	..	50 0 0	" Contributions to other Science Academies under Rule 19	..	..	1,056 0 0
" Sale of Authors' extra copies and publications	..	..	409 7 0	" Honoraria, etc. for preparing Abstracts for 'Indian Science Abstracts'	..	..	550 0 0
" Sale of 'Indian Science Abstracts'	..	..	124 0 0	" Postage	..	..	437 13 6
" Interest on Investments	..	..	1,505 1 0	" Stationery	..	..	159 1 9
" Grants-in-aid—	..	..	..	" Audit Fee	..	..	50 0 0
Government of India	..	7,000 0 0	..	" Travelling	..	..	87 6 0
Universities	..	1,000 0 0	8,000 0 0	" Rent of Office	..	..	600 0 0
" Miscellaneous Receipts	..	..	7 4 0	" Miscellaneous Expenses	..	..	83 12 0
				" Bank Charges	..	..	18 15 0
				" Cash and Other Balances—	..	..	..
				Investments—	..	..	..
				3½% G.P. Notes 1842/43	..	5,000	..
				3½% " 1854/55	..	2,000	..
				3½% " 1865	..	6,000	..
				3½% " 1879	..	2,000	..
				3½% " 1900/01	..	8,000	..
				4% Loan 1960/70	..	17,000	..
					..	40,000	..
				At cost	..	40,786 13 10	..
				With Imperial Bank of India—	..	..	..
				On Savings Bank	Rs.	A.	P.
				Account	..	5,713 9 0	..
				On Current Account	4,818 12 9	..	..
					10,532 5 9	..	..
				In hand	..	14 3 0	..
					..	51,333 6 7	..
TOTAL	..	..	63,347 11 10	TOTAL	..	..	63,347 11 10

Examined with the Books and Vouchers and found in accordance therewith.

PRICE, WATERHOUSE, PEAT & CO. }  
 Chartered Accountants, }  
 Registered Accountants. } Auditors.

CALCUTTA,  
 8th December, 1941.

## APPENDIX VI.

## BUDGET ESTIMATES.

	1940-41 Estimates.	1940-41 Actuals.	1941-42 Estimates.
<i>Ordinary Receipts.</i>			
	Rs.	Rs.	Rs.
Subscription .. .. .	5,500	5,373	5,500
Interest .. .. .	1,400	1,505	1,500
Contributions towards publication of 'Indian Science Abstracts' ..	1,500	50	100
Sale of publications including 'Indian Science Abstracts' ..	800	533	500
Grants-in-aid from Universities ..	1,000	1,000	1,000
Grants-in-aid from Government of India .. .. .	7,000	7,000	7,000
Miscellaneous Receipts .. ..	..	7	..
Contributions from General Fund ..	700	..	3,800
	<u>17,700</u>	<u>15,468</u>	<u>19,400</u>
<i>Extraordinary Receipts.</i>			
Admission Fees .. .. .	320	320	320
Compounding Fees .. .. .	131	131	..
	<u>451</u>	<u>451</u>	<u>320</u>
<i>Ordinary Payments.</i>			
Salaries and allowances .. ..	3,300	3,171	3,300
Publications including 'Indian Science Abstracts' and Circulars ..	10,000	5,800	12,000*
Contributions to co-operating academies under Rule 19 .. .. .	1,200	1,056	1,200
Honoraria, etc., for preparing abstracts for 'Indian Science Abstracts' ..	1,000	550	1,000
Furniture .. .. .	300	..	..
Postage .. .. .	600	438	600
Stationery .. .. .	150	159	150
Audit Fee .. .. .	50	50	50
Travelling .. .. .	400	87	400
Office rent .. .. .	600	600	600
Miscellaneous (including bank charges)	100	103	100
Refunded to General Fund .. ..	..	3,454	..
	<u>17,700</u>	<u>15,468</u>	<u>19,400</u>
<i>Extraordinary Payments.</i>			
Funding of Admission Fees and Com- pounding Subscription .. .. .	451	451	320

\* Additional provision has been made to cover the increased cost of paper and publications.

# Annual Address to the National Institute of Sciences of India.

BARODA, 1942.

By DR. B. PRASHAD, *D.Sc., F.R.S.E., F.L.S., F.Z.S., F.R.A.S.B.*

## ZOOGEOGRAPHY OF INDIA.

### I. GENERAL.

I have first of all to express my appreciation and thanks to the Council and the Fellows of the National Institute for the high honour they did me by electing me as the President of the Institute. During the year under review I have tried, as far as possible, to carry on the traditions of my distinguished predecessors in this office, and this would not have been possible but for the whole-hearted support and co-operation of my colleagues on the Council.

Since our last meeting at Benares the affairs of the Institute have progressed satisfactorily, and notwithstanding the great stress of the economic conditions as a result of the war there has been no marked change in our material prosperity during this period. It is unfortunate that the Institute has not received any fresh donations during the year, but it is hoped that this lack of support will not seriously hinder the progress of our work. The record of our activities during the past year, as detailed in the Annual Report, reflects credit on the administrative officers and the Council of the Institute for the skilful handling of its affairs.

The number of Fellows on our roll at the beginning of the year was 170 Ordinary and 21 Honorary Fellows. At the end of the year this number stood at 179 Ordinary and 23 Honorary Fellows. During the year two Fellows resigned, and through death we lost two Honorary and three Ordinary Fellows. As was remarked by my distinguished predecessor Sir Ram Nath Chopra in his Address last year, the number of active Fellows of the Institute, considering the prevailing conditions in the country and the statutory limitations in regard to new elections, is satisfactory, but the Council for some time had been considering the question of increasing the number of new elections with a view to be able to maintain and extend the activities of the Institute. With this end in view a change in the rules was suggested after very careful consideration. This change, which was adopted in the Benares meeting, has made it possible for an increase in the number of elections from 10 as laid down in Rule 7(B) to a number not

exceeding 15, dependent on the vacancies occurring during the previous year by resignation, death or otherwise, until the maximum of 250 is reached. As a result of this change 14 new Ordinary Fellows and 4 Honorary Fellows were elected in 1941.

Two Ordinary General Meetings of the Institute were held during the year.

**Meetings of the Institute.** The first was held in the Physics Lecture Theatre of the Delhi University on the 19th of April, 1941 and was followed by a Symposium on 'Heavy Chemical Industries in India';

in this meeting a number of interesting papers were read and discussed. Unfortunately I found it impossible to be present at this meeting, and we are grateful to Sir Shanti Swarup Bhatnagar for so kindly arranging the symposium, and to the authorities of the Delhi University and in particular to Prof. D. S. Kothari, Professor of Physics, for making the necessary arrangements for the meeting at Delhi. The second meeting was held in Calcutta in the rooms of the Royal Asiatic Society of Bengal on the 29th of August, 1941. In this meeting a number of papers were read and discussed, but the special lecture arranged for the meeting had unfortunately to be cancelled.

The Council for the year was elected at the sixth Annual Meeting held at Benares on the 2nd of January, 1941 and has served throughout the year without any change. Seven Ordinary meetings and two emergency meetings were held during the year; the attendance of the members in these meetings was fairly satisfactory.

**Council.**

Three numbers of the *Proceedings*, one number of the *Transactions* and one number of *Indian Science Abstracts* were published during the year under review. The preparation of the material for, and the editing of the *Indian Science Abstracts* involves a great deal of work, and the printing of this publication is also very expensive. Owing to the war the cost of printing in general has increased materially, and the Council has been faced with the serious situation of finding ways and means for the continuance of the activities of the Institute in this connection. We are particularly grateful to the Government of India for sanctioning an increase in their annual grant from Rs.6,000 to Rs.7,000 from the current financial year.

**Publications.**

As a result of my experience of running the publications of the Institute since its foundation I am definitely of the opinion that it is not possible for any one person to run the publications of a learned Society like ours without the active help of a number of editors and workers all over the country, while for the *Indian Science Abstracts* the question of having a permanent staff for looking after their preparation and publication is becoming more and more patent.

The preparation of a Quinquennial Review dealing with the progress of science in the country, to which a reference was made by Sir Ram Nath Chopra in his Address at Benares, could not unfortunately be taken up, but I hope the Council will arrange for its compilation this year.

The financial position of the Institute is detailed in the Balance Sheet appended to the Annual Report. Though the position is in no way alarming, there can be no question that our expenses are definitely on the high side, more particularly in connection with our publications. This in view of the daily increasing cost of publication is a serious matter, and attempts will have to be made, if we are to continue our activities, to have the annual grants-in-aid, which we receive from the Government of India and the Universities, increased. In this connection special mention may be made of a grant-in-aid of Rs.500 which was sanctioned by the Punjab University for the publication of a specially expensive paper in the *Transactions* of the Institute. I have already referred to the increase in the annual grant from the Government of India from Rs.6,000 to Rs.7,000 which was sanctioned from the beginning of the current financial year. In addition we have received the following grants during the year:—

- (1) Rs.500 from the Calcutta University.
- (2) Rs.300 from the Osmania University.
- (3) Rs.200 from the Dacca University.

We are grateful to the authorities of these Universities for their support, and I hope that other Universities in the country will also help us to carry on the work of the Institute by sanctioning grants-in-aid.

I have already referred to the sad loss by death during the year of two of our Honorary and three Ordinary Fellows, and short references to their career would not be out of place here:

(1) Sir Albert C. Seward, D.Sc., Hon. LL.D., F.R.S., formerly Master of the Downing College and the Emeritus Professor of Botany in the University of Cambridge, was elected as an Honorary Fellow in 1936. He was born in 1863 and died on April 11, 1941, at the age of 77. Sir Albert has rightly been described as the founder of modern Palaeobotany, and was well known as a teacher, research worker, author and administrator. Though he did not contribute any articles to our publications he was the author of several important papers on the Palaeobotany of India. Indian Botany owes a great deal to his example and teaching, and Science is much the poorer by his early death.

(2) Sir James G. Frazer, O.M., D.C.L., LL.D., Trinity College, Cambridge, was elected an Honorary Fellow in 1937. Sir James Frazer died at Cambridge on May 7th at the age of 87 years. Sir James's fame was world-wide as the author of that cyclopaedic work 'The Golden Bough' and many other studies dealing with primitive beliefs and institutions; Anthropology has lost an outstanding exponent by his death.

(3) Sir Shah Muhammad Sulaiman was elected as a Fellow in 1937. After passing the B.Sc. examination from the Allahabad University he received a State Scholarship for studies abroad, and took the Mathematics Tripos of the Cambridge University. After practising for some years in the mofussil



and the Allahabad High Court, he was elevated to the Bench in 1920 at the early age of 34, and after officiating on several occasions was appointed the Chief Justice in 1932. In 1937 he was appointed as a Judge in the Federal Court of India. He died at the early age of 56. By his sudden and untimely death India has lost not only a great jurist and a great scholar, but a true patron of learning. In spite of being taken up with legal work he made valuable contributions on the Theory of Relativity, the problem of the deviation of light, etc. He also published one paper in our *Proceedings*. As the Vice-Chancellor of the Muslim University, Aligarh, he not only put new life into the work of the institution, but, what is probably more important, he established it on a firm financial footing. His sad death cut short a very promising career.

(4) Dr. P. K. Koshy was one of the Founder Fellows of the National Institute. He was born in 1885 and breathed his last on the 19th March, 1941. Dr. Koshy was well known for his anatomical work and was a distinguished teacher. The Anatomy museum of the Madras Medical College owes a great deal to his untiring zeal and energy, and is in fact one of the best Anatomy museums in the East. In recognition of his researches he was elected a Fellow of the Royal College of Physicians at Edinburgh.

(5) Dr. B. L. Bhatia was elected a Fellow of the National Institute in 1937. He was one of the pioneers among the students of Biology in the Punjab, and as a teacher played a very important part in popularising the study of Biology in the province. During his active service of some 25 years in the Punjab Educational Service he occupied various posts as an Assistant Professor, Lecturer and Professor of Zoology in the Government College, Lahore, and finally as the Principal of the Government Intermediate College, Hoshiarpur. After his retirement he started an Indian Science News Agency, but had to give up this work on being appointed as the Principal of the Jind State College, Sangrur. He was one of the founders of the Society for Promoting Scientific Knowledge at Lahore, and for a time was the editor of its journal the 'Raushani'. He was a great organiser and was connected with the management of several educational institutions. He published a number of papers on Protozoa, and was the author of two volumes dealing with the Indian forms in the *Fauna of British India* series.

Sir Ram Nath Chopra in his Presidential Address at Madras in January 1940 briefly discussed the organisation and development of scientific studies and research in India and suggested a scheme for a body 'which could draw up a comprehensive scheme of scientific and industrial research, mobilise all available talent in the country by allotting problems to scientists and institutes best suited for their solution, provide necessary research facilities and adequate grants, and finally deal *in extenso* with all scientific and industrial problems of the entire country'.

**Development  
of Scientific Re-  
search.**

The abnormal conditions resulting from the war are probably responsible for very little attention having been paid to the highly important question of the development of research in pure science, but a great headway has been made in connection with industrial research.

In his Address at Benares last year Sir Ram Nath referred to the establishment of a Board of Scientific and Industrial Research by the Central Government. Since its inception and more particularly during the year under review the Board of Scientific and Industrial Research has carried out very important and highly valuable work under the distinguished directorship of our Fellow Sir Shanti Swarup Bhatnagar. He and his associates have initiated and developed various research schemes, several of which have already found application in industry in connection with the war, while others are likely to play a very important part in the industrial development of the country as a whole. In accordance with the policy adopted for the Board the results of these researches have been made available to private industrialists in the country for the development of industry, and it is gratifying to note that as a result of these researches several industrial undertakings have been started in different parts of the country. This great development is undoubtedly to be attributed to the far-seeing policy and active interest of all members of the Board, as also the team-work of the various Research Committees which have been working under its aegis. The Government of India realising the great value of the work carried out by the Board have decided to constitute it on a permanent basis. With this end in view Sir Shanti Swarup Bhatnagar has been confirmed in his appointment as the Director, and the Board is to be financed from an Industrial Research Fund, which will receive grants of 10 lakhs of rupees a year for a period of five years. It will be managed by a Board of Trustees consisting of some officials, and prominent scientists and industrialists, and its main function will be the fostering of industrial development in the country. A resolution to this effect was passed by the Central Legislative Assembly at Delhi in its November session. For this highly satisfactory state of affairs the country is indebted to the untiring efforts of the Hon'ble Diwan Bahadur Sir A. Ramaswami Mudaliar, Member in charge of the Department of Commerce and Labour, who is also the Chairman of the Board.

This Board brings industrial research in line with other agencies in the country dealing with special branches, such as the Indian **Other Research Organisations.** Research Fund Association for medical research, the Imperial Council of Agricultural Research for agriculture and animal husbandry, the Indian Cotton Committee for cotton, the Indian Jute Association for jute, the Lac Cess Committee for lac, etc. The name 'Board of Scientific and Industrial Research' as applied to the Board referred to above, however, is not strictly accurate, as the major part of the activities of the Board

will be directed, as has been remarked above, towards fostering industrial developments in the country.

In connection with scientific planning it has become essential in almost all civilised countries to think not of individual and sectional problems only, but of all scientific problems as they concern the country and community as a whole. These problems can roughly be grouped under two main heads: (i) those that concern the internal organisation of science, and (ii) those dealing with the relationship between all scientific work and developments in the country. The very complicated problems connected with the work and future of the workers who are employed in research on the one hand and of the multiplicity of sciences, institutes, universities and other cognate research agencies on the other have created the necessity for setting up organisations not only for organising, developing and directing their activities but safeguarding the interests of these scientific workers; these functions cannot be performed by bodies interested in one or other branch only. The phrase 'organisation of research', as that great biological philosopher, the late Professor William Morton Wheeler so aptly described, 'is nonsense if we take "research" in its abstract sense, for an abstraction, of course, is one of the things that cannot be organised. All we can mean by the term is the organisation of the actual processes of research, or investigation, and since these processes are essentially nothing but the living, functioning investigators themselves, organisation of research can mean only the organisation of the investigators'. All the same, the developments in the country in regard to applied research are so rapid and the conditions under which these are taking place so abnormal, mainly owing to the stress of the war, that it will not be out of place to repeat here the note of warning from an editorial in *Nature* published in 1938: 'the research organisations of the country should be truly national and responsible to the Federal Government alone. Even in an Empire the size of India, where the resources and needs of various provinces are widely different, it would seem that centralised organisation of research is the only way of avoiding waste of money and effort. The detailed planning of research must be in the hands of those with the necessary specialised knowledge, and they must be able to act without suspicion of political or racial influence'. This, in other words, stresses the necessity for having a central co-ordinating and directing agency, and I would again very strongly urge for the consideration of the authorities the constitution of a truly representative National Research Council in India on the lines of the body which has been rendering such useful service in Great Britain ever since its constitution. Similar bodies are also doing invaluable work in Canada, South Africa, Australia, etc. As I stated on an earlier occasion, 'The functions of this Council should not only include the defining of scientific policy but it should also act as an expert advisory body for planning and co-ordinating all scientific research in the country. The planning of scientific policy and co-ordination of research should

be so arranged as to preclude duplication and avoid wastage of talent and available funds, but without restricting the normal work of the universities, scientific departments and institutions, or in any way curbing individual initiative which is so essential for high class research. Such an authoritative body should also be able to help in bringing about the necessary reforms in the existing system of scientific education'.

The National Institute of Sciences of India was started in 1935 in response to the keenly felt need for a body which could co-ordinate the work of all scientific societies, institutions, Government Scientific Departments and Services, and cognate agencies throughout the country. One of the main items of the programme laid down for the Institute was

'to act through properly constituted National Committees in which other learned academies and societies will be associated as the National Research Council of India, for undertaking such scientific work of national and international importance as the Council may be called upon to perform by the public and by Government.'

Unfortunately all efforts of the Institute for the establishment of a National Research Council for India have been unsuccessful. The need for such a body in connection with the organisation, healthy and normal development and co-ordination of scientific research in the country is, however, too patent to require any further justification, and the Institute will be failing in its duty if it does not continue to press for the constitution of such a Council at an early date.

## II. ZOOGEOGRAPHY OF INDIA.

In the second part of my address I propose to discuss briefly the Zoogeography of India. Zoogeographic studies can be carried out along different lines in accordance with the ideals in view, but the *raison d'être* of all such studies is the elucidation of the constitution of the fauna of any particular area, its distribution, origin and relationships.

Older authorities on Zoogeography like Wallace, Huxley, Selater, Sharp, Heilprin and others mainly considered the present-day distribution of the various groups of animals, with casual references to their geological history, and from the data thus obtained attempted to divide the surface of the earth into zoogeographical regions or realms. In fact, as Ortmann<sup>1</sup> remarked, 'any research in this direction is deemed incomplete that is not finished by the creation or discussion of "regions"'. This method resulted in the division of the earth's surface into a varying number of realms or regions, 21 according to Schmarda<sup>2</sup>, 6 according

<sup>1</sup> *Proc. Amer. Phil. Soc.*, XLI, p. 271, (1902).

<sup>2</sup> Schmarda, K., *Die Geographische Verbreitung der Tiere*, (Wien, 1853).

to Solater <sup>1</sup> and Wallace <sup>2</sup>, 2 according to Huxley <sup>3</sup>, 7 according to Blyth <sup>4</sup>, 9 according to Gill <sup>5</sup>, 3 according to Blanford <sup>6</sup>, 4 according to Dahl <sup>7</sup>, and various others. The regions were further subdivided into subregions or provinces, but the divisions were based mainly on the distribution of mammals or birds. In spite of Wallace's assertion <sup>8</sup> that his slightly modified scheme of Solater is applicable to all groups of the Animal Kingdom, there is little doubt that no one scheme can serve equally for all the groups.

As Blanford <sup>9</sup>, one of our most distinguished geologists and zoogeographers, remarked, 'For the study of zoological distribution there are few, if any, regions on the earth's surface that exceed British India and its dependencies in interest. The area is large, nearly 1,800,000 square miles, and although the vertebrate fauna is by no means thoroughly explored, it is well known throughout the greater part of the area . . . . . The variety in elevation and of climate is remarkable; the country is bounded on the north by the highest of known mountain ranges, and by the loftiest plateau on the earth's surface, and it includes within its limits both the almost rainless area of the Sind Desert, and the locality in the Khasi Hills distinguished by the heaviest rainfall known. Another element of interest is the fact that the Peninsula of India is a land of great geological antiquity, there being no evidence to show that it has ever been submerged, although the greater part of the Himalayas and Burma have at times been beneath the sea.' Blanford <sup>10</sup> admirably defined the limits of the area as consisting 'of the dependencies of India with the addition of Ceylon, which, although British, is not under the Indian Government. Within the limit thus defined are comprised the whole of India proper and the Himalayas, the Punjab, Sind, Baluchistan, all the Kashmir territories with Gilgit, Ladak, etc., Nepal, Sikkim, Bhutan and other cis-Himalayan States, Assam, the countries between Assam and Burma, such as the Garo, Khasi and the Naga Hills and Manipur, the whole of Burma with Karenni, and of course Tenasserim and the Mergui Archipelago, and last the Andaman and Nicobar Islands.' With this we have also to include the Laccadive and Maldive Islands, which not only are under the Indian Government, but the fauna of which shows very distinct affinities with that of the Indian area. On the other hand Burma, which administratively is now a separate entity, must still in view of the faunistic relationships be included within the Indian area.

<sup>1</sup> *Journ. Proc. Linn. Soc. London (Zool.)*, II, pp. 130-145, (1858).

<sup>2</sup> Wallace, A. R., *The Geographical Distribution of Animals*, Vols. I, II, (London, 1876).

<sup>3</sup> *Proc. Zool. Soc. London*, pp. 294-319, (1868).

<sup>4</sup> *Nature*, III, pp. 427-429, (1871).

<sup>5</sup> *Proc. Biol. Soc. Washington*, II, pp. 1-39, (1884).

<sup>6</sup> *Proc. Geol. Soc. London*, pp. 76, 77, (1890).

<sup>7</sup> Dahl, F., *Oekologische Tiergeographie*, I, pp. 102-106, (1921).

<sup>8</sup> *Nature*, XLIX, pp. 610-613, (1894).

<sup>9</sup> *Phil. Trans. Roy. Soc. London*, CXCIV, p. 336, (1901).

<sup>10</sup> Blanford, W. T., *Faun. Brit. Ind., Mammalia*, p. iv, (1889).

It will be presumptuous to claim that we are, by any means, fully acquainted with the forms of animal life which inhabit this vast subcontinent, but one would not be far wrong in saying that we are today fairly well informed about the main features, and in many cases, even the details of its fauna. The limits of India, as defined above, fall mainly within the Oriental Region of Wallace or the Eastern Palaetropical Region of some authors. Probably, however, as Blanford suggested, the best name for the region, owing to the earlier use of the name Oriental by the botanists for South-western Asia and Persia, is Indo-Malay, as explored by Elwes for Birds. This name also is not very suitable, as practically the whole of the Western Frontier Province, the greater part of the Punjab, and the Western Himalayan area to the western limit of Nepal with Gilgit and Ladak should undoubtedly be included in the Holarctic or the Palaearctic Region rather than the Indo-Malay. Further, parts of the Indo-Gangetic Plain show closer affinities to the Western Frontier territory than to the rest of the Indo-Malayan area.

Owing to the heterogeneous nature of the faunas of the different parts the division of this vast area into subregions is not an easy task. The affinities of the faunas of the different areas are very complicated and probably the best course under the circumstances is to take physiographical rather than zoogeographical tracts as the basis for the consideration of the faunas of different parts. In this connection it will be useful to consider here briefly the history of the various attempts that have been made by earlier workers for subdividing the Indian area into subregions. Jordon<sup>1</sup> taking the Birds and Günther<sup>2</sup> the Reptiles, as the bases for their conclusions, divided India into several subregions, but their subdivisions were based mainly on geographical units rather than on the available zoological data. Blanford<sup>3</sup> basing his scheme on the distribution of the Land Mollusca divided India into four Provinces which he designated: (1) the Punjab Province; (2) the Indian Province proper; (3) the Eastern Bengal Province; and (4) the Malabar Province with Southern Ceylon. The Indian Province proper was subdivided into four sub-provinces. Elwes<sup>4</sup> who considered India with Malay Peninsula as a single unit (Indo-Malay Region) for Birds, divided it into three subregions: (1) Himalayan or Himalo-Chinese; (2) Indian; and (3) Malay. Wallace<sup>5</sup> from a general consideration of the distribution of all the groups of animals divided the Oriental region into: (1) Hindustan or the Indian subregion consisting of the whole of the Peninsula from the foot of the Himalayas on the north to somewhere near Seringapatam on the south-east and Goa on the south-west; (2) Ceylon and South India;

<sup>1</sup> Jordon, T. C., *Birds of India*, p. xxxix, (1882).

<sup>2</sup> Günther, A. C. L. G., *Reptiles of British India*, p. vii, (1864).

<sup>3</sup> *Jour. As. Soc. Bengal*, XXXIX, pt. ii, p. 336, (1870).

<sup>4</sup> Elwes, H. J., *Proc. Zool. Soc. London*, pp. 652-682, (1873).

<sup>5</sup> Wallace, A. R., *op. cit.*, I, pp. 81, 82, 321-334.

(3) Himalayan or Indo-Chinese subregion comprising the *Himalayas* as far west as Kashmir from the base to an elevation of 9,000–10,000 feet, and the countries east of the Bay of Bengal, Assam, Burma, Southern China, Siam and Cochin China; and (4) Indo-Malaya or the Malayan subregion consisting of the Malaya Peninsula and the Archipelago. Kobelt<sup>1</sup> basing his conclusions mainly on the distribution of the Mollusca divided it into: (1) the north-western area of the Indus Plateau limited in the south-east by a boundary running almost in line with the Aravalli mountain range; (2) the greater part of the Peninsula in the south bounded by a line from Goa on the west to Madras on the east, on the north-west by the Aravalli range and including almost the greater part of the Gangetic shed—the latter bordered on the north by the Himalayan chain and on the east by a line running from the eastern border of Nepal to a little to the west of Calcutta; and (3) the Basin of the Brahmaputra including a part of Bengal, the whole of Assam and the hill areas of the Garos, Nagas, etc., and bounded on the east by a line running from Cape Negrais along the Arrakan Yomas and then running further east along the Irawadi river to Tibet. He did not include Burma and Tenasserim in this account. Sharpe<sup>2</sup> from the distribution of the Birds divided the Indian region into: (1) Indian Peninsular subregion; (2) Indo-Malay subregion; (3) Indo-Chinese subregion; (4) Himalo-Malayan subregion; and (5) Himalo-Chinese subregion. Blanford<sup>3</sup> in the Introduction to the Mammalia in the *Fauna of British India* divided the region into six subregions: (1) Tibetan; (2) Himalayan; (3) Indian; (4) Malabar or Ceylonese; (5) Burmese; and (6) South Tenasserim. Newton<sup>4</sup> and Gadow<sup>5</sup> in discussing the distribution of Birds and W. L. Sclater<sup>6</sup> of the Mammals, followed Wallace, but united his Indian and Ceylonese regions into a single unit. Blanford<sup>7</sup> in his classical work on the Distribution of the Vertebrates of India, divided the whole area into 5 subdivisions: (1) The Indo-Gangetic Plain; (2) the Indian Peninsula; (3) Ceylon; (4) the Himalayas; and (5) Assam and Burma, and further subdivided these into 19 tracts. Alcock<sup>8</sup> taking the freshwater Crabs as the basis for his work divided India into 6 territories: (1) The Western Frontier territory; (2) Western Himalayan territory; (3) North-Eastern Frontier or Eastern Himalayan or Eastern sub-Himalayan territory; (4) Burma-Malay territory; (5) Peninsular territory; and (6) Indo-Gangetic Plain. Annandale<sup>9</sup> found that

<sup>1</sup> Kobelt, W., *Ber. Senckenberg. naturf. Gesel. Frankfurt a. M.*, pp. 89–104, (1899).

<sup>2</sup> *Nat. Sci.*, III, p. 108, (1893).

<sup>3</sup> Blanford, W. T., *Faun. Brit. Ind., Mammalia*, p. iv, (1888).

<sup>4</sup> Newton, A., *Dictionary of Birds*, p. 356, (1893).

<sup>5</sup> Gadow, H., *Bronn's Klass. Ord. Thier., Vogel*, p. 296, (1893).

<sup>6</sup> Sclater, W. L., *Geogr. Journ.*, VII, p. 380, (1896); also see Sclater, W. L. and Sclater, P. L., *The Geography of Mammals*, (1899).

<sup>7</sup> *Phil. Trans. Roy. Soc. London*, CXIV, pp. 343–348, (1901).

<sup>8</sup> Alcock, A. W., *Cat. Ind. Dec. Crust. Coll. Ind. Mus.*, pt. i, fasc. ii, pp. 9–14, (1910).

<sup>9</sup> Annandale, N., *Faun. Brit. Ind., Freshw. Sponges, Hydroids and Polyzoa*, pp. 7–10, (1911).

the distribution of the freshwater Sponges and Polyzoa confirmed Alcock's conclusions, but it was necessary to divide the Peninsular territory into (a) the main area consisting of the Peninsula east of Western Ghats, and (b) Malabar zone including the Western Ghats from Taptee River to Cape Comorin and eastwards to the sea. He also considered Ceylon as a separate territory. Stephenson<sup>1</sup> in discussing the Geographical Distribution of the Oligochaeta opined that in addition to the territories recognised by Annandale it was necessary to separate the narrow southern end of the Peninsula below the level of Goa and south of the fifteenth parallel from the eastern to the western shore as a distinct region. Christophers<sup>2</sup> for the Anopheline mosquitoes divided India into 6 areas: (1) Trans-Indus area; (2) Indo-Gangetic area; (3) Peninsular area; (4) Malabar and Ceylon; (5) Assam and Burma; and (6) Himalayan area. Taking into consideration the results of systematic work on various groups of animals I<sup>3</sup> suggested the following scheme: (1) Western Frontier Territory including Baluchistan, the North-Western Frontier Province and the greater part of the Punjab; (2) the Himalayas consisting of the Upper Indus Valley with Ladak, Gilgit, etc., the Western Himalayas from Hazara to the western limit of Nepal, and the Eastern Himalayas from the limit of the Western Himalayas to the Mishmi Hills above the Assam Valley; (3) Assam and Burma comprising the greater part of the Lower Brahmaputra Drainage System and the Burmese territory including Tenasserim; (4) the Gangetic Plain to the east of Delhi, and including the whole of the United Provinces, Bengal, and parts of Assam up to the base of the Assam Hills, together with the plain of the Brahmaputra as far as Goalpara and Cachar, Sylhet and the plains of Tipperah; and (5) Peninsular India, with the Malabar zone as a very distinct subdivision, and Ceylon. Malcolm Smith<sup>4</sup> suggested the division of the Indian subregion into: (1) the Desert Area or North-West India including Baluchistan, the North-West Frontier Province, the Punjab, western Rajputana as far as the Aravalli range, and Sind; (2) Kashmir and the Western Himalayas as far east as, but not including, Nepal; (3) the Gangetic Plain, extending from the valley of the Indus in Sind to the right bank of the Brahmaputra in Bengal; (4) Central India—the tract of country lying between the Gangetic Plain and the Deccan and bounded on the west by the Aravalli range and on the east by the Chota Nagpur area; (5) the Deccan, consisting of the greater part of the Peninsula of India between 12° and 21° north latitude; (6) the Mountains of the Malabar Tract and Ceylon; and (7) the Chota Nagpur Area, consisting of Bihar south of the Gangetic Plain, the northern part of Orissa and the eastern part of the Central Provinces. Recently Mahendra<sup>5</sup> from a study of the distribution of the amphibian and reptilian species divided India into ten provinces: (1) the arid

<sup>1</sup> Stephenson, J., *Faun. Brit. Ind., Oligochaeta*, pp. 12-13, (1923).

<sup>2</sup> Christophers, S. R., *Proc. Fourth Entomol. Meeting*, pp. 206-208, (1921).

<sup>3</sup> Prashad, B., *The Indian Empire*, pp. 190, 191, (Calcutta, 1927).

<sup>4</sup> Smith, Malcolm, A., *Faun. Brit. Ind., Reptiles and Amphibia*, I, pp. 18-21, (1931).

<sup>5</sup> *Science and Culture*, IV, pp. 374-377, (1939).



or semi-arid Province of North India; (2) the Western Himalayas; (3) the Trans-Gangetic Province; (4) Southern Burmese Province; (5) the Gangetic Plain and the adjacent country as far south as 20° latitude; (6) South India below 20° latitude excluding the Travancore Province; (7) the Travancore Province; (8) Ceylon; (9) the Andaman Islands; and (10) the Nicobar Islands.

These attempts to divide the vast area of continental India, useful as they are, have unfortunately not helped materially in unravelling completely the very complicated questions of the origin, distribution and relationships of its fauna. In what follows I propose to give a brief outline of the faunal constitution and their relationships for the different parts in accordance with my scheme referred to above.

The fauna of the Western Frontier Territory is markedly different from that of the rest of the area. Practically all the genera of the Vertebrates are either Palaearctic (Holarctic), or are peculiar to this subregion; the relationships of the latter are also with the Palaearctic rather than with the Indo-Malayan forms.

Blanford basing his views on the distribution of the Vertebrates suggested that this subregion should be classified with the Eremian or Mediterranean subregion of the Palaearctic, and this view has been fully confirmed by the distribution of the various groups of the Invertebrates that have been studied since 1901. Some forms of the Gangetic Plain have also migrated into this subregion, but they are of no importance from the zoogeographic point of view. The Western Frontier Territory consists of desert or semi-desert tracts, except near the rivers or the artificially irrigated and cultivated parts. The annual rainfall is not heavy, and the fauna on the whole is poor.

In the Himalayan subregion the ranges above the forest limits, a part of the Tibetan plateau and the Upper Indus Valley including Ladak, Gilgit, etc., constitute a distinct division. This area is very bare, the mountains are perpetually covered with snow, and there is a very great difference in the altitudes of the mountainous ranges on the one hand, and of the intervening valleys on the other; the annual rainfall is generally low. Our information about the fauna of this part is not sufficiently detailed, but in the main it is almost entirely Palaearctic. In view of these faunistic affinities this division may later have to be included with the Western Frontier Territory. The second division consists of the forest zone of the Himalayas from near the base to an altitude between 10,000-14,000 feet, the uppermost limit of the forest zone. It forms a belt of varying breadth between the higher mountain ranges and the Indo-Gangetic Plain. The rainfall in this division is heavier, more so in the eastern than in the western parts, and the forests of the eastern ranges are also more extensive, richer and truly tropical. A fair number of Palaearctic animals from the higher mountain ranges wander down into the forests, while a few species penetrate northwards into the rather warmer valleys from the plains in the south. The western forest region has a predominantly Palaearctic

arctic fauna, while the eastern, which has a very marked Malayan element, was on this account separated with Assam, Burma, etc., into what Blanford designated as the Trans-Gangetic subregion.

In Assam and Burma the northern region, comprising the northern part of the drainage area of the Brahmaputra and Assam, consists of hilly tracts with dense forests except in the plains of Assam; the annual rainfall in this tract is fairly heavy. Physiographically, parts of this area belong to the Indo-Gangetic Plain, but its fauna is distinctly Burmese. In Upper Burma, which is roughly the drainage area of the Irawadi, there is a large number of hills thickly covered by forests, while the undulating ground between the mountains is densely overgrown by brushwood and high grass; the annual rainfall in this region is pretty heavy. The Tenasserim area consists of two distinct tracts, (i) the northern, covered by thick forests on a hilly ground and with a fauna of the Burmese type; and (ii) the southern area which in its physiography is similar to the northern; the annual rainfall in this tract is not so heavy as in the northern area, and its fauna is distinctly Malayan. The Andaman and Nicobar Islands, which are also included in this subregion, are covered by dense forests and have a heavy rainfall. The fauna of these islands is by no means identical; the Andamans having an impoverished Burmese fauna, while that of the Nicobars is undoubtedly Malayan.

Since the main part of the Indus Plain has been separately considered above in the Western Frontier Territory, I use the name Gangetic Plain. Gangetic Plain for the rest of the Indo-Gangetic watershed. Its extent has been noted already, and its physical features only need be considered. Most of the western area is cleared and used for cultivation, and only some of the uncleared areas are covered by tall grasses. The annual rainfall generally is not very heavy. In the eastern part of the area, except for the Sunderban forests in the deltaic region of the Ganges, the country is similar to that in the north-western part, but the rainfall is heavier, and there are more extensive tracts of uncleared land. The fauna of the area is generally of the same type as that of Peninsular India, but in the north-eastern parts there is a large admixture of the eastern or Blanford's Trans-Gangetic types. The freshwater fauna shows a very marked similarity and in many cases actual identity with the forms occurring in the Indus System.

The greater part of Peninsular India, with the exception of the Malabar Tract, consists of either cultivated land or low hilly country covered with brushwood or thin forests; the average rainfall is from 35-50 inches. In the Malabar Tract, on the other hand, we have the high mountain ranges of the Western Ghats and the west coastal area of the Peninsula. Most of this part is covered with thick tropical forests, though there are many places near the coast which are cleared and cultivated. The island of Ceylon, like Peninsular India, consists of two types of country. About three-fourths of the island along the north and the

east resembles the main area of Peninsular India, and is almost plain or only slightly undulating country of no great elevation, with an average annual rainfall of about 50 inches. The rest or the south-western part of Ceylon, like the Malabar Tract, is hilly, with rich tropical forests and an average rainfall of over 100 inches.

In this area a peculiar admixture of the different faunas seems to have taken place. In main characteristics the fauna of this area differs from that of Blanford's Trans-Gangetic partly in the absence of numerous Eastern Types, and partly by the presence of two other distinct constituents, which form, especially in the forests, the majority of the animal population of the area. One of these constituents to which Blanford gave the appropriate name—the Aryan faunal element—consists of certain genera of mammals, birds and reptiles. The typical genera of this Aryan element are, for the most part, represented in the tropics of Africa at the present day, but do not occur in Western Asia or Northern Africa. Other genera of the Aryan element found in Peninsular India occur in Western Asia and are represented at the present day by allied species. Both these groups of genera are well represented in the Pliocene Siwalik Fauna of the Himalayan foothills, and it appears probable that most of them are descended from animals which appeared in India, so far as we know at present, in the Pliocene period; a few, however, may be later migrants. On the whole, this Aryan element is subtropical rather than tropical, and is best developed in parts where the rainfall is moderate. Several of its most conspicuous and characteristic members, such as the Antelope and Nilgai, are not found in the extreme south of India or in Ceylon, and they are inhabitants of the grassy and bush-covered plains with scattered trees, not of dense forests and bamboo-jungle in which the gaur and the elephant flourish. The second constituent of this fauna is the Indo-Malayan or the Oriental element. It is more diffuse and much more richly represented in the damp tropical forests of Malabar and Ceylon than in the drier parts of the Peninsula. The diffusion of the Indo-Malayan element seems to indicate that it is older than the Aryan element mentioned already, but there can be little doubt that it is an immigrant and not an indigenous element, for it is only an impoverished representative of the typical Oriental life found in the countries to the east of the Bay of Bengal. Its main representatives are amongst birds and mammals, and like the Aryan it appears to have migrated into Peninsular India about the Miocene times driving the earlier Dravidian into high ranges of hills, etc. Some authors have opined that the Oriental or the Indo-Malayan fauna, owing to the presence in it of representatives of the Lower Miocene and Oligocene faunas of Europe, is of Palaearctic origin and that it was driven down into the tropics by the diminishing temperature of the Holarctic region in the Miocene times. The third element in this fauna that can be recognised distinctly from the other two is what Blanford termed Dravidian. It is thoroughly tropical and damp-loving, and is only represented by lower groups of the Animal Kingdom, *viz.*, reptiles and batrachians. It is probable

that this is the oldest element and may have inhabited the country since India was connected in Mesozoic and early Cenozoic times with Madagascar and South Africa, across what is now the Indian Ocean.

In the fauna of the Peninsula in Malabar and Ceylon there is a much greater concentration of the Oriental element. There are, for example, various mammals, reptiles, batrachians, fishes, and invertebrates, which are represented in Burma and the Malay countries but not in northern India. There is also the occurrence of certain Himalayan species on the mountains of Southern India and in Burma and even further south but not in the intervening area. These faunal anomalies have been explained as a result of the Glacial Epoch, but the explanation is not quite satisfactory, though it is hard to understand how otherwise the animals of temperate Himalayan types could have migrated to the hills of Southern India and Ceylon on the one hand, and those of Burma and the Malay Peninsula on the other. After the Glacial Epoch when the country became warmer, the Oriental fauna must have migrated rapidly from the south-east into Eastern Himalayas. At the present day the comparatively narrow plain of the Brahmaputra in Assam is far more extensively covered with forests than the much broader Gangetic Plain, and if, as is probable, the same differences existed at the close of the Glacial Epoch, it is easy to understand why the Trans-Gangetic fauna of Burma and the south-east had greater chances of occupying the vacant region of the Himalayas than the Cis-Gangetic fauna which had been driven much further south by the cold. A reference may here be made to the Aethiopian element in the fauna of Peninsular India. As was pointed out by Annandale<sup>1</sup>, several groups of Invertebrates, Sponges, Polyzoa, Hydroids, Oligochaetes, Crustacea and Mollusca, found in the Malabar tract, show a very great affinity, if not distinct identity, with the forms found in Africa.

Finally, reference may be made to some palaeogeographic facts in regard to the origin of the Indian fauna. The early Tertiary or placental mammals of Europe, and presumably also those of Asia north of the Circum-continental sea, the Tethys, drifted either as such or as their descendants by certain routes—of which we have only indications—into the fragments of Gondwanaland represented by Aethiopian Africa on the one hand and Peninsular India on the other. Meantime, evolution went on rapidly to the north of the Tethys giving rise to the more modern and highly evolved types of mammals. About the end of Tertiary times, as a result of the receding of the Tethys, communication between the northern with the southern lands seems to have become easier, and this, combined with the climatic changes, led to a great rush southwards of the more modern types. These overwhelmed the earlier fauna in the southern lands, driving its few representatives into the more outlying or upland areas, or wiping them out altogether off the face of the earth. In the

<sup>1</sup> Annandale, N., *Proc. Ninth Congr. Internat. Zool. Monaco*, pp. 579-588, (1914).

case of the Oriental region the Central Himalayas which had meanwhile risen as the mighty mountain chain of Asia and the Tibetan plateaux to their north formed a real barrier. In the north-west, where this mountain chain is comparatively less higher and less continuous, this barrier was not so effective, but the Afro-Asian arid belt which is continued into India as the Sindh desert, formed a very efficient barrier. Through the passes in the north-west of the Himalayas the recently evolved mammals found their way into India, but naturally only forms which could withstand arid conditions or were adapted to mountain life, were able to use this route. The areas further to the east, which have been clothed for a long time with forests and are without high mountain barriers, offered greater facilities for the spread of animals adapted to wooded regions. India proper may thus be conceived as having had two converging streams of immigrants, one coming from the north-west and the other from the north-east. In view of the fact that the Indian Peninsula narrows southwards, it is clear that very few representatives of the Tertiary fauna in this area could successfully withstand the inroads of the more highly evolved immigrants from the north. The area to the east of the Assam neck, or the region where the Bay of Bengal pushes upwards towards the Himalayas narrowing the country into a bottle-neck shape, was, however, more favourably placed in this respect, as only a few immigrants were able to traverse the Assam neck. Further, as the members of the earlier fauna were pushed southwards by the incomers into an area of almost equatorial climate, it is not difficult to surmise that survival was possible only for such forms as could adapt themselves to the highly specialised climate and surroundings. As a result this earlier element of the fauna was mainly wiped out, and at the present day is only poorly represented in the area.

In this account I have not considered the very interesting cases of the occurrence of identical aquatic species in the Indus and the Ganges river systems, which at the present day constitute quite distinct and unconnected systems. This has been explained on the hypothesis of a continuous river in place of the two river systems during the Tertiary times. The mighty river, which has been designated the Indobrahm by Pascoe or the Siwalik River by Pilgrim, is supposed to have run from the east to the west and broken up into three river systems with the elevation of the Himalayas, resulting in similar forms being left in the different river systems<sup>1</sup>. Similarly closely allied, if not identical, aquatic species which occur in Bengal-Assam region on the one hand and Peninsular India on the other, are to be explained on the basis of very different river systems during the Tertiary times in these areas, and the changes that occurred during recent geological times due to river captures, beheading of rivers, etc. In this connection the continuity of the mountain ranges of the Chota Nagpur Plateau

<sup>1</sup> For a detailed discussion of the present position in reference to this Tertiary river, see Prashad, B., *Rec. Geol. Surv. Ind.*, LXXIV, pp. 555-561, (1932).

westwards to the Satpura range and eastwards to the Himalayas has also been suggested, and it is surmised that along this continuous chain of mountain ranges the migration of the Himalayan aquatic fauna to Peninsular India took place. Further work in connection with these problems is, however, necessary before they can be satisfactorily dealt with. Similarly the occurrence of *Typhloperipatus* in the Abor Hills of Assam, *Herpele* in Assam, *Pseudomulleria* in the Kadir Hills of Mysore and other archaic types needs a great deal more of intensive zoological work before their relationships and distribution can be properly understood.



## RADIO-ACTIVITY OF RUBIDIUM.

By P. K. SEN-CHOWDHURY, *M.Sc., Research Scholar, Palit Research Laboratory,  
University College of Science, Calcutta.*

(Communicated by Prof. M. N. Saha, F.R.S.)

(Read January 1, 1942.)

### INTRODUCTION.

Since the discovery of radio-activity of rubidium by Campbell and Wood (1906) much work has been done to elucidate this nuclear process and though a good deal of information has been obtained the problem is far from being closed. The points which have to be tackled may be enumerated as follows:—

- (1) The particular isotope of rubidium which is responsible for the  $\beta$ -activity.
- (2) Half-life of the radio-active isotope.
- (3)  $\beta$ -Ray energy-spectrum, the maximum energy of the emitted  $\beta$ -rays and also whether any  $\gamma$ -ray is emitted.
- (4) The spin changes in the nucleus giving rise to the  $\beta$ -ray emission, and the discussion of the continuous energy-distribution curve from the theoretical standpoint.

These points are taken one after another.

#### (1) Rb-isotope responsible for $\beta$ -activity.

Rubidium has two isotopes, viz.  $\text{Rb}^{85}$  (73%) and  $\text{Rb}^{87}$  (27%). It has been conclusively proved that  $\beta$ -emission is due to  $\text{Rb}^{87}$ , and a brief reference to the works leading to the conclusion may be given. Klemperer (1935a) and Hevesy (1935b) suggested that the radio-activity of rubidium was due to the active isotope  $\text{Rb}^{86}$ , whereas Nier (1936) and Sitte (1935c) gave arguments in favour of  $\text{Rb}^{87}$ . Hahn, Strassman, Walling and Mattauch (1937a) have however definitely proved that the active isotope is  $\text{Rb}^{87}$ . They separated strontium from a specimen of mica geologically very old and containing a little rubidium, and found by mass-spectrographic analysis of the sample that the separated strontium was almost 100%  $\text{Sr}^{87}$ . The naturally occurring abundant isotope of strontium is however  $\text{Sr}^{88}$  of frequency 83%. This conclusively proved that  $\text{Sr}^{87}$ , which is found in the mica, must have arisen from a  $\beta$ -ray body which must be  $\text{Rb}^{87}$ , and is therefore the active isotope. Smythe and Hemmendinger (1937b) have also confirmed this by separating the isotope  $\text{Rb}^{87}$  by a high intensity mass spectrometer.



(2) *Half-life of Rb.*

The half-life of rubidium has been determined by Hahn and Rothenbach (1919), Holmes and Lawson (1926), Mühlhoff (1930), Orban (1931) and Hahn, Strassman and others (1937c), and their values are given below:—

Hahn and Rothenbach	..	..	..	$7.5 \times 10^{10}$ years.
Holmes and Lawson	..	..	..	$1.4 \times 10^{11}$ „
Mühlhoff	..	..	..	$4.3 \times 10^{11}$ „
Orban	..	..	..	$1.6 \times 10^{11}$ „
Hahn, Strassman, <i>et al.</i>	..	..	..	$3.15 \times 10^{10}$ „

All these values are much larger than the half lives of Ur ( $4.5 \times 10^9$  years) or of Th ( $16.5 \times 10^9$  years).

The methods used by them are all based on the law

$$\frac{dN}{dt} = -\lambda N \quad \dots \quad (a)$$

$$\text{and} \quad T = \frac{\log_e 2}{\lambda} \quad \dots \quad (b)$$

We have to take a definite quantity of rubidium and find out the number of  $\beta$ -rays emitted per sec. Then  $\lambda$  is directly obtained from (a).

Though the theory is simple, its application is attended with considerable difficulties. As the emitted  $\beta$ -rays are of very low intensity and low energy, it is very difficult to count them accurately. The energy spectrum of Rb reveals that some of the emitted electrons will be stopped even by a thin layer of the substance itself of a thickness of only a few milligrams per sq. cm. It is very difficult to prepare a uniform thin layer of this order of thickness.

Hahn and Rothenbach obtained the value of half-life from the ratio of the ionisation current due to thin layers of uranium and rubidium. From this ratio they found that the number of  $\beta$ -rays emitted by the same quantity of rubidium and uranium is in the ratio 1 : 15. Holmes and Lawson from all the existent data at that time calculated half-life and made some correction on Hahn and Rothenbach's value. Mühlhoff introduced a thin layer of the salt inside a Geiger-Müller tube counter and from the rate of counting he determined the number of  $\beta$ -rays emitted by a known weight of the salt. Orban determined the half-life of rubidium by counting the number of tracks in a Wilson Chamber in which a thin layer of Rb salt was introduced. He made allowance for absorption in Rb-layer by determining the value of average mass-absorption coefficient ' $\mu/\rho$ ' of the emitted  $\beta$ -rays. But the half-life was calculated in all these cases on the assumption that all the atoms of Rb are radio-active as the radio-active isotope  $\text{Rb}^{87}$ . Their values are therefore to be reduced proportionately.

Hahn, Strassman and others (*loc. cit.*) have indirectly obtained the value of half-life for rubidium from the geological data which proved that  $\text{Rb}^{87}$  is the active isotope. Their method of calculating the half-life is very instructive

and the account may be repeated here. On chemical analysis of one kilogram of a very old mica mineral whose age was estimated between 500 to 1,000 million years they found that it contained 2 to 3% of rubidium and 250 milligrams of strontium carbonate. Ninety-nine per cent of this strontium as shown by a mass spectrograph was  $\text{Sr}^{87}$ . Taking the percentage of rubidium present to be 2.5% and the frequency of  $\text{Rb}^{87}$  to be 27%,  $\text{Rb}^{87}$  present in one kilogram of the mineral is

$$\frac{25 \times 27}{100} = 6.75 \text{ gm.}$$

Again 250 milligrams of  $\text{SrCO}_3$  contain 148 milligrams of strontium and since the mass number of strontium and rubidium in this case is the same therefore

$$\frac{\text{No. of } \text{Rb}^{87} \text{ atoms transformed}}{\text{No. of } \text{Rb}^{87} \text{ atoms present}} = \frac{0.148}{6.75} = \frac{1}{45} \text{ approximately.}$$

Now by the relation (a) and (b)

$$\frac{dN}{N} = \lambda t = \frac{0.69t}{T} = \frac{1}{45}$$

Taking  $t = 1,000$  million years,  $T = 0.69 \times 45 \times 10^6 = 3.15 \times 10^{10}$  years.

Taking  $t = 500$  „ „  $T = 1.58 \times 10^{10}$  years.

But there is an amount of uncertainty due to their assumption of the geological age of the mineral. This as is well known may vary within wide limits.

Though the values for half-life of Rb has been determined by so many workers there seems to be considerable disagreement in the values obtained by different workers. An attempt has been made in the present investigation to determine the value of half-life of rubidium using a moderately thick layer and correcting for absorption by the method of Orban.

(3)  *$\beta$ -ray energy spectrum, the maximum energy of emitted  $\beta$ -rays and also whether any  $\gamma$ -ray is emitted.*

The problem of determining the energy spectrum has not been attacked as yet due to experimental difficulties. As the emitted  $\beta$ -rays are of very low-energy and low intensity, magnetic spectrograph cannot be satisfactorily used for deducing the energy distribution curve. An attempt has been made to deduce the approximate shape of the continuous energy spectrum of Rb by a new method suggested by Occhialini (1931).

The maximum energy of the emitted  $\beta$ -rays has been determined by Klemperer (*loc. cit.*) and Libby and Lee (1939). Klemperer calculated the maximum energy from the absorption coefficient as determined by Mühlhoff

(*loc. cit.*). Libby and Lee used the magnetic deflection method as has been used by us. Their values are given below:—

Klemperer	..	..	$0.25 \times 10^6$	electron volts.
Libby and Lee	..	..	$(0.13 \pm 0.02) \times 10^6$	" "

The two values are then extremely discordant.

(4) *The spin changes in the nucleus giving rise to the  $\beta$ -emission, and the discussion of energy-distribution curve from the theoretical basis.*

The  $\beta$ -activity of rubidium like the other light alkali metal potassium has some peculiarities which are not as yet very clear. From the experimentally determined maximum energy and half-life of rubidium it is observed that it does not fall on the two main lines ( $\log \lambda$  against  $\log E_{\max}$  curve) of Sargent's curve (1933a) corresponding to  $\Delta i = 0$  or 1, where  $\Delta i$  is the spin change of the nucleus in the transition,

$$n^0 \rightarrow P^+ + \beta^- + \text{neutrino.}$$

Heyden and others (1938), by hyperfine-structure analysis, have determined the spin of  $\text{Rb}^{87}$  and  $\text{Sr}^{87}$  to be  $3/2$  and  $9/2$  respectively. This shows that in the  $\beta$ -emission from rubidium  $\Delta i = 3$ . This type of transition again involving such a high spin change is highly forbidden by both Fermi's (1934a) theory and Konopinski, Uhlenbeck (1935d) theory of  $\beta$ -decay. In order to explain these anomalies Gamow (1934b) suggested three alternative schemes for the  $\beta$ -decay of Rb. But all of them were shown by Klemperer (*loc. cit.*) to be incorrect.

#### EXPERIMENTAL TECHNIQUE.

The experimental method followed here was first suggested and used by Occhialini and Bocciaireli (1932, 1933) to determine the energy of the  $\beta$ -rays emitted by potassium and rubidium. In recent years this method has been much improved and used by Libby and Lee (*loc. cit.*) of the California University. A screen-wall Geiger-Müller counter is placed co-axially inside another brass cylinder on the inner surface of which the substance under investigation is placed below the screen-wall as shown in fig. 1. The screen-wall counter is

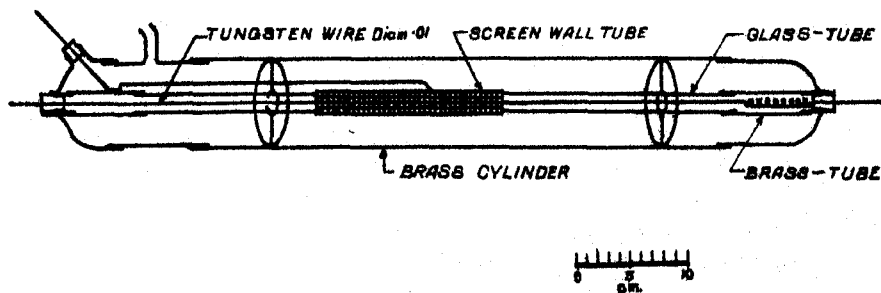


FIG. 1.

nothing but an ordinary tube counter with the difference that the tube is made of copper wire gauze-screen with widely separated meshes so that the emitted  $\beta$ -rays can enter the counter without any absorption. The whole chamber is evacuated and kept at a pressure of a few cm. of mercury for the working of the counter. To determine the energy of the emitted  $\beta$ -rays, a magnetic field is applied in a direction parallel to the axis of the counter. It is evident that the  $\beta$ -rays entering the counter will be bent into circles in a plane perpendicular to the direction of the magnetic field, and the radius of curvature for a particular energy will be inversely proportional to the strength of the magnetic field. As this is increased it follows that the softer components of the emitted  $\beta$ -rays, whose radius of curvature is less than half the distance between the sample-surface and screen-wall, will be gradually cut off and when the field is so much increased that the radius of curvature of the electron of maximum energy is just less than half the distance between the screen-wall and the sample surface, no electron will be able to enter the counter and the rate of counting will be only due to the background of cosmic rays and radio-active impurities if any. From this limiting  $H\rho$ -value the maximum energy of the emitted  $\beta$ -rays can be calculated.

A screen-wall counter has the same type of characteristic curve as an ordinary Geiger counter with the only difference that it is necessary to keep the sample cylinder about 50 volts positive with respect to the screen-wall by an insulated battery in order to prevent the accumulation of ions in the intermediate space between the screen-wall and the cylinder, which ultimately stops the working of the counter. Another fact about this type of counter is that as the magnetic field is increased, there is a slight reduction of the background counting due to cosmic rays and other radio-active impurities. In calculating energy this must be taken into account. Within the range of the magnetic field used in this experiment the maximum number of counts reduced was only 8 per minute, in a background effect of 80 per minute.

#### APPARATUS.

The apparatus which was used is shown in fig. 1. The screen-wall counter is 2 cm. in diameter and made of copper screen with 7 wires per cm. each of diameter 0.031 cm. The central wire is of tungsten 0.01 cm. in diameter. The internal diameter of the external brass cylinder is 8.4 cm. At the two ends the brass cylinder was ground joined with the two glass pieces. The whole chamber could be evacuated through a side tube in one of the glass pieces as shown in the figure and then a suitable gas-mixture could be introduced at a suitable pressure for the working of the counter. The other glass piece was opened whenever it was necessary to take out or introduce radio-active materials under investigation. Hydrogen mixed with a small amount of petroleum-ether has been used as the counter gas to minimise the scattering effect. For many days the counter was worked with different proportions of

hydrogen and petroleum-ether at different pressure to ascertain the best condition of working and ultimately it was found to work satisfactorily at a pressure of 10 cm. of mercury with hydrogen and petroleum-ether, in the ratio of 2 : 1. At this pressure, the counter was standardised for several days and found to have a plateau of 70 to 90 volts starting at about 1,200 volts. The rate of counting due to cosmic rays and radio-active impurities within this plateau region was found to be about 80 per minute on the average. The characteristic curve of the counter is shown in fig. 2.

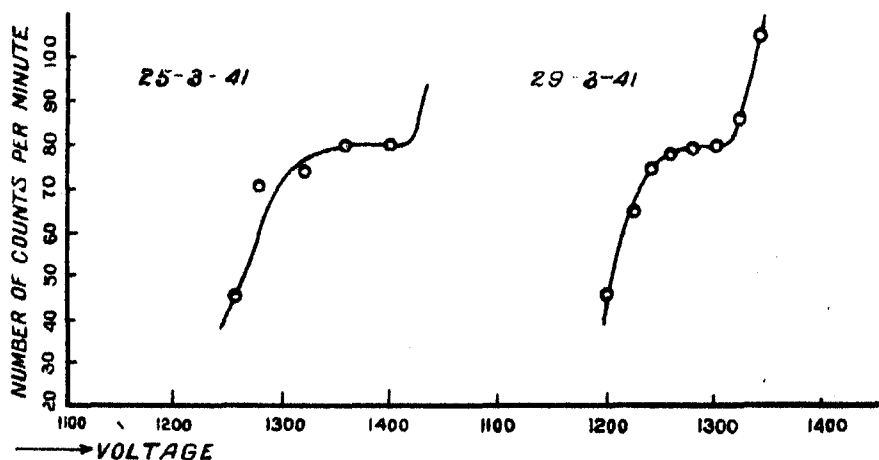


FIG. 2.

The whole counter was placed co-axially inside the coils of a large Weissmagnet from which the pole pieces were removed. This magnet is of Helmholtz coil pattern of about 10 cm. internal diameter with a gap of 10 cm. between the two parallel coils. The magnetic field within this gap was found by an exploring coil to be nearly uniform. The field increased linearly with the increase of the current through the coil. The coils were constantly cooled by circulating water round them. The magnet was carefully calibrated by an exploring coil for different current and a calibration curve (a straight line) of magnetic field in gauss against the corresponding current through the coil was drawn as shown in fig. 3.

The pulses from the counter were amplified by a three-stage valve amplifier of the Neher and Pickering\* model. This amplifier has been found to be very satisfactory in cosmic-ray work of this laboratory. Each pulse was automatically recorded by a mechanical counter worked by a thyratron valve.

\* Our thanks are due to Drs. Pickering and Neher for instructing us in the use of the amplifier during their visit to this laboratory in 1940.

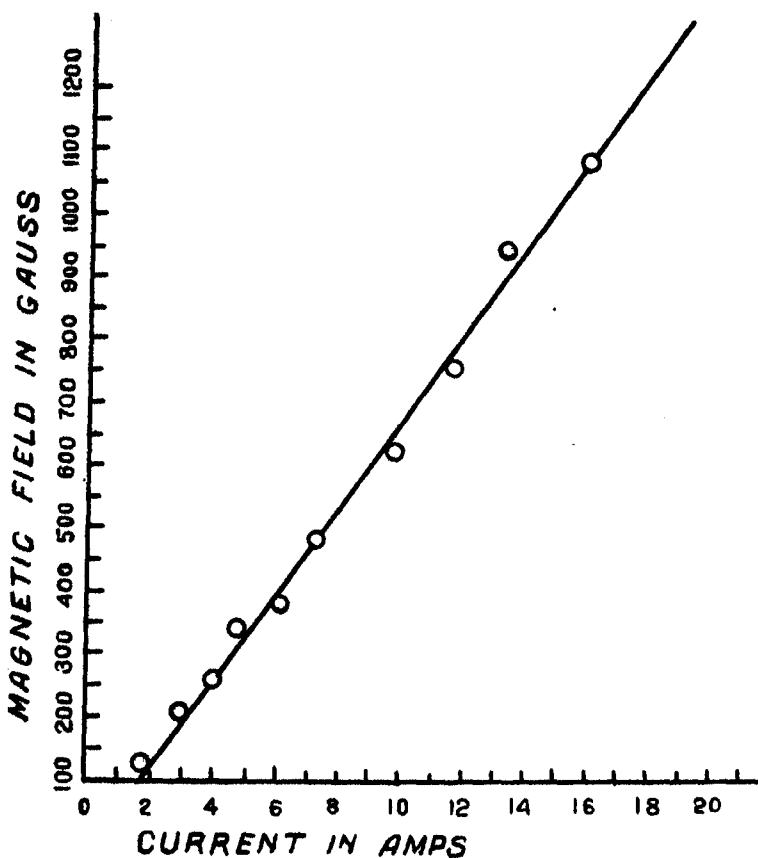


FIG. 3.

## EXPERIMENTAL RESULTS.

*Half-life of Rubidium.*

The value of half-life has been obtained by counting the number of  $\beta$ -rays emitted from the surface of a thick layer of salt and correcting for self-absorption by Orban's method (*loc. cit.*). Orban has shown that the number of  $\beta$ -rays 'n' emitted per sec. from 1 sq. cm. of a thick layer is given by

$$n = \frac{\lambda K}{2M} \cdot \frac{\rho}{\mu} \cdot 6.07 \times 10^{23} \quad \dots \quad (c)$$

where  $\lambda$  = disintegration constant,  $M$  = molecular weight of the salt,  $K$  = number of radio-active atoms in a molecule,  $\rho$  = density of the salt, and  $\mu$  = absorption coefficient of the emitted  $\beta$ -rays.

This expression can be easily deduced from the relation (a), assuming  $1/\mu$  to be the average range of the emitted  $\beta$ -rays and remembering that only half of the emitted  $\beta$ -rays will be transmitted upward.

In our experiment about 12 gms. of pure RbCl was uniformly spread over a flat aluminium dish 4 cm. by 10 cm. in dimension and the dish was introduced into the counter below the screen tube. The characteristic curve of the counter with RbCl was again determined as shown in fig. 4 under the

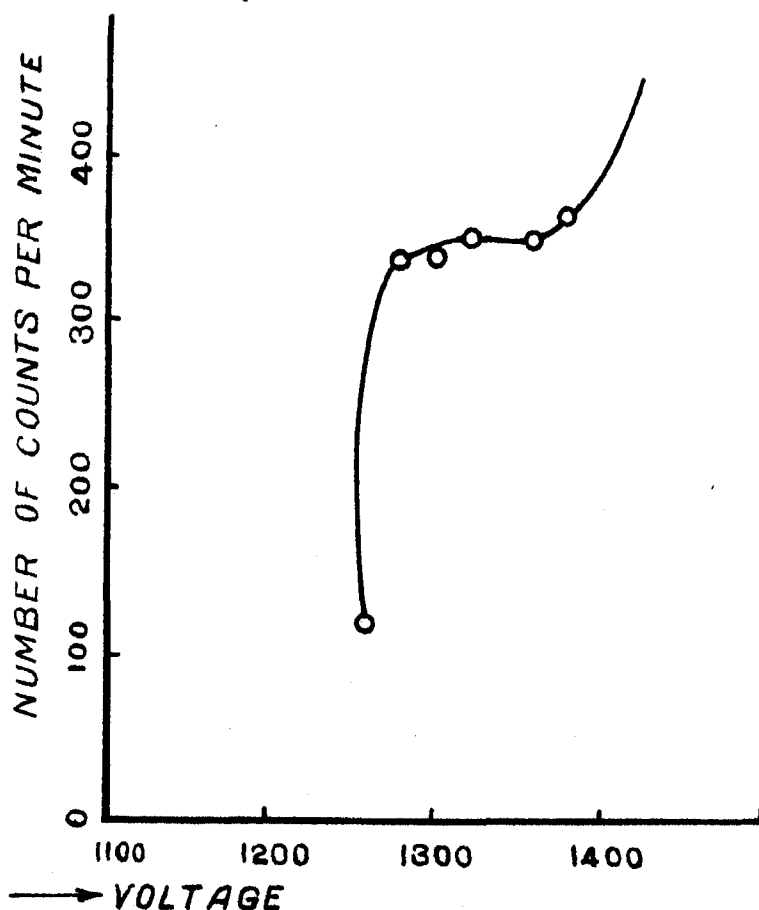


FIG. 4.

same condition with the background. It is observed from the curve that the rate of counting in the plateau region is about 350 per minute. Subtracting the background rate of counting 80 from this, the number of  $\beta$ -rays recorded by the counter is 270 per minute.

For finding out the efficiency and geometry of the counter, it was calibrated using a thin layer of uranium nitrate. 4.462 mg. of  $\text{UO}_2(\text{NO}_3)_2 \cdot 6\text{H}_2\text{O}$  dissolved

in ether was uniformly spread on a dish 4 cm. by 10 cm. in dimension and the dish was introduced into the counter below the screen-wall. 266 counts per minute were obtained over the background counting. Rutherford and Geiger (1910) showed that 1 gm. of uranium emits  $1.43 \times 10^6$   $\alpha$ -rays per minute. As uranium contains two  $\alpha$ -emitters  $U_1$  and  $U_{11}$  and two  $\beta$ -emitters  $Ux_1$  and  $Ux_2$  in equilibrium therefore  $1.43 \times 2 \times 10^6$   $\alpha$  and  $\beta$  particles are emitted by 1 gm. of uranium per minute. As there are  $1.116 \times 10^{-4}$  gm. of uranium nitrate per square cm. it follows from the number of counts obtained that only 8.794% of the particles emitted from 1 sq. cm. are recorded. Calibration was repeated again with  $8.372 \times 10^{-5}$  gm. of  $UO_2(NO_3)_2 \cdot 6H_2O$  per sq. cm. and the percentage recorded was found to be 8.984. The mean of these two values 8.884% are used for calculating the half-life.

With the above experimental data, the value of disintegration constant  $\lambda$  and hence  $T$  are calculated from the relation (c). The value of ' $\rho/\mu$ ', the reciprocal of the average mass-absorption coefficient of the emitted  $\beta$ -rays from rubidium, is taken to be 1/160 as found by Orban. The value obtained for  $\lambda$  and  $T$  are as follows:—

$$\lambda = 8.065 \times 10^{-20} \text{ sec}^{-1}.$$

$$T = 2.763 \times 10^{11} \text{ years}.$$

As the abundance of the active isotope  $Rb^{87}$  is 27%, therefore correcting for this factor:—

$$\lambda = 2.986 \times 10^{-19} \text{ sec}^{-1}.$$

$$T = 7.459 \times 10^{10} \text{ years}.$$

The value of half-life obtained by this experiment is nearly the mean of the values obtained by Mühlhoff and Orban assuming all the Rb-atoms to be active. When corrected for the isotope frequency, the value of half-life is of the same order as predicted by the geological evidence of Hahn and others. There is, however, some error in the value obtained due to the fact that the relation (c) deduced by Orban appears to be not very rigorous. Moreover, there will be a little error due to back-scattering which may be, as shown by Schonland (1923, 1925), about 13% in the very low energy region.

The maximum energy and the continuous energy-distribution of the emitted  $\beta$ -particles from rubidium will be published and discussed from a theoretical point of view in a subsequent paper.

In conclusion, with great pleasure I express my deep gratitude and thanks to Prof. M. N. Saha, D.Sc., F.R.S., whose constant encouragement and guidance enabled me to complete this work. My thanks are also due to Dr. N. N. Dasgupta and to Dr. S. C. Sirkar for many helpful discussions, and to Dr. G. P. Dube for kindly helping me in mathematical calculations. I wish also to express my thanks to Messrs. Scientific Indian Glass Co., particularly to Prof. N. C. Nag, and to Mr. Sirkar of the above Company, who have very kindly constructed the glass pieces of our apparatus in their factory.



## SUMMARY.

A brief reference to all the information available at present about the radio-activity of rubidium is given in the introduction. The half-life of rubidium has been calculated from the recent geological data of Hahn and others and the value obtained suggests that the present accepted value is too high. Therefore, the half-life was again determined with a screen-wall Geiger-Counter. The value obtained when corrected for the abundance of active isotope is  $7.459 \times 10^{10}$  years approximately.

## REFERENCES.

- Campbell and Wood (1906), *Proc. Cam. Phil. Soc.*, **14**, 15.  
 Eddy (1929), *Proc. Camb. Phil. Soc.*, **25**, 50.  
 Fermi (1934a), *Zs. f. Phys.*, **88**, 161.  
 Gapow (1934b), *Nature*, **133**, 746.  
 Hahn, Strassman, Walling and Mattauch (1937), *Naturwiss.*, **25**, 189.  
 Hahn and Rothenbach (1919), *Phys. Zeits.*, **20**, 194.  
 Hevesy (1935b), *Naturwiss.*, **23**, 583.  
 Heyden and others (1938), *Zs. f. Phys.*, **108**, 232.  
 Holmes and Lawson (1926), *Phil. Mag.*, **2**, 1218.  
 Klemperer (1935a), *Proc. Roy. Soc. A.*, **148**, 638.  
 Konopinski, Uhlenbeck (1935d), *Phys. Rev.*, **48**, 7.  
 Libby and Lee (1939), *Phys. Rev.*, **55**, 245.  
 Mühlhoff (1930), *Ann. Phys.*, **7**, 205.  
 Nier (1936), *Phys. Rev.*, **50**, 1041.  
 Occhialini (1931), *R.C. Acad. Linc.*, **15**, 103.  
 Occhialini and Bocciaireli (1933), *R.C. Acad. Linc.*, **17**, 830.  
 Orban (1931), *Akad. O. Wiss. Wien.*, **140**, 121.  
 Rutherford and Geiger (1910), *Phil. Mag.*, **20**, 5, 691.  
 Sargent (1933), *Proc. Roy. Soc., A.*, **138**, 659.  
 Schonland (1923), *Proc. Roy. Soc., A.*, **104**, 235.  
 ——— (1925), *Proc. Roy. Soc., A.*, **108**, 187.  
 Sitte (1935c), *Zs. f. Phys.*, **96**, 593.  
 Smyth and Hemmendinger (1937b), *Phys. Rev.*, **51**, 1052.

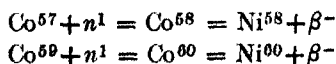
# ON THE EXISTENCE OF AN ISOTOPE OF COBALT, $\text{Co}^{57}$

By P. K. SEN-CHOWDHURY, *M.Sc., Research Scholar, Palit Research Laboratory, University College of Science, Calcutta.*

(Communicated by Prof. M. N. Saha, F.R.S.)

(Read January 1, 1942.)

Since Sampson and Bleakney (1936a) reported that cobalt, besides having a main isotope of weight 59, has an isotope of mass No. 57 and frequency of about 0.2%, there has been a certain amount of controversy over the existence of this stable isotope  $\text{Co}^{57}$ . Working with their magnetic mass-spectrograph and using anhydrous cobalt chloride, Sampson and Bleakney obtained a peak at the mass No. 92. This peak they interpreted to be due to  $\text{Co}^{57}\text{Cl}^{35}$ . From the relative height of the peak they calculated the abundance of  $\text{Co}^{57}$  to be about 0.2%. They also supported their conclusion from the fact that two artificially radio-active isotopes of ordinary cobalt, namely  $\text{Co}^{58}$  and  $\text{Co}^{60}$ , are obtained by bombarding ordinary cobalt with fast and slow neutrons. They assume (1936b) that these two are produced by the neutron capture of the two isotopes according to the nuclear process:

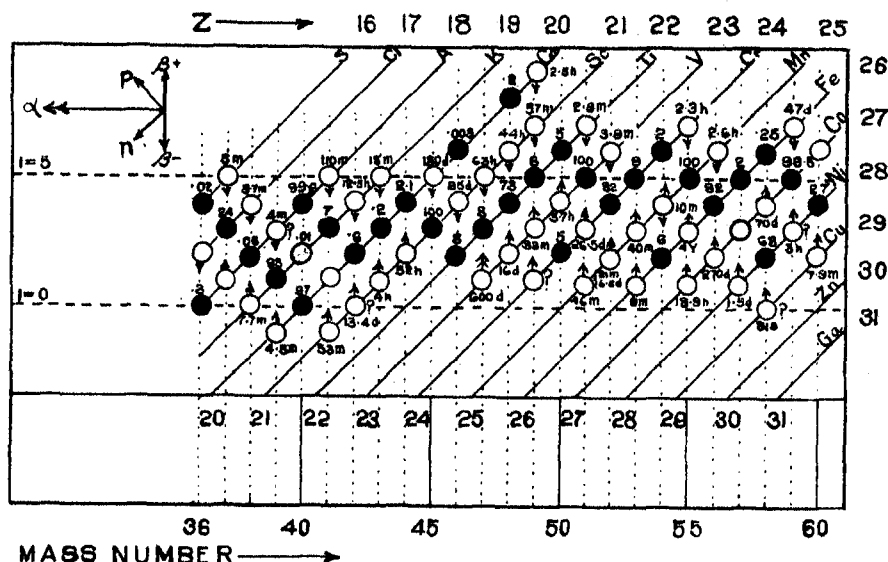


From the empirical chart of nuclei of Saha, Sirkar and Mukherji (1940), however, it follows that if  $\text{Co}^{57}$  exists, it should be at least naturally radio-active and emit positrons according to the nuclear process:



Further, if it really occurs in natural cobalt to the extent of 1 : 500, it should be a long-lived one like  ${}_{19}\text{K}^{40}$  or  ${}_{37}\text{Rb}^{87}$  and emit very slow  $\beta$ -rays. The relevant portion of the nuclear chart is illustrated on p. 56.

It will be observed that  $\text{Co}^{57}$  lies on the horizontal line corresponding to the isotope number  $1 = 3$ , and the characteristic of the lines having odd isotope number is that there are a number of stable elements in the middle, flanked by  $\beta^-$ -emitting elements on the left, and  $\beta^+$ -emitting elements on the right. In line  $1 = 3$ , the stable isotopes are  ${}_{17}\text{Cl}^{37}$ ,  ${}_{19}\text{K}^{41}$ ,  ${}_{20}\text{Ca}^{48}$ ,  ${}_{21}\text{Sc}^{45}$  and  ${}_{22}\text{Ti}^{47}$  ( $\text{A}^{50}$ —not yet discovered). From  ${}_{23}\text{V}^{49}$  onwards, all isotopes are  $\beta^+$ -active up to  ${}_{30}\text{Zn}^{68}$ , the only exception seems to be  ${}_{27}\text{Co}^{57}$ . Saha, Sirkar and Mukherji pointed out that if  $\text{Co}^{57}$  really occurred in natural cobalt to the extent of 0.2%, ordinary cobalt should show feeble radio-activity due to this isotope, just like potassium, in which radio-activity is due to  ${}_{19}\text{K}^{40}$  occurring in the proportion of 1 : 8000.



In this chart the abscissae represent mass-number  $A$ , the ordinate represents  $I$ , the isotope number which is defined as the excess of neutrons over protons in the nucleus. The parallel lines at  $45^\circ$ , to be called the  $Z$ -lines, represent atomic number ' $Z$ '. Thus all isotopes of same  $Z$  are to be found on the same  $Z$ -line. Each isotope is represented by a circle. Solid circles represent stable nuclei. Hollow circles with an arrow pointing up,  $\sigma$ , represent  $\beta^+$  (positron) emitting nuclei, when the arrow points down,  $\rho$ , they indicate  $\beta^-$  (electron) emitting nuclei.

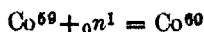
To detect if there is any feeble radio-activity of ordinary cobalt due to the isotope  $\text{Co}^{57}$  (of assumed abundance 0.2%) a very sensitive  $\beta$ -ray analyser consisting of screen-wall Geiger-Müller Counter mounted radially in a uniform magnetic field as described by Libby (1939) and others was built up in this laboratory. It is described in the previous paper. This Counter as tested with rubidium and potassium (using a magnetic field) is capable of detecting efficiently emitted electrons having as small an energy as one Kilovolt. Using about 10 gms. of cobalt oxide and other salts of cobalt (Mercks' preparation) with this Counter and giving prolonged exposure no increase in the counting rate over the background rate was observed. From this it is concluded that there is probably no feebly active isotope of cobalt in Nature and like  $^{23}\text{Na}$  and certain other elements with odd mass number and odd charge, it has only one stable isotope, of weight 59 and having 100% frequency.

It may be further mentioned that Aston (1933) has found no trace of any isotope of cobalt. He is of the opinion that cobalt is a simple atom of mass-number 59. Hahn is also of the opinion that the peak obtained by Bleakney and Sampson is due to some impurities and that there is no stable  $\text{Co}^{57}$ . The peak obtained by them at 92 may be due to  $^{55}\text{Mn}$ ? Moreover the radio-active isotope of cobalt, e.g.  $\text{Co}^{58}$  of about 20 m. period as stated above by Bleakney

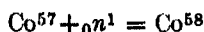
and Sampson in support of their conclusion to be formed by the neutron capture of Co<sup>57</sup> seems to be incorrect, for a study of the original report of Rotblat (1935) to which reference has been made by Bleakney, etc., it is found that the former at first obtained the radio-active cobalt of period about 20 minutes by bombarding nickel by neutron from a Radon-Beryllium source. Rotblat assumed the active isotope to be formed according to the nuclear reaction:—



He confirmed it by bombarding cobalt with slow neutron when a similar period was obtained which he attributed to the reaction:—

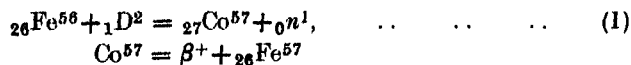


Bleakney and Sampson however assume it to be due to the reaction:—

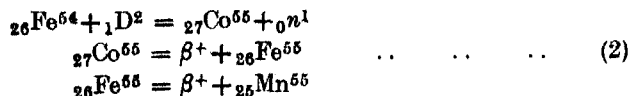


But the assignment of the 20 minute period to Co<sup>58</sup> seems to be wrong from the experiments of Livingwood, Seaborg, Fairbrothers (1938) and Barresi and Cacciapuoti (1939) who obtained Co<sup>58</sup> by the reaction Mn<sup>55</sup>-α-n, and Fe<sup>57</sup>-D-n, and found Co<sup>58</sup> obtained in both the cases have a half-life 70 days and not 20 minutes. Therefore Rotblat's result if correct suggests that either there was some nickel impurities in cobalt or Co<sup>60</sup> must have an isomer.

Again assuming that there is no naturally radio-active isotope Co<sup>57</sup>, it should be obtained artificially. The nuclear chart of Saha, Sirkar and Mukherji (*loc. cit.*) suggests that Co<sup>57</sup> may be obtained by bombarding iron with deuteron according to the nuclear reaction (Fe-D-n)



A reaction of this type has been actually observed first by Darling, Cartis, Cork (1937) and subsequently by others by bombarding iron with deuteron. They, however, probably assuming Co<sup>57</sup> to be stable interpreted it by the reaction



According to this reaction there is double positron emission in each process. From the continuous energy spectra of radio-active cobalt obtained by Lawson (1939) nothing can be concluded definitely. From this it may be said that either Co<sup>57</sup> rather than Co<sup>55</sup> is obtained by the Fe<sup>57</sup>-D-n reaction. Or probably both the reaction Fe<sup>54</sup>-D-n and Fe<sup>56</sup>-D-n, producing Co<sup>55</sup> and Co<sup>57</sup> respectively, occur on bombarding iron with deuteron. As a matter of fact this may explain the existence of more than one half-period in the cobalt portion separated from iron bombarded with deuteron as pointed out in the works of Livingwood, Seaborg, Fairbrothers (1937) and others. These different periods they conclude to be due to some unidentified isotope. One of this is probably

$\text{Co}^{57}$ . This alternative possibility (1) and (2) can be further tested by separating the two isotopes of iron  $\text{Fe}^{56}$  (90%) and  $\text{Fe}^{54}$  (6%) by some process like thermal diffusion and then bombarding the separated isotope with deuteron.

This work has been done under the constant direction and guidance of Prof. M. N. Saha, F.R.S., to whom I express my deep gratitude. I wish also to express my thanks to Messrs. Scientific Indian Glass Co., particularly to Prof. N. C. Nag, Technical Expert of the above Works, who have very kindly constructed the apparatus for us in their factory.

#### SUMMARY.

An attempt has been made to clear the controversial existence of an isotope of cobalt  $\text{Co}^{57}$  (0.2%) in Nature. Saha, Sirkar and Mukherji's empirical chart of nuclei suggests that  $\text{Co}^{57}$  should be positron-active and have a long life like  $\text{K}^{40}$  in natural potassium. Therefore the positron activity of natural cobalt was searched very carefully using a screen-wall Geiger Counter but no activity was detected. From this as well as from a study of some observed nuclear reactions it is concluded that there is no  $\text{Co}^{57}$  in Nature and probably one of the unidentified artificially radio-active isotopes in the cobalt fraction separated from iron bombarded with deuteron is  $\text{Co}^{57}$ . These nuclear reactions also suggest that probably  $\text{Co}^{60}$  has an isomeric pair.

#### REFERENCES.

- Aston (1933), *Mass-Spectra and Isotopes*, p. 156.  
 Barresi and Cacciapuoti (1939), *Rivista Scient.*, **10**, 404.  
 Darling, Cartis and Cork (1937), *P.R.*, **51**, 1010.  
 Lawson (1939), *P.R.*, **56**, 131.  
 Libby and others (1939), *P.R.*, **55**, 245.  
 Livingwood and Seaborg (1938), *P.R.*, **53**, 847.  
 Livingwood and Seaborg (1937), *P.R.*, **52**, 135.  
 Rotblat (1935), *Nature*, **136**, 515.  
 Saha, Sirkar and Mukherji (1940), *Proc. Nat. Inst. Sc. Ind.*, **6**, 45-63.  
 Sampson and Bleakney (1936a), *P.R.*, **50**, 735.  
 Sampson, Bleakney and Ridenour (1936b), *P.R.*, **50**, 382.

DEVELOPMENT OF EMBRYO-SAC AND ENDOSPERM-HAUSTORIA IN  
*TETTRANEMA MEXICANA* BENTH. AND *VERBASCUM*  
*THAPSUS* LINN.

By C. V. KRISHNA IYENGAR, M.Sc., Department of Botany, University of Mysore.

(Communicated by Dr. P. Maheshwari, D.Sc., F.N.I.)

(Read January 1, 1942.)

In the course of my investigations on Scrophulariaceae (Krishna Iyengar, 1937, 1939a, 1939b, 1939c, 1940a, 1940b, 1940c, 1941b and 1941c) several interesting features were noticed during the pre- and post-fertilization stages of the embryo-sac. In the second paper of this series (Krishna Iyengar, 1939a) I described the formation of the chalazal nutritive tissue and endosperm haustoria in *Isoplexis canariensis* and *Celsia coromandeliana*, and explained how the integumentary tapetum plays a significant nutritional rôle in the latter member. This has also been reported in the various species of *Verbascum*, *Digitalis* and *Celsia* by previous investigators like Balicka Iwanowska (1899), Hakansson (1926) and Schmid (1906). A paper on *Tetranema* was read by me (1941a) at the Indian Science Congress, 1941. On account of the endospermal similarities existing between *Tetranema* and *Verbascum* both have been included in the present paper.

MATERIAL AND METHODS.

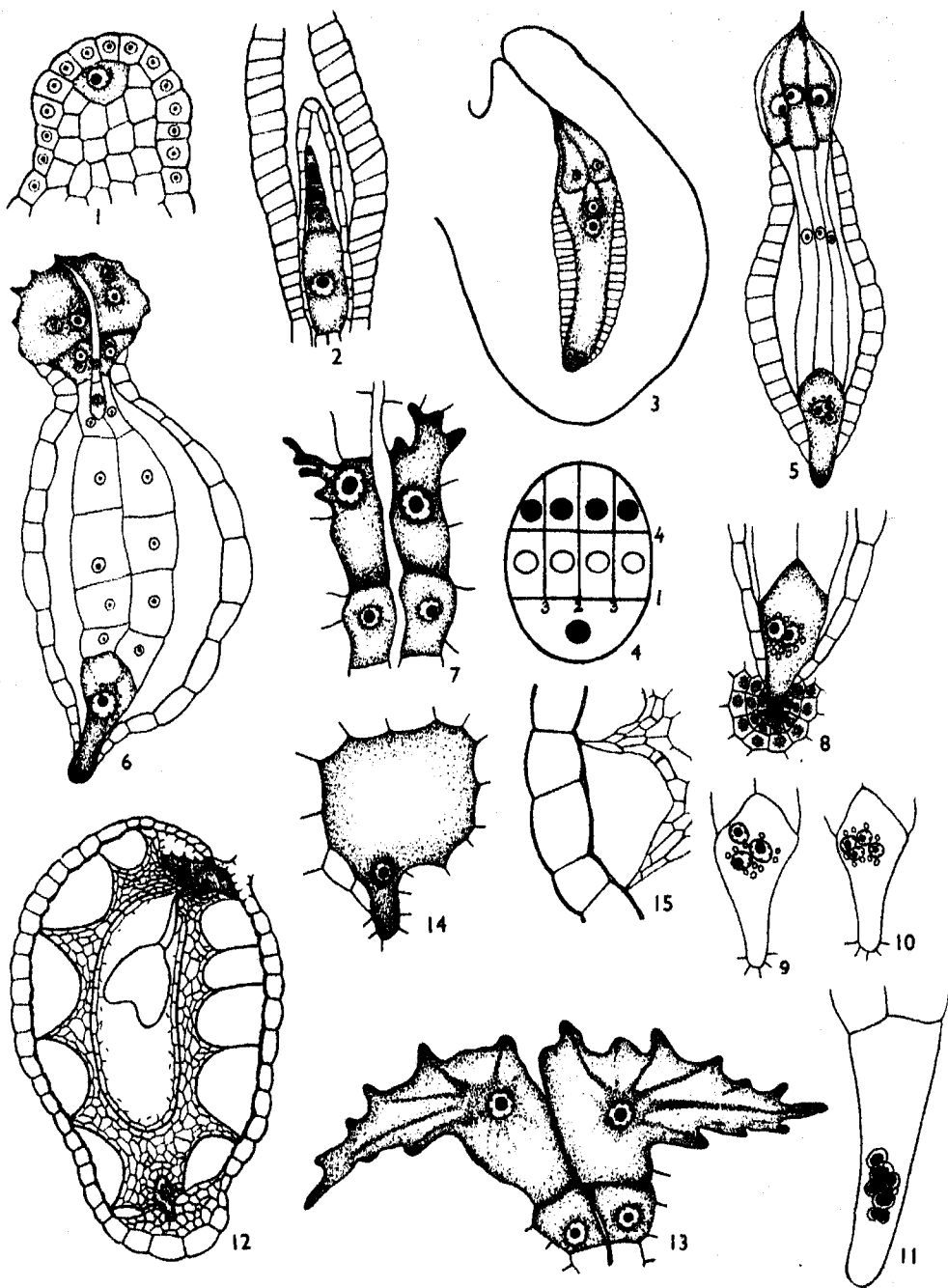
The material for this investigation was collected from the Government Horticultural Gardens, Bangalore, and the Ayurvedic Gardens, Mysore, and fixed in Bouin's fluid. The sections were cut 8 $\mu$  thick for embryo-sac and 10 $\mu$  for endosperm development, and were stained in Heidenhain's iron-alum haematoxylin.

OVULE.

The ovules are anatropous, indefinite in number and arranged on a massive placenta rich in starch. A well-defined hypostase with rich cell-contents is present at the chalazal region. Even here there is a conspicuous deposition of starch. A single thick integument and reduced nucellus are seen in both members.

*Tetranema Mexicana* Benth.

*Embryo-Sac*.—The large hypodermal archesporial cell directly functions as the megaspore mother cell (Fig. 1). A linear tetrad of megaspores is produced as usual (Fig. 2), and the chalazal megaspore develops into the normal eight-nucleate embryo-sac (Fig. 3). The micropylar part of the sac is dilated and



*Tetranema mexicana* Benth.

Fig. 1. Archesporial cell.  $\times 480$ . Fig. 2. Linear tetrad.  $\times 640$ . Fig. 3. Embryo-sac.  $\times 320$ . Fig. 4. A diagram showing the sequence of divisions in endosperm. Fig. 5. Embryo-sac showing differentiation of haustoria and endosperm.  $\times 320$ . Fig. 6. Formation of endosperm and haustoria.  $\times 320$ . Fig. 7. Micropylar haustorium enlarged.  $\times 730$ . Fig. 8. Chalazal haustorium enlarged. Bi-nucleate condition.  $\times 320$ . Fig. 9. Tri-nucleate chalazal haustorium.  $\times 320$ . Fig. 10. Tetra-nucleate chalazal haustorium.  $\times 320$ . Fig. 11. Chalazal haustorium with nine nuclei.  $\times 480$ . Fig. 12. Long. Section of an almost mature seed showing the embryo, endosperm haustoria and tapetum.  $\times 92.5$ . Fig. 13. Old micropylar haustoria with the darkly stained nuclei and rich deposition of cellulose.  $\times 480$ . Fig. 14. Old chalazal haustorium.  $\times 480$ . Fig. 15. Tapetal cells enlarged.  $\times 160$ .

contains the egg-apparatus with the large synergids, while the narrow chalazal part includes the three small antipodal nuclei. The two polar nuclei situated in the middle fuse just before fertilization. The cells of the nucellar jacket go on degenerating till at last at the mature embryo-sac stage even their last traces disappear. Thus the integumentary tapetum lines the sac directly. Although originally surrounding the whole of the linear tetrad, the tapetum in later stages sheathes only the non-dilated lower part of the sac. Accumulation of nutritive material, however, is noticed in the integumentary tissue in the neighbourhood of the dilated micropylar end of the sac.

*Embryo and Endosperm.*—The antipodal nuclei degenerate immediately after fertilization. The first division of the primary endosperm nucleus which is transverse is succeeded by a wall and separates a chalazal haustorial chamber from the micropylar one. Further divisions are restricted to the micropylar chamber resulting in four rows of cells of which the terminal become haustorial (Fig. 5). Fig. 4 is a diagram to indicate the sequence of divisions in the early development of the endosperm. The middle cells by further divisions form the body of the endosperm (Fig. 6), which finally becomes differentiated into the two terminal regions composed of smaller cells and the centrally placed region with larger cells, the former probably serving to transport nutritive material from the haustoria to the centre (Fig. 12). Only four of the endosperm cells next to the micropylar haustoria assume a noteworthy size (Figs. 6, 7 and 12). Starch is abundantly deposited in the large endosperm cells.

*Endosperm Haustoria.*—The four cells towards the micropyle develop into aggressive uni-nucleate haustoria. They show significant enlargement, their contents are highly granulated and their nuclei also assume a larger size (Fig. 7). Their ends eat their way into the integumentary tissue probably with the help of their several short processes. Often the digestion of the major part of the adjacent tissue has also been noticed. Older haustoria show darkly staining amoeboid nuclei which appear as dark bodies on account of high chromatic concentration. A rich deposition of cellulose in the form of rods has also been noticed in these haustoria (Fig. 13).

The chalazal chamber develops directly into a non-aggressive haustorium. Its nucleus often divides resulting in a binucleate body (Fig. 8). At times four nuclei are also seen (Fig. 10). In two cases three nuclei were noticed and one case showed as many as nine nuclei of various sizes (Fig. 11). Thus all grades from the uni-nucleate (Fig. 6) to a multi-nucleate condition are met with in this plant. The size of the haustorial nuclei depends on their number, the uni-nucleate haustorium having the largest nucleus. The occasional multi-nucleate condition seen in this region reminds one of the basal apparatus of some members of the families with *Helobiales*-type of endosperm.

*Integumentary Tapetum.*—The integumentary tapetum plays a significant nutritional rôle. During pre-fertilization stages of the embryo-sac it acts as a repository for food material and with the commencement of endosperm formation it shows an enlargement of its cells (Figs. 12 and 15). All the cells



except those towards the two ends assume considerable size at the time of senility of the haustoria. Their size, rich contents and thin-walled nature and their proximity to the digested and absorbed cells of the integument indicate their probable haustorial action to assist in the nutrition of the developing endosperm and embryo.

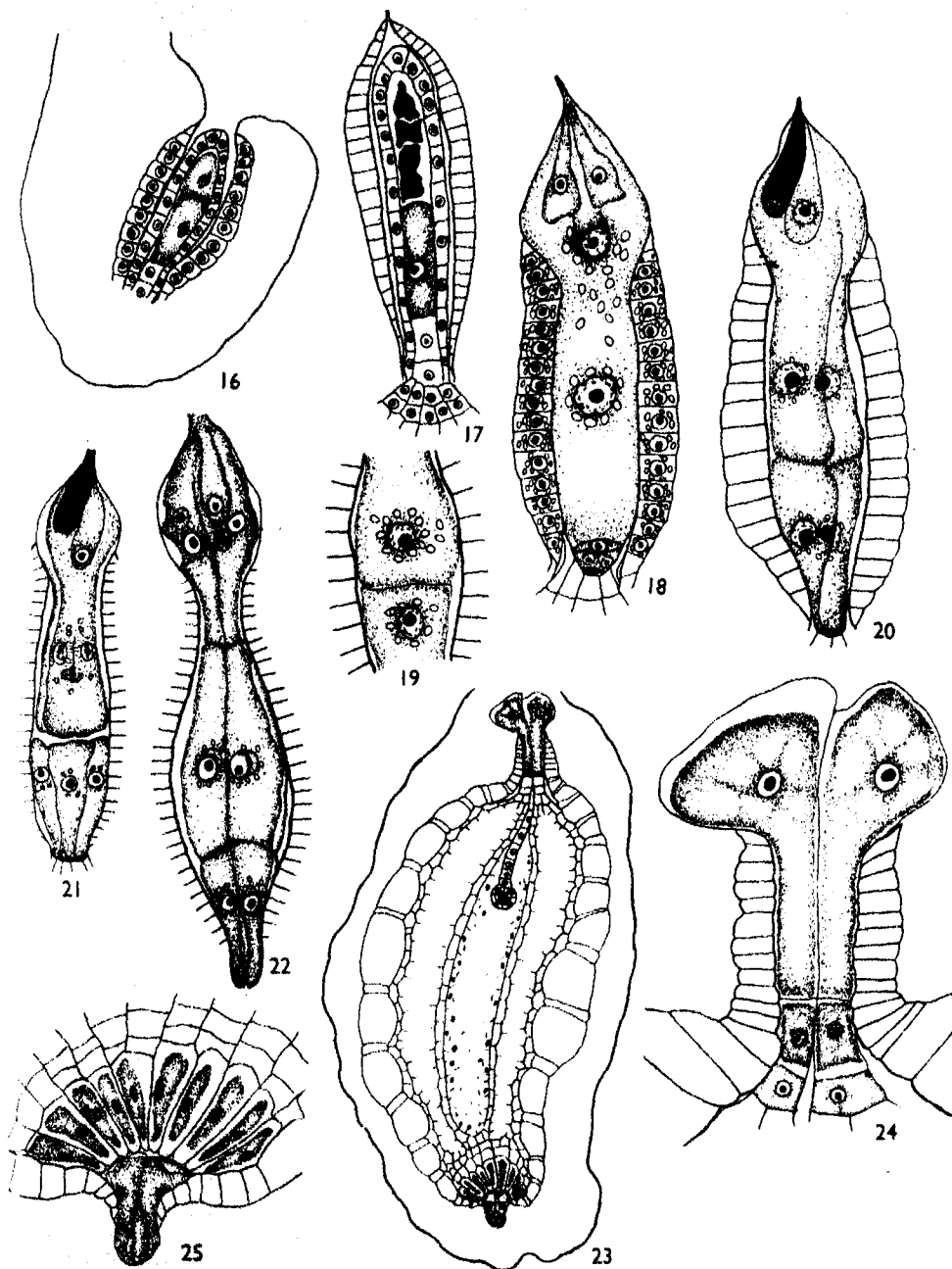
*Verbascum thapsus* Linn.

*Embryo-Sac*.—Just as in the previous species a large hypodermal cell of the nucellus directly functions as the megaspore mother cell and gives rise to a linear tetrad of megaspores (Fig. 17). Of these the chalazal develops into the normal eight-nucleate embryo-sac (Fig. 18), while the other three degenerate. The degeneration of these starts from the interior so that the micropylar megaspore degenerates last. The structure of the embryo-sac is similar to that of *Tetranema*. The dilated micropylar end contains the large synergids and the egg, while the slightly narrow chalazal part has three antipodal cells instead of nuclei (Fig. 18). There is a constriction just below the dilated micropylar end, and in its neighbourhood lie the two polar nuclei, which fuse to form the secondary nucleus when the embryo-sac is mature. The embryo-sac and, as already stated before, the tissue surrounding it is filled with starch grains. The nucellar jacket gets absorbed and almost disappears, only a few cells persisting at the base and forming a patch with darkly stained contents.

*Endosperm and Embryo*.—Although pollen tubes were frequently noticed, stages in fertilization were not available. The post-fertilization stages can be described as follows:—

The primary endosperm nucleus divides transversely resulting in the formation of the chalazal and micropylar chambers as in Fig. 19. The next two divisions which are longitudinal occur in both chambers (Figs. 20 and 21). Thus there are four cells towards the chalaza, which directly become the haustoria, and four cells towards the micropyle from which a subsequent transverse division cuts off the four micropylar haustorial initials (Fig. 22). The four cells forming the middle tier divide further, giving rise to the endosperm tissue (Fig. 23), with two clearly defined regions. The region towards the two ends is composed of cells with rich protoplasmic contents and perhaps with a food conducting rôle, while that towards the middle is composed of larger cells with a rich deposition of starch and forming the body of the endosperm as in Fig. 23.

Even in the tissue towards the two ends there is considerable difference. The conducting endosperm tissue towards the chalaza is composed of smaller as well as larger cells; the latter lie in direct contact with the chalazal haustorial cells, have richer contents and are almost as large as the haustoria (Fig. 25). This is a peculiar feature not met with in any other Scrophulariaceae till now, although many instances are known where a few cells towards the micropylar end are as large as the haustoria, as for instance in *Tetranema*.



*Verbascum thapsus* Linn.

Fig. 16. Dyad cells dividing.  $\times 320$ . Fig. 17. Formation of the linear tetrad.  $\times 480$ . Fig. 18. Section showing embryo-sac, tapetum and hypostase.  $\times 480$ . Fig. 19. First division of the primary endosperm nucleus.  $\times 480$ . Fig. 20. Second division of the same.  $\times 480$ . Fig. 21. Third division of the same.  $\times 320$ . Fig. 22. Fourth division of the same and the organisation of haustoria and endosperm.  $\times 320$ . Fig. 23. Long. Section of an almost mature seed showing the various parts.  $\times 92.5$ . Fig. 24. Old micropylar haustoria.  $\times 480$ . Fig. 25. Old chalazal haustoria with the conducting cells of the endosperm.  $\times 320$ .

*Endosperm Haustoria.*—The chalazal haustoria are formed earlier. They are composed of four uni-nucleate tubular and non-aggressive cells which do not enlarge. Starch grains are noticed in these cells from the commencement till a late stage in their activity, the disappearance of these coinciding with the senility of the haustoria. The haustoria neither show a high degree of development nor appreciable haustorial activity (Figs. 21 and 25). The compact nutritive tissue at the base of these cells may come in the way of their free development or it might be that the presence of a well-defined nutritive tissue makes the extra development of the haustoria unnecessary. A similar feature is met with in *Celsia* (Krishna Iyengar, 1939a) and other members. The degeneration of these haustoria sets in very early, long before the endosperm and embryo are well developed.

The four micropylar haustoria are also non-aggressive and uni-nucleate. Their outer ends enlarge and become bulbous, but compared with the size of the endosperm the haustoria are rather small, leading one to suspect their efficiency as adequate nutritive organs. They persist till a late stage in the embryo and endosperm formation, and show large nuclei with rich chromatin material and highly vacuolated dense protoplasm.

*Integumentary Tapetum.*—The tapetum is organized from the innermost layer of the integument and its cells act as a reservoir of food material, while the embryo-sac is developing. The two ends of the tapetal sheath are here invariably composed of smaller cells, while the most pronounced development of the cells is confined to the middle part (Fig. 23). Here the larger and smaller cells alternate as in *Verbascum montanum* (Schmid, 1906). The enlargement of alternate cells may be explained as due to the limited nature of the available space. The structure of the tapetal cells during post-fertilization stages indicates their importance as digesting and absorbing organs. Since the tapetal cells towards the micropyle are somewhat thick-walled, the transportation of material takes place mainly through the chalaza. While the closely adpressed nature of the endosperm tissue and the tapetum, and the thin separating wall may as well indicate the possibility of a direct transportation of food materials, the presence of large conducting endosperm cells next to the chalazal haustoria points towards a movement of the nutritional stream through this part of the sac.

#### DISCUSSION.

Just as in the other members of the family, the archesporial cell directly becomes the megaspore mother cell and gives rise to a linear tetrad of megaspores. The embryo-sac develops quite normally from the chalazal megaspore. The presence of the hypostase at the chalaza is a noteworthy feature. This is also met with in *Isoplexis* and *Celsia* (Krishna Iyengar, 1939a) and its organization is associated with the limited development and activity of the chalazal haustoria in these two members.

There is much in common between *Tetranema* and *Verbascum* as regards the number of the micropylar haustoria, their formation and sequence of development. The chalazal haustoria are the earlier to appear as also the first to degenerate, while the micropylar persist till a late stage in endosperm formation.

The chalazal haustorium of *Tetranema* is likely to shed some light on the evolutionary tendencies of the organ. The frequent occurrence of a uni- or bi-nucleate haustorium indicates its affinity to *Vandellia* (Krishna Iyengar, 1940a), while the occurrence of a tetra-nucleate body indicates its transitional position between *Verbascum* with four uni-nucleate haustoria and the other members with a single bi- or uni-nucleate haustorium.

The tetra-nucleate stage of *Tetranema* is the result of free nuclear divisions of the nucleus in the chalazal chamber, while the accompanying wall-formation results in the *Verbascum*-type. At times there is no division of the nucleus, while at other times there are one or more divisions, thus resulting in all stages from the uni-nucleate to the multi-nucleate condition. The general condition being the uni- or bi-nucleate one, it appears that there is a tendency towards reduction in the number of divisions without wall-formation at any stage (see the chart below). The former feature is very clearly seen in the bi-nucleate

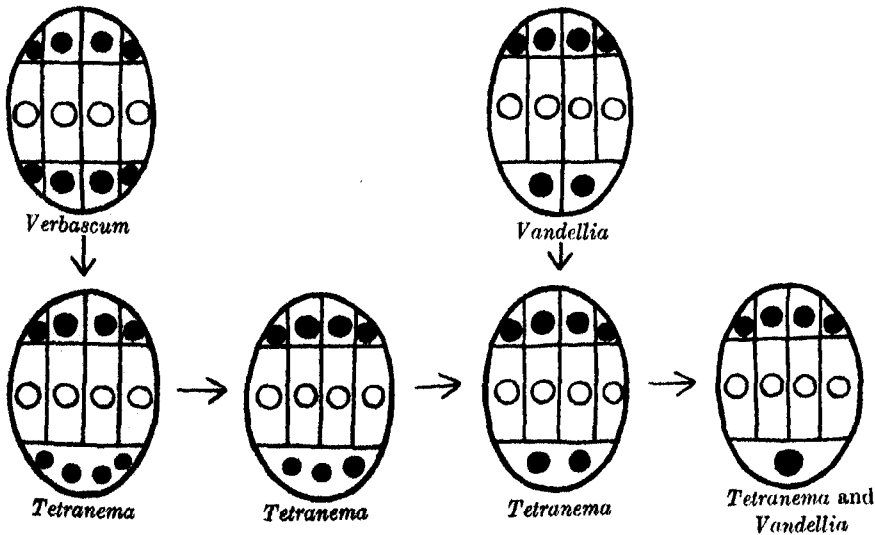


Chart to illustrate the affinities between *Tetranema* and other allied members.

condition where one of the two nuclei resulting from the first division does not divide, its larger size bearing testimony to this assumption. Thus the largest nucleus is seen in the uni-nucleate haustorium, while an increase in number is accompanied by a proportionate diminution in size. A similar feature is met with in *Vandellia*, but this has either two haustorial cells which coalesce to

form a bi-nucleate body or a uni- or bi-nucleate body is formed from the commencement. Here also the trend seems to be in favour of omission of wall-formation, or its dissolution when this is formed. Thus the absence of wall-formation in the antipodals and haustorium forms a noteworthy feature of *Tetranema*. A similar feature, i.e. absence of wall-formation in the antipodals is partially noticed in *Alectorolophus* (Schmid, 1906), where there are only two antipodals, one being bi-nucleate.

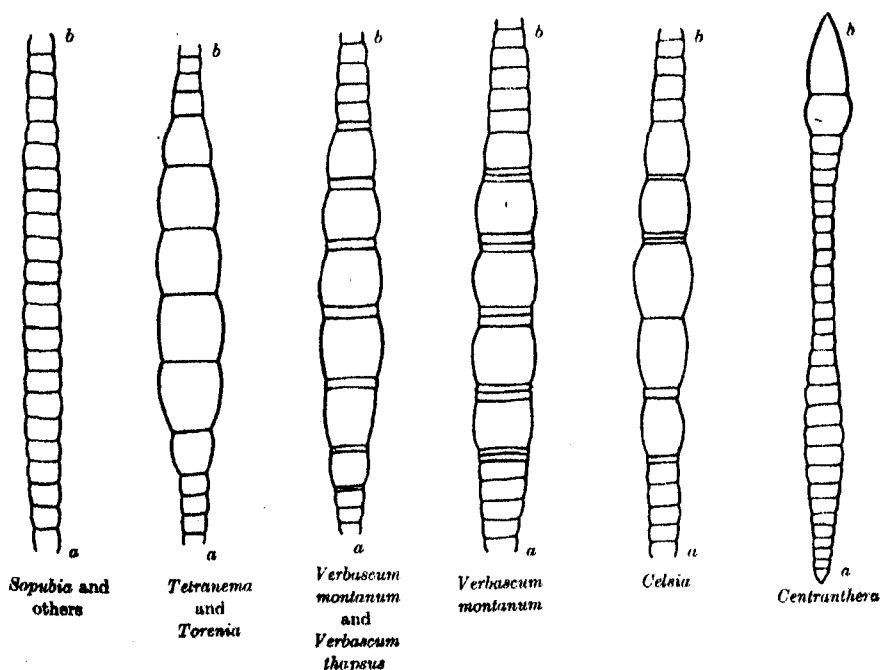
The presence of several free endosperm nuclei in the chalazal haustorium reminds one of the 'basal apparatus' met with in members with *Helobiales*-type of endosperm. Both are structures formed during post-fertilization stages and have a significant rôle in the nutritional physiology of the endosperm and embryo.

*Integumentary Tapetum*.—An integumentary tapetum is a common feature of sympetalous families, and its nutritional value during post-fertilization stages is well known. During the development of the embryo-sac, this sheathes only the lower part of the sac, the micropylar being generally free. It is suggested that the compact cuticularised sheath lining the chalazal part of the sac prevents its free enlargement and consequently affects the size and arrangement of the antipodal cells. The dilated nature of the micropylar part of the sac is attributed to the absence of the sheath towards this part and the consequent freedom for this end to expand. As opposed to this view there is the fact that the tapetum develops by intercalary growth during post-fertilization stages providing adequate space for the enlargement of the endosperm. This introduces the possibility of spacial consideration and not cuticular resistance as responsible for this shape of the embryo-sac.

Although the tapetum is generally the repository for food material and can absorb nutrition from the integumentary tissue, the direct transfer of food materials from this layer to the embryo-sac seems to be difficult in view of the presence of a cuticle of varying thickness. Thus the food current can mostly pass only through the chalaza and partly through the dilated micropylar part of the sac.

There are various grades in the development of the integumentary tapetum in the family as a whole. In several members the tapetum loses its contents as the endosperm and embryo are being formed, and may be completely obliterated. In some members although reduced in size this will show itself by the formation of a thick cuticle. *Alonsoa* (Krishna Iyengar, 1937) and *Isoplexis* (Krishna Iyengar, 1939a) and others are instances of this kind. In other cases the tapetal cells attain significant development and play a prominent rôle in the nutrition of the endosperm and embryo. The accompanying diagrams indicate the different types of tapetum met with during my investigations on several members of Scrophularineae. The first condition happens to be the one most commonly met with. In this case the chalazal and micropylar ends of the tapetal sheath are generally composed of smaller cells, while the larger cells are confined to the middle of the sheath. *Torenia*

(Krishna Iyengar, 1941) shows alternating rows of larger and of smaller cells. In *Tetranema* all the cells in the middle are large, while in *Verbascum* the larger and smaller cells regularly alternate, the smaller cells being single as in *V. thapsus* and *V. montanum* or in pairs as in the latter (Schmid, 1906). In *Celsia* (Krishna Iyengar, 1939a) this regularity is wanting. The intercalation of smaller cells may or may not be found and when these are present they may be either solitary or in pairs. The last figure in the series is that of *Centranthera* (Krishna Iyengar, 1939c) with the highest degree of specialization. The largest cells of the row are towards the chalazal end in the neighbourhood



Diagrammatic representation of the Integumentary Tapetum in some members of Scrophulariaceae.

(a) Micropylar end.

(b) Chalazal end.

of the chalazal haustorium, which is here the least efficient as a haustorium. Next to these are smaller cells which develop a thick cuticle and protect the developing endosperm. Towards the micropyle are some large cells which are rich in cell-contents and which are often pierced by the secondary endosperm haustoria, thus appearing to have a rôle in the stimulation of haustorial formation. Thus the tapetum undergoes several structural changes, especially during the post-fertilization stages to fulfil its functions of digestion, absorption, storage and protection.

## SUMMARY.

1. In *Tetranema mexicana* Benth. and *Verbascum thapsus* Linn. the hypodermal archesporial cell directly forms the megaspore mother cell and gives rise to a linear tetrad of megaspores. The chalazal megaspore develops into the normal eight-nucleate embryo-sac.

2. A well-developed nutritive tissue composed of compactly arranged radiating cells is present at the chalaza.

3. The chalazal part of the embryo-sac is narrow and is sheathed by the integumentary tapetum composed of cells with rich contents.

4. The first division of the primary endosperm nucleus is transverse and this results in the formation of the chalazal and micropylar chambers. The next two divisions are longitudinal and may be confined only to the micropylar chamber as in *Tetranema* or occur in both the chambers as in *Verbascum*. The fourth division is confined to the micropylar chamber only, resulting in the separation of a micropylar tier which forms the four uni-nucleate haustoria.

6. The micropylar haustoria become bulbous and aggressive and show short processes in *Tetranema*, while in *Verbascum* these are non-aggressive and differentiated into the long and tubular inner part and the bulbous outer part. Cellulose rods are met with in the older haustoria of *Tetranema*.

7. The chalazal chamber in *Tetranema* develops directly into a haustorium with one to four nuclei. In *Verbascum* there are four non-aggressive, tubular and uni-nucleate chalazal haustoria. In both cases the chalazal haustoria degenerate very early.

8. The endosperm tissue shows smaller cells towards the two ends, but some of the cells towards the chalaza are appreciably large in *Verbascum*.

9. The tapetal cells enlarge while the endosperm is developing and take an important part in the nutritional mechanism of endosperm and embryo.

10. The alternation of larger and smaller cells in the tapetum forms a distinctive feature of *Verbascum*.

The author expresses his indebtedness to Dr. M. A. Sampathkumaran, M.A., Ph.D., S.M., Professor of Botany, Central College, Bangalore, for facilities and encouragement, and to Dr. P. Maheshwari, D.Sc., F.N.I., F.A.Sc., of Dacca University for his kind perusal of the manuscript and invaluable suggestions. Sincere thanks are due to the authorities of the Government Horticultural Gardens, Bangalore City, and the Ayurvedic Gardens, Mysore, for enabling the author to collect the material for investigation.

## REFERENCES.

- BALIOGA IWANOWSKA, G., 1899. Contribution à l'étude du sac embryonnaire chez certaines Gamopétales. *Flora*, 86: 47-71.
- Hakanason, A., 1926. Zur Zytologie von *Celsia* und *Verbascum*. *Lunds. Univ. Årsskrift*, N.F. Avd. 2, 21, Nr. 10.
- Krishna Iyengar, C. V., 1937. Development of embryo-sac and endosperm haustoria in some members of Scrophulariaceae. I. *Sopubia delphinifolia* G. Don and *Alonsoa* sp. *Jour. Ind. Bot. Soc.*, 16: 99-109.

- Krishna Iyengar, C. V., 1939a. Development of embryo-sac and endosperm haustoria in some members of Scrophularineae. II. *Isoplexis canariensis* Lindl. and *Celsia coromandeliana* Vahl. *Ibid.*, 18: 13-20.
- 1939b. Development of embryo-sac and endosperm haustoria in some members of Scrophularineae. III. *Limnophila heterophylla* Benth. and *Stemodia viscosa* Roxb. *Ibid.*, 18: 35-42.
- 1939c. A note on the embryo-sac and endosperm-haustoria in some members of Scrophularineae. *Curr. Sci.*, 8: 261-263.
- 1940a. Development of embryo-sac and endosperm haustoria in some members of Scrophularineae. IV. *Vanitellia hirsuta* Ham. and *V. scabra* Benth. *Jour. Ind. Bot. Soc.*, 18: 179-189.
- 1940b. Development of embryo-sac and endosperm haustoria in some members of Scrophularineae, V. *Ilysanthes hyssopioides* Benth. and *Bonnaya tenuifolia* Spreng. *Ibid.*, 19: 5-17.
- 1940c. Structure and development of seed in *Sopubia trifida* Ham. *Ibid.*, 19: 251-261.
- 1941a. Development of embryo-sac and endosperm haustoria in *Tetranema mexicana* Benth. *Proc. Ind. Sci. Congress*, Part 5, 1941.
- 1941b. Development of embryo-sac and endosperm haustoria in *Torenia cordifolia* Roxb. and *T. hirsuta* Benth. *Proc. Nat. Inst. Sci. India*, 7, No. 1, 16-71.
- 1941c. Development of embryo-sac and endosperm haustoria in *Rehmannia angulata* Hemsl. (In the press.)
- Schmid, E., 1906. Beiträge zur Entwicklungsgeschichte der Scrophulariaceen. *Beih. Bot. Cbl.*, 20A: 175-299.





## STUDIES IN FLORAL ANATOMY.

### II. FLORAL ANATOMY OF THE MORINGACEAE WITH SPECIAL REFERENCE TO GYNAECIUM CONSTITUTION.<sup>1</sup>

By V. PURI, D.Sc., Meerut College, Meerut.

(Communicated by Dr. P. Maheshwari.)

(Read January 1, 1942.)

#### INTRODUCTION.

The Moringaceae is a small family confined to the tropics and occurring mainly in North Africa, India and the East Indies. The only genus, *Moringa*, contains about ten species. The systematic position of the family has long been a debated question. Jussieu (1789)<sup>2</sup> placed *Moringa* in the family Leguminosae. It was Lindley (1836)<sup>2</sup> who first recognised the family Moringaceae and included it in the Violales, while putting the Cruciferae, the Capparidaceae and the Resedaceae in the Cruciales and the Papaveraceae with the sub-family Fumariaceae in the Ranales. Bentham and Hooker (1862) regarded the family as anomalous and provisionally placed it next to the Coriariaceae after the Sapindales. Wettstein (1924/1935) puts it at the end of the Rhoadales along with the Papaveraceae, Tovariaceae, Capparidaceae, Cruciferae and Resedaceae. Hutchinson's (1926) Rhoadales includes only the Papaveraceae and Fumariaceae, while the Capparidaceae, Moringaceae and Tovariaceae are grouped under the Capparidales and the Cruciferae under the Cruciales. The most recent arrangement is that of Harms (Engler and Prantl, 1936) who divides the Rhoadales into five sub-orders:—

1. Rhoadineae (Papaveraceae).
2. Capparidineae (Capparidaceae, Tovariaceae and Cruciferae).
3. Resedineae (Resedaceae).
4. Moringineae (Moringaceae).
5. Bretschneiderineae (Bretschneideraceae).

The lack of agreement among these authors, all of whom have relied mainly upon the usual taxonomical data (i.e., flower structure) emphasises the need of evaluating evidence from other sources like anatomy (floral as well as vegetative<sup>3</sup>) and embryology for the solution of the problem. Having

---

<sup>1</sup> Part of the thesis approved for a D.Sc. degree of the Agra University.

<sup>2</sup> Quoted from Engler-Prantl.

<sup>3</sup> Some three years ago Professor S. J. Record of the Yale University wrote to me that he was studying the wood structure in this and the allied families.

done with the embryology (Puri, 1941a), I propose to describe in detail the floral anatomy of *Moringa oleifera*, which is very commonly seen in N. India as a planted tree.

#### EXTERNAL MORPHOLOGY OF THE FLOWER.

The inflorescence is an axillary panicle whose ultimate ramifications end in cymes consisting of three flowers of which the central is the oldest (Fig. 2, A). The flower is slightly zygomorphic owing partly to the variation in size of members of the same whorl and partly to the difference in the level of origin of the floral leaves on the anterior and posterior sides. The thalamus forms a cup-shaped structure with the ovary inserted somewhere in the bottom and the other whorls on its edge. Posteriorly highest, the wall of the cup goes on decreasing towards the anterior side (Fig. 2, K).

There are five, spatulate, reflexed and unequal sepals which remain free from one another and almost equal the petals at maturity. The cells of epidermal layers are radially elongated and often produced into uni-cellular hairs, especially abundant on the inner surface (Fig. 1, A). Stomata are

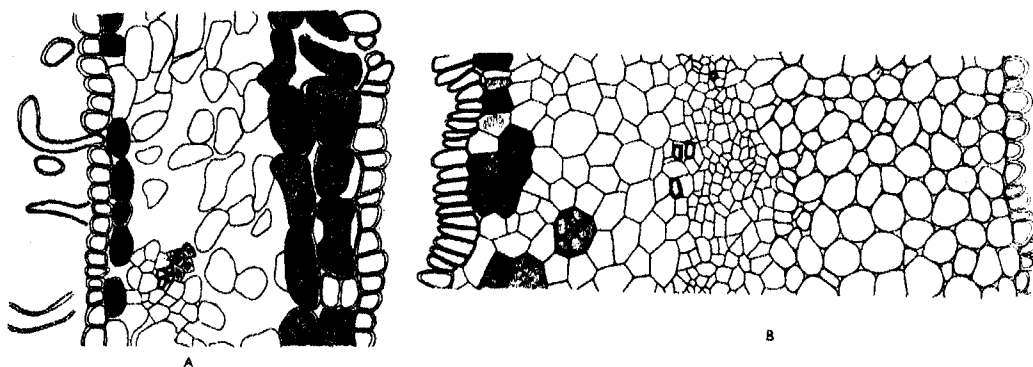


FIG. 1. ( $\times 100$ .)

A & B.—Sections of sepal and petal respectively through the middle region.

present only on the outer side. The mesophyll tissue is more or less spongy and the hypodermal layers are very rich in a dark brown substance [myrosin, according to Solereder (1908)], which becomes precipitated in alcohol. Usually there are two such layers below the outer epidermis and one below the inner. Sometimes some of the myrosin cells are scattered more or less irregularly in the mesophyll tissue.

The petals have no definite mid-rib but a cross section shows that the middle region is the thickest in size and the richest in food material. The two posterior petals are the smallest and become more reflexed than the others. They have a dense coating of hair on their inner surface, while on the other petals this is very scanty or even absent. Myrosin, whenever present, is confined to the inner hypodermis (Fig. 1, B).

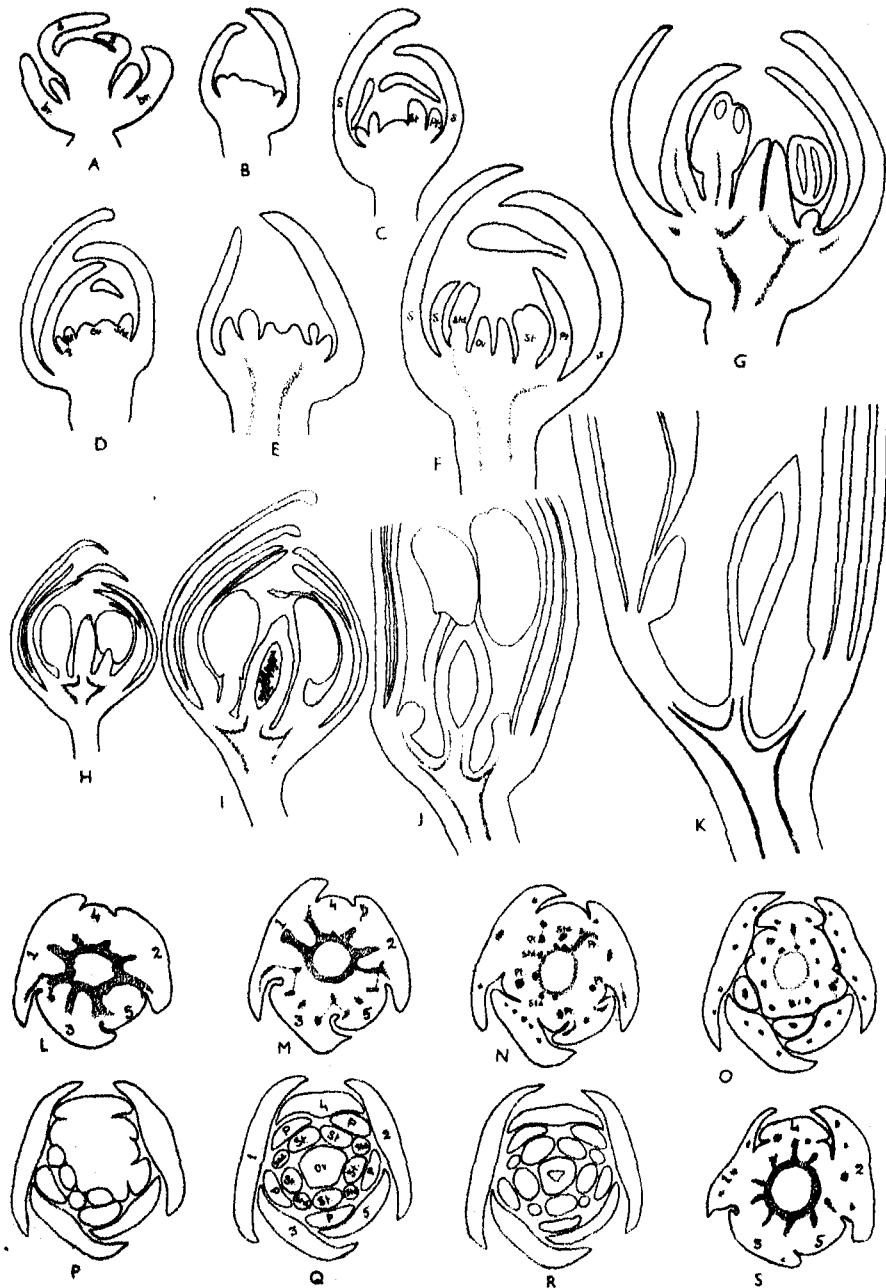


FIG. 2, A-S. ( $\times 26$ .)

A.—Vertical section through a young cymule; each of the lateral buds is situated in the axil of a large bract. B-G.—Vertical sections through buds of varying ages showing the acropetal origin and differentiation of floral leaves. H-K.—Drawings from free-hand sections of buds to show the formation of the floral cup as also the course of the vascular tissue entering the gynophore ( $\times 12$ ). L-R.—T.s. of a young bud from base upward. For explanation see text. S.—T.s. of a younger bud showing sepals arising in regular order.

The five stamens have swollen papillose bases. The posterior ones are the longest (about 1 cm.) while the others gradually decrease in length towards the anterior side. The anthers are one-celled and bent downward forming a sort of hood through which the style protrudes out at maturity. Alternating with the stamens and forming an outer whorl are 3-5 staminodes which also have swollen papillose bases. The missing staminodes were always those of the posterior side.

The gynaecium is tri-carpellary, syncarpous and is borne on a small gynophore usually arising from the posterior wall of the floral cup. The place of origin of the gynophore is, however, not fixed. In some flowers it arises very close to the bottom of the floral cup while in others it separates at a comparatively higher level. The ovary is continued into a long hollow style which is narrowest in the basal region.

The gynophore, the ovary and the style are all covered with fine hairs which are seen even in the interior of the ovary. These are similar to the hairs borne on other parts of the flower. The myosin usually occurs in one or two hypodermal layers. Running along the whole length of the ovary there are three grooves, which according to the current view correspond in position to the mid-ribs of the three carpels (Fig. 4, K-L). The ovules are borne in two longitudinal rows on the placentae.

#### ORGANOGENY.

The younger flower bud is a small protuberance consisting of homogeneous cells and arising in the axil of a bract, large enough to cover it completely on the anterior side (Fig. 2, A). The floral organs arise in the usual, acropetal succession. The first sepal arises on the left side (Fig. 2, Q). Subsequently others also appear and by the time the primordia of the other organs can be made out the sepals have increased enough to overlap one another on the top (Fig. 2, B). Thus the period which elapses between the appearance of the first sepal and the primordia of the next whorl seems to be quite long.

The petals which are the next to arise are closely followed by staminodes and stamens (Fig. 2, C-E). It is curious that for a time the staminodes and the stamens grow quicker than the petals so that they protrude out of them. But later on the petals elongate more rapidly and finally cover the stamens on the top. Soon after, the central apical part of the axis becomes inactive and around it appears an annular outgrowth which forms the gynaecium (Fig. 2, F-G).

A young bud shows the typical hypogynous condition with the ovary in the centre and the other parts around it at a somewhat lower level (Fig. 2, H). The sepals are arranged spirally with a divergence of  $144^\circ$ , while petals and stamens show the cyclic arrangement.

When all the parts have differentiated, the peripheral region of the receptacle bearing sepals, petals and stamens undergoes rapid elongation and forms

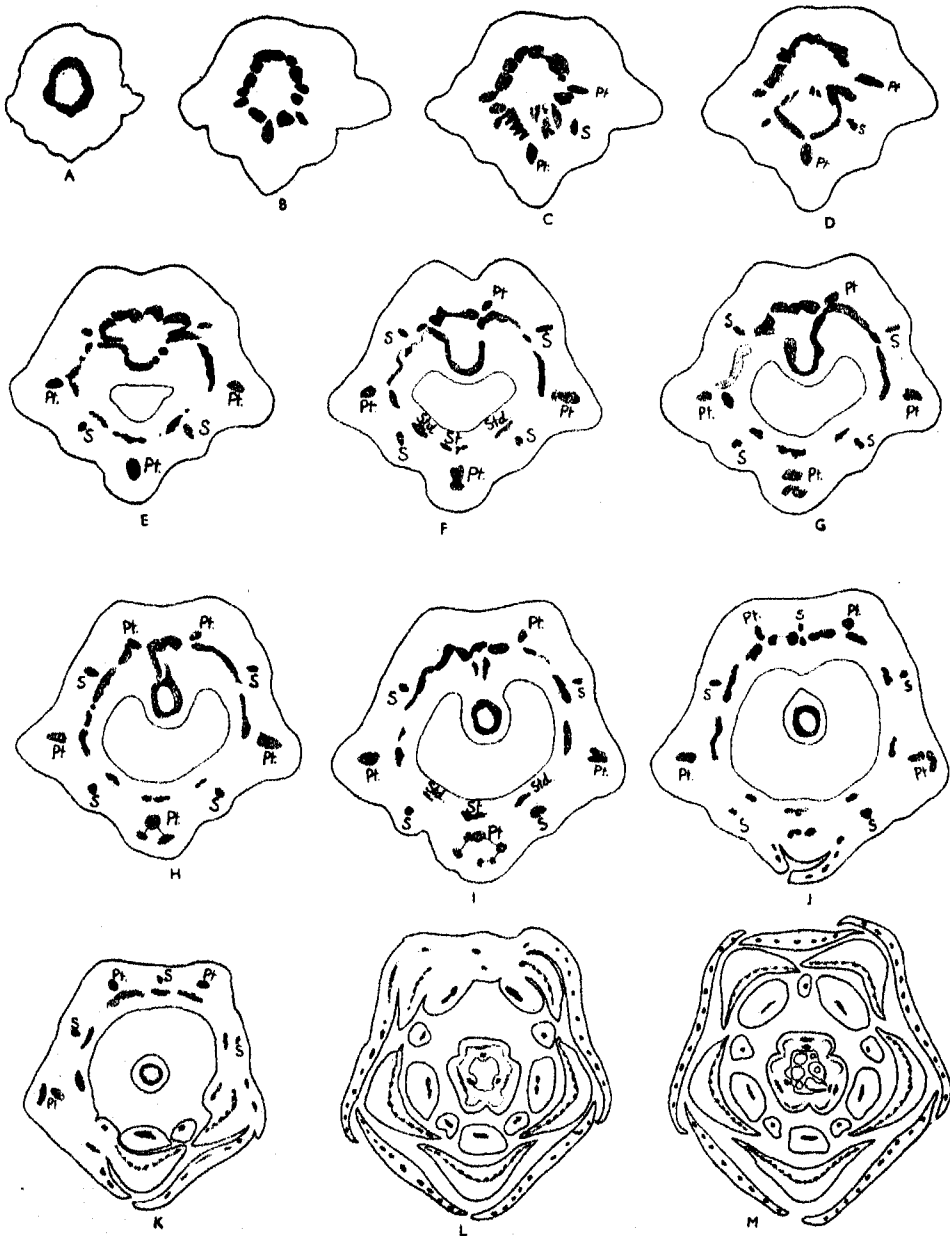


FIG. 3, A-J. ( $\times 18$ .) K-M. ( $\times 12$ .)

Serial microtome sections of a bud from base upward. For explanation see text.

a cup round the ovary. This elongation is, however, not uniform all round. On the posterior side it is more and this is probably responsible for carrying the ovary to a higher level along this side (Fig. 2, I-K). The effect of this unequal growth is noticeable even in so young a stage as shown in fig. 2, L-R, where the fourth sepal, occurring on the posterior side, separates after the fifth. While in younger buds, where the peripheral region of the receptacle has not undergone this growth, the five sepals arise in regular order (Fig. 2, S).

#### VASCULAR SUPPLY OF THE FLORAL ORGANS.

The pedicel of the flower contains an unbroken siphonostele (Fig. 3, A), which later on expands and begins to give out traces, first on the anterior side and then on the posterior. Bundles are given out on both the sepal and petal radii almost simultaneously (Fig. 3, B-E).

*Sepal.*—Every one of the sepals primarily receives three traces. The mid-rib bundle leaves a distinct gap in the stele, while the two marginal veins are derived from adjoining petal trunk cords (Pt.). Every one of the petal trunk cords splits up into three bundles, the central, destined to supply the petal and a marginal for a sepal on either side (Fig. 3, G-H). All these three bundles may be formed simultaneously or the trunk cord may first divide into an inner and an outer bundle and then the latter may again divide into two marginal veins. All the three sepal traces are approximately of an equal size and every one of them divides several times (Fig. 3, K-M). Towards the tip these bundles diminish in size and ultimately disappear.

Such a common origin for sepal marginals and petal mid-ribs is reported to be a very common feature in the Cruciferae (Arber, 1931) and in many other families (Saunders, 1934, and others).

*Petal.*—The petal trace whose origin has already been traced above, frequently tends to become concentric. Like the sepal traces it undergoes several divisions to form a continuous band of vascular tissue running through the whole breadth of the petal as seen in transverse section (Fig. 3, L-M). Higher up this band separates into smaller bundles which finally fade away.

*Stamen.*—Every one of the 3-5 antherless staminodes receives one trace given out on the sepal radius. The missing staminodes are often represented by stubs of vascular tissue which can be observed to come out for a short distance and then disappear. The stamens also receive one trace each. The staminal trace is usually more massive than that of a staminode and higher up it gives rise to several distinct groups of vascular elements, three being the commonest number.

Saunders' observations (1937) that in the Moringaceae the staminal bundles pass out conjoint with the perianth mid-ribs could not be confirmed by the writer.

*Gynaeceum.*—Though occurring usually on the posterior side of the cup, the gynaeceum receives its vascular supply from all sides. On the anterior side traces for sepals and petals are the first to be given out. They are followed

by those for the staminodes and the stamens. The remaining vascular tissue from this side runs more or less obliquely or in some cases horizontally across the centre to reach the posterior side to enter the gynophore. In some extreme cases it separates off from the staminal traces at a level higher than that of the origin of the floral cup. Naturally then it has to take a 'dip' to come out on the posterior side. It is for this reason that the stelar tissue on this side is cut twice in fig. 3, D.

The behaviour of the vascular tissue supplied to the gynophore from the posterior side is somewhat different. Although traces for sepals and petals are usually the first to be given out yet in some cases those for the gynæceum separate off first. This is evidently connected with the position of the ovary. If it is situated at a higher level the sepal and petal traces will pass out first but if it is lower down it will receive the first traces. Further it has been observed that the vascular tissue from this side does not directly enter the gynophore but goes up a little beyond the level of the latter and then bends downwards to pass into it (Figs. 2, K and 3, H-I).

A young bud presents, however, a comparatively simple appearance. Traces for sepals and petals arise almost simultaneously on all sides (Fig. 2, S). Traces for staminodes and stamens arise as usual. The remaining vascular tissue from all sides now passes in almost horizontally and forms a narrower ring for the gynophore in the centre (Fig. 2, H). The 'bending' in the course of the vascular tissue entering the gynophore seems, therefore, to be induced by further growth in the peripheral region of the receptacle (Fig. 2, I-K).

At the base of the gynophore there is a complete ring of vascular tissue (Fig. 4, B). A little higher up it becomes triangular in cross-section (Fig. 4, C) and then from each of the three angles two bundles begin to pass in (Fig. 4, D-E). The vascular triangle is thereby broken into three more or less straight bands of vascular tissue. The two bundles of each pair then swing apart in such a way that the adjacent two of adjacent pairs come to lie on the inner side of the corresponding band. Thus the bundles *a, b, d* approach *f, c, e* respectively and fuse in pairs to form inversely oriented bundles which give out traces to the ovules and remain quite distinct from the outer bundles (Fig. 4, E-H). As the bundles *a, b, c*, etc., proceed inward, they may be followed by some very small bundles which are of very short duration.

The vascular triangle is again completed. The gynophore now passes into the ovary and the connecting 'bridges' of the procambial tissue become invaginated, as it were, by the three grooves appearing on the outer side of the ovary (Fig. 4, I). Just opposite to each groove and somewhat on the inner side of each 'bridge' a very small bundle makes its appearance. It is very trivial in the region of the ovary, very often consisting of a single xylem element and a little phloem (Fig. 4, I-M, bundles X, Y & Z). But in the styler region it enlarges and finally becomes as prominent as other bundles.

Higher up in the ovary the vascular triangle again breaks up into separate bands which follow the contour of the ovary wall (Fig. 4, K-L). The bundles



$S_1$ ,  $S_2$  and  $S_3$  now decrease in size, while the three bundles supplying ovular traces become practically used up as the end of the ovary region is reached. If any traces of them are still left they approach the bundles on their outer

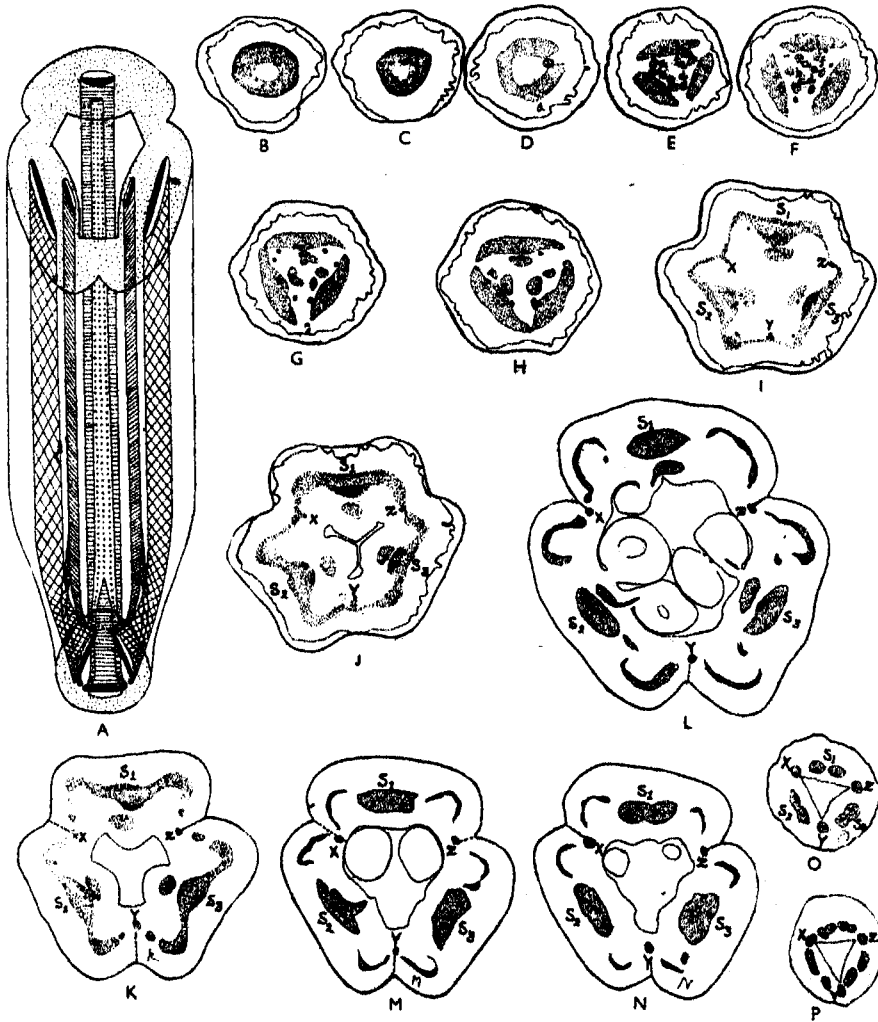


FIG. 4. A-P. ( $\times 26$ .)

A.—Diagrammatic representation of the ground-plan of *Moringa* ovary, with both ends out so as to face the observer. Every one of the placental bundles (smaller ones) is formed by the fusion of two marginal veins at the base. B-P.—T.s. of ovary from base upward. For explanation see text.

sides and ultimately fuse with them. This is clear not only from the concentric nature of the resulting bundles but also from the fact that some ovular traces may still be given out by these bundles (Fig. 4, M).

The base of the style contains six prominent bundles (Fig. 4, N). Of these,  $S_1$ ,  $S_2$  and  $S_3$  split up into two each (sometimes into three) by radial constrictions (Fig. 4, O-P). The daughter bundles thus formed continue up to 300-250 microns beneath the extreme tip. The remaining three bundles, X, Y and Z, continue undivided and disappear somewhat earlier than the other bundles.

**Ovule.**—The ovule is anatropous and bi-integumentary. To begin with it has a more or less circular outline in cross-section (Fig. 5, B), but after fertilization growth becomes more active at three equidistant places in the outer integument. This results in a triquetrous ovule which later on becomes three-winged.

A small procambial strand appears on the funicular side of the ovule at a stage long before fertilization. This runs along the inner region of the outer integument and may extend up to the chalazal end even at the two-nucleate stage of the embryo sac (Fig. 5, A). A transverse section of a young ovule,

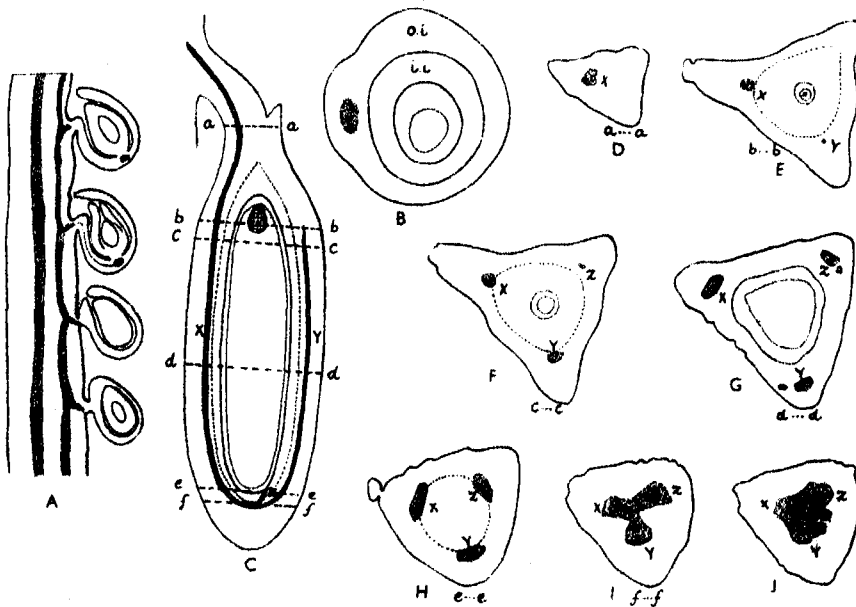


FIG. 5. A-J.

A.—Shows attachment of ovules to ovary wall: ovular traces have reached the chalazal end ( $\times 26$ ). B.—T.s. of a young ovule having only one bundle on the funicular side ( $\times 60$ ). C.—Diagrammatic representation of vascular plan of ovule. A single bundle (X) entering the ovule divides into two (Y & Z) at the chalazal end. D-J.—Serial microtome sections of an ovule cut approximately at levels marked in C. ( $\times 18$ .)

therefore, shows only a single vascular strand on one side (Fig. 5, B). At the mature embryo sac stage it splits up, in the chalazal region, into two daughter bundles, Y and Z (Fig. 5, C and I). These two branches elongate with age

and finally reach the micropylar end (Fig. 5, C). A transverse section at a later stage shows, therefore, three vascular bundles in the middle of the ovule (Fig. 5, F-H). Newman (1934) has also described a similar behaviour of the funicular bundle in *Acacia*.

For the sake of comparison I also cut some sections of *Moringa aptera* Gaertn. and *M. concanensis* Nimmo., only herbarium material of which was obtainable. The vascular ground-plan of both the species is almost identical with that of *M. oleifera*. Fig. 6, A-D shows the origin of various traces in

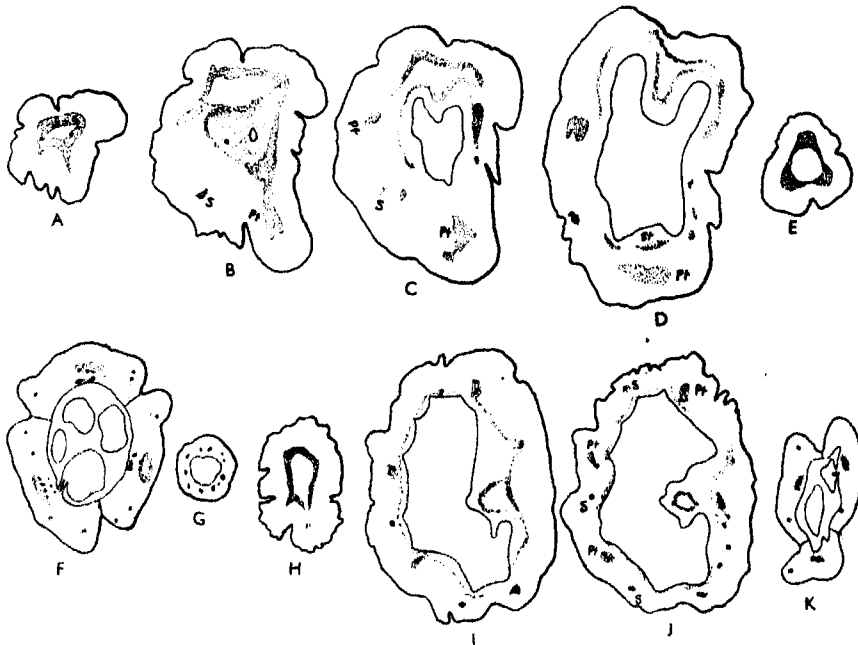


FIG. 6, A-K. ( $\times 26$ .)

A-D.—T.s. through base of a bud of *Moringa aptera*. Sepal mid-ribs and petal trunk cords pass out almost simultaneously on the anterior side. Petal trunk cords give off sepal marginals in the usual way. E.—Vascular triangle in the base of ovary. Mid-rib bundles differentiate at three angles. F.—Shows the inverted placental strands on the inner side of the mid-rib bundles. G.—A ring of vascular tissue in the style. H-J.—T.s. through the base of a bud of *M. concanensis*. Sepal mid-ribs and petal trunk cords arise as usual. K.—T.s. of ovary of the same. No placental bundles could be seen here but the attachment of an ovule on the inner side of mid-rib bundle indicates that they both lie on the same radius.

*M. aptera*. There is, however, a little difference in the arrangement of the vascular tissue in the basal part of the ovary. Just as in *M. oleifera*, the vascular tissue in the gynophore is arranged in the form of a triangle in transverse section (Fig. 6, E); but here the bundles corresponding to  $S_1$ ,  $S_2$  and  $S_3$  (see Fig. 4, L) differentiate at the three angles and not in the middle of the

sides. The course of the bundles corresponding to *a, b; c, d; and e, f* towards their ultimate positions could not be traced. The only thing noticeable is the occurrence of three inversely oriented bundles on the inner side of *S*<sub>1</sub>, *S*<sub>2</sub> and *S*<sub>3</sub> (Fig. 5, F). However, it seems quite evident that they arise in much the same manner as in *M. oleifera*. In the style the number of bundles varies from 9–12 (Fig. 6, G).

The material of *M. concanensis* proved to be even less satisfactory than that of *M. aptera*. For this reason the vascular supply of different parts could not be studied in detail; but enough has been observed to conclude that in broad outlines it corresponds to that of *M. oleifera* (Fig. 6, H–K).

#### DISCUSSION.

##### (i) Nature of the 'Floral-cup' and position of the gynæceum.

Although a misnomer, the term 'calyx-tube' is still retained by some taxonomists for the cup-shaped receptacle met with in the Rosaceae, Leguminosae, Moringaceae and many other families.

As a result of her studies on the floral anatomy of the Rosaceae, Jackson (1934) has concluded that in most of the genera having a superior ovary the floral-cup is appendicular and is formed by the fused basal portions of the sepals, petals and stamens. In *Rosa* itself only the upper part of the cup is appendicular while the lower is axial. She presumes that in course of phylogeny an invagination of the terminal portion of the floral axis has taken place here with the result that the carpels have come to be situated at a lower level than the other organs of the flower.

The condition in *Moringa oleifera* is very much similar to that in *Rosa*. On the posterior side, where the wall of the cup is higher than on the other side, the lower portion of the cup is traversed by stelar bundles which give out traces to the various floral organs at a somewhat higher level. Naturally, therefore, this portion of the cup on the posterior side has to be regarded as receptacular. On the anterior side, though the vascular traces for different whorls are usually cut off even before the level of the cup is reached, it cannot be argued that immediately after their detachment from the stele they begin to run in the tissue of the organs they have to supply. For some distance at least they must pass through the tissue of the receptacle. Finally the receptacular tissue passes insensibly into sepals, petals and stamens whose bases fuse together to form the rim of the cup.

In determining the position of an organ considerable significance has been attached to the 'down-turning' in the course of the vascular tissue entering it. Thus Bechtel (1921) reported that the ovular trace in *Boehmeria* (Urticaceae) does not pass out directly into the ovule but ascends the ovary wall for a short distance and then turns abruptly down and descends to the base of the ovule. This unusual behaviour of the vascular trace was interpreted by him

to indicate that the ovule, which is basal now, has descended from an originally lateral position in the course of evolution. The ovule itself does not give any clue into its past history but the vascular bundle has slightly lagged behind, as it were, in the race of evolution and is believed to give evidence of the former high position once occupied by its recipient, the ovule, by first going up and then bending down!

Jackson (1934) has also observed such a down-turning in the course of the vascular traces entering the carpels in certain Rosaceae and she also interprets this as the natural outcome of the descending down of the ovaries from higher positions.

This also appears to be the most logical and plausible interpretation of the down-turning in *Moringa* and the present-day position of the gynæceum in this species is, therefore, a derived one.

#### (ii) Nature of the Carpels.

(a) *The Current View*.—The gynæceum in the Moringaceae is usually believed to be composed of three valve carpels fusing by their margins. The mid-ribs of the carpels are believed to correspond in position to the three longitudinal grooves running in the wall of the ovary and the swollen placental regions are interpreted as the fused margins of the adjacent carpels. The bundles X, Y and Z (Fig. 4, L) are the dorsals while the two bundles with opposite orientation in the placental region have to be regarded as branches of the same placental strand. This view is represented diagrammatically in fig. 7, A.

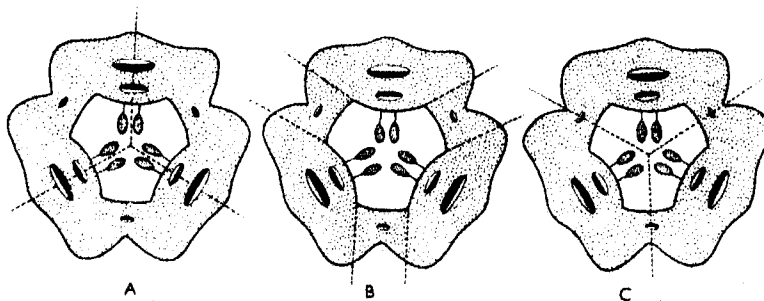


FIG. 7, A-C.

Diagrammatic representation of the various interpretations of the *Moringa* gynæceum. Dotted lines in A, B and C respectively delimit the carpels according to *Current view*, *Saunders' view* and the *Author's view*.

Such an interpretation is, however, not supported either by the external morphology of the gynæceum or by its vascular supply. There are, of course, only three carpels but their nature and limits have to be differently interpreted.

The point upon which the acceptance or the non-acceptance of this current view mainly depends is the determination of the nature of the two bundles

in the placental region. As mentioned above, these have so far been regarded as branches of the same placental strand<sup>1</sup>. There is, however, no reason to support such a presumption; for, none of them is a branch of the other, each arising quite independently from the stelar tissue (see Fig. 4, E-1). If this is so, the next question that arises is: 'which of them is the placental bundle?'. It is well known that the latter is usually formed by the fusion of two marginal bundles and that this alone supplies traces to the ovules. Further, it often disappears beyond the region of the ovules. Out of the two bundles in the placental region it is only the inner one which fulfils all these conditions and, therefore, it is this that should be regarded as the placental strand. In other words this means that the bundles *a, b*; *c, d*; and *e, f* (Fig. 4, E) should be interpreted as marginal bundles.

This, the most logical and reasonable interpretation of the nature of these bundles, leads us, nevertheless, to certain difficulties which are obviously unsurmountable on the basis of the current view.

In all cases of the usual type of parietal placentation the marginal bundles of the adjacent carpels fuse into normally oriented placental strands which occur alternately with the mid-ribs but in the same ring. In *Moringa*, on the other hand, the bundles supplying the ovules are always inversely oriented and always lie on the inner side of other bundles which will presently be shown to be mid-rib bundles. Such a behaviour on their part cannot be satisfactorily explained by the supporters of the current view.

Again, according to this view the bundles *a, b* and similarly *c, d* and *e, f* (Fig. 4, E) have to be regarded as marginal bundles of the same carpel; for then alone the placental strands would be formed by marginals coming from two different carpels, as the current view demands. It is difficult to imagine how in such open carpels as are believed to be present in *Moringa*, the marginal bundles of the same carpel could arise from the same gap when ordinarily they leave quite different gaps, one on either side of the mid-rib.

The last but not the least important is the interpretation of the bundles *S*<sub>1</sub>, *S*<sub>2</sub> and *S*<sub>3</sub>, which occur on the outer side of the placental strands. They are undoubtedly the most prominent bundles. It has already been pointed out that they cannot be regarded as branches of the placental strand and no other suitable interpretation of them can be offered on the basis of the current view.

(b) *Saunders' View*.—Saunders (1937) holds that there are six carpels in the Moringaceae, three being 'semi-solid' and fertile and three 'solid' sterile (Fig. 7, B). The expanded placental regions are interpreted as the 'semi-solid' carpels and the vascular bundles *X, Y* and *Z* (Fig. 4, K) with the surrounding tissue are regarded as constituting the 'solid' sterile carpels.

---

<sup>1</sup> This is how such bundles have been explained by the supporters of the bi-carpellary theory of the Crucifer gynaeceum (see Arber, 1931 and 1937).

In the first place my conception of a carpel is fundamentally different from that of Miss Saunders. I cannot regard it as axiomatic that every bundle represents a carpel. On the other hand, I believe that a carpel is primarily a 'three-traced organ'. Besides, I have shown that the bundles, X, Y and Z, are too insignificant at the place of their origin to be given the status of mid-rib bundles. As will be shown later, they are best interpreted as secondary marginal bundles.

(c) *Author's View*.—It is a well known fact that in ovaries with axile placentation the marginal bundles of the same carpel fuse together to form the placental strand which occurs in the central column of the ovary with its xylem directed outwards (i.e. inversely oriented with reference to the dorsal bundle). Such an orientation and position of the placental strand with respect to the mid-rib bundle are characteristic features of the closed carpels, where the margins of the same carpel fuse together to enclose a loculus.

A closer examination of the vascular supply of the *Moringa* gynæceum reveals clearly that exactly similar conditions are obtained here. The bundles  $S_1$ ,  $S_2$  and  $S_3$  are the mid-rib bundles while  $a, f$ ;  $b, c$  and  $d, e$  are the marginals of the three carpels. The two margins of the same carpel fuse together and form an inversely oriented placental strand on the inner side of the mid-rib bundle. As stated above, such a relation between the placental strands and the mid-rib bundles constitutes a sound basis for regarding the carpels in *Moringa* as of the closed type. The realisation of such a condition has been rendered somewhat difficult by the so-called solidification of the carpels resulting in the extrusion of the ovules and complete elimination of the loculus.

According to such an interpretation the nature of the remaining three bundles, X, Y and Z, can also be satisfactorily explained. They can easily be regarded as the fusion products of the secondary marginal veins, given off after the passing in of the first marginal veins to form the placental strands. Their fusion has gone down so 'deep' that separate components can no longer be distinguished now.

Thus, on this view, which is diagrammatically represented in fig. 7, C, the behaviour and nature of all the bundles seen in the base of the ovary can be satisfactorily explained. It is to be noted, therefore, that the Moringaceae is peculiar in having all the three carpels of the solid type while in the Cruciferae the solid carpels alternate with the sterile valves.

### (iii) *Solidification of the Carpels and extrusion of the Ovules.*

Fig. 8, A-H is intended to show the probable way in which solidification of the carpels in *Moringa* may have taken place. The main factor which appears to have been responsible for solidification is perhaps the swelling of the mid-rib, which encroached upon the loculus and reduced the space therein to such an extent that the ovules were forced out through the opened margins into the central cavity (Fig. 8, E). Later on the margins fused together and closed

the loculus whose cavity became further reduced and finally disappeared completely (Fig. 8, F-H). The ovules are thus extra-carpellary in the sense

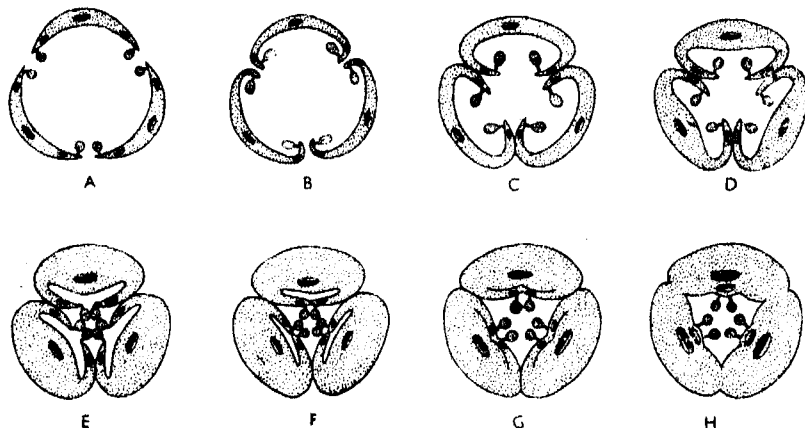


FIG. 8, A-H.

Theoretical diagrams to show the probable way in which the *Moringa* gynaeceum may have evolved from an ancestor with three valve carpels.

that they do not lie inside the loculus of the carpel which bears them. Eames and Wilson (1930) have already drawn attention to the extra-carpellary nature of the ovules in the Cruciferae. But they have suggested a different mode of extrusion of the ovules there (see Puri, 1941b).

Early stages in the process of solidification, as outlined above, are evidenced to a certain extent in *Reseda luteola*, a member of a closely related family, the Resedaceae. In this species the gynaeceum consists of three carpels which are fused below but free in the upper region. The margins of each of the carpels swing in and approach one another, much in the same way as shown in fig. 8, B-D. But they do not fuse, so that the loculus still opens on the inner side. Here, the only thing to be desired to make an approach to the gynaeceum of *Moringa* is the reduction in the size of the loculus to the extent at which the ovules may be expelled into the common central cavity.

Dickson (1934) and Arber (1938) have actually observed such an expulsion of the ovules in *Platystemon californicus*, a member of the Papaveraceae. The ovary here is polycarpellary and each carpel has a loculus of its own, opening into a common central cavity. Both these authors report that in some cases, owing to lack of enough space in the loculus, some of the ovules were seen pushed out into the central cavity (cf. Fig. 8, E).

In view of these cases it should not be at all surprising that ancestors of *Moringa* gynaeceum had such a tendency to expel their ovules into the common central cavity. When once the loculi became empty their complete elimination would be a logical consequence. The disappearance of the loculus, or in other words, the solidification of the carpels in such cases need not be



materially different from that of those which have lost their ovules altogether. Woodson and Moore (1938) have described an interesting series of stages of the solidification of sterile carpels in *Pleiocarpa mutica*. In one of the three flowers examined by them the ovary was found to be composed of four fertile carpels each having a loculus of its own. In the second flower there were only two fertile carpels, the third carpel had a loculus but no ovule and the fourth had lost even its loculus and become solid. In the third case again, there were only two fertile carpels while the other two had become solid carpellobes.

Cases of such solidification are frequently seen in the styler region. In *Platystemon californicus*, for instance, the margins of each carpel fuse together to enclose a loculus which, a little higher up, disappears completely leaving what may be called solid styles. Arber (1937) has also reported similar cases of solid styles in *Hypericum hirsutum*. And then a little search into the literature will reveal many more cases of this type. But it is not the purpose here to cite all the literature on the subject. What is more important for me is to illustrate the practicability of the scheme of solidification suggested here. That purpose, it is hoped, is served by the few cases cited above.

#### (iv) *Placentation.*

In accordance with the view suggested here, we have in *Moringa* three closed and solid carpels and the margins of every one of them have fused together to bear a placenta having extra-carpellary ovules.

This mode of placentation is to be clearly distinguished from parietal and axile placentations. In the former case each placenta is formed at the point of fusion of the two adjacent margins of two carpels and ovules lie in the common central cavity. Thus each placenta is formed by contributions of two different carpels. In axile placentation ovules are borne on the fused margins of the same carpel and they lie within the loculus of that very carpel. But in the case under discussion the placenta is formed by the margins of one carpel and not by  $\frac{1}{2} + \frac{1}{2}$  carpels as in parietal placentation and yet the ovules are contained in the common central cavity.

As this condition appears to be quite common in the Rhocadales (Eames and Wilson 1928; Puri, 1941b) it is desirable that it should be given a definite name. For this purpose I venture to suggest the 'extra-carpellary' placentation.

The presence of this new type of placentation demands a more restricted use of the term 'loculus'. So far it has been used for any cavity or 'chamber' containing ovules. The carpels in *Moringa*, as also the solidified ones in the Crucifers and Capparids (Eames and Wilson, 1928) have lost their loculi and yet the term is retained in the description of ovary, which is unfortunate. It is, therefore, necessary to suggest that the term 'loculus' should be applied only to the cavity enclosed by a single carpel as in axile placentation. The cavity enclosed by more than one carpel, as is the case in parietal and 'extra-carpellary' placentations, may be described as 'ovarian chamber'.

(v) *Systematic position of the Moringaceae.*

From the introductory paragraph of the paper it is evident that the systematic position of the Moringaceae up till recently was doubtful. Of late systematists have agreed to place it in the Order Rhœadales. It is to be seen whether or not the present study strengthens its inclusion in the order.

One fact which emerges out most clearly from the present study is that the carpels in the Moringaceae are not of the usual type. They are all solid in the sense that after having pushed their ovules into the common central cavity or 'ovarian chamber' they have lost their loculi completely. Nevertheless, this difference is not of kind but of degree. The solid carpel is still a three-traced organ like so many carpels of the ordinary type.

Such a specialization of the carpels is indeed a very important feature. It is so far very rare, having been reported only in the Order Rhœadales (Bancroft, 1935), specially in the Cruciferae and Capparidaceae (Eames and Wilson, 1928, 1930). Its occurrence in the Moringaceae furnishes additional corroborative evidence for the inclusion of this family in the Rhœadales. The position of the family within the Order will be discussed in a later paper of the series.

SUMMARY.

The different floral whorls arise in the usual acropetal succession.

The 'floral-cup' is believed to be receptacular at the base and appendicular at the top and the 'down-turning' in the course of the vascular tissue entering the gynophore is interpreted to indicate that the gynoecium has descended from an originally high position.

The gynoecium consists of three carpels which are shown to be fertile and solid in the sense that they have lost their loculi by reduction. The grooves in the ovary wall which have so far been regarded as corresponding to the mid-ribs of the carpels are shown here to mark the limits between the adjacent carpels. The evidence, upon which such a conclusion is based, rests mainly upon the vascular ground-plan in the base of the ovary.

The ovules are extra-carpellary in the sense that they lie outside the loculus of the carpel which bears them. They are believed to have extruded long before the margins of the carpels fused together to close the loculus.

The peculiar type of placentation is described as 'extra-carpellary' and the term 'loculus' is suggested to be used only for the cavity enclosed by a single carpel. For the central cavity enclosed by more than one carpel the term 'ovarian chamber' is suggested.

The inclusion of the family Moringaceae in the Order Rhœadales is further strengthened.

I take this opportunity of offering my sincere thanks to Dr. P. Maheshwari for his helpful criticism. I am also grateful to Professor A. J. Eames of Cornell University for examining some of my slides and confirming my observations. To Miss E. R. Saunders I am indebted for some useful suggestions. Although

my interpretations differ from her, she has very kindly confirmed most of my observations in a general way.

#### LITERATURE CITED.

- Arber, A. (1931)—Studies in floral morphology. I. On some structural features of the cruciferous flower. *New Phyt.*, 30 : 11–41.
- Arber, A. (1937)—The interpretation of the flower: A study of some aspects of morphological thought. *Biol. Rev.*, 12 : 157–184.
- Arber, A. (1938)—Studies in flower structure. IV. On the gynæceum of *Papaver* and related genera. *Ann. Bot.*, N.S. 2 : 649–664.
- Bancroft, H. (1935)—A review of researches concerning floral morphology. *Bot. Rev.*, 1 : 77–99.
- Bechtel, A. R. (1921)—The floral anatomy of the Urticales. *Amer. Jour. Bot.*, 8 : 386–410.
- Bentham, G. and Hooker, J. D. (1862)—*Genera Plantarum*, Vol. 1.
- Dickson, J. (1934)—Studies in floral anatomy. II. The floral anatomy of *Glaucium flavum* with reference to other members of the Papaveraceae. *Proc. Linn. Soc.*, 1 : 175–224.
- Eames, A. J. and Wilson, C. L. (1928)—Carpel morphology in the Cruciferae. *Amer. Jour. Bot.*, 15 : 251–270.
- Eames, A. J. and Wilson, C. L. (1930)—Crucifer carpels. *Amer. Jour. Bot.*, 17 : 638–656.
- Harms, H. (1936)—Engler-Prantl—Die natürliche Pflanzenfamilien. 17b. Leipzig.
- Hutchinson, J. (1926)—Families of Flowering Plants. I. Dicotyledons. London.
- Jackson, Gema (1934)—The morphology of the flower of *Rosa* and certain closely related genera. *Amer. Jour. Bot.*, 21 : 453–466.
- Newman, I. V. (1934)—Studies in the Australian Acacias. IV. The life-history of *Acacia baileyana* F.V.M. Part 2. *Proc. Linn. Soc. N.S.W.*, 59 : 277–313.
- Puri, V. (1941a)—Life-history of *Moringa oleifera* Lamk. *Jour. Ind. Bot. Soc.*, 20 : 263–284.
- Puri, V. (1941b)—Studies in floral anatomy. I. Gynæceum constitution in the Cruciferae. *Proc. Ind. Acad. Sci.*, 14 : 166–187.
- Saunders, E. R. (1934)—On carpel polymorphism. VI. *Ann. Bot.*, 48 : 645–692.
- Saunders, E. R. (1937)—*Floral Morphology*. Cambridge.
- Solereder, H. (1908)—*Systematic Anatomy of Dicotyledons* (Eng. Trans.).
- Wettstein, R. (1924/1935)—*Handbuch der systematischen Botanik*. 3 & 4 Aufl. Wien u. Leipzig.
- Woodson, R. E. (Jr.) and Moore J. A. (1938)—The vascular anatomy and comparative morphology of apocynaceous flowers. *Bull. Torrey Bot. Club*, 65 : 135–166.

#### POSTSCRIPT.

When this paper was in press I found out on re-examination of my slides that the bundles X, Y and Z (Fig. 4) arise almost simultaneously with the bundles a, b, c, d, e and f; but due to their very insignificant size they were overlooked in sections below the one drawn in fig. 4, I.

# THE RELATION OF GAS PRESSURE TO RADIATION PRESSURE IN A BOSE-EINSTEIN GAS.

By B. N. SINGH and A. G. CHOWDBI, *University of Delhi.*

(Communicated by Dr. D. S. Kothari.)

(Read January 1, 1942.)

The thermodynamical properties of Bose-Einstein gas have been discussed by several authors. In this paper we shall examine the ratio of black-body radiation pressure to gas pressure for an assembly of Bose-Einstein particles at temperature  $T$ . The gas pressure is given by

$$p = nkT \left( 1 - \frac{A_1}{2^{s+1}} - \dots \right) \quad \dots \quad \dots \quad (1)$$

in the non-degenerate case; and by

$$p = \Gamma(s) C (kT)^{s+1} \zeta(s+1) \quad \dots \quad \dots \quad (2)$$

in the degenerate case, where  $n$  is the number of particles per unit volume,  $k$  is the Boltzman's constant and  $T$  the absolute temperature. Further, in the non-relativistic case

$$C = \frac{2\pi g(2m)^{\frac{3}{2}}}{h^3}, \quad s = \frac{3}{2} \quad \text{and} \quad A_1 = A_0 = \frac{n h^3}{g(2\pi m k T)^{\frac{3}{2}}},$$

and in the relativistic case

$$C = \frac{4\pi g}{c^3 h^3}, \quad s = 3 \quad \text{and} \quad A_1 = A_0 = \left( \frac{ch}{kT} \right)^3 \frac{n}{8\pi g}.$$

$\zeta(s)$  is the Riemann zeta function defined by

$$\zeta(s) = \sum_{n=1}^{n=\infty} \frac{1}{n^s}.$$

In the non-relativistic case the average energy per particle is much smaller than its rest mass energy and in the relativistic case it is the opposite.  $A_0$  and  $A_0^R$  are the degeneracy discriminants in the non-relativistic and relativistic cases respectively. When  $A_0$  is less than  $\zeta(\frac{3}{2})$  the gas is non-degenerate and degeneracy sets in when  $A_0$  is greater than  $\zeta(\frac{3}{2}) = 2.612$ . For the relativistic case the critical value of  $A_0$  is  $\zeta(3) = 1.202$ .

The black-body radiation pressure in the system will be

$$p_r = \frac{1}{3} a T^4 \quad \dots \quad (3)$$

• where 
$$a = \frac{8\pi^5}{15} \frac{k^4}{c^3 h^3}.$$

We shall now derive expressions for  $\delta$  the ratio of the gas pressure to radiation pressure for the different cases. The physical meaning is discussed later. As usual this includes two sub-cases, viz.: (1) the non-relativistic case, and (2) the relativistic case.

*Case 1.* Non-relativistic non-degenerate case.

$$\left( y = \frac{mc^2}{kT} \gg 1, A_0 \ll 1 \right)$$

In this case we have from equations (1) and (3) by giving  $s$  the value  $\frac{3}{2}$ ,

$$\delta = \frac{45}{2^{\frac{3}{2}} \pi^{\frac{1}{2}}} \left( \frac{mc^2}{kT} \right)^{\frac{3}{2}} A_0 \quad \dots \quad (4)$$

*Case 2.* Relativistic non-degenerate case ( $y \ll 1, A_0 \ll 1$ ). We obtain as before from equations (1) and (3) giving  $s$  the value 3,

$$\delta = \frac{45}{\pi^{\frac{1}{2}}} A_0^R \quad \dots \quad (5)$$

*Degenerate case* ( $A_1 \gg \zeta(s)$ ).

In the degenerate case  $\delta$  is determined in a similar way. From equations (2) and (3) we have for the non-relativistic case ( $s = \frac{3}{2}$ ),

$$\delta = \frac{45g}{2^{\frac{3}{2}} \pi^{\frac{1}{2}}} \left( \frac{mc^2}{kT} \right)^{\frac{3}{2}} \zeta\left(\frac{3}{2}\right) \quad \dots \quad (6)$$

and in the relativistic case ( $s = 3$ ) we get

$$\delta = 1 \quad \dots \quad (7)$$

The variation of  $\delta$  in the various cases is best represented graphically. In figure 1 the abscissa represents  $\log A_1$ , and the ordinate  $\log y$ . On the upper side of the line  $RR$  the abscissa scale is for  $\log A_0$  and on the lower side for  $\log A_0^R$ . The continuous curves are the curves along which  $\delta$  remains constant and its value is noted on the curves. The space above the line  $RR$  ( $\log y = 0$ ) denotes the non-relativistic region and below it the relativistic region. The broken line  $D_1D_1$  divides the degenerate region from the non-degenerate region. The degenerate region is to the right of the line. Similarly, the broken line  $D_2D_2$  ( $\log A_0^R = \zeta(3)$ ) divides the non-degenerate from degenerate region in the relativistic part of the diagram. It will be seen that  $D_1D_1$  and  $D_2D_2$  are almost in a line.

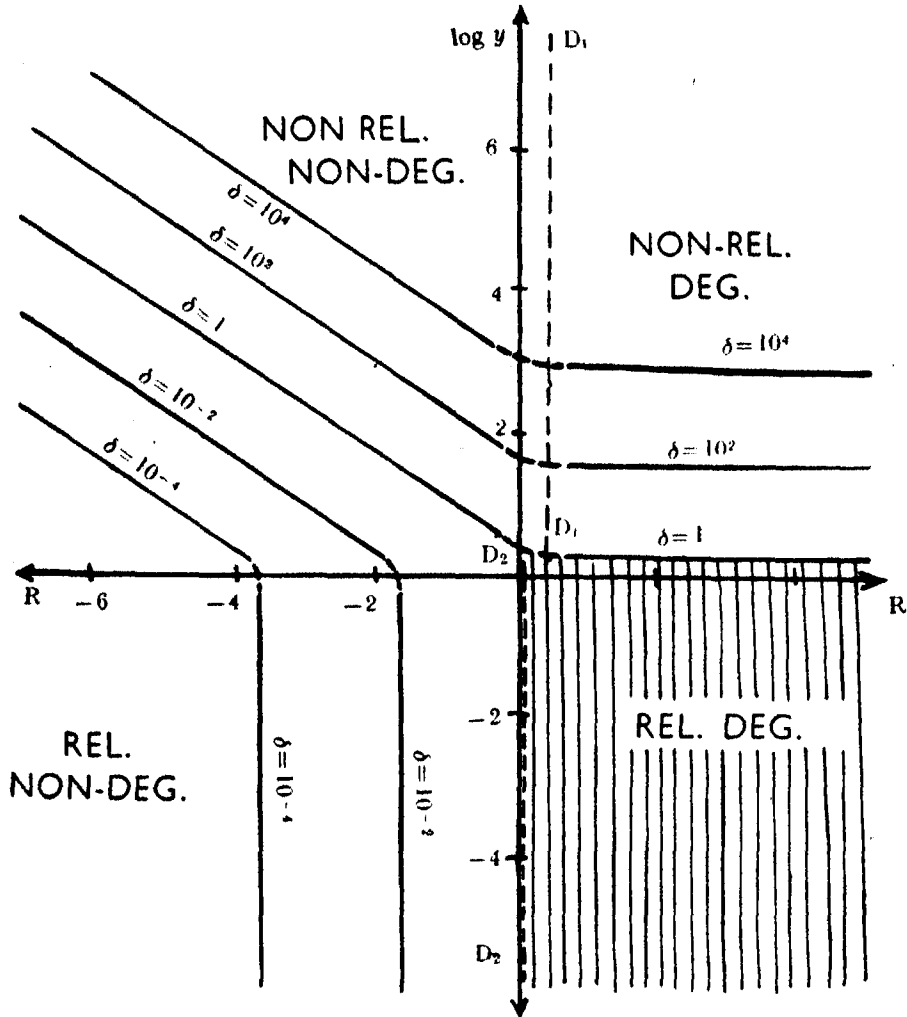


FIG. 1. Showing the variation of the ratio  $\delta$  of the gas pressure to radiation pressure. The ordinate represents  $\log y$  ( $y = \frac{mc^2}{kT}$ ) and the abscissa  $\log A_0$  and  $\log A_0^H$  for the spaces above and below the line  $RR$  respectively. Thus each of the usual four sub-cases occupy almost a quadrant, viz.,

- the non-relativistic degenerate case in the first quadrant;
- the non-relativistic non-degenerate case in the second quadrant;
- the relativistic non-degenerate case in the third quadrant;
- and the relativistic degenerate case in the fourth quadrant (where  $\delta = 1$ ).

It is clear from the figure that in the *relativistic* case gas pressure is smaller than the radiation pressure, and they become equal to each other in degeneracy. This region where the two pressures are equal is shown shaded in the figure.

In the non-relativistic case, the gas pressure is always greater than radiation pressure in degeneracy, but can be greater or smaller in non-degeneracy.

It follows, therefore, that when  $\delta < 1$  the gas is necessarily non-degenerate but the converse is not true, that is, in a non-degenerate gas  $\delta$  may be less than, equal to, or greater than, unity. When the gas is degenerate  $\delta$  is greater than unity in the non-relativistic case, but is equal to unity in the relativistic case. These results are similar to those obtained in Fermi-Dirac Statistics but with the difference that the ratio of gas pressure to the radiation pressure becomes equal to unity in the relativistic degenerate case for Bose-Einstein gas, whereas in the Fermi-Dirac degenerate gas  $\delta$  is always greater than unity. This is to be expected since the radiation itself behaves as a relativistic degenerate Bose-Einstein gas.

Our thanks are due to Dr. D. S. Kothari for his kind interest in this work.

# PROPERTIES OF A CONFLUENT HYPER-GEOMETRIC FUNCTION.

By B. MOHAN, Benares Hindu University.

(Communicated by Prof. V. V. Narlikar.)

(Read January 1, 1942.)

1. In a recent paper \* I have studied the properties of the function

$$f_{\nu}(x) = \sum_0^{\infty} \frac{(-1)^{\gamma} x^{\nu+2\gamma}}{2^{\nu+2\gamma} \Gamma(\nu+\gamma+1)}.$$

This has led me to study, in this note, the properties of the analogous function

$$g_{\nu}(x) = \sum_0^{\infty} \frac{x^{\nu+2\gamma}}{2^{\nu+2\gamma} \Gamma(\nu+\gamma+1)}. \quad \dots \quad (1.1)$$

To begin with, the series (1.1) is absolutely and uniformly convergent in any finite interval of values of  $x$ . It is also obvious that

$$g_0(x) = e^{\frac{1}{2}x^2} \quad \dots \quad (1.2)$$

$$g_{\nu}(x) = \frac{\left(\frac{1}{2}x\right)^{\nu}}{\Gamma(\nu+1)} {}_1F_1\left(1; \nu+1; \frac{1}{4}x^2\right) \quad R(\nu) > -1. \quad \dots \quad (1.3)$$

2. Differentiating (1.1) with respect to  $x$  we have

$$\begin{aligned} g_{\nu}'(x) &= \sum_0^{\infty} \frac{(\nu+2\gamma)x^{\nu+2\gamma-1}}{2^{\nu+2\gamma} \Gamma(\nu+\gamma+1)} \\ &= \sum_0^{\infty} \frac{(2\nu+2\gamma)x^{\nu+2\gamma-1}}{2^{\nu+2\gamma} \Gamma(\nu+\gamma+1)} - \nu \sum_0^{\infty} \frac{x^{\nu+2\gamma-1}}{2^{\nu+2\gamma} \Gamma(\nu+\gamma+1)} \\ &= \sum_0^{\infty} \frac{x^{\nu+2\gamma-1}}{2^{\nu+2\gamma-1} \Gamma(\nu+\gamma)} - \frac{\nu}{x} \sum_0^{\infty} \frac{x^{\nu+2\gamma}}{2^{\nu+2\gamma} \Gamma(\nu+\gamma+1)}. \end{aligned}$$

It follows that

$$g_{\nu}'(x) = g_{\nu-1}(x) - \frac{\nu}{x} g_{\nu}(x).$$

---

\* 'A Confluent Hyper-geometric Function.'—*Proc. Nat. Inst. Sci. India*, VII, 177-82, (1941).



$$\begin{aligned}
\text{Again, } & \left(\frac{x}{2} + \frac{\nu}{x}\right) g_\nu(x) \\
&= \left(\frac{x}{2} + \frac{\nu}{x}\right) \sum_0^\infty \frac{x^{\nu+2\gamma}}{2^{\nu+2\gamma} \Gamma(\nu+\gamma+1)} \\
&= \sum_0^\infty \frac{x^{\nu+2\gamma+1}}{2^{\nu+2\gamma+1} \Gamma(\nu+\gamma+1)} + \nu \sum_0^\infty \frac{x^{\nu+2\gamma-1}}{2^{\nu+2\gamma} \Gamma(\nu+\gamma+1)} \\
&= \sum_0^\infty \frac{x^{\nu+2\gamma+1}}{2^{\nu+2\gamma+1} \Gamma(\nu+\gamma+1)} + \sum_0^\infty \frac{(\nu+2\gamma)x^{\nu+2\gamma-1}}{2^{\nu+2\gamma} \Gamma(\nu+\gamma+1)} \\
&\quad - \sum_1^\infty \frac{px^{\nu+2p-1}}{2^{\nu+2p-1} \Gamma(\nu+p+1)} \\
&= g'_\nu(x) + \sum_0^\infty \frac{x^{\nu+2\gamma+1}}{2^{\nu+2\gamma+1} \Gamma(\nu+\gamma+1)} - \sum_0^\infty \frac{(\gamma+1)x^{\nu+2\gamma+1}}{2^{\nu+2\gamma+1} \Gamma(\nu+\gamma+2)} \\
&= g'_\nu(x) + \sum_0^\infty \frac{x^{\nu+2\gamma+1}}{2^{\nu+2\gamma+1} \Gamma(\nu+\gamma+1)} \left(1 - \frac{\gamma+1}{\nu+\gamma+1}\right).
\end{aligned}$$

Thus, we have

$$\left(\frac{x}{2} + \frac{\nu}{x}\right) g_\nu(x) = \nu g_{\nu+1}(x) + g'_\nu(x). \quad \dots \quad (2.2)$$

As a particular case,

$$g_0'(x) = \frac{1}{2} x g_0(x). \quad \dots \quad (2.3)$$

Now, from (2.1) we have

$$g_\nu'' = g'_{\nu-1} - \frac{\nu}{x} g_\nu' + \frac{\nu}{x^2} g_\nu.$$

Also, from (2.2) we have

$$\left(\frac{x}{2} + \frac{\nu-1}{x}\right) g_{\nu-1} = g'_{\nu-1} + (\nu-1) g_\nu.$$

$\therefore$  Subtracting, we have

$$g_\nu'' - \left(\frac{x}{2} + \frac{\nu-1}{x}\right) g_{\nu-1} = -\frac{\nu}{x} g_\nu' + \left(\frac{\nu}{x^2} - \nu + 1\right) g_\nu.$$

That is,

$$g_\nu'' - \left(\frac{x}{2} + \frac{\nu-1}{x}\right) (g_\nu' + \frac{\nu}{x} g_\nu) + \frac{\nu}{x} g_\nu' + \left(\nu - 1 - \frac{\nu}{x^2}\right) g_\nu = 0,$$

on using (2.1). Thus, we get

$$g_\nu'' + \left(\frac{1}{x} - \frac{x}{2}\right) g_\nu' + \left(\frac{1}{2} \nu - 1 - \frac{\nu^2}{x^2}\right) g_\nu = 0. \quad \dots \quad (2.4)$$

This result could also be arrived at by starting with (1.3) and making use of the differential equation satisfied by the function  ${}_1F_1$ .

Other results that can be easily derived from the above formulae are:

$$\left(\frac{x^2}{2\nu} + 1\right) g_{\nu-1} - \left(\frac{x^2}{2\nu} + 2\right) g_{\nu}' = \nu g_{\nu+1} \quad \dots \quad (2.5)$$

$$\left(\frac{x}{2} + \frac{2\nu}{x}\right) g_{\nu} - g_{\nu-1} = \nu g_{\nu+1} \quad \dots \quad (2.6)$$

$$g_{\nu}'' = g_{\nu-2} - \frac{2\nu-1}{x} g_{\nu-1} + \frac{\nu(\nu+1)}{x^2} g_{\nu} \quad \dots \quad (2.7)$$

$$\left(\frac{d}{x dx}\right)^m (x^{\nu} g_{\nu}) = x^{\nu-m} g_{\nu-m}, \quad \dots \quad (2.8)$$

where  $m$  is a +ve integer.

$$\frac{d}{x dx} (x^{-\nu} g_{\nu}) = \frac{1}{2} x^{-\nu} g_{\nu} - \nu x^{-\nu-1} g_{\nu+1},$$

$$\left(\frac{d}{x dx}\right)^2 (x^{-\nu} g_{\nu}) = \frac{1}{4} x^{-\nu} g_{\nu} - \nu x^{-\nu-1} g_{\nu+1} + \nu(\nu+1) x^{-\nu-2} g_{\nu+2}.$$

$$\begin{aligned} 3. \quad g_{\nu}(x) &= \sum_0^{\infty} \frac{\left(\frac{1}{2}x\right)^{\nu}}{\Gamma(\nu) |\underline{\gamma}|} \cdot \frac{x^{2\gamma}}{2^{2\gamma}} \cdot \frac{\Gamma(\nu)\Gamma(\gamma+1)}{\Gamma(\nu+\gamma+1)} \\ &= \sum_0^{\infty} \frac{\left(\frac{1}{2}x\right)^{\nu}}{\Gamma(\nu) |\underline{\gamma}|} \cdot \frac{x^{2\gamma}}{2^{2\gamma}} \int_0^1 t^{\nu-1} (1-t)^{\gamma} dt \quad R(\nu) > 0 \\ &= \frac{\left(\frac{1}{2}x\right)^{\nu}}{\Gamma(\nu)} \int_0^1 t^{\nu-1} \sum_0^{\infty} \frac{x^{2\gamma}}{2^{2\gamma} |\underline{\gamma}|} (1-t)^{\gamma} dt, \end{aligned}$$

a process easily justifiable. Hence

$$\begin{aligned} g_{\nu}(x) &= \frac{\left(\frac{1}{2}x\right)^{\nu}}{\Gamma(\nu)} \int_0^1 t^{\nu-1} e^{\frac{1}{2}x^2(1-t)} dt \quad \dots \quad (3.1) \\ &= \frac{\left(\frac{1}{2}x\right)^{\nu}}{\Gamma(\nu)} \int_0^1 (1-u)^{\nu-1} e^{\frac{1}{2}x^2 u} du. \end{aligned}$$

These results may also be thrown into the forms

$$\begin{aligned} g_\nu(2\sqrt{\omega}) &= \frac{\omega^{\frac{1}{2}\nu}}{\Gamma(\nu)} \int_0^1 t^{\nu-1} e^{\omega(1-t)} dt, \\ &= \frac{\omega^{\frac{1}{2}\nu}}{\Gamma(\nu)} \int_0^1 (1-u)^{\nu-1} e^{\omega u} du. \end{aligned}$$

(3.1) is also equivalent to

$$g_\nu(x) = 2 \cdot \frac{\left(\frac{1}{2}x\right)^\nu}{\Gamma(\nu)} \int_0^{\frac{\pi}{2}} \sin^{2\nu-1} \theta \cos \theta e^{\frac{1}{2}x^2 \cos^2 \theta} d\theta.$$

Finally, from (3.1) we have

$$\begin{aligned} g_\nu(x) &= \frac{x^{-\nu} e^{\frac{1}{2}x^2}}{2^\nu \Gamma(\nu)} \int_0^{x^2} u^{\nu-1} e^{-\frac{1}{2}u} du \\ &\sim x^{-\nu} e^{\frac{1}{2}x^2} \text{ for large } x \text{ and } R(\nu) > 0. \end{aligned}$$

4. Let us evaluate the integral

$$I = \int_0^\infty x^{p-1} e^{-ax^2} g_\nu(bx) dx,$$

where  $4R(a) > R(b^2) > 0$ ;  $R(\nu+p) > 0$ . we have

$$\begin{aligned} I &= \int_0^\infty x^{p-1} e^{-ax^2} \sum_0^\infty \frac{(bx)^{\nu+2\gamma}}{2^{\nu+2\gamma} \Gamma(\nu+\gamma+1)} dx \\ &= \sum_0^\infty \frac{b^{\nu+2\gamma}}{2^{\nu+2\gamma} \Gamma(\nu+\gamma+1)} \int_0^\infty e^{-ax^2} x^{p+\nu+2\gamma-1} dx, \end{aligned}$$

a process easy to justify. Hence

$$\begin{aligned} I &= \sum_0^\infty \frac{b^{\nu+2\gamma} \Gamma\left(\frac{1}{2}p + \frac{1}{2}\nu + \gamma\right)}{2^{\nu+2\gamma+1} \Gamma(\nu+\gamma+1) a^{\frac{1}{2}p + \frac{1}{2}\nu + \gamma}} \\ &= \frac{b^\nu}{2^{\nu+1} a^{\frac{1}{2}p + \frac{1}{2}\nu}} \sum_0^\infty \frac{\Gamma\left(\frac{1}{2}p + \frac{1}{2}\nu\right) \Gamma\left(\frac{1}{2}p + \frac{1}{2}\nu + \gamma\right)}{\Gamma(\nu+1) \Gamma(\nu+1, \gamma)} \left(\frac{b^2}{4a}\right)^\gamma. \end{aligned}$$

Thus we find that

$$\begin{aligned} \int_0^\infty x^{p-1} e^{-ax^2} g_\nu(bx) dx \quad & 4R(a) > R(b^2) > 0; R(\nu+p) > 0 \\ & = \frac{b^\nu \Gamma\left(\frac{1}{2}p + \frac{1}{2}\nu\right)}{2^{\nu+1} a^{\frac{1}{2}p + \frac{1}{2}\nu} \Gamma(\nu+1)} F\left(1, \frac{1}{2}p + \frac{1}{2}\nu; \nu+1; \frac{b^2}{4a}\right). \quad \dots (4.1) \end{aligned}$$

*Particular Cases :*

(i)  $p = \nu + 2$

$$\begin{aligned} \int_0^\infty x^{\nu+1} e^{-ax^2} g_\nu(bx) dx \quad & R(\nu) > -1; 4R(a) > R(b^2) > 0 \\ & = 2^{1-\nu} \left(\frac{b}{a}\right)^\nu \frac{1}{4a-b^2}. \quad \dots \dots \dots (4.2) \end{aligned}$$

Further, putting  $a = \frac{1}{2} b^2$ , we get

$$\int_0^\infty x^{\nu+1} e^{-\frac{1}{2}b^2x^2} g_\nu(bx) dx = \frac{2}{b^{\nu+2}} \quad R(\nu) > -1; R(b) > 0 \quad \dots (4.3)$$

In particular, when  $b = 1$ ,

$$\int_0^\infty x^{\nu+1} e^{-\frac{1}{2}x^2} g_\nu(x) dx = 2. \quad \dots \dots \dots (4.4)$$

(ii)  $p = 1$

$$\begin{aligned} \int_0^\infty e^{-ax^2} g_\nu(bx) dx \quad & 4R(a) > R(b^2) > 0; R(\nu) > -1 \\ & = \frac{b^\nu \Gamma\left(\frac{1}{2} + \frac{1}{2}\nu\right)}{2^{\nu+1} a^{\frac{1}{2} + \frac{1}{2}\nu} \Gamma(1+\nu)} F\left(1, \frac{1}{2} + \frac{1}{2}\nu; 1+\nu; \frac{b^2}{4a}\right) \quad \dots \dots (4.5) \end{aligned}$$

If in (4.1) we put  $\nu = 0$  and make use of (1.2) we arrive at the familiar result

$$\int_0^\infty x^{p-1} e^{-(a - \frac{1}{2}b^2)x^2} dx = \frac{2^{p-1} \Gamma\left(\frac{1}{2}p\right)}{(4a-b^2)^{\frac{1}{2}p}},$$

where  $R(p) > 0; 4R(a) > R(b^2) > 0$ .



## ON A PHYSICAL THEORY OF THE SOLAR CORONA.

By M. N. SAHA, D.Sc., F.R.S., F.N.I., Palit Professor of Physics,  
Calcutta University.

(Received January 14, 1942.)

### SUMMARY.

The paper presents a 'Physical Theory of the Solar Corona' based on the discovery of Grotrian and Edlen that the coronal lines are due to forbidden transitions of atoms of iron, nickel and calcium, stripped of a large number of electrons, and presenting the electron-composition  $(3p)^x$  ( $x = 1$  to  $5$ ) for iron and nickel,  $(2p)^x$  for calcium. It is shown that such ions can be due to some kind of nuclear reaction only, similar to Uranium Fission, occurring at some depth below the chromosphere and they are not certainly due to large scale meteor flashes. The range, and energy balance of such high speed particles (i.e. the cross-sections for loss of electrons, and capture of electrons from solar atoms) are calculated and discussed. It is shown that they are in good accord with observed facts. The formation of the outer corona is suggested to be due to the constant stream of  $\delta$ -rays ejected from the solar atoms by the high speed ions. A programme for further work is indicated.

### § 1. INTRODUCTION.

The problem of the solar corona has baffled astronomers and physicists ever since physical science began to be applied for an understanding of its mechanism. The available knowledge, and the different theories up to 1936 are summarised in the *Handbuch der Astrophysik*, Band IV, p. 315, and Band VII, p. 395, and subsequent theoretical attempts are given in the references under the headings Anderson (1926), Minnaert (1930), Grotrian (1931 and 1934), and Thackeray (1940). It will be seen from a perusal of these references that there are two distinct but associated problems involved which may be termed respectively as:—

- (1) The problem of the Coronium.
- (2) The problem of the Corona.

In the Coronium problem, we have to find out the element or elements responsible for the lines 5303, 6374, and others (*vide* Table I) which are found to occur in the inner corona (from the top layers of the chromosphere up to heights of 5' to 8' from the disc), and which used formerly to be ascribed to a hypothetical element 'Coronium'; and the nature of electronic transition giving rise to these lines.

TABLE 1.  
*Lines in the Solar Corona.*

Wavelength.	Frequency.	Intensity.	Origin.	Remarks.
3328	30039.46	2.8	....	....
(3359)	29762.24	..	....	....
3388.10	29506.62	44.4	$\text{Fe}^{+12} \dots 3p^2 \ ^3P_2 - ^1D_2$	....
3454.13	28942.59	5.6	....	....
(3461)	28885.14	..	....	....
(3505)	28522.54	..	....	....
(3534)	28288.49	..	....	....
3601.00	27762.17	4.4	$\text{Ni}^{+15} \dots 3p \ ^2P_{\frac{1}{2}} - ^2P_{\frac{3}{2}}$	....
(3626)	27570.76	..	....	....
(3641)	27457.18	..	....	....
3642.9	27442.86	..	....	....
(3648)	27404.50	..	....	....
(3651)	27381.98	..	....	....
3800.8	26302.81	..	....	....
3865	25865.91	..	$\text{Fe}^{+10} \dots 3p^4 \ ^3P_1 - ^1D_2$	Bowen (1940) obtains a line at $\lambda 3871.0$ , and assigns it to the transition given here.
(3891)	25693.08	..	....	....
3986.9	25075.07	0.8	....	....
4086.3	24465.13	1.2	....	....
(4130)	24206.27	..	....	....
(4131.4)	24298.06	..	....	....
4231.4	23626.21	3.2	....	....
(4244.8)	23551.62	..	....	....
4311.0	23189.97	..	$\text{Ni}^{+11} \dots 3p^5 \ ^2P_{\frac{1}{2}} - ^2P_{\frac{3}{2}}$	(?)
4359.0	22934.61	< 0.8	$\text{Co}^{+14} \dots 3p \ ^2P_{\frac{1}{2}} - ^2P_{\frac{3}{2}}$	Identified by D. Kundu (1941).
(4398)	22731.24	..	....	....
(4533.4)	22054.28	..	....	....
4567.0	21890.09	1.2	....	....
4586	21799.40	..	....	....
(4722)	21171.56	..	....	....
(4725)	21158.12	..	....	....
(4779)	20919.04	..	....	....
(5073)	19706.72	..	....	....
5116.03	19540.98	4.8	....	....
5302.86	18852.52	110	$\text{Fe}^{+13} \dots 3p \ ^2P_{\frac{1}{2}} - ^2P_{\frac{3}{2}}$	Discovered in 1868 by Harkness and Young. See further.
5536	18058.58	..	....	....
(5694.0)	17557.48	..	....	....
6374.51	15683.15	28	$\text{Fe}^{+9} \dots 3p^5 \ ^2P_{\frac{1}{2}} - ^2P_{\frac{3}{2}}$	Discovered in 1914. Identification due to Grotrian (1931a).
6704.83	14910.51	3.3	....	Discovered in 1929 by Grotrian (1931a).
7059.6	14161.21	4	....	....
7891.94	12667.68	29	$\text{Fe}^{+10} \dots 3p^4 \ ^3P_2 - ^3P_1$	....
8024.2	12458.88	1.3	....	....
10746.8	9314.4	240	$\text{Fe}^{+12} \dots 3p^2 \ ^3P_0 - ^3P_1$	Discovered by Lyot (1934) by means of the Coronagraph.
10797.9	9261.0	150	$\text{Fe}^{+12} \dots 3p^2 \ ^3P_1 - ^3P_2$	"

NOTE.—The wavelengths are taken from a table given by Dyson and Woolley, *Eclipses of the Sun and the Moon*, p. 132. The intensities are calculated in units of  $10^{-6}$  of the intensity at the same wavelength of photospheric emission, comprised within 1 Å. Lines of doubtful occurrence are given within circular brackets. The identifications as far as they could be inferred from Russell's (1941) short account, and Mr. D. Kundu's investigations are given in column (3). As regards the intensities of the lines, it is well known that they are subject to wide fluctuations. The intensity of the green coronal line 5303 has been found by Lyot (1934) to vary between 3 to  $70 \times 10^{-6}$  of the Fraunhofer spectrum as defined above. The identification of 4359 to  $\text{Co}^{+14} \dots 1s^2 2s^2 2p^6 3s^2 3p \ ^2P_{1/2} - ^3P_{1/2}$  is due to D. Kundu (1942) and should be confirmed. Lines due to forbidden transitions of  $\text{Fe}^{+11}$  are not in the available range.

It is now needless to add that all previous speculations regarding the origin of the coronal lines proved to be wrong. The right clue to identification of the origin of the lines was suggested by Bowen's discovery that the nebular lines can be traced to forbidden transitions of once or multiply ionised light atoms. It was felt that the coronal lines would be found to have a similar origin. The author of the present paper, and probably many others spent considerable time in ransacking the available literature for forbidden lines of elements which may coincide with some of the coronal lines, but without the least success.

The hunt was confined to only singly and doubly, and sometimes trebly ionised atoms, because it was considered improbable that more highly ionised atoms can, without violating ordinary laws of physics, occur in the corona. It was therefore a matter of some surprise when Grotrian, in 1937, announced that the red corona line 6374 had a frequency which was nearly coincident with the frequency difference between the  $^2P_{3/2}$  and  $^2P_{1/2}$  terms of  $\text{Fe}^{+9} \dots 3p^5$ , which has a chlorine-like structure, and the faint infra-red line 7892 had the frequency corresponding to the difference  $^3P_2 - ^3P_1$  of  $\text{Fe}^{+10} \dots 3p^4$ . This identification was not taken very seriously at the time, because we cannot see how, if the laws of physics continue to hold good, we can have iron atoms stripped of as many as nine or ten electrons occurring in the inner corona. But the clue was taken up by Dr. Bengt Edlen (Russell, 1941), and he has succeeded in tracing the most important coronal lines to forbidden transitions of highly stripped medium-weight atoms, viz. to  $\text{Fe}^{+9}$ ,  $\text{Fe}^{+10}$ ,  $\text{Fe}^{+12}$  and  $\text{Fe}^{+13}$  possessing  $3p^5$ ,  $3p^4$ ,  $3f^2$ ,  $3p^1$  structures; and stripped ions of Ni and Ca having similar structures. Details of this identification, as far as available, are given in Tables 1 and 5. The claim is considered a good one by Prof. H. N. Russell, Dr. D. B. Menzel, and other Harvard astrophysicists. It may be mentioned here that these 'lines' have not been actually produced in the laboratory, \* only their frequencies have been calculated from the term-values obtained from the spectra of highly stripped atoms. The author of the

---

\* In fact none of the nebular lines has yet been actually observed in any laboratory experiment. Only the green auroral line 5577 due to  $\text{O} \dots 2p^4 \ ^1D_2 - ^1S_0$  has been obtained in the laboratory.



present note along with Mr. D. Kundu has re-examined all the published data, and finds no reason for doubting the identification. It appears therefore almost certain that the problem of the origin of the coronal lines has been finally solved, and the present paper takes up the study from this point onwards.

## § 2. THE CORONA PROBLEM.

The discovery that the 'coronium lines' are due to metastable transitions of very highly stripped heavy atoms considerably enhances the difficulties which have been experienced for the last 80 years in formulating a reasonable physical theory of the 'Solar Envelope'. We use this term in a comprehensive sense after Rosseland (1934), to denote the totality of the phenomena known under the terms: the Reversing Layer, the Chromosphere and the Corona, and consider their problems together as these cannot be dissociated from each other. The composition of the solar envelope is given in Table 2, which is compiled from data given by Unsöld, *Sternatmosphäre* (p. 348). It has not been considered necessary to enter into a critical discussion about the correctness of these values, as the arguments are not likely to be much modified thereby. Full details will be found in Unsöld, *loc. cit.*

TABLE 2.

Element.	Reversing Layer.	Chromosphere.	Inner corona.
H-atoms ..	$1.8 \times 10^{22}$	$3.6 \times 10^{20}$	....
O-atoms ..	$7 \times 10^{20}$	....	....
Metals or C-atoms ..	$7 \times 10^{20}$	$7 \times 10^{19}$	....
Free electrons ..	$6 \times 10^{20}$	....	$7 \times 10^7$ per cm. <sup>2</sup> at 1'.

The figures under 'Reversing Layer' represent the total number of atoms over one cm.<sup>2</sup> of the photosphere. Hydrogen and oxygen are taken to be mostly unionised. The metals or C-atoms of Menzel (1931) are taken to be 80% ionised, and the free electrons are the result of their thermal ionisation. The 'Reversing Layer' may have a depth of 100–150 kilometres, over which we have the chromosphere extending over  $10^4$  km. The number of atoms over 1 cm.<sup>2</sup> of the base of the 'Chromosphere' (Menzel, 1931) is taken to be roughly 1/1000 of the number in the reversing layer. The inner corona starts from the top of the chromosphere, and show the lines ascribed to 'coronium' usually up to heights of 5', but occasionally in the case of coronal streamers up to heights of 8' to 10' and more. The inner corona also shows a continuous spectrum from which the Fraunhofer lines are absent or blurred out. The outer corona shows a pure continuous spectrum in which the Fraunhofer lines re-appear and it extends usually in the quiescent stage up to 15' but in disturbed times, and in the case of streamers up to several solar diameters.

The continuous spectrum in the inner or outer corona was ascribed by Schwarzschild to Rayleigh scattering of photospheric light by free electrons, and subsequent investigations have confirmed it [Grotrian (1934), Minnaert

(1930) and Bumbauch (1937)]. The number of free electrons at different heights is calculated by Minnaert (1930) from photometric measurements of the intensity of the continuous coronal light at different heights. The number-density in the quiescent stage is shown in Table 3, but very considerable fluctuations take place occasionally, particularly over coronal streamers.

TABLE 3.

$\rho$	..	1	1.03	1.06	1.10	1.2	1.3	1.4	1.6	1.8	2.0
log N	..	8.66	8.49	8.36	8.19	7.85	7.58	7.38	7.05	6.79	6.57
$\rho$	..	2.2	2.4	2.6	2.8	3.0	3.5	4.0	5.0	6.0	8.0
log N	..	6.40	6.25	6.13	6.04	5.96	5.80	5.71	5.58	5.40	5.21

$\rho$ , the distance from the sun's centre is given in units of solar radius. Thus  $\rho = 1.03$  denotes 0.48' from the disc, i.e. nearly  $2 \times 10^5$  km. from the photosphere. The electron density per  $\text{cm}^3$  at this point is  $3 \times 10^8$ . It reduces to  $\approx 10^6$  per  $\text{cm}^3$  at a distance 7 radii, i.e.  $5 \times 10^6$  km. The table is taken from Unsöld, *Sternatmosphäre*, p. 440, where it is quoted from a paper by Bumbauch (1937).

*The Problems of the Solar Chromosphere.*

The abnormal heights reached by the H, K lines of Ca have been known for a long time to astrophysicists. In recent years quantitative measurements of gradient of density distributions of the different elements have been made by Pannekoek (1928), S. A. Mitchell and E. J. R. Williams (1933), Cillie and Menzel (1935). The figures of the latter are reproduced in Table 4.

TABLE 4.  
*Density-Gradient in the Chromosphere.*

	Neutral.		Ionised.		Remarks.
H	6563	$1.54 \times 10^{-8}$ $\text{cm.}^{-1}$	....	..	....
He	5876 $1s\ 2p\ ^3P - 1s\ 3d\ ^3D$	0.78	4686	0.30	<i>Vide remarks in text.</i>
Mg	....	2.50	4481	—	....
Al	3961, 3944 $3p\ ^2P_{\frac{1}{2}}, \frac{3}{2} - 4s^2\ S_{\frac{1}{2}}$	2.77	....	—	....
Ca	4227 $4s^2\ ^1S_0 - 4s\ 4p\ ^1P$	$> 2.11$	3934 $4p\ 2s_{\frac{1}{2}} - 4p\ ^2P_{\frac{1}{2}}$	1.51	....
Sc	....	—	....	4.20	....
Ti	....	—	....	3.32	....
Cr	....	$> 2.07$	....	1.72	....
Mn	....	2.95	....	1.60	....
Fe	....	2.48	....	1.69	....
Sr	4607 $5s^2\ ^1S_0 - 5s\ 5p\ ^1P_1$	..	4077, 4215 $5s^2\ S_{\frac{1}{2}} = 5p^2\ P$	1.06	....

The gradients are far smaller than  $5.44 \times 10^{-8} \text{ cm.}^{-1}$  ( $\alpha = \frac{mg}{kT}$ ) which is the value for an element of weight unity and for a temperature of  $6000^\circ$ . There appears to be some 'force of levity' in action. The origin of this has been looked for in Selective Radiation Pressure (Milne, 1925), Electrical Force, etc., Turbulence (McCrae, 1929). But what is most disconcerting is the fact that the density gradient appears to have the same value for elements widely differing in weight, e.g. for Mg. (A.W. = 24), and Fe (A.W. = 58) and is not much larger than that for hydrogen. What 'mysterious forces' reduce the weight of Mg and Ca to almost the same value as that of H is still a problem.

An important constituent of the chromosphere is Helium, which is not observed in the Fraunhofer spectrum but occurs only in the chromosphere as emission lines; though in recent years 10830.3,  $1s\ 2s\ ^3S-1s\ 2p\ ^3P$  has been observed by Babcock (1934) as a faint absorption line, and 5876,  $1s\ 2p\ ^3P-1s\ 3d\ ^3D$  was observed by Nagaraja Aiyar to occur as an absorption line in the penumbra of spots. As a matter of fact, Evershed (1898) noted that helium lines tended to vanish as we approach the 'Reversing Layer'. Following this Pannekoek and Minnaert (1928) and Perepelkin and Melnikov (1935) have determined the distribution of He-atoms emitting  $D_3$  and 4471 ( $1s\ 2p\ ^3P-1s\ 3d\ ^3D$ ,  $1s\ 2p-1s\ 4d\ ^3D$ ) with height. They observe that the intensity of the lines tend to vanish at the base of the chromosphere, rises to a maximum at a height of 2,500 km. and then gradually vanish, but can be traced up to a height of 7,500 km. Another anomaly discovered by A. Fowler was the occurrence of  $\text{He}^+$  4686, having an excitation potential of 73-volts in the lower chromosphere (2,500 km.).

The reversing layer and the chromosphere show plenty of strong lines of Fe, and  $\text{Fe}^+$  and some  $\text{Fe}^{++}$ -lines have been suspected and the excitation of these lines are satisfactorily explained on the theory of thermal ionisation. But no extranuclear process can deprive the iron atom of thirteen, and possibly of more electrons, at least not in the coronal heights of the sun.

Temperatures of the order of  $2 \times 10^7^\circ\text{C}$ . or photoelectric light of wavelength 1 to 10 Å.U. in sufficient strength would be needed. In fact, Prof. H. N. Russell (1941) remarks:—

'It is hard to see how these stripped atoms can maintain so high a degree of ionisation if the corona, as has generally been supposed, contains many free electrons. But apparent difficulties of this sort often turn out to be guide-posts directing to new knowledge.'

We must add to this that the greatest difficulty has been encountered in finding out a source for these electrons. They cannot arise from thermal or photo-electric ionisation as we have then to postulate, in coronal heights, the existence of atoms and ions; this is impossible on dynamical grounds. Reviewing several theories, Minnaert (1930) remarks: 'Anderson has shown that the corona cannot be in equilibrium if the ordinary physical laws are

valid. Instead of assuming, as he does, that very hypothetical modified laws must be applied, we may attempt to account for the corona by assuming that it really is not in equilibrium, and *that its particles are continuously projected towards space.*'

We shall see later that Minnaert has been right in giving up the equilibrium theory. We have to find out what forces impel the electrons towards outside space. In fact difficulties of such a serious nature have been encountered in finding out the origin of coronal electrons, that at one time, it was seriously thought that the coronal glow was due to scattering of light quanta by the light quanta themselves. The scattering cross-section for this effect was in fact calculated by Heisenberg and Euler (1934), but was found to have the extremely small value of  $10^{-70}$  cm.<sup>2</sup> for the average solar radiation. This requires an enormous number of light quanta for the observed effect, and therefore the hypothesis had to be given up.

In addition to the question of origin, the stability of electron clouds in the corona has engaged the attention of physicists, for a cloud of electrons would disperse to nothing in a very short interval of time due to mutual electrostatic repulsion. Anderson at one time pointed out that the presence of an equal number of positrons might ease the situation, but the query about the origin of the hypothetical positrons has never been answered. It is difficult to see how positrons can occur in the corona, for then electrons and positrons would annihilate each other, forming annihilation radiation. There is no indication that such a process ever takes place in the corona.

Another difficulty was pointed out by Moore (1934) and further investigated by Grottrian (1934). Moore showed that though Fraunhofer lines are blurred out from the inner corona, they reappear in the outer corona. Grottrian (1934) found that the continuous spectrum of the scattered radiation from the inner corona shows depressions in regions corresponding to Fraunhofer absorption, but displaced by about 100 Å.U., but the lines appear again in the outer corona. He sought to explain the first of these observations by the hypothesis that electrons in the inner corona are moving outwards with velocities of the order of 4,000 km. (corresponding to a temperature of  $4.8 \times 10^5$ ). But for the reappearance of Fraunhofer lines in the outer corona, he had to postulate the existence of 'Cosmic Dust'.

But Astrophysicists have never been able to understand how cosmic dust of the size postulated by Grottrian can exist at such close proximity to the sun without vaporising completely. The phenomena may as well be explained by the hypothesis that the electrons in the outer corona are, at least partly, nearly at rest.

### § 3. PRELIMINARY EXAMINATION OF DIFFERENT HYPOTHESIS REGARDING ORIGIN OF HIGHLY STRIPPED ATOMS IN THE SOLAR CORONA.

Two suggestions may be made regarding the origin of highly stripped iron and other atoms in the solar corona.

(1) That the production of highly stripped iron, nickel and calcium atoms is due to the bombardment of the solar atmosphere by 'Cosmic Dust' which is meteoric matter, consisting mainly of elements which occur in great abundance in stony and iron meteorites, viz. Fe, Ni, Ca, Mg, etc. The 'Dust' or 'Meteors' enter the solar atmosphere with a velocity of the order of  $6.22 \times 10^7$  cm./sec. (velocity of escape from the surface of the sun) which is much larger than  $3 \times 10^6$  cm., the average velocity of entry of cosmic particle into the Earth's atmosphere. In the case of the meteors it is well known that these get incandescent by friction in the Earth's atmosphere, and give out characteristic lines of neutral and once-ionised atoms of Ca, Fe, Mg, Si (Millmann, 1933) and other elements that they are composed of. In the sun, it may be assumed that on account of the much higher energy, the elements are stripped off of many of their electrons.

According to this view, the coronal lines are due to large scale meteoric flashes, and are caused by the passage of the sun through a cloud of cosmic dust. This hypothesis is examined in § 4 and found to be opposed to facts.

(2) We can assume that the highly ionised iron and other atoms are being constantly produced somewhere in the solar envelope by some kind of *nuclear* reaction, similar to Uranium Fission, or some other type of nuclear reaction still undiscovered, and projected upwards with energies of the order of millions of volts, through the higher chromosphere. The ion may even start as a bare nucleus, and its passage through the higher chromosphere may be compared to that of an  $\alpha$ -particle or better of uranium fission fragments through the cloud chamber. During its passage, the Fe-ion goes on capturing and losing electrons, and ejecting electrons from the atoms and ions it encounters (Ionisation by Collision). The capture of electrons by the Fe-ion is illustrated by the emission of the coronal lines and electrons ejected from higher chromospheric atoms and ions probably from the outer corona.

We may call this the  $\delta$ -ray theory of the origin of coronal electrons. It appears to be in fair agreement with all that we know of the outer corona; the  $\delta$ -rays, i.e. electrons liberated by the heavy Fe and other ions will have a maximum velocity of twice the amount possessed by the original ions and can therefore rise to four times the height of the heavy ions, and thus we require no heavy ions or atoms for the production of the electron atmosphere which gives rise to the outer corona.

If this view be correct, the solution of the coronium problem has also led to that of the corona problem.

#### § 4. CRITICAL EXAMINATION OF THE METEOR FLASH HYPOTHESIS.

*Whether the emitters of Coronal lines are streaming in or streaming out.*

Decision may be arrived between the two views by finding out whether the emitters of coronal lines are streaming out or streaming in. Fortunately, we are in a position to give a definite answer to this point.

Grottrian (1931a) was the first to find out that the coronal line 5303 has a rather large breadth (of the order of  $1 \text{ \AA.U.}$ ). This has been confirmed by Lyot (1934 and 1936) in his Coronagraph observations and he finds for the three most prominent coronal lines the following half-breadths:—

Line.	Half-breadth.	Ratio.
5303	0.80	$1.50 \times 10^{-4}$
6376	0.97	$1.52 \times 10^{-4}$
6703	1.07	$1.60 \times 10^{-4}$

If these breadths are due to Maxwellian motion, the mean velocity is 32 km. per second. Lyot was under the impression that the lines were due to oxygen and he deduced that this signified a temperature of  $6.6 \times 10^5$  degrees C. Taking the emitters to be iron-ions, the temperature ought to be  $2.34 \times 10^6$  degrees. Such temperatures are of course unthinkable on the surface of the sun, and Waldemeier (1938) has shown that the width curve of Lyot can be explained on the supposition that the emitters of coronal lines are streaming radially outwards with a mean velocity of 60 km. per sec. Lyot (1934, see Fig. 5) has further found that the width is largest when the emitters are nearest the sun's limb, and become narrower as the height increases. This combined with Waldemeier's suggestion points out that the velocity of atoms emitting coronal lines increases inwards, i.e. towards the solar limb.

Let us now try to interpret these facts. Waldemeier's suggestion is quite in agreement with Minnaert's quoted above (page 105, line 3). Further, though his conclusions hold equally well whether the emitters are streaming in or streaming out, the fact that they have a mean velocity of the order of 60 km. per sec. in the inner corona shows that they cannot arise from the ionisation of meteoric matter coming from space. In that case the velocity of entry would be of the order of 600 km./sec. It may be supposed that this velocity diminishes in the inner corona to 60 km. on account of the resistance, but this is not very probable, because, the resisting force would be working far more strongly as the particles plunge inwards, and the velocity would therefore diminish inwards. This is irreconcilable with Lyot's finding that the velocity of the emitters is largest nearest the sun's limb, and diminish outwards.

Russell (1929) considered the dynamics and physical state of meteoric matter near the stars, particularly the sun. His conclusion may be quoted:

'Masses of stone or iron will be completely volatilised by the sun's heat, before they reach the surface, unless they were originally a foot or more in diameter. But the atoms resulting from volatilisation will proceed with unaltered speed, and fall into the sun unless repelled by radiation pressure. . . . Further, the meteoric matter falling into the sun may scatter enough to account for a small fraction of brightness of the corona, but cannot exert enough effective absorption in the spectrum to produce the equivalent of a single narrow Fraunhofer line' (equivalent width  $10^{-3} \text{ \AA.U.}$ ).

It can be easily seen that an iron-atom moving through the sun's atmosphere with a velocity of  $6 \times 10^2$  km./sec. cannot lose any electron by collision with the free electrons of the upper corona, for the effect is the same as if the iron-atom was at rest, and the electrons were moving past it with a velocity of  $6 \times 10^2$  km./sec. For an electron, the equivalent energy is merely one-electron volt and is too low to cause even the loss of a single electron from the Fe-atom. It would be otherwise in case of collision with protons, or heavier nuclei (say  $\alpha$ -particle or heavier ions). In the case of encounter with protons, it is equivalent to bombarding the iron-atoms with protons of about 2,000 volt energy, and about 13 collisions are sufficient to relieve the iron-atom of 13 electrons. But neither hydrogen lines nor lines of any other familiar elements have been observed beyond a height of 14,000 km. (top of the chromosphere), and as Anderson (1930-1932) has shown it is dynamically not possible that any atom or ion can, under the usual conditions prevailing in the sun, rise to the height of the inner corona (i.e. from the top of the chromosphere to a height of 3' to 5', i.e.  $1.30 \times 10^5$  to  $2.17 \times 10^5$  km.). It is therefore almost certain that an iron-atom vaporised from a meteor striking the sun with the usual velocity cannot be relieved of as many as 13 or 14 electrons while passing to the inner corona. We must look for the origin of these highly stripped atoms elsewhere.

#### § 5. NUCLEAR REACTION THEORY OF CORONAL EXCITATION.

We shall now develop the ideas of nuclear reaction theory of coronal excitation briefly sketched in § 3. It may be mentioned here that there is already a certain volume of opinion in favour of such a view. Thus Rosseland (1933), after reviewing at length the numerous anomalous results in the solar envelope, points out that some of these anomalies may be explained, by assuming that some kind of radioactive process is in action, *which forces charged particles radially outwards through the envelope*. Naturally enough, no attempt was made to define the nature of this radioactive process, and the reaction of the charged particles with the atoms and ions in the solar envelope.

From the evidence so far available, forbidden lines of  $\text{Fe}^{+9} \dots \text{Fe}^{+18}$ , having the constitution  $2p^x$  ( $x = 5$  to 1), and lines of Ca and Ni having similar constitution have been identified in the corona. It is quite possible that there may be still more highly charged  $\text{Fe}^{+}$ -ions, viz.  $\text{Fe}^{+14}$  ( $3s^2$ )  $\text{Fe}^{+15}$  ( $\dots 3s$ ),  $\text{Fe}^{+16}$  ( $2p^6$ ). But as these have no metastable levels, there are no means of detecting their presence in the corona.  $\text{Fe}^{+17}$  ( $2p^6$ ) does not appear to have been yet spectroscopically investigated, but on extrapolation from known data, the forbidden line  $^2P_{\frac{3}{2}} - ^3P_{\frac{1}{2}}$  is expected to have a wavelength of 900 Å.U. This being in a region not available to observation the presence of  $\text{Fe}^{+17}$  cannot be detected. It can be proved that no other ion of higher charge can emit a metastable line within visible range; hence even if they are present in the corona or lower, in the solar envelope, it is not possible for us to detect their presence.

TABLE 5.

*Stripped Iron-ions and their Electron-Structure, etc.*

Ion	Electron Structure.	Funda- mental State.	Value of the lowest terms in volts	$\sqrt{\frac{\text{I. P.}}{13.54}} = \frac{z_1}{n}$	Remarks.
Fe <sup>24</sup> I	.. 3d <sup>6</sup> 4s <sup>2</sup>	<sup>5</sup> D <sub>4</sub>	7.83	0.76	....
Fe II	.. 3d <sup>6</sup> 4s	<sup>6</sup> D <sub>4½</sub>	16.5	1.10	Forbidden lines found in η-Carina. Bowen (1936).
Fe III	.. 3d <sup>6</sup>	<sup>6</sup> D	30.48	1.50	....
Fe IV	.. 3d <sup>5</sup>	<sup>6</sup> S	56.8	2.05	....
Fe V	.. 3d <sup>4</sup>	<sup>5</sup> D <sub>0</sub>	..	(2.37) *	Bowen (1940) gives metastable lines found in nebulae. D. Kundu thinks that some of these lines may occur in the corona.
Fe VI	.. 3d <sup>3</sup>	<sup>4</sup> F <sub>¾</sub>	..	(2.69)	"
Fe VII	.. 3d <sup>2</sup>	<sup>3</sup> F	..	(3.01)	"
Fe VIII	.. 3d	<sup>2</sup> D	150.4	3.33	<sup>2</sup> D <sub>¾</sub> - <sup>2</sup> D <sub>½</sub> = 1875 cm. <sup>-1</sup> No metastable line available.
Fe IX	.. 3p <sup>6</sup>	<sup>1</sup> S <sub>0</sub>	233.5	4.15	No metastable state.
Fe X	.. 3p <sup>5</sup>	<sup>2</sup> P	261	4.39	λ 6374.75 <sup>2</sup> P <sub>¾</sub> ← <sup>2</sup> P <sub>½</sub>
Fe XI	.. 3p <sup>4</sup>	<sup>3</sup> P	288.9	4.62	λ 7892
Fe XII	.. 3p <sup>3</sup>	<sup>4</sup> S	320	(4.91)	Has no metastable line in the available range.
Fe XIII	.. 3p <sup>2</sup>	<sup>3</sup> P <sub>012</sub>	346	(5.06)	10746.80 } 10797.95 }
Fe XIV	.. 3p	<sup>2</sup> P	373	5.25	λ 5303 <sup>2</sup> P <sub>½</sub> - <sup>2</sup> P <sub>¾</sub>
Fe XV	.. 3s <sup>2</sup>	<sup>1</sup> S <sub>0</sub>	454	5.79	No metastable state.
Fe XVI	.. 3s	<sup>2</sup> S <sub>½</sub>	487	5.99	"
Fe XVII	.. 2p <sup>6</sup>	<sup>1</sup> S <sub>0</sub>	1259.7	9.65	"

\* Parentheses ( ) denote that the value is extrapolated.

We shall now give certain arguments which appear to point out that the probability of occurrence of ions more highly stripped than Fe<sup>+16</sup> or Ni<sup>+18</sup> is extremely small. For this purpose, we refer the reader to Table 5, in which the ionisation potentials of iron, as far as available, are given.

A glance at Table 5 shows that the ionisation potentials of Fe-ions from Fe<sup>+8</sup> to Fe<sup>+15</sup> corresponding to the removal of electrons from 3p, and 3s-shells, vary in continuous gradation from 233 volts to 487 volts. There is a sudden jump at Fe<sup>+16</sup> (2p<sup>6</sup>) where the I.P. jumps up to 1250 volts. This is as expected, because now the electron has to be detached for the first time from the 2p-shell. We calculate the orbital velocities of electrons in the



different shells on the assumption that  $V = \sqrt{\frac{\text{I.P.}}{13.56}} cf$ , where  $c$  = velocity of light,  $f$  = Sommerfeld fine-structure constant,  $cf$  = velocity of the electron in the H-atom. We find (*vide* column 5 of Table 5) that  $z/n$  varies from 4.15 for  $\text{Fe}^{+8}..3p^6$  to 5.99 for  $\text{Fe}^{+15}..3s$  in a continuous sequence, but suddenly jumps to 9.65  $cf$  for the next ion  $\text{Fe}^{+16}$ .

In a Uranium Fission process the fragments are formed with energies of the order of 80 to 100 mev. (mev = million-electron-volts). Elements like Fe and Ni can be formed only in a threefold or fourfold fission process, of heaviest elements  $\text{U}^{239}$ ,  $\text{U}^{235}$ , Prot. Act.<sup>231</sup>, or  $\text{Th}^{232}$ , which alone, according to Bohr and Wheeler (1939), are capable of fission. These processes, however, have not yet been observed, but are quite possible on energetic grounds.

If an iron-atom is formed in such a process, its kinetic energy will be of the order 60 mev., corresponding to a velocity of 6.4  $cf$ . If the velocity is 10  $cf$  the energy would be 140 mev., which is impossible on energetic grounds. Let us now ask what will be the number of electrons which will be retained by the fission-fragment? Now Bohr (1940, 1941), Knipp and Teller (1941), and Lamb (1941) have discussed this point in connection with the problem of finding out the net charge carried by a fission-fragment and have shown that the number of electrons retained is limited by the condition that the orbital velocity of the outermost electrons retained by the ion, i.e.  $V_i$  should be larger than that of the fragment as a whole, viz.  $V_f$  where  $\frac{1}{2}M.V_f^2$  = energy of fission. This points out that the fission fragment can be at most  $\text{Fe}^{+15}$ , but not  $\text{Fe}^{+16}$ . As  $\text{Fe}^{+15}..3s$ , and  $\text{Fe}^{+14}..3p^6$  have no metastable levels, they cannot be detected. We can detect ions ranging from  $\text{Fe}^{+13}..2p$  to  $\text{Fe}^{+9}..2p^6$ , as already noted by Russell (1941).

#### § 6. PASSAGE OF HIGHLY CHARGED (STRIPPED) IONS THROUGH THE SOLAR ENVELOPE.

In this section, the passage of highly charged iron-ions through the solar envelope will be considered. To start with, we do not make any *a priori* assumption regarding the exact point where the stripped ions originate, but merely assume that it happens somewhere in the reversing layer. As a first approximation we consider the envelope to consist mainly of H-atoms, in accordance with considerations given in § 2.

The various possible reactions of a highly stripped iron atom with H-atoms in the solar envelope are:

(1) That the Fe-ions, etc., release electrons from the H-atom by the process known as ionisation by collision [Thomson (1930), Bohr, Bethe (1932), Bloch (1933)].

As we shall see presently, this is the main factor for the reduction in energy of the ion.

(2) When the velocity slows down, due to electron-capture, there may be liberation of the proton (nuclear process).

The loss due to this effect is usually of the order of  $10^{-3}$  times the first, but may be comparable when  $V_i \simeq cf$ .

(3) The ion may have its charge reduced by capture of free electrons, or electrons from the H-atom.

This process must be taking place in the reversing layer and the chromosphere, and as a result, the Fe-ion goes on losing its net charge as we actually observe ( $\text{Fe}^{+13}$  to  $\text{Fe}^{+9}$ ).

### Energy loss due to ionisation by collision.

The energy-loss of the Fe-ion due to liberation of an electron from the H-atom is given by Livingstone and Bethe, 1937

$$-\frac{dE}{dx} = \frac{4\pi n e^4 z_i^2}{m V^2} \ln \left( \frac{2m V^2}{I} \right) \quad \dots \quad (1)$$

where  $E$  = energy of the particle =  $\frac{1}{2} M V^2$

$z_i$  = effective charge of the ion

$I$  = average excitation potential of the H-atom.

The effective charge of the Fe-ion varies from  $z_i = 6$  for  $\text{Fe}^{+15}$  to  $z_i = 4$  for  $\text{Fe}^{+8}$ . We shall, in the first instance, assume  $z_i$  to have the average value 5.

The quantity  $I$  is not the Ionisation Potential  $\frac{2\pi^2 e^4 m}{h^2} = I_0$ , but is  $y I_0$ , for particles are usually released with some velocity. The value of  $y$  has been found experimentally for  $\text{N}_2$ ,  $\text{O}_2$ ,  $\text{H}$ ,  $\text{A}$  (Lehmann, 1927), but naturally no experiment can be carried out for  $\text{H}$ . We have taken  $y = 2$ , and  $y = 1.2$  rather arbitrarily.

After some work, the formula (1) can be put in the form

$$-\frac{dE}{dx} = n \cdot \sigma_e \cdot mc^2 \quad \dots \quad (2)$$

where  $\sigma_e$  may be called 'the electron-release cross-section' and is given by

$$\sigma_e = 2\pi r_0^2 z_i^2 \left( \frac{Mc^2}{E} \right) \left\{ \ln E + \ln \left( \frac{4m}{My I_0} \right) \right\} \quad \dots \quad (3)$$

where  $r_0 = \frac{e^2}{mc^2}$  = nuclear radius.

Expressed in electron-volts, we have

$$\sigma_e \cdot mc^2 = 8.37 \cdot 10^{-7} \cdot \frac{\log E - 5.858}{E} \cdot \text{ev. cm.}^2 \quad \dots \quad (3a)$$

In using this formula,  $E$  should be expressed in electron-volts. A plot of  $\log \sigma_e$  against  $\log E$  is given in Fig. 1.

*Energy-loss due to proton-release.*

Let us next find out the energy-loss suffered by the ion due to communication of energy to the proton. According to Bohr (1940) this is given by:—

$$-\frac{dE}{dx} = n\sigma_p mc^2 \quad \dots \quad (4)$$

where  $\sigma_p$  = proton-release cross-section and is given by:—

$$\sigma_p mc^2 = \frac{4\pi e^4 z_1^2 z_2^2}{M_2 V^2} \cdot \ln \left( \frac{M_1 M_2}{M_1 + M_2} \cdot \frac{V^2 a_{12}}{z_1 z_2 e^2} \right) \quad \dots \quad (5)$$

where  $z_1$  .. Charge of the ionising particle; here  $z_i$ .

$z_2$  .. " " " nucleus of atom; here = 1.

$M_1$  .. Mass of the particle, i.e. of Fe-ion.

$M_2$  .. " " " atom; here  $M_H$

$a_{12}$  .. Effective radius of collision.

Since  $M_2 = M_H$  (mass of proton), and  $M_1 = 58 M_H$ , we can put

$$\frac{M_1 M_2}{M_1 + M_2} = M_2 = M_H$$

$$a_{12} \simeq a_B \left( \text{Bohr-radius} = \frac{h^2}{4\pi^2 e^2 m} \right).$$

After some work, it can be shown that

$$\sigma_p = 2\pi r_0^2 \frac{m}{M_H} \cdot z_i^2 \left( \frac{Mc^2}{E} \right) \left[ \ln E + \ln \left( \frac{M_H}{M z_i I_0} \right) \right] \quad \dots \quad (6)$$

In deducing this formula, we have made use of the relation  $e^2/a_B = 2I_0$ .

Expressed in electron-volts, the expression reduces to

$$\sigma_p mc^2 = 4.56 \times 10^{-10} \left\{ \frac{\log E - 3.594}{E} \right\} \cdot \text{ev. cm.}^2 \quad \dots \quad (6a)$$

A plot of  $\log (\sigma_p mc^2)$  against  $\log E$  is shown in Fig. 1. It is easily seen that  $\sigma_p$  is about  $\frac{1}{2000} \sigma_s$  at high values of  $E$ , but the two become comparable when  $E \simeq 10^6$  ev.

We have in fact

$$\frac{\sigma_s}{\sigma_p} = \frac{m_H}{m} \left( \frac{\log E - 5.858}{\log E - 3.594} \right)$$

Formula (3a) is inapplicable when  $E$  is  $< 10^6$  ev. We have then  $V_i \simeq 0.8$  cf, i.e. Fe-ion will by this time acquire electrons, the value of  $z_i$  would go down, and formula (3a) ceases to apply.

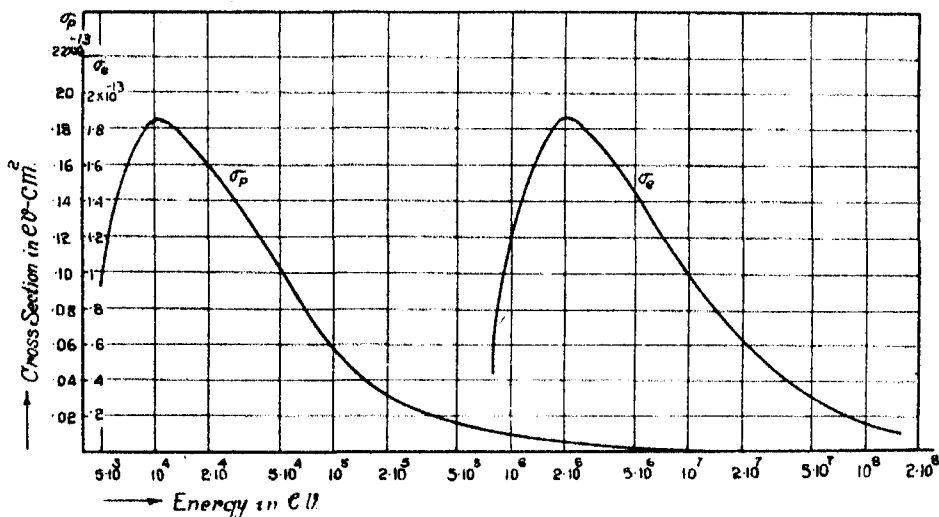


FIG. 1. Electron-release cross-section ( $\sigma_e$ ) and proton-release cross-section  $\sigma_p$  of a stripped iron atom at different energies ( $z_i = 5$ ,  $y = 2$ ).

*Depth of the Layer which can be penetrated by the Fe-ion.*

We shall now calculate 'the Range' of the highly stripped ions in the solar envelope. The results of the calculation are rendered somewhat uncertain by the fact that we have to choose  $z_i$  and  $y$  rather arbitrarily. But this is unavoidable at the present stage.

Following a procedure adopted by P. C. Bhattacharyya (1941), (1) can be put in the form

$$n dx = - \frac{My^2}{128 \pi m z_i^2} \cdot \frac{1}{a_B^2} \cdot \frac{d\epsilon}{\ln \epsilon} \quad \dots \quad (7)$$

where

$$a_B = \text{Bohr-radius} = \frac{h^2}{4\pi^2 e^2 m}, \quad \epsilon = \left( \frac{4m}{M} \cdot \frac{E}{yI_0} \right)^2$$

We can as a preliminary measure neglect the other causes of energy loss. These are: losses due to proton release, to gravity, and to collisions with other atoms, viz. Oxygen and C-atoms. We take  $z_i = 5$ ,  $y = 2$ ; we can then apply (7) to find out the number of H-atoms which the  $\text{Fe}^+$ -ion can traverse before it loses its energy. We obtain

$$\begin{aligned} \int n dx &= N(x_0) - N(x) = \frac{My^2}{128 \pi m z_i^2} \cdot \frac{1}{a_B^2} \int_{\epsilon_0}^{\epsilon_{\max}} \frac{d\epsilon}{\ln \epsilon} \\ &= 1.46 \times 10^{18} [E_i(\log \epsilon_{\max}) - E_i(\log \epsilon_0)] \quad \dots \quad (8) \end{aligned}$$

For  $E_m = 60$  mev.,  $\epsilon_{max} = (83.26)^2$ ,  $\log \epsilon_m = 8.833$ ,  $E_i(\log \epsilon_m) = 900$  in round numbers.

Let us take the lower limit  $E_0 = 1$  mev., corresponding to  $V_i = 2 \times 10^8$  cm./sec.  $\simeq cf$ . At this stage, the Fe-ion will have captured electrons from the H-atom, and would have most of its charge neutralized.  $E_i(\log \epsilon_0) = 0$ , i.e. the formula (8), is inapplicable at this stage.

We find that with these assumptions

$$N = \int n dx = 1.3 \times 10^{21} \quad \dots \quad (9)$$

i.e. an  $\text{Fe}^{+}$ -ion of net charge  $z_i = 5$  and having an initial energy of 60 mev. can pass through  $1.3 \times 10^{21}$  H-atoms before it loses the whole of its energy by electron-release. A reference to Table 2 shows that this is 1/15 of the number of H-atoms over the photosphere. Hence the Fe-ion has to originate rather high up in the reversing layer, but far below the base of the chromosphere. If the Fe-ion has to originate on the photosphere, a rough calculation shows that  $E_m$  should be 280 ev., and  $V_i = 13$  cf and the iron-ion should be  $\text{Fe}^{+22} \dots 1s^2, 2s^2$ .

The probable value of 'y' in the case of different gases has been considered by Rutherford, Chadwick and Ellis (*Radiations for Radioactive Substances*, p. 81, Table). For diatomic gases the experimental value of  $y = 2$ , and for monatomic gases, we have for He,  $y = 1.13$ , for Ne, A, Kr,  $y = 1.3, 1.6, 1.75$ , respectively. Atomic hydrogen resembles He most, as it has the smallest number of electrons next to He, and its radiation potential is high like He. A value of  $y = 1.12$  is likely therefore to be more correct for H-atoms.

Taking this value of  $y$ , we get

$$\sigma_i = 8.37 \times 10^{-7} \frac{\log E - 5.606}{E} \text{ ev. cm.}^2 \quad \dots \quad (10)$$

i.e. the constant is 5.606 instead of 5.858 in formula (3a)

Putting this value of  $y$  in the formula for calculation of range, we find that

$$\int n dz = 4.74 \times 10^{17} [E_i(\log \epsilon_m) - E_i(\log \epsilon_0)] \quad \dots \quad (11)$$

The value of  $\epsilon$ 's, however, is different. For  $E = 60$  mev.,  $\log \epsilon_m = 9.987$ , and  $E_i(9.987) \simeq 2400$ ; the value of  $E_0$ , the lowest energy at which the formula ceases to hold now becomes  $5 \times 10^5$  volts. We have

$$N = 1.12 \times 10^{21} \quad \dots \quad (12)$$

so that the total number of particles which can be traversed remain pretty nearly the same.

The value of  $z_i$  varies from 6 to 4. In Fig. 2, the  $\log N/\log E$  curves for different values of  $z_i$ , and for  $y = 1.12$ , and for  $z_i = 5, y = 2$  are drawn.

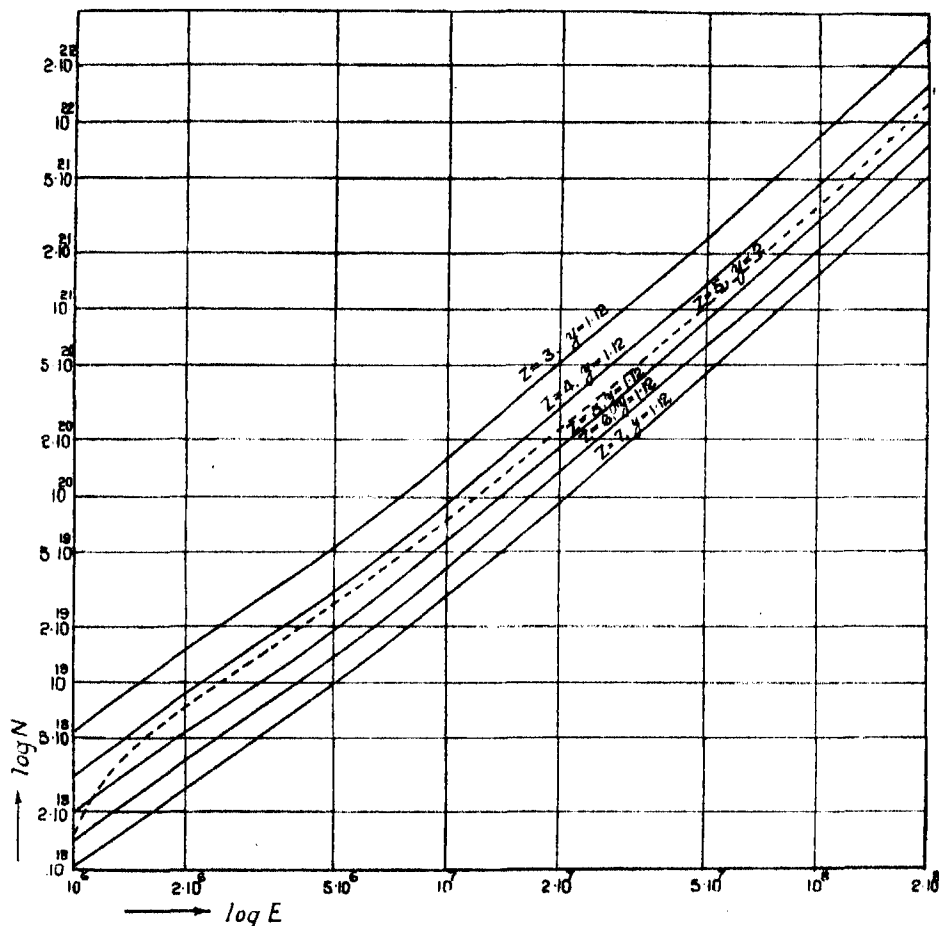


FIG. 2. Total range of a stripped iron atom at different energies for various values of the effective charge. Range has been expressed as the total number of H-atoms traversed.

### § 7. CAPTURE AND LOSS OF ELECTRONS BY THE SWIFTLY MOVING IONS.

We have assumed in the foregoing treatment that the iron-ion takes its birth in the reversing layer as an  $\text{Fe}^{+16} 1s^2 2s^2 2p^6$ -ion, with an energy of ca 60 mev. and gradually loses this energy on its passage through an atmosphere composed mainly of H-atoms. In course of this passage the ions have a chance of not only capturing free electrons but also electrons from the H-atoms and other atoms and ions; further, it can also lose electrons by collision. Let us now consider this electron exchange phenomena.

The only parallel case in experimental physics is the phenomenon discovered by Henderson (1922) that the  $\alpha$ -ray, while passing through the last one cm. of its range in air, can capture an electron from the molecules, and become

$\text{He}^+$ , which then might lose an electron by collision. Rutherford showed that this kind of alternate capture and loss takes place nearly two thousand times during the last 1 cm. of the path of the  $\alpha$ -particle. Towards the extreme end of the track,  $\text{He}^+$  may capture an electron and become neutral He, which may again lose an electron by collision. These cases have been treated by Rutherford (1923) and Jacobsen (1930). A preliminary account may be found in *Radiations from Radioactive Substances* by Rutherford, Chadwick and Ellis (p. 124 *et seq.*).

It has been shown by these authors that if  $N(\text{He}^{++})$  be the number of  $\alpha$ -particles,  $N(\text{He}^+)$  the number of  $\alpha$ -particles which have caught an electron,  $\sigma_c$  is the capture cross-section of an electron from air molecules by  $\text{He}^{++}$ , and  $\sigma_l$  is the loss cross-section of an electron from  $\text{He}^+$ , then we have for equilibrium

$$N(\text{He}^{++}) \sigma_c = N(\text{He}^+) \sigma_l \quad \dots \quad (13)$$

In place of  $\sigma_c$ ,  $\sigma_l$ , we can introduce  $\lambda_c$ , and  $\lambda_l$ , the mean free-paths for capture, and loss. It is clear that  $\lambda_c = \frac{1}{N\sigma_c}$ ,  $\lambda_l = \frac{1}{N\sigma_l}$  where  $N$  is the number of air molecules per c.c. From this relation, we have

$$N(\text{He}^{++})/\lambda_c = N(\text{He}^+)/\lambda_l \quad \dots \quad (14)$$

$\lambda_l$  is obtained from experiments, and  $\lambda_c$  from observed ratios of  $N(\text{He}^{++})$  to  $N(\text{He}^+)$ . Kramers and Brinkmann (1930) have developed a theory of capture of electrons from air molecules by the  $\text{He}^{++}$ -particle, and find that subject to certain assumptions, their results are in agreement with the data given by Rutherford *et al.* Jacobsen (1930) has given a method of calculating  $\lambda_l$  independently.

Let us now turn to the present case. We have supposed that the iron-ion starts its career as an  $\text{Fe}^{+16} \dots 1s^2 2s^2 2p^6$ -ion, with a velocity slightly greater than 6 cf. Let us calculate first  $\sigma_l$  for any ion, by following the method given by Jacobsen. We can suppose that the ion is at rest, and the H-atoms are rushing past it with the velocity of the ion,  $V_i$ , which is slightly larger than 6 cf. Then an electron can be knocked out of the  $\text{Fe}^{+16} \dots 1s^2 2s^2 2p^6$  by either the electron of the H-atom or its nucleus. According to the formula developed by J. J. Thompson (1932), the energy communicated to the electron is given by

$$Q = \frac{2E^2e^2}{mV_i^2(p^2+d^2)} \quad \dots \quad (15)$$

where  $E$ ,  $M$  are the charge and mass of the ray (i.e. either the electron, or the nucleus of the H-atom).

$e$ ,  $m$  are the charge and mass of the electron belonging to  $\text{Fe}^{+16}$ .

$p$  = collision distance.

Case (1):

In the first case (ionisation by electron of the H-atom),  $E = e$ ,  $M = m$ ,  
 $\therefore Q = \frac{2e^4}{mV_i^2(p^2+d^2)}$  and  $d = \frac{eE(M+m)}{mMV^2} = \frac{2e^2}{mV^2}$ . So  $Q_0$  which is the value  
 of  $Q$  for  $p = 0$  and the maximum energy which can be imparted to the electron  
 by the ionising particle equals  $\frac{2e^4}{mV^2} \left( \frac{mV^2}{2e^2} \right)^2 = \frac{1}{2} mV^2$ .

From (15), we obtain

$$2\pi p dp = -\pi \frac{dp^2}{dQ} dQ = \frac{2\pi e^4}{mV^2} \frac{\delta Q}{Q^2} \quad \dots \quad (16)$$

The total ionising cross-section is obtained by integrating this expression within the limiting values of  $Q$ . These are the maximum energy communicated when  $p = 0$ , and  $W_i$ , the energy needed to release an electron from the  $\text{Fe}^{+16}$ -ion. We have then

$$\sigma_i^e = \frac{2\pi e^4}{mV^2} \left[ \frac{1}{W_i} - \frac{1}{Q_0} \right] \quad \dots \quad (17)$$

In the case of ionisation by the proton, or any heavy particle it can be shown by a similar procedure that  $Q_{\max} = 2 mV^2 = 4Q_0$ . So we have

$$\sigma_i^p = \frac{2\pi e^4}{mV^2} \left[ \frac{1}{W_i} - \frac{1}{4Q_0} \right] \quad \dots \quad (18)$$

So we have

$$\sigma_i = \sigma_i^e + \sigma_i^p = \frac{4\pi e^4}{mV^2} \left[ \frac{1}{W_i} - \frac{5}{8Q_0} \right] \quad \dots \quad (19)$$

Now, if we put  $V_i = scf$  we have, since  $\frac{1}{2} mc^2 f^2 = e^2/a_B$ ,  $W_i = z_i^2 \frac{e^2}{2a_B}$ ,  
 $Q_0 = \frac{1}{2} mV^2$

$$\sigma_i = 8\pi a_B^2 \cdot \frac{s^2 - \frac{5}{8} z_i^2}{s^4 z_i^2} \quad \dots \quad (19a)$$

According to Table 2, we have in the solar envelope 90% H-atoms, 3.5% O-atoms, 3.5% C-atoms, and 3% electrons. The O-atoms have each 8 electrons, and each one of these electrons can ionise the  $\text{Fe}^{+}$ -ion, and similarly some of the electrons of the C-atoms. So the number  $n$  of electrons per c.c. which can ionise the  $\text{Fe}^{+}$ -ion is given by

$$n = n_H + n_O z_1 + n_C z_2 + n_e$$

where  $n_H$ ,  $n_O$ ,  $n_C$  are the number of H, O and C-atoms.  $n_e$  = number of free electrons.

Taking  $z_1, z_2 = 8$ , we have  $n = 90 + 8 \times 3.5 + 8 \times 3.5 + 3 = 150$  nearly for 100 solar atoms.



The number of heavy molecules, on the other hand, remain 100. Hence we have

$$\sigma_l = \sigma_l' + \sigma_l^\wedge = 1.50 \left[ \frac{1}{W_i} - \frac{1}{Q_0} \right] + \left[ \frac{1}{W_i} - \frac{1}{4Q_0} \right] = 2.50 \left[ \frac{1}{W_i} - \frac{0.7}{Q_0} \right]$$

So we have the effective cross-section

$$\frac{\sigma_l}{2.5} = 8\pi a_B^2 \frac{\{s^2 - \alpha z_i^2\}}{s^4 z_i^2} \quad \dots \quad (20)$$

If we multiply this quantity by  $n$ , the number of atoms per c.c.

$$\lambda_l = \frac{1}{2.5n\sigma_l} = \frac{1}{20\pi a_B^2} \left( \frac{s^4 z_i^2}{s^2 - \alpha z_i^2} \right) \quad \dots \quad (21)$$

Under the assumptions made here  $\alpha = 0.7$ , but it can have any value from 0.7 or a somewhat higher value to 0.625 for a purely hydrogen atmosphere.

We have not applied the correction introduced in the ionisation formula by Thomas and E. J. Williams (1933) due to the orbital motion of the electrons as the theory is not yet much developed. The introduction of these corrections may modify the argument substantially.

The value  $\log(\sigma/a_B^2)$ , for different values of ' $s$ ' and  $z_i$  are shown in fig. 3.

The general features of these  $\sigma_l$ -curves for the iron-ions may be noted.

We find that there is a critical velocity  $s_c$  below which  $\sigma_l$  vanishes. The value of  $s_c = \sqrt{\alpha} z_i$ . These critical values of velocity and the corresponding energies of the iron-ion are given in the second and third rows of Table 6.

TABLE 6.

Fe <sup>+</sup> ..	16	15	14	13	12	11	10	9	8
$s$ ..	8.072	5.010	4.844	4.392	4.234	4.108	3.865	3.673	3.471
$E$ (in mev.)	92.26	35.55	33.22	27.32	25.37	23.89	21.14	19.10	17.06
$s_m$ ..	11.41	7.086	6.850	6.212	5.987	5.809	5.466	5.194	4.909
$E$ (in mev.)	184.5	71.09	66.43	54.63	50.75	47.77	42.29	38.19	34.12

The maximum value of  $\sigma_l$  occurs at  $s = \sqrt{2\alpha} z_i$ , i.e. at 0.99 $z_i$ , i.e. very nearly at  $s = z_i$ . The value of  $\sigma_l$  (called  $\sigma_{lm}$ ) at this point is given by  $(\sigma_{lm}/a_B^2) = 7.1\pi/z_i^4$ . The value of  $s_m$  for the different ions is given in the fourth row of Table 6.

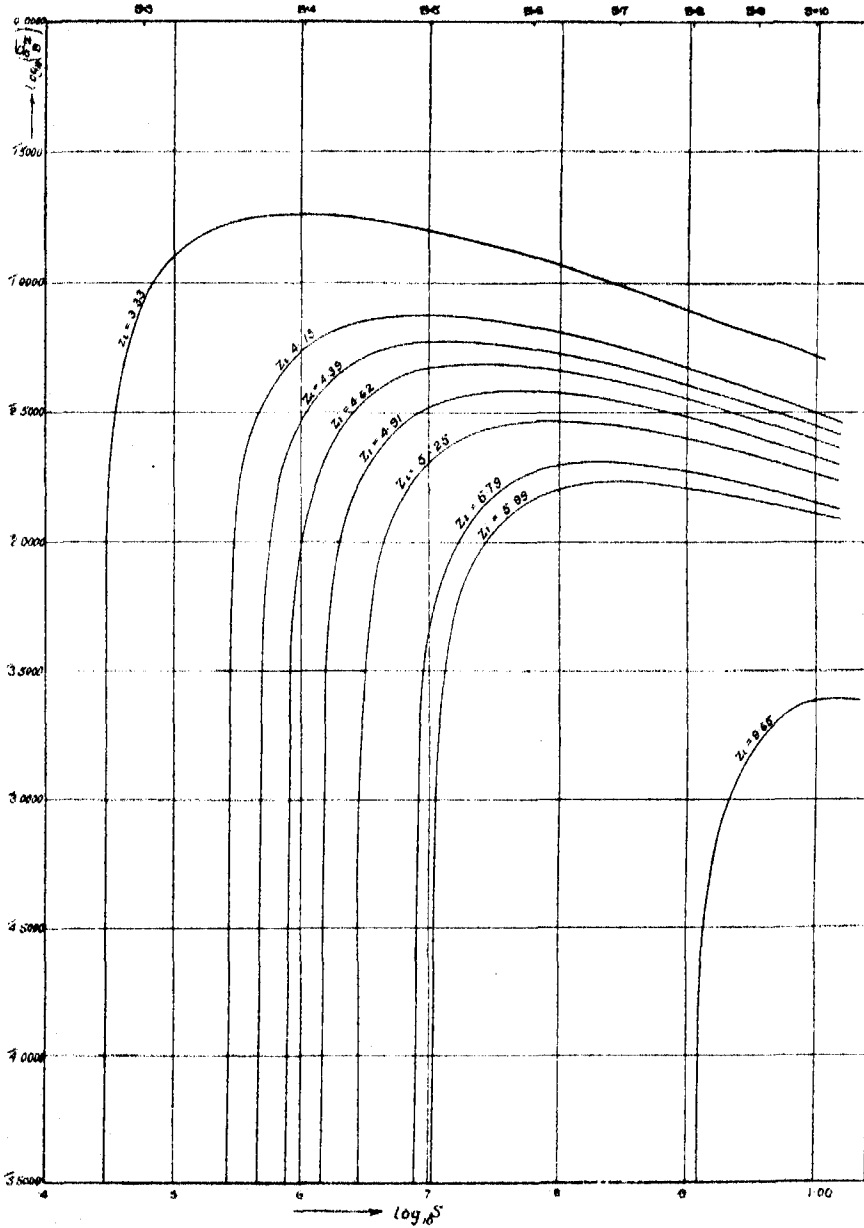


FIG. 3.

The  $\log \left( \sigma_l / a_B^2 \right) - \log s$  curves are drawn in fig. 3. We note that  $\log \left( \sigma_l / a_B^2 \right)$  rise from  $-\infty$  (i.e.  $\sigma_l = 0$ ) at  $s_c$  very steeply to the maximum value at  $s_m = \sqrt{2} s_c$ , and then falls down in a very gentle slope.

*Electron-capture by the Fe-ions.*

In this section, the cross-section for electron-capture by the Fe-ions are calculated. The electron captured may be :—

- (1) a free electron,
- (2) electron bound to the H-atom in the 1s-state,
- (3) electron bound to the C-atoms, oxygen and other constituents of the solar envelope.

*Capture of Free Electrons.*

The problem of capture of free electrons by hydrogen-like ions has been very fully treated by Stobbe (1930). He has given tables of the capture cross-sections of free electrons moving with the velocity ' $V$ ', relative to a stationary hydrogen-like ion with the charge  $z_i$ , the capture being effected in the  $ns$ ,  $np$ ,  $nd$  orbits.

In our present case, the ion is moving through the solar envelope with the velocity  $V_i = c.f.s.$  The velocity of the electrons relative to the  $Fe^+$ -ion is given by  $\vec{V} = \vec{V}_i - \vec{V}_e$ , where  $\vec{V}_e$  is the velocity of the free electron.

Now  $|V_i| \gg |V_e|$ , hence we can put  $\vec{V} = \vec{V}_i$  (*vide* Stobbe's table, p. 687).

Stobbe expresses his capture cross-sections in the form of functions of a quantity  $x$  which in our notation  $= \frac{ns}{z_i}$ , where  $n$  is the total quantum number. With the aid of these tables, we can attempt an estimate of the cross-section for the capture of free electrons by Fe-ions.

For  $Fe^{+16} \dots 1s^2 2s^2 2p^6$ , we have  $z_i/3 = 5.99$ , and ' $s$ ' may be supposed to vary from 6 downwards. We have, therefore,  $x = \frac{ns}{z_i} = 1 \dots \dots \dots$  to 0.16, the lower limit being for  $s = 1$ . According to Stobbe's tables,  $\sigma_{25}$  ( $q_{30}$  in Stobbe's notation) varies from  $4.06 \times 10^{-26} \text{ cm.}^2$  to  $\approx 5 \times 10^{-21} \text{ cm.}^2$

Since there are probably not more than  $6 \times 10^{20}$  electrons in the solar envelope, we see that the probability of capture of free electrons by the  $Fe^{+16}$  ion is extremely small, except when the velocity has fallen to  $V_i \approx cf$ . But this takes place in the high chromosphere, where there are not sufficient electrons to capture.

It can be shown in a similar way that the capture cross-section of free electrons by  $Fe^{+15} \dots 3s$  is of the same order.

When we come to the Fe-ions,  $Fe^{+14}$  to  $Fe^{+9}$ , the capture takes place in the  $3p$ -orbit. As a first step, the problem may be treated as hydrogen-like, the value of  $x = \frac{ns}{z_i}$  being obtained from the known values of  $(z_i/n)$ , given in Table 5. The value of  $q_{3p}$  is obtained from Stobbe's tables (p. 687),

it =  $q_{31}$  in his notation. At low velocities, these values are larger than  $q_{3s}$ , but at high velocities they are smaller. For  $\text{Fe}^{+9}$ ,  $z_i/3 = 4.39$ ,  $\frac{ns}{z_i} = 0.228$ ,  $q_{3p} \simeq 5 \times 10^{-22} \text{ cm}^2$ . Hence the probability of capture of free electrons by  $\text{Fe}^{+9}$ -ions is generally very small.

### Case (2).

The general case of electron capture by a swiftly moving ion from any type of ion or atom has not yet been solved. Kramers and Brinkmann (1930) have given a solution of the problem of capture of an electron moving in the  $s$ -orbit of some atom by a charged-particle into its own  $s$ -orbit, both being regarded hydrogen-like. These results have been applied by them to the data of Rutherford (1923) and Jacobsen (1930) on the capture and loss of electrons by  $\text{He}^{++}$ -particles with good success.

The capture cross-section from one  $1s$ -orbit to another  $1s$ -orbit is given by the formula,\*

$$\frac{\sigma}{a_B^2} = \frac{\pi}{5} \cdot 2^{20} \cdot z^5 \cdot z'^3 \cdot s^8 / [s^2 + (z+z')^2]^5 [s^2 + (z-z')^2]^5 \quad \dots (22)$$

Here the atom-ion is assumed to have the charge  $z'$ , and moves with the velocity  $V = cz$ .

$z$  = charge on the atom from which the electron is captured.

When the capture is from an  $1s$ -orbit to an  $ns$ -orbit, we have

$$\sigma_n = n^2 \sigma_1(z, z'/n) \quad \dots \dots \dots (23)$$

In the present case, the  $\text{Fe}^{+16}$ -ion is capturing an electron into the  $3s$ -orbit from the H-atom, the electron there being in the  $1s$ -orbit. We have put  $n = 3$ ,  $z'/3 = z_i$  of Table 5 = 5.99,  $z = 1$ . Hence we have for  $\text{Fe}^{+16}$

$$\frac{\sigma}{a_B^2} = 3^3 \cdot \frac{\pi}{5} \cdot 2^{20} \cdot 5.99^3 \cdot \frac{s^8}{[s^2 + 6.99^2]^5 [s^2 + 4.99^2]^5} \quad \dots (22a)$$

We can apply the same formula for the capture of an electron by the  $\text{Fe}^{+16} \dots 1s^2 \cdot 2s^2 \cdot 2p^6 \cdot 3s$  thus completing the  $3s^2$ -shell. We have to put  $z_i = 5.79$ . We have then

$$\left( \frac{\sigma_c}{a_B^2} \right) = \frac{3^2 \cdot \pi \cdot 2^{20}}{5} \cdot (5.79)^3 \cdot \frac{s^8}{[s^2 + 6.79^2]^5 [s^2 + 4.79^2]^5} \quad \dots (22b)$$

Values of  $\sigma_c$  for  $\text{Fe}^{+16}$  and  $\text{Fe}^{+15}$  different values of ' $s$ ' are given in Table 7.

---

\* This formula is different from K. and B.'s No. (4), by the factor  $\frac{2^3}{z'^3}$ . As K. and B. treat a case where  $z' = 2$ , their calculations remain unchanged.

TABLE 7.  
 $\sigma_c$ -Values.

$\log (v_c / \alpha_B^2)$ \ $s$	8	7	6	5	4	3	2	1
Fe <sup>+16</sup> ..	4.3214	4.5694	4.7632	4.8636	4.8024	4.4584	5.5921	7.5491
Fe <sup>+15</sup> ..	4.3803	4.6453	4.8621	4.9800	4.9593	4.6483	5.8160	7.7990

*Electron Balance of the Fe-ions on passage through the Solar envelope.*

From the above results on the loss and capture cross-sections of highly ionised atom-ions, we can visualise to some extent the problem of their electron-balance, as they pass through the solar envelope. We assume that the Fe<sup>+16</sup>-ion is formed with an energy of 60 mev.,  $V = 6.5$  cf. According to (17), the Fe<sup>+16</sup> can never lose any further electron as this velocity is  $< 8.06$  which is the critical value of  $s$  for this ion (*vide* Table 6).

But the Fe<sup>+16</sup>-ion can capture an electron, for at this velocity we find from Table 7 that  $\sigma_c \simeq 1.4 \times 10^{-20}$  cm.<sup>2</sup> and the value increases as the velocity falls. The capture takes place after the Fe<sup>+16</sup>-ion has traversed approximately  $7 \times 10^{19}$  H-atoms, or even less. By this time we calculate from (3a) that the energy falls to  $\simeq 58$  mev. and the velocity to  $s = 6.4$ .

*Career of the Fe<sup>+15</sup>-ion.*

For the Fe<sup>+15</sup>-ion, the critical velocity for loss is  $s = 5.01$  cf. But the Fe<sup>+15</sup>-ion may start with a velocity of 6.4 cf and  $\sigma_l$  at this point  $= 1.3 \times 10^{-18}$  cm.<sup>2</sup>. This is a rather large value, and Fe<sup>+15</sup> has a chance of losing the electron as soon as it is captured. This may happen, but all this while, the ion goes on losing energy, and the process is repeated, but with lesser chances for loss and increasing chances of capture. So during the stretch  $s = 6.4$  to  $s = 5.01$ , Fe<sup>+15</sup> may lose and capture electrons a large number of times till ultimately at  $s = 5.01$  corresponding to the energy 35.55 mev.  $\sigma_l$  vanishes altogether. The ion, by now, has traversed nearly  $4 \times 10^{20}$  H-atoms (*vide* Fig. 1). There are still about  $7 \times 10^{20}$  H-atoms to traverse.

*The Fe<sup>+14</sup> ion.*

From  $s = 5.01$  to 4.84,  $E = 35.55$  mev. to 33.22 mev. the Fe<sup>+14</sup>-ion will have a career similar to that of the Fe<sup>+15</sup>-ion. The loss cross-section for Fe<sup>+14</sup> at  $s = 5.01$  amounts to  $1.37 \times 10^{-19}$  cm.<sup>2</sup>. The capture cross-section cannot be estimated as the capture is now in the 3p-orbit. Let us

suppose that it is  $1/10$  that for the  $3s$ -orbit for a similar ion, with  $s = 5.01$ . Then we have  $\sigma_c \simeq 5 \times 10^{-21}$  cm.<sup>2</sup> and this varies rather gently with velocity. So at first  $\text{Fe}^{+14}$ -ion will lose electrons more frequently than it captures but as the velocity falls to  $s = 4.84$ ,  $\sigma_l$  vanishes and  $\text{Fe}^{+14}$  can only capture an electron, and be converted to  $\text{Fe}^{+13}$  either in the  $3p\ 2P_{\frac{1}{2}}$  or in the  $3p\ 2P_{\frac{3}{2}}$ -state. But on account of the smaller value of  $\sigma_c$ , viz.  $5 \times 10^{-21}$  cm.<sup>2</sup> the  $\text{Fe}^{+13}$ -ions have a chance of reaching greater heights, i.e. even a region where H-atoms do not exist, with small velocities. If the capture is in the  $3p\ 2P_{\frac{3}{2}}$ -orbit, conditions are favourable for a forbidden transition to  $3p\ 2P_{\frac{1}{2}}$ , for the time of flight is nearly 10 seconds, and there are very few electrons or atoms to encounter. Following the general procedure laid down by Condon and Shortley, Pasternack (1940) has calculated the values of transition probabilities of the metastable levels arising from  $p^2$ -combinations ( $x = 1$  to 5). From the values of these transition probabilities and the intensity of the coronal lines, it will be possible to calculate the number of  $\text{Fe}^{+13}$ -ions streaming through the solar envelope, and thus forming an estimate of the contribution of this process to the total energy production in the sun. But these considerations are postponed pending calculations of the capture cross-sections in the  $3p$ -orbits.

The formation of the other iron-ions with lower net charge, viz. of  $\text{Fe}^{+12}$   $3p^2$ ,  $\text{Fe}^{+11}$   $3p^3$ ,  $\text{Fe}^{+10}$   $3p^4$ ,  $\text{Fe}^{+9}$   $3p^5$ .....takes place according to the same process as is described for  $\text{Fe}^{+13}$ , by successive capture of electrons, after the velocity of the ion has been reduced by the ionisation-loss to the critical values. A detailed discussion is postponed pending the calculation of  $p$ -capture cross-sections.

From this discussion, it appears that  $\text{Fe}^{+13}$ -ion will be formed usually at a lower level than the succeeding ions, and the  $\text{Fe}^{+9}$ -ion will be formed at the highest level. But these formation processes all take place in the highest level chromosphere, and the technique is probably not sufficiently advanced to enable astrophysicists to find out the levels where these lines originate.

#### CONCLUSION.

If the considerations presented in this paper be correct, the occurrence of the coronium lines in the solar corona form the first clear fingerpost that nuclear reactions are not confined to the interior of the stars, as already postulated with a certain amount of success by Gamow (1939), and Bethe (1938), and others, but they also take place on the surface of the Sun, and therefore generally on stars as well, and modify in varying degrees the phenomena taking place there. In this connection, the following intuitive remarks of the late Lord Rutherford may be quoted:

'In the furnace of the Sun and other hot stars, the electrons, protons, neutrons, and atoms present must be endowed with high average velocities owing to thermal agitation. It is thus to be expected that the processes both

of disintegration and aggregation of nuclei, such as are observed in the laboratory, should be operative on a vast scale for all nuclei, and that a kind of equilibrium should be set up between these two opposing agencies of dissociation and association for each type of atomic nucleus.'

But it is obvious that before we can go to the root of the problems raised by the extraordinary discovery of the origin of coronal lines by Grotrian and Edlen, a large amount of theoretical work and practical observations and work is needed. As the writer of the present paper will not be in a position to tackle all these problems single-handed, or resume these studies for some time, a brief résumé of some of these problems is given:—

(1) The production of stripped iron and other atoms has been supposed to be due to some kind of nuclear reaction, analogous to Uranium Fission, but the heaviest elements so far discovered on the Sun are  $\text{Ra}^{226}$  (this is considered doubtful by some). Osmium and Platinum, Uranium and Thorium lines have not so far been discovered, probably because the spectra of these elements have not been so far analysed and classified. It will be a useful task to get the lines of the fission elements classified and look for their occurrence in the Sun.

With respect to the probability of threefold or fourfold fission, fresh experiments are obvious suggestions; if the Fe and Ni-ions responsible for the coronium lines consist of the usual isotopes they should be the end-products of a successive series of  $\alpha$ -ray disintegrations, and hence the primary product of fission may be some element with a lesser charge, say  ${}_{23}\text{V}^{60}$  or  ${}_{24}\text{Cr}^{60}$  but with an extraordinarily large mass, far larger than that of the isotopes of these elements occurring in Nature. This may occur from the fission of the A-products or B-products (Saha, 1941), some of which have very large mass and may therefore possess an inherent instability for fission.

This subject belongs obviously to nuclear physics and has been treated in detail by Bohr and Wheeler (1939), and Flüge (1939).

(2) We require a better knowledge of the composition and density-gradient of the elements in the reversing layer, the chromosphere, and the corona. Our knowledge of the transition layer between the top of the chromosphere (14") and the beginning of the inner corona (48") is particularly defective. Very good work on this line can be done during total solar eclipses, when attempts should be made to photograph fainter coronal lines and prove or disprove their presence. The transitional region may be investigated by means of a powerful Lyot coronagraph at good heights, say at Kodaikanal.

(3) Some progress has been made on the explanation of the peculiarities of the inner and the outer corona on the basis of the  $\delta$ -ray theory, briefly referred to in § 3, but the matter is so extensive that it can be taken up only in a separate article.

The author expects to return to these and other problems which obviously suggest themselves to an astrophysicist, as soon as circumstances allow him to do so.

It is a great pleasure to record my thanks to my pupils who have taken part in the discussions and helped in the calculations. Mr. D. Kundu has gone through the spectroscopic data as far as available; Messrs. P. C. Bhattacharyya and S. K. Ghosh have checked the calculations and helped in drawing the figures.

## REFERENCES.

- Anderson, 1926, *Zs. f. Physik*, **37**, 342 (previous references will be found there).  
 Babcock, 1934, *Proc. Ast. Soc. Pac.*, **46**, 132.  
 Bethe, 1932, *Zs. f. Physik*, **76**, 293.  
 1938, *Phys. Rev.*, **54**, 436.  
 Bhattacharyya, P. C., 1941, *Proc. Nat. Inst. Sci.*, **7**, 275.  
 Bloch, 1933, *Ann. d. Physik*, **16**, 285.  
 Bohr and Wheeler, 1939, *Phys. Rev.*, **56**, 426.  
 Bohr, 1940, *Phys. Rev.*, **58**, 650.  
 1941, " " **59**, 270.  
 Bowen, 1936, *Rev. Mod. Phys.*, **8**, 55.  
 Bowen and Wyse, 1940, *Lick Obs. Bull.*, **19**, 1.  
 Bumbauch, 1937, *A.N.*, 263.  
 Cillié and Menzel, 1935, *Harvard Circular*, 410.  
 Condon and Shortley, *The Theory of Atomic Spectra*.  
 Flügge, 1939, *Zs. f. Phys. Chemie*, B, **42**, 274.  
 Gamow, 1939, *Phys. Rev.*, **55**, 718.  
 Grotrian, 1931(a), *Zs. f. Ast. Physik*, **2**, 106.  
 1931(b), " " " " **3**, 199.  
 1933, " " " " **7**, 26.  
 1934, " " " " **8**, 124.  
 Henderson, 1923, *P.R.S.L. (A)*, **102**, 496.  
 Heisenberg and Euler, 1934, *Naturwissenschaften*.  
 Jacobsen, 1930, *Phil. Mag.*, **10**, 401.  
 Knipp and Teller, 1941, *Phys. Rev.*, **59**, 659.  
 Kramers and Brinkmann, 1930, *Proc. K. A. Amsterdam*, **30**, 973.  
 Kundu, 1942, *Science and Culture*, **7**, 364.  
 Lamb Jr., 1941, *Phys. Rev.*, **58**, 696.  
 Lehmann, 1927, *P.R.S.L. (A)*, **115**, 624.  
 Livingstone and Bethe, 1937, *Rev. Mod. Phys.*, **9**.  
 Lyot, 1934, *Zs. f. Ast. Physik*, **5**, 73.  
 1936, *M.N.R.A.S.*, **99**, 580.  
 1937, *L'Astronomie*, **51**, 203.  
 McCrea, 1929, *M.N.R.A.S.*, **89**, 483.  
 1934, " " **95**, 80.  
 Menzel, 1931, *Lick Observatory Bull.*, **17**, 348.  
 Millmann, 1933, *Pop. Astr.*, **41**, 298.  
 Milne, 1921, *M.N.R.A.S.*, **81**, 375 and onwards.  
 Minnaert, 1930, *Zs. f. Ast. Physik*, **1**, 226.  
 Mitchell and E. T. R. Williams, 1933, *Astro. Jour.*, **77**, 197.  
 Moore, 1934, *Proc. Ast. Soc. Pac.*, **46**, 298.  
 Nagaraja Aiyar, Pringsheim, *Physik der Sonne*.  
 Pannekoek and Minnaert, 1928, *Verh. Akad. Wet. Amsterdam*, **13**.  
 Pasternack, 1940, *Ast. Phy. Jour.*, **92**, 129.  
 Perepelkin and Melnikov, 1935, *Pulkovo Bulletin*, No. 122, 14.



- Rosseland, 1933, *Pub. Obs. Univ. Oslo*, No. 5.  
 1934, *Theoretical Astrophysics*, Chap. XIV.  
 Russell, 1929, *Astrph. Jour.*, **69**, 49.  
 1929, „ „ **70**, 11.  
 1941, *Scien. American*, August.  
 Saha, 1941, *Science and Culture*, **7**.  
 Stobbe, 1930, *Ann. d. Physik*, **7**, 661.  
 Thackery, 1941, *Report on Solar Physics* (Progress of Physics, Physical Society, London),  
**7**, 160.  
 Thompson, J. J., 1932, *Conduction of Electricity through Gases*, p. 97.  
 Unsöld, *Physik der Sternatmosphäre*, Kap., **17**.  
 Waldemeier, 1938, *Zs. f. Ast. Physik*, **15**, 44.  
 Williams, 1932, *P.R.S.L. (A)*, **135**, 108.

## X-RAY STUDIES IN INDIAN COALS. PART I.

By J. DHAR, *M.Sc., A.Inst.P.* and B. B. NIVOGI, *B.Sc., A.I.C., Indian School of Mines, Dhanbad.*

(Communicated by Dr. K. Banerjee, D.Sc., F.N.I.)

(Read January 1, 1942.)

### ABSTRACT.

Several samples of vitrains and of a few other constituents of coal have been studied by the X-ray diffraction method. The vitrains so far examined indicate the presence of two characteristic rings of mean spacings  $3.7\text{--}3.8\text{\AA}$  and  $2.1\text{--}2.3\text{\AA}$  which are analogous to the spacings of corresponding prominent rings in the case of graphite. A strong small-angle scattering is invariably present. The diffraction pictures of vitrain, durain and fusain are distinctive among themselves. The durain picture is a superposition of the pictures of graphite and ash. The pictures of vitrains from the Jharis and Raniganj field suggest a striking difference in rank and quality. This is in accord with the findings from chemical analysis.

### I. INTRODUCTION.

Since the discovery of X-rays in 1895, among the numerous important uses has been that of the application to the examination of coal. In this type of investigation the pioneer was H. Couriot<sup>1</sup> who, in 1898, submitted anthracite, bituminous coal and other fuels to X-rays and obtained in their radiographs nearly every detail of the intimate structure of the mineral matter. Some attempts were later made to apply X-rays to the study of coals<sup>2</sup> by shadow photographs and to correlate the results with chemical analysis. But it has only been since 1924 that radiographic and radio-densimetric methods were systematically and extensively employed, with improved technique, by C. Norman Kemp<sup>3</sup> to the study of coal structures. Owing to the varying absorptive power of the ash of a coal, the shadow photographs obtained indicate in a remarkable manner the distribution of ash in coal and hence enable the variation of such distribution in coals from various coal-seams to be traced.

Forrester,<sup>4</sup> availing himself of the X-ray equipment of Norman Kemp, took radiographs of twenty-four samples of Indian coals in order to compare them with the result of washability tests.

In 1927 C. Mahadevan<sup>5</sup> commenced a systematic study of Indian coals from various seams widely scattered, by the Debye-Scherrer method of X-ray diffraction. In a series of interesting articles he drew certain important conclusions on the subject quite in accord with the findings of Sir Lewis Fermor from chemical and other sources. Since then no further X-ray studies on coal have been attempted, so far as the present authors are aware.



TABLE I. *X-ray Results*—(continued).  
 Spacings observed in Å units.

Serial No.	Nature of coal.	Source of coal.	$d_1$	$d_2$	$d_3$	$d_4$	$d_5$	$d_6$	$d_7$	$d_8$	$d_9$	$d_{10}$	$d_{11}$
11	Vitrain (Fig. 2).	Singareni Colliery (Hyderabad).	3.79 s.	2.60 m.	..	..	..	..	..	..	..	..	..
12	Durain (Fig. 7).	Do. do.	7.65 m.	4.40 m.	3.87 w.	3.50 v.s.	2.89 v.w.	2.61 w.	2.36 w.	2.18 v.w.	2.03 w.	1.86 w.	1.69 v.w.
13	Fusain (Fig. 8).	Do. do.	4.12 s.	3.15 m.	2.60 w.	2.35 v.w.	2.12 v.w.	1.95 w.	1.78 v.w.	..	..	..	..
14	Fusain (Fig. 4).	X Seam. Jharia	4.44 m.	3.56 s.	2.54 w.	2.08 v.w.	..	..	..	..	..	..	..

TABLE II. *Vitrinite*.

Serial No.	Source of Coal.	PROXIMATE CHEMICAL ANALYSIS.				X-RAY ANALYSIS.	
		Moisture.	Volatile matter.	Fixed carbon.	Ash.	Description of X-ray pattern.	Width of the strongest characteristic halo observed in mm.
1	XII Seam. Dharia-Jobe Colliery (Jharia field).	0.04	23.37	74.65	1.34	Interspace clear; first ring strong and well-defined but the second ring diffuse and weak.	5.5
2	VII Seam. Golmukdih Colliery (Jharia field).	0.88	23.17	73.91	2.04	Do. do. (Fig. 1.)	5.7
3	X Seam. Gandrudih Colliery (Jharia field).	0.83	21.90	76.25	1.12	Do. do.	6.0
4	Ghusick Colliery (Raniganj).	4.23	36.70	53.33	5.74	Interspace not very distinct; first ring sharp; second ring very broad and several other sharp rings weak in intensity. (Fig. 3.)	11
5	Satpukuria Colliery (Raniganj).	5.10	33.47	56.76	4.67	Do. do.	10.5
6	X Seam. Alkusa South (Jharia field).	1.50	24.02	73.26	1.22	Interspace fairly clear; first ring sharp and well-defined; second ring diffuse and weak.	4.8

TABLE II. *Vitrinite*—(continued).

Serial No.	Source of Coal.	PROXIMATE CHEMICAL ANALYSIS.				X-RAY ANALYSIS.	
		Moisture.	Volatile matter.	Fixed carbon.	Ash.	Description of X-ray pattern.	Width of the strongest characteristic halo observed in mm.
7	XII Seam. Alkusa South (Jharia field).	1.44	23.80	73.66	1.10	Interspace quite indistinct; first ring very strong; second ring weak but distinct; third ring very diffuse and weak.	7.0
8	XI Seam. Alkusa North (Jharia field).	1.48	22.48	74.49	1.55	Interspace fairly clear; first ring strong and sharp. (Fig. 5.)	9.0
9	XII Seam. Alkusa North (Jharia field).	1.32	24.22	73.06	1.40	Interspace quite indistinct. First ring very strong; second ring spread out and weak; third ring very diffuse and very weak. (Fig. 6.)	9.0
10	XIIIA Seam. South Kustore (Jharia field).	1.78	23.38	73.86	0.98	Interspace fairly clear; first ring sharp but second ring weak and broad.	7.5
11	Singareni Colliery (Hyderabad).	*	*	*	4.29	Interspace almost indistinct even in filtered radiation; first ring broad and second ring weak but sharp. (Fig. 2.)	14

\* The substance at our disposal is too meagre to allow full chemical analysis.

As coal is an important mineral of industry and its systematic study may lead to vast possibilities from both academic and industrial points of view, the authors have taken up a systematic and extensive study of the coal structure on similar lines to and in continuation of Mahadevan's work with a more powerful X-ray-unit and larger substance-to-plate distances.

Vitrain is generally regarded as representing the fundamental coal-substance. It is, therefore, considered that an exhaustive study, by means of X-rays, of vitrains from different seams of the same district as well as of different districts may throw some light on the rank and quality of the coal substance. This paper presents a preliminary report of the results of this investigation. An attempt is also made to correlate the X-ray diffraction patterns of the various samples of vitrain with their composition as ascertained by proximate chemical analysis. A few other constituents of coal have also been studied in this connection.

## 2. EXPERIMENTAL.

The X-rays used for the examination of coals were the Cu-K radiations emitted from the target of a Siegbahn-Hadding tube. The copper anticathode is cooled by means of tap water but the aluminium cathode by a pumping arrangement suspended from the ceiling. The high tension as supplied by an oil-cooled transformer to the cathode of the X-ray tube is rectified by a kenotrone. The high vacuum was obtained by a four-stage mercury-diffusion pump backed by a Cenco pump. The leak was maintained by the needle-valve on the low vacuum side. The tube runs smoothly when the primary of the transformer is supplied with an A.C. supply of 140 volts. The secondary current was 15 milliamps and the high tension supply usually 35-40 k.v.

A very intense X-ray beam is usually obtained under these conditions and the X-ray tube runs smoothly almost without attention. The time-exposure needed is usually 1 hour, or 2 hours when a nickel-filter is used.

The camera consists essentially of a platform carrying at one end a brass rod with a fine circular hole bored along the axis and at the other end a plate-holder. The hole opens out wider at the end close to the plate holder. X-ray-duplitised film is cut into suitable size, enclosed in a black-paper cover and then secured inside the plate-holder by screw attachments. A brass disc about 2 mm. thick has a circular orifice at the centre much wider than the opening of the slit. This orifice serves as the container of the substance. The disc can be attached with great ease to the end of the slit farther from the window of the X-ray tube.

The coal samples were first of all finely powdered and then inserted into the hole of the brass disc which was then placed on the slit. The powder was then exposed for an hour or so. To cut off the direct beam a lead-shield is used and is shifted for a while at the end of each exposure to register the direct beam. Wherever necessary the same sample was exposed for longer

periods using the Ni-filter. When the background showed general blackening, the filter was invariably used. The exposed films were all developed in Rodinal developer for 5 mins. at 18°C.

The photographs show the Debye-Scherrer patterns in the form of concentric rings. The inner and outer radii of the rings were carefully measured. The spacings corresponding to each ring were then calculated from  $\lambda = 2d \sin \theta$  where  $\tan 2\theta = \frac{R}{D}$  where  $R$  is the mean radius of the ring and  $D$  the substance-to-film distance, and the other terms have their usual significance.

TABLE III.

Substance.	Spacings calculated in Å	Reflecting planes.	Remarks on intensity.
Graphite <sup>6</sup>	3.40	(002)	v.s.
	2.13	(100)	s.
	2.03	(101)	s.
	1.81	(102)	w.
	1.70	(004)	m.
	1.55	(103)	w.
	1.23	(110)	s.
	1.16	(112)	s.
SiO <sub>2</sub> (Silica)	4.25	(100)	..
	4.25	(010)	..
	3.35	(011)	..
Al <sub>2</sub> O <sub>3</sub> (Alumina)	4.01	(100)	..
	4.01	(010)	..
	3.54	(011)	..

### 3. RESULTS.

Several samples of vitrain have been subjected to X-ray and chemical examination and the results have been embodied in Tables I and II. For comparative analysis of the different constituents of coal the vitrain, durain and fusain of Singareni Colliery have also been examined. The results of these and of the fusain of X seam Jharia are also entered in Table I.

All the diffraction pictures of vitrains as well as of the other constituents of coal exhibit a strong scattering at a small angle corresponding to a spacing



of nearly  $12.3\text{\AA}$  which is probably due to the presence of a carbon complex of large molecular units. For the complete elucidation of this phenomenon a separate investigation into small-angle scattering would need to be carried out. The vitrains so far examined have two characteristic rings which correspond to the mean spacings  $3.7\text{--}3.8\text{\AA}$  and  $2.1\text{--}2.3\text{\AA}$ . The first ring is much stronger and sharper than the second ring. These spacings are analogous to the spacings  $3.4\text{\AA}$  and  $2.1\text{\AA}$  characteristic of graphite. The spacing  $3.7\text{--}3.8\text{\AA}$  refers to the inter-layer distance between hexagonal networks of carbon and is in accordance with the fact that the minimum distance of approach between carbon atoms in adjacent organic molecules<sup>6</sup> lies between  $3.4\text{--}3.9\text{\AA}$ .

On careful scrutiny of the tables and the X-ray pictures it would appear that the characteristic diffraction rings of Raniganj Series vitrains are distinctly broader than those of the same from the Jharia coalfield although they are all broader and more diffuse than the corresponding rings characteristic of graphite. This shows that the crystallinity of carbon is less perfect in these vitrains than in the graphitic carbon and as crystallinity matures with age the vitrains from the Jharia field are older than those from the Raniganj field. This is evident on reference to column 8 of Table II. It seems probable therefore that the X-ray diffraction patterns may enable us to distinguish between vitrains of the Jharia and Raniganj fields. The examination of a larger number and range of specimens would be desirable.

In general the interspaces between rings in pictures of vitrains belonging to the Jharia field are much clearer than those of the vitrains from the Raniganj field. An exception has, however, been observed in the sample from XII seam Alkusa (North and South). Diffraction pictures for vitrains Nos. 4 and 5 possess other sharp but weak rings indicating comparatively high ash-content.

This is in accord with the chemical analysis which also points to the comparatively high ash-content, high moisture and high volatile matter but low fixed carbon in the vitrains from the Raniganj field as compared with those from the Jharia field so far examined.

The diffraction pictures for durain and fusain from Singareni Colliery are themselves distinctive. The picture of fusain from X Seam Jharia also differs from that of Singareni Colliery. The pictures indicate that the durain and fusains contain large percentages of ash. In durain the spacings  $3.87\text{\AA}$  and  $2.89\text{\AA}$  are due to  $\text{Cu K}_\beta$  reflection, whereas the spacings  $7.65\text{\AA}$ ,  $4.40\text{\AA}$ ,  $2.61\text{\AA}$  and  $2.36\text{\AA}$  refer to the ash content and the remaining to the graphitic carbon. In fusain of Singareni Colliery the spacings  $4.12\text{\AA}$ ,  $2.6\text{\AA}$ ,  $2.35\text{\AA}$  are ascribed to ash while in fusain of X Seam Jharia only  $4.44\text{\AA}$  and  $2.54\text{\AA}$  refer to ash, the remaining spacings in each case refer to graphitic carbon. The fusain of X Seam Jharia seems to possess a lower ash-content compared with that from Singareni. The ash-content of durain and fusain is mostly silica and alumina. This is in accordance with the data in Tables I and III.

The work is in progress.

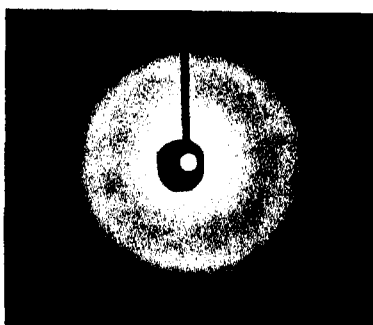
## ACKNOWLEDGMENT.

The authors are indebted to Principal Dr. C. Forrester and Dr. B. B. Banerji, of the Indian School of Mines as well as to Prof. S. N. Bose and Dr. K. Banerjee of the University of Dacca for kindly granting all facilities for this work. Our heartfelt thanks are also due to Mr. R. K. Sen, B.Sc., of the Dacca University for helping in taking the X-ray photographs.

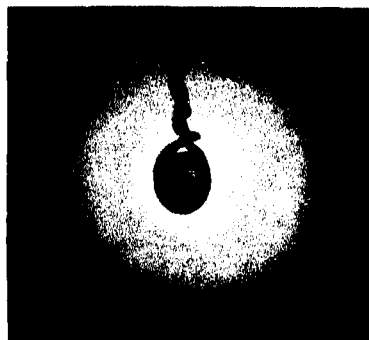
## REFERENCES.

- <sup>1</sup> Couriot, *Bull. de la Soc. Indus Minérale*, **12**, 713 (1898).
- <sup>2</sup> Daniel, *Ann. Mines de Belgique*, **4**, 3 (1899).  
Garret and Burton, *Trans. Inst. Min. Engrs.*, **43**, 295 (1912).
- <sup>3</sup> Kemp, *Trans. Inst. Min. Engrs.*, **67**, 59 (1924) and **77**, 175 (1929).
- <sup>4</sup> Forrester, *Trans. Min. Geol. Inst. Ind.*, **30**, 174 (1936).
- <sup>5</sup> Mahadevan, *Ind. Journ. Phys.*, **4**, 79 (1929).  
----- *Ind. Journ. Phys.*, **4**, 457 (1930).  
----- *Ind. Journ. Phys.*, **5**, 525 (1930).  
----- *Quart. Journ. Geol. Min. Met. Soc. Ind.*, **7**, 1 (1935).  
----- *Proc. Nat. Inst. Sci. Ind.*, **6**, 569 (1940).
- <sup>6</sup> Riley, *Trans. Inst. Min. Engrs.*, **95**, 57 (1938).
- <sup>7</sup> Hendricks, *Chem. Rev.*, **7**, 474 (1930).

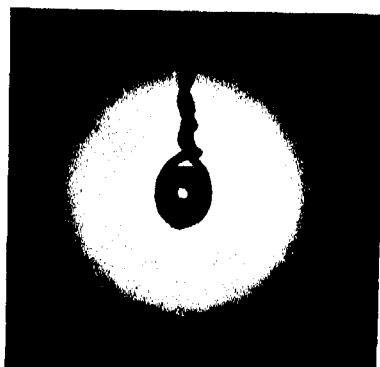




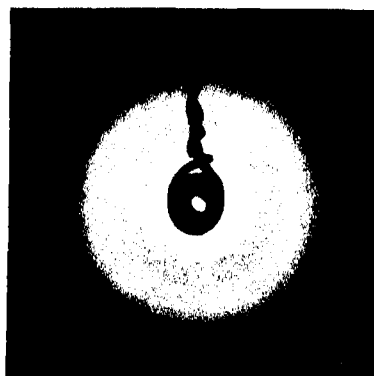
Vitrain (1)  
VII Seam Goluckdih Colliery (Jharia)



Vitrain (2)  
Singareni Colliery (Hyderabad)



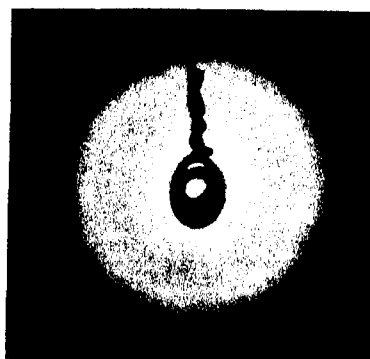
Vitrain (3)  
Ghusick Colliery (Raniganj)



Fusain (4)  
X Seam (Jharia)

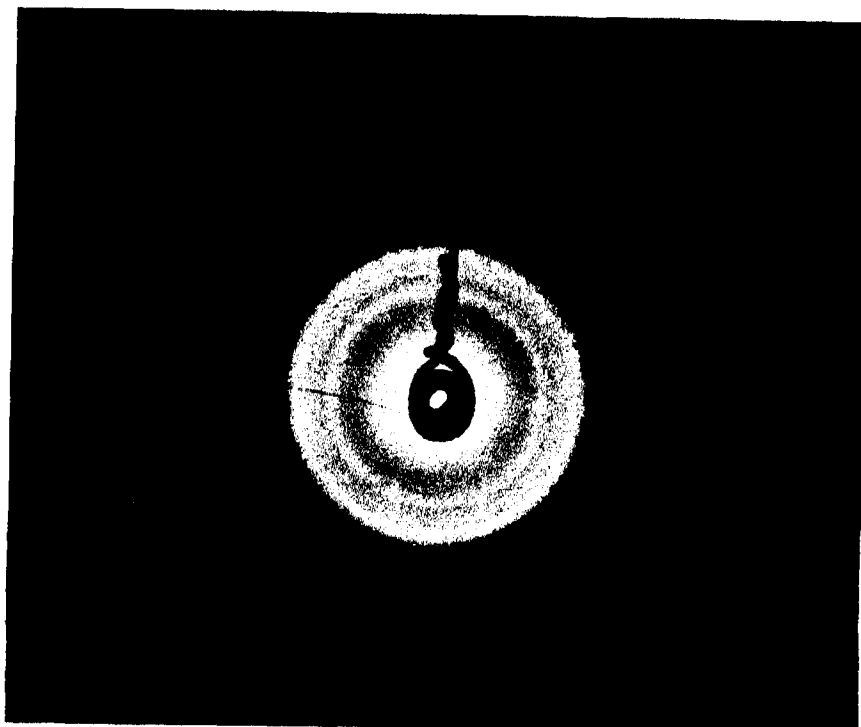


Vitrain (5)  
XI Seam Alkusa North

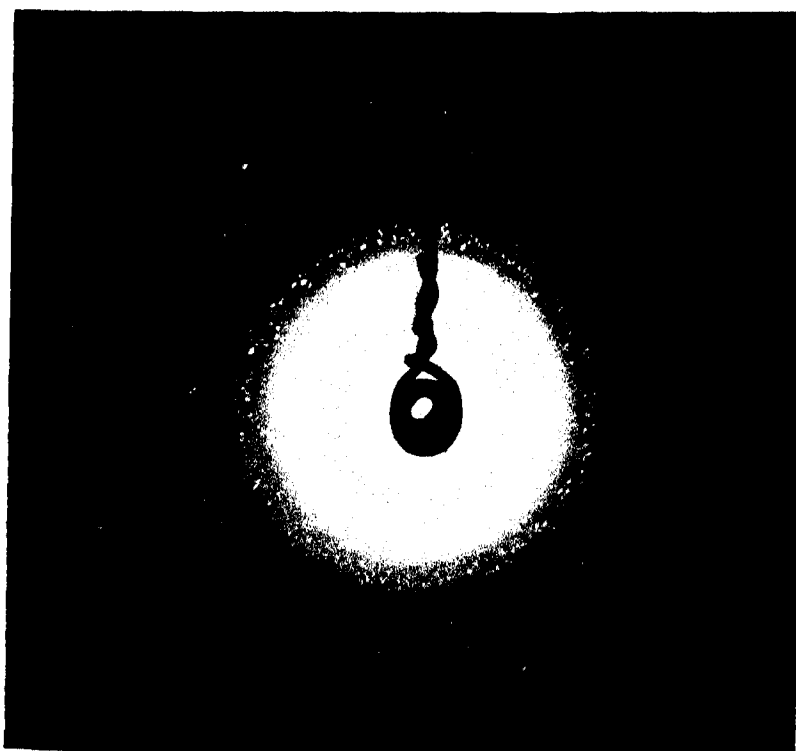


Vitrain (6)  
XII Seam Alkusa North





Durain (7)  
Singareni Colliery (Hyderabad)





## INDUCED REACTIONS WITH ASCORBIC ACID AS INDUCTOR.

By G. GOPALA RAO and T. V. SUBBA RAO, *Andhra University, Waltair.*

(Communicated by Prof. N. R. Dhar.)

(Received April 29, 1941.)

Whenever the reaction between a substance A and the substance B brings about the reaction between the substance C and the substance B, then the first reaction is said to induce the second reaction. In the absence of A from the reaction system, the substance B does not interact with the substance C under the conditions in which A interacts with B. But, when all the three substances, A, B and C are brought together, A and B react and this reaction provokes or induces the reaction between B and C. This phenomenon is called chemical induction. The reaction between A and B which occurs unaided is called the primary change and the reaction between B and C which does not occur in the absence of A is called the secondary change. An example will make this clear. Sodium sulphite (A) in dilute aqueous solution undergoes ready oxidation by interaction with atmospheric oxygen (B), while sodium arsenite (C) does not undergo reaction with oxygen under the same conditions. According to the customary nomenclature, the substance A which induces the chemical change is known as the 'inductor', and the substance B which takes part in both the changes is called the 'acceptor'.

A large number of reactions have been studied with sodium sulphite as inductor by various investigators. Only one reaction has so far been reported, where sodium sulphite acts as the acceptor. Gordon (*J. Phys. Chem.*, 1913, 17, 47) and W. D. Bancroft (*J. Phys. Chem.*, 1929, 33, 1188) suggested that the process of photographic development involves chemical induction. Verma and Dhar (*J. Phys. Chem.*, 1931, 35, 1770) and Pandalai and Gopala Rao (*Z. anorg. Chem.*, 1933, 215, 23) showed that in this reaction sodium sulphite acts as the acceptor. The primary reaction between the organic reducer (such as hydroquinone, pyrogallol, *p*-amino-phenol, etc.) and the silver halide induces the secondary reaction, namely the reduction of silver halide by sodium sulphite. Pandalai and Gopala Rao have also been able to elucidate the mechanism of this induced reaction. Recently, Gopala Rao and Subba Rao (*Current Science*, 1941, 10, 24) have discovered another example where sodium sulphite acts as an acceptor. They have found that the reduction of silver chloride by ascorbic acid induces the reaction between silver chloride and sodium sulphite.

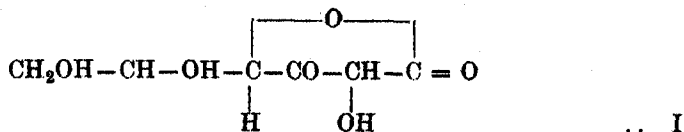
In the examples of chemical induction referred to in the preceding paragraphs, we were concerned with two reducing agents and one oxidizing agent ;



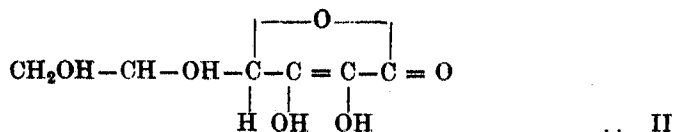
one of the reducing agents acts as the inductor while the other reducing agent acts as the acceptor. The oxidizing agent is shared between the two. There is another type of chemical induction discovered by Dhar (*J. Chem. Soc.*, 1917, *III*, 690) in which we have to deal with two oxidizing agents and one reducing agent. When an aqueous solution of mercuric chloride is boiled with oxalic acid, there is no reduction of the mercuric chloride to the mercurous state. But if we add a small quantity of a dilute (N/10) solution of potassium permanganate, there appears a copious formation of mercurous chloride. Dhar has shown this phenomenon to be of quite common occurrence. The primary change between the oxalic acid and the permanganate induces the reaction between the oxalic acid and the mercuric chloride. The phenomenon of chemical induction is of great importance. Dhar and collaborators (Dhar, Presidential Address, *Eleventh Annual General Meeting of the Indian Chemical Society*, Jan. 4, 1935, Calcutta) have in a large number of publications elaborated the idea that biological oxidation processes involve chemical induction. They have demonstrated that various substances like glucose, fructose, cane sugar, tartrate, citrate, etc., which are not directly oxidized by atmospheric oxygen at ordinary temperatures, can be oxidized by passing air through aqueous solutions of these substances in the presence of sodium sulphite, or freshly precipitated ferrous, cerous, manganous or other hydroxides, all of which undergo oxidation readily. The results of Dhar, that (1) all sugars are readily oxidized to carbon dioxide and water by air in the presence of cerous hydroxide, and that (2) the cerous hydroxide employed acts as a simple inductor, have been confirmed by Ghosh and Rakshit (*J. Ind. Chem. Soc.*, 1935, *12*, 358) using the refined manometric technique of Warburg. Ghosh and Rakshit also made the important observation that amino-acids retard the oxidation of sugars. This lends support to the theory of Dhar that proteins act as negative catalysts in the oxidation of carbohydrates and vice versa in the animal body.

There exist in the animal and plant tissues autoxidizable substances like glutathione, insulin, ascorbic acid, carotene, lactoflavine, cytochrome, etc. It is probable that these substances act as inductors for the oxidation of the metabolites, in the same way as sodium sulphite, cerous hydroxide, etc. It was, therefore, thought desirable to study a large number of induced reactions with inductors of biochemical significance. The study of such reactions and their mechanisms will help us in unravelling the mystery of life.

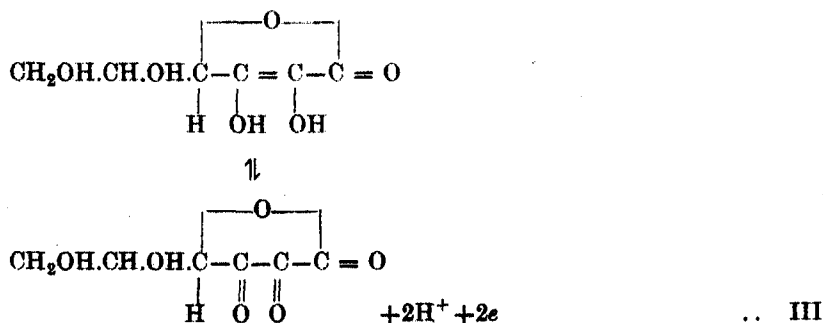
It is with this aim that the present investigation with ascorbic acid was undertaken. Ever since the isolation in the pure state of ascorbic acid by Szent Györgyi and the elucidation of its constitution and synthesis by W. N. Haworth and co-workers, it has been a compound of much absorbing interest to chemists and biochemists. The constitution of ascorbic acid as given in I) is now generally accepted as correct.



This enolizes in solution into form (II)



The hydroxy groups attached to the doubly linked carbon atoms have the remarkable property that they are both capable of easy dehydrogenation (oxidation) and stepwise dissociation into  $\text{H}^+$  ions. Ascorbic acid is capable of reversible oxidation and reduction according to the equation.



Ascorbic acid thus easily passes into dehydroascorbic acid III by losing two hydrogen atoms; and the reaction can be easily reversed. We conceived the idea that this property of ascorbic acid will make it an excellent inductor for several reactions, including those of biochemical interest.

We found that ascorbic acid works as an excellent inductor for the reduction of silver chloride by sodium sulphite. Under the conditions of our experiments sodium sulphite does not reduce silver chloride, while ascorbic acid does so readily. But when ascorbic acid and sodium sulphite are present together, a given amount of ascorbic acid produces a much larger reduction of the silver halide than when it is alone. The results of this investigation are presented in detail in this paper.

#### EXPERIMENTAL.

The ascorbic acid employed in the present investigation was the synthetic product supplied by the British Drug Houses, Ltd. The other chemicals such

as sodium sulphite, silver nitrate, potassium chloride, etc., were of Merck's A.R. quality.

The experiments were conducted in brown bottles and silver chloride was formed *in situ* by adding to each bottle 10 ml. of 0.1N silver nitrate and 10 ml. of 0.1N potassium chloride solution. The requisite volumes of sodium sulphite solution and ascorbic acid solution were then added, followed by enough distilled water to make up the total volume to 50 ml. After three to three and a half hours, the contents of each bottle were poured through a filter (Whatman No. 42, for fine precipitates). The residue on the filter was carefully washed until free from the soluble salts. The funnel with the filter is then put over a 250 ml. volumetric flask and the residue on the filter treated with 1:1 dilute analytical nitric acid. The corresponding brown bottle was also treated similarly and the liquid poured on the same filter. The treatment was repeated three times to ensure complete solution of any metallic silver formed by reduction. It is well known that silver chloride does not dissolve in 1:1 nitric acid. The filtrate in the 250 ml. flask was made up to the mark and the amount of silver in an aliquot portion estimated volumetrically by titration with standard potassium thiocyanate solution, using ferric alum as the indicator.

In the following table are recorded the results on the influence of time on the reduction of silver chloride by ascorbic acid.

TABLE I.

5 ml. of ascorbic acid (5 mgms.).

Time.	Amount of AgCl in terms of mgms. Ag.	Amount of Ag obtained by reduction, in mgms.
1 hour	107.9	1.13
2 hours	107.9	2.05
3 hours	107.9	2.26
4 hours	107.9	2.26

It will be seen from the above table that the reaction is complete in three to four hours. Experiments have been made to see if sodium sulphite alone can reduce silver chloride with negative results. Even by microchemical qualitative tests we could not demonstrate any reduction of silver chloride by sodium sulphite. The results in the following table show that in the presence of sodium sulphite a given amount of ascorbic acid produces a much larger reduction of the silver halide than when it is alone.

TABLE II.

Experiment. Time $3\frac{1}{2}$ hrs. Total volume 50 ml.	Amount of AgCl in terms of mgms. Ag.	Amount of Ag obtained by reduction in mgms.
10 ml. of $\text{Na}_2\text{SO}_3$ (0.025 Molar)	107.9	Nil.
5 mgms. of ascorbic acid	107.9	2.28
5 mgms. of ascorbic acid +10 ml. of $\text{Na}_2\text{SO}_3$ (0.025 Molar)	107.9	9.04

The results indicate that ascorbic acid induces the reduction of silver chloride by sodium sulphite. The primary reaction between silver chloride and the organic reducer ascorbic acid provokes the secondary reaction between sodium sulphite and the silver chloride. Hence ascorbic acid is the inductor, sodium sulphite is the acceptor and silver chloride is the actor, according to the nomenclature mentioned in the introduction.

If we now vary the concentration of the acceptor, keeping the concentration of the inductor constant we find that the rate of reduction of silver chloride increases. This is shown by the results in the following table.

TABLE III.

5 mgms. of ascorbic acid. Time of experiment  $3\frac{1}{2}$  hours.

Volume of $\text{Na}_2\text{SO}_3$ solution. (0.025 Molar).	Amount of AgCl in terms of mgms. Ag.	Amount of Ag obtained by reduction in mgms.
0	107.9	2.88
5 ml.	107.9	6.26
10 ml.	107.9	9.04
15 ml.	107.9	9.71

If we keep the concentration of the acceptor ( $\text{Na}_2\text{SO}_3$ ) constant and vary the concentration of the inductor (ascorbic acid) then also the rate of reduction of silver chloride is increased, as shown by the results in the following table.

TABLE IV.

Total Volume 50 ml. Concentration of Sodium sulphate 0.05 Molar.

Amount of ascorbic acid.	Amount of AgCl in terms of mgms. Ag.	Amount of Ag obtained by reduction in mgms. (3 hrs.)
5 mgms.	107.9	7.08
10 mgms.	107.9	12.13
15 mgms.	107.9	17.00

## INFLUENCE OF pH.

In the following experiments 2 ml. of N/2 silver nitrate solution and 2 ml. of N/2 potassium chloride solution were added to each brown bottle, then 40 ml. of the requisite buffer solution followed by 1 ml. of ascorbic acid solution (containing 5 milligrams per ml.) and enough water (5 ml.) to bring the total volume to 50 ml. The bottles were kept in the thermostat for three hours with occasional shaking. At the end of three hours the contents of each bottle were analysed according to the method already described for determining the amount of silver formed by reduction.

In another series of experiments the reaction was allowed to proceed in the presence of sodium sulphite. The bottles were set up exactly as described above, but with the addition of 5 ml. of N/10 sodium sulphite solution in place of 5 ml. of water.

TABLE V.

Influence of pH.

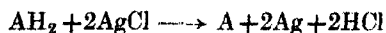
pH	Milligrams of silver formed by reduction.	
	With ascorbic acid alone.	With ascorbic acid + sodium sulphite.
4.047	2.23	2.83
7.0	3.53	5.64
8.0	3.98	6.22

From these results it is evident that as the pH is increased (as the reaction of the solution is made increasingly alkaline) the reduction of silver salt by ascorbic acid is facilitated. Even in the alkaline solutions there is greater reduction in the presence of sodium sulphite than in its absence. The influence

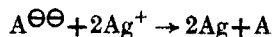
of sodium sulphite in increasing the amount of silver formed by reduction is thus due to a true induced reaction and not merely due to its capacity to raise the pH of the solution slightly.

## DISCUSSION OF RESULTS.

From our results it will be seen that silver chloride can be reduced to metallic silver by ascorbic acid. In this property ascorbic acid resembles hydroquinone, pyrogallol, *p*-amino-phenol, etc. The reduction is greater in alkaline than in acid *pH*. If we represent the organic reducing agent as  $AH_2$ , the reduction of silver chloride can be represented as

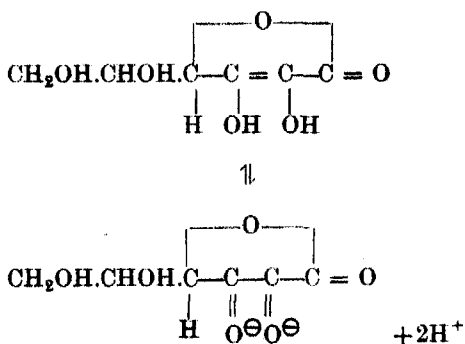


It is more rational to express oxidation-reduction processes in terms of transference of electrons. Ascorbic acid undergoes reversible dissociation.



The silver ions take up electrons from the anion of the reducing agent and are reduced to metallic silver.

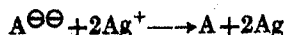
Ascorbic acid can be regarded as a dibasic acid undergoing reversible dissociation represented by the following equation :—



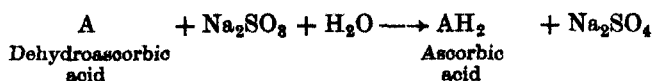
or simply



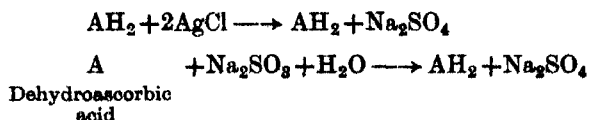
This ionization will be favoured by an alkaline pH, for then the  $H^+$  ions combine with the  $OH^-$  ions to form undissociated water. We have a higher concentration of the anion of the organic reducer in alkaline than in acid pH. Hence the following reaction resulting in the reduction of ionic  $Ag^+$  to metallic silver occurs more readily in alkaline than in an acid pH.



Our results show that the amount of silver obtained in the presence of sodium sulphite is much greater than in its absence. We may conclude in the customary nomenclature that the reduction of silver halide by ascorbic acid induces the reaction between silver halide and sodium sulphite which normally does not occur. To investigate the mechanism of this induced reaction, we have made experiments to study the influence of dehydroascorbic acid on silver halide. We have found that while dehydroascorbic acid is unable to reduce silver halide by itself, it can do so when sodium sulphite is also present. These results suggest the following reaction:—



Ascorbic acid by itself can reduce silver halide to metallic silver, becoming itself oxidized to dehydroascorbic acid.



The sodium sulphite regenerates the ascorbic acid from the dehydroascorbic acid. Thus in the presence of sodium sulphite a given amount of ascorbic acid produces greater reduction than in the absence of sodium sulphite.

The dehydroascorbic acid used in our work was prepared by the catalytic oxidation of ascorbic acid in the presence of dilute acetic acid with Norit charcoal as the catalyst.

Perhaps our view explains the results of B.I. Tanovskaya (*Voprosy Pitaniya*, 1935, 4, 51) who found that the process of sulfiting black currant juice for storage seemed to preserve the vitamin C activity, which was lost in the untreated, stored juice. S. N. Matzko (*ibid.*, p. 59) found that the expressed juice from cooked, dried, white cabbage, which had been sulfited for storage protected guinea-pigs from scurvy.

Ascorbic acid is easily oxidized by atmospheric oxygen *in vitro*. Yet the vitamin occurs in its reduced form in the plant and animal tissues, a fact which is attributed to the presence of stabilizing substances which reduce the auto-oxidation to the minimum. To the authors it seems that it is more rational to assume the presence in living tissues of reducing mechanisms through which the oxidized form of ascorbic acid, the dehydroascorbic acid, is converted by reduction to ascorbic acid. F. G. Hopkins and E. J. Morgan (*Biochem. J.*, 1936, 30, 1446) and H. Borsook and C. E. P. Jeffreys (*Science*, 1936, 83, 397) find that glutathione can reduce dehydroascorbic acid, Hopkins and Morgan believe that the reduction of dehydroascorbic acid to ascorbic acid is catalyzed by the enzyme, ascorbic acid oxidase. According

to Borsook and Jeffreys the reduction of dehydroascorbic acid by glutathione can be rapidly effected by glutathione, when it is present in concentrations of 100-200 mg. per cent. The failure of previous workers to find any significant amount of reduction is attributed by Borsook and Jeffreys to their having worked at a low pH and without sufficient excess of glutathione. Z. I. Kertesz (*Biochem. J.*, 1938, 32, 621) found that the rate of reduction of dehydroascorbic acid by glutathione at pH 7.4 was slower than the rate of oxidation of ascorbic acid. Contrary to the findings of Hopkins and Morgan he did not observe any catalytic effect of ascorbic acid oxidase (from cucumber and cauliflower juice), on the rate of reduction. He observed that glutathione does not inhibit the oxidation of ascorbic acid at pH 6.0, while it does so at pH 7.4.

Jorissen (*Chem. Weekblad.*, 1931, 28, 337) stated that the induced oxidation of lactic acid by air can be effected by using sodium sulphite as inductor. Jorissen and Belifante (*Rec. tra. Chim.*, 1936, 55, 374) found that in dilute buffered solutions at 30°, the oxidation of lactic acid is induced by the slow auto-oxidation of glucuronic acid or ascorbic acid. They also found that ascorbic acid induces the oxidation of arsenite. In each case, the amounts of oxygen taken up by the inductor and acceptor are nearly the same. They believe that their results are of significance in the treatment of cancer. The ingestion of ascorbic acid may facilitate the oxidation of lactic acid in tumours, thus keeping the tumour from developing.

P. Holtz (*Naturwissenschaften*, 1937, 24, 14) found that on passing air or oxygen through 10 ml. of an aqueous solution of 200 mg. of histidine and 50 mg. of ascorbic acid in neutral reaction and at body temperature, the resulting deep brown solution exhibited the physiological effect (blood pressure drop) of 1γ histamine per ml. The author suggests that in the presence of ascorbic acid, histamine is formed from histidine by decarboxylation as well as deamination. We are inclined to believe that this is a case of induced reaction.

Holtz (*Arch. exp'tl. Path. Pharmacol.*, 1936, 182, 98) also found that ascorbic acid strongly accelerates the auto-oxidation of linseed oil. It may also be of interest to note here that Lemberg, Cortis-Jones and Norrie (*Biochem. J.*, 1938, 32, 149) have shown that ascorbic acid and haematin undergo coupled oxidation in dilute pyridine solution. Pyridine-haemochromogen catalyses the oxidation of ascorbic acid, which is not autoxidizable under these conditions; and ascorbic acid induces the oxidation of haematin to verdohaematin, a bile pigment iron complex. The main product of the oxidation of ascorbic acid is dehydroascorbic acid.

The above discussion will indicate the interest that is attached to reactions induced by ascorbic acid, and the need for further work in this field.

In conclusion, the authors desire to express their profound thanks to Prof. N. R. Dhar, D.Sc., Dr. es. Sci., F.I.C., I.E.S., of Allahabad for his kind interest in this investigation. One of us (T.V.S.R.) is grateful to the authorities



of the Andhra University for the award of the Dr. C. R. Reddy Research Fellowship in chemistry.

SUMMARY.

1. We have found that ascorbic acid induces the reaction between sodium sulphite and silver halide. This is one of the few reactions in which sodium sulphite acts as an acceptor.

2. Dehydroascorbic acid cannot by itself reduce silver halide, whereas it can do so in the presence of sodium sulphite.

3. The mechanism of the induced reaction is discussed.

Physico-Chemical Laboratories,  
University College of Science and  
Technology,  
Andhra University, Waltair.

# WHITE DWARF AND HARMONIC OSCILLATOR.

By F. C. AULUCK, *Dyal Singh College, Lahore.*

(Communicated by Dr. D. S. Kothari.)

(Read January 1, 1942.)

## SUMMARY.

As is well known, the *cold* stellar bodies, viz. white dwarf stars and planets, have provided one of the most fertile fields for the application of the new Quantum Statistics. It was realised that under certain simplified conditions, the state of an electron inside a *cold* stellar mass could be represented by the wave-functions of a simple harmonic oscillator and a further development of this idea led to a discussion of the usual (i.e. non-relativistic) and the relativistic harmonic oscillator subject to artificial-boundary conditions. The fundamental formula of the white dwarf theory has been derived from the standpoint of the bounded oscillator. When the relativistic theory of the oscillator is used, it is found that, for a mass exceeding a critical mass  $M_0$ , the radius of the equilibrium configuration tends to vanish.

1. *Introduction.*—The fundamental mass-radius relation of the white dwarf theory, first given by Milne (1932), is

$$R = \alpha_1 \frac{L_0}{\mu_0^{\frac{1}{3}}} \left( \frac{\odot}{M} \right)^{\frac{1}{3}}, \quad \dots \quad (1)$$

where  $L_0$  is the characteristic length of the white dwarf theory,

$$L_0 = \frac{h^2}{4\pi^2 m m_H^{\frac{1}{3}} G \odot^{\frac{1}{3}}} \sim 6.18 \times 10^8 \text{ cm.} \quad \dots \quad (2)$$

and  $\alpha_1$  is a numerical constant,\*

$$\alpha_1 = \frac{(\omega_{\frac{1}{2}}^0)^{\frac{1}{3}} (3\pi)^{\frac{1}{3}}}{2^{\frac{1}{3}}} \sim 4.512 \quad \dots \quad (3)$$

$\mu_0$  denotes the mean molecular weight per free electron,  $m$  is the mass of the proton, and the other symbols have their usual meaning. If the stellar material be assumed to be composed of an element of atomic weight  $A$  and atomic number  $Z$ , then because of complete ionization (in accordance with the theory of pressure ionization)  $\mu_0 = \frac{A}{Z}$ .

---

\*  $\omega_{\frac{1}{2}}^0$  is a constant characteristic of the Emden solution of Emden's equation of index  $\frac{1}{2}$ ;  $\omega_{\frac{1}{2}}^0 = 132.39$ .

It will be noticed that in the expression (1), the dependence of the radius  $R$  on the chemical nature of the material is through the ratio  $\mu_0 = A/Z$  and therefore so far as the composition of a white dwarf is concerned, we need distinguish only between hydrogen ( $A/Z = 1$ ) and non-hydrogen elements (for which  $A/Z$  is approximately 2 except for  $\text{He}^3$ , for which it is 1.5). For any assigned mass, the computed radius given by (1) will vary between two limits, the maximum being for  $\mu_0 = 1$  (all hydrogen) and the minimum for  $\mu_0 = 2$  (no hydrogen). It is a significant fact that the observed radii for all the known white dwarfs lie between these two limits. In fact the observed radius can be made to agree exactly with the theoretical value by assuming a suitable proportion of hydrogen and non-hydrogen elements. If the proportion, by weight, of hydrogen,  $\text{He}^3$ , and other elements be  $x$ ,  $y$ , and  $1-x-y$ , respectively, then  $\mu_0$  for the mixture is easily seen to be,

$$\mu_0 = \frac{6}{3+3x+y}, \quad \dots \quad (4)$$

or ignoring  $\text{He}^3$

$$\mu_0 = \frac{2}{1+x} \quad \dots \quad (4')$$

Thus, if we take the case of Sirius B, for which the observational data are most reliable, the observed radius, as was first pointed out by Mitra (1932), agrees with the calculated value for  $\mu_0 = 1.2$ , i.e.  $x = \frac{2}{3}$  or about 70% by weight of hydrogen.

A couple of years ago, this result was considered satisfactory but the recent work [Kothari (1938), Wildhack (1940)] on the energy-generation inside white dwarfs has made it imperative to abandon, for them, the hypothesis of hydrogen-abundance. A white dwarf star cannot contain any appreciable amount of hydrogen, for otherwise the energy generated in it due to the proton-proton reaction ( $\text{H}^1 + \text{H}^1 \rightarrow \text{He}^4 + U$ ) will be tremendously large compared to its observed luminosity. In fact, at the present moment, the problem of white dwarfs constitutes a serious dilemma: for, (i) if hydrogen-abundance is assumed to make the observed radius agree with the theoretical value, then the computed luminosity will be in violent disagreement with the observed value, and (ii) if no hydrogen be assumed so as to reconcile the observed and the theoretical luminosities, then the radius given by formula (1) is smaller than the observed value by a factor comparable to 3.

No satisfactory solution to resolve this dilemma has so far appeared. Bethe, though realising that it is very unlikely, has suggested the possibility of a flaw in the theory of energy-generation, whereas Gamow and Kuiper consider that there is a chance of the observed radius being in error. The third alternative, that the formula (1) is faulty, can also be dismissed as extremely unlikely. All the same it seems worth while to examine, if possible, the basic formula (1) from a point of view different from the usual one. An instructive treatment, differing from the usual derivation, is provided

by realising that the motion of an electron inside a white dwarf can be represented under certain assumptions as that of a simple harmonic oscillator.

2. *Free-oscillator and the white dwarf star.\**—In a way the connection between an oscillator and a white dwarf should appear natural enough, for crudely speaking it depends on the elementary result, that a particle moving inside a frictionless tunnel passing through a spherical mass and subject to the gravitational force is oscillatory. This crude physical picture has to be translated in terms of wave-mechanics, and account must also be taken of the electrical field set up in the ionized material constituting the white dwarf star.

Let us consider, for simplicity, a model of uniform density. As pointed out by Roseland, an electrical field is set up in a star which prevents any appreciable separation between the free electrons and the atomic nuclei, and in the case of a model of uniform density we have

$$Am_H u + Zev = 0 \quad \dagger, \quad \dots \dots \dots (5)$$

where  $u$  is the gravitational and  $v$  the electrostatic potential both measured from the centre  $-u = v = 0$  at  $r = 0$ . For a sphere of uniform density it is seen that

$$u = \frac{GM}{2R^3} r^2, \quad \dots \dots \dots (6)$$

and therefore from (5),

$$v = -\frac{\mu_0 m_H}{2e} \frac{GM}{R^3} r^2. \quad \dagger \dots \dots \dots (7)$$

The Schrodinger equation for an electron inside a white dwarf will be

$$\nabla^2 \psi + \frac{8\pi^2 m}{h^2} (W - mu + ev) \psi = 0, \quad \dots \dots \dots (8)$$

\* This section is based on Kothari (1940). By free-oscillator is meant a simple harmonic oscillator subject to the natural boundary condition  $\psi \rightarrow 0$  as  $r \rightarrow \infty$ . The artificially bounded oscillator is considered in the next section.

† The atomic nuclei, because of their large mass, behave as a non-degenerate gas, though the free electrons constitute a degenerate gas. The distribution of the nuclei

will, therefore, follow the Boltzmann Law  $N = N_0 e^{\frac{-\chi r}{kT}}$  where  $N_0$  is the concentration for  $r = 0$  and  $N$ , the concentration at a distance  $r$ ;  $\chi$  is the potential energy of the particle at  $r$  ( $\chi$  denotes the work done in carrying the particle from  $r = 0$  to  $r$ ). For uniform distribution the variation of  $N$  with  $r$  should be negligible and hence  $\chi$  must be zero. When electrical and gravitational fields both are present, the gravitational potential energy is  $Am_H u$  and the electrical potential energy is  $+Zev$ ,  $+Ze$  being the charge of the nucleus. Therefore  $\chi = Am_H u + Zev$ .

† At the boundary of the white dwarf, the electrical potential will be

$$v_1 = -\frac{\mu_0 m_H GM}{2eR},$$

i.e. it is of the order of  $10^4$  volts.

where  $W$  is the eigen-value of the energy. Substituting for  $u$  and  $v$ , we obtain

$$\nabla^2 \psi + \frac{8\pi^2 m}{h^2} \left( W - \frac{1}{2} \alpha r^2 \right) \psi = 0, \quad \dots \quad (9)$$

where

$$\alpha = \mu m_H \frac{GM}{R^3}. \quad \dots \quad (10)$$

This is the well-known equation of a harmonic oscillator and its eigen-values are given by  $W_q = \frac{h}{2\pi} \left( \frac{\alpha}{m} \right)^{\frac{1}{2}} \left( q + \frac{1}{2} \right)$  where  $q$  is any positive integer including zero. The number of independent wave-functions associated with the eigen-value  $W_q$  is  $g \frac{q(q+1)}{2}$  where  $g (= 2)$  is the weight factor.

In the degenerate case, because of the exclusion principle, all levels from  $q = 0$  to  $q = q_0$  will be completely filled where  $q_0$  will depend upon the total number of electrons and will be defined by

$$\frac{M}{\mu_0 m_H} = \sum_{q=0}^{q_0} q(q+1) \sim \frac{q_0^3}{3},$$

or

$$q_0 = \left( \frac{3M}{\mu_0 m_H} \right)^{\frac{1}{3}}. \quad \dots \quad (11)$$

Identifying with the radius of the star, the 'amplitude' of the oscillator corresponding to the energy  $W_{q_0}$  we have

$$W_{q_0} = \frac{h}{2\pi} \left( \frac{\alpha}{m} \right)^{\frac{1}{2}} \left( q_0 + \frac{1}{2} \right) = \frac{1}{2} \alpha R^2, \quad \dots \quad (12)$$

Substituting for  $\alpha$  we obtain for the maximum energy  $W_{q_0}$ ,

$$W_{q_0} = \frac{\pi^2 (\mu_0 m_H)^{\frac{1}{2}} G^2 m}{2.3^{\frac{1}{2}} h^2} M^{\frac{1}{2}}, \quad \dots \quad (13)$$

and the mass-radius relation,

$$R = (24)^{\frac{1}{2}} \frac{L_0}{\mu_0^{\frac{1}{2}}} \left( \frac{\odot}{M} \right)^{\frac{1}{2}}, \quad \dots \quad (14)$$

where  $L_0$  is given by the relation (2). Equation (14) is the fundamental equation of the white dwarf theory and it is indeed satisfactory that a viewpoint, widely different from the usual theory, gives a relation which agrees with Milne's formula (1) except for a somewhat different numerical factor. In the case of Sirius B, the calculated radius from the above relation comes out to be, for  $\mu_0 = 2$  (no hydrogen)  $1.6 \times 10^9$  cm. This may be compared with the value  $0.8 \times 10^9$  given by Milne's theory. The observed value is  $2 \times 10^9$  cm.

3. *Artificially-bounded oscillator.*—The above investigation is, however, admittedly rough and needs to be refined in many ways. For example, the effect of electron collisions should be taken into account and this could be done on lines similar to the theory of diamagnetism of metals. Perhaps a more serious objection is the use of the equation (12) in a wave-mechanical treatment. The value of  $W_{q_0}$  taken in the theory corresponds to that of a free-oscillator whose wave-function  $\psi$  satisfies the boundary  $\psi \rightarrow 0$  as  $r \rightarrow \infty$  whereas the equation (12), introducing as it does a *classical* concept of amplitude, assumes that the electrons do not go beyond the stellar boundary  $r = R$ . Though equation (12) is plausible, still the underlying physical incompatibility between its L.H.S., which is interpreted in terms of quantum mechanics, and the R.H.S., which admits only a *classical* description, is obvious. The very idea of a boundary at a finite distance is foreign to the usual theory of the oscillator. It is evident, therefore, that for a complete wave-mechanical treatment of the problem, we must consider the wave-function of the oscillator subject not to the natural boundary condition  $\psi \rightarrow 0$  as  $r \rightarrow \infty$  but to the artificial-boundary condition  $\psi = 0$  at  $r = R$ .

The significance of an artificial-boundary condition was not appreciated till very recently. The treatment of an oscillator subject to an artificial boundary condition has been given in two papers by the author (1941)\*. It is interesting to note in this connection that, during the last three years, Sommerfeld (1938, 1940) and his collaborators have discussed the Kepler problem and the rotator subjected to artificial boundary conditions. The results of the Kepler problem are significant for the theory of pressure ionization, and in fact it was the possibility of this application that led Sommerfeld and Welker (1938) to introduce the artificial-boundary conditions for the hydrogen atom (Kepler problem).

It need hardly be remarked that the generalized study of the oscillator undertaken in the papers referred to has, besides astrophysical applications, its own intrinsic interest.

The Schrodinger equation for a linear oscillator † is

$$\frac{d^2\psi}{dx^2} + \frac{8\pi^2m}{h^2} \left( W_q - \frac{1}{2} \alpha x^2 \right) \psi = 0, \quad \dots \dots \dots (15)$$

where  $m$  is the mass of the particle and  $\frac{1}{2} \alpha x^2$  its potential energy for a displacement  $x$ , the proper frequency  $\nu_0$  being defined by

$$\nu_0 = \frac{1}{2\pi} \left( \frac{\alpha}{m} \right)^{\frac{1}{2}} \quad \dots \dots \dots (16)$$

\* These papers will be referred to as AI and AII respectively.

† For a detailed treatment see Auluck, 1941. For the sake of completeness results relevant to the present paper are given here.

The equation (15) can be written in the form

$$\frac{d^2\psi}{dz^2} + \left(n + \frac{1}{2} - \frac{1}{4}z^2\right)\psi = 0, \quad \dots \quad (17)$$

where

$$W_q = h\nu_0 \left(n + \frac{1}{2}\right), \quad \dots \quad (18)$$

and

$$z = \left(\frac{4\pi}{h}\right)^{\frac{1}{2}} (\alpha m)^{\frac{1}{2}} x. \quad \dots \quad (19)$$

The natural boundary condition is  $\psi \rightarrow 0$  as  $x \rightarrow \pm \infty$  and for this case  $n$  is a positive integer including zero, and  $\psi$  is a Hermitian function. For the ground state the energy  $W_0$  is  $\frac{1}{2}h\nu_0$ , for the first excited state  $W_1 = \frac{3}{2}h\nu_0$  and so on.

When we impose the artificial-boundary condition:  $\psi = 0$  at  $x = \pm \frac{l}{2}$ , the energy of the stationary states depends on  $l$  and is no longer given by integral values of  $n$  in formula (18). It increases with increasing  $l$  and tends to the asymptotic formula

$$W_q = \frac{h^2 q^2}{8ml^2}. \quad \dots \quad (20)$$

To take a particular example, consider the ground state ( $q = 1$ )—similar results with obvious modifications will of course hold for the higher excited states. Though strictly the eigen-value of the energy for the ground state is  $\frac{1}{2}h\nu_0$ , only when the boundary is at infinity ( $l \rightarrow \infty$ ), still the difference from this value is less than 5% so long as  $l > 3l_0$  where  $l_0$  is defined by

$$l_0 = \left(\frac{h}{2\pi^2\nu_0 m}\right)^{\frac{1}{2}}. \quad \dots \quad (21)$$

In the other extreme case when  $l$  is very small compared to  $l_0$ , the energy approximates to  $\frac{h^2}{8ml^2}$ . Our discussion therefore assigns, as if it were, a 'size' to an oscillator which for the ground state is comparable to  $3l_0$ . The eigen-value will be practically  $\frac{1}{2}h\nu_0$  only, so long as the oscillator is not confined within a space less than  $3l_0$ , but when it is restricted to a smaller space, the energy will depend upon the dimensions of this space.\*

---

\* It would be of interest to note here that, for the Kepler problem, Sommerfeld and Welker (1938) found that the eigen-value of the energy becomes positive when the radius ' $a$ ' of the sphere enclosing the hydrogen atom and constituting its artificial boundary becomes less than  $1.835 a_H$ ,  $a_H$  being the radius of the first Bohr orbit.

4. *Bounded oscillator and the white dwarfs.*—We now return to the application of the oscillator to the white dwarfs. It has already been seen that if all energy levels from  $q = 0$  to  $q = q_0$  are completely filled then

$$q_0 = \left( \frac{3M}{\mu_0 m_H} \right)^{\frac{1}{3}}.$$

As already remarked, the solution of the oscillator equation subject to an artificial-boundary condition gives a relation between energy and the position of the boundary for the different states. Figure 1 shows this relation in a qualitative way—the ordinate represents  $z_0$  which corresponds to the position of the boundary.

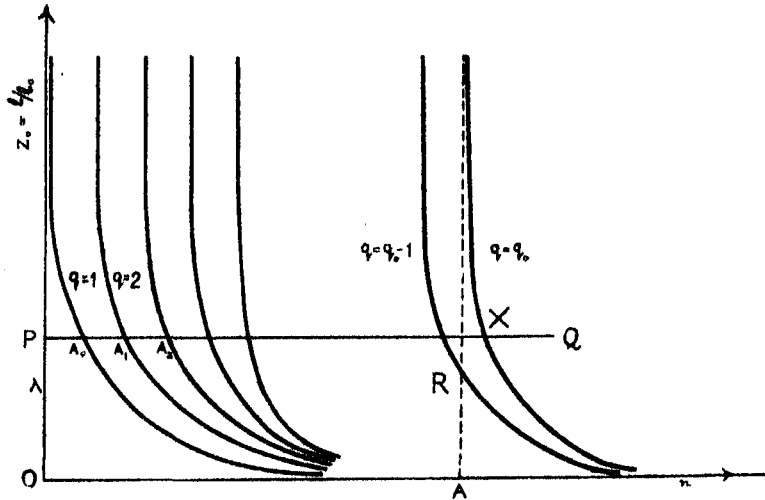


FIG. 1

The boundary occurs at  $x = \pm \frac{l}{2}$  and  $z_0$  is defined to be

$$z_0 = \frac{l}{l_0} = l \left( \frac{2\pi^2 \nu_0 m}{h} \right)^{\frac{1}{3}} \quad \dots \quad (22)$$

The abscissa, instead of representing direct energy, denotes  $n$  which is connected with the energy by the usual relation  $W_q = h\nu_0 \left( n + \frac{1}{2} \right)$ . The curve marked  $q = 1$  is for the ground state, those marked with  $q = 2, q = 3$ , etc. are for the successive higher states.

Every curve has two asymptotes—the axis  $z_0 = 0$  being the common asymptote for all of them. The other asymptote is different for the different curves. For the ground state it is  $n = 0$ , for the first excited state  $n = 1$ , and for the  $q$ th excited state  $n = q$ . Consider a line  $PQ$  represented by  $z_0 = \lambda$ ,



$\lambda$  being a constant. Then the eigen-values for the different states, in the case of the oscillator which is subjected to the boundary corresponding to the value  $\lambda$  for  $z_0$  (i.e. boundary placed at  $x = \pm \frac{\lambda l_0}{2}$ ) will be  $PA_0, PA_1, PA_2, \dots$  and let  $PX$  be the value corresponding  $q_0$ th state. For a given mass  $M$ , the value of  $q_0$  is already fixed and is given by  $q_0 = \left(\frac{3M}{\mu_0 n \pi}\right)^{\frac{1}{2}}$ . As we seek to determine the configuration of least possible energy, we note that the minimum value of  $PX$  is obviously  $OA = q_0$  (corresponding to the asymptote  $n = q_0$ ). The interval  $AR$  is cut by all curves before  $q_0$ , i.e. it has  $q_0 - 1$  cuts. Any value of  $\lambda$  greater than  $AR$  will have the same  $q_0 - 1$  cuts but  $AR$  is the minimum value to possess these number of cuts. The value  $\lambda$ , so that the interval  $AR$  ( $= \lambda$ ) will possess  $q_0 - 1$  cuts and no more, is easily given by applying Sturm's theorem to the oscillator equation (17) and remembering that our boundary positions correspond to the zeros of the equation (17). Since  $n = q_0$ , for  $q_0 - 1$  zeros to lie within the interval  $z_0 = 0$  to  $z_0 = \lambda$  we must have

$$q_0 - 1 + \frac{1}{2} - \frac{1}{4}\lambda^2 < 0,$$

or

$$\lambda > 2\sqrt{q_0}, \quad \dots \dots \dots (23)$$

as  $q_0$  is large. After substituting for  $q_0$  and identifying  $l$  with

$$2R \left( \lambda = \frac{l}{l_0} = \frac{2R}{l_0} \right)$$

we finally obtain,

$$R > (24)^{\frac{1}{2}} \frac{L_0}{\mu_0^{\frac{1}{2}}} \left( \frac{\odot}{M} \right)^{\frac{1}{2}} \dots \dots \dots (24)$$

Instead of the equality (14) which is obtained in the semi-classical treatment, we have here obtained the inequality (24), and this need cause no surprise; for, what the exact treatment here presented determines, is not the radius of the star but the distance at which the artificial boundary (wholly impermeable to the electrons) can be placed. Naturally, to be consistent with the data of the problem, the boundary could be placed anywhere but not inside the star, for otherwise it will exclude some of the electrons, whereas by hypothesis we obtain those possible positions of the boundary which will include all the electrons.

5. *Relativistic bounded oscillator.*—So far our treatment has been completely non-relativistic and, though for most of the known white dwarfs and especially those for which the observational data are most reliable, the relativistic effect is negligible, still for the sake of completeness, a complete relativistic treatment of the oscillator is also desirable. The condition, for which the relativistic effect will be appreciable, can easily be found with the help

of the equation (13). For the relativistic correction to be significant,  $W_{q_0}$  should become comparable to  $mc^2$  and thus we have  $W_{q_0} > mc^2$ ,

$$\text{or } M > M_0, \quad \dots \quad (25)$$

where

$$\frac{M_0}{\odot} = \frac{1}{\mu_0^2} \left\{ \frac{8^{1/2} \cdot 3^{1/2}}{m_{II} \odot} \left( \frac{ch}{2\pi G} \right)^{1/2} \right\}, \quad \dots \quad (26)$$

$$\sim \frac{15 \cdot 26}{\mu_0^2}.$$

The relativistic effect will be important for masses comparable to  $M_0$  and can be neglected for masses fairly smaller than this.

The relativistic oscillator, even for the natural boundary condition, has so far received scanty attention [Nikolsky (1930)]. In the paper A II, the problem is studied using Schrodinger's relativistic equation subject to an artificial boundary condition. Some representative cases have been numerically worked out. As in every relativistic treatment, the negative energy states occur here as well. One rather significant point (also found by Nikolsky who worked with Dirac's equation but using only the natural boundary condition) is that, for the boundary at infinity, stationary states for the oscillator do not exist. In fact the stationary states for an oscillator, taking effect of relativistic mechanics, have been obtained, for the first time, in paper A II by imposing an artificial boundary condition. Even when  $\frac{h\nu_0}{2m_0c^2}$  is very small (i.e. tending

to the non-relativistic case), the curves between  $\frac{W}{h\nu_0}$  and  $z_0$ , given by the relativistic treatment, differ in a most important respect from the corresponding curves given in paper A I. The non-relativistic curves (i.e. the curves given in paper A I) have asymptotes  $\frac{W}{h\nu_0} = \frac{1}{2}, \frac{3}{2}, \frac{5}{2}, \dots$  but the curves given by the relativistic treatment, though they run nearly parallel to the non-relativistic curves for sometime, finally, for sufficiently large values of  $z_0$ , cut the  $z_0$ -axis and then continue their run to negative energy-values. In the relativistic treatment, it is only a bounded oscillator which has stationary states though the boundary can be placed at a considerable distance but never at infinity.

The inspection of the curves in the figures III and IV of paper A II shows that, in the relativistic case, if we seek the lowest energy configuration for a large number of oscillators (corresponding to the large number of electrons inside the star), then it will correspond to zero-energy-value for all the oscillators because all the curves (for the ground state and the higher excited states) cut the  $z_0$ -axis. It will also be seen that the minimum value  $\lambda$  of  $z_0$  such that a given number of curves will cut the  $z_0$ -axis in the interval  $z_0 = 0$  to  $z_0 = \lambda$ , becomes smaller and smaller as  $\frac{h\nu_0}{2m_0c^2}$  becomes larger and larger, and finally

when  $\frac{\hbar\nu_0}{2m_0c^2} \rightarrow \infty$ , which corresponds to the completely relativistic case,  $\lambda \rightarrow 0$ .\*

We therefore verify, in a most interesting way, the Stoner-Chandrasekhar conclusion of the white-dwarf theory, that when the relativistic effect is dominant (i.e. the average energy of a particle is very large compared to its rest-mass energy), the radius for the equilibrium configuration tends to vanish. From what has been said before, it follows that the critical mass beyond which the equilibrium configuration will sink to a vanishing radius will be comparable

$$\text{to } \frac{M_0}{\odot} = \frac{15.26}{\mu_0^2}.$$

It is a pleasure to express my thanks to Dr. D. S. Kothari for his help and interest in the preparation of the paper.

#### REFERENCES.

- Auluck, F. C. 1941. (A I) *Proc. Nat. Inst. Sci. India*, 7, 133.  
 (A II) *Proc. Nat. Inst. Sci. India*, 7, 383.  
 Kothari, D. S. 1938. *Nature*, 142, 916.  
 1940. *Nature*, 146, 24.  
 Milne, E. A. 1932. *Monthly Notices, R.A.S.*, 92, 610.  
 Mitra, S. N. 1932. *Zs. f. Astrophysik*, 4, 329.  
 Nikolaky, K. 1930. *Zs. f. Physik*, 62, 677.  
 Sommerfeld, A. and Welker, H. 1938. *Ann. d. Physik*, 32, 56.  
 Sommerfeld, A. 1940. *Ann. d. Phys.*  
 Wildhack, W. A. 1940. *Phys. Review*, 57, 81.

---

\* This result holds good also for a configuration for any non-zero value of the energy.

# DEGENERATE GAS AND THE MOTION OF A PARTICLE IN A UNIFORM FIELD.

By D. S. KOTIARI and F. C. AULUCK, *University of Delhi.*

(Read January 1, 1942.)

## ABSTRACT.

The density distribution for a completely degenerate Fermi-Dirac gas in a uniform field is obtained (i) by using the thermodynamical theorem connecting Gibb's free energy and potential, and (ii) directly from the wave-equation of a particle in a uniform field and subject to the appropriate boundary condition. The two results are, of course, identical. The meaning of degeneracy temperature for a Fermi-Dirac gas in a field of force is discussed.

1. The present paper deals, from two different points of view, with the density distribution in a Fermi-Dirac (non-relativistic) *degenerate* gas placed in a uniform field of force. The starting point in section (2) is the expression for Gibb's free energy for a Fermi-Dirac gas in the absence of the field and then the distribution in the presence of the field is determined with the help of the well-known thermodynamical theorem connecting the difference in Gibb's free energy with the difference of potential. In section (3), the wave-mechanical problem of a particle, moving in a uniform field and subject to appropriate boundary conditions is considered. The eigen-values for the energy of the stationary states are determined, and the number of independent wave-functions corresponding to eigen-values less than any assigned value is found. The density distribution for a completely degenerate gas is then easily obtained. The final results of the two sections are, of course, identical.<sup>1</sup> Section (4) deals with the degeneracy-temperature ( $T_0$ ) for a Fermi-Dirac gas placed in a field of force.

*The degeneracy-temperature increases with the field strength and the total number of particles.* The physical meaning of the degeneracy-temperature ( $T_0$ ) is, that the gas is degenerate if its temperature is low compared to  $T_0$ , and is non-degenerate if its temperature is large compared to  $T_0$ .

---

<sup>1</sup> The interest of the problem partly lies in the fact that recently two alternative derivations—one based on the pressure of a degenerate gas and the other using the idea of a harmonic oscillator—for the fundamental mass-radius relation for a white dwarf have been given. The final results are identical except for a numerical factor of the order unity. In the white dwarf theory several simplifying assumptions are to be made to make the problem amenable to two alternative treatments. The simple problem taken in this paper has the merit that it permits of an exact treatment in both the cases.

2. Let us consider an assembly of Fermi-Dirac particles at temperature  $T$  and occupying a field-free region of volume  $V$ . The number of wave-functions for a particle, when its kinetic energy lies within  $\epsilon$  and  $\epsilon + d\epsilon$ , is

$$a(\epsilon) d\epsilon = \frac{2\pi g}{h^3} (2m)^{\frac{3}{2}} V \epsilon^{\frac{1}{2}} d\epsilon, \quad \dots \quad (1)^1$$

where  $m$  is the mass of the particle,  $g$  its weight factor, and  $h$  is Planck's constant. If  $n(\epsilon) d\epsilon$  represents the number of particles per unit volume of the assembly and having their kinetic energy within the range  $\epsilon$  to  $\epsilon + d\epsilon$ , the distribution law is

$$V \cdot n(\epsilon) d\epsilon = \frac{a(\epsilon) d\epsilon}{\frac{1}{A} e^{\epsilon/kT} + 1}, \quad \dots \quad (2)$$

and

$$Vn = \int_0^\infty \frac{a(\epsilon) d\epsilon}{\frac{1}{A} e^{\epsilon/kT} + 1}, \quad \dots \quad (3)$$

$n$  being the concentration.  $A$  is called the *absolute activity*. The Gibb's free energy per particle is connected with  $A$  by the relation

$$\zeta = kT \log A. \quad \dots \quad (4)$$

For the completely non-degenerate <sup>2</sup> or *classical* case ( $A \rightarrow 0$ ),

$$\zeta^+ = kT \log \frac{nh^3}{g(2\pi mkT)^{\frac{3}{2}}}, \quad \dots \quad (5)$$

and for the completely degenerate case ( $A \rightarrow \infty$ )

$$\zeta^- = \frac{h^2}{2m} \left( \frac{3n}{4\pi g} \right)^{\frac{2}{3}}. \quad \dots \quad (6)$$

We shall now consider the gas placed in a field of force directed along the  $x$ -axis which we shall suppose to be vertical. The density distribution of the gas is, then, given by the well-known thermodynamical theorem

$$\zeta(x_1) - \zeta(x_2) = W(x_1, x_2), \quad \dots \quad (7)$$

where  $\zeta(x)$  denotes the value of the Gibb's free energy at  $x$  and  $W(x_1, x_2)$  is the work done, against the field, in carrying a particle from  $x_1$  to  $x_2$ .

For a classical gas in a uniform field, we then have the usual Boltzmann law

$$n(x) = n_0 e^{-\alpha x/kT}, \quad \dots \quad (8)$$

where  $n(x)$  is the concentration at  $x$  and  $n_0$  the concentration at  $x = 0$ , and  $\alpha$  is the force acting on a particle—the direction of the force is along the

<sup>1</sup> In this paper we treat only the completely non-relativistic case.

<sup>2</sup> The + suffix attached to a quantity denotes its value in the non-degenerate case, and the - suffix refers to the degenerate case.

negative  $x$ -axis. If  $\bar{n}$  denotes the number of particles contained in a vertical cylinder of unit cross-section and extending from  $x = 0$  to  $x \rightarrow \infty$ , then

$$\bar{n} = \int_0^{\infty} n_0 e^{-\alpha x/kT} dx = \frac{n_0 kT}{\alpha}, \quad \dots \quad (9)$$

and hence

$$n(x) = \frac{\bar{n}\alpha}{kT} e^{-\alpha x/kT} \dots \quad (10)$$

The concentration for a classical gas, at any assigned value of  $x$ , is directly proportional to  $\bar{n}$  (or  $n_0$ ) and vanishes for  $x \rightarrow \infty$ . However, for a *completely degenerate* gas the situation is entirely different. The concentration, for a given  $x$ , is not directly proportional to  $\bar{n}$  (or  $n_0$ ), and the distribution, instead of extending up to infinity, is confined within a finite interval  $x = 0$  to  $x = l$ ,  $l$  depending on  $\bar{n}$ . This is easily seen as follows.

Substituting the expression (6) in (7) we have

$$\frac{\hbar^2}{2m} \left( \frac{3n_0}{4\pi g} \right)^{\frac{2}{3}} - \frac{\hbar^2}{2m} \left( \frac{3n}{4\pi g} \right)^{\frac{2}{3}} = \alpha x, \quad \dots \quad (11)$$

and hence the distribution extends from  $x = 0$  to  $x = l$  (i.e.  $n$  vanishes at  $x = l$ ), where  $l$  is given by

$$l = \frac{\hbar^2}{2m\alpha} \left( \frac{3n_0}{4\pi g} \right)^{\frac{2}{3}}, \quad \dots \quad (12)$$

and (11) becomes

$$n = \frac{4\pi g}{3} \left( \frac{2m\alpha}{\hbar^2} \right)^{\frac{3}{2}} (l-x)^{\frac{3}{2}}. \quad \dots \quad (13)$$

The total number of particles contained within a vertical cylinder of unit cross-section is

$$\bar{n} = \int_0^l n dx = \left( \frac{3}{4\pi g} \right)^{\frac{2}{3}} \frac{\hbar^2}{5m\alpha} n_0^{\frac{4}{3}} = \frac{2}{5} n_0 l, \quad \dots \quad (14)$$

and substituting for  $n_0$  in terms of  $l$ , we have

$$\bar{n} = \frac{8\pi g}{15} \left( \frac{2m}{\hbar^2} \right)^{\frac{3}{2}} \alpha^{\frac{1}{2}} l^{\frac{4}{3}}. \quad \dots \quad (15)$$

Equation (15) gives the extent  $l$  of the distribution in terms of the total number of particles lying above unit area.

The above expressions refer to a 3-dimensional case. It is sometimes of interest [Singh (1941)] to consider explicitly 2- or 1-dimensional case. However, as the general case referring to any number of dimensions is equally easy, it will be better to give the results in terms of  $v$ ,  $v$  being the number of

dimensions. The Gibb's free energy for a completely degenerate gas, in the case of a  $v$ -dimensional space, is easily found to be

$$\bar{\epsilon}_v = \frac{h^2}{2\pi m} \left\{ \frac{n_0}{g} \Gamma\left(\frac{v}{2} + 1\right) \right\}^{\frac{2}{v}}, \quad \dots \quad (16)$$

where  $n_v$  denotes the concentration per unit content in the  $v$ -dimensional space. Using (16) in place of (6) we obtain, instead of (15),

$$\bar{n}_v = g \left( \frac{2\pi m \alpha}{h^2} \right)^{\frac{v}{2}} \frac{l^{\frac{v}{2}+1}}{\Gamma\left(\frac{v}{2} + 2\right)}, \quad \dots \quad (17)$$

$\bar{n}_v$  being the number of particles lying in a column of unit 'cross-section' (which is of  $v-1$  dimensions) and of length  $l$  along the  $x$ -axis. For  $v = 3$ , (17) reduces to (15).

3. We shall now discuss the distribution law by directly considering the Schrodinger equation for the motion of a particle in a uniform field of force.<sup>1</sup> Consider a particle enclosed inside a cylinder extending from  $x = 0$  to  $x \rightarrow \infty$ , the end at  $x = 0$  being closed. The cross-section of the cylinder is a rectangle of sides  $a_2$  and  $a_3$  parallel to the  $y$  and  $z$  axes respectively, one of its corners being at the origin. The Schrodinger equation is

$$\nabla^2 \psi + \frac{8\pi^2 m}{h^2} (W - \alpha x) \psi = 0. \quad \dots \quad (18)$$

This equation is separable in the three variables and, therefore,  $\psi$  will be

$$\psi = C \sin \frac{\pi n_2 y}{a_2} \sin \frac{\pi n_3 z}{a_3} X(x); \quad \dots \quad (19)$$

( $n_2, n_3 = 1, 2, 3, \dots$ )

$X(x)$  satisfies the equation

$$\frac{d^2 X}{dx^2} + \frac{8\pi^2 m}{h^2} \left( W - \frac{h^2}{8m} \frac{n_2^2}{a_2^2} - \frac{h^2}{8m} \frac{n_3^2}{a_3^2} - \alpha x \right) \psi = 0. \quad \dots \quad (20)$$

Writing

$$W - \frac{h^2}{8m} \left( \frac{n_2}{a_2} \right)^2 - \frac{h^2}{8m} \left( \frac{n_3}{a_3} \right)^2 - \alpha x = \left( \frac{h^2 \alpha^2}{8\pi^2 m} \right)^{\frac{1}{2}} u, \quad \dots \quad (21)$$

we have

$$\frac{d^2 X}{du^2} + u X = 0. \quad \dots \quad (22)$$

<sup>1</sup> Also see Condon and Morse, pp. 45-47.

This equation is a standard form of Bessel's equation and its solution is

$$X(u) = u^{\frac{1}{2}} J_{\frac{1}{2}}\left(\frac{2}{3} u^{\frac{3}{2}}\right), \quad \dots \quad (23)$$

where  $J_{\frac{1}{2}}(u)$  is a Bessel function of order  $\frac{1}{2}$ . The eigen-values of  $W$  can now be found by imposing on (23) the boundary condition

$$X(u) = 0 \quad \text{for } x = 0,$$

i.e. for 
$$u = \left(\frac{8\pi^2 m}{h^2 \alpha^2}\right)^{\frac{1}{2}} \left\{ W - \frac{h^2}{8m} \left(\frac{n_2}{a_2}\right)^2 - \frac{h^2}{8m} \left(\frac{n_3}{a_3}\right)^2 \right\}. \quad \dots \quad (24)$$

For large values of the argument

$$J_p(x) \sim \left(\frac{2}{\pi x}\right)^{\frac{1}{2}} \left\{ \cos\left(x - \frac{2p+1}{4}\pi\right) - \frac{4p^2-1}{8x} \sin\left(x - \frac{2p+1}{4}\pi\right) \dots \right\}, \quad (25)$$

and hence for large  $u$  we have<sup>1</sup>

$$X(u) \sim \left(\frac{3}{\pi}\right)^{\frac{1}{2}} \frac{1}{u^{\frac{1}{2}}} \cos\left(\frac{2}{3} u^{\frac{3}{2}} - \frac{5\pi}{12}\right). \quad \dots \quad (26)$$

From (24) and (26), therefore, we have

$$\left(\frac{8\pi^2 m}{h^2 \alpha^2}\right)^{\frac{1}{2}} \left\{ W - \frac{h^2}{8m} \left(\frac{n_2}{a_2}\right)^2 - \frac{h^2}{8m} \left(\frac{n_3}{a_3}\right)^2 \right\} = \left(\frac{3}{2} n_1 \pi\right)^{\frac{3}{2}}, \quad \dots \quad (27)$$

or 
$$W = \frac{h^2}{8m} \left(\frac{n_2}{a_2}\right)^2 + \frac{h^2}{8m} \left(\frac{n_3}{a_3}\right)^2 + \left(\frac{9h^2 \alpha^2}{32m} n_1^2\right)^{\frac{1}{2}}, \quad \dots \quad (27)$$

where  $n_1$  is a positive integer. Equation (27) gives the eigen-values of the energy  $W$ .

A particle with energy  $W$  will not be found at any appreciable distance beyond  $l = \frac{W}{\alpha}$ , for, by (21) if  $x$  be greater than  $\frac{W}{\alpha}$ ,  $u$  becomes negative and the asymptotic expansion for  $X(u)$  decreases exponentially:

$$X(u) \sim i^{-\frac{1}{2}} \left(\frac{3}{4\pi}\right)^{\frac{1}{2}} \frac{1}{(-u)^{\frac{1}{2}}} e^{-\frac{2}{3}(-u)^{\frac{3}{2}}}. \quad \dots \quad (28)$$

<sup>1</sup> For determining the eigen-values, we require the behaviour of  $X(x)$  in the neighbourhood of  $x = 0$ . The assumption, that for  $x = 0$ ,  $u$  is large, is always valid except for those energy states for which  $n_1$  is small. For determining the eigen-values for the lowest energy levels, the behaviour of  $X(u)$  in the neighbourhood of  $u = 0$  is required.



We shall now enumerate the number of eigen-functions corresponding to all values of energy less than or equal to a certain assigned value of  $W = \alpha l$ . Writing

$$\beta^2 = \frac{8mW}{h^2} \text{ and } \gamma = \frac{h^2}{12m\alpha}, \quad \dots \dots \dots (29)$$

(27) reduces to

$$\left(\frac{n_1}{\gamma}\right)^{\frac{2}{3}} + \left(\frac{n_2}{a_2}\right)^2 + \left(\frac{n_3}{a_3}\right)^2 = \beta^2. \quad \dots \dots \dots (30)$$

The number of eigen-functions for energies  $\leq W$  is the volume of the space bounded by the surface described by (30) and the three co-ordinate planes, and for which  $n_1$ ,  $n_2$ , and  $n_3$  are all positive. If  $g$  is the weight factor for the particle, then the number of wave-functions is  $g$  times the above value. If, for a moment, we suppose  $n_1$  fixed and  $n_2$ ,  $n_3$  varied, then the area of the positive quadrant of the elliptical section is

$$\frac{\pi}{4} a_2 a_3 \left\{ \beta^2 - \left(\frac{n_1}{\gamma}\right)^{\frac{2}{3}} \right\}, \quad \dots \dots \dots (31)$$

and hence the required volume is

$$\frac{\pi}{4} a_2 a_3 \int_{n_1=0}^{\gamma\beta^3} \left\{ \beta^2 - \left(\frac{n_1}{\gamma}\right)^{\frac{2}{3}} \right\} dn_1 = \frac{\pi}{10} a_2 a_3 \gamma \beta^5. \quad \dots \dots \dots (32)$$

Remembering that, for the completely degenerate case, the number of particles is equal to the number of independent wave-functions, we have

$$\begin{aligned} n &= g \cdot \frac{\pi}{10} \gamma \beta^5 \\ &= \frac{8\pi g}{15} \left(\frac{2m}{h^2}\right)^{\frac{5}{2}} \alpha^{\frac{3}{2}} l^{\frac{5}{2}}. \quad \dots \dots \dots (33) \end{aligned}$$

The above treatment can be easily generalised to hold for any number of dimensions. In the case of  $v$ -dimensions (30) will be replaced by

$$\left(\frac{n_1}{\gamma}\right)^{\frac{2}{3}} + \sum_{i=2}^v \left(\frac{n_i}{a_i}\right)^2 = \beta^2. \quad \dots \dots \dots (34)$$

The content, corresponding to the positive values of  $n_2, n_3, \dots, n_v$ , of the hyper-ellipsoid in  $(v-1)$ -dimensions will be

$$\frac{\pi^{\frac{v-1}{2}}}{2^{v-1} \Gamma\left(\frac{v+1}{2}\right)} \left\{ \beta^2 - \left(\frac{n_1}{\gamma}\right)^{\frac{2}{3}} \right\}^{\frac{v-1}{2}} (a_2 a_3 \dots a_v), \quad \dots \dots \dots (35)$$

and hence the number of wave-functions is

$$\begin{aligned}
 &= g \cdot \frac{\pi^{\frac{v-1}{2}}}{2^{v-1} \Gamma\left(\frac{v+1}{2}\right)} (a_2 a_3 \dots a_v) \int_0^{\gamma \beta^2} \left\{ \beta^2 - \left(\frac{n_1}{\gamma}\right)^{\frac{2}{3}} \right\}^{\frac{v-1}{2}} dn_1 \\
 &= g (a_2 a_3 \dots a_v) \frac{\pi^{\frac{v}{2}}}{\Gamma\left(\frac{v}{2} + 2\right)} \alpha^{\frac{v}{2}} l^{\frac{v}{2} + 1} \left(\frac{2m}{\hbar^2}\right)^{\frac{v}{2}}. \quad \dots \dots \dots (36)
 \end{aligned}$$

Therefore, finally, we have for the  $v$ -dimensional case

$$\bar{n}_v = g \left( \frac{2\pi m \alpha}{\hbar^2} \right)^{\frac{v}{2}} \frac{l^{\frac{v}{2} + 1}}{\Gamma\left(\frac{v}{2} + 2\right)}, \quad \dots \dots \dots (37)$$

a result which is identical with that of section (2).

4. In the foregoing sections we have discussed the density distribution of a Fermi-Dirac gas in the presence of a field. We shall now derive an expression for the average kinetic energy per particle, and then discuss the *degeneracy-temperature* and its dependence on the field strength.

For a classical gas, the average kinetic energy is  $\frac{3}{2} kT$  and is unaffected by the field. For a completely degenerate gas the average kinetic energy ( $\bar{\epsilon}$ ) per particle is

$$\bar{\epsilon} = \frac{1}{\bar{n}} \int_0^\infty \epsilon_0 n dx,$$

where the null-point energy  $\epsilon_0$  is given by the usual expression,

$$\epsilon_0 = \frac{3}{10} \frac{\hbar^2}{m} \left( \frac{3n}{4\pi g} \right)^{\frac{2}{3}},$$

and hence using (13), (14), and (15) we obtain <sup>1</sup>

$$\begin{aligned}
 \bar{\epsilon} &= \frac{3}{7} \alpha l = \frac{3}{14} \frac{\hbar^2}{m} \left( \frac{3n_0}{4\pi g} \right)^{\frac{2}{3}} \\
 &= \frac{3}{14} \frac{\hbar^2}{m} \left( \frac{15\bar{n}}{8\pi g l} \right)^{\frac{2}{3}}, \quad \dots \dots \dots (38)
 \end{aligned}$$

<sup>1</sup> The total energy per particle (i.e. the sum of the kinetic and potential energies) is easily found to be  $\frac{5}{7} \alpha l$  for the degenerate gas. For the non-degenerate case the total energy is  $\frac{5}{2} kT$ .

and the expression in terms of  $\bar{n}$  and  $\alpha$ , which is the most useful in practice, is

$$\bar{\epsilon} = \frac{3}{7} \left( \frac{\hbar^2}{2m} \right)^{\frac{1}{2}} \left( \frac{15\alpha\bar{n}}{8\pi g} \right)^{\frac{1}{2}}. \quad \dots \dots \dots (39)$$

Let us define the degeneracy-temperature  $T_0$  by the relation,

$$T_0 = \frac{\bar{\epsilon}}{k}, \quad \dots \dots \dots (40)$$

$k$  being the Boltzmann constant. In a degenerate gas, the average energy per particle is much larger compared to  $kT$  and hence the criterion for degeneracy is

$$T \ll T_0. \quad \dots \dots \dots (41)$$

The temperature  $T_0$  can be expressed with the help of equations (38) and (40) either in terms of  $n_0$  or any two of the three quantities  $\alpha$ ,  $l$ , and  $\bar{n}$ . Taking  $\bar{n}$  and  $\alpha$  for example, we have

$$T_0 = \frac{3}{7k} \left( \frac{\hbar^2}{2m} \right)^{\frac{1}{2}} \left( \frac{15\alpha\bar{n}}{8\pi g} \right)^{\frac{1}{2}}, \quad \dots \dots \dots (42)$$

$\bar{n}$ , as defined before, denotes the number of particles contained in a cylinder of unit cross-section, its axis being parallel to the field. Equation (42) shows the effect of the field strength on the degeneracy-temperature—the temperature decreasing with decreasing field strength.

#### REFERENCES.

- Condon, E. U. and Morse, P. M. *Quantum Mechanics* (McGraw Hill).  
Singh, B. N. 1941. *Ind. Jour. Phys.*, **15**, 73.

# FERMI-DIRAC AND BOSE-EINSTEIN GAS IN A UNIFORM FIELD OF FORCE.

By D. S. KOTHARI and F. C. AULUCK, *University of Delhi.*

(Read January 1, 1942.)

## ABSTRACT.

The density distribution of a Fermi-Dirac and a Bose-Einstein gas, both for the relativistic and non-relativistic cases, in the presence of a uniform field of force, is considered. The average kinetic and potential energy, per particle, is determined, and a general theorem regarding their ratio is discussed. The condensation phenomenon, in the presence of a uniform field, for a Bose-Einstein gas is treated in the last section. The specific heat is found to be discontinuous at the critical point.

1. When an ideal Fermi-Dirac or Bose-Einstein gas is placed in a uniform field of force, which we assume to be acting along the  $x$ -axis and extending from  $x = 0$  to  $x \rightarrow \infty$ , then the density distribution of the gas is described by the relation,

$$\eta(x_1) - \eta(x_2) = \alpha(x_2 - x_1), \quad \dots \quad (1)$$

where  $\eta(x)$  denotes the value of the Gibb's free energy at  $x$ , and  $\alpha$  is the force acting on a particle—the force is along the negative  $x$ -axis. If  $n(x)$  denotes the number of particles per unit volume, i.e. the concentration at  $x$ , then  $\eta(x)$  and  $n(x)$  are connected by the relation,

$$n(x) = \int_0^\infty n(\epsilon) d\epsilon = \int_0^\infty \frac{a(\epsilon) d\epsilon}{\beta + \exp. \frac{\epsilon - \eta(x)}{kT}}. \quad \dots \quad (2)$$

$a(\epsilon) d\epsilon$  represents the number of wave-functions for a particle when its kinetic energy lies within  $\epsilon$  and  $\epsilon + d\epsilon$ .

$$a(\epsilon) d\epsilon = \frac{4\pi g}{c^3 h^3} (\epsilon^2 + 2\epsilon mc)^{\frac{1}{2}} (\epsilon + mc^2), \quad \dots \quad (2')$$

where  $m$  is the mass of the particle,  $g$  its weight factor;  $c$  is the velocity of light and  $h$  is Planck's constant, and  $\beta = 0$  for classical statistics,  $\beta = 1$  for Fermi-Dirac statistics and  $\beta = -1$  for Bose-Einstein statistics.

If  $\bar{n}$  denotes the number of particles contained in a vertical cylinder (we suppose the  $x$ -axis to be vertical) of unit cross-section and extending from  $x = 0$  to  $x \rightarrow \infty$ , then

$$\bar{n} = \int_0^\infty n(x) dx = \int_0^\infty \int_0^\infty \frac{a(\epsilon) d\epsilon dx}{\beta + \exp. \frac{1}{kT} \{ \epsilon - \eta(0) + \alpha x \}}, \quad \dots \quad (3)$$

where  $\eta(0)$  is the value of  $\eta(x)$  at  $x = 0$ . Let  $\bar{\epsilon}$  denote the average kinetic energy per particle, then

$$\bar{\epsilon} = \frac{1}{\bar{n}} \int_0^\infty \int_0^\infty \frac{\epsilon a(\epsilon) d\epsilon dx}{\beta + \exp. \frac{1}{kT} \{\epsilon - \eta(0) + \alpha x\}},$$

and integrating twice by parts we obtain

$$\bar{\epsilon} = \frac{1}{\bar{n}} \int_0^\infty \int_0^\infty \frac{\alpha x \frac{d}{d\epsilon} [\epsilon a(\epsilon)] d\epsilon dx}{\beta + \exp. \frac{1}{kT} \{\epsilon - \eta(0) + \alpha x\}}, \quad \dots \quad (4)$$

provided  $a(\epsilon) = 0$  at  $\epsilon = 0$ . If  $\bar{W}$  be the average potential energy per particle then

$$\bar{W} = \frac{1}{\bar{n}} \int_0^\infty \int_0^\infty \frac{\alpha x a(\epsilon) d\epsilon dx}{\beta + \exp. \frac{1}{kT} \{\epsilon - \eta(0) + \alpha x\}}. \quad \dots \quad (5)$$

It is usual to consider two extreme cases: (i) the completely non-relativistic case, for which the average kinetic energy per particle is negligible compared to its rest-mass energy, and (ii) the completely relativistic case for which the rest-mass energy is negligible compared to its average kinetic energy. In the non-relativistic case

$$a(\epsilon) d\epsilon = \frac{2\pi g}{h^3} (2m)^{\frac{3}{2}} \epsilon^{\frac{1}{2}} d\epsilon, \quad \dots \quad (6)$$

and in the relativistic case

$$a(\epsilon) d\epsilon = \frac{4\pi g}{(ch)^3} \epsilon^2 d\epsilon, \quad \dots \quad (6')$$

and, therefore, we have from (4) and (5)

$$\frac{\bar{\epsilon}}{\bar{W}} = \begin{cases} \frac{3}{2}, & \text{for the non-relativistic case} \\ 3, & \text{for the relativistic case.} \end{cases} \quad \dots \quad (7)$$

It should be noticed that the above result is independent of the statistics obeyed by the gas, the field strength and the actual location of the plane  $x = 0$  (this plane defines the zero-level for measuring potential energy—and only particles lying above this plane are taken in considering the average values  $\bar{\epsilon}$  and  $\bar{W}$ ).

2. The density distribution for a Fermi-Dirac gas in the non-relativistic case has already been discussed in a previous paper (Kothari and Auluck, 1942). We shall, therefore, treat only the relativistic case for a Fermi-Dirac gas. The Bose-Einstein case is treated in the next section.

For the relativistic (completely) non-degenerate (or classical) case, we have the usual Boltzmann law,

$$n(x) = n_0 e^{-\alpha x/kT}, \dots \dots \dots (8)$$

$n_0$  being the concentration at  $x = 0$ , and further

$$\bar{n} = \int_0^\infty n_0 e^{-\alpha x/kT} dx = \frac{n_0 kT}{\alpha}, \dots \dots \dots (9)$$

$$\text{and} \quad \bar{\epsilon} = 3kT. \dots \dots \dots (10)$$

The concentration for a non-degenerate gas, at any assigned value of  $x$ , is directly proportional to  $\bar{n}$  (or  $n_0$ ) and vanishes for  $x \rightarrow \infty$ . However, for a completely degenerate gas the situation is different. The density distribution, instead of extending to infinity, is confined within  $x = 0$  and  $x = l$ ,  $l$  depending on  $\bar{n}$ . In the case of a relativistic completely degenerate Fermi-Dirac gas (2) and (2') give

$$\eta(x) = ch \left\{ \frac{3n(x)}{4\pi g} \right\}^{\frac{1}{3}}, \dots \dots \dots (11)$$

where  $n(x)$  is the concentration at  $x$ , and hence substituting in (1) we obtain

$$ch \left( \frac{3n_0}{4\pi g} \right)^{\frac{1}{3}} - ch \left( \frac{3n(x)}{4\pi g} \right)^{\frac{1}{3}} = \alpha x, \dots \dots \dots (12)$$

where  $n_0$  is the concentration at  $x = 0$ . The distribution will, therefore, extend from  $x = 0$  to  $x = l$  (i.e.  $x$  vanishes at  $x = l$ ) where  $l$  is given by

$$l = \frac{ch}{\alpha} \left( \frac{3n_0}{4\pi g} \right)^{\frac{1}{3}}, \dots \dots \dots (13)$$

and therefore, from (12) we get

$$n(x) = \frac{4\pi g}{3} \left( \frac{\alpha}{ch} \right)^3 (l-x)^3. \dots \dots \dots (14)$$

We, therefore, have for  $\bar{n}$ , and  $\bar{\epsilon}$ ,

$$\bar{n} = \frac{\pi g}{3} \left( \frac{\alpha}{ch} \right)^3 l^4 = \frac{\pi g ch}{3\alpha} \left( \frac{3n_0}{4\pi g} \right)^{\frac{4}{3}} = \frac{1}{4} n_0 l, \dots \dots \dots (15)$$

$$\begin{aligned} \bar{\epsilon} &= \frac{3}{5} \alpha l = \frac{3}{5} ch \left( \frac{3n_0}{4\pi g} \right)^{\frac{1}{3}} \\ &= \frac{3}{5} ch \left( \frac{3\bar{n}}{\pi g l} \right)^{\frac{1}{3}} = \frac{3}{5} ch \left( \frac{3\bar{n}\alpha}{\pi g ch} \right)^{\frac{1}{3}}, \dots \dots \dots (16) \end{aligned}$$

and  $l$  in terms of  $\bar{n}$  and  $\alpha$  is

$$l = \left( \frac{3\bar{n}}{\pi g} \right)^{\frac{1}{4}} \left( \frac{ch}{\alpha} \right)^{\frac{1}{4}}. \dots \dots \dots (17)$$

For the sake of completeness, we may note that, for the completely degenerate non-relativistic Fermi-Dirac gas, the corresponding formulae are

$$\bar{n} = \left(\frac{3}{4\pi g}\right)^{\frac{1}{3}} \frac{\hbar^2}{5m\alpha} n_0^{\frac{2}{3}} = \frac{8\pi g}{15} \left(\frac{2m}{\hbar^2}\right)^{\frac{1}{3}} \alpha^{\frac{1}{3}} l^{\frac{2}{3}} = \frac{2}{5} n_0 l, \quad \dots \quad (15')$$

and 
$$\bar{\epsilon} = \frac{3}{7} \alpha l = \frac{3}{14} \frac{\hbar^2}{m} \left(\frac{3n_0}{4\pi g}\right)^{\frac{1}{3}} \dots \dots \dots (16')$$

$$= \frac{3}{14} \frac{\hbar^2}{m} \left(\frac{15\bar{n}}{8\pi g l}\right)^{\frac{1}{3}} = \frac{3}{7} \left(\frac{\hbar^2}{2m}\right)^{\frac{1}{3}} \left(\frac{15\alpha\bar{n}}{8\pi g}\right)^{\frac{2}{3}},$$

and 
$$l = \left(\frac{15\bar{n}}{8\pi g}\right)^{\frac{1}{3}} \left(\frac{\hbar^2}{2m\alpha}\right)^{\frac{1}{3}} \dots \dots \dots (17')$$

3. We shall now take up the case of Bose-Einstein gas and discuss how the peculiar condensation phenomenon, first mentioned by Einstein and recently discussed in detail by London (1938-39), Goldstein (1941) and Kothari and Singh (1941) and others, is affected by a field of force. In the case of a Bose-Einstein gas ( $\beta = -1$ ),  $\eta(x)$  can never be positive, otherwise the number of particles  $n(\epsilon)$ , occupying a state of kinetic energy  $\epsilon$ , would be negative for some value of  $\epsilon$ , which is inadmissible. For Bose-Einstein statistics, the non-degeneracy is characterised by  $\eta < 0$ , and the degeneracy by  $\eta = 0$ . Writing, as usual,

$$\eta(x) = \eta(0) - \alpha x, \quad \dots \dots \dots (18)$$

we have from equation (2)

$$n(x) = \sum_{s=1}^{\infty} \int_0^{\infty} e^{-s\{\epsilon - \eta(0) + \alpha x\}/kT} \cdot u(\epsilon) d\epsilon, \quad \dots \dots (19)$$

and, therefore, in the non-relativistic case

$$n(x) = \frac{g}{\hbar^3} (2\pi m kT)^{\frac{3}{2}} \sum_{s=1}^{\infty} \frac{1}{s^{\frac{3}{2}}} e^{\left[\frac{\eta(0) - \alpha x}{kT}\right]s}, \quad \dots \dots (20)$$

and in the relativistic case

$$n(x) = 8\pi g \left(\frac{kT}{ch}\right)^3 \sum_{s=1}^{\infty} \frac{1}{s^3} e^{\frac{\eta(0) - \alpha x}{kT} s}. \quad \dots \dots (21)$$

Hence we have for  $\bar{n}$ , in the non-relativistic case

$$\bar{n} = \frac{g}{\hbar^3} (2\pi m kT)^{\frac{3}{2}} \frac{kT}{\alpha} \sum_{s=1}^{\infty} \frac{1}{s^{\frac{3}{2}}} e^{\frac{\eta(0)}{kT} s}, \quad \dots \dots (22)$$

and in the relativistic case

$$\bar{n} = 8\pi g \left( \frac{kT}{ch} \right)^3 \frac{kT}{\alpha} \sum_1^{\infty} \frac{1}{s^4} e^{\frac{\eta(0)}{kT}} \dots \dots \dots (22')$$

The R.H.S. in (22) or (22') attains its maximum value when  $\eta(0) = 0$ , and, therefore,  $\eta(x) = -\alpha x$ . This means that the Bose-Einstein gas is degenerate only at the level  $x = 0$ . Denoting the maximum value of the R.H.S. of (22) by  $n^*$ , we have

$$n^* = \frac{g}{h^3} (2\pi mkT)^{\frac{3}{2}} \frac{kT}{\alpha} \zeta\left(\frac{5}{2}\right), \dots \dots \dots (23)$$

and similarly from (22')

$$n^* = 8\pi g \left( \frac{kT}{ch} \right)^3 \frac{kT}{\alpha} \zeta(4), \dots \dots \dots (23')$$

$\zeta(s)$  being Riemann's zeta function. When the actual number of particles lying per unit area above the plane  $x = 0$  exceeds  $n^*$ , then it follows, from arguments familiar in connection with the discussion of the condensation phenomenon for a Bose-Einstein gas, that the difference  $(\bar{n} - n^*)$  represents the number of particles in the zero-energy state, and these will be all situated at the level  $x = 0$ .

Defining the critical temperature  $T_0$  by the relation

$$T_0 = \begin{cases} \left[ \frac{h^3 \bar{n}}{g(2\pi mk)^{\frac{3}{2}}} \frac{\alpha}{k\zeta(\frac{5}{2})} \right]^{\frac{2}{5}}, & \text{(non-relativistic)} \\ \left[ \frac{\bar{n}}{8\pi g} \left( \frac{ch}{k} \right)^3 \frac{\alpha}{k\zeta(4)} \right]^{\frac{1}{4}}, & \text{(relativistic)} \end{cases} \dots \dots \dots (24)$$

we see that so long as  $T > T_0$  (i.e.  $\bar{n} < n^*$ ), the gas is non-degenerate throughout the entire space. But for  $T < T_0$  (i.e.  $\bar{n} > n^*$ ), the gas is degenerate at the level  $x = 0$  and non-degenerate above it; and the number of particles in the zero-energy state which are all located at the level  $x = 0$  is given by

$$(\bar{n} - n^*) = \begin{cases} \bar{n} \left[ 1 - \left( \frac{T}{T_0} \right)^{\frac{5}{2}} \right] & \text{(non-relativistic)} \\ \bar{n} \left[ 1 - \left( \frac{T}{T_0} \right)^4 \right] & \text{(relativistic).} \end{cases} \dots \dots \dots (25)$$

It should be particularly noted that whereas in the absence of the field the condensed phase (i.e. particles in the zero-energy state) is present throughout the mass of the gas, in the presence of the field the condensed phase is only present within a restricted region of space.<sup>1</sup>

<sup>1</sup> In the foregoing treatment the thickness of the layer, in which the condensed phase is present, is zero because we have assumed that for the zero-energy state  $\epsilon_0 = 0$ , but due to the uncertainty relation the zero-state has always a small but non-vanishing energy.



It now remains to derive the expression for the average kinetic energy per particle and this is easily found to be, for the case  $T > T_0$ ,

$$E = \bar{n}\bar{\epsilon} = \frac{3g}{2h^3} (2\pi mkT)^{\frac{3}{2}} \left(\frac{kT}{\alpha}\right)^2 \sum_1^{\infty} \frac{1}{s^{\frac{5}{2}}} e^{\frac{\eta(0)}{kT} s}, \text{ (non-relativistic) } \dots (26)$$

and

$$E = \bar{n}\bar{\epsilon} = 24\pi g \left(\frac{kT}{ch}\right)^3 \frac{(kT)^2}{\alpha} \sum_1^{\infty} \frac{1}{s^6} e^{\frac{\eta(0)}{kT} s}, \text{ (relativistic) } \dots (26')$$

and hence

$$\bar{\epsilon} = \frac{3}{2} kT \frac{\sum_1^{\infty} \frac{1}{s^{\frac{5}{2}}} e^{\frac{\eta(0)}{kT} s}}{\sum_1^{\infty} \frac{1}{s^{\frac{3}{2}}} e^{\frac{\eta(0)}{kT} s}}, \text{ (non-relativistic) } \dots (27)$$

and

$$\bar{\epsilon} = 3kT \frac{\sum_1^{\infty} \frac{1}{s^6} e^{\frac{\eta(0)}{kT} s}}{\sum_1^{\infty} \frac{1}{s^4} e^{\frac{\eta(0)}{kT} s}}, \text{ (relativistic) } \dots (27')$$

In the degenerate case ( $T < T_0$ ) we have

$$E = \begin{cases} \frac{3g}{2h^3} (2\pi mkT)^{\frac{3}{2}} \frac{(kT)^2}{\alpha} \zeta(\frac{5}{2}) & \text{(non-relativistic)} \\ 24\pi g \left(\frac{kT}{ch}\right)^3 \frac{(kT)^2}{\alpha} \zeta(5) & \text{(relativistic)} \end{cases} \dots (28)$$

and

$$\bar{\epsilon} = \begin{cases} \frac{3}{2} kT \frac{\zeta(\frac{5}{2})}{\zeta(\frac{3}{2})} & \text{(non-relativistic)} \\ 3kT \frac{\zeta(5)}{\zeta(4)} & \text{(relativistic)} \end{cases} \dots (29)$$

The constant-volume specific heat  $C_v$  at the point  $T = T_0$  is easily shown to be discontinuous. This is to be contrasted with the case of no field where the discontinuity lies in the temperature-derivative of the specific heat and not

in the specific heat itself. The ratio of the specific heats at the point of discontinuity is found to be

$$\frac{[C_v]_{\text{at } T_0+0}}{[C_v]_{\text{at } T_0-0}} = \begin{cases} 1 - \frac{5}{7} \frac{[\zeta(\frac{5}{2})]^2}{\zeta(\frac{3}{2})\zeta(\frac{7}{2})} & \text{(non-relativistic)} \\ 1 - \frac{4}{5} \frac{[\zeta(4)]^2}{\zeta(3)\zeta(5)} & \text{(relativistic)} \end{cases} \quad \dots (30)$$

The condensation phenomenon for a Bose-Einstein degenerate gas, due largely to the recent work of London, has acquired physical significance because of its possible connection with the peculiar properties of liquid He II. The possible applications of the foregoing results will be considered elsewhere.

## REFERENCES.

- Goldstein, L. 1941. *Jour. Chem. Phys.*, **9**, 273.  
 Kothari, D. S. and Singh, B. N. 1941. *Proc. Roy. Soc.*, **178**, 135.  
 Kothari, D. S. and Auluck, F. C. 1942. *Proc. Nat. Inst. Sci. India*, **8**, 157.  
 London, F. 1938. *Phys. Rev.*, **54**, 947.  
 1939. *Jour. Physical Chemistry U.S.A.*, **43**, 49.



# THE INSTABILITY OF RADIAL OSCILLATIONS OF A VARIABLE STAR AND THE ORIGIN OF THE SOLAR SYSTEM.

By A. C. BANERJI, *M.A. (Cantab.), F.N.I.*

(Received February, 9, 1942.)

## ABSTRACT.

No existing tidal theory can satisfactorily explain the origin of the solar system and account for the angular momentum and energy possessed by the planets. To obviate the difficulties of the tidal theories, the Sun in the present theory is supposed to be originally a part of a Cepheid variable of about nine times the Sun's mass, which oscillated with small amplitude. The near-by passage of a star of about the Cepheid's mass increased the amplitude of the oscillations rendering them unstable. That this could have been possible has been mathematically shewn in this paper. Matter was consequently thrown out, which condensed into the Sun and the planets. Enough energy for this is available in the parent Cepheid. The Sun is shown to have taken about two-fifths of the energy of the parent Cepheid. It has also been shown that the encounter need not be very close, nor need the intruding star have an inordinately large velocity, to give the requisite angular momentum to the Sun and its planets and enough energy to the Solar System to escape from the parent Cepheid.

We shall briefly allude to some of the modern theories which have been proposed from time to time to explain the origin of the Solar System. The planetesimal theory of Chamberlin (1916) and Moulton (1906) and the tidal theory of Jeans (1919) and Jeffreys (1929) undoubtedly possess certain distinct advantages in explaining the dynamical arrangement of the bodies which form our Solar System, but they are also open to some grave objections. In both these theories it is supposed that the Sun and a passing star narrowly missed each other. Jeffreys later on supposed that there was grazing collision between the two bodies. It is also surmised that the angular momentum of the planets was obtained at the expense of the small fraction of what had originally been possessed by the passing star. But Russell (1935) has pointed out the grave difficulty which arises when the distribution of angular momentum per unit mass of the passing star as well as of the planets is considered. If  $l$  be the semi-latus rectum of the orbit of a body, whether a planet or a passing star, relative to the Sun, we find that the angular momentum per unit mass of the body is proportional to  $\sqrt{l(1+x)}$ , where  $x$  is the ratio of the mass of the body to that of the Sun. Now to produce tidal eruptions in the Sun, the encounter must have been very close, and the parameter  $l$  may be taken to be of the order of 0.03 astronomical unit. If we take  $x$  to be one, we find that the angular momentum per unit mass of the passing star would be 0.25 unit, taking that of the earth per unit mass to be unity. On the same scale

we find that the angular momentum per unit mass varies from 0.61 unit in case of Mercury to 5.49 units for Neptune. The weighted average for all the planets is calculated to be about 2.63 units, which is ten times greater than the amount which the star can possess due to its motion round the Sun and at the same time produce tidal eruptions for which a close encounter is necessary. It appears to be highly improbable, if not impossible, that so much angular momentum can be put into the material ejected from the Sun by the passing star during the encounter.

Recently there has been a number of new lines of attack on this problem. It has been suggested (Russell, *loc. cit.*, p. 135) that our Sun might have been a binary star having a companion much smaller than itself which revolved in an orbit about the Sun at a distance comparable with those of the major planets. A collision between this companion and a passing star broke the former into fragments which were condensed into the present planets. Russell abandoned this hypothesis as unpromising, as it is not possible to explain satisfactorily how the collision would be capable of breaking up a single mass into several planets of comparable size. Moreover, it is unlikely that the plane of orbit of the original companion about the Sun and that of the intruding star would be roughly parallel. Lyttleton (1936) tried to give a mathematical treatment of the above suggestion. He studied the particular case when the three stars were of equal mass. Luyten and Hill (1937) have pointed out two main difficulties in Lyttleton's theory. The first is that the energy required to form the planets is very large and the intruding star must have an initial velocity of 100 km./sec. at least relative to the Sun at a great distance from the Sun, which is a rare occurrence in Nature. The centre of the planetary ribbon which may be formed between the Sun's companion and the intruding star would acquire a velocity much greater than the velocity of escape relative to the Sun. The second difficulty is that, after the encounter, the subsequent action of these two colliding stars, that is, the Sun's companion and the intruding star, on the planetary ribbon, cannot be neglected. Luyten and Hill have shown that about 94 per cent of the total length of the ribbon would be retained by these two stars, and so only 6 per cent of the length of the filament becomes available for possible capture by the Sun and subsequent formation into planets.

To avoid the requirements of a very large velocity for the intruding star, Lyttleton (1938), in a later theory, assumed that the intruding star was much more massive than the Sun. But Luyten (1939) has shown that even with the above assumption no favourable case for formation of our planetary system can be established. Luyten has shown the possibility that, in order that the Sun could capture a part of the filament between its companion and the intruding star, 'the Sun must have been running parallel to the filament for some time, and must itself have suffered a close approach or collision with the intruder.' In the above case, the Sun itself would be captured by the more massive intruder.

It can be mathematically shown that rapidly rotating stars break up by fission preferentially in the vicinity of another star. Ross Gunn (1941) has considered the case of a rapidly rotating star, with angular velocity of rotation slightly less than the critical value for fission, which approaches another star. When they are sufficiently near together, both are deformed by tidal forces. Tidal forces acting in conjunction with the centrifugal forces break up the rapidly rotating star. Condensed masses of planetary size from outermost zones leave the surface of the star which has broken up into components. Now tidal forces between the stellar components and the second star reduce their angular velocity of rotation. Gunn believes that the resulting slowly rotating outer component finally proceeds to infinity, accompanied by two different families of satellites all marked by definite asymmetries. He maintains that no serious inconsistency of energy or momentum will occur, and that a stellar encounter of the type considered above will produce a distribution remarkably like the Solar System.

The main difficulty of this theory is that such close encounters in which one of the approaching stars is rapidly rotating with angular velocity almost equal to its critical value of fission are highly improbable. The suggestion that such encounters might have occurred in the early stages of evolution when our Universe was much more compact and the stars were very close together seems also to be too far-fetched.

Very recently Lyttleton (1941) has also considered the question of planetary formation resulting from the break-up of a single stellar mass due to rotational instability. He regards the Sun as the distant companion of a close double star whose components had first merged into a single body and then this mass broke up into a pair of stars due to rotational instability, and a planetary filament was produced between them as they were separated from one another. The initial system was thus a triple star, and Lyttleton maintains that a single mass which could be obtained by combining the two components of a double star would have sufficient angular momentum to cause instability, fission, and ultimate formation into a planetary filament. Lyttleton further suggests that the two new components separate from the Sun with hyperbolic velocity, leaving the filament to be captured by the latter. This part of his theory is open to the same objection as his earlier theory of planetary formation depending on encounters. Moreover, it is not clear how the decrease of separation between the two components of the double star can be brought about so that they would ultimately coalesce into a single body. It seems rather far-fetched to suggest that this process of coalescence was brought about by accretion of inter-stellar matter. It is also difficult to see how the close passage of a third star can be responsible for gradual merging of the two components of the double star into a single body. In all probability such a process may result in catastrophic collisions between the two components.

In a recent paper, P. L. Bhatnagar (1940) has studied the changes that would take place in the velocity of the Sun and also its distance from its companion due to the encounter of the latter with the intruding star. He has shewn that even in the most favourable cases there is hardly any possibility for the formation of the planetary ribbon, as in such cases an actual collision between the Sun, its companion, and the intruding star cannot be avoided.

It may be mentioned now that from astrophysical considerations Spitzer (1939) has proved that even if the desired planetary ribbon is assumed to be formed by a close encounter between two stars, it would acquire sufficient velocity of expansion to dissipate in a period of the order of an hour at the most at stellar temperatures without giving birth to any planets. Thus from two entirely different considerations we find that the existing tidal theories are unable to explain the formation of the Solar System.

It may be mentioned here that in reply to Spitzer, Lyttleton (1941) states that it is not permissible to regard the filament as conditioned solely by its own gravitational effect. On the other hand, the filament would be under the combined gravitational field of the stars concerned. Moreover, he maintains that a temperature greatly in excess of that likely to be reached at any point of a star similar to the Sun is required to give thermal velocities equal to the escape velocities of the particles in the filament.

We have now seen that it is hardly possible for an intruding star to supply most of the energy and momentum required for the formation of planets. It has been suggested that the raw material which ultimately formed planets was shot out from the Sun by powerful internal forces. If there were sufficient initial impulse, the planets could easily have been formed at their present distances while the attraction of a passing star would set them revolving in their present orbits. But the main difficulty is how such powerful internal forces came to exist. We have to examine the possibility whether the requisite amount of energy for formation of planets can be obtained from available subatomic sources due to thermo-nuclear reactions. We have further to examine how a state of dynamic instability can be brought about, which would result in ejection of matter to planetary distances. Cepheid variables constitute a well-known class of periodic variables having short periods. Cepheid variables lurch (Merrill, 1938*a*) towards us when they are bright, away from us when they are faint. The accepted interpretation is that of pulsation which holds the field now as the best working hypothesis. Jeans (1929) suggested that changes in brightness of variable stars depend on the rotation of a pear-shaped body. This explanation in which the orientation of the star's axis plays an important part is not acceptable to the astronomers for any standard type of variables, for they are of the opinion that a variable star has approximate spherical symmetry so that it would look the same at all times from all directions and would not depend on the location of the observer (Merrill, 1938*b*).

Gaposchkin (1938) mentions that the Cepheids are in fact among the most luminous objects of their spectral classes, and may appropriately be called 'supergiants'. Gamow (1939a) suggests that the pulsation phenomena observed for Cepheid variables are due to instability during the transitions from the giant branch into the main sequence. Further, he is of the opinion that the pulsative instability of the stars near the limiting line of R-L diagram (radius-luminosity diagram) is due to the conditions existing during the transition from the state of thermo-nuclear evolution into the state of purely gravitational contraction.

It will be useful to investigate how dynamical instability of pulsation of a Cepheid variable can be brought about, and to find out when this state of instability has been attained, whether sufficient sub-atomic energy can be obtained in the Cepheid to eject matter to planetary distances to be condensed into planets. It has to be seen whether a passing star (a close encounter not necessarily being required) can bring about this state of instability by producing tidal disturbances. It may be remarked that if the planets are once formed, the attraction of the passing star would set them moving sidewise.

We may also examine the case of pulsating instability of a Cepheid variable having mass considerably greater than that of the Sun with the possibility that an amount of matter having mass more or less equal to that of the Sun might have been thrown out to a distance where this ejected material would ultimately escape from the parent's body with part of the ribbon which had initially joined the two, and thus become our Sun with planets formed out of this partial ribbon. The parent Cepheid as well as the passing star would give the necessary angular momentum to the planets to go round the Sun in their orbits.

Eddington (1926) has considered the adiabatic pulsations of a variable star, which are symmetrical about the centre. The star as it expands and contracts remains spherical in shape. He only considered small radial oscillations, the square of whose amplitude could be neglected, and so all the variations could be represented by simple harmonic terms.

Sterne (1937) has considered three models of oscillating stars for which the square of the amplitude was neglected, viz.

- (1) the star of uniform density;
- (2) the star in which the density varies inversely as the square of the distance from the centre up to a very small distance from the centre within which the density is constant; and
- (3) the model in which nearly all the mass is contained in a particle at the centre and in the remaining portion of the star the density varies inversely as the square of the distance from the centre.

We shall now retain the square of the amplitude in our equations and try to investigate their solutions.



For radial oscillations of a star, the equation of motion, in general, is

$$\ddot{\xi} = -\frac{g_0 \xi_0^2}{\xi^2} - \frac{1}{\rho} \frac{dP}{d\xi}, \quad \dots \quad (1)$$

where  $\xi$ ,  $g$ ,  $\rho$  and  $P$  denote distance from centre, gravity, density and pressure respectively, at a point, and  $\xi_0$ ,  $g_0$ ,  $\rho_0$  and  $P_0$  are the corresponding values at the same point in the undisturbed state of the star.

Define  $\xi_1$ ,  $\rho_1$  and  $P_1$  by

$$\xi = \xi_0(1 + \xi_1), \quad \rho = \rho_0(1 + \rho_1) \text{ and } P = P_0(1 + P_1), \quad \dots \quad (2)$$

where  $\xi_1$ ,  $\rho_1$  and  $P_1$  are small quantities.

We shall keep later on small quantities of the second order, that is, up to  $\xi_1^2$ , etc.

During the motion the following equation remains true:

$$\rho_0 \xi_0^2 d\xi_0 = \rho \xi^2 d\xi. \quad \dots \quad (3)$$

For adiabatic oscillation, the relation

$$P = K\rho^\gamma \quad \dots \quad (4)$$

holds good, where  $\gamma$  is the effective ratio of the specific heats (regarding the matter and enclosed radiation as one system).

We get from (2), (3) and (4)

$$1 + \rho_1 = \frac{1}{(1 + \xi_1)^2 (1 + \xi_1 + \xi_0 \xi_1')} \quad \dots \quad (5)$$

and

$$1 + P_1 = \frac{1}{(1 + \xi_1)^{2\gamma} (1 + \xi_1 + \xi_0 \xi_1')^\gamma}, \quad \dots \quad (6)$$

where

$$\xi_1' = \frac{d\xi_1}{d\xi_0}.$$

We therefore have

$$\ddot{\xi} = -\frac{g_0}{(1 + \xi_1)^2} - \frac{(1 + \xi_1)^2}{\rho_0} \left\{ (1 + P_1) \frac{dP_0}{d\xi_0} + P_0 \frac{dP_1}{d\xi_0} \right\}. \quad \dots \quad (7)$$

From equation of undisturbed state we get

$$\frac{dP_0}{d\xi_0} = -g_0 \rho_0.$$

The equation (7) may now be put into the form

$$\ddot{\xi} = -g_0 \left[ \frac{1}{(1 + \xi_1)^2} - \frac{1}{(1 + \xi_1)^{2\gamma-2} (1 + \xi_1 + \xi_0 \xi_1')^\gamma} \right] - \frac{P_0}{\rho_0} (1 + \xi_1)^2 \frac{d}{d\xi_0} \left[ \frac{1}{(1 + \xi_1)^{2\gamma} (1 + \xi_1 + \xi_0 \xi_1')^\gamma} \right]. \quad \dots \quad (8)$$

### Approximations.

We shall neglect higher powers of  $\xi_1$ , etc., than the second. Following the method of P. L. Bhatnagar (see later) we get:—

$$(1+P_1) = 1 - \gamma(3\xi_1 + \xi_0\xi_1') + \left\{ \frac{\gamma(\gamma+1)}{2} \xi_0^2 \xi_1'^2 + \frac{3}{2} \gamma(3\gamma+1) \xi_1^2 + \gamma(3\gamma+1) \xi_0 \xi_1 \xi_1' \right\},$$

$$\begin{aligned} \frac{dP_1}{d\xi_0} = & -\gamma(4\xi_1' + \xi_0\xi_1'') + [\gamma(4\gamma+2)\xi_0\xi_1'^2 + \gamma(\gamma+1)\xi_0^2\xi_1'\xi_1'' \\ & + 4\gamma(3\gamma+1)\xi_1\xi_1' + \gamma(3\gamma+1)\xi_0\xi_1\xi_1''], \text{ where } \xi_1'' = \frac{d^2\xi_1}{d\xi_0^2}. \end{aligned}$$

$$\begin{aligned} \text{Hence} \quad (1+P_1)(1+\xi_1)^2 = & 1 - \{ (3\gamma-2)\xi_1 + \gamma\xi_0\xi_1' \} \\ & + \left\{ \left( \frac{9}{2}\gamma^2 - \frac{9}{2}\gamma + 1 \right) \xi_1^2 + \gamma(3\gamma-1)\xi_0\xi_1\xi_1' + \frac{\gamma(\gamma+1)}{2} \xi_0^2 \xi_1'^2 \right\}. \\ (1+\xi_1)^2 \frac{dP_1}{d\xi_0} = & -\gamma(4\xi_1' + \xi_0\xi_1'') + \{ 4\gamma(3\gamma-1)\xi_1\xi_1' \\ & + 2\gamma(2\gamma+1)\xi_0\xi_1'^2 + \gamma(3\gamma-1)\xi_0\xi_1\xi_1'' \\ & + \gamma(\gamma+1)\xi_0^2\xi_1'\xi_1'' \}. \end{aligned}$$

We get, therefore, from equation (7),

$$\begin{aligned} \ddot{\xi} = g_0 \left[ \left\{ -(3\gamma-4)\xi_1 - \gamma\xi_0\xi_1' \right\} + \left\{ \left( \frac{9}{2}\gamma^2 - \frac{9}{2}\gamma - 2 \right) \xi_1^2 \right. \right. \\ \left. \left. + \gamma(3\gamma-1)\xi_0\xi_1\xi_1' + \frac{\gamma(\gamma+1)}{2} \xi_0^2 \xi_1'^2 \right\} \right] \\ + \frac{P_0}{\rho_0} \gamma \left[ (4\xi_1' + \xi_0\xi_1'') - \{ 4(3\gamma-1)\xi_1\xi_1' + 2(2\gamma+1)\xi_0\xi_1'^2 \right. \\ \left. + (3\gamma-1)\xi_0\xi_1\xi_1'' + (\gamma+1)\xi_0^2\xi_1'\xi_1'' \} \right]. \quad \dots \quad (8') \end{aligned}$$

Let us assume in the *beginning* that  $\xi_1$  is small and that

$$\xi_1 = a_1(\xi_0) \cos nt - a_2(\xi_0) \cos 2nt - a_3(\xi_0), \quad \dots \quad (9)$$

where  $a_1(\xi_0)$  is a small quantity of the first order and  $a_2(\xi_0)$  and  $a_3(\xi_0)$  are small quantities of the second order in  $\xi_1$ . We shall neglect small quantities of the third and higher orders.  $a_3(\xi_0)$  has been introduced for the vanishing of certain quantities of second order which are left over after equating coefficients of  $\cos nt$  and  $\cos 2nt$  to zero.

We have

$$\xi = \xi_0(1+\xi_1), \text{ where } \dot{\xi} = \frac{d\xi}{dt}, \ddot{\xi} = \frac{d^2\xi}{dt^2}.$$

$$\text{Hence} \quad \ddot{\xi} = \xi_0 \ddot{\xi}_1 = -n^2 \xi_0 \{a_1(\xi_0) \cos nt - 4a_2(\xi_0) \cos 2nt\}. \quad \dots (10)$$

$$\dot{\xi}_1 = a_1'(\xi_0) \cos nt - a_2'(\xi_0) \cos 2nt - a_3'(\xi_0). \quad \dots (11)$$

$$\dot{\xi}_1 = \dot{a}_1 \cos nt - \dot{a}_2 \cos 2nt - \dot{a}_3, \quad \dots (12)$$

$$\text{where } \dot{\xi}_1 = \frac{d\xi_1}{d\xi_0}, \dot{\xi}_1 = \frac{d^2\xi_1}{d\xi_0^2}, \text{ etc.}$$

Substituting in (8) we have

$$\begin{aligned} & \left[ n^2 a_1 \xi_0 + g_0 \{ -(3\gamma - 4)a_1 - \gamma \xi_0 a_1' \} + \frac{P_0 \gamma}{\rho_0} \{ 4a_1' + \xi_0 a_1'' \} \right] \cos nt \\ & + \left[ -4n^2 \xi_0 a_2 + g_0 \{ (3\gamma - 4)a_2 + \gamma \xi_0 a_2' + \frac{1}{4} (3\gamma - 4)(3\gamma + 1)a_1^2 \right. \\ & + \frac{1}{2} \gamma (3\gamma - 1) \xi_0 a_1 a_1' + \frac{1}{4} \gamma (\gamma + 1) \xi_0 a_1'^2 \} + \frac{P_0 \gamma}{\rho_0} \{ -4a_2' - \xi_0 a_2'' \\ & - 2(3\gamma - 1)a_1 a_1' - (2\gamma + 1) \xi_0 a_1'^2 - \frac{1}{2} (3\gamma - 1) \xi_0 a_1 a_1'' - \frac{1}{2} (\gamma + 1) \xi_0^2 a_1' a_1'' \} \left. \right] \cos 2nt \\ & + \left[ g_0 \{ (3\gamma - 4)a_3 + \gamma \xi_0 a_3' + \frac{1}{4} (3\gamma - 4)(3\gamma + 1)a_1^2 + \frac{1}{2} \gamma (3\gamma - 1) \xi_0 a_1 a_1' \right. \\ & + \frac{1}{4} \gamma (\gamma + 1) \xi_0^2 a_1'^2 \} + \frac{P_0 \gamma}{\rho_0} \{ -4a_3' - \xi_0 a_3'' - 2(3\gamma - 1)a_1 a_1' \\ & \left. - (2\gamma + 1) \xi_0 a_1'^2 - \frac{1}{2} (3\gamma - 1) \xi_0 a_1 a_1'' - \frac{1}{2} (\gamma + 1) \xi_0^2 a_1' a_1'' \} \right] = 0. \quad \dots (13) \end{aligned}$$

Putting the coefficients of  $\cos nt$ ,  $\cos 2nt$  and the terms independent of time to be separately zero we get

$$a_1' + \frac{4-\nu}{\xi_0} a_1 + \left\{ \frac{n^2 \rho_0}{P_0 \gamma} - \frac{\alpha \nu}{\xi_0^2} \right\} a_1 = 0, \quad \dots (14)$$

$$a_2' + \frac{4-\nu}{\xi_0} a_2 + \left\{ \frac{4n^2 \rho_0}{P_0 \gamma} - \frac{\alpha \nu}{\xi_0^2} \right\} a_2 = Q, \quad \dots (15)$$

and

$$a_3' + \frac{4-\nu}{\xi_0} a_3 - \frac{\alpha \nu}{\xi_0^2} a_3 = Q, \quad \dots (16)$$

where

$$\nu = \frac{g_0 \rho_0 \xi_0}{P_0}, \alpha = 3 - \frac{4}{\gamma}, \quad \dots (17)$$

and

$$\begin{aligned}
 Q = & \left\{ \frac{1}{2}(3\gamma-1) \frac{n^2 \rho_0}{P_0 \gamma} - \frac{3}{4}(\gamma-1) \frac{\alpha \nu}{\xi_0^2} \right\} a_1^2 \\
 & + \frac{1}{2}(\gamma+1) \left\{ \frac{n^2 \rho_0}{P_0 \gamma} - \frac{\alpha \nu}{\xi_0^2} \right\} \xi_0 u_1 a_1' \\
 & + \left\{ 1 - \frac{1}{4}(\gamma+1)\nu \right\} a_1'^2. \quad \dots \quad \dots \quad (18)
 \end{aligned}$$

These equations have also been obtained by my research scholar, P. L. Bhatnagar, in his unpublished thesis for the D. Phil. degree of the Allahabad University.

*Boundary conditions.*

From equation (1) we get

$$\frac{(1+\xi_1)^2}{\rho_0} \frac{d(P_0 P_1)}{d\xi_0} = g_0 \left\{ -\frac{1}{(1+\xi_1)^2} + (1+\xi_1)^2 \right\} - \ddot{\xi}. \quad \dots \quad (19)$$

Remembering that

$$\frac{1}{\rho_0} \frac{dP_0}{d\xi_0} = -g_0,$$

we find that

$$(1+\xi_1)^2 \frac{d(P_0 P_1)}{dP_0} = \left\{ \frac{1}{(1+\xi_1)^2} - (1+\xi_1)^2 \right\} + \frac{\ddot{\xi}}{g_0}. \quad \dots \quad (20)$$

At the boundary  $P_0$  is infinitesimally small, and

$$\frac{d(P_0 P_1)}{dP_0} = P_1.$$

Hence, at the boundary

$$(1+\xi_1)^2 P_1 = \left\{ \frac{1}{(1+\xi_1)^2} - (1+\xi_1)^2 \right\} + \frac{\ddot{\xi}}{g_0}, \quad \dots \quad (21)$$

where  $\xi_1, g_0, \ddot{\xi}$  have their corresponding values at the boundary.

(21) may be put in the form

$$(1+P_1)(1+\xi_1)^2 = \frac{1}{(1+\xi_1)^2} + \frac{\ddot{\xi}}{g_0}. \quad \dots \quad (22)$$

Now, we have, up to small quantities of second order,

$$\begin{aligned}
 P_1 = & -\gamma(3\xi_1 + \xi_0 \xi_1') + \left\{ \frac{1}{2} \gamma(\gamma+1) \xi_0^2 \xi_1'^2 \right. \\
 & \left. + \gamma(3\gamma+1) \xi_0 \xi_1 \xi_1' + \frac{3}{2} \gamma(3\gamma+1) \xi_1^2 \right\}.
 \end{aligned}$$

Now, substituting in (22), we get at the boundary

$$\frac{\ddot{\xi}}{g_0} = - \left\{ (3\gamma - 4)\xi_1 + \gamma\xi_0\xi_1' \right\} + \left\{ \frac{1}{2}(3\gamma - 4)(3\gamma + 1)\xi_1^2 + \gamma(3\gamma - 1)\xi_0\xi_1\xi_1' + \frac{1}{2}\gamma(\gamma + 1)\xi_0^2\xi_1'^2 \right\}. \quad \dots \quad (23)$$

Now, substituting for  $\xi_1$ ,  $\xi_1'$ ,  $\xi_1''$  and  $\ddot{\xi}$  from (9), (10) and (12), and equating the coefficients of  $\cos nt$ ,  $\cos 2nt$  and the term independent of them separately to zero, we get at  $\xi_0 = R$ ,

$$a_1' + \left( \frac{\alpha}{\xi_0} - \frac{n^2}{\gamma g_0} \right) a_1 = 0, \quad \dots \quad (24)$$

$$a_2' + \left( \frac{\alpha}{\xi_0} - \frac{4n^2}{\gamma g_0} \right) a_2 + \frac{1}{4} \frac{\alpha(3\gamma + 1)}{\xi_0} a_1^2 + \frac{1}{2} (3\gamma - 1) a_1 a_1' + \frac{1}{4} (\gamma + 1) \xi_0 a_1'^2 = 0, \quad (25)$$

$$\text{and} \quad a_3' + \frac{\alpha}{\xi_0} a_3 + \frac{1}{4} \frac{\alpha(3\gamma + 1)}{\xi_0} a_1^2 + \frac{1}{2} (3\gamma - 1) a_1 a_1' + \frac{1}{4} (\gamma + 1) \xi_0 a_1'^2 = 0. \quad (26)$$

These conditions have also been obtained by P. L. Bhatnagar.

#### Case I. Sphere of uniform density.

We consider a sphere of undisturbed uniform density  $\rho$ . The mass within radius  $\xi_0$  is  $\frac{4}{3}\pi\rho\xi_0^3$ ; the undisturbed value of gravity and pressure are  $g_0 = \frac{4\pi}{3}G\rho\xi_0$  and  $P_0 = \frac{2\pi}{3}G\rho^2(R^2 - \xi_0^2)$ , where  $G$  is the constant of gravitation and  $R$ , the radius of the undisturbed star.

We have  $\nu = \frac{2x^2}{1-x^2}$ , where  $\xi_0 = Rx$ .

Substituting the values of  $g_0$ ,  $P_0$  and  $\nu$  and putting  $\xi_0 = Rx$  in (14), (15) and (16), we get

$$(1-x^2) \frac{d^2 a_1}{dx^2} + \frac{1}{x} (4-6x^2) \frac{da_1}{dx} + (\beta - 2\alpha) a_1 = 0, \quad \dots \quad (27)$$

$$(1-x^2) \frac{d^2 a_2}{dx^2} + \frac{1}{x} (4-6x^2) \frac{da_2}{dx} + (4\beta - 2\alpha) a_2 = Q_0, \quad \dots \quad (28)$$

$$\text{and} \quad (1-x^2) \frac{d^2 a_3}{dx^2} + \frac{1}{x} (4-6x^2) \frac{da_3}{dx} - \frac{2}{\gamma} a_3 = Q_0, \quad \dots \quad (29)$$

where

$$Q_0 = \left\{ \frac{1}{2} (3\gamma - 1) \beta - \frac{3}{2} (\gamma - 1) \alpha \right\} a_1^2 + \frac{1}{2} (\gamma + 1) (\beta - 2\alpha) x a_1 \frac{da_1}{dx} + \left\{ 1 - \frac{1}{2} (\gamma + 3) x^2 \right\} \left( \frac{da_1}{dx} \right)^2, \quad \dots \quad (30)$$

$$\text{and} \quad \beta = \frac{3n^2}{2\pi G \rho \gamma} \quad \dots \quad (31)$$

Let us now put dashes for differentiation with respect to  $x$ .  
The boundary conditions are at  $x = 1$

$$2a_1' + (2\alpha - \beta) a_1 = 0, \quad \dots \quad (32)$$

$$\begin{aligned} 2a_2' + (2\alpha - 4\beta) a_2 + \frac{1}{2} \alpha (3\gamma + 1) a_1^2 \\ + (3\gamma - 1) a_1 a_1' + \frac{1}{2} (\gamma + 1) a_1'^2 = 0, \quad \dots \quad (33) \end{aligned}$$

$$\begin{aligned} \text{and} \quad 2a_3' + 2\alpha a_3 + \frac{1}{2} \alpha (3\gamma + 1) a_1^2 \\ + (3\gamma - 1) a_1 a_1' + \frac{1}{2} (\gamma + 1) a_1'^2 = 0, \quad \dots \quad (34) \end{aligned}$$

where  $a_1, a_1'$ , etc. have their relevant values at  $x = 1$ .

We shall now get the solution in series of the equation (27) and investigate the convergence of the series in the interval  $0 < x < 1$ .

It is evident from the form of (27) that the boundary condition (32) is satisfied if  $\frac{d^2 a_1}{dx^2}$  remains finite at  $x = 1$ .

The roots of the indicial equation for (27) are 0 and  $-3$ . The negative value gives a singularity at the origin. We, therefore, choose the former value (0) and expand the solution about the origin in a power series of the form

$$a_1 = \sum_0^{\infty} b_{\lambda} x^{\lambda}, \quad \dots \quad (35)$$

where we assume arbitrarily  $b_0 = 1$  (as the equation is linear).

It is found by substitution that the terms in odd powers of  $x$  vanish, and that the coefficients of the even terms satisfy the recurrence formula

$$b_{2\lambda+2} = b_{2\lambda} \frac{2\lambda(2\lambda+5) - \beta + 2\alpha}{(2\lambda+2)(2\lambda+5)} \quad \dots \quad (36)$$

The series (35) will terminate provided

$$\beta - 2\alpha = 2\lambda(2\lambda+5). \quad \dots \quad (37)$$

Otherwise, (35) will be an infinite series whose coefficients are ultimately all of the same sign, and which, by the recurrence formula (36), can be easily shown to be divergent at  $x = 1$ , and convergent for  $x < 1$ .

Hence it is impossible for the boundary condition (32) to be satisfied, and at the same time for  $a_1$  to be finite at  $x = 1$ , unless condition (37) were satisfied.

Let us suppose that condition (37) holds good and that the series for  $a_1$  terminates.

We shall now find out the complementary function of (28). The roots of the indicial equation are again 0 and  $-3$ . Choosing the former, as before, we assume for the complementary function of (28) the series

$$\sum_0^{\infty} c_{\lambda} x^{\lambda}. \quad \dots \quad \dots \quad \dots \quad \dots \quad (38)$$

By substitution we find as before that the terms in odd powers of  $x$  vanish and that the coefficients of the even terms satisfy the recurrence formula

$$c_{2\lambda+2} = c_{2\lambda} \frac{2\lambda(2\lambda+5) - 4\beta + 2\alpha}{(2\lambda+2)(2\lambda+5)}. \quad \dots \quad \dots \quad (39)$$

It is quite possible that for particular values of  $\lambda$  both  $a_1$  and the complementary function of  $a_2$  may terminate, e.g.  $\alpha = \frac{1}{3}$ ,  $\lambda_1 = 3$  and  $\lambda_2 = 7$ .

For the particular integral of (28) we assume the series

$$\sum_0^{\infty} c'_{\lambda} x^{\lambda}. \quad \dots \quad \dots \quad \dots \quad \dots \quad (40)$$

We note from (30) that as, according to our assumption,  $a_1$  is a terminating series, so is  $Q_0$ . Hence, the coefficients of (40) will ultimately follow the same law as those of (38), that is, the terms in odd powers of  $x$  will vanish and the coefficients of the even terms will satisfy the recurrence formula (39).

Reasoning as before, we conclude that it is impossible for the boundary condition (33) to be satisfied and at the same time for  $a_2$  to be finite at  $x = 1$ , unless the following condition were satisfied

$$4\beta - 2\alpha = 2\lambda(2\lambda+5). \quad \dots \quad \dots \quad \dots \quad (41)$$

We shall now suppose that both conditions (37) and (41) were satisfied and the series for  $a_1$  and  $a_2$  both terminate.

The indicial equation for the complementary function of (29) gives again the roots 0 and  $-3$ . Choosing, as before, the first root, and assuming the series to be expanded in the form

$$\sum_0^{\infty} d_{\lambda} x^{\lambda}, \quad \dots \quad \dots \quad \dots \quad \dots \quad (42)$$

we find that the terms in odd powers of  $x$  vanish and the coefficients of the even terms satisfy the recurrence formula

$$d_{2\lambda+2} = d_{2\lambda} \frac{2\lambda(2\lambda+5) + \frac{2}{\gamma}}{(2\lambda+2)(2\lambda+5)}. \quad \dots \quad \dots \quad \dots \quad (43)$$

The series (42) will, therefore, never terminate and for  $x = 1$  can be shown to be divergent. The same remarks will apply to the series assumed for the

particular integral of (29), as its coefficients will ultimately satisfy the recurrence formula (43).

Hence, even if conditions (37) and (41) were satisfied, it is impossible for the boundary condition (34) to be satisfied, as  $a_3$  does not remain finite at  $x = 1$ .

As  $a_1$  is a first order term, while  $a_2$  and  $a_3$  are of the second order, it is impossible for  $a_1$  to remain finite if  $a_2$  and  $a_3$  were not so.

Hence we see that  $\xi_1$  given by (9) cannot remain finite, and the conclusion is that no radial mode of oscillation is possible in this case.

## Case II.

The density varies inversely as the  $p$ th power of the distance from the centre (where  $p$  is a positive integer excluding 1 and 3), except in a small, finite core of constant density surrounding the centre.

Let a small core of radius  $a$  inside the star of radius  $R$  have uniform density, and let the density  $\rho_0$  of the undisturbed state outside the core be  $k/\xi_0^p$  at a distance  $\xi_0$  from the centre ( $a < \xi_0 < R$ ). Let  $\rho_a$  be the uniform density of the core in the undisturbed state and  $\bar{\rho}$  be the mean density of the envelope.

$$\text{Let } \mu = \frac{a}{R}.$$

$$\text{Hence } \rho_a = \frac{k}{a^p} = \frac{k}{R^p \mu^p}.$$

$$\text{Now } \frac{4\pi\bar{\rho}}{3} (R^3 - a^3) = \frac{4\pi k}{p-3} \left( \frac{1}{a^{p-3}} - \frac{1}{R^{p-3}} \right), \text{ if } p \neq 3.$$

$$\text{Hence } k = \frac{\bar{\rho}(p-3)(R^3 - a^3) a^{p-3} R^{p-3}}{3(R^{p-3} - a^{p-3})} = \frac{\bar{\rho}(p-3)\mu^{p-3}(1-\mu^3) R^p}{3(1-\mu^{p-3})} \quad \dots (44)$$

$$\text{and } \bar{\rho} = \frac{3k(1-\mu^{p-3})}{(p-3)(1-\mu^3)\mu^{p-3}R^p} = \frac{3\rho_a(1-\mu^{p-3})\mu^3}{(p-3)(1-\mu^3)}, \quad \dots (45)$$

if  $p \neq 3$ .

The value of gravity at a distance  $\xi_0$  from the origin in the undisturbed state is  $g_0$ , where

$$g_0 = \frac{\frac{4}{3}\pi\rho_a a^3 G + \frac{4\pi k}{p-3} \left[ \frac{1}{a^{p-3}} - \frac{1}{\xi_0^{p-3}} \right] G}{\xi_0^2},$$

[where  $G$  is the gravitational constant],

$$= \frac{4}{3} \frac{\pi k G}{p-3} \frac{1}{\xi_0^2} \left( \frac{p}{a^{p-3}} - \frac{3}{\xi_0^{p-3}} \right), \text{ as } \rho_a = \frac{k}{a^p}.$$

Put  $\xi_0 = Rx$ , where  $\mu < x < 1$ .



Therefore, we have

$$g_0 = \frac{4\pi kG}{3(p-3)R^{p-1}x^2} \left( \frac{p}{\mu^{p-3}} - \frac{3}{x^{p-3}} \right), \quad \dots \quad (46)$$

if  $p \neq 3$  or 1.

Now, in the undisturbed state,

$$\frac{dP_0}{d\xi_0} = -g_0\rho_0.$$

Integrating and remembering that pressure is zero when  $\xi_0 = R$ , we have at a distance  $\xi_0$  from the centre the pressure  $P_0$  given by

$$P_0 = \frac{4\pi k^2 G}{3(p-3)R^{2p-2}} \left\{ \frac{p}{(p+1)\mu^{p-3}} \left( \frac{1}{x^{p+1}} - 1 \right) - \frac{3}{(2p-2)} \left( \frac{1}{x^{2p-2}} - 1 \right) \right\}. \quad (47)$$

Now

$$\begin{aligned} \nu &= \frac{g_0\rho_0\xi_0}{P_0} \\ &= \frac{(p+1)(2p-2)(px^{p-3}-3\mu^{p-3})}{p(2p-2)x^{p-3}(1-x^{p+1})-3(p+1)\mu^{p-3}(1-x^{2p-2})}, \quad \dots \quad (48) \end{aligned}$$

when  $p \neq 3$  or 1.

We have  $\alpha = 3 - \frac{4}{\gamma}$  as before. (49)

Also  $P_0$ ,  $\nu$  and  $k$  are given by equations (47), (48) and (44).

Substituting these in equation (14), we have for the *annular* region:—

$$\begin{aligned} &[-3(p+1)\mu^{p-3}x^2 + p(2p-2)x^{p-1} - \{p(2p-2) - 3(p+1)\mu^{p-3}\}x^{2p}] \frac{d^2a_1}{dx^2} \\ &+ [6(p+1)(p-3)\mu^{p-3}x + (3-p)p(2p-2)x^{p-2} - 4\{p(2p-2) \\ &- 3(p+1)\mu^{p-3}\}x^{2p-1}] \frac{da_1}{dx} + [3\alpha(p+1)(2p-2)\mu^{p-3} \\ &- \alpha p(p+1)(2p-2)x^{p-3} + fx^p]a_1 = 0, \quad \dots \quad (51) \end{aligned}$$

where  $f = \frac{6n^2}{4\pi kG\gamma} (p^2-1)(p-3)R^p\mu^{p-3}$  .. .. (52)

Let  $a_1 = x^q \sum_{\lambda=0}^{\infty} b_{\lambda} x^{\lambda}$  satisfy (51) .. .. (53)

The indicial equation gives

$$q = \frac{(2p-5) \pm \sqrt{(2p-5)^2 + 8\alpha(p-1)}}{2}, \quad \dots \quad (54)$$

that is, two real roots, one positive, the other negative. We keep both the roots as  $\mu$  though small is finite.

Equating the coefficients of  $x^{q+\lambda}$  to zero, we arrive at the following recurrence formula:

$$\begin{aligned} fb_{\lambda-p} - \{p(2p-2) - 3(p+1)\mu^{p-3}\}(\lambda+q-2p+2)(\lambda+q-2p+5)b_{\lambda-2p+2} \\ + p(2p-2)\{(\lambda+q-p+3)(\lambda+q-2p+5) - \alpha(p+1)\}b_{\lambda-p+3} \\ - 3(p+1)\mu^{p-3}\{(\lambda+q-2p+5)(\lambda+q) - \alpha(2p-2)\}b_{\lambda} = 0. \end{aligned} \quad (55)$$

From (55) we have

$$\begin{aligned} fb_{\lambda-p} = \lambda^2[\{p(2p-2) - 3(p+1)\mu^{p-3}\}b_{\lambda-2p+2} \\ - p(2p-2)b_{\lambda-p+3} + 3(p+1)\mu^{p-3}b_{\lambda}] \\ + \lambda[\{p(2p-2) - 3(p+1)\mu^{p-3}\}(2q-4p+7)b_{\lambda-2p+2} \\ - p(2p-2)(2q-3p+8)b_{\lambda-p+3} + 3(p+1)\mu^{p-3}(2q+5-2p)b_{\lambda}] \\ + [\{p(2p-2) - 3(p+1)\mu^{p-3}\}(q-2p+2)(q-2p+5)b_{\lambda-2p+2} \\ - p(2p-2)\{(q-p+3)(q-2p+5) - \alpha(p+1)\}b_{\lambda-p+3} \\ + 3(p+1)\mu^{p-3}\{q(5+q-2p) - \alpha(2p-2)\}b_{\lambda}]. \end{aligned} \quad (56)$$

The coefficients of  $\lambda^2$  and  $\lambda$  on the right hand side of (56) will be simultaneously zero, provided the following equations are simultaneously satisfied:

$$\{p(2p-2) - 3(p+1)\mu^{p-3}\}x - p(2p-2)y + 3(p+1)\mu^{p-3} = 0, \quad (57)$$

$$\begin{aligned} \text{and } \{p(2p-2) - 3(p+1)\mu^{p-3}\}(2q-4p+7)x - p(2p-2)(2q-3p+8)y \\ + 3(p+1)\mu^{p-3}(2q+5-2p) = 0, \end{aligned} \quad (58)$$

$$\text{where } x = \frac{b_{\lambda-2p+2}}{b_{\lambda}} \quad \text{and} \quad y = \frac{b_{\lambda-p+3}}{b_{\lambda}}.$$

Solving (57) and (58), we get

$$x = \frac{3(p-3)\mu^{p-3}}{p(2p-2) - 3(p+1)\mu^{p-3}}$$

$$\text{and } y = \frac{3\mu^{p-3}}{p}.$$

This makes  $x$  and  $y$  both less than 1, so long as  $p > 3$  (as  $\mu$  is much less than 1). For  $p = 2$ , we have  $x = \frac{6}{9-4\mu}$ , which  $< 1$ , if  $\mu < \frac{3}{4}$ , and  $y > 1$ .

It should be noted that the values of  $x$  and  $y$  which we have obtained are independent of  $\lambda$ , and at least one of them we have proved to be always less than 1 if  $\mu < \frac{3}{4}$ . But, for the convergence of the series (53) when  $x = 1$ , both  $x$  and  $y$  ought ultimately to be greater than 1 for  $p > 3$ , as  $b_{\lambda}$  is a later term to both  $b_{\lambda-2p+2}$  and  $b_{\lambda-p+3}$ ; and for  $p = 2$ ,  $x$  ought to be  $> 1$  and  $y < 1$ .

It is impossible, therefore, for the coefficients of  $\lambda^2$  and  $\lambda$  in the right hand side of (56) to vanish simultaneously, if the series is to be convergent.

As the Cepheids have all finite periods and we are not considering an infinitesimal core, both  $n$  and  $\mu$  are finite. Hence  $f$  given by (52) is finite.

Hence the ratio  $\frac{b_{\lambda-p}}{b_{\lambda-2p+2}}$  is of the order of  $\lambda^2$  or  $\lambda$  and the series (53) diverges when  $x = 1$ . This is because when  $p > 3$ ,  $b_{\lambda-p}$  is a later term than  $b_{\lambda-2p+2}$  and the ratio  $\frac{b_{\lambda-p}}{b_{\lambda-2p+2}}$  must be less than 1 for convergence. When  $p = 2$  the ratio  $\frac{b_{\lambda-p}}{b_{\lambda-2p+2}}$  must be 1, hence coefficients of  $\lambda^2$  and  $\lambda$  must vanish in this case, and the series would again be divergent.

It need hardly be mentioned that the series cannot terminate.

H. K. Sen has given an independent proof of this result in a paper to be published.

With proper substitutions equation (15) becomes

$$\begin{aligned} & [-3(p+1)\mu^{p-3}x^2 + p(2p-2)x^{p-1} - \{p(2p-2) - 3(p+1)\mu^{p-3}\}x^{2p}] \frac{d^2a_2}{dx^2} \\ & + [6(p+1)(p-3)\mu^{p-3}x + (3-p)p(2p-2)x^{p-2} - 4\{p(2p-2) - 3(p+1)\mu^{p-3}\} \\ & \quad \quad \quad x^{2p-1}] \frac{da_2}{dx} \\ & + [3\alpha(p+1)(2p-2)\mu^{p-3} - \alpha p(p+1)(2p-2)x^{p-3} + f'x^p]a_2 = Q, \quad \dots \quad (59) \end{aligned}$$

where 
$$f' = \frac{6n^2}{\pi k G \gamma} (p^2 - 1)(p - 3)R^p \mu^{p-3},$$

and  $Q$  is given by (18).

As in the case of equation (51), we can show the series for the complementary function of (59) to be divergent.

For the particular integral of (59) we note that  $Q$  is a function of  $a_1$ , and, hence, diverges, as we have proved  $a_1$  to be divergent. Hence the particular integral of (59) is divergent.

Therefore no convergent series solution for (59) can be found.

The equation (16) reduces to

$$\begin{aligned} & [-3(p+1)\mu^{p-3}x^2 + p(2p-2)x^{p-1} - \{p(2p-2) - 3(p+1)\mu^{p-3}\}x^{2p}] \frac{d^2a_3}{dx^2} \\ & + [6(p+1)(p-3)\mu^{p-3}x + (3-p)p(2p-2)x^{p-2} - 4\{p(2p-2) - 3(p+1)\mu^{p-3}\} \\ & \quad \quad \quad x^{2p-1}] \frac{da_3}{dx} \\ & + [3\alpha(p+1)(2p-2)\mu^{p-3} - \alpha p(p+1)(2p-2)x^{p-3}]a_3 = Q, \quad \dots \quad (60) \end{aligned}$$

where  $Q$  is given by (18).

The series solution for (60) can similarly be shown to be divergent.

Hence none of  $a_1$ ,  $a_2$  and  $a_3$  in the expression (9) for  $\xi_1$  is finite.

The boundary conditions (24), (25) and (26) follow from the equations (14), (15) and (16) when  $a_1$ ,  $a_2$  and  $a_3$  are finite.

This we show as follows. Dividing each of the equations (14), (15) and (16) by  $\nu$ , we have

$$\frac{a_1''}{\nu} + \frac{4-\nu}{\xi_0 \nu} a_1' + \left\{ \frac{n^2 \rho_0}{P_0 \nu \gamma} - \frac{\alpha}{\xi_0^2} \right\} a_1 = 0, \quad \dots \dots \dots (61)$$

$$\begin{aligned} \frac{a_2''}{\nu} + \frac{4-\nu}{\xi_0 \nu} a_2' + \left\{ \frac{4n^2 \rho_0}{P_0 \nu \gamma} - \frac{\alpha}{\xi_0^2} \right\} a_2 = & \left\{ \frac{1}{2} (3\gamma-1) \frac{n^2 \rho_0}{P_0 \nu \gamma} - \frac{3}{4} (\gamma-1) \frac{\alpha}{\xi_0^2} \right\} a_1^2 \\ & + \frac{1}{2} (\gamma+1) \left\{ \frac{n^2 \rho_0}{P_0 \nu \gamma} - \frac{\alpha}{\xi_0^2} \right\} \xi_0 a_1 a_1' \\ & + \left\{ \frac{1}{\nu} - \frac{1}{4} (\gamma+1) \right\} a_1'^2 \quad \dots \dots \dots (62) \end{aligned}$$

$$\begin{aligned} \text{and} \quad \frac{a_3''}{\nu} + \frac{4-\nu}{\xi_0 \nu} a_3' - \frac{\alpha}{\xi_0^2} a_3 = & \left\{ \frac{1}{2} (3\gamma-1) \frac{n^2 \rho_0}{P_0 \nu \gamma} - \frac{3}{4} (\gamma-1) \frac{\alpha}{\xi_0^2} \right\} a_1^2 \\ & + \frac{1}{2} (\gamma+1) \left\{ \frac{n^2 \rho_0}{P_0 \nu \gamma} - \frac{\alpha}{\xi_0^2} \right\} \xi_0 a_1 a_1' \\ & + \left\{ \frac{1}{\nu} - \frac{1}{4} (\gamma+1) \right\} a_1'^2. \quad \dots \dots \dots (63) \end{aligned}$$

Now when  $x = 1$ ,

$$P_0 = 0,$$

$$\begin{aligned} P_0 \nu = g_0 \rho_0 \xi_0 = & \left[ \frac{4\pi k^2 G}{3(p-3)R^{2p-2}} \frac{px^{p-3} - 3\mu^{p-3}}{x^{2p-2}\mu^{p-3}} \right]_{x=1} \\ = & \frac{4\pi k^2 G(p-3\mu^{p-3})}{3(p-3)R^{2p-2}\mu^{p-3}}, \end{aligned}$$

a finite quantity,

and  $\nu \rightarrow \infty$ , as  $P_0 = 0$ .

Hence, equations (61) and (62) become for finite  $a_1$ ,  $a_2$ ,

$$a_1' + \left( \frac{\alpha}{\xi_0} - \frac{n^2}{\gamma g_0} \right) a_1 = 0 \quad \dots \dots \dots (64)$$

$$\begin{aligned} \text{and} \quad a_2' + \left( \frac{\alpha}{\xi_0} - \frac{4n^2}{\gamma g_0} \right) a_2 + \left\{ \frac{1}{2} (3\gamma-1) \frac{n^2}{\gamma g_0} - \frac{3}{4} (\gamma-1) \frac{\alpha}{\xi_0} \right\} a_1^2 \\ + \frac{1}{2} (\gamma+1) \left\{ \frac{n^2}{\gamma g_0} - \frac{\alpha}{\xi_0} \right\} \xi_0 a_1 a_1' - \frac{1}{4} (\gamma+1) \xi_0 a_1'^2 = 0. \quad \dots \dots \dots (65) \end{aligned}$$

Now from (64) we have

$$\frac{n^2}{\gamma g_0} a_1^2 = a_1' a_1 + \frac{\alpha}{\xi_0} a_1^2.$$

Hence we have

$$\begin{aligned} & \frac{1}{2} (3\gamma - 1) \frac{n^2}{\gamma g_0} a_1^2 - \frac{3}{4} (\gamma - 1) \frac{\alpha}{\xi_0} a_1^2 \\ &= \left\{ \frac{1}{2} (3\gamma - 1) - \frac{3}{4} (\gamma - 1) \right\} \frac{\alpha}{\xi_0} a_1^2 + \frac{1}{2} (3\gamma - 1) a_1 a_1' \\ &= \frac{1}{4} \frac{\alpha (3\gamma + 1)}{\xi_0} a_1^2 + \frac{1}{2} (3\gamma - 1) a_1 a_1'. \end{aligned}$$

Also we have from (64)

$$a_1'^2 = \left( \frac{n^2}{\gamma g_0} - \frac{\alpha}{\xi_0} \right) a_1 a_1'.$$

Hence we have

$$\begin{aligned} & \frac{1}{2} (\gamma + 1) \left\{ \frac{n^2}{\gamma g_0} - \frac{\alpha}{\xi_0} \right\} \xi_0 a_1 a_1' - \frac{1}{4} (\gamma + 1) \xi_0 a_1'^2 \\ &= \frac{1}{2} (\gamma + 1) \xi_0 a_1'^2 - \frac{1}{4} (\gamma + 1) \xi_0 a_1'^2 \\ &= \frac{1}{4} (\gamma + 1) \xi_0 a_1'^2. \end{aligned}$$

Therefore, equation (65) becomes

$$a_2' + \left( \frac{\alpha}{\xi_0} - \frac{4n^2}{\gamma g_0} \right) a_2 + \frac{1}{4} \frac{\alpha (3\gamma + 1)}{\xi_0} a_1^2 + \frac{1}{2} (3\gamma - 1) a_1 a_1' + \frac{1}{4} (\gamma + 1) \xi_0 a_1'^2 = 0. \quad (66)$$

Similarly we have, when  $a_3$  is finite,

$$a_3' + \frac{\alpha}{\xi_0} a_3 + \frac{1}{4} \frac{\alpha (3\gamma + 1)}{\xi_0} a_1^2 + \frac{1}{2} (3\gamma - 1) a_1 a_1' + \frac{1}{4} (\gamma + 1) \xi_0 a_1'^2 = 0. \quad (67)$$

Equations (64), (66) and (67) are the same as the boundary conditions (24), (25) and (26).

Hence it is impossible for the boundary conditions to be satisfied, as  $a_1, a_2, a_3$  do not remain finite at  $x = 1$ .

As  $a_1$  is the predominating first order term in the expression for  $\xi_1$  in (9),  $\xi_1$  becomes infinitely great when  $x = 1$ .

The conclusion, therefore, is that no mode of radial oscillation is possible in this case too.

As regards the variation of density in stellar configurations, some discussion seems to be necessary here. The Trumpler's (Chandrasekhar, 1938) stars are very massive stars. Inference from observation leads to the conclusion that these stars are more or less homogeneous gaseous configurations. But Trumpler's stars are not Variable stars. Kopal (1938) states, 'If the hypotheses involved in the present state of the pulsation theory are correct, the density condensation of Cepheids must depend widely on their spectral class. With advancing spectral type the central condensations seem rapidly

to diminish, and the  $\delta$  Cephei- $F_5$  stars seem to approach the limit of homogeneity.' Chandrasekhar (1936) states 'the giants should be expected to be more homogeneous than the main series stars'. 'The Cepheids and the Cluster-type Variables' which occur in the 'Super-giant' region of the Hertzsprung-Russell diagram must be much less concentrated towards the centre than the typical main series stars. Eddington has also emphasised that the Cepheids should necessarily be more homogeneous than ordinary stars.

Eddington (1941) has enumerated two outstanding difficulties in the Pulsation theory of Cepheid Variables, viz., (1) the quarter-period retardation of phase between the flow of heat in the main part of the interior and the outflow from the surface; and (2) the existence of a period-luminosity law.

Eddington believes that a close connection exists between the period-luminosity law and the quarter-period retardation, and that there is a critical hydrogen layer not far below the photosphere where 'the hydrogen is in the mid-stage of ionisation so that it is ionised and de-ionised in the course of pulsation'. He thinks that the period-luminosity law can only be explained on the hypothesis of a critical ionisation in a layer near the photosphere. Now, the period is affected by the changes of density, and the luminosity depends upon the mass of the star. Hence, a period-luminosity law is effectively a density-mass relation. It implies that for a *given mass, there is a narrow range of density for which the star can pulsate*. For this reason some modification of stellar material is required. He thinks that there is a sharp drop in the ratio of specific heats at the midstage of ionisation in the critical hydrogen layer. This critical layer stores in the form of ionisation the temporary excess of radiant energy accumulating during quarter-period delay in emission. The maintaining energy of the pulsation comes from the change in the rate of liberation of sub-atomic energy which varies with temperature and density. Due to this variation, mechanical work is produced through the same process as that of a thermodynamic engine. Heat is thus added to the material when it is at a high temperature and subtracted when it is at a low temperature. If this maintaining energy exceeds dissipation, then only pulsation can occur. The excess of this energy may be due either to a sudden increase of maintaining energy or to a sudden decrease of dissipation. This maintaining energy can increase if there be a source of sub-atomic energy which is especially sensitive to temperature. But Eddington thinks that this cannot explain the existing sequence of Cepheids in which the stars of short period have much higher internal temperatures than those of long period. He believes that Cepheid pulsation is associated with a transient decrease of dissipation.

It may be mentioned here that it is found from observations that the period of pulsation of many Cepheid Variables changes less than 0.00002 per cent per year from which it may be concluded that on the basis of general pulsation theory the radius of such a star remains approximately constant within the same limit. Gamow (1939b) therefore concludes that the energy-liberation in Cepheid Variables which are red giants is due to some 'nuclear reaction

which is going faster and at a lower temperature than the reaction in the stars of the main sequence'. It is also surmised that the Cepheid Variable would contain in the interior a comparatively large amount of light elements such as lithium, beryllium and boron. These become consumed by the time Cepheid Variables cease to be pulsating stars and reach the main sequence.

In another paper, my research scholar, H. K. Sen, will show that, in the case of radial oscillations of a star, except for (i) uniform density and (ii) density varying inversely as the square of the distance from the centre, the series for  $a_1$  would become divergent even when we neglect terms of the order of  $\xi_1^2$ . So our pulsating stars must either be homogeneous or have density varying inversely as the square of the distance from the centre.

As shown before dynamically, a passing star will bring about some sort of resonance phenomenon, by increasing the amplitude of pulsation through tidal influence and making the system unstable, so that matter is ejected to suitable distances to be formed into planets.

Now, let us calculate approximately the kinetic energy in ergs that must be imparted to the planets so that they may revolve round the Sun and rotate about their own axis.

Taking the mass of the earth, semi-axis major of earth's orbit, and the earth's radius to be unity, we have approximately from observations (Russell *et al.*, 1926)

TABLE I.

Planets.		Semi-Axis major of Orbit.	Sidereal period in years.	Axial rotation in sidereal days.	Mass.	Radius.
Mercury	..	0.39	0.24	88	.04	0.39
Venus	..	0.72	0.62	0.96	0.81	0.97
Earth	..	1	1	1	1	1
Mars	..	1.5	1.9	1.05	0.11	0.53
Jupiter	..	5.2	11.9	0.42	317	11
Saturn	..	9.5	29.5	0.42	95	9
Uranus	..	19.2	84	0.42	14.7	4
Neptune	..	30	165	0.63	17.2	3.9
Pluto	..	40	249	..	0.1	..

Now, if  $M_E$  be the mass of the Earth,  $r_E$  the semi-axis major of the Earth's orbit,  $T_E$  the sidereal period of the Earth's revolution round the Sun,  $t_E$  the period of the Earth's axial rotation and  $K_E$  the Earth's mean radius, we have (Russell *et al.*, 1926)

$$M_E \sim 6 \times 10^{27} \text{ gms.}$$

$$r_E \sim 1.5 \times 10^{13} \text{ cms.}$$

$$T_E \sim 3.16 \times 10^7 \text{ secs.}$$

$$t_E \sim 23.9 \times 60^2 \text{ secs.}$$

$$K_E \sim 6.37 \times 10^8 \text{ cms.}$$

Now the kinetic energy of revolution of the planets round the Sun is  $I_1 = \frac{1}{2} \sum M r^2 \omega^2$ , where  $M$  is the mass of a planet,  $r$  the mean radius of its orbit round the Sun, and  $\omega$  its orbital angular velocity.

Hence we have

$$I_1 = \frac{1}{2} \sum M r^2 \omega^2 = 2\pi^2 \sum \frac{M r^2}{T^2},$$

[where  $T$  is the orbital period]  $= \frac{2\pi^2 r_E^3}{T_E^3} \sum \frac{M}{r}$ , by Kepler's Third Law.

Hence we have

$I_1 \sim \frac{2\pi^2 r_E^3}{T_E^3} \cdot \frac{M_E}{r_E} \times 75$  ergs, from Table I, i.e.  $I_1 \sim 2 \times 10^{42}$  ergs, on substituting for  $M_E$ ,  $r_E$  and  $T_E$ .

Taking account of the asteroids and the satellites, we can put

$$I_1 < 3 \times 10^{42} \text{ ergs.}$$

Now the kinetic energy of the planets due to axial rotation is  $I_2 = \frac{1}{5} \sum M k^2 \phi'^2$ , where  $M$  is the mass and  $k$  the radius of a planet, and  $\phi'$  is its angular velocity round its axis.

Hence we have

$$I_2 = \frac{4\pi^2}{5} \sum \frac{M k^2}{t^2}, \text{ where } t \text{ is the period for axial rotation of a planet.}$$

Therefore,  $I_2 \sim \frac{4\pi^2}{5} \frac{M_E k_E^2}{t_E^2} \times 3 \times 10^5$  ergs, from Table I.

Substituting for  $M_E$ ,  $k_E$  and  $t_E$  and taking account of asteroids and planets we can put  $I_2 < 10^{42}$  ergs.

The gravitational energy of the planets,  $W = \frac{1}{2} \sum V M$ , where  $V$  is the gravitational potential at the planet of mass  $M$  due to the Sun's attraction  $= \frac{\gamma}{2} \odot \sum \frac{M}{r}$ , where  $\odot$  is the Sun's mass and  $\gamma$  is the constant of gravitation.

Now,  $\odot = 1.983 \times 10^{33}$  gms.

and  $\gamma = 6.673 \times 10^{-8}$  C.G.S. units.

Hence we have  $W \sim \frac{\gamma}{2} \odot \frac{M_E}{r_E} \times 75$  ergs  
 $\sim 2 \times 10^{42}$  ergs.



Hence the total energy of the planetary system

$$\begin{aligned} &= I_1 + I_2 + W \\ &< 6 \times 10^{42} \text{ ergs.} \end{aligned}$$

Now, according to Eddington (Int. Const. Stars, p. 289), the total store of available heat energy of the Sun consists of  $2.97 \times 10^{48}$  ergs in the form of material kinetic energy and radiant energy and an unknown amount of energy of ionisation and excitation which is less than  $2.7 \times 10^{48}$  ergs.

It will not be unreasonable to take the total available energy *at least* to be  $3 \times 10^{48}$  ergs.

The total mass of the planets would lie between  $\odot/500$  and  $\odot/1000$ .

Hence the total energy stored up in them, when they were not separated from the Sun, would be at least  $3 \times 10^{45}$  ergs. This is at least 500 times the present energy of the planets.

There is also no difficulty about the angular momentum. In order that Pluto, which is at a distance of about 42 astronomical units from the Sun, may not be captured by a passing star whose mass is equal to that of the Sun, the star must at least be at a distance of 100 astronomical units from the Sun. Now, taking the angular momentum per unit mass of the Earth to be unity, and using the formula  $\sqrt{l(1+x)}$  for angular momentum per unit mass of the star where  $l$  = semi-latus rectum = 200 astronomical units, and  $x$  = ratio of mass of the star to that of the Sun = 1, we get the angular momentum per unit mass of the passing star to be  $\sqrt{400} = 20$  units. This is more than sufficient to give the necessary angular momentum to the planets to revolve round the Sun, as the average angular momentum per unit mass for the planetary system is 2.63 units.

We first picture the Sun as a Cepheid Variable, oscillating with a small amplitude. The near-by passage of a star—the passage, be it noted need not be grazing, or even very near, but only sufficiently near to produce appreciable tidal disturbance in the Sun—increases the amplitude of the oscillations, which consequently become unstable, as we have mathematically shown. This results in ejection of matter, which subsequently condenses into planets. We have already shown that the total energy which can be availed of by ejected matter exceeds by far that which is required for the formation of the planets. Only a part is utilised for this purpose, the rest is dissipated by radiation and escape of material.

Instability having ensued by the passage of the star, the Sun would draw on its sub-nuclear sources to provide enough energy for the ejection of material and return to a stable state. This energy is, as we have seen, a very small fraction of the total energy of the Sun, and would be utilised in part to form the planets. The consequent loss of mass would perhaps hasten the passage of the Sun from the giant to the main-sequence stage (Gamow, *loc. cit.*, p. 718) and the oscillations of the Sun would ultimately die out.

The passing star would, as we have already said, give orbital momentum to the planets, and the rest of the development of the planetary system would be as in previous theories. The main difficulty with these theories has been, as we have seen, the supply of sufficient orbital energy and angular momentum to the planets, and I have, therefore, specially considered this aspect of the case in the theory developed here, which I believe to be the first of its kind in the field.

A cogent objection may be raised on the ground that we have taken the mass of the parent Cepheid star to be equal to that of the Sun, whereas the mass of a Cepheid varies generally from five to twenty times the Sun's mass. To meet this objection we can formulate an alternative hypothesis and examine its feasibility.

Let us take the mass of the parent Cepheid to be that of the representative Cepheid,  $\delta$  Cephei, which is nine times the Sun's mass. Now, taking Eddington's (Int. Const. Stars, p. 146) figures, we have the radius  $R$  of the star  $= 2.32 \times 10^{12}$  cm.

The negative gravitational potential energy in contracting from infinite diffusion to present radius  $= \frac{3}{2} \gamma \frac{(9\odot)^2}{R} \sim 1.4 \times 10^{49}$  ergs, from which we get material kinetic energy, radiant energy and energy of ionisation and excitation.

Now, on account of dynamical instability caused by near-by passage of a star of mass of the same order as  $\delta$  Cephei, material will be ejected from the parent Cepheid. Let us calculate the energy required in ejecting material of mass more or less equal to that of the Sun to a sufficient distance so that both the Sun and a part of the planetary ribbon that is formed may escape recapture by the parent star.

The average (Smart, 1938) differential velocity between two stars is about 20 km./sec. As the ejected material had originally been a part of the parent star, the differential velocity between the parent star and the ejected material due to near-by passage of a star can hardly exceed 10 km./sec.

If we take the differential velocity to be 8 km./sec. for the ejected material with a part of the ribbon, then in order to escape capture by the parent Cepheid it must be ejected to a distance greater than  $d$  given by

$$v^2 = 2\gamma \frac{(8\odot + \odot)}{d}, \text{ where } v = 8 \text{ km./sec.};$$

$$\begin{aligned} \text{whence we have } d &= \frac{18\gamma\odot}{v^2} \\ &\sim 3.6 \times 10^{15} \text{ cms.} \end{aligned}$$

The radius of the parent Cepheid being  $2.32 \times 10^{12}$  cm., the material equal to the Sun's mass will have to be ejected to a distance at least 1600 times the radius of the parent star in order to avoid recapture by it.

Our hypothesis is that this ejected material with part of the ribbon ultimately condensed into our Sun and the planets, the passing star as well as the

parent Cepheid being responsible for giving orbital motion of the planets round the Sun.

Now Pluto is at a distance  $6 \times 10^{14}$  cms. from the Sun. If at any instant it comes between the parent Cepheid and the Sun, its distance from the parent Cepheid would be at least of the order of  $3 \times 10^{15}$  cms.

As  $\frac{8\odot}{(3 \times 10^{15})^2} < \frac{\odot}{(6 \times 10^{14})^2}$ , there was no chance of Pluto being recaptured by the parent Cepheid.

According to this theory, the parent Cepheid would also have a planetary system round it.

The energy required by the Sun to be ejected to the distance of escape and to have a velocity of 8 km./sec. is given by

$$W = \frac{1}{2} \odot v^2 + \frac{2}{5} \odot a^2 \omega^2 + \frac{3}{2} \gamma \frac{\odot^2}{a} + \frac{1}{2} \gamma \frac{8\odot^2}{d},$$

where  $a$  is the radius of the Sun  $= 6.95 \times 10^{10}$  cm.,

$$v = 8 \text{ km./sec.}$$

and  $\omega$  = angular velocity

$$= \frac{2\pi}{28 \times 24 \times 60^2} \text{ C.G.S. units,}$$

as period of the Sun's axial rotation is about 28 days.

Substituting these values, we have

$$W < 6 \times 10^{48} \text{ ergs.}$$

The Sun has therefore taken about two-fifths of the energy of the parent Cepheid.

As the passage of the star by the representative Cepheid need not be grazing or even very near, and as only two bodies are involved, the theory makes a less number of assumptions than any other recent theory, and is definitely more probable. One conclusion seems to be irresistible: If the theory be correct in its essentials, there may be more planetary systems than at present supposed, and, if life on this earth be the result of an orderly natural process, some of these other planets may be inhabited by beings like us.

We hope to consider the details of the dynamical configuration of the planetary system in a subsequent paper.

My thanks are due to Mr. H. K. Sen for kindly revising the paper and giving useful suggestions.

#### REFERENCES.

- Bhatnagar, P. L.—On the Origin of the Solar System. *Ind. Journ. Phys.*, Vol. 14, pp. 253–281, (1940).  
Chamberlin, T. C.—The Origin of the Earth. Chic. Univ. Press, (1916).

- Chandrasekhar, S.—The Equilibrium of Stellar Envelopes and the Central Condensations of Stars. *M. N. Roy. Astro. Soc.*, Vol. 96, p. 656, (1936).
- Chandrasekhar, S.—Introduction to the Study of Stellar Structure. Chic. Univ. Press, pp. 313-314, (1938).
- Eddington, A. S.—The Internal Constitution of Stars. Camb. Univ. Press., Chap. VIII, pp. 180-215, (1926).
- Eddington, A. S.—On the Cause of Cepheid Pulsation. *M. N. Roy. Astro. Soc.*, Vol. 101, pp. 182-194, (1941).
- Gamow, G.—Physical possibilities of Stellar Evolution. *Phys. Rev.*, Vol. 55, p. 718, (1939a).
- Gamow, G.—*loc. cit.*, pp. 724-725, (1939b).
- Goposchkin, S.—Variable Stars. *Harvard Observatory Monograph*, No. 5, p. 203, (1938).
- Gunn, R.—Origin of the Solar System. *Phys. Rev.*, Vol. 59, p. 690, (1941).
- Jeans, J. H.—The Problems of Cosmogony and Stellar Dynamics. Camb. Univ. Press, pp. 275-285, (1919).
- Jeans, J. H.—Astronomy and Cosmogony. Camb. Univ. Press, pp. 388-389, (1929).
- Jeffreys, H.—The Earth. Camb. Univ. Press, pp. 16-35, (1929).
- Kopal, J.—On the density condensations of Cepheid Variables. *M. N. Roy. Astro. Soc.*, Vol. 99, p. 38, (1938).
- Luyten, W. J. and Hill, E. L.—On the Origin of the Solar System. *Astro. Phys. Journ.*, Vol. 86, p. 470, (1937).
- Luyten, W. J.—On the Origin of the Solar System. *M. N. Roy. Astro. Soc.*, Vol. 99, pp. 692-696, (1939).
- Lyttleton, R. A.—The Origin of the Solar System. *M. N. Roy. Astro. Soc.*, Vol. 96, pp. 559-568, (1936).
- Lyttleton, R. A.—On the Origin of the Planets. *M. N. Roy. Astro. Soc.*, Vol. 98, pp. 136-139, (1938).
- Lyttleton, R. A.—On the Origin of the Solar System. *M. N. Roy. Astro. Soc.*, Vol. 101, pp. 216-226, (1941).
- Merrill, P. W.—Nature of Variable Stars, Macmillan Company, p. 105, (1938a).
- Merrill, P. W.—*loc. cit.*, p. 109, (1938b).
- Moulton, F. R.—An Introduction to Astronomy (New York), p. 463, (1906).
- Russell, H. N.—The Solar System and its Origin, pp. 113-114, (1935).
- Russell, H. N., Dugan, R. S. and Stewart, J. Q.—Astronomy. Vol. I, Appendix, (1926).
- Smart, W. M.—Spherical Astronomy, Camb. Univ. Press, Appendix C, (1931).
- Smart, W. M.—Stellar Dynamics, Camb. Univ. Press, p. 318, (1938).
- Spitzer, L.—Dissipation of Planetary Ribbons. *Astro. Phys. Journ.*, Vol. 90, p. 675-680, (1939).
- Sterne, T. E.—Modes of Radial Oscillations. *M. N. Roy. Astro. Soc.*, Vol. 97, pp. 582-593, (1937).



## ON THE COLLISION BETWEEN MESON AND ELECTRON.

By S. GUPTA, *Department of Applied Mathematics, Calcutta University, and*  
R. C. MAJUMDAR, *Bose Research Institute, Calcutta.*

(Received December 2, 1941.)

### ABSTRACT.

The cross-sections for the meson-electron collision for different values of spin of meson are investigated from quantum electrodynamics. In the first article the Hamiltonian containing the interaction of meson with the electromagnetic field is given, and in the second article the matrix elements of the interaction between meson and electron for different polarisations of meson are calculated. The cross-sections are then evaluated in the third article and in the fourth article the bearing of the results on the spin of the meson is discussed.

### INTRODUCTION.

The cascade showers observed under a great thickness of matter are known to be soft secondaries produced by the meson component of cosmic radiation. It was first suggested by Bhabha (1938a) that these showers are produced in ordinary cascade process by the electrons which are knocked out of the atoms by the incident meson. The interaction between the two charged particles, which is involved in the calculation of the collision cross-section for this knock-on process, was first successfully worked out by Møller (1932) from the scheme of quantum mechanics by a correspondence method. He calculated the interaction between two electrons and found out the corresponding collision cross-section. In Møller's theory one first constructs the retarded potentials which are produced by the charge and current densities due to the transition of the first electron and these potentials are then considered to act as a perturbation on the second electron causing its transition. The retarded potentials are determined from the time dependent Poisson's equations as is usually the practice in classical electrodynamics. The connection between Møller's retardation or correspondence method and that of quantum electrodynamics was first shown by Fermi and Bethe (1932), who had been able to deduce Møller's interaction from the latter method. The collision cross-section for the knock-on process could be easily taken over from Møller's work of the scattering of electron by electron if we assumed the meson to be possessed of spin half. This was done by Bhabha. But if the meson obeys Bose-statistics and has spin one, the corresponding calculation of collision cross-section becomes complicated, for then the three states of polarisations of meson have to be properly taken into account in considering its interaction with the electron. Recently, however, Massey and Corben (1939) have worked out the collision cross-section of a meson of spin one with the electron following

closely the correspondence method of Møller. The calculation runs exactly parallel to that of Møller because, as shown by them, the matrix elements of the interaction energy of the meson with the electron can be expressed in the same form as that between the two electrons in Møller's theory. This can be easily seen by expressing the interaction Hamiltonian between the meson of spin one and the electromagnetic field in terms of the charge and current densities of the meson, taking thereby the scalar and vector potentials of the field to be produced by the charge and current densities due to the electron transition. Now the effect of retardation in Møller's theory is, in fact, responsible for the relativity correction to the denominator of the interaction matrix making it an invariant to Lorentz transformation. The retardation is therefore already included in the interaction Hamiltonian in quantum electrodynamics, which gives rise to mutual emission and absorption of photons between the charged particles. It may, therefore, be of some interest to work out the interaction between a meson and an electron and their collision cross-section directly from quantum electrodynamics. This treatment will obviously present a clearer picture of the interaction process and also simplify the calculations. As there has been some confusion in recent years about the values of the spin of meson, we have in the following articles calculated the interaction energies and the collision cross-section of the meson of spins zero, half and one with the electron and the nature of the variation of these cross-sections are shown explicitly in the accompanying figures. A discussion on the results obtained together with their bearing on the spin of the meson will be found in the last article.

### §1. *Interaction energy of meson with radiation field.*

We shall first write down the Hamiltonian containing the interaction of meson with the electromagnetic field. This has been given by various authors (Kemmer, 1938; Fröhlich, Heitler and Kemmer, 1938; Bhabha, 1938b; Yukawa, Sakata and Taketani, 1938; Kobayasi and Okayama, 1939; Fröhlich, Heitler and Kahn, 1940) and we shall follow in the present article the notations used by Heitler. If  $\mathbf{A}$  and  $V$  are the electromagnetic vector and scalar potentials and  $\phi$  and  $\psi$  are vectors representing the wave functions of the transverse and longitudinal mesons respectively, then we can express the interaction terms in the Hamiltonian in the following way:—

$$H^1 = - \frac{ie}{4\pi\hbar c} \int \left\{ \operatorname{div} \psi^* \left( \mathbf{A}, \psi + \frac{1}{\lambda c} \dot{\phi} \right) + \left( \operatorname{rot} \phi^* \cdot \left[ \mathbf{A}, \phi - \frac{1}{\lambda c} \dot{\psi} \right] \right) \right. \\ \left. - \text{conjugate terms} \right\} d\tau^*, \quad \dots \dots (1)$$

$$H^2 = \frac{ie}{4\pi\hbar c} \int \left\{ V \left( \lambda \psi + \frac{1}{c} \dot{\phi}, \phi^* - \frac{1}{\lambda c} \dot{\psi}^* \right) - \text{conjugate terms} \right\} d\tau \dots (2)$$

---

\*  $\hbar$  denotes the Planck's constant divided by  $2\pi$ .

We have neglected thereby the terms proportional to  $A^2$ . We now expand the wave functions of the meson into plane waves and quantise their amplitudes by the Pauli-Weisskopf (1934) method and obtain

$$\left. \begin{aligned} \phi &= i\hbar c \sum_k \sqrt{\frac{2\pi}{E_k}} (a_k - b_k^*) \mathbf{j} e^{i(\mathbf{k}, \mathbf{r})} \\ \psi &= i\hbar c \sum_k \sqrt{\frac{2\pi}{E_k}} (A_k - B_k^*) \frac{\mathbf{k}}{k} e^{i(\mathbf{k}, \mathbf{r})} \\ \dot{\phi} &= c \sum_k \sqrt{2\pi E_k} (a_k + b_k^*) \mathbf{j} e^{i(\mathbf{k}, \mathbf{r})} \\ \dot{\psi} &= c \sum_k \sqrt{2\pi E_k} (A_k + B_k^*) \frac{\mathbf{k}}{k} e^{i(\mathbf{k}, \mathbf{r})} \end{aligned} \right\} \dots (3)$$

Here  $\mathbf{k}$  is the wave vector in the direction of motion and  $\mathbf{j}$  is the unit vector in the direction of polarisation of transverse mesons. The operators  $a, a^*, A, A^*$ , etc., were introduced by Pauli-Weisskopf and have the following meanings:

$a_k^*$  increases the number of transverse positive meson by one,  
 $b_k^*$  „ „ „ „ transverse negative meson „ „  
 $A_k^*$  „ „ „ „ longitudinal positive meson „ „  
 $B_k^*$  „ „ „ „ longitudinal negative meson „ „

Similarly, the operators  $a, b, A, B$  without asterisk decrease the corresponding number of mesons by one. Further we have

$$E_k = \hbar c \sqrt{k^2 + \lambda^2}, \quad \lambda = \frac{Mc}{\hbar} \quad \dots \dots \dots (4)$$

where  $M$  denotes the mass of the meson. The wave vector  $\mathbf{k}$  is connected with the momentum  $\mathbf{p}$  of the meson in a different way for positive and negative mesons.

For positive meson :  $\mathbf{p} = c\hbar\mathbf{k}$ ,

For negative meson :  $\mathbf{p} = -c\hbar\mathbf{k} \quad \dots \dots \dots (5)$

For the light quantum the corresponding relation is

$$\kappa = \hbar\nu = c\hbar\mathbf{q} \quad \dots \dots \dots (6)$$

where  $\mathbf{q}$  is the wave vector of the photon. The introduction of wave vector instead of the momentum, as will be seen later, ensures the symmetry between the positive and negative mesons.

We can as usual eliminate the longitudinal part of the electromagnetic field and replace the scalar potential by Coulomb interaction.  $\mathbf{A}$  then represents the transverse part of the vector potential only and can be expanded as a Fourier series

$$\mathbf{A} = \sum_{\mathbf{q}} \sqrt{\frac{2\pi c\hbar}{q}} \mathbf{e}_{\mathbf{q}} (C_{\mathbf{q}} e^{i(\mathbf{q}, \mathbf{r})} + C_{\mathbf{q}}^* e^{-i(\mathbf{q}, \mathbf{r})}) \dots \dots \dots (7)$$



where  $\mathbf{e}_q$  is a unit vector in the direction of polarisation of the wave vector  $\mathbf{q}$ .  
 $C_q$  and  $C_q^*$  are operators which signify

$$\begin{aligned} C_q^* &\text{ increases the number of photons by one,} \\ C_q &\text{ decreases ,, ,, ,, ,, ,, } \end{aligned}$$

Now inserting the values of  $\mathbf{A}$ ,  $\psi$ ,  $\phi$ , etc., as given by (7) and (3), in (1) and (2) we obtain

$$\begin{aligned} H^1 = & \sum_k \sum_{k'} \sum_q \sqrt{\frac{2\pi}{E_k E_{k'} c \hbar q}} \left\{ C_q \delta(\mathbf{k} - \mathbf{k}' + \mathbf{q}) + C_q^* \delta(\mathbf{k} - \mathbf{k}' - \mathbf{q}) \right\} \\ & \times \left[ -\frac{e\hbar^2 c^2}{2} \left\{ \left( \frac{k'}{k} (\mathbf{e}\mathbf{k}) + \frac{k}{k'} (\mathbf{e}\mathbf{k}') \right) (A_k A_{k'}^* + B_k^* B_{k'} - B_k^* A_{k'}^* - A_k B_{k'}) \right. \right. \\ & + (([\mathbf{j}'\mathbf{k}'] \cdot [\mathbf{j}\mathbf{e}]) + ([\mathbf{j}\mathbf{k}] \cdot [\mathbf{j}'\mathbf{e}])) (a_k a_{k'}^* + b_k^* b_{k'} - b_k^* a_{k'}^* - a_k b_{k'}) \left. \right\} \\ & + \frac{ie\hbar c}{2\lambda} \left\{ (E_k k' (\mathbf{e}\mathbf{j}) - \frac{E_{k'}}{k'} ([\mathbf{j}\mathbf{k}] \cdot [\mathbf{e}\mathbf{k}'])) (a_k A_{k'}^* - b_k^* B_{k'}) \right. \\ & - (E_k k' (\mathbf{e}\mathbf{j}) + \frac{E_{k'}}{k'} ([\mathbf{j}\mathbf{k}] [\mathbf{e}\mathbf{k}'])) (a_k B_{k'} - b_k^* A_{k'}^*) \\ & - (E_k k (\mathbf{e}\mathbf{j}') - \frac{E_k}{k} ([\mathbf{j}'\mathbf{k}'] [\mathbf{e}\mathbf{k}])) (A_k a_{k'}^* - B_k^* b_{k'}) \\ & \left. \left. - (E_k k (\mathbf{e}\mathbf{j}') + \frac{E_k}{k} ([\mathbf{j}'\mathbf{k}'] [\mathbf{e}\mathbf{k}])) (A_k b_{k'} - B_k^* a_{k'}^*) \right\} \right] \quad \dots \quad (8) \end{aligned}$$

and

$$\begin{aligned} H^2 = & \sum_k \sum_{k'} \frac{e}{2} \frac{V_{\mathbf{k}\mathbf{k}'}}{\sqrt{E_k E_{k'}}} \left[ \frac{(\mathbf{k}\mathbf{k}')}{kk'} \left\{ (E_k + E_{k'}) (A_k A_{k'}^* - B_k^* B_{k'}) \right. \right. \\ & \left. \left. + (E_k - E_{k'}) (B_k^* A_{k'}^* - A_k B_{k'}) \right\} \right. \\ & + (\mathbf{j}\mathbf{j}') \left\{ (E_k + E_{k'}) (a_k a_{k'}^* - b_k^* b_{k'}) + (E_k - E_{k'}) (b_k^* a_{k'}^* - a_k b_{k'}) \right\} \\ & - i \lambda \hbar c \left\{ \frac{(\mathbf{k}\mathbf{j}')}{k} \left( -\left(1 + \frac{E_k E_{k'}}{\lambda^2 \hbar^2 c^2}\right) (A_k a_{k'}^* + B_k^* b_{k'}) \right. \right. \\ & \left. \left. + \left(1 - \frac{E_k E_{k'}}{\lambda^2 \hbar^2 c^2}\right) (B_k^* a_{k'}^* + A_k b_{k'}) \right) \right. \\ & \left. \left. + \frac{(\mathbf{k}'\mathbf{j})}{k'} \left( \left(1 + \frac{E_k E_{k'}}{\lambda^2 \hbar^2 c^2}\right) (a_k A_{k'}^* + b_k^* B_{k'}) \right. \right. \right. \\ & \left. \left. \left. - \left(1 - \frac{E_k E_{k'}}{\lambda^2 \hbar^2 c^2}\right) (b_k^* A_{k'}^* + a_k B_{k'}) \right) \right\} \right] \quad \dots \quad (9) \end{aligned}$$

where

$$V_{\mathbf{k}\mathbf{k}'} = \int V e^{i(\mathbf{k}-\mathbf{k}', \mathbf{r})} d\tau \quad \dots \quad (10)$$

If we assume a pure Coulomb potential between the meson and electron then this reduces to

$$V_{kk'} = \frac{4\pi e^2}{|\mathbf{k} - \mathbf{k}'|^2} \dots \dots \dots (11)$$

The interaction  $H^1$  gives rise to various transitions involving light quanta. In this paper we shall, however, be interested only in the matrix elements of  $H^1$  for the transitions in which a photon is emitted or absorbed by the meson. The interaction  $H^2$  causes transitions in the electrostatic field between the meson and the electron.

§2. *Total matrix element of the interaction between the meson and the electron.*

The total matrix element for the transition from the initial state  $A$ , in which the meson and electron have wave vectors  $\mathbf{k}$  and  $\mathbf{k}_e$ , to the final state  $F$  with the wave vectors  $\mathbf{k}'$  and  $\mathbf{k}'_e$  consists of two parts. The first part is the matrix element of the Coulomb interaction between the particles which causes direct transition to the final state. The second part is the matrix element of the interaction of the particles with the radiation field and the transition from initial to final states takes place through an intermediate state. We have thus

$$H_{AF} = H_{AF}^2 + \sum_n \frac{H_{An}^1 H_{nF}^1}{E_A - E_n} \dots \dots \dots (12)$$

where the summation has to be taken over all the intermediate states  $n$  which we shall denote by I, II and also over all directions of polarisation of the quantum  $q$ .

We consider the following sets of transitions:

*Initial meson longitudinal, final meson longitudinal.*

1. A longitudinal meson (positive or negative) with wave vector  $\mathbf{k}$  emits a photon with wave vector  $\mathbf{q}$  and goes over to the longitudinal state with wave vector  $\mathbf{k}'$ . The law of conservation of momentum gives

$$\left. \begin{array}{l} \text{for positive meson: } \mathbf{k}' = \mathbf{k} - \mathbf{q} \\ \text{for negative meson: } \mathbf{k}' = \mathbf{k} + \mathbf{q} \end{array} \right\} \dots \dots \dots (13)$$

We obtain the corresponding matrix element from (8)

$$H_{AI}^1 = -\frac{eA^2c^2}{2} \sqrt{\frac{2\pi}{EE'\hbar c q}} \left\{ \frac{k}{k'} (\mathbf{e}\mathbf{k}') + \frac{k'}{k} (\mathbf{e}\mathbf{k}) \right\} \dots \dots \dots (14)$$

The photon  $q$  is then absorbed by the electron with wave vector  $\mathbf{k}_e$  (momentum  $\mathbf{p}_e$ ) which goes over the state  $\mathbf{k}'_e$  (momentum  $\mathbf{p}'_e$ ). We have from the conservation of momentum

$$-\kappa = \mathbf{p}_e - \mathbf{p}'_e = -(\mathbf{p} - \mathbf{p}') \dots \dots \dots (15)$$

$$\left. \begin{array}{l} \text{i.e. for positive meson: } -\mathbf{q} = +(\mathbf{k}_e - \mathbf{k}'_e) = -(\mathbf{k} - \mathbf{k}') \\ \text{for negative meson: } -\mathbf{q} = (\mathbf{k}_e - \mathbf{k}'_e) = (\mathbf{k} - \mathbf{k}') \end{array} \right\} \quad \dots \quad (16)$$

The corresponding matrix element is as usual given by

$$H_{IF} = -e \sqrt{\frac{2\pi\hbar c}{q}} (u^{*'}(\boldsymbol{\alpha}\mathbf{e})u) \quad \dots \quad (17)$$

where  $u$  and  $u'$  are the amplitudes of Dirac's wave functions of electron for the initial and final states and the vector  $\boldsymbol{\alpha}$  is Dirac's matrix.

2. The electron first emits a photon  $\mathbf{q}'$  which is then absorbed by the meson  $\mathbf{k}$ . This is the second intermediate state II. From conservation of momentum we have

$$\kappa' = \mathbf{p}_e - \mathbf{p}'_e = -\kappa; \quad \mathbf{q}' = -\mathbf{q} \quad \dots \quad (18)$$

The matrix elements are the same as case 1.

3. The transition from the initial to the final state  $A \rightarrow F$  may also take place directly in the mutual field of the particles due to interaction  $H^2$  without involving any emission or absorption. We get from (9)

$$H_{AF}^2 = \frac{2\pi e^2 \hbar^2 c^2}{\kappa^2} \frac{E+E'}{\sqrt{EE'}} \frac{(\mathbf{k}\mathbf{k}')}{kk'} (u^{*'}u) \quad \dots \quad (19)$$

The energy differences  $E_A - E_n$  are

$$E_A - E_I = E - E' - \kappa, \quad E_A - E_{II} = E_e - E'_e - \kappa \quad \dots \quad (20)$$

whereas the conservation of energy gives

$$E - E' = -(E_e - E'_e) = \epsilon \quad \dots \quad (21)$$

The total matrix element (12) thus becomes

$$H_{AF}^{\text{long-long}} = \frac{2\pi e^2 \hbar^2 c^2}{\sqrt{EE'}} \left[ \frac{E+E'}{\kappa^2} (\mathbf{n}\mathbf{n}') (u^{*'}u) + \frac{\hbar c}{\epsilon^2 - \kappa^2} \{ k(\mathbf{e}\mathbf{n}') + k'(\mathbf{e}\mathbf{n}) \} (u^{*'}(\boldsymbol{\alpha}\mathbf{e})u) \right] \quad \dots \quad (22)$$

where  $\mathbf{n}$  and  $\mathbf{n}'$  are the unit vectors in direction of the wave vector of the meson in the initial and final states and given by

$$\mathbf{n} = \frac{\mathbf{k}}{k}, \quad \mathbf{n}' = \frac{\mathbf{k}'}{k'} \quad \dots \quad (23)$$

We shall now have to sum over both directions of polarisation of the photon. Let  $\mathbf{e}_1$  and  $\mathbf{e}_2$  be two unit vectors in the direction of polarisation. Then if  $\mathbf{A}$  and  $\mathbf{B}$  be any two vectors, we have

$$\sum_{\mathbf{e}_1 \mathbf{e}_2} (\mathbf{e}\mathbf{A})(\mathbf{e}\mathbf{B}) = (\mathbf{A}\mathbf{B}) - \frac{(\mathbf{k}\mathbf{A})(\mathbf{k}\mathbf{B})}{k^2} \quad \dots \quad (24)$$

Applying this to (22) we obtain finally

$$H^{\text{long-long}} = \frac{2\pi e^2 \hbar^2 c^2}{(\kappa^2 - \epsilon^2)} \frac{1}{\sqrt{EE'}} [(E + E')(\mathbf{nn}') (u^* u) - \hbar c \{ (k\mathbf{n}' + k'\mathbf{n}) \cdot (u^* \alpha u) \}] \quad \dots \quad (25)$$

*Initial meson transverse, final meson transverse.*

1. A transverse meson (positive or negative) with wave vector  $\mathbf{k}$  emits a photon with wave vector  $\mathbf{q}$  and goes over to the transverse state  $\mathbf{k}'$ . The matrix element is

$$H_{AI}^1 = -\frac{e\hbar^2 c^2}{2} \sqrt{\frac{2\pi}{EE' \hbar c q}} \{ ([\mathbf{j}\mathbf{k}] \cdot [\mathbf{j}'\mathbf{e}]) + ([\mathbf{j}'\mathbf{k}'] \cdot [\mathbf{j}\mathbf{e}]) \} \quad \dots \quad (26)$$

The photon  $\mathbf{q}$  is then absorbed by the electron  $\mathbf{k}_e$  which changes to  $\mathbf{k}'_e$  and so

$$H_{IF} = -e \sqrt{\frac{2\pi \hbar c}{q}} (u^* (\alpha \mathbf{e}) u) \quad \dots \quad (17)$$

2. The electron  $\mathbf{k}_e$  first emits a photon  $\mathbf{q}$  which is then absorbed by the transverse meson  $\mathbf{k}$ .

The matrix elements are the same as in (1).

3. The transition  $A \rightarrow F$  takes place directly due to Coulomb interaction. The matrix element is

$$H_{AF} = \frac{2\pi e^2 \hbar^2 c^2}{\kappa^2} \frac{E + E'}{\sqrt{EE'}} (\mathbf{j}\mathbf{j}') (u^* u) \quad \dots \quad (27)$$

The total matrix element (12) thus becomes

$$H^{\text{trans-trans}} = \frac{2\pi e^2 \hbar^2 c^2}{\sqrt{EE'}} \left[ \frac{E + E'}{\kappa^2} (\mathbf{j}\mathbf{j}') (u^* u) + \frac{\hbar c}{\epsilon^2 - \kappa^2} \{ k([\mathbf{j}\mathbf{n}] \cdot [\mathbf{j}'\mathbf{e}]) + k'([\mathbf{j}'\mathbf{n}'] \cdot [\mathbf{j}\mathbf{e}]) \} (u^* (\alpha \mathbf{e}) u) \right] \quad \dots \quad (28)$$

If we now sum over the directions of polarisation of the photon, we obtain

$$H^{\text{trans-trans}} = \frac{2\pi e^2 \hbar^2 c^2}{(\kappa^2 - \epsilon^2)} \frac{1}{\sqrt{EE'}} [(E + E')(\mathbf{j}\mathbf{j}') (u^* u) - \hbar c (k([\mathbf{j}\mathbf{n}]\mathbf{j}') + k'([\mathbf{j}'\mathbf{n}']\mathbf{j}) \cdot (u^* \alpha u))] \quad \dots \quad (29)$$

*Initial meson longitudinal, final meson transverse.*

1. A longitudinal meson (positive or negative) with wave vector  $\mathbf{k}$  emits a photon with wave vector  $\mathbf{q}$  and transforms into a transverse meson with wave vector  $\mathbf{k}'$ . The matrix element is

$$H_{AI}^1 = -\frac{ie\hbar c}{2\lambda} \sqrt{\frac{2\pi}{EE' \hbar c q}} \left\{ E' k(\mathbf{e}\mathbf{j}') - \frac{E}{k} ([\mathbf{j}'\mathbf{k}'] \cdot [\mathbf{e}\mathbf{k}]) \right\} \quad \dots \quad (30)$$

The photon  $q$  is then absorbed by the electron  $k$ , which thereby goes to the state  $k'$ , whence we have

$$H_{IF} = -e \sqrt{\frac{2\pi\hbar c}{q}} (u^* (\alpha \mathbf{e}) u) \quad \dots \quad (17)$$

2. The electron  $k$ , first emits a photon  $q$  which is then absorbed by the longitudinal meson  $k$ .

The matrix elements are the same as 1.

3. The transition  $A \rightarrow F$  takes place directly due to Coulomb interaction, and so we have

$$H_{AF}^2 = \frac{i2\pi e^2 \hbar c}{\lambda \kappa^2} \frac{1}{\sqrt{EE'}} (\hbar^2 c^2 \lambda^2 + EE') (\mathbf{n} \mathbf{j}') (u^* u) \quad \dots \quad (31)$$

The total matrix element (12) becomes

$$H^{\text{long-trans}} = \frac{i2\pi e^2 \hbar c}{\lambda \sqrt{EE'}} \left[ \frac{(\hbar^2 c^2 \lambda^2 + EE')}{\kappa^2} (\mathbf{n} \mathbf{j}') (u^* u) + \frac{\hbar c}{\epsilon^2 - \kappa^2} \{ E' k(\mathbf{e} \mathbf{j}') - E k'([\mathbf{j}' \mathbf{n}'] \cdot [\mathbf{e} \mathbf{n}]) \} (u^* (\alpha \mathbf{e}) u) \right] \quad \dots \quad (32)$$

On summing over the polarisations of the photon we get

$$H^{\text{long-trans}} = \frac{i2\pi e^2 \hbar c}{\lambda (\kappa^2 - \epsilon^2)} \cdot \frac{1}{\sqrt{EE'}} [(\hbar^2 c^2 \lambda^2 + EE') (\mathbf{n} \mathbf{j}') (u^* u) - \hbar c (E' k \mathbf{j}' + E k' ([\mathbf{j}' \mathbf{n}'] \cdot \mathbf{n})) (u^* \alpha u)] \quad \dots \quad (33)$$

*Initial meson transverse, final meson longitudinal.*

The total matrix element in this case is the same as when the initial meson longitudinal, final meson transverse with the roles of the dashed and undashed quantities interchanged.

We therefore obtain

$$H^{\text{trans-long}} = \frac{i2\pi e^2 \hbar c}{\lambda (\kappa^2 - \epsilon^2)} \frac{1}{\sqrt{EE'}} [(\hbar^2 c^2 \lambda^2 + EE') (\mathbf{n} \mathbf{j}') (u^* u) - \hbar c (E k' \mathbf{j} + E' k([\mathbf{j} \mathbf{n}] \cdot \mathbf{n}')) (u^* \alpha u)] \quad \dots \quad (34)$$

It is to be noted that in the interaction matrix elements (25), (29), (33) and (34) the denominators are invariant as they form the sum of the squares of the four vectors of energy and momentum. Since the numerators are also invariant, being the product of four vectors forming the charge and current of meson and electron, the complete interaction matrix element is invariant. For the sake of comparison we now give the corresponding interaction matrices for the interaction of meson of spins zero and half with the electron.

The Hamiltonian for the interaction of meson of spin zero with the electromagnetic field has been given by Pauli-Weisskopf (1934).

$$H^1 = -\frac{e\hbar^2 c^2}{2} \sum_k \sum_{k'} \sum_q \sqrt{\frac{2\pi}{E_k E_{k'} \hbar c q}} \{ C_q \delta(\mathbf{k}-\mathbf{k}'+\mathbf{q}) + C_q^* \delta(\mathbf{k}-\mathbf{k}'-\mathbf{q}) \} \\ \times ((\mathbf{ek}) + (\mathbf{ek}')) (A_k A_{k'}^* + B_k^* B_{k'} - B_k^* A_{k'} - A_k B_{k'}) \quad \dots \quad (35)$$

$$H^2 = \frac{1}{2} \sum_k \sum_{k'} \frac{V_{kk'}}{\sqrt{EE'}} [(E_k + E_{k'}) (A_k A_{k'}^* - B_k^* B_{k'}) \\ + (E_k - E_{k'}) (B_k^* A_{k'}^* - A_k B_{k'})] \quad \dots \quad (36)$$

Working out as before we obtain the total matrix element

$$H = \frac{2\pi e^2 \hbar^2 c^2}{(\kappa^2 - \epsilon^2)} \frac{1}{\sqrt{EE'}} [(E + E')(u''u) - \hbar c(\mathbf{k}\mathbf{n}' + \mathbf{k}'\mathbf{n}) \cdot (u^* \alpha u)] \quad (37)$$

The total matrix element of the interaction between the meson of spin half and the electron can be at once obtained from Möller's result. It is given by (Heitler, 1936)

$$H = \frac{4\pi e^2 \hbar^2 c^2}{(\kappa^2 - \epsilon^2)} [(u_m^* u_m)(u''u) - (u_m^* \alpha_m u_m) \cdot (u^* \alpha u)] \quad \dots \quad (38)$$

where the suffix *m* refers to the meson.

### §3. Calculation of the collision cross-sections.

We consider the collision between meson-electron in a co-ordinate system *L* in which the meson is moving with velocity *v* along the *z*-axis and the electron is initially at rest. There is no loss of generality in doing this since any other case can be obtained from this by a Lorentz transformation. The differential cross-section for the scattering of mesons through an angle  $\theta$  and  $\theta + d\theta$  about its initial direction of motion is given by

$$d\phi = \frac{|H|^2}{4\pi^2 \hbar^4 c^3 v} p'^2 \frac{dp'}{dE_p} 2\pi \sin \theta d\theta \quad \dots \quad (39)$$

*H* is the interaction matrix which has been already given in the last section.  $E_p'$  is the total energy in the final state. Since the differential cross-section (39) is an invariant for a Lorentz transformation if we pass from system *L* to another system *L*<sup>\*</sup> in which the meson and the electron are moving in opposite directions along the *z*-axis with equal momentum, we shall, for convenience, calculate the differential cross-section in the system *L*<sup>\*</sup> for the scattering of meson through an angle  $\theta^*$  and  $\theta^* + d\theta^*$ . In the subsequent discussions suffix *e* refers to the quantities for the electron and the dash refers to the quantities after the collision. Further from now on we shall express all the expressions in terms of the momentum *p* and it can be easily seen that the final results shall be still valid both for positive and negative mesons. Since in the system *L*<sup>\*</sup> the momenta of the meson and the electron are also equal and opposite after the collision we have the following relations for that system:—

$$\mathbf{p}_e^* = -\mathbf{p}^*, \mathbf{p}_e'^* = -\mathbf{p}'^*, |\mathbf{p}^*| = |\mathbf{p}'^*| = Mc^2 \alpha \sqrt{\gamma^{*2} - 1} \quad \dots \quad (40)$$

and

$$E_e^* = E_e'^* = Mc^2\alpha\gamma^*; E = E^* = Mc^2\gamma^* \frac{\alpha\gamma+1}{\alpha+\gamma} \quad \dots \quad (41)$$

Further  $\theta$  is connected with  $\theta^*$  by the formula

$$\tan \theta = \frac{1}{\gamma^*} \tan \frac{\theta^*}{2} \quad \dots \quad (42)$$

where

$$\gamma^* = \frac{\gamma+\alpha}{(\alpha^2+2\alpha\gamma+1)^{\frac{1}{2}}}; \gamma = \frac{E}{Mc^2} = \frac{1}{\sqrt{1-\frac{v^2}{c^2}}}; \alpha = \frac{m}{M} \quad \dots \quad (43)$$

$m$  being the mass of the electron.

The differential cross-section in the system  $L^*$  is thus

$$d\phi^* = \frac{1}{2\pi\hbar^4c^4} \frac{E^{*2}E_e'^{*2}}{(E^*+E_e^*)^2} |H^*|^2 \sin \theta^* d\theta^* \quad \dots \quad (44)$$

Now in order to obtain the result which is of physical interest we shall have to average over initial, and sum over the final, spins of the electron and polarisations of the meson in (44). For the electron this summation and averaging is well known. For the case of meson we have actually to sum over two independent polarisations of scattered meson and average over the three polarisations of the incident meson. If we denote this operation by a bar, the following relations are obtained

$$\begin{aligned} \overline{(j'j')^2} &= \frac{1}{3} (1 + \cos^2 \theta^*), \quad \overline{(n'j')^2} = \overline{(n'j)^2} = \frac{2}{3} \sin^2 \theta^*, \\ \overline{(n'j')(n'j)(j'j')} &= -\frac{1}{3} \cos \theta^* \sin^2 \theta^*, \quad \overline{(n'j')^2(n'j)^2} = \frac{1}{3} \sin^4 \theta^* \quad \dots \quad (45) \end{aligned}$$

Then after some calculation we get

$$\begin{aligned} |H^{\text{long-long}}|^2 &= \frac{\pi^2 e^4 \hbar^4 c^4}{6p^{*4}(1-\cos \theta^*)^2} \frac{1}{E^{*2}E_e'^{*2}} [4E^{*2} \cos^2 \theta^* (p^{*2} \cos \theta^* \\ &+ \alpha^2 M^2 c^4 + E_e'^{*2}) + 8p^{*2} E_e^* E^* \cos \theta^* (1 + \cos \theta^*) + 4p^{*4} (1 + \cos \theta^*)], \quad \dots \quad (46) \end{aligned}$$

$$\begin{aligned} |H^{\text{trans-trans}}|^2 &= \frac{\pi^2 e^4 \hbar^4 c^4}{6p^{*4}(1-\cos \theta^*)^2} \frac{1}{E^{*2}E_e'^{*2}} [4E^{*2} (p^{*2} \cos \theta^* \\ &+ \alpha^2 M^2 c^4 + E_e'^{*2}) (1 + \cos^2 \theta^*) + 8p^{*2} E_e^* E^* (1 + \cos \theta^*)^2 \\ &+ 2p^{*4} \{4(1 + \cos \theta^*) + \sin^2 \theta^* (1 - \cos \theta^*)\}], \quad \dots \quad (47) \end{aligned}$$

$$\begin{aligned}
|H^{\text{long-trans}}|^2 &= |H^{\text{trans-long}}|^2 \\
&= \frac{\pi^2 e^4 \hbar^4 c^4}{6 p^{*4} (1 - \cos \theta^*)^2} \frac{1}{E^{*2} E_e^{*2}} \left[ M^2 c^4 \left( 1 + \frac{E^{*2}}{M^2 c^4} \right)^2 (p^{*2} \cos \theta^* + \alpha^2 M^2 c^4 + E_e^{*2}) \sin^2 \theta^* \right. \\
&\quad + \frac{2 E^{*2} p^{*4}}{M^2 c^4} (1 - \cos \theta^*)^3 + \frac{E^{*2} p^{*4}}{M^2 c^4} (3 - \cos \theta^*) \sin^2 \theta^* \\
&\quad \left. + 4 \left( 1 + \frac{E^{*2}}{M^2 c^4} \right) E^* E_e^* p^{*2} \sin^2 \theta^* \right] \dots \dots \dots (48)
\end{aligned}$$

With the substitution of these values in (44) the differential cross-section finally reduces to

$$\begin{aligned}
d\phi^* &= \frac{\pi e^4}{6} \frac{\sin \theta^* d\theta^*}{(1 - \cos \theta^*)^2} \frac{1}{(E^* + E_e^*)^2} \left[ \frac{2 E^{*2}}{p^{*2}} \left\{ 1 + \cos \theta^* + \frac{2 \alpha^2 M^2 c^4}{p^{*2}} \right\} (1 + 2 \cos^2 \theta^*) \right. \\
&\quad + \frac{M^2 c^4}{p^{*2}} \left( 1 + \frac{E^{*2}}{M^2 c^4} \right)^2 \left\{ 1 + \cos \theta^* + \frac{2 \alpha^2 M^2 c^4}{p^{*2}} \right\} \sin^2 \theta^* \\
&\quad + \frac{4 E^* E_e^*}{p^{*2}} (1 + \cos \theta^*) \left\{ 1 + 2 \cos \theta^* + \left( 1 + \frac{E^{*2}}{M^2 c^4} \right) (1 - \cos \theta^*) \right\} \\
&\quad + \{ 6 + (1 - \cos \theta^*)^2 \} (1 + \cos \theta^*) + \frac{E^{*2}}{M^2 c^4} \{ 2(1 - \cos \theta^*)^2 \\
&\quad \left. + (3 - \cos \theta^*) (1 + \cos \theta^*) \} (1 - \cos \theta^*) \right] \dots \dots \dots (49)
\end{aligned}$$

Similarly, the collision cross-section between meson-electron for meson of spin zero can be calculated. We have thus

$$\begin{aligned}
d\phi^* &= \frac{\pi e^4}{2} \frac{\sin \theta^* d\theta^*}{(1 - \cos \theta^*)^2} \frac{1}{(E^* + E_e^*)^2} \left[ \frac{2 E^{*2}}{p^{*2}} \left( 1 + \cos \theta^* + \frac{2 \alpha^2 M^2 c^4}{p^{*2}} \right) \right. \\
&\quad \left. + \frac{4 E^* E_e^*}{p^{*2}} (1 + \cos \theta^*) + 2(1 + \cos \theta^*) \right] \dots (50)
\end{aligned}$$

The differential cross-section for the meson-electron collision when the meson has spin half is given by

$$\begin{aligned}
d\phi^* &= \frac{\pi e^4}{2} \frac{\sin \theta^* d\theta^*}{(1 - \cos \theta^*)^2} \frac{1}{(E^* + E_e^*)^2} \left[ 2(1 + \cos^2 \theta^*) \right. \\
&\quad + \frac{1}{p^{*2}} \{ 2 M^2 c^4 (1 + \alpha^2) + 4 E^* E_e^* \} \cos \theta^* + \frac{4 E^* E_e^*}{p^{*2}} \left( 1 + \frac{E^* E_e^*}{p^{*2}} \right) \\
&\quad \left. + \frac{2 M^2 c^4}{p^{*4}} (2 \alpha^2 M^2 c^4 - E_e^{*2} - \alpha^2 E^{*2}) \right] \dots \dots \dots (51)
\end{aligned}$$

The cross-section is most conveniently expressed in terms of the fraction of the initial kinetic energy of the meson that has been transferred to electron



on collision. If  $\varepsilon$  be the ratio of the kinetic energy of the knocked-on electron to the initial kinetic energy of the colliding meson in the system  $L$ , then

$$\varepsilon = \frac{E'_e - mc^2}{E - Mc^2} = \frac{\varepsilon_m}{2} (1 - \cos \theta^*) \quad \dots \quad (52)$$

since

$$E'_e = \alpha Mc^2 \{ \gamma^{*2} - (\gamma^{*2} - 1) \cos \theta^* \}, \quad E = \gamma Mc^2 \quad \dots \quad (53)$$

Here  $\varepsilon_m$  is the maximum fraction of energy which can be taken up by the knocked-on electron and is given by

$$\varepsilon_m = \frac{2\alpha(\gamma+1)}{\alpha^2 + 2\alpha\gamma + 1} \quad \dots \quad (54)$$

$\varepsilon_{\max}$  tends to unity for sufficiently large  $\gamma$ , however large  $M$  may be.

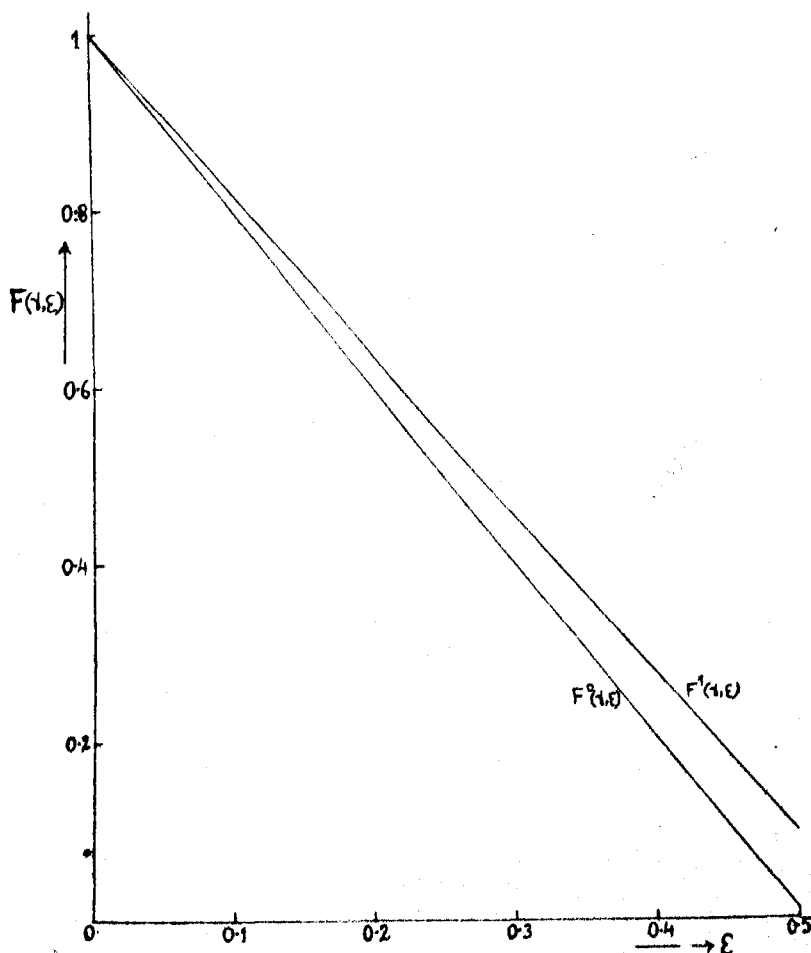


FIG. 1.  $\gamma = 10^2$ ,  $\varepsilon_m = 0.505$ .

The cross-section for the production of secondary electron of kinetic energy  $\varepsilon$  and  $\varepsilon + d\varepsilon$  by the meson of the total energy  $E$  thus reduces to

$$d\phi = 2\pi \left( \frac{e^2}{mc^2} \right)^2 \frac{\alpha \gamma^2}{(\gamma-1)(\gamma^2-1)} \frac{d\varepsilon}{\varepsilon^2} F(\varepsilon, \gamma) \quad \dots \quad (55)$$

where we have—

(i) for meson of spin one

$$F^1(\varepsilon, \gamma) = 1 - \frac{\gamma^2-1}{\gamma^2} \frac{\varepsilon}{\varepsilon_m} + \frac{\alpha(2\gamma^2+1)(\gamma-1)}{6\gamma^2} \varepsilon + \left( \frac{1}{\gamma+1} - \frac{\alpha}{\varepsilon_m} \right) \frac{(\gamma-1)(\gamma^2-1)}{\gamma^2} \frac{\varepsilon^2}{3} + \frac{\alpha(\gamma-1)^3}{6\gamma^2} \varepsilon^3 \quad \dots \quad (56)$$

(ii) for meson of spin zero

$$F^0(\varepsilon, \gamma) = 1 - \frac{\gamma^2-1}{\gamma^2} \frac{\varepsilon}{\varepsilon_m} + \frac{\alpha(\gamma-1)}{2\gamma^2} \varepsilon \quad \dots \quad (57)$$

(iii) for meson of spin half

$$F^{\frac{1}{2}}(\varepsilon, \gamma) = 1 - \frac{\gamma^2-1}{\gamma^2} \frac{\varepsilon}{\varepsilon_m} + \frac{1}{2} \frac{(\gamma-1)^2}{\gamma^2} \varepsilon^2 \quad \dots \quad (58)$$

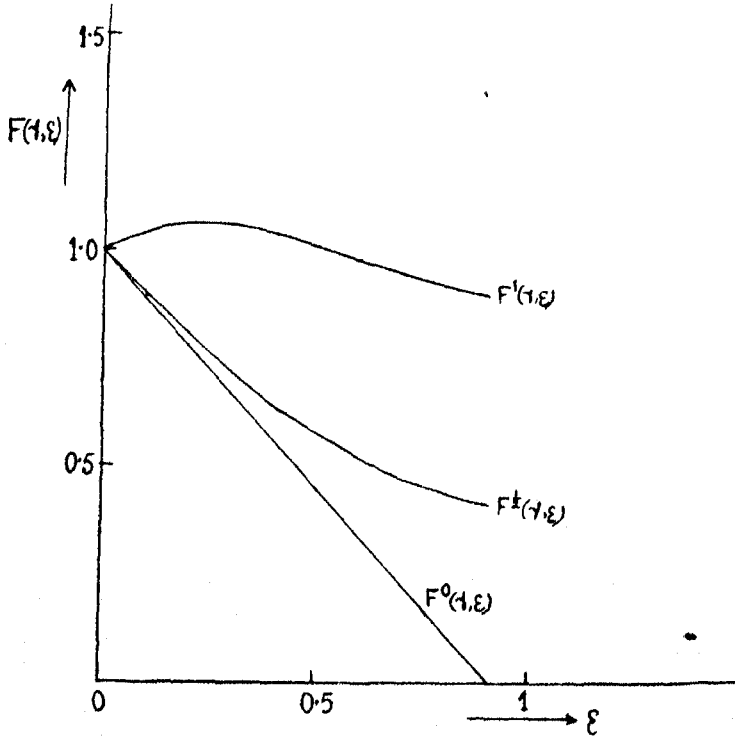
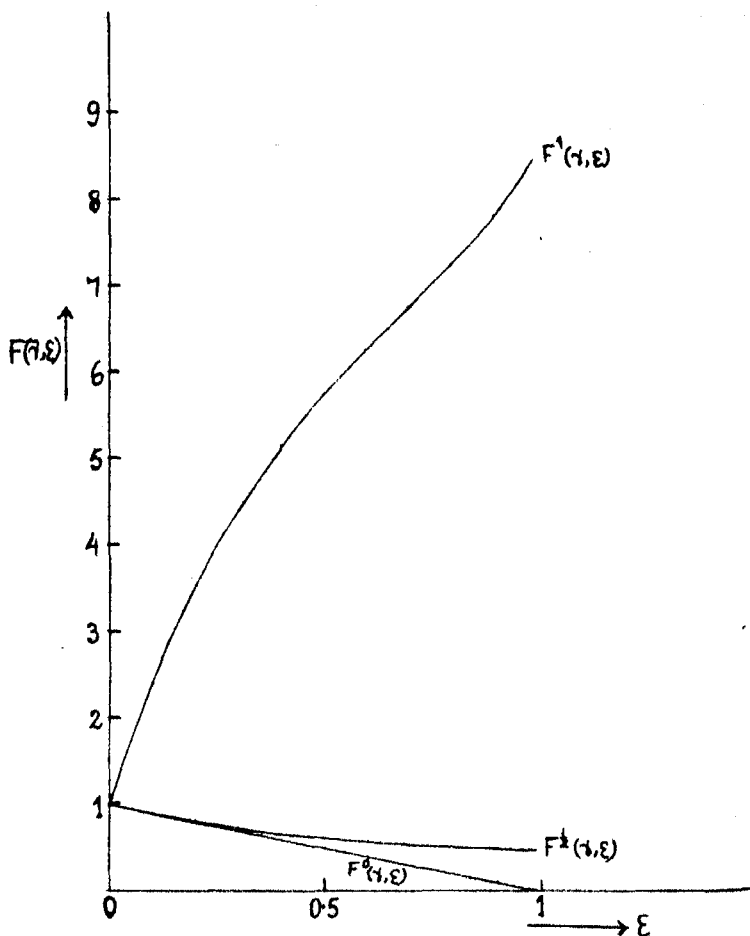


FIG. 2.  $\gamma = 10^2$ ,  $\varepsilon_m = 0.01$ .

FIG. 3.  $\gamma = 10^4$ ,  $\varepsilon_m = 0.99$ .

## §4. Discussion.

An inspection of the equations (56), (57) and (58) shows that the effect of the spin is practically negligible for small energies of the meson. But when the energy of the meson is very large compared with its rest energy, i.e.  $\gamma \gg 1$ , the contribution due to the spin begins to be important. We have for  $\gamma \gg 1$

$$F^1(\varepsilon, \gamma) \sim 1 - \frac{\varepsilon}{\varepsilon_m} + \frac{\varepsilon^2}{3} + \frac{\alpha\gamma\varepsilon}{3} \left( 1 - \frac{\varepsilon}{\varepsilon_m} + \frac{\varepsilon^2}{2} \right) \quad \dots \quad (59)$$

$$F^0(\varepsilon, \gamma) \sim 1 - \frac{\varepsilon}{\varepsilon_m} \quad \dots \quad (60)$$

$$F^{1/2}(\varepsilon, \gamma) \sim 1 - \frac{\varepsilon}{\varepsilon_m} + \frac{1}{2}\varepsilon^2 \quad \dots \quad (61)$$

We thus notice that in this region of high energy  $F^0(\varepsilon, \gamma)$  against  $\varepsilon$  is a straight line decreasing from 1 to 0, whereas  $F^1(\varepsilon, \gamma)$  against  $\varepsilon$  is a parabola with vertex at  $\left(1 - \frac{1}{2\varepsilon_m^2}, \frac{1}{\varepsilon_m}\right)$  decreasing in value throughout the range  $\varepsilon = 0$  to  $\varepsilon = \varepsilon_m$ . But as  $\varepsilon_m \gtrsim 1$  the vertex of the parabola cannot be reached. The behaviour of  $F^1(\varepsilon, \gamma)$  is rather complicated. It follows at once from (59) that the effect of the spin one becomes considerable when  $\frac{\alpha\gamma\varepsilon}{3} \gg 1$ , i.e. when the energy loss  $\varepsilon E \gg 6 \times 10^{10}$  e.v. The curve of  $F^1(\varepsilon, \gamma)$  against  $\varepsilon$  has the form of a cubic parabola and first rises for small  $\varepsilon$  as proportional to  $\varepsilon$ ; then the term proportional

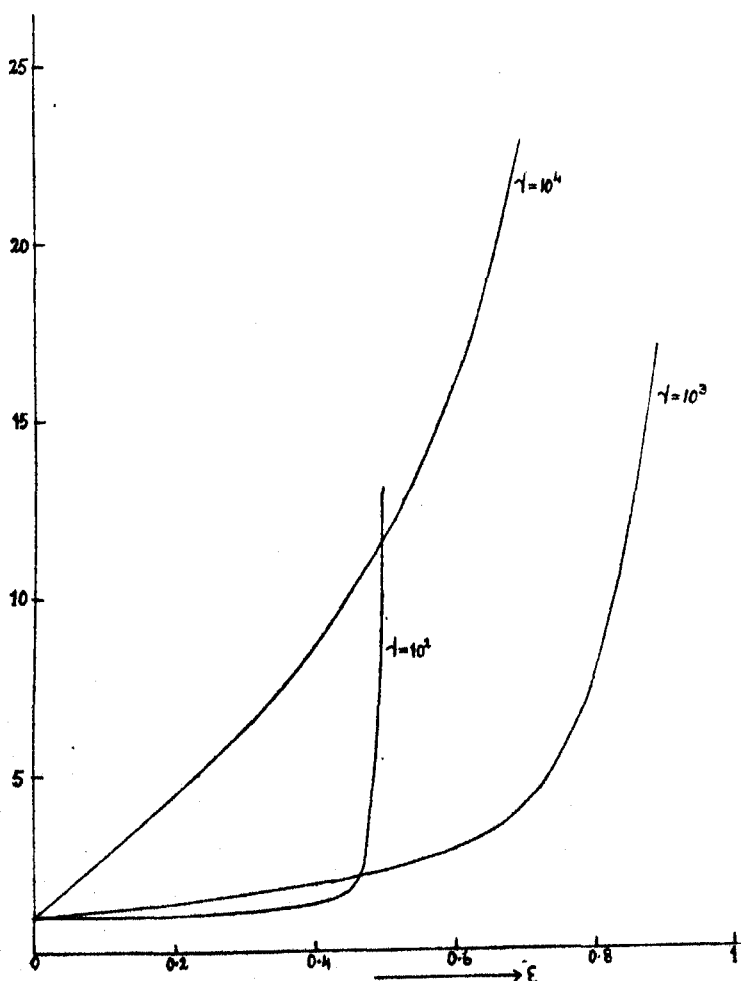


FIG. 4. The ordinate =  $\frac{\text{Differential cross-section for spin one}}{\text{Differential cross-section for spin zero}}$ .

to  $\varepsilon^2$  begins to compete with it resulting in a change in the slope of the  $F^1(\varepsilon, \gamma)$  curve until finally near  $\varepsilon_{\max}$  the terms proportional to  $\varepsilon$  and  $\varepsilon^2$  practically cancel one another and the curve behaves as  $\sim \gamma \varepsilon^3$  due to the last term. The behaviour of  $F(\gamma, \varepsilon)$  against  $\varepsilon$  as given by (56), (57) and (58) is shown in figures 1-3. It is to be noticed that the characteristic rise of  $F^1(\varepsilon, \gamma)$  with the incident energy of the meson above an energy loss of  $6 \times 10^{10}$  e.v. is remarkable and is due to the transition of the meson from its transverse to the longitudinal state or vice versa during the meson-electron collision. The ratio of the scattering cross-sections of meson of spins one and zero, and spins one and half have been drawn in figures 4 and 5 against the fraction of the energy taken up by

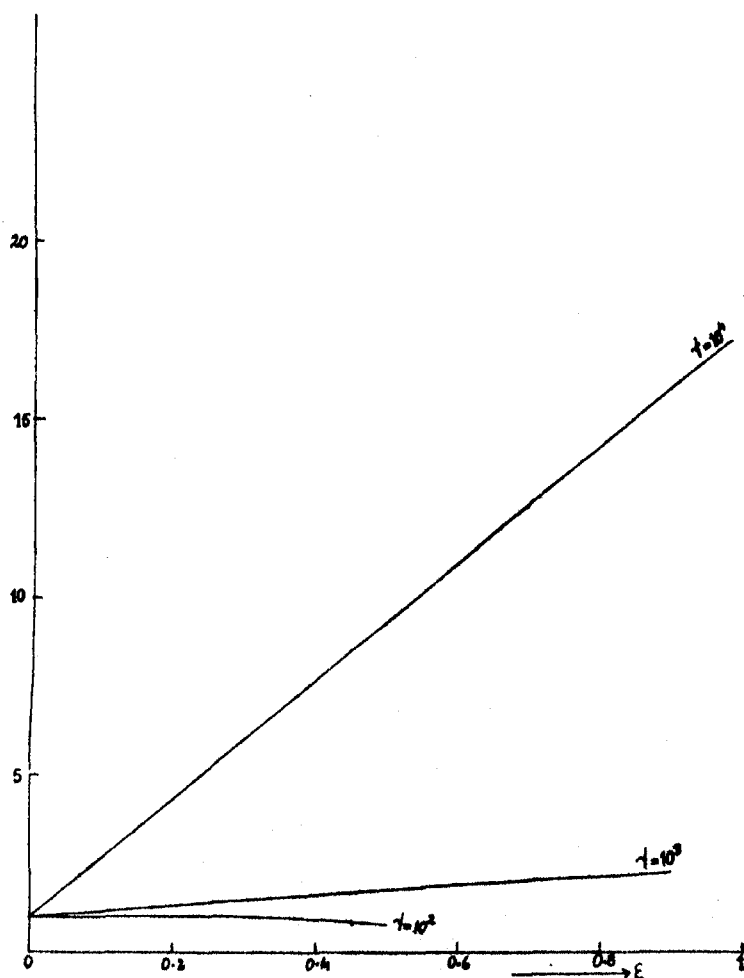


FIG. 5. The ordinate =  $\frac{\text{Differential cross-section for spin one}}{\text{Differential cross-section for spin half}}$ .

the secondary electron, i.e.  $\epsilon$  for different meson energies. We find from figure 4 that there is a sudden enormous increase in the scattering ratio at  $\epsilon \sim \epsilon_m$  which is 0.505 for  $\gamma = 10^2$ , 0.91 for  $\gamma = 10^3$  and 0.99 for  $\gamma = 10^4$ .

This is due to the factor  $1 - \frac{\epsilon}{\epsilon_m}$  or more rigorously  $1 - \frac{\gamma^2 - 1}{\gamma^2} \frac{\epsilon}{\epsilon_m}$  which occurs in the denominator of the ratio of the cross-section. The corresponding scattering ratio for meson of spin one and half increases for an energy loss  $\epsilon E \gg 6 \times 10^{10}$  e.v. as  $\frac{mE\epsilon}{3M^2c^2}$ . This large energy transfer is perhaps responsible for

the increase of the energy loss of the penetrating component of cosmic radiation with the energy for energies greater than  $10^{10}$  e.v.—a fact which had been observed by Blackett (1937) and could not be reconciled with the ionisation loss calculated from Bloch's formula. This favours the meson of having a spin one. Further evidence for attributing spin one to meson may be furnished by the observation on cosmic ray bursts produced by the penetrating component in different materials. The bursts are produced in cascade process by the high energy electrons knocked on by the mesons as discussed above and the frequency-size distribution of bursts as well as its dependence on different materials seem to support that the meson has spin one (Oppenheimer, 1939; Oppenheimer, Snyder and Serber, 1940; Bhabha, Carmichael and Chou, 1939; Lovell, 1939). But a quantitative analysis of the theory of bursts and its comparison with the experiments of Schein and Gill (1939) on the frequency-size distribution of bursts, which have been recently made by Christy and Kusaka (1941), favour spin zero or possibly half and tend to exclude spin one for the meson. The theoretical calculations of Christy and Kusaka contain, however, some amount of uncertainty which require careful consideration before any conclusion can be reached. As for example a pure Coulomb interaction between meson and electron has been assumed in the deduction of collision cross-section for the knock-on process. But the closest distance of approach in collision for an energy loss  $\epsilon E$  is of the order of

$$137 \left( \frac{e^2}{mc^2} \right) \left( \frac{mc^2}{\epsilon E} \right)^{\frac{1}{2}}$$

and thus when the energy acquired by the knock-on electron exceeds  $10^{10}$  e.v. this becomes of the order of the dimension of the electron and the deviation from the Coulomb field is to be taken into account. Further the Cascade theory of showers and the form of the fluctuations as assumed by Christy and Kusaka require revision. The contribution to the bursts from the low energy electrons should also be properly taken into consideration. We shall discuss this elsewhere in a separate paper.

#### REFERENCES.

- Bethe, H., and Fermi, E.—Über die Wechselwirkung von zwei Elektronen. *Zs. f. Phys.*, vol. 77, p. 296, (1932).

- Bhabha, H. J.—On the penetrating component of Cosmic Radiation. *Proc. Roy. Soc. (A)*, vol. **164**, p. 257, (1938a).
- Bhabha, H. J.—On the theory of heavy electrons and nuclear forces. *Proc. Roy. Soc. (A)*, vol. **166**, p. 501, (1938b).
- Bhabha, H. J., Carmichael, H., and Chou, C. N.—Production of Bursts and Spin of the Meson. *Proc. Ind. Acad. Sci. (A)*, vol. **10**, p. 221, (1939).
- Blackett, P. M. S.—The Energy-Range Relation for Cosmic-Ray Particles. *Proc. Roy. Soc. (A)*, vol. **159**, p. 19, (1937).
- Christy, R. F., and Kusaka, S.—Burst production by Mesotrons. *Phys. Rev.*, vol. **59**, p. 414, (1941).
- Fröhlich, H., Heitler, W., and Kemmer, N.—On the nuclear forces and the magnetic moments of the neutron and the proton. *Proc. Roy. Soc. (A)*, vol. **166**, p. 154, (1938).
- Fröhlich, H., Heitler, W., and Kahn, B.—The photodisintegration of the deuteron in the meson theory. *Proc. Roy. Soc. (A)*, vol. **174**, p. 85, (1940).
- Heitler, W.—Quantum Theory of Radiation, Oxford, p. 101, (1936).
- Kemmer, N.—Quantum theory of Einstein-Bose particles and nuclear interaction. *Proc. Roy. Soc. (A)*, vol. **166**, p. 127, (1938).
- Kobayasi, M., and Okayama, T.—On the Creation and Annihilation of Heavy Quanta in Matter. *Proc. Phys.-Math. Soc., Japan*, vol. **21**, p. 1, (1939).
- Lovell, A. C.—Shower production by penetrating cosmic rays. *Proc. Roy. Soc. (A)*, vol. **172**, p. 589, (1939).
- Massey, S. W., and Corben, H. C.—Elastic collisions of Mesons with Electrons and Protons. *Proc. Camb. Phil. Soc.*, vol. **35**, p. 463, (1939).
- Møller, C.—Zur Theorie des Durchgangs schneller Elektronen durch Materie. *Ann. d. Phys.*, vol. **14**, p. 531, (1932).
- Oppenheimer, J. R.—Discussion on High Energy Electrons in the Cosmic Radiation. *Rev. Mod. Phys.*, vol. **11**, p. 264, (1939).
- Oppenheimer, J. R., Snyder, H., and Serber, R.—The production of soft secondaries by Mesotrons. *Phys. Rev.*, vol. **57**, p. 75, (1940).
- Pauli, W., and Weisskopf, V.—Über die Quantisierung der skalaren relativistischen Wellengleichung. *Helv. Physica. Acta.*, vol. **7**, p. 709, (1934).
- Schein, M., and Gill, P. S.—Burst Frequency as a Function of Energy. *Rev. Mod. Phys.*, vol. **11**, p. 267, (1939).
- Yukawa, H., Sakata, S., and Taketani, M.—On the Interaction of Elementary Particles. III. *Proc. Phys.-Math. Soc., Japan*, vol. **20**, p. 319, 1938.

## ON THE ORIGIN OF EXTRA SPOTS IN LAUE PHOTOGRAPHS.

*By S. C. SARKAR, D.Sc., and B. M. BISHUI, M.Sc., Palit Laboratory of Physics,  
University College of Science, Calcutta.*

(Communicated by Prof. M. N. Saha, F.R.S.)

(Received February 18, 1942.)

### INTRODUCTION.

Numerous investigations, both theoretical and experimental, have been carried out during the last two years to explain the origin of extra spots in Laue photographs and various explanations have been offered. Since there is difference of opinion regarding the actual origin of these extra spots, and the explanations offered have not yet passed the controversial stage, it is proposed to discuss in the present paper numerous experimental results which have been published recently and also those which have been obtained by the present authors, in the light of the existing theories. In view of the large volume of literature which has accumulated recently dealing with this problem, it was, however, thought worthwhile to include a brief historical review which might be helpful in understanding the significance of the various results which have already been published.

### BRIEF HISTORICAL REVIEW.

The appearance of extra diffuse radial streaks starting from the central spot in Laue photographs was first observed by Friedrich (1913), and Faxen (1923) first suggested that these streaks might be due to diffuse scattering of incident continuous X-rays by Debye heat waves produced in the crystal by thermal agitation. Faxen further showed that when a monochromatic beam of X-rays of wavelength  $\lambda$  is incident at a glancing angle  $\theta$  on a set of lattice planes having the spacing  $d$ , there is a maximum in the intensity of the diffuse scattering which lies in the neighbourhood of the Laue spot in a direction in the plane of incidence making a glancing angle  $\phi$  with the said set of planes, where

$$d (\sin \theta + \cos \theta \tan \phi) = \lambda. \quad \dots \dots \dots (1)$$

Waller (1925) also investigated theoretically the same problem introducing the normal co-ordinates of the lattice given by Born and Karman and obtained an expression for the intensity of diffuse scattering analogous to Faxen's expression. No systematic attempt, however, was made at that time to verify these theories experimentally.



Wadlund (1938) first observed intense but diffuse extra spots accompanied by streaks in the Laue photographs of NaCl and Zachariasen (1938) put forward the hypothesis that scattering by two-dimensional lattice produced these extra spots and streaks. Preston (1939) made a careful investigation of the problem by studying the Laue photographs of a few crystals, e.g. NaCl, Al, diamond, Zn, etc., at different temperatures and using monochromatic as well as continuous X-radiation. He observed that the intensity of the extra spots in the Laue photograph of NaCl increased very much on heating the crystal to 500°C. and that the extra spots in the case of a crystal of Al were produced even when monochromatic radiation was used. Thus it was first proved by Preston experimentally that the extra spots were due to monochromatic radiation. He discussed his results in the light of Zachariasen's theory and showed that the results did not agree with the said theory. He further put forward a new theory to explain the extra spots. According to this theory the extra spots are due to independent scattering by small groups of atoms, there being no phase relation among different groups. The temperature effect observed by him was explained by assuming that the number of such groups of atoms increases with the increase of temperature, the phase relation among some of them being destroyed by increase in the thermal agitation. Laval (1939) also had studied the same problem experimentally a little earlier than Preston and had determined the intensity of scattering in the neighbourhood of some of the points in the reciprocal lattice using an X-ray spectrometer provided with an ionisation chamber.

Raman and Nilakantan (1940a) starting investigations in this line observed some extra spots and streamers first in the Laue photograph of diamond obtained with X-rays from Cu anti-cathode incident in a direction almost normal to the 111 cleavage plane of the crystal. They described the phenomenon as a 'new X-ray effect' and made an attempt to explain it by assuming that the vibration of the two interpenetrating lattices of diamond is excited by the impact of the incident photon with the lattice, and thereby a *dynamic stratification* is produced which is inclined to the 111 set of planes. Consequently, even when the static 111 planes do not satisfy the Bragg relation, the dynamic stratification may do so and there may be Bragg reflection from these dynamic stratifications. Their claim to the discovery of a new phenomenon was, however, disputed by many workers and particularly by Knaggs *et al.* (1940b) who pointed out that the results published by previous workers mentioned above had been overlooked by Raman and Nilakantan (1940a), as they had not mentioned these results while reporting their own results on diamond. Raman and Nilakantan (1940b) next observed that in the case of diamond, the directions of reflections producing the extra spots satisfied the empirical relation

$$\lambda^* \sin (\theta + \phi) = \lambda \cos \phi, \quad \dots \dots \dots (2)$$

where  $\lambda^*$  is the spacing of the 111 planes,  $\theta$  is the glancing angle of incidence,  $\phi$ , that of the reflected rays and  $\lambda$  the wavelength of incident monochromatic

X-rays. It can be seen that equation (2) is identical with the Faxen formula (1) but this was not mentioned by Raman and Nilakantan (1940*b*) who claimed it as a new discovery. It was Lonsdale (1940*a*), however, who pointed out that it was merely Faxen's formula which was apparently overlooked by Raman and Nilakantan (1940*b*).

Zachariasen (1940*a*), on the other hand, prior to the publication of the results on diamond by Raman and Nilakantan (1940*a*) had investigated theoretically the distribution of intensity in the diffuse scattering of monochromatic X-rays by cubic crystals, in which the atoms might be vibrating owing to thermal agitation. Assuming the velocity of elastic waves to be the same along all the cube edges, he showed that in the case of a simple cubic lattice there is a maximum in the intensity of the diffuse scattering in the direction making an angle  $2\theta_m$  with the incident rays in the plane of incidence given approximately by the relation

$$2\theta_m = 2\theta_B + 2(\theta_i - \theta_B) \sin^2 \theta_B, \dots \dots \dots (3)$$

where  $\theta_i$  and  $\theta_B$  are respectively the glancing angles of incidence and of Bragg reflection. It was pointed out by Zachariasen (1940*b*) and also by Sirkar and Gupta (1940) that the results on diamond published by Raman and Nilakantan agreed with Zachariasen's simplified formula (3). Siegel and Zachariasen (1940) had already shown that the position of the maximum in diffuse scattering observed by them in the case of NaCl agreed with the above formula (3). Raman and Nilakantan next extended the investigations to other crystals and studied the Laue patterns of the  $\text{NaNO}_3$  crystal at room temperature and at higher temperatures up to  $275^\circ\text{C}$ . Extra spots and streaks were observed in all the patterns and the intensity of some of these spots increased while that of others diminished with the rise of the temperature of the crystal. It was further observed that in this particular case the relation

$$2d \sin \frac{1}{2}(\theta + \phi) = \lambda \dots \dots \dots (4)$$

was satisfied more closely than the asymmetric relation (2).

A geometrical theory was next put forward by Raman and Nath (1940) who showed that the geometrical relationship (4) is obtained when the propa-

gation vector  $\vec{1/\Delta}$  for the optical vibration of the lattice is small and perpendicular to the radius vector of the point in question in the reciprocal lattice,  $\Delta$  being the spacing of the dynamic stratification. Similarly, formula (2) was deduced geometrically by assuming that the scalar magnitude of  $1/\Delta$  was minimum.

Lonsdale (1940*a*) investigated the Laue patterns of a large number of crystals including diamond at different temperatures and observed that except in the case of diamond the extra spots almost disappeared in all other cases at the temperature of liquid oxygen. In the case of diamond the extra spots due to 111 planes diminished in intensity only very slightly when the crystal

was cooled down to  $-180^{\circ}\text{C}$ . It was pointed out by her that since the extra spots disappear in most cases at low temperatures they are due to diffuse scattering by elastic waves and cannot be due to reflection from dynamic stratification caused by incident photon as postulated by Raman and Nilakantan. She also pointed out that the characteristic temperature of diamond being extremely high the intensity of the extra spots does not diminish considerably with a lowering of temperature by about  $200^{\circ}\text{C}$ .

The Laue pattern of rocksalt was studied by Raman and Nilakantan (1940*d*) in order to find out which of the two relations (2) and (4) was satisfied by the observed extra spots. It was concluded from the results observed by them that the extra spots in this case satisfied the symmetrical formula (4) and not the asymmetric Faxen formula (2) and hence they also concluded that the extra spots could not be due to diffuse scattering. As these results were contradictory to the observation by Siegel and Zachariasen (1940), the latter (1941) pointed out that the results of measurement of angles of incidence and scattering corresponding to the observed maxima reproduced by Raman and Nilakantan actually agreed more closely with the asymmetric formula (3) than with the symmetrical relation (4).

Sir William Bragg (1940*a*) on the other hand examined Preston's (1939) hypothesis quantitatively and deduced an expression for the intensity of diffuse scattering in the case of a group of eight similar atoms situated at the corners of a simple cube. The intensity  $I$  of the scattered beam in a direction having direction cosines  $q_1, q_2, q_3$  is given by

$$I = \text{const.} \times \cos \pi a \frac{(\cos i - q_1)}{\lambda} \cdot \cos (-\pi a) \frac{(\sin i + q_2)}{\lambda} \cdot \cos \frac{(-\pi a q_3)}{\lambda} \dots \quad (5)$$

where the edges  $a$  of the cube are parallel to the  $x, y, z$  axes and the incident rays are in the  $xy$  plane making an angle  $i$  with the  $x$  axis. Jauncey (1941) further examined the Bragg formula (5) for the shift in the position of the diffraction maximum with the turning away of the group from the position for the Laue maximum. He deduced an expression which is identical with formula (2) and Zachariasen's approximate formula (3).

The geometrical relationship between the direction of the incident beam and that of the maximum in the diffuse scattering was further investigated experimentally with the help of X-ray spectrometers by Siegel (1941) in the case of KCl, by Kirkpatrick (1941) in the case of diamond and calcite and by Jauncey and Baltzer (1941) in the case of rocksalt. Siegel varied the value of  $\theta_i - \theta_B$  from  $6'$  up to  $41'$  and observed that the experimental results agreed with Zachariasen's simplified formula (3). Kirkpatrick (1941) observed that in the case of diamond the angle between the direction of maximum in the diffuse scattering and that of incidence agreed with Zachariasen's formula (3) for values of  $\theta_i - \theta_B$  only up to about  $\pm 2.5^{\circ}$ . For greater values of  $\theta_i - \theta_B$  the deviation was much larger or smaller than that indicated by the said formula according as  $\theta_i - \theta_B$  was positive or negative. In the case of calcite

he observed no new maxima with untreated cleavage faces and the reflected line was quite sharp, but when the face was lightly ground with an abrasive the intensity in the reflected beam extended over a much wider region. This was attributed to the presence of disarranged crystal particles on the ground surface. Jauncey and Baltzer (1941) observed that in the case of rock salt the positions of extra spots satisfy Zachariasen's simplified formula (3) only when  $\theta_i - \theta_B = 1^\circ$ , and for larger or smaller values of  $\theta_i - \theta_B$ , the values of  $2\theta_m - 2\theta_B$  are much smaller than those indicated by the said formula. On the other hand Jahn and Lonsdale (1941) observed that in the case of diamond when the value of  $\theta_i$  was varied from  $-16.8^\circ$  to  $-26.8^\circ$  in the neighbourhood of  $-\theta_B$  for the 111 plane and the *Cu K $\alpha$*  radiation, the diffuse maxima consisted of three spots situated at the corners of a triangle, there being diffuse scattering at the centre of the triangle. It was also pointed out that the size of the triangle increased as the difference  $\theta_i - \theta_B$  increased and the position of the centre of the triangle satisfied the Faxen formula (1) and that this structure of the diffuse maximum could be explained by Waller's (1925) theory.

Raman and Nilakantan (1941*a*) also pointed out that the Faxen formula (1) is not satisfied by the observed directions of new maxima when the values of  $\theta_i - \theta_B$  are large. They further showed that the observed results could be explained by the more general expression deduced by Raman and Nath (1941), viz.,

$$2d \sin \psi \sin (\theta + \epsilon) = n\lambda \sin \theta, \quad \dots \quad (6)$$

where  $\psi$  is the glancing angle of incident beam with dynamic stratifications,  $\theta$  and  $\epsilon$  are the angles which the crystal planes make respectively with the phase-waves due to optical vibration and the dynamic stratifications and  $d$  is the spacing of 111 planes. It was pointed out that equation (6) agrees with observed facts if the value of  $\theta$  be taken as  $54^\circ 44'$  and from this fact it was concluded that the phase-waves are parallel to the 100 planes normal to the plane of incidence. They further pointed out that these facts, along with the persistence of the extra spots even with the lowering of the temperature of the specimen of diamond to  $-180^\circ\text{C}$ . observed earlier by them (Raman and Nilakantan, 1940*e*), definitely supported the theory of quantum reflection put forward by them and contradicted the theories of diffuse scattering.

Zachariasen (1941*b*), however, put forward a revised theory of diffuse scattering by a cubic lattice in which the velocities of elastic wave along different directions were not assumed to be the same. The expressions deduced by him for the intensity of diffuse scattering are different for different limiting relative values of the elastic constants. It was shown by him that one of these expressions which could be used in the case of diamond could explain all the observed facts including the directions of maxima, the triangular pattern and the streamers mentioned earlier.

Some new results were published recently by Lonsdale and Smith (1941*a*) who investigated the Laue patterns of a few specimens of diamond which had

been studied by Robertson, Fox and Martin (1934) and divided into two groups. Those belonging to group I, which showed some absorption band at  $8\mu$  and also absorbed the near ultraviolet region, produced very intense streamers. But the streamers were absent in the case of specimens of diamond belonging to group II, which are known to be mosaic in character. After the publication of Zachariasen's modified theory, Pisharoty (1941) put forward a geometrical theory of quantum reflection of X-rays and tried to explain the phenomena observed in the case of diamond basing his arguments on the theory put forward by Raman and Nath (1941) and assuming, as pointed out by Raman and Nilakantan (1941a), that the phase-waves are parallel to the 100 planes. According to this theory the streamers owe their origin to the finite divergence of the incident beam; but it has been recently pointed out by the present authors (Sirkar and Bishui, 1941) that experimental facts do not support this conclusion of Pisharoty's theory. Further details of the said theory will be discussed later in the present paper.

In a report of the discussion held in the Royal Society, London, Lonsdale and Smith (1941b) have reported the results of an exhaustive investigation on the diffuse scattering of X-rays by crystals of a large number of substances. Some of these crystals have been studied at room temperature as well as at the temperature of liquid oxygen. Also, both continuous as well as monochromatic radiations have been used as incident X-rays. The results furnish important information regarding the various properties of the extra spots some of which will be discussed later. In the same report Born and Sarginson (1941) have published a wavemechanical theory on the effect of thermal vibration of atoms in the crystal on the scattering of X-rays. They have deduced expressions in the case of cubic lattices for the directions and the integrated intensity of the maxima in the background scattering, the expression for the intensity being valid only for maxima not lying too near the Laue spot. The intensity is found to be a function of  $T$  the absolute temperature,  $\lambda$ , the wavelength of incident radiation,  $\mu$ , the atomic weight,  $a$ , the atomic distance,  $\theta$ , the characteristic temperature of the crystal and  $\phi$  the angle of rotation of the crystal about one of the edges of the cube from the position for Laue diffraction. The expressions for the direction of the maxima can be reduced to the Faxen formula under certain approximations, but they furnish further information regarding the azimuthal displacement. Sir William Bragg (1941a) has developed in detail the theory of scattering by small groups of atoms and has compared the conclusions of his theory with the observed results for KCl, diamond and calcite. He has also shown (Bragg, 1941b) that all the details of the experimental results obtained by Lonsdale and Smith (1941a) in the case of diamond can be explained by his theory. The said report also contains a few more papers by other authors.

In a special issue of the Proceedings of the Indian Academy of Sciences entitled 'Symposium of papers on the quantum theory of X-ray reflection' fifteen papers dealing with different aspects of quantum theory of X-ray

reflection have been published by Sir C. V. Raman and others working under him. In all these papers attempts have been made to prove that the extra spots and streaks observed in the case of diamond and other crystals do not owe their origin to diffuse scattering, but they are produced by quantum reflection of X-rays from dynamic stratification caused by the excitation of optical vibrations by the incident X-rays, as first pointed out by Raman and Nilakantan (1940*a*) and further worked out by Raman and Nath and by Pisharoty. Some of the main experimental evidences in support of this view have been stated by Raman and Nilakantan (1941*b*) to be as follows:—

- (1) The geometric law of quantum reflection deduced by Raman and Nath (1940) agrees with the results obtained in the case of diamond more closely than the Faxen formula.
- (2) There is displacement of the direction of maxima from the plane of incidence and this can be explained by Pisharoty's (1941) theory applied to the case of diamond.
- (3) The structure of the triangular extra spot observed by Jahn and Lonsdale (1940) in the case of diamond as well as the streamers can be explained by Pisharoty's theory very satisfactorily. This fact according to them confirms the hypothesis of quantum reflection.
- (4) The relative intensities of classical and quantum reflection are not affected by change in the volume of the crystal irradiated. Also the intensity remains constant in the case of diamond even when the crystal is cooled down from room temperature up to  $-180^{\circ}\text{C}$ .
- (5) The diffuse halo surrounding the central spot observed in the case of diamond is found not to be due to thermal vibration, because it persists in liquid air temperature. It is concluded that this halo is due to quantum reflections from stratifications caused by vibrations of lower frequencies excited by the incident radiation.

These conclusions are discussed below in the light of the recent theoretical and experimental results.

#### DISCUSSIONS OF EXPERIMENTAL RESULTS.

##### (a) *The position of extra spots.*

It has already been pointed out that a revised theory of diffuse scattering has been published by Zachariasen (1941*b*). According to this theory in the case of diamond the intensity of diffuse scattering is given by

$$J_2 \approx K \frac{3[\sum \alpha_j \beta_j]^2}{(\Delta \sin^2 \theta_B)^2 \Sigma H_j^2} \sum_j \frac{H_j^2}{1 + (g-1) \alpha_j^2} \quad \dots \quad (7)$$

where

$$K = \frac{4I_a kT \sin^2 \theta_B}{3\Omega^2 C_{12}} \delta V,$$

$\delta V$  is the volume of scattering,  $I_a$  is the intensity of scattering from a single atom,  $H_j$  are Millerian indices,  $\Omega$  is the volume of unit cell,  $g$  is the ratio  $C_{11}/C_{12}$

where  $C_{11}$  and  $C_{12}$  are elastic constants,  $\alpha_1, \alpha_2, \alpha_3$  are the direction cosines of the unit vector normal to the elastic wave relative to the cube edges and  $\beta_1, \beta_2, \beta_3$  are those of the vector  $\lambda r_{\min}$  and are approximately equal to the direction cosines of the scattering direction and  $\Delta = \theta_i - \theta_B$ . It has been shown by Zachariasen that this expression gives three maxima corresponding to the three sets of values of  $\alpha_1, \alpha_2, \alpha_3$ , viz., 1, 0, 0; 0, 1, 0 and 0, 0, 1 and the intensities of the three maxima are respectively proportional to  $\beta_1^2, \beta_2^2$  and  $\beta_3^2$ . This explains the structure of the maxima observed in the case of diamond with the rays incident in the neighbourhood of  $+\theta_B$  and  $-\theta_B$  by Jahn and Lonsdale (1941), because the values of  $\beta_1, \beta_2, \beta_3$  are almost equal in the latter case, and  $\beta_1$  is much larger than  $\beta_2$  or  $\beta_3$  in the former case. It has also been shown by Zachariasen that for  $Cu K\alpha$  and  $K\beta$  radiations the following formulae regarding the directions of maxima hold good when

$$Cu K\alpha, \quad 2\theta_m^A \approx 43^\circ 58' + 0.444\Delta \quad \dots \dots \dots (8)$$

$$Cu K\beta, \quad 2\theta_m^A \approx 39^\circ 30' + 0.405\Delta \quad \dots \dots \dots (9)$$

These relations (8) and (9) have been shown to agree with the results observed by Raman and Nilakantan. The present authors have obtained some results which are given below. The corresponding Laue photographs are reproduced in figures 1 and 2, plate III.

TABLE I.

$\theta_i$	Radiation $Cu K$	$\Delta$	$2\theta_m^A$ observed.	$2\theta_m^A$ calculated.
$21^\circ 17'$	$\alpha$	$-41'$	$43^\circ 37'$	$43^\circ 38'$
$20^\circ 18'$	$\alpha$	$-1^\circ 40'$	$43^\circ 1'$	$43^\circ 12'$
$19^\circ 42'$	$\alpha$	$-2^\circ 16'$	$42^\circ 50'$	$42^\circ 56'$
$17^\circ 5'$	$\alpha$	$-4^\circ 53'$	$41^\circ 38'$	$41^\circ 46'$
$17^\circ 5'$	$\beta$	$-2^\circ 40'$	$38^\circ 13'$	$38^\circ 25'$

As the central spot was recorded on each Laue photograph with feeble density by using an absorber of suitable thickness placed in contact with the film, the angles could be measured with an accuracy of about  $\pm 7$  minutes of arc.

The results in Table I show that the observed values of  $2\theta_m^A$  do not differ systematically from those calculated from Zachariasen's recent theory. The total angle of divergence of the incident beam used was  $1^\circ 30'$ , i.e.  $45'$  on each side. The variations observed are within experimental error. Thus the observed directions of maximum intensity in the background scattering in the Laue photograph of diamond are in agreement not only with those calculated from the theory of Raman and Nath (1940) but also with those calculated from

Zachariasen's recent theory. Hence it is not possible from considerations of the directions of maxima alone to accept one of these theories and to reject the other, as has been done by Raman and Nilakantan (1941b). The formula deduced by Born and Sarginson (1941) for the directions of maxima in the background scattering also gives the azimuthal displacement and it is evident that this displacement is a property not only of the quantum reflection but also of the diffuse scattering.

*(b) Origin of the triangular spot and streamers accompanying the diffuse maximum due to 111 plane of diamond.*

It has been mentioned by Raman and Nilakantan (1941b) that the geometrical theory of quantum reflection explains the origin of the triangle consisting of three spots observed by Jahn and Lonsdale (1941) and of the streamers observed by Raman and Nilakantan (1940b). The streamers, according to Pisharoty's theory, are due to the finite divergence of the incident beam and would be almost absent if the divergence could be reduced to a few minutes of arc. Also, according to his theory the intensity of the streamers should be comparable to the diffuse maximum which they accompany when  $\theta_i$  is slightly less than  $\theta_B$ . The intensity of each of the streamers would be slightly smaller than that of the said maximum because the total intensity in the streamer is distributed over a larger area than in the case of the maximum which it accompanies.

Both these conclusions of Pisharoty's theory, however, are definitely contradicted by experimental observations. First, it can be seen from the pattern due to a diamond plate 0.88 mm. thick, reproduced in fig. 1, plate III, that the streamers are extremely feeble in comparison with the maximum which they accompany, and in fig. 2, in which the pattern due to a thinner plate of diamond is reproduced, the streamers are completely absent although the diffuse maximum is very intense. The values of  $\theta_i$  in figs. 1 and 2 are  $20^\circ 18'$  and  $21^\circ 17'$  respectively. The angular length of the streamers in figure 1 is about  $10^\circ$ , although the divergence of the beam used was about  $1^\circ 30'$ . According to Pisharoty's theory the streamers would disappear if the value of  $\theta_i$  would be  $19^\circ 58'$  and the maximum angular length in the case of the thicker specimen of diamond would be  $4^\circ 53'$ . The length of the streamer expected from this theory in the case of the thinner crystal (fig. 2) ought to have been a little larger, but actually the streamer is absent in this case. Again in the case of a particular specimen of diamond studied by Lonsdale and Smith (1941a) the total length of each of the streamers is about  $10^\circ$  for  $\theta_i = +\theta_B$  although the total divergence of the incident beam as shown by the size of the Laue spots cannot exceed  $30'$  of arc. This fact combined with the results of the present investigation discussed above definitely proves that the length of the streamers is rather constant and does not depend on the divergence of the incident beam. This fact, therefore, also contradicts the view held by Pisharoty that the streamers are due to quantum reflection by dynamic



stratifications. These streamers are, however, explained satisfactorily by the theory of Zachariasen according to which the maxima corresponding to sets of values of  $\alpha_1, \alpha_2, \alpha_3$  equal to 1, 0, 0; 0, 1, 0 and 0, 0, 1 are connected by saddle shaped ridges of intensity much less than that of the maximum and these appear as streamers when  $\alpha_2 = \alpha_3 = 0$ . The length of the streamers thus does not depend on the angle of divergence of the incident beam and also the intensity is smaller than that of the maximum. The observed facts are thus explained satisfactorily by Zachariasen's theory and the streamers may be assumed to be entirely due to diffuse scattering and not due to quantum reflection.

It has already been mentioned that the triangle consisting of three spots observed by Jahn and Lonsdale (1941) when  $\theta_i = -\theta_B$  can be explained by Zachariasen's modified expression for the intensity of diffuse scattering applicable to the case of diamond. It has also been mentioned that Pisharoty has given a geometrical theory to explain this pattern. According to the latter theory, however, each of the three spots would be circular in shape, the size depending on the divergence of the incident beam. The small intensity in the regions in between these three spots actually observed by Lonsdale and Smith (1941b) cannot be explained by Pisharoty's theory, but it is explained by Zachariasen's theory. Again it has been observed by the present authors, as can be seen from figure 3 that when  $\theta_i$  is slightly less than  $\theta_B$  in the case of the 111 plane of diamond, the shape of the extra spot is not exactly circular, but it is triangular with its apex towards the Laue spot, and this fact shows that this spot is the projection of the larger triangular pattern indicated by Zachariasen's theory. Hence in this case also the theory of quantum reflection fails to explain the observed phenomena in detail while that of diffuse scattering explains them satisfactorily.

(c) *Intensity of the extra spots.*

As pointed out first by Raman and Nilakantan (1941a) the intensity of quantum reflection should depend in  $N^2$  and that of diffuse maximum on  $N$ , the number of unit cells taking part in the scattering. In order to investigate the dependence of the intensity on the volume irradiated, Venkateswaran (1941) studied the Laue patterns of specimens of NaCl of different thicknesses using different widths of the slit. It has been argued by him that due to primary and secondary extinctions the intensity of the Laue diffraction as well as that of quantum reflection should not increase with the increase in the thickness of the crystal beyond a certain limiting thickness. In the case of diffuse scattering, however, the extinction is absent and the intensity should increase with the increase in the volume of the crystal irradiated. He has, observed that the relative intensities of the Laue spots and the extra spots remain constant even when the volume of irradiated portion of the crystal is increased twelve times. From this he concludes that the extra spots cannot be due to diffuse scattering but they are due to quantum reflection. He has,

however, not investigated whether with the thicknesses 0.25 mm. and 0.5 mm. the crystals of NaCl used by him actually exhibited primary extinction. Further, in figs. 1 and 3 of his paper are reproduced the patterns obtained with the different thicknesses of the specimens but with the same slit-width. The settings, however, are slightly different from each other in the two cases and the densities of the spots in the two patterns are so widely different from each other that no conclusion can be drawn from these photographs. Again, the Laue spots are due to the continuous radiation and the extra spots due to the  $Mo K\alpha$  and  $K\beta$  radiations, and except for the exact Bragg setting, the intensity of quantum reflection is very small and hence the effect of extinction would be negligible in the case of the extra spots observed by him even if they were due to quantum reflection as postulated by him. In fact, however, even for the Laue spots the primary extinction is negligible in the case of NaCl as has been discussed by Compton and Allison (1935). For the thickness used by Venkateswaran the secondary extinction also has very small effect. But nothing can be said definitely unless the secondary extinction is estimated for the specimens used. This has not been done by Venkateswaran and therefore the results on which he has based his conclusions have very little significance.

Investigations of a similar nature have been carried out by the present authors using two plates of diamond the thickness of one being 0.42 mm. and that of the other 0.88 mm. Laue patterns were photographed with the incident X-ray beam nearly normal to the 111 plane and using the same setting, the width of the slit and exposure in both the cases. In each case two exposures, one short and one long were used. The Hadding tube used was kept quite steady by a regulated continuous circulation of air from a reservoir at a low pressure. The voltage used was about 38 K.V. The films were developed under similar conditions in the same developer. The Laue patterns obtained with the thin and the thicker crystal and with the shorter exposure are reproduced in figures 4 and 5 respectively. It can be seen that the Laue spots due to the  $\bar{1}\bar{1}\bar{1}$ ,  $\bar{1}\bar{1}\bar{1}$  and  $\bar{1}\bar{1}\bar{1}$  planes of the thicker crystal are not appreciably more intense than the corresponding spots due to the thin crystal. This fact shows that the influence of absorption and secondary extinction is quite appreciable in the case of the thicker crystal. It is, however, seen from figures 6 and 7, in which the Laue photographs obtained with the longer exposure are reproduced, that the diffuse maximum accompanying the Laue spot due to  $\bar{1}\bar{1}\bar{1}$  plane is more intense in the case of the thicker crystal than in the case of the thin crystal. Thus the ratio of the intensity of the diffuse maximum to that of the corresponding Laue spot is larger in the case of the thick crystal than in the case of the thinner crystal. This fact clearly contradicts the conclusion arrived at by Venkateswaran that the said intensity ratio does not increase with the increase in the volume of the crystal irradiated and shows that when secondary extinction is effective the said intensity ratio actually increases with the increase in the said volume. This observed fact thus supports the theory of diffuse scattering.

(d) *The origin of the halo round the direct beam.*

As already mentioned, it was first pointed out by Raman and Nilakantan (1940b) that the halo round the direct beam observed in the case of diamond might be due to some quantum mechanical effect in which the monochromatic X-rays might excite the vibrations of diamond lattice having much lower frequency than  $1332\text{ cm}^{-1}$ . Lonsdale and Smith (1941b), on the other hand, have observed that this halo disappears when monochromatic X-rays are used as incident radiation. Hence the hypothesis of Raman and Nilakantan is not supported by experimental observations. It has been shown by Zachariasen (1941b), however, that his theory of diffuse scattering predicts the absence of any halo round the direct beam. Thus the observed facts support the view that the observed phenomena are due to diffuse scattering.

Hence it can be concluded that even in the simple case of diamond, the observed phenomena mentioned above support the theories of diffuse scattering and do not agree in detail with the predictions of the theory of quantum reflection.

(e) *Influence of Temperature on the intensity of extra spots.*

According to the theory put forward by Sir C. V. Raman (1941) the temperature factor  $f(T)$  for the intensity of the quantum reflection is given by

$$f(T) = \frac{e^{h\nu^*/kT} + 1}{e^{h\nu^*/kT} - 1} \quad \dots \quad (10)$$

where  $\nu^*$  is the frequency of optical vibration of the lattice, and in the case of diamond for ordinary and low temperatures  $f(T) = 1$ . According to the theory of diffuse scattering put forward by Zachariasen (1941b)  $f(T) \propto T$ , and in the expression for the maximum in the diffuse scattering deduced by Born and Sarginson (1941) the factor explicitly containing temperature  $T$  is

$$f'(T) = \frac{T}{\theta} \log \frac{\sinh \theta/T}{\sinh \theta w_0/T} \quad \dots \quad (11)$$

where  $w_0$  is a factor independent of temperature and  $\theta$  is the characteristic temperature of the crystal. There is also another factor  $f''(T)$  in the said expression which is the same as the Debye factor,  $\exp. (-2M)$ . Hence the two factors together indicate a slower variation of the intensity with temperature than that indicated by any one of the two factors. But when the characteristic temperature  $\theta$  is very large so that  $\theta \gg T$ , as it is in the case of diamond,

$$\frac{T}{\theta} \log \frac{\sinh \theta/T}{\sinh \theta w_0/T} \approx \frac{T}{\theta} \left( \frac{\theta}{T} - \frac{w_0 \theta}{T} \right) \approx 1 - w_0.$$

Thus in this case the temperature effect is given by the Debye factor,  $\exp. (-2M)$  of (11) alone and the intensity is expected to diminish only slightly with the diminution of the temperature, when  $\theta \gg T$ . In the case of diamond if  $\theta = 2340^\circ$  as given by Lonsdale and Smith (1941b), the ratio,  $\exp. (-2M_{20})/$

exp. ( $-2M_{300}$ ) is approximately 1.009. This change in the intensity of the diffuse spots can hardly be detected experimentally. Thus the intensity should remain constant even when the crystal is cooled down from room temperature up to  $90^{\circ}\text{K}$ .

The influence of temperature on the intensity of the extra spots in the Laue photograph of diamond was studied by Lonsdale and Smith (1941b) and Raman and Nilakantan (1941b). While the former authors point out that the intensity of the extra spots seems to diminish slightly when the crystal is cooled down from room temperature to  $-180^{\circ}\text{C}$ ., the latter authors do not observe any sensible difference between the intensities observed at the two temperatures mentioned above. If actually the intensity would slightly diminish with the diminution of temperature as observed by Lonsdale and Smith (1941b), this fact would be contradictory to the theory of background scattering developed by Born and Sarginson (1941). But Lonsdale and Smith have not concluded definitely that the intensity diminishes at the lower temperature.

#### ACKNOWLEDGMENT.

The authors express their gratitude to Prof. M. N. Saha, F.R.S., for his kind encouragement and interest during the progress of the work.

#### SUMMARY.

The experimental results published by previous workers and those obtained by the authors themselves on the various properties of the extra spots in Laue photographs have been discussed in the light of the various theories of diffuse scattering and that of quantum reflection. It is shown that the length of the streamers and the structure of the extra spots observed in the case of diamond with particular glancing angles of incidence cannot be explained by the theory of quantum reflection, put forward by Raman and Nilakantan, but the details can be explained by the theory of diffuse scattering put forward recently by Zachariasen. In the case of diamond the observed directions of maxima also agree with Zachariasen's theory and the observed influence of temperature is given satisfactorily by the wavemechanical theory put forward by Born and Sarginson. The ratio of the intensity of diffuse scattering to that of Laue spot due to the  $\{111\}$  plane of diamond is observed to increase with the increase of thickness of the crystal. It is pointed out that these results are contradictory to the theory of quantum reflection and also to the results obtained by Venkateswaran in the case of NaCl.

#### REFERENCES.

- Born, M. and Sarginson, K. (1941). The effect of thermal vibrations, etc. *Proc. Roy. Soc., A*, **179**, 69.  
Bragg, Sir William (1940). The extra spots of Laue photographs, etc. *Nature*, **146**, 509.  
Bragg, Sir William (1941a). The diffuse spots, etc. *Proc. Roy. Soc., A*, **179**, 51.

- Bragg, Sir William (1941b). The diffuse spots, etc. *Ibid.*, A. 179, 94.
- Compton, A. H. and Allison, S. K. (1935). *X-rays*, etc., p. 426.
- Faxen, H. (1923). Die bei Interferenz Röntgenstrahlen, etc. *Z. f. Phys.*, 17, 266.
- Friedrich, W. (1913). Interference of X-rays. *Physikal Z.*, 14, 1082.
- Jahn, H. A. and Lonsdale, K. (1941). Diffuse reflections from diamond. *Nature*, 147, 88.
- Jauncey, G. E. M. (1941). Note on the theory of the modified reflection, etc. *Phys. Rev.*, 59, 456.
- Jauncey, G. E. M. and Baltzer, O. J. (1941). Non-Laue maxima in the diffraction of X-rays, etc. *Phys. Rev.*, 59, 699.
- Kirkpatrick, P. (1941). X-ray diffraction maxima at other than Bragg angles. *Phys. Rev.*, 59, 462.
- Knaggs, I. E., Lonsdale, K., Muller, A. and Ubbelohde, A. R. (1940). Anomalous X-ray reflections, etc. *Nature*, 145, 820.
- Laval, J. (1939). *Bull. Soc. Francaise, Min.*, 62, 137.
- Lonsdale, K. (1940a). Diffuse reflections on Laue photographs. *Nature*, 146, 332 and 806.
- Lonsdale, K. and Smith, H. (1941a). Diffuse X-ray diffraction from two types of diamond. *Nature*, 148, 112.
- Lonsdale, K. and Smith, H. (1941b). An experimental study of diffuse X-rays, etc. *Proc. Roy. Soc.*, A. 179, 8.
- Pisharoty, P. R. (1941). On the geometry of quantum reflection, etc. *Proc. Ind. Acad. Sci.*, 14, 56.
- Preston, G. D. (1939). Diffraction of X-rays by crystals, etc. *Proc. Roy. Soc.*, 172, 116; *Nature*, 143, 76.
- Raman, Sir C. V. (1941). Quantum theory of X-ray reflection, etc. *Proc. Ind. Acad. Sci.*, Symposium, p. 350.
- Raman, Sir C. V. and Nath Nagendra, N. S. (1940a). Quantum theory of X-ray reflection and scattering. *Proc. Ind. Acad. Sci.*, 12, 83.
- Raman, Sir C. V. and Nath Nagendra, N. S. (1940b). The two types of X-ray reflections, etc. *Proc. Ind. Acad. Sci.*, 12, 427.
- Raman, Sir C. V. and Nilakantan, P., (1940a). Specular reflection of X-rays, etc. *Nature*, 145, 667; A new X-ray effect. *Current Science*, 9, 165.
- Raman, Sir C. V. and Nilakantan, P. (1940b). Reflection of X-rays with change of frequency. *Proc. Ind. Acad. Sci.*, 11, 389.
- Raman, Sir C. V. and Nilakantan, P. (1940c). Reflection of X-rays, etc. *Ibid.*, 11, 398.
- Raman, Sir C. V. and Nilakantan, P. (1940d). Reflection of X-rays, etc. *Ibid.*, 12, 141.
- Raman, Sir C. V. and Nilakantan, P. (1940e). Classical and quantum reflection of X-rays. *Nature*, 146, 686.
- Raman, Sir C. V. and Nilakantan, P. (1941a). The quantum theory of X-ray reflection. *Current Science*, 10, 241.
- Raman, Sir C. V. and Nilakantan, P. (1941b). Quantum theory of X-ray reflection, etc. *Proc. Ind. Acad. Sci.*, Symposium, p. 356.
- Robertson, Sir R., Fox, J. J. and Martin, A. E. (1934). Two types of diamond. *Phil. Trans.*, 232, 463.
- Robertson, Sir R., Fox, J. J. and Martin, A. E. (1936). Further work on two types of diamond. *Proc. Roy. Soc.*, A. 157, 579.
- Siegel, S. (1941). Experimental study of the diffuse scattering, etc. *Phys. Rev.*, 59, 371.
- Siegel, S. and Zachariasen, W. H. (1940). Preliminary experimental study, etc. *Phys. Rev.*, 57, 795.

- Sirkar, S. C. and Bishui, B. M. (1941). On Pisharoty's Theory, etc. *Science and Culture*, **7**, 314.
- Sirkar, S. C. and Gupta J. (1940). On new diffraction maxima, etc. *Science and Culture*, **6**, 187.
- Sirkar, S. C. and Gupta, J. (1940). On the new diffraction maxima, etc. *Proc. Nat. Inst. Sci. Ind.*, **6**, 705.
- Venkateswaran, C. S. (1941). The quantum reflection and quantum scattering, etc. *Proc. Ind. Acad. Sci.*, Symposium, p. 395.
- Wadlund, A. P. R. (1938). Radial lines in Laue spot photographs. *Phys. Rev.*, **53**, 843.
- Waller, I. (1925). *Dissertation, Uppsala*.
- Waller, I. (1923). Zur Frage der Einwirkung, etc. *Z. f. Phys.*, **17**, 398.
- Zachariasen, W. H. (1938). Comments on the article by A. P. R. Wadlund. *Phys. Rev.*, **53**, 844.
- Zachariasen, W. H. (1940a). A theoretical study of diffuse scattering, etc. *Phys. Rev.*, **57**, 597.
- Zachariasen, W. H. (1940b). Diffraction maxima in X-ray photographs. *Nature*, **145**, 1019.
- Zachariasen, W. H. (1941a). On the diffuse X-ray diffraction maxima. *Phys. Rev.*, **59**, 207.
- Zachariasen, W. H. (1941b). Temperature diffuse scattering, etc. *Phys. Rev.*, **59**, 860.



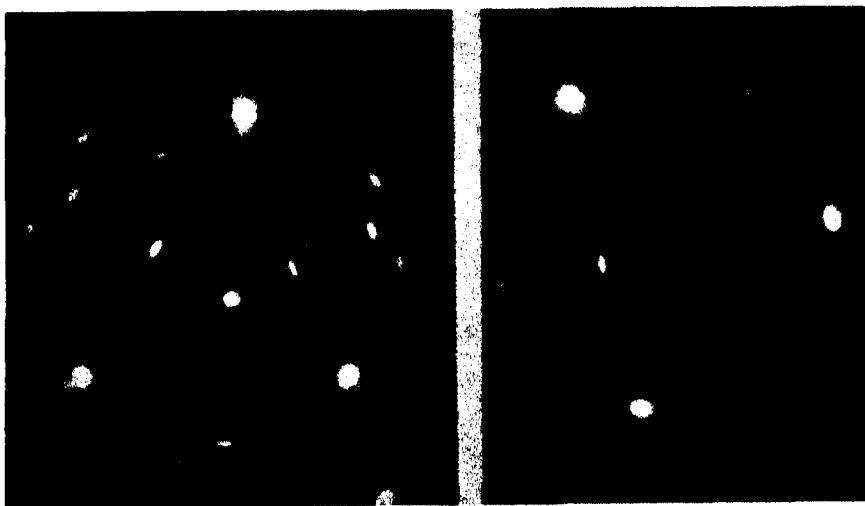


Fig. 1

Fig. 2

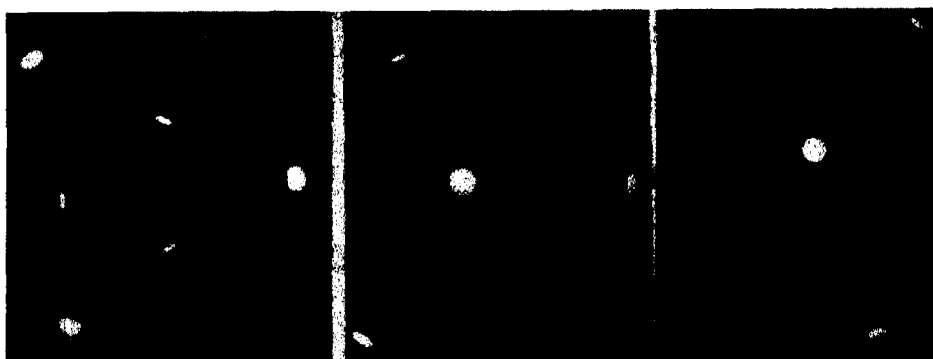


Fig. 3

Fig. 4 ( thin crystal )

Fig. 5 ( thick crystal )

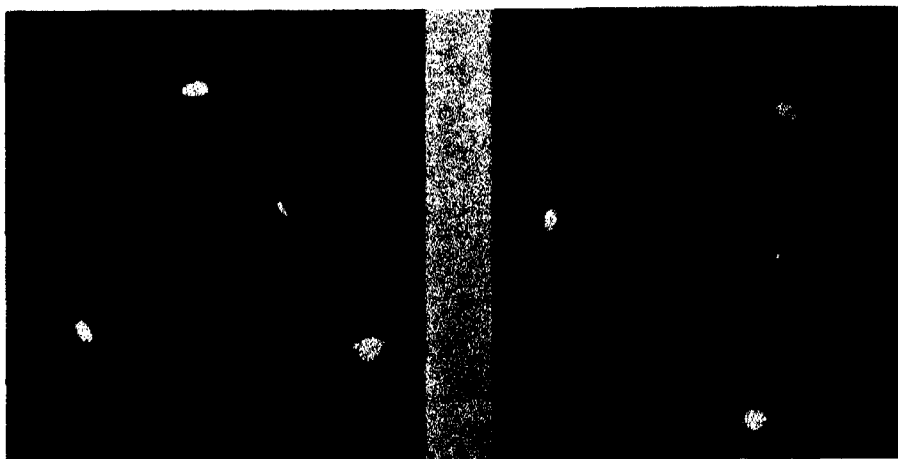


Fig. 6 ( thin crystal )

Fig. 7 ( thick crystal )





# ON THE PRODUCTION OF MESONS BY NON-IONISING AGENTS IN COSMIC RAYS.

By S. C. SIKKAR, *D.Sc.*, and S. K. GHOSH, *M.Sc.*

(Communicated by Prof. M. N. Saha, *F.R.S.*)

(Received March 10, 1942.)

## INTRODUCTION.

Rossi (1931) used a twofold coincidence counter telescope and observed the number of coincidences with an absorber of lead placed first between the counters (position 1) and then above the counters (position 2) as shown in Fig. 1. The number of coincidences in the arrangement (2) was found to be

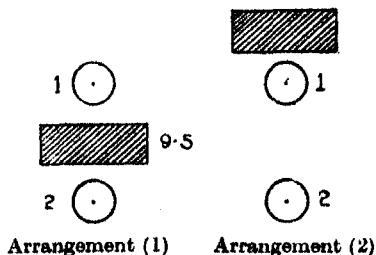


FIG. 1.

slightly larger than that in arrangement (1). This difference was ascribed to the production of secondary ionising particles in the absorber by photons.

Hsiung (1934) repeated the experiment using a modified arrangement shown in Fig. 2. Counter 3 is shielded by lead 2.5 cm. thick. A is a Pb-

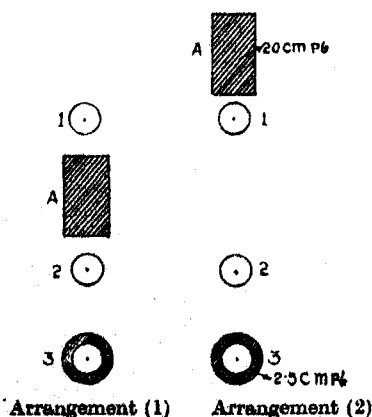


FIG. 2.

absorber 20 cm. thick, which was placed alternately between counters 1 and 2 (position 1) and above all the counters (position 2). The ratio of threefold coincidences in position (2) to those in position (1) was found to be 1.06. If counter 3 was removed, i.e. the experiment described in para. 1 was repeated now with 20 cm. of Pb, the ratio increased to 1.14. Hsiung interpreted these results by assuming that the ratio is 1.06 in threefold coincidence, because in position (2) some primary may be producing a pair of secondaries in the absorber *A*, which may pass through counters 1 and 2 respectively but not through 3, which is traversed by the primary itself. But the chance of this kind of coincidence is much less in position (1). The extra amount recorded in twofold coincidences was taken by Hsiung to arise from some soft components which are produced in the absorber *A*, but are usually absorbed by the Pb-shield of the counter 3. Another alternative proposal, viz. that the extra number of threefold coincidences in position (2) may be due to photons producing charged particles in *A* was also discussed by Hsiung, but it was concluded that the probability of such a mechanism was negligible.

Maass (1936) working at sea level measured the absorption of single cosmic ray particles by a counter telescope placing an iron block *A* of *varying* thickness between the counters (position 1) and above the counters (position 2), as shown in Fig. 3. He observed that the ratio of the number of coincidences

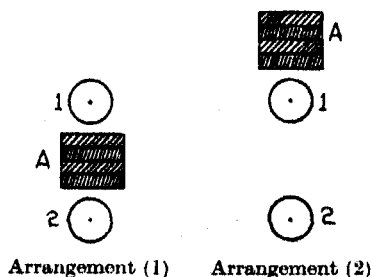


FIG. 3.

with the arrangement (2) to that with the arrangement (1) was almost unity for smaller thickness of *A* but increased to about 1.2 for an absorber of 30 cm. of Fe. Maass also observed that the presence of absorbers on the sides of the telescope affected considerably the number of coincidences. It was concluded by him that the penetrating ionising particles were created in the absorber *A*, in the arrangement (2) of the counters, by energetic photons present in cosmic rays. This, however, is in contradiction to what Hsiung concluded.

Arley and Heitler (1938) pointed out that the increase in the number of coincidences in Maass's experiment with the shift of the absorber from the middle to the top of the counters might be due to the production of mesons by penetrating neutral particles instead of by the photons. They were of opinion that those penetrating neutral particles are 'uncharged mesons' and identified them with the 'neutrettos' of the meson theory.

Schein and Wilson (1939) sent a fourfold coincidence counter telescope up to an altitude of 25,000 ft. in an aeroplane, in order to investigate the production of mesons in the atmosphere. The arrangement of counters used by them is shown in Fig. 4. The bottom tube was shielded from soft shower

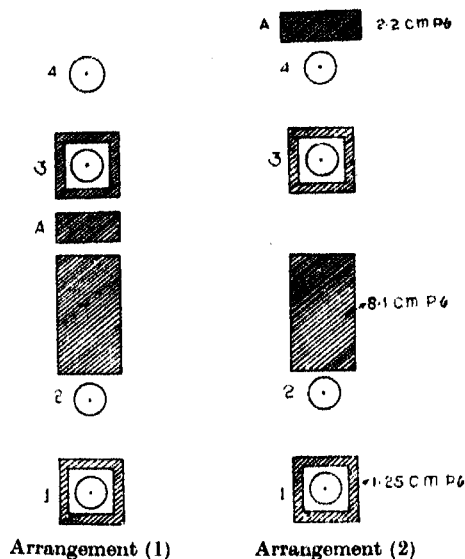


FIG. 4.

particles by 1.25 cm. of Pb. Counter 3 was shielded with Pb sheets 0.625 cm. thick, to absorb Compton recoil electrons produced in the Pb plate below. 8.1 cms. of Pb were placed between counters 2 and 3 to absorb the soft radiation, thus enabling to record only the penetrating rays, coming vertically.

The ratio of fourfold coincidences in the arrangement (2) with a Pb block A 2.2 cm. thick placed above all the counters to those in the arrangement (1) with the same Pb block placed between the counters 2 and 3 was found to change with height above sea level. Up to 20,000 ft. the ratio of the number of fourfold coincidences in the two arrangements remained almost equal to unity. Above that height the ratio was appreciably greater than unity, being 1.5 at about 22,000 ft. and 2.1 at 25,000 ft.

They interpreted this result by stating that mesons are produced by photons only above 20,000 ft.; they also say that the results obtained are in good agreement with Heitler's (1938) assumption that the mesons are formed by secondary photons which are abundant at high altitudes.

Shonka (1939) performed a similar experiment at an altitude of 14,200 ft. with a fourfold coincidence array of Geiger Müller counters in a vertical position. A thickness of 12.7 to 17.3 cm. of Pb served as absorber for the soft secondary particles, in between the counters 4 and 1 (Fig. 5). Additional

varying thicknesses  $A$  were placed alternately above the counters (arrangement 2) and between the counters 3 and 2 (arrangement 1). For a small thickness of  $A$  of only 0.32 cm. the ratio of the counts with the arrangement

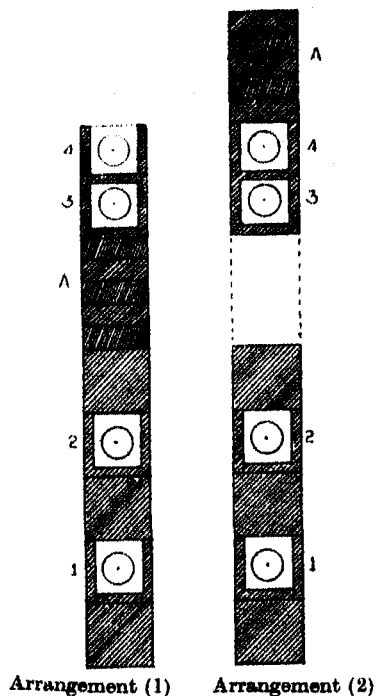


FIG. 5.

(2) to those with the arrangement (1) was only  $1.012 \pm 0.012$ ; and for large thickness of  $A$  equal to 23.18 cm. the value of the ratio was  $1.059 \pm 0.013$ .

Since most of the photons are absorbed in two cm. of Pb only the small and hardly significant difference of  $1.2 \pm 0.1\%$  observed with the shifting of thinner layer 0.32 cm. of Pb can be ascribed to mesons produced in the absorber  $A$  by primary photons. The much greater difference of  $5.9 \pm 1.6\%$  observed with the shifting of thicker layers of 23.18 cm. of Pb should thus be ascribed to mesons produced by neutral particles that are much more penetrating than photons. These rays penetrate 20 cm. of Pb without any considerable absorption. The high penetrating power suggests their identification with 'neutrettos' postulated by Arley and Heitler (1938).

Schein, Jesse and Wollan (1940) made two free balloon flights with a coincidence counter apparatus designed to record the vertical meson intensity and also the number of mesons produced in a 2 cm. Pb block by a non-ionising radiation. The detailed arrangement of the counter set used by them is shown in Fig. 6.

Counters 1, 2 and 3 represent one coincidence set, and counters 2, 3 and 4 constitute another set. Since a particle which passes through either set of counters must penetrate at least 8 cm. of Pb the coincidences registered must be due to mesons. The top set of counters consisting of the counters 1, 2

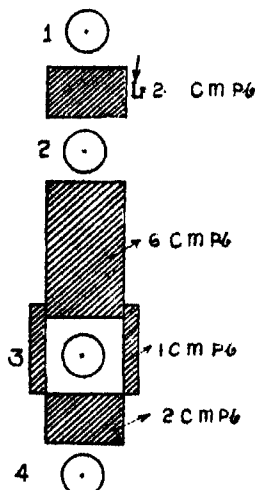


FIG. 6.

and 3 can be actuated only by mesons which have originated outside the apparatus, whereas the lower set comprising the counters 2, 3 and 4 can be set off either by a meson entering from outside or by one which is produced in the Pb block *L*, 2 cm. in thickness.

Thus the excess of the counts in the lower set, over those in the upper set, gives us the number only of those mesons which are produced in *L*, and which can pass through the three counters 2, 3 and 4.

Schein, Jesse and Wollan have found that the production of mesons in Pb block *L* becomes noticeable at about 35 cm. pressure and increases with altitude, attaining at an altitude corresponding to a pressure of 6.6 cm. of Hg, a value of about 25% of the total meson intensity at that altitude.

This rate of production of mesons increases at about the same rate as does the soft component. This is the evidence that photons are the agents responsible for a large part of the observed creation of mesons in the Pb block *L*. On this assumption, they have calculated a cross-section for this meson creation process by photons:  $\sigma_{ph} = 0.7 \times 10^{-27} \text{ cm.}^2$  per nuclear particle in Pb.

Lovell (1939), on the other hand, while studying cosmic-ray showers at sea level did not obtain even a single photograph of a meson track produced by a 'neutretto', although 500 photographs were obtained by him in which the primary particles traversed 10 cm. of Pb. Since, according to Arley and Heitler (1938), the mean free path of a 'neutretto' in Pb is only 5 cm. it was

concluded by Lovell that the number of neutrettos in cosmic radiation at sea level must be very much smaller than the number of mesons. He also concluded that probably there are no 'neutrettos' at sea level.

Rossi, Janossy, Rochester and Bound (1940) made a careful investigation of the problem, using a system of counter arrangement in such a way that fourfold and threefold coincidences could be recorded simultaneously. In position (2) as well as in position (1) of their arrangement as shown in Fig. 7,

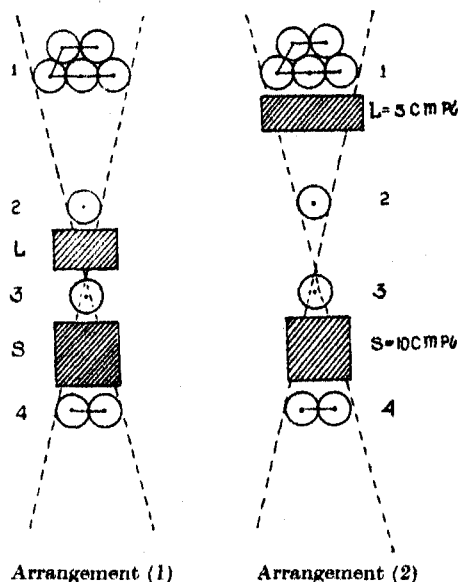


FIG. 7

a Pb block  $S$ , 10 cm. in thickness was placed between the counters 3 and 4, so that the coincidences recorded were all due to mesons. In arrangement (2) a Pb block  $L$  5 cm. thick was placed between the counters 1 and 2, while in arrangement (1) the block  $L$  was placed between 2 and 3.

If some penetrating ionising particles are produced in  $L$ , by any non-ionising agent in cosmic rays, the number of threefold coincidences (234) in the arrangement (2) should be greater than (234) in arrangement (1). The difference would be a measure of the number of ionising penetrating particles which are produced by non-ionising agents in  $L$  and are able to discharge the counters 2, 3 and 4.

They have observed that the number of threefold coincidences (234) is  $1.6 \pm 0.5\%$  larger in the position (2) than in the position (1). But the difference between the number of threefold coincidences (234) and the fourfold coincidences (1234) increased by only  $0.18\%$  with such a shift of the absorber  $L$ . This increase ought to have been the same as that for the threefold coincidences. They concluded from these results that at

sea level the number of penetrating ionising particles created by non-ionising agents in cosmic rays is negligibly small, and the positive results reported by previous workers might be due to some spurious phenomena such as side showers, etc.

The facts mentioned above clearly indicate that the results obtained by different workers regarding the creation of mesotrons by non-ionising agents, photons as well as 'neutrettos' in cosmic rays, are not in agreement with each other and no definite proof of the creation of mesons by 'neutrettos' at sea level has yet been obtained by any of the observers. It was therefore thought worth while to repeat the investigation in Calcutta using an anti-coincidence circuit, which is different from that used by Rossi, Janossy, Rochester and Bound. The results obtained in Calcutta, however, do not agree with those obtained by Rossi, Janossy, Rochester and Bound.

#### EXPERIMENTAL TECHNIQUE.

##### (a) *The anti-coincidence circuit.*

With an arrangement used by Rossi, Janossy, Rochester and Bound as is shown in Fig. 7 the number of coincidences (1234) and that of the threefold coincidences (234) recorded simultaneously are almost the same, but when the lead plate placed between 2 and 3 is removed to the position between 1 and 2, the number of threefold coincidences (234) increases. The difference between the threefold coincidences and the fourfold coincidences (234-1234) gives a measure of the non-ionising rays producing the ionising rays in the lead block passing through 2, 3 and 4.

If, however, a circuit is designed in which only threefold coincidences (234) will be recorded while the fourfold coincidences (1234) do not energize the recorder at all, the simultaneous counting of the threefold and fourfold coincidences can be avoided. This will greatly simplify the experimental work and will produce more reliable results. Such a circuit is called the anti-coincidence circuit. Herzog (1940) described a circuit made on this principle. While this work was in progress Rossi and Regener (1940) reported the results of investigations similar to ours in which an anti-coincidence circuit was used. They carried out the investigation at an altitude of 4,300 metres and obtained positive results regarding the creation of mesotrons by neutral particles. In the present investigation an anti-coincidence circuit was designed in which only threefold coincidences (234) and no fourfold coincidences (1234) could energize the recorder.

The diagram of the circuit used in the present investigation is shown in Fig. 8. Just as in the case of Rossi's coincidence circuit the three tubes  $T_2$ ,  $T_3$  and  $T_4$  are connected in parallel and are then connected through a common anode resistance  $R_{12}$  to the positive terminal of the 220 volt supply (D.C.) for the plate voltage. These tubes are kept in a conducting stage, so that there is originally a potential drop across  $R_{12}$ . When a charged particle



passes through the three Geiger Müller counters  $Z_2$ ,  $Z_3$  and  $Z_4$  the potentials at the points  $A_2$ ,  $A_3$  and  $A_4$  decrease momentarily so that negative pulses are transmitted to the grids of the tubes  $T_2$ ,  $T_3$  and  $T_4$ . Thus the tubes come to a non-conducting stage from a conducting one and at once the potential at the point  $B$  increases. A positive pulse is thus sent to the grid of the thyatron  $T_5$ , which is kept in a non-conducting state by a negative bias of 16 volts. This positive pulse drives the grid of the thyatron positive with respect to its cathode, so that the thyatron at once flashes and the mechanical counter (a telephone call counter) inserted in the plate circuit of the thyatron is energized. Thus the threefold coincidence is automatically registered. If, however, a discharge passes through only one or two of the three counters  $Z_2$ ,

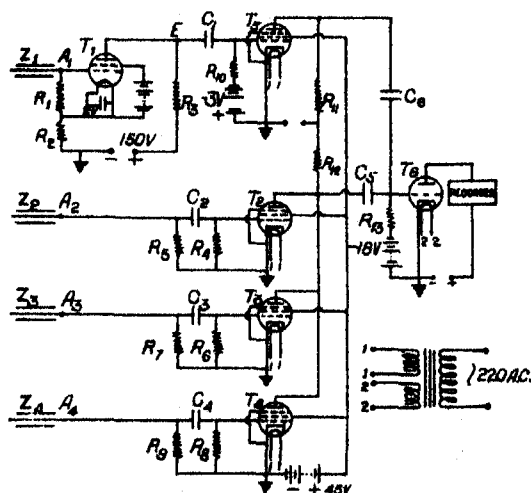


FIG. 8.

$$\begin{aligned}
 C_1 = C_2 = C_3 = C_4 &= 0.001 \mu F, \quad C_5 = C_6 = 0.01 \mu F, \\
 R_2 = R_3 &= 1 M\Omega, \quad R_5 = R_7 = R_9 = R_{11} = 2 M\Omega, \\
 R_{10} = R_4 = R_6 &= R_8 = R_{12} = 25 M\Omega, \\
 R_1 &= 10 M\Omega, \quad R_{13} = 0.4 M\Omega, \quad T_1 = RCA.32, \\
 T_2 = GT_1C, \quad T_3 = T_4 &= T_5 = RCA.57
 \end{aligned}$$

$Z_3$  and  $Z_4$ , the thyatron relay is not actuated, because in this case due to the parallel connection of the three tubes  $T_2$ ,  $T_3$  and  $T_4$  the change in the potential at the plate of  $T_2$  is very small. Hence neither the twofold coincidence nor the independent discharge of any of the three counters is recorded. When, however, a charged particle passes only through the counter  $Z_1$  the grid of the tube  $T_1$  receives a negative pulse. Thus the tube  $T_1$ , originally maintained in a conducting stage, becomes momentarily non-conducting, thereby creating a positive pulse at  $E$  which is transmitted to the grid of  $T_5$ . Since  $T_5$  is originally kept just in a non-conducting state by a negative bias of 3 volts only, the positive pulse brings it to a conducting stage. A negative pulse is thereby impressed on the grid of the thyatron. Thus a discharge in counter  $Z_1$

which sends only a negative pulse to the grid of the thyatron is never recorded in the call counter.

Therefore, when a single charged particle passes through all the four Geiger Müller counters  $Z_1$ ,  $Z_2$ ,  $Z_3$  and  $Z_4$ , two pulses, one negative due to the discharge of  $Z_1$  and the other positive due to the discharge of  $Z_2$ ,  $Z_3$  and  $Z_4$ , are impressed simultaneously on the grid of the thyatron. When the strength of the negative pulse is either equal to or greater than that of the positive pulse the thyatron does not flash and so the fourfold coincidence is never recorded. When, however, an ionising particle passes only through the three counters  $Z_2$ ,  $Z_3$  and  $Z_4$  and not through  $Z_1$  a positive pulse is delivered to the grid of  $T_6$  so that the call counter is energized. Thus it is found that with this circuit, only threefold coincidences  $Z_2Z_3Z_4$  can be recorded. The counter  $Z_1$  will be called the anticounter while  $Z_2$ ,  $Z_3$  and  $Z_4$  will be called coincidence counters. Thus, with an arrangement of counters as shown in Fig. 7 having the topmost counter as anticounter, called  $Z_1$ , and with a lead absorber  $L$  between  $Z_1$  and the next counter  $Z_2$ , the passage of a neutral particle through  $Z_1$ ,  $Z_2$ ,  $Z_3$  and  $Z_4$  will be recorded if it produces an ionising particle in  $L$  which discharges  $Z_2$ ,  $Z_3$  and  $Z_4$ , because the counters  $Z_1$  cannot be discharged by the neutral particle.

To bring the circuit into a working condition careful attention was paid to the fact that the negative pulse delivered to the grid of the thyatron through the capacity  $C_6$  was never smaller than the positive pulse transmitted through  $C_8^*$ . This condition was obtained by using a large value of  $R_1$  ( $\sim 10^7\Omega$ ) and  $R_{11}$  ( $\sim 2 \times 10^6\Omega$ ) and amplifying the negative pulse from the counter  $Z_1$  one stage more than the pulses from the counters  $Z_2$ ,  $Z_3$  and  $Z_4$ . The strength and shape of the pulses were tested with a cathode ray oscillograph. The nature of the pulses on the oscillograph screen also indicated that the negative pulses were of a little longer duration than the positive ones. This ensured the neutralization of the positive pulse even when a very small time-lag between the positive and the negative pulses might exist owing to a little difference in the characteristics of the two circuits producing these two pulses.

In the actual construction of the circuit arrangements are also made so that either only threefold coincidence, twofold coincidence or single countings can be recorded whenever desired. The circuit is also completely shielded from external radiations.

#### (b) Counters used.

The counters used are of the self-quenching type and were prepared in this laboratory. The outer electrodes, cylindrical in shape, are of thin copper sheet oxidised to black oxide of copper. The central wire is of tungsten of diameter .02 cm. The envelope is made of pyrex glass tubes. The copper-oxide electrode has a length of 15 cm. and an internal diameter of 3.5 cm.

\* The authors' thanks are due to Dr. R. L. Sen Gupta for pointing out the necessity of this condition being satisfied for getting anti-coincidence.

The gas mixture used consists of argon and petroleum ether in the ratio of 2 : 1 with a total pressure of 5.4 cm. of Hg.\*

The first voltage stabiliser circuit of Neher and Pickering was used to get a source of steady high voltage necessary for the counters.

The counters used start at very nearly the same potential of about 1,150 volts and have a plateau of about 300 volts between 1,200 volts and 1,500 volts. They were operated at 1,250 volts during the experiments.

The efficiency of the counters has been measured according to the methods of Street and Woodward (1934) by measuring the triple coincidences of three counters placed in a vertical plane and then measuring the double coincidences, with the middle counter removed and the two end-counters kept in the same position. Triple accidental coincidences as also the double accidental coincidences of the two end-counters have also been determined. The efficiency of the middle counter is given by the ratio of the real triple coincidence counts to that of the real double coincidence counts.

The efficiency of all the four counters used together was found to be above about 99.5%.

The time constant of the twofold coincidence circuit comprising the tubes  $T_2$ ,  $T_3$ ,  $T_6$  and the counters  $Z_2$  and  $Z_3$  was determined from the rate of double accidental coincidences, and the single countings of the two Geiger Müller counters. The number of double accidental coincidences per second is  $A_{32} = 2N_3N_2\tau$  (Johnson and Street, 1933) where  $N_3$  and  $N_2$  are the single countings of the counters per second and  $\tau$  is the time constant of the circuit in seconds. The experimental value of  $\tau$  was  $4.97 \times 10^{-5}$  sec.

The efficiency of the anti-coincidence circuit is determined with an arrangement of counters as shown in Fig. 9.  $Z_1$  is the anti-counter. All the rays

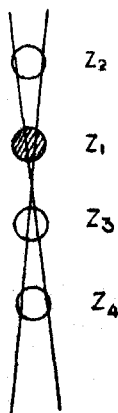


FIG. 9.

\* The counters were prepared according to the instruction kindly given by Drs. Neher and Pickering who visited this laboratory during their recent tour in India with Prof. Millikan.

passing through  $Z_2$ ,  $Z_3$  and  $Z_4$  must also pass through  $Z_1$ , so that whenever a charged particle passes through  $Z_2$ ,  $Z_3$  and  $Z_4$  a positive and a negative pulse are simultaneously impressed on the grid of the thyatron so that the thyatron relay is not actuated. Thus no fourfold coincidence should be registered with this arrangement of the counters.

Therefore if  $n_1$  be the number of the triple coincidence per unit time for the counter telescope  $Z_2Z_3Z_4$  without the anti-counter  $Z_1$  and  $n_2$  the number of fourfold coincidences per unit time with the anti-counter  $Z_1$  placed between  $Z_2$  and  $Z_3$ , the efficiency of the circuit is given by the ratio  $(n_1 - n_2)/n_1$ .

Hence with the arrangement of the counters as shown in the Fig. 10,  $n_1$  and  $n_2$  were determined without using any absorber between the counters and from these values of  $n_1$  and  $n_2$  the efficiency of the anti-coincidence circuit was determined, and was found to be 99.33%.

As already mentioned, Herzog (1940) as also Rossi, Janossy, Rochester and Bound (1940) have published two different anti-coincidence circuits. Herzog's circuit is very much similar to ours and the efficiency of his circuit is stated to be more than 98%. Rossi and others claim a cent per cent efficiency of their circuit. Their circuit is however very complicated. The anti-coincidence circuit used in the present investigation is very simple and yet quite efficient.

#### EXPERIMENTAL ARRANGEMENT AND RESULTS.

The arrangement shown diagrammatically in figure 10 was used for investigating the non-ionising component of the cosmic rays capable of producing ionising penetrating particles while passing through an absorber of lead. The

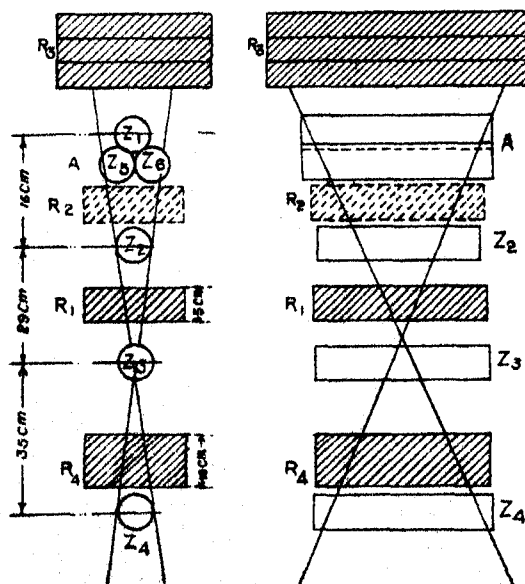


FIG. 10.

counter battery  $A$  consists of three counters  $Z_1, Z_3, Z_6$  connected in parallel and forms the anti-counter which when discharged imparts a negative pulse to the grid of the thyratron. The total width of the counter battery  $A$  just covers the angle subtended by the diameter of  $Z_2$  at  $Z_3$ .  $R_4$  is a lead block 10 cm. thick placed permanently between  $Z_3$  and  $Z_4$ . A lead block 5 cm. thick is first placed at  $R_1$  between  $Z_2$  and  $Z_3$  and is next shifted to  $R_2$  between  $A$  and  $Z_2$ .  $R_3$  is a lead block the thickness of which has been varied from 0 to 25 cm. in order to investigate the absorption of the incident non-ionising component which produces ionising penetrating particles in  $R_2$ . With the arrangement used in the present investigation the resultant pulse due to the passage of a charged particle through all the four counters,  $A, Z_2, Z_3, Z_4$ , does not energize the thyratron and hence the recording instrument (a telephone call counter), but the positive pulse due to the coincidence of  $Z_2, Z_3$  and  $Z_4$  not accompanied by the discharge of the counter  $A$  are recorded. These later coincidences will be called the anti-coincidences  $Z_2Z_3Z_4-A$ . The experiment was carried out in a one storied building having a light roof. The counters and the absorbers were placed in the respective positions on an iron frame. The results obtained with various disposition of the absorbers are given in Table I. Standard statistical errors are also included in these results.

TABLE I.

Disposition of absorbers.	Total time of experiment in hours.	Total number of counts ( $Z_2Z_3Z_4-A$ )	Counts ( $Z_2Z_3Z_4-A$ ) per hour.
$R_1 = 5$ cm.; $R_2 = R_3 = 0$ cm. . .	40.42	85	$2.10 \pm 0.228$
$R_1 = 5$ cm.; $R_2 = 0$ cm.; $R_3 = 2.5$ cm. . .	43	91	$2.116 \pm 0.222$
$R_1 = 5$ cm.; $R_2 = 0$ cm.; $R_3 = 5$ cm. . .	34	73	$2.147 \pm 0.251$
$R_1 = 0$ cm.; $R_2 = 5$ cm.; $R_3 = 0$ cm. . .	97	352	$3.63 \pm 0.194$
$R_1 = 0$ cm.; $R_2 = 5$ cm.; $R_3 = 2.5$ cm. . .	104	343	$3.298 \pm 0.178$
$R_1 = 0$ cm.; $R_2 = 5$ cm.; $R_3 = 5$ cm. . .	101	310	$3.069 \pm 0.174$
$R_1 = 0$ cm.; $R_2 = 5$ cm.; $R_3 = 10$ cm. . .	105	294	$2.80 \pm 0.163$
$R_1 = 0$ cm.; $R_2 = 5$ cm.; $R_3 = 15$ cm. . .	75	209	$2.786 \pm 0.193$
$R_1 = 0$ cm.; $R_2 = 5$ cm.; $R_3 = 25$ cm. . .	96	267	$2.781 \pm 0.170$

## DISCUSSION OF RESULTS.

The results in Table I show that the number of anti-coincidences, i.e. the number of events in which the three counters  $Z_2, Z_3, Z_4$  are discharged simultaneously while the counter system  $A$  remains unaffected, increases from  $2.1 \pm 0.228$  to  $3.63 \pm 0.194$  per hour on shifting the lead absorber, 5 cm. thick, from  $R_1$  to  $R_2$ . This may be interpreted in two ways: (1) a non-ionising component

of cosmic rays creates, while traversing  $R_2$ , a charged particle which passes through the counters  $Z_2$ ,  $Z_3$  and  $Z_4$  and can thus penetrate 10 cm. of Pb and (2) side showers discharge  $Z_2$ ,  $Z_3$  and  $Z_4$  without striking the counter system  $A$  and the number of such incidents increases on shifting the absorber from  $R_1$  to  $R_2$ . Let us first consider the possibility (2). From the results of their investigation Rossi, Janossy, Rochester and Bound (1940) came to the conclusion that the side showers were responsible in their arrangement for the increase by about 1.4% of the threefold coincidences  $Z_2Z_3Z_4$  when the absorber was shifted from  $R_1$  to  $R_2$ . They recorded the fourfold  $Z_1Z_2Z_3Z_4$  and threefold  $Z_2Z_3Z_4$  coincidences simultaneously and thus found out the number of threefold coincidences not accompanied by the fourfold coincidence. These events (called anti-coincidences by them), however, were found to increase only by about .18% of the threefold coincidences. If charged penetrating particles produced by the non-ionising component in the absorber at  $R_2$  were responsible for the increase in the threefold coincidences  $Z_2Z_3Z_4$ , the number of anti-coincidences should have increased by the same amount. Since the number of anti-coincidence was observed not to increase by more than 0.18% the major portion of the increase in the number of threefold coincidences was ascribed to side showers. The presence of side showers was further demonstrated by placing a Wilson chamber between  $Z_2$  and  $Z_3$  and photographing such showers, but removing the absorber  $R_4$  so that even electrons and positrons of the side showers could discharge the two counters below the chamber.

In the present investigation, the presence of side showers was investigated by displacing the counters in the horizontal directions at right angles to their lengths, so that they did not form a counter telescope. The side showers in this case also had an equal chance of causing the threefold coincidence without discharging  $Z_1$  as in the case of the counter telescope. The results given in Table II, however, show that the observed number of side showers being only  $0.37 \pm .019$  per hour when 5 cm. of Pb is placed at  $R_2$  and  $0.17 \pm .01$  per hour when the absorber  $R_2$  is absent, the increase in the number of anti-coincidences with the shift of absorber from  $R_1$  to  $R_2$  cannot be accounted for by the side showers. Also the increase is much greater than the standard statistical error. Hence the results lead to the conclusions that the observed increase in the number of anti-coincidences with the shift of the absorber is due to the non-ionising component of the cosmic rays which produces charged particles in the absorber at  $R_2$ .

TABLE II.

	No. of hours.	No. of anti-coincidences $Z_2Z_3Z_4-A$ due to side showers.	No. of $Z_2Z_3Z_4-A$ per hour.
$R_2 = 5$ cms. . . . .	30	11	$0.37 \pm .019$
$R_2 = 0$ . . . . .	41.5	7	$0.17 \pm .01$

It was observed that with the same arrangement of the counters  $Z_1$ ,  $Z_3$ ,  $Z_4$  as described above but with the circuit of the counter  $A$  disconnected from the grid of the thyratron the number of triple coincidences with  $R_3$  in the position shown was  $24.41 \pm 3.1$  per hour. Hence the neutral component being 1.3 per hour was about 5.4% of the total penetrating ionising component of the cosmic rays. This is much higher than that reported by Rossi, Janossy, Rochester and Bound who observed the neutral component to be only 0.18% of the total penetrating component. In the present investigation, the background with no absorber at  $R_2$  is 2.1 counts per hour which is very large. As explained above, this background was not due to side showers but was due to the length of counter  $Z_2$  being much larger than what would remain entirely within the solid angle subtended by the anti-counter at the counter  $Z_3$ . This stray effect was, however, constantly present for all the thicknesses of the absorber  $R_3$  and hence it can be presumed that it remained constant when the absorber was put at  $R_2$  and consequently there is a genuine increase in the anti-coincidence with the shift of the absorber from  $R_1$  to  $R_2$ . Further, the increase was much less when a Pb absorber of thickness 10 cm. was placed at  $R_3$ . Further increase in the thickness of  $R_3$  does not appreciably affect the number of anti-coincidences observed with the absorber in  $R_2$ . This fact shows definitely that there is a non-ionising component capable of producing ionising penetrating particles in  $R_2$  and that part of this non-ionising component is completely absorbed by 10 cm of lead and the remaining part is not absorbed by 25 cm. of lead. The former part is probably the photon component and the latter part may consist of neutrettos. If this interpretation is assumed to be correct then the percentage of these neutral particles producing mesotrons at sea level is only about 2.1% of the total number of mesons. Rossi and Regener observed that at an altitude of 4,300 metres these neutrettos which produce mesotrons are less than one per cent of the total mesotron intensity.

The results of the present investigation are apparently contradictory to those of Rossi, Janossy, Rochester and Bound (1940). The circuit used by the latter authors, however, was not actually an anti-coincidence circuit and the side showers might be responsible for increase in the number of fourfold coincidences with the shift of the absorber from  $s_1$  to  $s_2$  and in that case the difference between the fourfold and threefold coincidences recorded by them would be diminished. The results reported by them actually indicate that the number of fourfold coincidences ( $ABCD$ ) increased with the shift of the absorber from  $s_1$  to  $s_2$ , because while the number of threefold coincidences increased by 1.6%, the difference between the numbers of threefold and fourfold coincidences increased only by .18%. Such spurious fourfold coincidences would not affect the total number of anti-coincidences recorded with the circuit used in the present investigation. Probably this explains the discrepancy between the results of the present investigation and those of Rossi, Janossy, Rochester and Bound.

In conclusion the authors take this opportunity of expressing their gratitude to Prof. M. N. Saha, F.R.S., for his kind interest and guidance during the progress of the work.

#### SUMMARY.

The production of mesons by non-ionising agents in cosmic rays has been investigated using an anti-coincidence circuit consisting of four horizontal counter systems placed one below the other to form a vertical counter telescope. The topmost system formed the anti-counter imparting, on passage of a charged particle through it, a negative pulse to the grid of the thyatron of the recording circuit, while the lower three systems formed a threefold coincidence circuit imparting a positive pulse to the said grid. It has been observed that with a lead absorber 10 cm. thick between the bottom and the third counter and on shifting a lead absorber 2 cm. thick from its position between the second and the third counter to a position between the topmost counter and the second, the number of anti-coincidences increased by 5% of the total vertical intensity of the mesons. On placing an absorber of lead 10 cm. thick on the top of the anti-counter, this increase was only 2% of the said mesotron intensity. It is concluded that the latter increase might be due to production of mesons by neutrettos in the lead absorber between the first and the second counter while the total increase of 5% might be that due to both photons and neutrettos.

#### REFERENCES.

- Arley, N. and Heitler, W. 1938. Neutral particles in cosmic radiation. *Nature*, **142**, 158.  
 Heitler, W. 1937. On the analysis of cosmic rays. *Proc. Roy. Soc.*, **161A**, 261.  
 Heitler, W. 1938. Shower produced by the penetrating, etc. *Proc. Roy. Soc.*, **166A**, 529.  
 Herzog, G. 1940. Cloud chamber photographs, etc. *Phys. Rev.*, **57**, 337.  
 Herzog, G. Circuit for anti-coincidences, etc. *Rev. Sc. Inst.*, **11**, 84.  
 Hsiung, D. S. 1934. A coincidence test of the corpuscular hypothesis, etc. *Phys. Rev.*, **46**, 653.  
 Johnson, T. H. and Street, J. C. 1933. Circuit for recording, etc. *Jour. Franklin Institute*, **215**, 239.  
 Lovell, A. C. B. 1939. Shower production by penetrating, etc. *Proc. Roy. Soc.*, **172A**, 568.  
 Maass, H. 1936. Über eine harte Sekundär strahlung. *Ann. der. Phys.*, **27**, 507.  
 Rossi, B. 1931. Über den Ursprung, etc. *Z.f. Phys.*, **68**, 64.  
 Rossi, B., Janossy, L., Rochester, G. and Bound, M. 1940. On the production of secondary ionising, etc. *Phys. Rev.*, **58**, 761.  
 Rossi, B. and Regener, V. 1940. Production of mesotrons, etc. *Phys. Rev.*, **58**, 837.  
 Schein, M., Jesse, W. P. and Wollan, E. O. 1940. Intensity and rate of production, etc. *Phys. Rev.*, **57**, 847.  
 Schein, M. and Wilson, V. C. 1939. Evidence for the production, etc. *Phys. Rev.*, **54**, 304.  
 Shonka, F. R. 1939. New evidence for existence of, etc. *Phys. Rev.*, **55**, 24.  
 Street, J. C. and Woodward, R. H. 1934. Counter-calibration, etc. *Phys. Rev.*, **46**, 1029.





# DEVELOPMENT OF SEED AND ITS NUTRITIONAL MECHANISM IN SCROPHULARIACEAE.

## PART I.

*Rhamphicarpa longiflora* Benth., *Centranthera hispida* Br., and *Pedicularis zeylanica* Benth.

By C. V. KRISHNA IYENGAR, *Department of Botany, University of Mysore, Mysore.*

(Communicated by Dr. P. Maheshwari, D.Sc., F.A.Sc., F.N.A.Sc., F.N.I.)

(Received January 19, 1942.)

The author has already studied the development of the embryo-sac and endosperm haustoria in several members of Scrophulariaceae (Krishna Iyengar, 1937, 1939a-c, 1940a-c, 1941, and 1942a-b) of which two are parasitic. This paper deals with three additional parasitic members of the family.

Several parasitic genera have been studied by various investigators from time to time. Balicka Iwanowska's (1899) is an early contribution of great significance in this line. Schmid's (1906) work happens to be of an outstanding nature, and this includes several parasites like *Euphrasia*, *Lathraea*, *Melampyrum*, *Pedicularis*, *Alectorolophus* and *Tozzia*. Michell (1915) describes the formation of the chalazal haustorium and basal cell haustorium in *Striga lutea*, and Glišić (1932) has given a very thorough account of *Lathraea squamaria*. A point of special interest in his paper is the sequence of the early divisions during endosperm formation. While Schmid (1906) mentions that the second division is usually transverse, Glišić contends that this is often longitudinal. A more recent paper by Glišić (1936-37) deals with the various types of endosperm in Scrophulariaceae with a view to trace their relationships and evolutionary tendencies.

## MATERIALS AND METHODS.

*Centranthera* was collected from the marshes and neglected paddy fields, and *Rhamphicarpa* from the grassy slopes round about Agumbe. *Pedicularis* was collected from Doddabetta near Ootacamund. The first two materials were fixed in chromo-acetic acid solution with some osmic acid and the last in Bouin's fluid. Sections were cut between 7 and 12 microns according to the required stages and stained in Heidenhain's iron-alum haematoxylin.

## OVULE.

The ovules are anatropous in *Rhamphicarpa* and *Centranthera* but campylotropous in *Pedicularis* and arranged on the thick placenta, which in *Rham-*

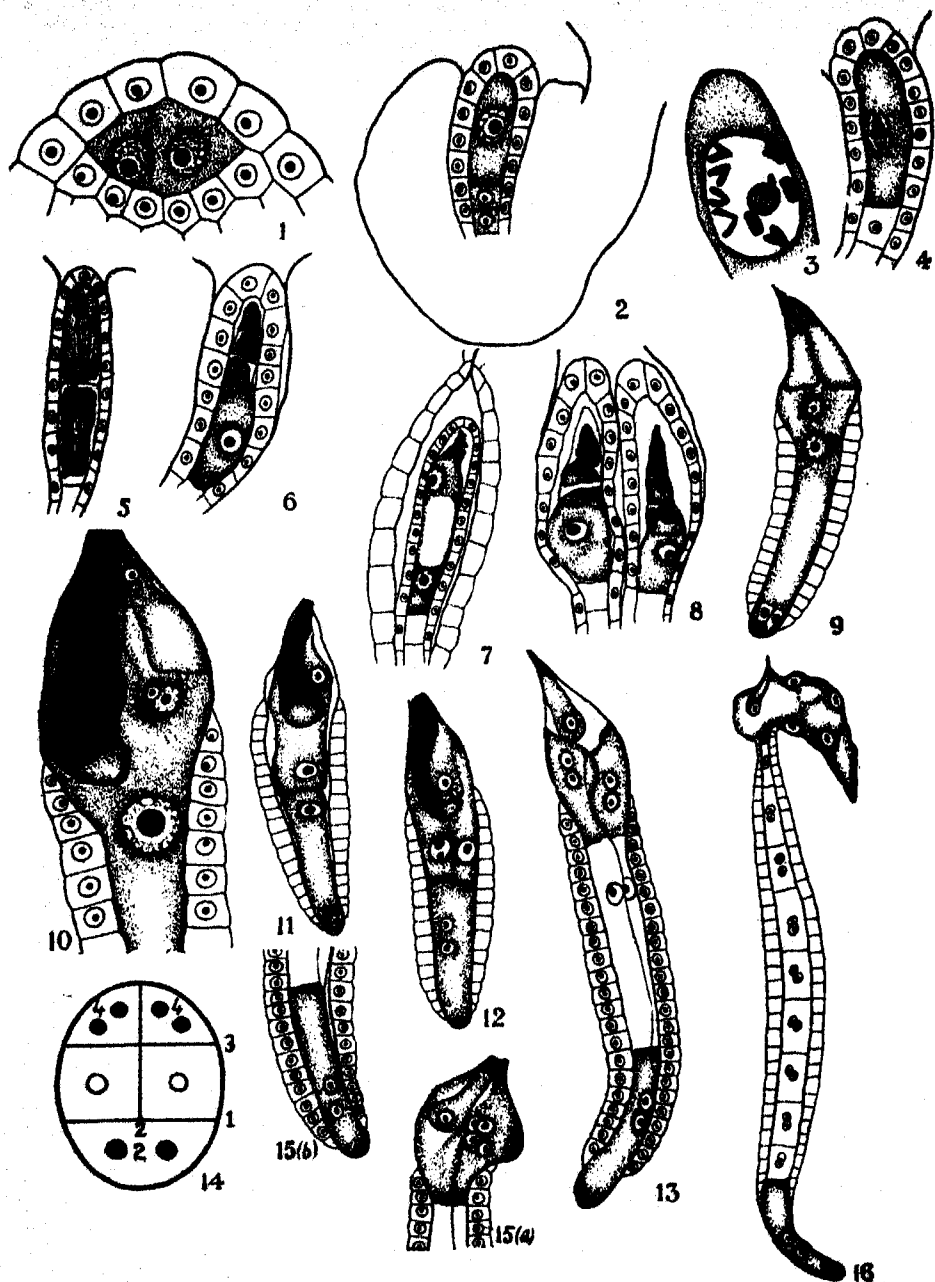
*phicarpa* shows a loose structure with large air spaces. The ovule is composed of a reduced nucellus and a single thick integument characteristic of the family in general. The integument comprises three regions, the two epidermal layers with a thick tissue in the middle having stored food materials. Oil globules are abundantly deposited in the outer epidermal layer when the embryo-sac is mature. The inner epidermis develops into the tapetum which lines the developing megaspore mother cell and the megaspores. The nucellus is generally composed of a large archesporial cell and a single layer of jacket cells.

*Rhamphicarpa longiflora* Benth.

**Embryo-sac.**—The large hypodermal archesporial cell directly becomes the megaspore mother cell and begins to enlarge significantly. At times two archesporial cells have also been noticed, although the formation of two tetrads in the same nucellus was not observed. In one or two instances the ovule was binucellate and showed two tetrads as in Fig. 8. A few stages in the formation of the tetrad have been noticed. Nine bivalents were noticed at the diakinesis stage (Fig. 3). The second division takes place simultaneously in both the dyad cells (Fig. 5) resulting in a linear tetrad of megaspores. The outer three megaspores invariably degenerate while the innermost functions and gives rise to a normal eight nucleate embryo-sac (Fig. 9). Starch grains are present. The dilated micropylar part of the embryo-sac shows the egg-apparatus composed of two large tapering synergids having a small nucleus and a large vacuole. The egg, which is deeply placed, lies in the neighbourhood of the secondary nucleus, and a large vacuole makes its appearance between the antipodals and the secondary nucleus. During this period the cells of the nucellar jacket lose their contents and show a significant reduction in size. The integumentary tapetum which at first surrounded the entire nucellus is now confined only to the non-dilated part of the embryo-sac.

**Fertilization.**—The pollen tube enlarges very much in the embryo-sac and destroys one of the synergids. Of the two sperm nuclei discharged into the sac one approaches the egg and the other the secondary nucleus. Actual fusion was not seen but may be inferred from the position of the male gametes seen in Fig. 10. The antipodal cells degenerate shortly after fertilization.

**Endosperm.**—The first division of the primary endosperm nucleus is followed by a transverse wall resulting in the separation of a chalazal chamber from an outer one (Fig. 11). The second division, which is longitudinal, takes place only in the micropylar chamber (Fig. 12). In the chalazal chamber there is only a nuclear division resulting in a binucleate haustorial body. The third division, which is transverse, separates the two micropylar haustorial cells from the two middle cells (Fig. 13). A series of longitudinal and transverse divisions takes place in the latter resulting in a well-developed endosperm tissue. This is composed of smaller cells towards the two ends and larger cells in the middle, the latter with a rich deposition of starch in them. The



*Rhamphicarpa longiflora* Benth.

FIG. 1. Archesporial cell.  $\times 1095$ . FIG. 2. Megaspore mother cell and integument.  $\times 480$ . FIG. 3. Diakinesis in the megaspore mother cell.  $\times 1460$ . FIG. 4. Formation of the two dyads.  $\times 640$ . FIG. 5. Division of the dyads.  $\times 640$ . FIG. 6. A linear tetrad of megaspores.  $\times 640$ . FIG. 7. Two nucleate stage of the embryo-sac.  $\times 640$ . FIG. 8. Binucleate ovule with two tetrads.  $\times 640$ . FIG. 9. Mature embryo-sac.  $\times 320$ . FIG. 10. A stage in fertilization.  $\times 640$ . FIG. 11. First division of the primary endosperm nucleus.  $\times 320$ . FIG. 12. Second division of the same.  $\times 320$ . FIG. 13. Differentiation of the haustorial and endosperm cells.  $\times 320$ . FIG. 14. Diagram showing early divisions in the primary endosperm nucleus. FIG. 15. Formation of (a) tetra-nucleate micropylar and (b) binucleate chalazal haustoria.  $\times 320$ . FIG. 16. Formation of tetra-nucleate micropylar and a binucleate chalazal haustoria—slightly older stage.  $\times 160$ .

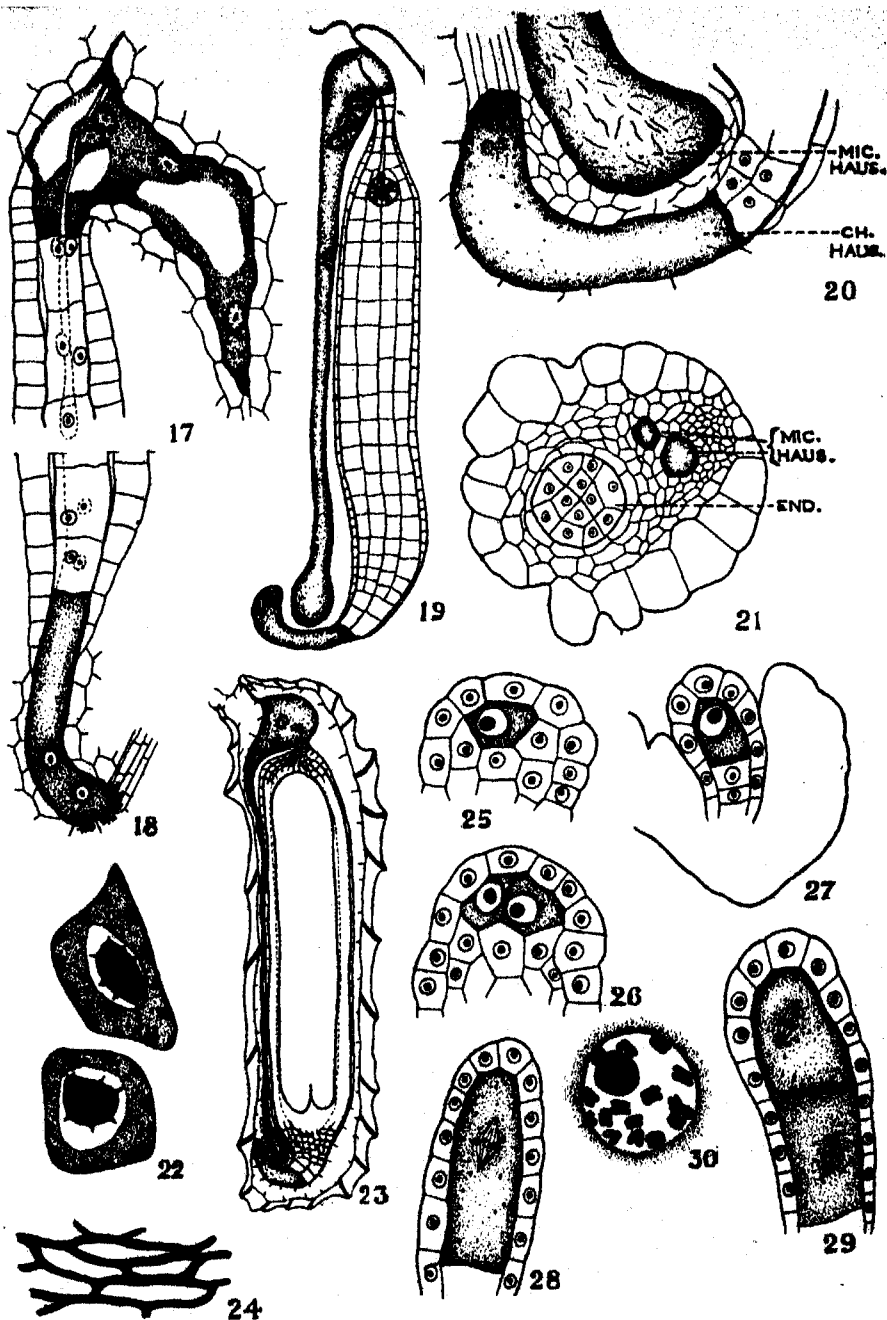


FIG. 17. Micropylar haustorium.  $\times 320$ . FIG. 18. Chalazal haustorium.  $\times 320$ . FIG. 19. Long. section of a young seed showing the various parts.  $\times 975$ . FIG. 20. Chalazal and micropylar (part) haustoria enlarged.  $\times 320$ . FIG. 21. Transverse section of a young seed to show the branches of micropylar haustorium, endosperm and other parts.  $\times 160$ . FIG. 22. Hypertrophied nuclei of micropylar haustorium.  $\times 730$ . FIG. 23. Long. section of an almost mature seed.  $\times 65$ . FIG. 24. Tangential section of epidermis.  $\times 65$ .

*Centranthera hispida* Br.

FIG. 25. Formation of the ovule.  $\times 640$ . FIG. 26. Ovule with two archesporial cells.  $\times 640$ . FIG. 27. Enlarging archesporial cell and integument.  $\times 640$ . FIG. 28. First division of the megaspore mother cell.  $\times 1095$ . FIG. 29. Second division of the megaspore mother cell.  $\times 1095$ . FIG. 30. Diakinesis in the microspore mother cell.  $\times 1095$ .

smaller cells have dense protoplasmic contents and are probably concerned with the transportation of nutritive material from the haustoria to the more deeply placed endosperm tissue. This peculiar function of the terminal endosperm cells seems to be a common feature in several members of Scrophulariaceae.

*Embryo*.—The fertilized egg remains as a short tubular structure for a long time. Its further development takes place only after the organisation of a rich endosperm tissue. At this stage the pro-embryo elongates considerably and makes its way through the tiers of endosperm cells. The stages observed indicate that its development is of the *Capsella*-type.

*Development of Haustoria*.—The chalazal haustorium is the first to be organised. As already reported there is only a nuclear division here resulting in a single binucleate organ (Fig. 18). This begins to elongate into a tubular body, and eats its way into the vascular traces of the integument. The terminal part is slightly bent and enlarged with the two nuclei migrating into it. The cells in its neighbourhood show all stages of disintegration, demonstrating the aggressive nature of the haustorium (as in Fig. 20). This haustorium is the first to commence its activity and also the first to degenerate.

The two micropylar cells become binucleate (Fig. 13) and fuse at a very early stage by the dissolution of their separating wall. This haustorial body is tetra-nucleate and grows towards the chalaza, along the vascular traces of the hilum, digesting and disorganising the tissue coming against it and finally finding its way into the bend formed by the chalazal haustorium and enlarging distally (Figs. 19 and 20). The micropylar haustorium is thus a highly aggressive tubular body. One or two nuclei are seen in this tube. At times the two haustoria (micropylar and chalazal) are so close and the disorganisation so thorough that they almost communicate with each other—a remarkable feature of this plant. It is also noticed that at times two haustorial tubes develop instead of one (Fig. 21). A similar situation is met with in *Melampyrum*. The micropylar haustorium is several times the size of the chalazal and its nuclei are also much larger.

Older micropylar haustoria show amoeboid and hypertrophied nuclei as represented in Fig. 22. A few outgrowths are seen all round the nucleolus. The contents of the haustorium are denser and stain deeply. Cellulose network is also present, a portion of which lying in the terminal part of the haustorium is represented in Fig. 20.

*Integument and seed coat*.—The tapetal wall remains unaltered for a long time, except for a thickening of the cuticle inside. While the endosperm and embryo are maturing the tapetal layer gets more and more reduced in size until at last it is almost obliterated. The middle layer of the integumentary tissue is also absorbed by the haustorial activity and at the mature embryo stage very little of it is left intact. The epidermis of the testa becomes thick walled (Figs. 23 and 24) and assumes a protective rôle.

*Centranthera hispida* Br.

A study of the pollen development was undertaken to count the chromosomes. The diakinesis stage shows 16 bivalents (Fig. 30).

*Development of Embryo-sac.*—A large hypodermal archesporial cell directly becomes the megaspore mother cell. Occasionally two such cells are noticed (Fig. 26). The formation of a linear tetrad, the invariable degeneration of three megaspores and the development of the innermost megaspore into a normal eight nucleate embryo-sac take place as usual. The synergids are large and the egg is deeply placed. The two polar nuclei fuse at an early stage giving rise to the large secondary nucleus (Fig. 32). The antipodal cells are small and confined to the tapering chalazal end. While the embryo-sac is developing, the nucellar jacket cells lose their contents and disappear so that the embryo-sac comes in contact with the tapetum. The tapetal cells which line the non-dilated part of the sac are large and rich in protoplasmic contents.

*Fertilization.*—Pollen tubes have been observed in the embryo-sac and the destruction of one of the synergids was also noticed. The antipodals persist for some time after fertilization, but degenerate and disappear during early stages in endosperm formation.

*Endosperm formation and embryo.*—The sequence of early divisions of the primary endosperm nucleus leading to the differentiation of the endosperm cells and haustoria (Figs. 33–35) and the formation of endosperm tissue and embryo are identical with those in *Rhamphicarpa*.

*Endosperm Haustoria.*—The binucleate chalazal cell is the first haustorium to be organised. This does not develop appreciably but remains small even in late stages of seed formation. Its poor cell-contents, reduced nuclei and non-aggressive nature even during older stages indicate that the cells have only a minor haustorial action.

The two micropylar cells show only nuclear division and become binucleate. An early dissolution of the separating wall between the two cells results in a tetra-nucleate body, but this also is only weakly haustorial (Fig. 40).

Some of the endosperm cells which are smaller become active at a very early stage and develop lateral haustorial tubes which eat their way into the tapetum (Fig. 38) and begin to digest the integumentary tissue (Fig. 37). These tubes are simple, unbranched, uninucleate and highly aggressive, ending just below the epidermis. Their growth seems to be lateral and then towards the chalaza. Even in the most advanced stages of seed formation a little tissue with poor cell-contents is persistent in the neighbourhood of the micropylar haustoria (Fig. 43). The term 'Secondary Haustoria' (Author, 1939c. was previously applied to such cells, but it seems that 'Lateral Haustoria' is more expressive. At times the ends of the haustoria coalesce as represented in Fig. 39, although these vermiform structures take a parallel course and present a rose\*te-like appearance in the fully formed seed. It is also noticed that all

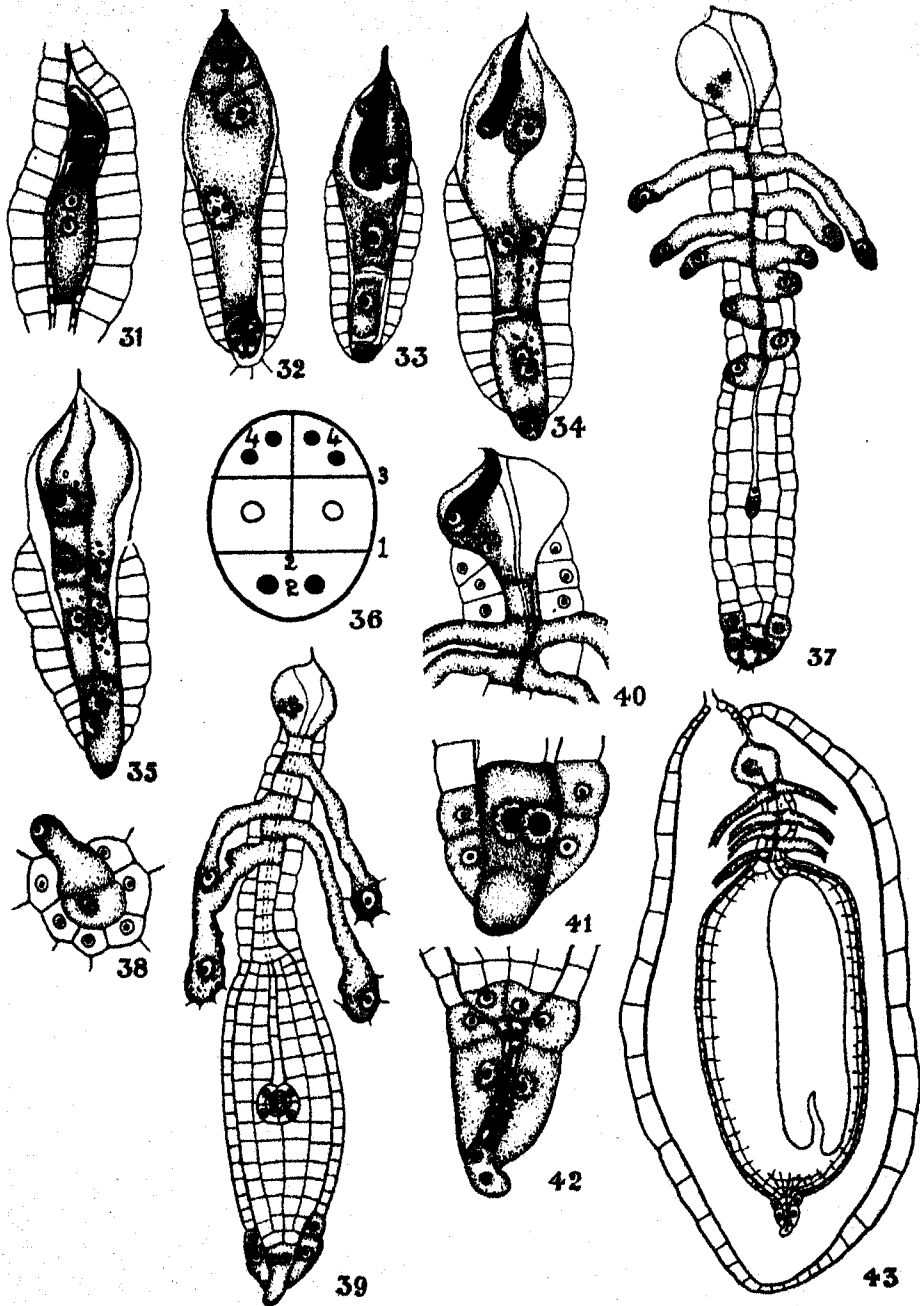
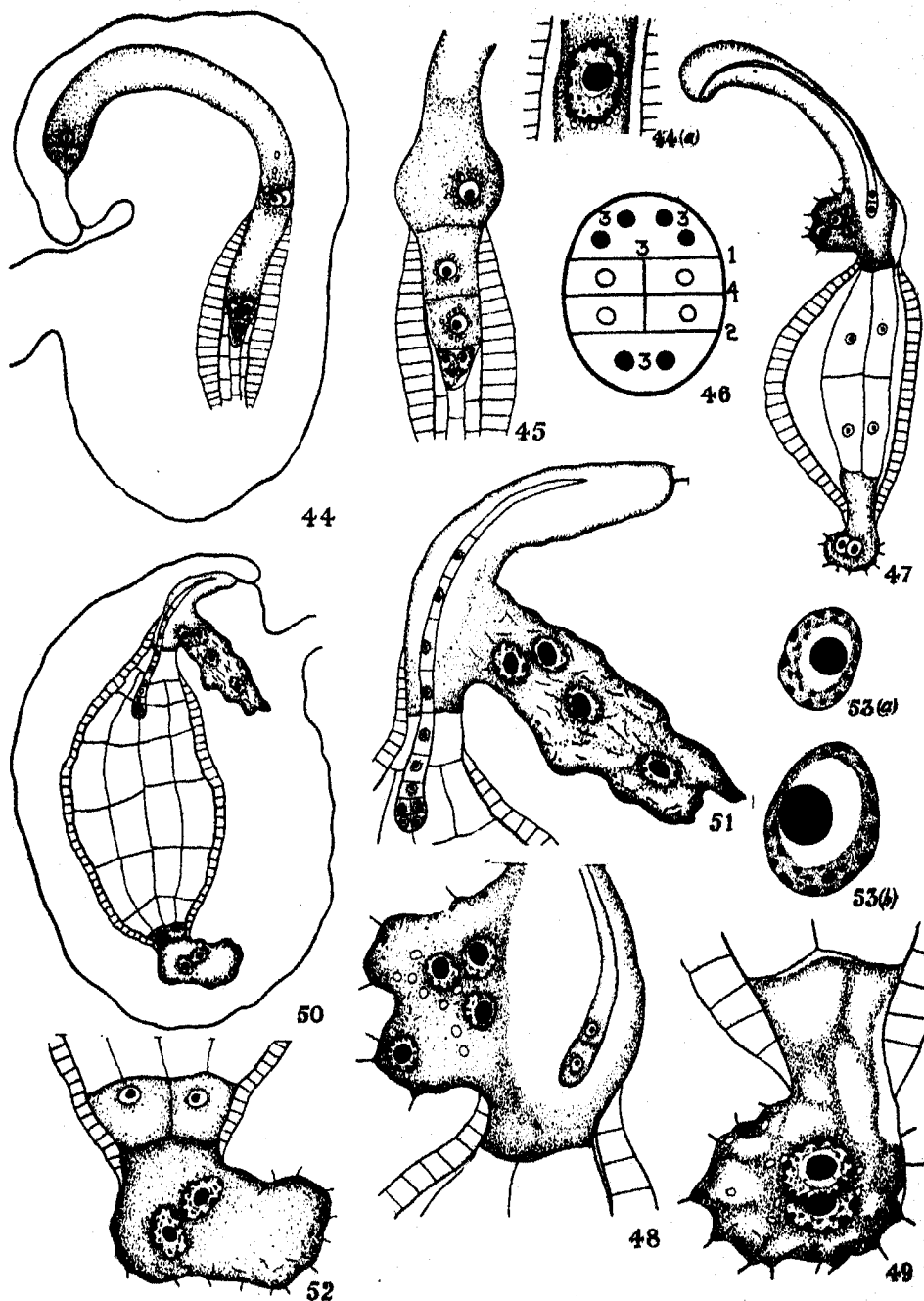


FIG. 31. Linear tetrad of megaspores.  $\times 640$ . FIG. 32. Mature embryo-sac.  $\times 480$ . FIG. 33. First division of the primary endosperm nucleus.  $\times 320$ . FIG. 34. Second division of the primary endosperm nucleus.  $\times 480$ . FIG. 35. Differentiation of the haustoria and endosperm.  $\times 480$ . FIG. 36. Diagram to show the sequence of divisions in the primary endosperm nucleus. FIG. 37. Long. section of young seed showing the endosperm and haustoria.  $\times 320$ . FIG. 38. Formation of secondary haustoria.  $\times 320$ . FIG. 39. Slightly older stage of Fig. 37.  $\times 160$ . FIG. 40. Almost non-functional micropylar haustorium.  $\times 365$ . FIG. 41. Non-functional chalazal haustorium.  $\times 730$ . FIG. 42. Degenerating chalazal haustorium and enlarged tapetal cell.  $\times 320$ . FIG. 43. Long. section of an almost mature seed.  $\times 97.5$ .





*Pedicularis zeylanica* Benth.

FIG. 44. Embryo-sac.  $\times 160$ . FIG. 44a. Primary endosperm nucleus.  $\times 320$ . FIG. 45. First and second divisions of the primary endosperm nucleus.  $\times 160$ . FIG. 46. Diagrammatic representation of the primary endosperm nucleus and its early divisions. FIG. 47. Long section showing the various parts.  $\times 97.5$ . FIG. 48. Micropylar haustorium.  $\times 320$ . FIG. 49. Chalazal haustorium.  $\times 320$ . FIG. 50. Long section of a young seed.  $\times 65$ . FIG. 51. Micropylar haustorium enlarged.  $\times 160$ . FIG. 52. Chalazal haustorium enlarged.  $\times 160$ . FIG. 53. Nuclei of micropylar (a) and chalazal (b) haustoria.  $\times 640$ .

these haustoria do not traverse the entire length of the ovule. Thus the chalazal part of the ovule is never attacked by the haustoria. Older haustoria show hypertrophied amoeboid nuclei with rich chromatin material.

*Tapetum*.—While the endosperm is developing the tapetum shows some differentiation in its size and structure. The cells in the vicinity of the prospective secondary endosperm haustoria become larger than those lining the endosperm tissue and also show richer contents (Fig. 37). The largest cells are however seen near the non-functional chalazal haustorium. These are six in number, broader towards the endosperm tissue and tapering towards the chalaza. They assume an enormous size—at times each of them becomes as large as the chalazal haustorium, and their nuclei are larger than those of the chalazal haustorium (Fig. 42). By their proximity to the richly staining chalazal tissue and by their rich contents, thin cell-wall and other features, it is reasonable to infer a probable haustorial function of these cells. It is thus a rare instance of a parasite where the tapetum shows such a high organisation and differentiation in its structure and functions. Thus the tapetum not only acts as a repository for food material but also assumes a digestive and absorptive as well as a partially protective rôle.

*Seed Coat*.—During the formation of the seed coat most of the integumentary tissue is digested and absorbed and the protective function is performed mostly by the thick-walled outer epidermis of the integument and partly by the thick cuticle of the tapetum.

#### *Pedicularis zeylanica* Benth.

*Embryo-sac*.—As in the preceding species, the nucellus is extremely reduced and the embryo-sac is of the normal eight-nucleate type (Fig. 44). The enlarged micropylar part of the sac is very much elongated and the chalazal is short and narrow. The integumentary tapetum, which is composed of large cells, lines only the narrow chalazal part, the persistent nucellar sheath being interposed between. Starch grains are abundantly deposited not only in the integument but also in the embryo-sac. Three small antipodal cells are present at the chalazal end of the sac, and the nucellar tissue in this region is rich in protoplasm. The two polar nuclei fuse to form the secondary nucleus. The egg-apparatus which is composed of two small synergids and an egg is surrounded by protoplasm with innumerable starch grains scattered in it. The integumentary tissue bordering the micropyle is specially rich in starch.

*Embryo and Endosperm*.—Just as in the other members of this family the fertilised egg becomes tubular and its further development takes place only after the organisation of the endosperm tissue. Some of the stages in the development of the embryo have been studied and these are similar to those in other members of the family already observed and reported by me.

The primary endosperm nucleus assumes a significant size (Fig. 44a) and undergoes two divisions followed by transversely placed walls resulting in a row of three cells, the micropylar, the middle and the chalazal (Fig. 45). The

third division which is longitudinal is confined to the middle chamber, while only nuclear divisions take place in the other two chambers which later develop into the haustoria. Fig. 46 gives a diagrammatic representation of the sequence of divisions. Subsequent divisions in the two middle cells form the endosperm tissue, which is differentiated into smaller cells towards the two ends (Fig. 50) and the centrally placed large cells.

*Endosperm haustoria*.—The nucleus of the micropylar chamber undergoes two divisions resulting in a tetra-nucleate aggressive haustorium. Although no separating wall is generally seen there are a few cases where an incomplete partition is noticed indicating thereby the probable two-celled ancestry of this haustorium (Fig. 48). Just above the level of the tapetum a tubular outgrowth begins to develop (Figs. 48 and 51) into the integumentary tissue and all the four nuclei gradually migrate into this. This becomes a conspicuous tubular unbranched body which is highly aggressive and shows a tendency to grow towards the chalaza (Fig. 51)—although not to the same extent as the 'Lateral Haustorium' of *Rhamphicarpa*. Older lateral haustoria are characterised by having large hypertrophied amoeboid nuclei and the deposition of cellulose, a feature met with in the other species of *Pedicularis* (Schmid, 1906).

The chalazal haustorium is a binucleate body forming a short aggressive tube growing into the tissue of chalaza and the vascular bundle of the hilum. It has rich protoplasmic contents and its amoeboid nuclei are larger than those of the micropylar haustorium (Fig. 53a and b). Degeneration of the chalazal haustorium takes place earlier.

#### DISCUSSION.

The affinities of *Rhamphicarpa*, *Centranthera* and *Pedicularis* to the other parasitic members of Scrophulariaceae can be summed up as follows:—

*Embryo-sac*.—In several parasitic members like *Alectorolophus*, *Pedicularis* (Schmid, 1906) and others more than one archesporial cell is often noticed, but the occasional occurrence of a binucellate ovule seems to be restricted only to *Rhamphicarpa*. The archesporial cell directly gives rise to the linear tetrad of megaspores of which the innermost develops into the normal eight-nucleate embryo-sac. Although the synergids are generally small, these are fairly large in *Rhamphicarpa* and *Centranthera*.

*Integumentary tapetum*.—The tapetum plays a prominent part in the nourishment of the embryo-sac during pre- and post-fertilization stages. In almost all members it is a layer with rich protoplasmic, starchy or fatty contents. Although this often lines the non-dilated part of the embryo-sac it is still capable of keeping pace with the enlarging embryo-sac by its intercalary growth during the post-fertilization stages. While in many parasitic members the development of outicle seems to be the only change in the tapetum during seed formation, it is noticed that in many non-parasitic members like *Celaia* (Krishna Iyengar, 1939a), *Vandellia* (Krishna Iyengar, 1940a) and others

this layer appears to have the rôles of digestion, absorption, storage and protection. *Centranthera* is unique among the parasites since this shows the most highly specialised tapetum with not only the above mentioned functions but also the stimulation of the secondary haustorial formation.

*Endosperm and endosperm haustoria*.—Just as in the other members, the first division of the primary endosperm nucleus is followed by a transverse wall resulting in the chalazal and micropylar chambers. The second division which is often restricted to the micropylar chamber is either transverse as in *Sopubia* (Krishna Iyengar, 1937, 1940c) and others or longitudinal as in *Rhamphicarpa* and *Centranthera*. Subsequent divisions will result in the separation of a middle tier from the micropylar, the former giving rise to the endosperm tissue, while the latter develops into the micropylar haustorium.

The chalazal chamber undergoes a nuclear or cell division and gives rise to the chalazal haustorium which is composed of two uninucleate cells or a binucleate body. In almost all the parasites this is an aggressive body, although in *Centranthera* this is almost non-functional. Older haustorium in all the parasites is binucleate.

In almost all the parasitic members of Scrophulariaceae the micropylar haustorium is a tetra-nucleate body either from the commencement or when fully formed. This may start as four uninucleate cells as in *Sopubia delphinifolia* (Krishna Iyengar, 1937) or as two binucleate cells as in *Sopubia trifida* (Krishna Iyengar, 1940c), *Rhamphicarpa*, *Centranthera* and others. Except in *Centranthera* and *Striga* (Michell, 1915) in all other members the micropylar haustorium is an aggressive body.

The occurrence of secondary endosperm haustoria seems to be an exceptional feature of *Centranthera*.

#### SUMMARY.

The development of the ovule, embryo-sac, endosperm and seed of three species, *Rhamphicarpa longiflora*, *Centranthera hispida* and *Pedicularis zeylanica*, is described in this paper.

The presence of more than one archesporial cell is occasionally noticed. One instance of a binucellate ovule has been noticed in *Rhamphicarpa*.

Chromosome counts have been made in *Rhamphicarpa longiflora* and *Centranthera hispida*, the haploid numbers being 9 and 16 respectively.

The hypodermal archesporial cell directly forms the megaspore mother cell and gives rise to a linear tetrad of megaspores in all the members. A normal eight-nucleate embryo-sac develops from the chalazal megaspore. The synergids are significantly large in *Rhamphicarpa* and *Centranthera*. The two polar nuclei fuse just before fertilization and the three small antipodal cells begin to degenerate soon after fertilization.

The first division of the primary endosperm nuclei is transverse in all the three members, separating a chalazal chamber from the micropylar one. The second division in *Rhamphicarpa* and *Centranthera* is longitudinal and the

third transverse and these divisions are confined to the micropylar chamber. In *Pedicularis* the second division is transverse and the third longitudinal, and both take place in the chalazal chamber. The three divisions, however, result in every case in the separation of a middle tier of two cells which gives rise to the endosperm tissue.

The chalazal haustorium is a binucleate tubular body which is aggressive in *Pedicularis* and *Rhamphicarpa*, but almost non-functional in *Centranthera*.

The micropylar haustorium is composed of two binucleate haustorial cells in *Rhamphicarpa* and *Centranthera*, these fusing very early to form a tetra-nucleate body. In *Pedicularis* this haustorium is tetra-nucleate from the very beginning.

In *Rhamphicarpa* and *Pedicularis* the micropylar haustorium is an aggressive body and shows lateral outgrowth developing into the integument and growing towards the chalaza, while in *Centranthera* even this seems to be almost non-functional.

In *Centranthera* aggressive secondary haustorial filaments develop from the primarily endosperm cells towards the micropylar end.

The tapetum in *Centranthera* shows enlarged and presumably haustorial cells towards the chalaza, protective cells towards the middle and cells probably with capacity to stimulate secondary haustorial formation towards the micropyle.

The epidermis of testa becomes lignified and functions as a protective layer in all the members.

I have very great pleasure in thanking Dr. M. A. Sampathkumaran, M.A., Ph.D., S.M. (Chicago), Professor of Botany, Central College, Bangalore, for giving the necessary facilities for this investigation and Dr. P. Maheshwari, D.Sc., F.A.Sc., F.N.A.Sc., F.N.I., of Dacca University for his kind perusal of the manuscript and helpful suggestions. My sincere thanks are due to Dr. L. Glišić of Belgrade for the literature he was kind enough to spare.

#### REFERENCES.

- Balička Iwanowska, G.—Contribution à l'étude du sac embryonnaire chez certaines Gamopétales. *Flora*, 86: 47-71, (1899).
- Glišić, Lj. M.—Zur Entwicklungsgeschichte von *Lathraea squamaria* L. *Bull. Inst. Jard. Bot. Univ. Belgrade*, 2: 20-56, (1932).
- Ein Versuch der Verwertung der Endospermmmerkmale für typologische und phylogenetische Zwecke innerhalb der Scrophulariaceen. *Bull. Inst. Jard. Bot. Univ. Belgrade*, 4: 42-73, (1936-37).
- Krishna Iyengar, C. V.—Development of the embryo-sac and endosperm haustoria in some members of Scrophularineae I. *Sopubia delphinifolia* G. Don and *Alonsoa* sp. *Jour. Ind. Bot. Soc.*, 16: 99-109, (1937).
- Development of the embryo-sac and endosperm haustoria in some members of Scrophularineae II. *Isoplexis canariensis* Lindl. and *Celastrum coromandeliana* Vahl. *Ibid.*, 18: 13-20, (1939a).
- A note on the embryo-sac and endosperm haustoria in some members of Scrophularineae. *Curr. Sci.*, 8: 261-263, (1939b).

- Krishna Iyengar, C. V.—Development of the embryo-sac and endosperm haustoria in some members of Scrophularineae III. *Limnophila heterophylla* Benth. and *Stemodia viscosa* Roxb. *Jour. Ind. Bot. Soc.*, **18**: 35-42, (1939c).
- Development of the embryo-sac and endosperm haustoria in some members of Scrophularineae IV. *Vandellia hirsuta* Ham. and *V. scabra* Benth. *Ibid.*, **18**: 179-189, (1940a).
- Development of the embryo-sac and endosperm haustoria in some members of Scrophularineae V. *Ilysanthes hyssopioides* Benth. and *Bonnaya tenuifolia* Spreng. *Ibid.*, **19**: 5-17, (1940b).
- Structure and development of seed in *Sopubia trifida* Ham. *Ibid.*, **19**: 251-261, (1940c).
- Development of the embryo-sac and endosperm-haustoria in *Torenia cordifolia* Roxb. and *T. hirsuta* Benth. *Proc. Nat. Inst. Sci. India*, **7**: 61-71, (1941).
- Development of embryo-sac and endosperm haustoria in *Rehmannia angulata* Hemsl. *Jour. Ind. Bot. Soc.*, **21**: 51-57, (1942a).
- Development of the embryo-sac and endosperm haustoria in \**Tetranema mexicana* Benth. and *Verbascum thapsus* Linn. *Proc. Nat. Inst. Sci. India*, **8**: 59-69, (1942b).
- Michell, M. R.—The embryo-sac and embryo of *Striga lutea*. *Bot. Gaz.*, **59**: 124-135, (1915).
- Schmid, E.—Beiträge zur Entwicklungsgeschichte der Scrophulariaceen. *Beih. Bot. Obl.*, **20A**: 175-299, (1906).

---

\* VI. Proc. Ind. Sci. Congr. Benares, (1941).



## EAST-WEST ASYMMETRY OF COSMIC RAYS AT CALCUTTA AND DARJEELING.

By P. C. BHATTACHARYA, *Palit Laboratory of Physics, University of Calcutta.*

(Communicated by Prof. M. N. Saha, F.R.S.)

(Received April 2, 1942.)

Since 1903 Carl Störmer has been trying to solve the mathematical problem of determining the orbits of the electrons in the magnetic field of the earth. He was led to this line from his interest in the problem of Aurora, which, according to the fundamental researches of Birkeland, were produced by the injection of streams of electrons into the earth's atmosphere.

Rossi (1930) first pointed out that if the primary cosmic rays were really electrons having an isotropic and homogeneous distribution in space far away from the earth's field and that if Störmer's theory were applicable to them then there should be greater intensity from the western sky if the particles were *positively charged*, and greater intensity from the eastern sky if they had a *negative charge*. If the energy distribution of the particles be the same and if they are equal in number then there should be no asymmetry.

The first experimental evidence of the existence of an asymmetry was produced in 1933 when Johnson and Street (1933) found that the western intensity at Mt. Washington ( $\lambda = 51^\circ$  N.,  $h = 6,288$  ft.) was greater than the eastern at  $30^\circ$  to  $40^\circ$  zenith angles. This experiment aroused a great deal of interest and various workers confirmed the result at various latitudes and at different altitudes. Mention may be made of the following:—

Alvarez and Compton (1933).

Auger, Leprince-Ringuet (1934).

Ehmert (1934).

Ghosh (1936).

Gill (1940).

Korff (1934).

Messerschmidt (1934).

Rossi (1934).

Seidl (1941).

Stevenson (1933).

The most extensive survey has been undertaken by Johnson (1935a) at various stations in Peru, Colorado, Panama and Mexico.

It is found that the asymmetry is maximum near the geomagnetic equator and amounts to  $\sim 15\%$  and then it decreases towards the higher latitudes, falling to  $2-3\%$  at  $\lambda = 50$  at sea-level.



These experiments appear to indicate a preponderance of positive electrons in the primary cosmic rays to the extent of 15% (the maximum value) at the geomagnetic equator, falling to 2-3% at the geomagnetic latitude of  $51^\circ$  N. It may be added that the particles need not necessarily be positive electrons but may as well be heavier particles such as protons or  $\alpha$ -particles, provided their energies lie in the field sensitive region, i.e. in the case of protons up to about 59 B.e.v.

But subsequent experiments by Johnson (1935) showed that the electrons themselves, which constitute the main soft component, seem to have a non-symmetric distribution. This was shown by studying the asymmetry of shower-producing particles. He placed three counters horizontally at the corners of an isosceles triangle 23 cm. in altitude and 9 cm. base with a 1.2 cm. thick lead cover over the upper counter. The lead plate was slightly larger than the cross-sectional area of a single counter. With this arrangement he could not detect any asymmetry at zenith angles of  $35^\circ$  and  $49^\circ$  at Nevado de Toluca in Mexico ( $\lambda = 29^\circ$ ,  $h = 4.3$  Km.). It is clear from this experiment that the shower-producing component (i.e. the soft component) is not asymmetric.

This experiment ought to be repeated at other latitudes and if the asymmetry is not found to exist, we can be sure of the conclusion that electrons do not show asymmetry. This experiment requires some time to perform but we can procure additional evidence by performing experiments in which soft rays are cut off by the use of thick absorbers.

At sea-level the soft component (electrons) forms about 25-30% of the total cosmic rays, so if we cut off the soft one with some absorber then the asymmetry should increase. Such experiments have been done, but the results are not conclusive and are rather contradictory.

Rossi (1934) finds at Asmara ( $\lambda = 11^\circ$ ,  $h = 2$  Km.) that the E.-W. asymmetry increases with 4 or 8 cm. lead between the counters at a zenith angle of  $45^\circ$ . But Korff (1934) finds at Mexico ( $\lambda = 29^\circ$  N.,  $h = 7,250$  ft.) and also at two stations in Peru that the E.-W. asymmetry is reduced by lead absorbers up to 30 cm. placed above the counter train. Johnson (1935a) finds at Cerro de Pesco ((Peru)  $\lambda = 0$ ,  $h = 4.3$  Km.) an increase of asymmetry while at El Pico Nevado de Toluca ( $\lambda = 29^\circ$ ,  $h = 4.3$  Km.) a decrease of asymmetry with lead absorber.

For tropical latitudes, very little work on E.-W. asymmetry has been reported so far. The following experiments on east-west asymmetry were undertaken at Calcutta ( $\lambda = 12^\circ$  N.,  $h = 80$  ft. above sea-level) and Darjeeling ( $\lambda = 16.5^\circ$  N.,  $h = 7,200$  ft. above sea-level) and the effects of lead absorbers on asymmetry have been studied at both the stations at different zenith angles.

#### *Experimental arrangement, etc.:—*

The amplifying circuit is of the Barasch (1935) type and is shown in fig. 1. The counters were used in Rossi parallel connection. The counters were filled with a mixture of commercially pure argon gas and petroleum

ether vapour to a total pressure of 6 cm. of Hg. The starting potential of each of these counters was about 1,200 volts with a plateau of about 350 volts.

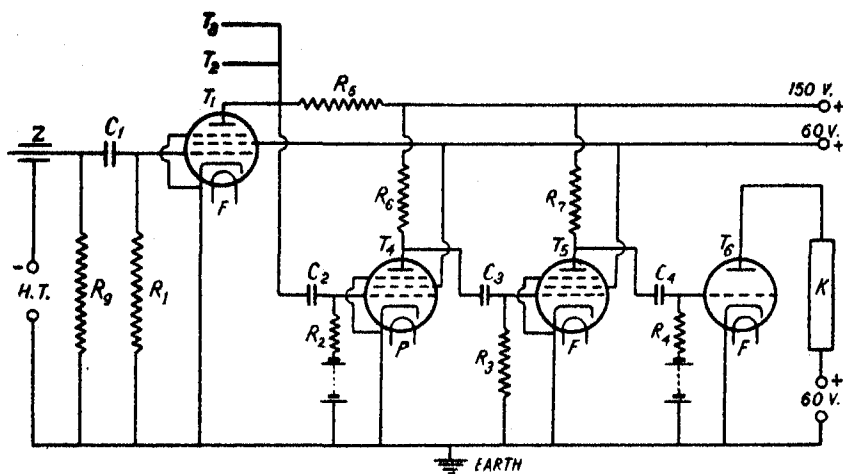


FIG. 1.

$C_1 = 50 \mu\mu F.$	$R_9 = 5 M\Omega.$	$T_1 = T_2 = T_3 = T_4 = T_5 \text{ MSP}_4.$
$C_2 = .002 \mu\mu F.$	$R_1 = R_7 = 1 M\Omega.$	$T_6 = G.T.1.$
$C_3 = .001 \mu\mu F.$	$R_2 = R_3 = R_4 = .5 M\Omega.$	$F = \text{Filament.}$
$C_4 = .01 \mu\mu F.$	$R_5 = .25 M\Omega.$	$K = \text{Recorder and Contact Breaker.}$
	$R_6 = 30,000 \Omega.$	$Z = G.M. \text{ Counter.}$
	$T_1, T_2, T_3 \text{ are in parallel (Rossi).}$	

The high tension for the counters was supplied from a H.T. stabilizer of the Street-Johnson type with Evan's modification of the screen grid battery.

The counter telescope (fig. 2) used in the E.-W. experiments consists of a light wooden frame supporting three pairs of counters, the distance between each pair being 50 cm. The counters in each pair are joined in parallel so that they act as a single counter. The wooden frame holding the counters is capable of rotation in the vertical plane, and the inclination of its axis (i.e. the axis of the counter telescope) to the vertical can at once be read with the help of a pointer moving over a protractor graduated in degrees. Each counter is 3.5 cm. in diameter and 15 cm. in length so that the counter telescope subtends an angle of  $8^\circ$  in the plane in which the system can rotate and an angle of  $17^\circ$  along the length of the central wire of the counters. Though the angular aperture along the diameter of the counters is  $8^\circ$ , it can be seen that more than 50% of the rays come through half the actual aperture. The instrument is placed in such a position that the axle of the framework is pointing north and south so that the telescope can rotate in the local magnetic east-west plane. Just above the lowermost counter there is a platform on which requisite thicknesses (10 cm. in our case) of lead can be put to cut off the soft component.

The exploration of the E.-W. plane is carried out by what is called the 'method of cycles', according to which each zenith angle is exposed to cosmic

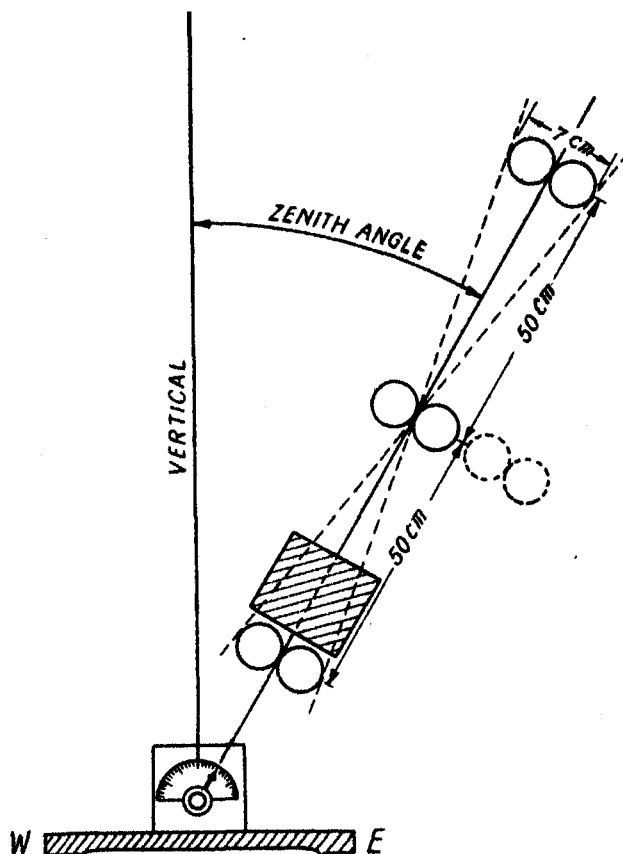


FIG. 2.

Counter Telescope.

rays for a short interval of time and the corresponding number of counts recorded and then the instrument is rotated to the next zenith angle and so on. This method has several advantages, for it avoids—

- (a) any instrumental selectivity,
- (b) any short period change of cosmic ray intensity,
- (c) any change of cosmic ray intensity due to sudden barometric change, magnetic disturbance or any such other cause.

In the experiment at both the stations at Darjeeling and Calcutta the time of 'exposure' at a zenith angle at a time was 20 minutes only.

The effect of showers was determined by displacing the central counter just outside the geometrical beam defined by the two outer ones (fig. 2, dotted

pair). It is found that the effect of showers is practically constant at all zenith angles and at both the azimuths.

At Darjeeling the experiment was performed in the Emerald Bank in Jalapahar (altitude 7,200 ft. above sea-level). The apparatus was placed in the drawing room having a roof of wood and corrugated tin sheet and the walls were of wood and window glass. In the eastern side of the house there is a hill which obscured the telescope if the zenith angle in that side exceeded about  $70^\circ$ .

In Calcutta ( $\lambda = 12^\circ$  N.,  $h = 80$  ft. above sea-level) the apparatus was placed in the topmost room of the main building of the University College of Science. This room has brick walls and ordinary tiled roof. All sides of this room are open.

Formerly, the E.-W. asymmetry ( $\alpha_{e-w}$ ) was computed in terms of the ratio of the west intensity ( $J_w$ ) to the east intensity ( $J_e$ ), i.e.  $\alpha = \frac{J_w}{J_e}$ .

But it will be seen that the statistical fluctuations of this quantity are not symmetric with respect to the value unity when  $J_w = J_e$ , and in the case of low counting rates and short time intervals Johnson (1935a) finds that there can be introduced in the calculation an appreciable false asymmetry favouring the west. For this reason it has become customary to define asymmetry as

$$\alpha = \frac{J_w - J_e}{\frac{J_w + J_e}{2}}$$

when it will be seen that the fluctuations are symmetric with respect to the value zero when  $J_w = J_e$ . In this paper we have followed the latter definition of  $\alpha$ .

The probable errors in this paper were calculated from the total number of counts, viz.  $R = \pm \frac{.68\sqrt{N}}{T}$ , where  $N$  is the total number of counts in time  $T$ .

## RESULTS.

TABLE I.

*E.-W. asymmetry of the unabsorbed radiation at Darjeeling ( $\lambda = 16^{\circ}5' N.$ ,  
 $h = 7,200$  ft.).*

Zenith angle.	Azimuth.	No. of counts/min. (corrected for showers).	Asymmetry $2 \frac{(J_w - J_e)}{J_w + J_e}$
$15^{\circ}$	West	$5693 \pm 0118$	$1112 \pm 0302$
	East	$5093 \pm 0113$	
$30^{\circ}$	West	$4343 \pm 0107$	$1844 \pm 0364$
	East	$3610 \pm 0098$	
$45^{\circ}$	West	$3151 \pm 0093$	$1692 \pm 0445$
	East	$2660 \pm 0090$	
$60^{\circ}$	West	$1035 \pm 0070$	$1104 \pm 0988$
	East	$0927 \pm 0068$	

TABLE II.

*E.-W. asymmetry of the penetrating component (Mesons) at Darjeeling.*

Zenith angle.	Azimuth.	No. of counts/min. (corrected for showers).	Asymmetry $2 \frac{J_w - J_e}{J_w + J_e}$
$15^{\circ}$	West	$3765 \pm 0085$	$1271 \pm 0329$
	East	$3315 \pm 0080$	
$30^{\circ}$	West	$3031 \pm 0078$	$1995 \pm 0385$
	East	$2481 \pm 0073$	
$45^{\circ}$	West	$2405 \pm 0067$	$1933 \pm 0430$
	East	$1981 \pm 0066$	
$60^{\circ}$	West	$0965 \pm 0055$	$1651 \pm 0843$
	East	$0815 \pm 0051$	

TABLE III.

*E.-W. asymmetry of the unabsorbed radiation at Calcutta ( $\lambda = 12^\circ$  N.,  
 $h = 80$  ft.).*

Zenith angle.	Azimuth.	No. of counts/min. (corrected for showers).	Asymmetry $2 \frac{J_w - J_e}{J_w + J_e}$
15°	West	$\cdot 3063 \pm \cdot 0066$	$\cdot 0869 \pm \cdot 0311$
	East	$\cdot 2808 \pm \cdot 0063$	
30°	West	$\cdot 2246 \pm \cdot 0058$	$\cdot 1371 \pm \cdot 0381$
	East	$\cdot 1958 \pm \cdot 0055$	
45°	West	$\cdot 1820 \pm \cdot 0053$	$\cdot 1132 \pm \cdot 0422$
	East	$\cdot 1625 \pm \cdot 0050$	
60°	West	$\cdot 0930 \pm \cdot 0040$	$\cdot 1196 \pm \cdot 0628$
	East	$\cdot 0825 \pm \cdot 0038$	

TABLE IV.

*E.-W. asymmetry of the penetrating component (Mesons) at Calcutta.*

Zenith angle.	Azimuth.	No. of counts/min. (corrected for showers).	Asymmetry $2 \frac{J_w - J_e}{J_w + J_e}$
15°	West	$\cdot 2458 \pm \cdot 0056$	$\cdot 1109 \pm \cdot 0336$
	East	$\cdot 2200 \pm \cdot 0055$	
30°	West	$\cdot 1866 \pm \cdot 0050$	$\cdot 1590 \pm \cdot 0392$
	East	$\cdot 1591 \pm \cdot 0046$	
45°	West	$\cdot 1528 \pm \cdot 0045$	$\cdot 1239 \pm \cdot 0432$
	East	$\cdot 1350 \pm \cdot 0043$	
60°	West	$\cdot 0816 \pm \cdot 0035$	$\cdot 0962 \pm \cdot 0598$
	East	$\cdot 0742 \pm \cdot 0031$	

## DISCUSSION.

Tables I-IV give the experimental results on the east-west asymmetry at Darjeeling ( $\lambda = 16^{\circ}5' \text{ N.}$ ,  $h = 7,200 \text{ ft.}$ ) and at Calcutta ( $\lambda = 12^{\circ} \text{ N.}$ ,  $h = 80 \text{ ft.}$ ). It can be seen that at both the stations the asymmetry increases with the increase of zenith angle up to about  $45^{\circ}$  and then again decreases in conformity with the results obtained by Johnson (1935a) and other workers at various other stations.

With 10 cm. lead between the counters (lead being placed just above the lowermost counter) the asymmetry increases at both the stations showing that the electrons contribute very little to the asymmetry. Our results agree with those of Rossi and Gill as well as those of Johnson (1935a) (one station only). At Calcutta, with zenith angle  $60^{\circ}$  there is a decrease of asymmetry with lead absorber.

The probable errors in the present experiment are rather large. This is because the angular aperture of the extreme counters is only  $8^{\circ}$  in the vertical plane, so the number of counts per unit time is rather small. In the experiments of the previous workers the angular aperture of the counter train was not so well defined. In the experiments of Rossi and Johnson the angular aperture was about  $23^{\circ}$ . In order to minimise the statistical fluctuations, readings were taken for 40 to 50 hours at each zenith angle (by the method of cycles) at Darjeeling, while at Calcutta about 60 hours at each zenith angle.

Johnson (1935a) has observed that asymmetry increases with altitude. It can be seen here that the asymmetry at Darjeeling at all the zenith angles is greater than that at Calcutta at the corresponding zenith angles. This increase is evidently due to the increase in the number of mesons between these two stations.

The conclusions from the experiments at Darjeeling and Calcutta, taken along with those of earlier workers are as follows:

- (1) That the electrons of either sign, which are identical with shower-producing particles, contribute very little to the E.-W. asymmetry.
- (2) That mesons which are produced in our atmosphere by the primary cosmic rays show a maximum asymmetry of  $\sim 20\%$  at Darjeeling ( $\lambda = 16^{\circ}30' \text{ N.}$ ,  $h = 7,200 \text{ ft.}$ ) for positive rays and about  $16\%$  at Calcutta ( $\lambda = 12^{\circ} \text{ N.}$ ,  $80 \text{ ft.}$ ). The maximum is reached between  $Z = 30^{\circ}$  to  $45^{\circ}$  and falls on either side.

Recent experiments of Schein, Jessey and Wollan (1941) at Missouri ( $\lambda = 51^{\circ}$ ) seem to indicate that electrons of energy between  $10^9 \text{ e.v.}$  and  $10^{12} \text{ e.v.}$  are absent in the upper atmosphere. The large number of electrons of energy below  $10^9 \text{ e.v.}$  that are found in the stratosphere are of secondary origin, for the minimum energy required by a primary electron to penetrate the earth's magnetic field at  $\lambda = 51^{\circ} \text{ N.}$  is about  $3 \times 10^9 \text{ e.v.}$  These secondary electrons are supposed to be due to decay of mesons, knock-on shower and cascade shower.

As regards the primary particles Johnson (1938), Swann (1940), Carlson and Schein (1941) are of opinion that they are protons. There is no satisfactory theory of the production of mesons by protons. According to Swann (1940) the primary protons, by an *unknown mechanism*, give rise to a number of mesons in the first one or half metre of water-equivalent depth of the atmosphere. The number of mesons that can be produced in a single 'explosion' can be as large as 8-10. These mesons are practically at rest so that their mean free path is  $\sim 300$  metres and the disintegration electrons from them come out in all directions. But the mesons which are produced by the protons in a greater depth of the atmosphere, having sufficient energy to maintain the original direction of the protons, give rise to all the geomagnetic effects such as E.-W. asymmetry, latitude effect, etc.

In conclusion, the author wishes to record his sincere thanks to Prof. M. N. Saha, D.Sc., F.R.S., for his kind interest and helpful discussions and criticisms throughout the progress of the work. His thanks are also due to Drs. S. C. Sirkar, N. N. Dasgupta, G. P. Dube and K. M. Basu for helpful discussions.

#### SUMMARY.

The east-west asymmetry of cosmic radiation at Darjeeling ( $\lambda = 16^\circ 30' \text{ N.}$ ,  $h = 7,200 \text{ ft.}$ ) and Calcutta ( $\lambda = 12^\circ \text{ N.}$ ,  $h = 80 \text{ ft.}$ ) at zenith angles of  $15^\circ$ ,  $30^\circ$ ,  $45^\circ$  and  $60^\circ$  has been measured with a triple coincidence counter telescope. The results agree with those of the previous workers at other stations. The asymmetry increases slightly with 10 cm. lead between the counters at both the places.

#### REFERENCES.

- Alvarez and Compton. 1933. A positively charged component of cosmic rays. *Phys. Rev.*, **43**, 835.
- Auger, P. and Leprince-Ringuet. 1934. Variation du Rayonnement cosmique suivant la latitude. *Nature*, **133**, 138.
- Barasch, H. P. 1935. Improved counting circuit. *Proc. Phys. Soc.*, **47**, 824.
- Carlson and Schein. 1941. On the production of Mesotron. *Phys. Rev.*, **59**, 840.
- Ehmert. 1934. Der Ost-West Effekt der Ultrastrahlung auf der Zugspitze. *Phys. Zeits.*, **35**, 20.
- Ghosh, R. 1936-37. On the angular distribution of cosmic rays. *Trans. Bose Inst.*, **11**, 159.
- Gill, P. S. 1940. East-west asymmetry of cosmic rays at  $40^\circ \text{ N.}$  latitude. *Phys. Rev.*, **57**, 68.
- Johnson, T. H. 1934. Coincidence counter studies of the corpuscular component of the cosmic radiation. *Phys. Rev.*, **45**, 569.
- Johnson, T. H. 1935. Coincidence counter studies of the corpuscular component of the cosmic radiation. *Phys. Rev.*, **45**, 569.
- Johnson, T. H. 1935a. Progress of the directional survey of cosmic ray intensities and its application to the analysis of the primary cosmic radiation. *Phys. Rev.*, **48**, 287.
- Johnson, T. H. 1938. A note on the nature of the primary cosmic radiation. *Phys. Rev.*, **54**, 385.



- Johnson and Street. 1933. The variation of cosmic ray intensities with azimuth on Mt. Washington. *Phys. Rev.*, **43**, 381.
- Korff, S. A. 1934. Penetrating power of asymmetric component of cosmic radiation. *Phys. Rev.*, **46**, 74.
- Messerschmidt. 1934. Über Schwankungsmessungen der Ultrastrahlung. Part III. *Zeits. f. Physik*, **87**, 800.
- Rossi, B. 1930. On the magnetic deflection of cosmic rays. *Phys. Rev.*, **36**, 606.
- Rossi, B. 1934. Directional measurements on the cosmic rays near the geomagnetic equator. *Phys. Rev.*, **45**, 212.
- Schein, Jessey and Wollan. 1941. The nature of the primary cosmic radiation and the origin of the mesotron. *Phys. Rev.*, **59**, 615.
- Seidl, F. G. P. 1941. The E.-W. asymmetry of cosmic radiation at high latitudes. *Phys. Rev.*, **59**, 7.
- Stevenson, E. C. 1933. Azimuthal asymmetry of the cosmic radiation in Colorado. *Phys. Rev.*, **44**, 855.
- Swann, W. F. G. 1941. A single component for the primary cosmic radiation. *Phys. Rev.*, **59**, 770.

## FINE STRUCTURE IN THE DIRECTIONAL INTENSITY OF COSMIC RAYS AT CALCUTTA ( $\lambda = 12^\circ$ N., $h = 80$ ft.).

By P. C. BHATTACHARYA, *Palit Laboratory of Physics, Calcutta University.*

(Communicated by Prof. M. N. Saha, F.R.S.)

(Received April 2, 1942.)

The theory of the motion of a charged particle in the earth's magnetic field has been developed by Störmer, Lemaitre, Vallarta and their associates. According to this theory, particles whose energy is greater than a certain minimum, corresponding to the particular geomagnetic latitude, may reach a place of observation on the earth, forming various types of cones of a complicated nature.

Those trajectories which come directly from infinity to the point of observation form the boundary of a cone called the 'main cone' or cone of full light (Lemaitre-Vallarta, 1936).

There are some trajectories which come from infinity but arrive at the point of observation only after having been tangential to the surface of the earth. There may be a number of loops in them. The simplest of these does not have any loop but is tangential to the earth only once before arriving at the place of observation. They give rise to what is called a 'shadow cone', outside of which all regions are forbidden. It may be pointed out that the shadow cone is due to the presence of the earth which is impenetrable to cosmic particles. All the trajectories which have a number of loops lie in the region between the main cone and the shadow cone. They give rise to what is called 'penumbra' which consists of alternate allowed and forbidden regions.

From a theoretical analysis of the banded structure of the penumbra Schremp (1938) predicted that there should be some anomaly in the directional intensity pattern of cosmic rays due to the presence of penumbra. The first experimental evidence of the existence of the penumbra was reported simultaneously by Cooper and Ribner in 1939. Cooper (1939) found three humps (i.e. sudden increase of intensity of cosmic rays) at zenith angles of  $7^\circ$ ,  $20^\circ$  and  $35^\circ$  in the eastern azimuth at Missouri while Ribner (1939) reported one pair of symmetrical prominences at zenith angle of  $20^\circ$  in both the eastern and western azimuths, and also some indication of peaks in the neighbourhood of  $Z = 10^\circ$  and  $40^\circ$ .

Schremp and Banos (1940) have also found such structure in the four principal azimuths, viz. N., S., E., and W. in Mexico city ( $\lambda = 29^\circ$ ,  $h = 2.24$  Km.). Recently they (1941) studied four additional azimuths, viz. N.E., S.E., S.W., N.W. The results show beyond doubt the existence of some irregularities in the zenith angle distribution of intensity of cosmic rays.

Vallarta (1939) has emphasised the importance of this kind of work as it provides a good method of analysis of the primary rays and their spectra. Hutner (1939) has given a detailed calculation of the structure of the penumbra for  $Z = 60^\circ$  and  $\lambda = 20^\circ$  and has shown that the position and magnitude of the prominences may supply sufficient data for the analysis of the energy spectrum of the primary particles, because the energy spectrum is very sensitive to the type of distribution function of the primary rays.\*

Schremp (1938a) has shown that the penumbra is absent at the equator but its effect begins to be felt in the neighbourhood of  $\lambda = 10^\circ$ . The geo-magnetic latitude of Calcutta is  $12^\circ$  N. So it was thought worth while to find experimentally how far their predictions regarding penumbra are correct and what are the nature and position of the prominences in the directional intensity at this place.

#### EXPERIMENT.

In order to study 'fine structure' in the directional intensity, the angular aperture of the counter telescope should be very small. The counters used were each 60 cm. long and 3.9 cm. in diameter. A triple coincidence circuit was used and the counters were placed 50 cm. one above the other, so that the angular aperture in the vertical plane was  $4.5^\circ$  while that in the lateral plane was  $62^\circ$ , so that the solid angle was  $\simeq \frac{1}{10}$ . Only the western azimuth was explored from the vertical up to  $45^\circ$ , in steps of  $5^\circ$ . Readings were taken by the 'method of cycles' and the apparatus was allowed to remain 15 minutes at a zenith angle at a time.

In order to avoid 'pick up' the first valve was placed very close to the corresponding counter in the same horizontal plane, and the counter together with the first valve was properly shielded.

The following table gives the result.

TABLE I.  
*Intensity of the unabsorbed radiation at different zenith angles in the western azimuth at Calcutta.*

Zenith angle.	Total No. of counts.	Counts per min.
$0^\circ$	2943	$2.84 \pm .036$
$5^\circ$	2746	$2.65 \pm .034$
$10^\circ$	2708	$2.61 \pm .034$
$15^\circ$	2519	$2.43 \pm .033$
$20^\circ$	2323	$2.24 \pm .031$
$25^\circ$	2204	$2.13 \pm .031$
$30^\circ$	1836	$1.77 \pm .028$
$35^\circ$	1855	$1.79 \pm .028$
$40^\circ$	1783	$1.72 \pm .028$
$45^\circ$	1543	$1.40 \pm .026$

\* Dr. Gill is trying to verify experimentally at Lahore ( $\lambda = 22^\circ$  N.) Hutner's predictions for  $\lambda = 20^\circ$  (vide *Phys. Rev.*, 60, 153).

In fig. 1 the number of counts per minute is plotted against the zenith angles in the western azimuth. The vertical lines indicate the probable errors.

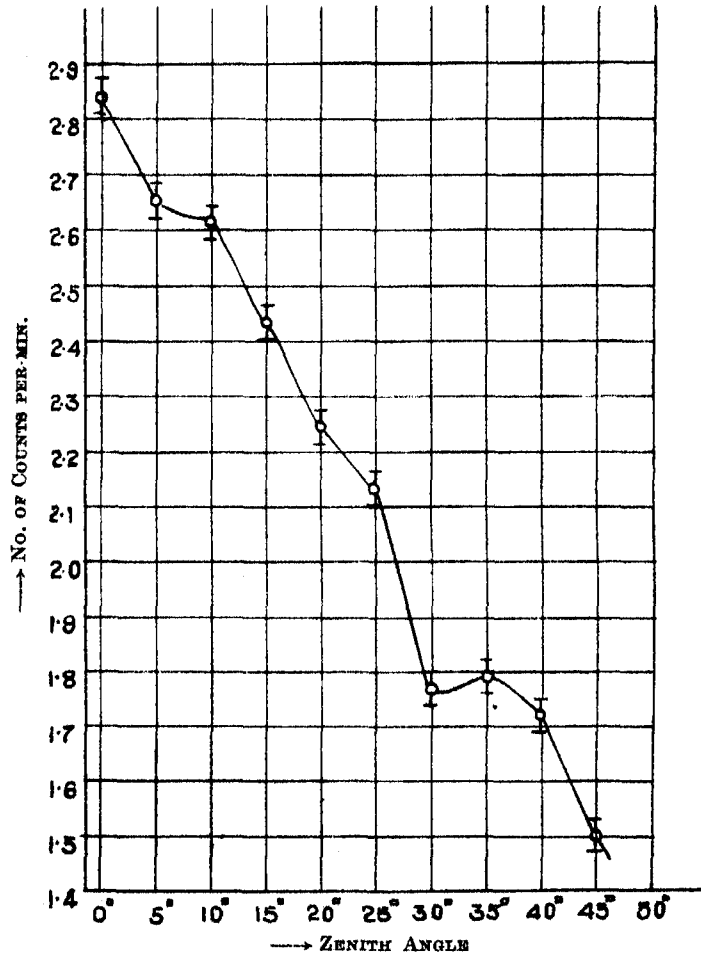


FIG. 1.

Intensity of cosmic rays at different zenith angles in the western azimuth at Calcutta ( $\lambda = 12^\circ \text{ N.}$ ,  $h = 80 \text{ ft.}$ ).

Fig. 1 shows two prominences, one at zenith angle  $10^\circ$  and the other at  $Z = 35^\circ$ . These peaks are just above the probable errors. There is, however, an indication of a peak at  $Z = 25^\circ$  which is within the statistical errors. The experiment thus shows for the first time the existence of penumbra even at the geomagnetic latitude of  $12^\circ \text{ N.}$  It remains to be seen whether these peaks are actually in the energy spectrum of the particles before their entrance into the atmosphere or whether they are produced in the atmosphere during the production of mesons or during their passage through the atmosphere.

The author is indebted to Prof. M. N. Saha, F.R.S., for his kind interest and helpful discussions throughout the progress of the work.

#### SUMMARY.

The intensity of cosmic radiation in the western azimuth at Calcutta ( $\lambda = 12^\circ$  N.,  $h = 80$  ft.) has been measured with a triple coincidence counter telescope of small aperture at various zenith angles from the vertical up to  $45^\circ$  at the intervals of  $5^\circ$ . The results show two prominences at  $Z = 10^\circ$  and  $35^\circ$  in the zenith angle distribution curve. There is a slight indication of a peak at  $Z = 25^\circ$ .

#### REFERENCES.

- Cooper, D. M. 1939. Fine structure in the zenith angle distribution of cosmic rays. *Phys. Rev.*, **55**, 1272.
- Hutner, R. A. 1939. The Penumbra at geomagnetic latitude  $20^\circ$  and the energy spectrum of primary cosmic radiation. *Phys. Rev.*, **55**, 614.
- G. Lemaître and M. S. Vallarta. 1936. On the geomagnetic analysis of cosmic radiation. *Phys. Rev.*, **49**, 719.
- Ribner, H. S. 1939. Anomalies in the directional intensity distribution of cosmic rays. *Phys. Rev.*, **55**, 1271.
- Schremp, E. J. 1938. General theory of the earth's shadow effect of cosmic radiation. Part I. *Phys. Rev.*, **54**, 153.
- Schremp, E. J. 1938a. General theory, etc. Part II. *Phys. Rev.*, **54**, 157.
- Schremp, E. J. and Banos, A. 1940. On the fine structure pattern of cosmic rays at Mexico city. *Phys. Rev.*, **58**, 662.
- Schremp, E. J. and Banos, A. 1941. Do. Part II. *Phys. Rev.*, **59**, 614.
- Vallarta, M. S. 1939. Determination of the energy spectrum of primary cosmic rays. *Rev. Mod. Phys.*, **11**, 239.

## STUDIES ON HELIUM-FILLED GEIGER-MÜLLER COUNTERS.

By H. R. SAENA, P. L. KAPUR, and CHARANJIT, *Physics Laboratory,  
Government College, Lahore.*

(Communicated by Prof. M. N. Saha, F.R.S., F.N.I.)

(Read January 1, 1942.)

### I. INTRODUCTION.

Geiger-Müller (G.M.) Counters are of two types: (a) those in which the discharge is extinguished by means of an external resistance put in series with the G.M. counter or by some other external device such as the Neher-Harper circuit, and (b) those in which the extinction is brought about by an internal mechanism. For an efficient use of counters of the first type the series resistance has to be quite large ( $\sim 10^9$  ohms) in order to keep the current during the discharge below a certain minimum value. It is only for very small values of the current that the discharge is unstable and is quickly stopped after its initiation, whereas if the current be higher than the minimum, the discharge is self-maintained and stable.

Apart from the difficulty of producing such a high resistance, its use in series with the counter puts a limitation on the maximum rate of recording as the recovery time of the counter-circuit after the discharge is directly proportional to the series resistance. In fact if  $t_g$  denotes the time for which the discharge lasts, the counter will not be ready for response to another incoming particle for an interval  $t_g + t_{rc}$  after the initiation of the discharge, where  $t_{rc}$  is the recovery time depending directly on both the series resistance  $r$  and the capacity  $c$  (made up of the capacity of the counter and other stray capacities) of the counter-circuit. In other words if two particles enter the counter at an interval less than  $t_g + t_{rc}$  they will not be appreciated as two distinct particles but only as one.

The second type (internally-quenched) of G.M. counters were first of all introduced by Trost (1937). Instead of filling the counter with some dry gas as nitrogen or hydrogen he used argon to which was added a certain percentage of alcohol vapour. The extinction of the discharge in such counters is brought about primarily by the mantle of the positive space charge produced around the wire by the ionisation of the organic vapour molecules. Since here the extinction is essentially due to an internal mechanism, the series resistance need not be large and can be just of the order of a megohm. Thus  $t_{rc}$  is considerably reduced and the counter becomes a faster one.

Trost investigated the behaviour of counters filled with argon and some organic vapour. In certain types of work, however, it may not be desirable

to use argon-filled counters, as argon becomes radioactive under neutron bombardment. So that if in any experiment involving neutrons an argon-filled G.M. tube is used, the number of counts recorded will be quite misleading. One is thus led to investigate the behaviour of counters in which gases other than argon are used. Curran and Petrzilka (1939) have investigated counters filled with He, Ne,  $H_2$ ,  $O_2$  and  $N_2$  using in all cases an admixture of 1 cm. ethyl alcohol in a total pressure of 10 cm. They find that helium and neon are as good as argon except that with helium a slightly ascending plateau is obtained. In certain cases the use of neon is open to the same type of objection as the use of argon; helium on the other hand is very stable against radioactive changes and should be very suitable (from the above point of view) for counter fillings. Moreover, helium is more easily available than other inert gases and so an investigation of the behaviour of helium-filled counters with admixtures of various organic compounds was taken in hand.

To make the study of helium-filled counters more detailed it was decided to investigate the effect of different types of organic compounds in a serial manner. In the present paper we report the behaviour of the counter when different percentages of the common aliphatic alcohols and ethyl ether are introduced in the G.M. counter atmosphere. In addition to studying the effect of different types of cylindrical surfaces it is also proposed to study the influence of the geometry of the counter on its behaviour and also to study the effect of time on a counter filled suitably. When the entire series have been finished we hope to throw some light on the mechanism of self-extinguishing counters.

## II. APPARATUS.

*The counter.*—The tube counter is made from pyrex glass and has tungsten electrodes. The central wire is of nickel, 0.1 mm. diameter, and is held along the axis of the tube by means of tungsten electrodes. The cylinder is of thin copper and is 2.3 cm. in diameter and 12.6 cm. in length. After the assemblage the copper surface of the cylinder was prepared according to the following treatment:—

The counter was first cleansed successively with six normal and 0.1 normal nitric acid, then washed with distilled water about ten times and dried. With dry air inside, the counter was next heated in a flame till the copper oxide turned brownish black in colour. It was then filled with dry nitric oxide gas and heated till the cylinder surface turned a dark velvety colour. The counter is then ready to be filled with the desired mixture.

*Filling of the counter.*—The apparatus used for this purpose is shown in fig. 1. By operating the stopcocks  $S_1$  and  $S_2$  organic vapour from the container  $B$  (which was surrounded by ice or some freezing mixture) was first introduced into the counter  $C$  and then evacuated, the process being repeated a number of times before finally filling the counter with the requisite pressure of the organic vapour. Then helium from  $A$  was introduced to

make a total pressure of 10 cm. in the counter as indicated by the mercury manometer. The helium used had been previously purified by connecting

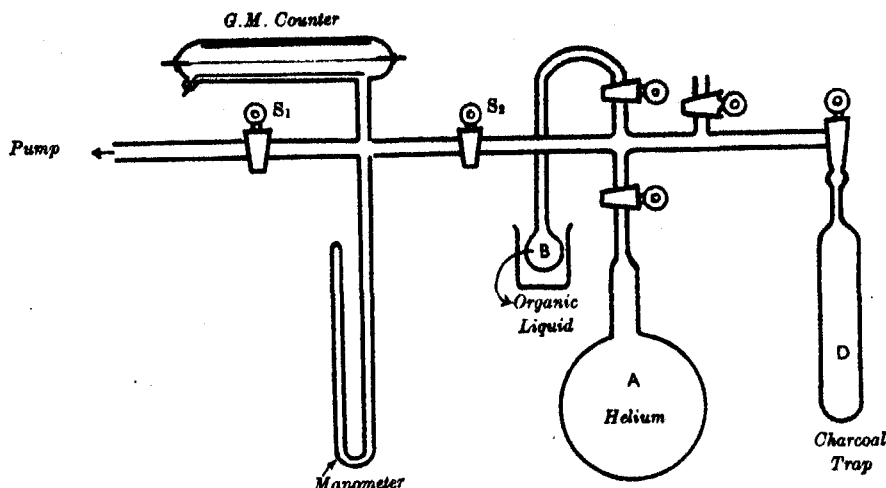


FIG. 1. Schematic diagram of the filling apparatus.

the flask *A* to the activated charcoal trap *D*, which was kept surrounded by liquid air for several hours.

*Voltage supply and recording.*—The stabilised high voltage for the counter wire was obtained from a circuit due to Evans (1934) and later modified by Gingrich (1936). It consists of a neon-sign transformer, an R.C.A. 866 rectifier, a suitable choke, condensers and a stabilising pentode (R.C.A. 47) tube. It is entirely mains operated and yields potentials up to 2,200 volts.

The electrical pulses from the counter were amplified by a circuit due to Gingrich (1936). It comprises an (R.C.A. 57) pentode tube as first stage amplifier, the plate-voltage changes of which flash a neon bulb and alter the voltage on the control grid of the output tube. It was noticed that with many of the common types of neon bulbs more counts were obtained in light than in darkness but with the Mazda neon-lamp, which was used ultimately in the apparatus, no such difference was observed.

For registering the amplified pulses we employed a clock recorder. An electro-magnet with a mumetal core was fitted on to a timepiece clock from which the hair-spring had been removed. To one end of the ratchet a small piece of the mumetal was attached, a spring of adjustable tension being fixed to the other end.

The arrival of a pulse in the output circuit energises the electro-magnet which attracts the mumetal piece attached to the ratchet, thus disengaging the toothed wheel which turns through one tooth. As the pulse dies out the ratchet moves back due to the action of the spring attached to its other end thereby again moving the toothed wheel through one tooth. Thus every



incoming pulse makes two clicks or in other words moves the seconds hand through one second. The sensitiveness of the arrangement depends upon the tension in the spring, the strength of the electro-magnet per unit current and upon the movement of the clock. In our case it was found that a current of only ten milliamperes in the output circuit was sufficient to actuate the clock recorder.

### III. RESULTS.

In the graphs of figures 2 to 5 are represented the number of counts per minute ( $N$ ) against the potential ( $V$ ) applied on the wire of the G.M. counter for different atmospheres in the counter. For each of the various organic vapours studied graphs have been drawn for increasing proportions of the vapour starting with a partial pressure of 0.5 cm. in a total of 10 cm. and going in steps of half-a-centimetre to 3.5 cm. or to a vapour pressure attainable at the room temperature. In all cases the container ( $B$ , fig. 1) with the liquid alcohol was surrounded with ice or some freezing mixture. If at this temperature the vapour pressure was not enough the container was kept at the lowest temperature consistent with the required pressure. This precaution was taken to keep the vapour pressure of water in the counter as small as possible, in any case negligible as compared to the vapour pressure of alcohol.

For comparative purposes graphs (fig. 6) are also drawn for mixtures of helium with methyl, ethyl, isopropyl alcohols and ethyl ether respectively at the same partial pressure of 3 cm. in a total pressure of 10 cm. The graphs show that helium-methyl alcohol mixture (7 cm. + 3 cm.) is best suited for G.M. counter fillings. Helium-ethyl alcohol mixture also gives an equally good plateau, though the threshold potential is higher.

It is a common feature of all the atmospheres studied that the quality and size of the plateau improves as the partial pressure of the organic vapour is increased up to a certain value usually 2.5 cm. to 3 cm. beyond which it again deteriorates.

A study of the time variation of the impulse from the counter by means of a cathode ray oscillograph revealed that the resolving time of the counter with its circuit was  $\sim 10^{-5}$  sec. A detailed account of the study of the impulse characteristics of the counter by a cathode ray oscillograph will be published later on.

*Helium-ethyl alcohol.*—The results are shown in fig. 2. Curran and Petrzilka observed that for He-alcohol filled counters the plateau was a slightly ascending one. They attributed it to the fact that the helium used by them was only commercially pure. We have used helium that was purified by being left in contact with activated charcoal at liquid air temperature but we find the same slightly ascending plateau for 0.5 cm. and 1.0 cm. of ethyl alcohol. As the partial pressure of alcohol is further increased the plateau, however, becomes

horizontal and increases in size becoming about 400 volts in length at a partial pressure of 3.0 cm. For higher concentrations of alcohol the plateau again

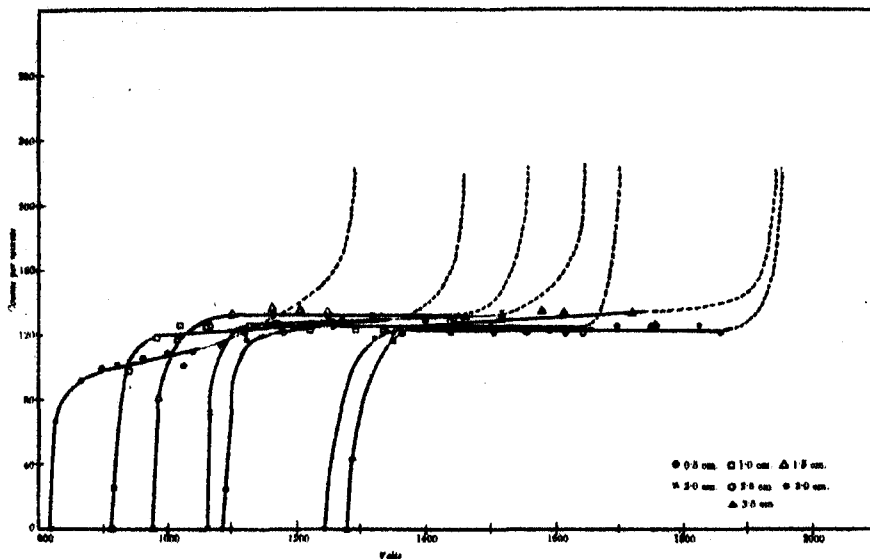


FIG. 2. Volts-counts graphs for ethyl alcohol at various partial pressures.

becomes an ascending one. The threshold potential increases with increasing percentages of the alcohol vapour present in the counter atmosphere.

*Helium-methyl alcohol.*—The results are shown in fig. 3. For all partial pressures of the vapour up to 3 cm. the plateau is horizontal. The region of

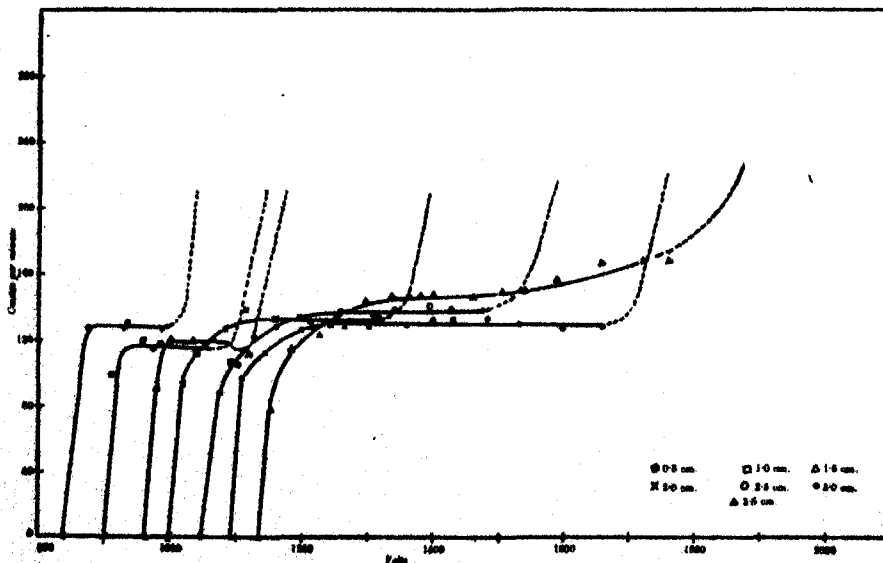


FIG. 3. Volts-counts graphs for methyl alcohol at various partial pressures.

constant counting increases with increasing concentrations of the alcohol admixture and is largest, extending over 400 volts for 3 cm. (for 2.5 cm. it extends over 325 volts). For concentration of and higher than 3.5 cm. the plateau becomes an ascending one, thus rendering such concentrations of alcohol unsuitable for counter filling.

The threshold potential increases with increasing percentages of the vapour in the counter atmosphere but for concentrations of the vapour greater than a partial pressure of 2 cm. the threshold potential values are consistently lower than their respective values for the case of helium ethyl-alcohol mixture.

*Helium-isopropyl alcohol.*—The results are given in fig. 4. Here also a satisfactory plateau is obtained for a partial pressure of 3 cm. of the alcohol

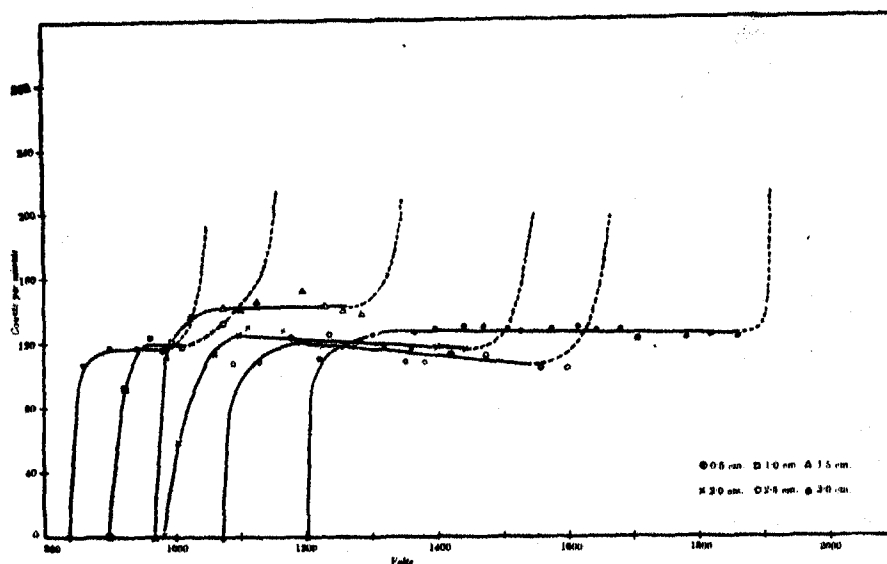


FIG. 4. Volts-counts graphs for isopropyl alcohol at various partial pressures.

vapour. For lower partial pressure, the points are scattered about, although for 2.5 cm. the scattering is less. As before the size of the plateau increases and the value of the threshold potential rises with increasing proportions of the vapour.

*Helium-N-butyl and helium-amyl alcohols (laboratory).*—With these only three concentrations of 0.5 cm., 1.0 cm. and 1.5 cm. vapour pressure were tried, as at ordinary room temperatures their vapour pressure is small. Of course, higher concentrations could be used by using a temperature bath for the G.M. tube counter, but no useful purpose would have been served as the object of these investigations was to find the best helium-organic vapour

mixture for G.M. counter fillings for Indian climates. The results are shown in fig. 5.

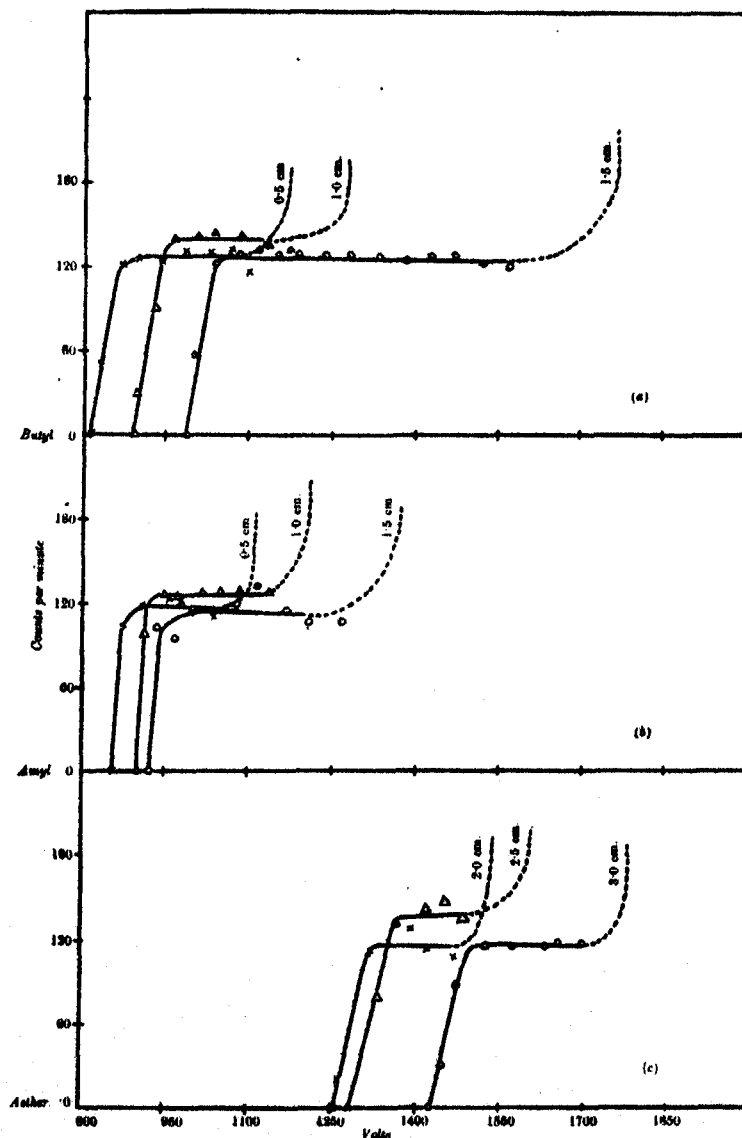


FIG. 5. Volts-counts graphs at various pressures for (a) *N*-butyl alcohol, (b) Laboratory amyl alcohol, (c) Ethyl ether.

*Helium-ethyl ether.*—With ether pressures of 2.0 cm., 2.5 cm. and 3.0 cm. were tried. The plateau, though flat, is not so good as for helium-methyl alcohol or helium-ethyl alcohol. The threshold potentials also are rather high.

## IV. DISCUSSION.

In all the cases studied it is observed that the value of the threshold potential goes on increasing with partial pressures of the vapour admixture in helium. Werner (1934) and Trost (1937) have both shown that the change of threshold potential with pressure in the G.M. counter can be expressed in terms of certain equations. Trost treats the counter as a coaxial cylinder and writes for the field at any point distant  $r$  from the axis of the wire,

$$E_r = \frac{V}{r \ln r_a/r_i},$$

where  $V$  is the potential on the wire and  $r_a$ ,  $r_i$  the radii of the cylinder and the wire respectively. The field inside the counter is not uniform radially, being stronger near the wire. At a certain potential (threshold potential) the ions produced in the counter atmosphere acquire sufficient energy to ionise other atoms or molecules by collision and thus a discharge is started. The free path in which the electrons have to acquire this energy depends inversely on the pressure, i.e.  $\lambda = \frac{k}{p}$ . Now if we suppose (as is found experimentally) that the minimum field  $E_0$  corresponding to a potential  $V_0$  on the wire is proportional to pressure, i.e.  $E_0 = p\epsilon_0$ , we get

$$E_0 = p\epsilon_0 = \frac{V_0}{\left(r_i + \frac{nk}{p}\right) \ln \frac{r_a}{r_i}}$$

or

$$V_0 = (pr_i + nk) \ln \frac{r_a}{r_i} \epsilon_0,$$

where  $n$  is the number of collisions which the electrons make from the position of minimum field to the wire, and  $\epsilon_0$  and  $k$  are constants. This gives a linear variation between  $V_0$  and  $p$ .

Trost varied the pressures for known concentrations of the mixture and found that the threshold-potential increased linearly with the pressure. We, on the other hand, have carried out all our investigations with a total pressure of 10 cm. in the counter, though the proportion of the organic vapour present was altered regularly from one set of observations to the next. Our experimental observations suggest a linear relationship between the threshold potential and the relative proportions of the organic vapour inside the counter. Trost has studied the characteristics of counters filled with argon and ethyl alcohol at different pressures and for different proportions of argon and alcohol. In any one run of observations he varied the total pressure inside the counter keeping the relative proportions of argon and ethyl alcohol the same and found the threshold potential to increase with increase of pressure. This he repeated for different proportions of the mixture. If from his observations we find the values of the threshold potential for different proportions of the argon-ethyl alcohol mixture at the same total pressure, namely of 10 cm., we again get a

linear relation between the threshold potential and the percentage of the alcohol vapour inside the counter. We are of opinion that this increase in

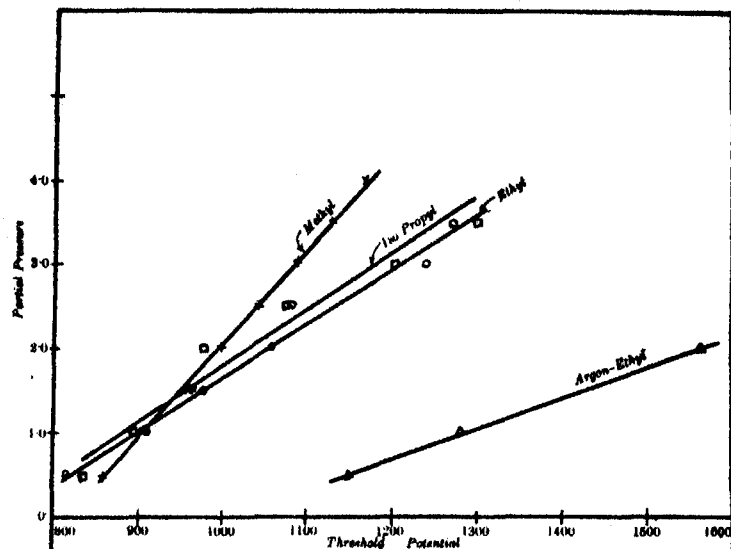


FIG. 7. Relation between partial pressure and threshold potential. Argon-Ethyl curve is obtained from Trost's observations.

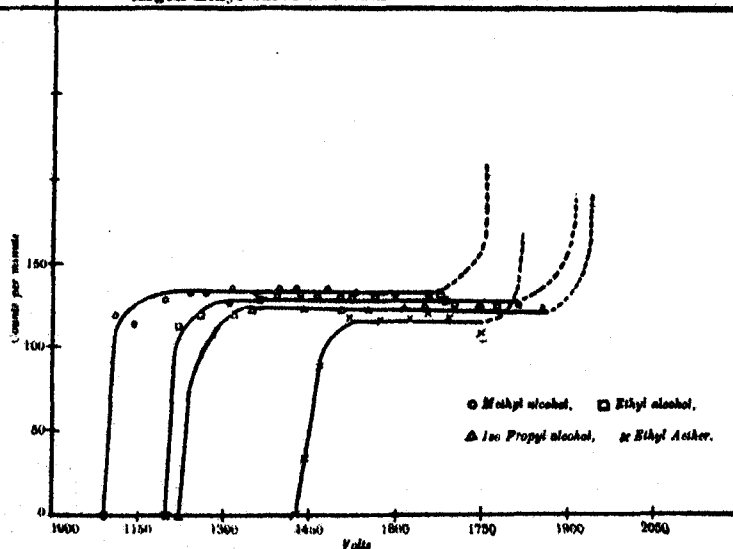


FIG. 6. Comparative graphs for various mixtures at partial pressure of 3.0 cm. in a total of 10.0 cm. pressure in the counter.

threshold potential is due to the fact that greater amounts of the organic vapour inside the counter decrease the effective mean free path for the ions by increasing their size considerably. In other words, the linear relationship

obtained by Trost between pressure and threshold potential is due to a superposition of two causes, namely (i) an increase of total pressure, and (ii) an increase in the quantity of the alcohol vapour inside. Moreover, the ionisation potential of the organic vapour being lower than that of the inert gas, it is the organic vapour atoms or molecules which will be easily ionised by collision and consequently if in any counter atmosphere the amount of the organic vapour present is smaller than a certain quantity, the threshold potential should increase even though the total pressure be decreased. This in fact was found to be the case by Trost. To determine, however, the exact relationship between threshold potential on the one hand and the percentage of the alcohol vapour on the other we require further study and analysis which we hope to undertake in the very near future.

The relationship between the threshold potential and the ratio of the alcohol vapour for the various mixtures studied is shown in fig. 7. The argon-ethyl alcohol curve is taken from Trost's observations. It is to be noticed that the threshold potential with helium-alcohol mixtures is consistently lower than that for argon-alcohol mixture and that for helium mixtures the curves are steeper.

We wish to express our gratitude to Professor J. B. Seth for the facilities given to us, to Dr. P. K. Kichlu and Mr. Balmokand for the supply of helium and to Mr. B. D. Chhabra for the use of the cathode ray oscillograph.

#### SUMMARY.

The characteristics of Geiger-Müller Counters filled with helium in mixture with vapours of organic alcohols have been studied with a view to finding the best proportions of the mixture for counter fillings. The counter consisted of a pyrex tube containing a thin oxidised copper cylinder (2.3 cm. diameter, and 12.6 cm. length) with a nickel wire (0.1 mm. diameter) running along its axis. Determinations of the threshold potentials and the nature and size of the plateau have been made. Vapours from ethyl, methyl, normal butyl, isopropyl and laboratory amyl alcohols have been used. The helium used had been previously purified by means of activated charcoal at liquid air temperature, and a total pressure of 10 cm. was kept in the counter. Starting with a 0.5 cm. admixture of alcohol vapour in a total pressure of 10 cm. it was found that the threshold potential increased with increasing proportions of the alcohol vapour, the length of the plateau also increased but as the vapour pressure increased beyond 3 cm. the plateau no longer remained horizontal but became an ascending one. As a result of our investigations we find that methyl and ethyl alcohols are the most suitable and that best results are obtained with them at 3 to 2.5 cm. partial pressures. The values of the threshold potentials for increasing proportion of the vapour have been compared with the formula given by Trost and a satisfactory agreement is noticed.

## REFERENCES.

- Curran, S. C. and Petrzilka, V. (1939). Methods of Construction of Geiger-Müller Counters and their use in Coincidence Experiments. *Proc. Camb. Phil. Soc.*, **35**, 309.
- Evans, R. D. (1934). Voltage Stabilizer controlled by a thermionic pentode. *Rev. Sci. Inst.*, **5**, 371.
- Gingrich, N. S. (1936). Voltage Stabilizer for amplifiers for Geiger Counters. *Rev. Sci. Inst.*, **7**, 207.
- Trost, Adolf (1937). Über Zahlrohr mit Dampfzusatz. *Zeit. für Physik*, **105**, 399.
- Werner, Sven (1934). Die Entladungsformen im Zylinderischen Zahlrohr. (i) *Zeit. für Physik*, **90**, 384; (ii) *Zeit. für Physik*, **92**, 705.





# THE ULTRA-VIOLET BAND SPECTRUM OF MERCURY IODIDE.

By M. G. SASTRY, *Research Fellow, Andhra University, Waltair.*

(Communicated by Dr. K. R. Rao, D.Sc., F.N.I.)

(Received February 3, 1942.)

## ABSTRACT.

In continuation of the work on HgCl and HgBr bands in the ultra-violet the author has investigated the bands of HgI in the same region. The Class I system reported by Wieland has been photographed with a Quartz Littrow spectrograph and measured. It is found to consist of two systems designated as  $\alpha_1$  and  $\beta_1$ , having a common final state, probably a  $^2\Sigma$ . The interval between the upper states is found as  $766\text{ cm}^{-1}$ .

A new system designated as Class A is obtained in the region  $\lambda 2540$  and is assigned to HgI. It is attributed to the electronic transition  $^2\Pi \rightarrow ^2\Sigma$ , showing four component heads  $P_1Q_1P_2Q_2$ , resembling the Class II system of HgCl. The electronic separation is  $126\text{ cm}^{-1}$ .

Vibrational formulae and constants for the three systems have been calculated.

## INTRODUCTION.

Numerous investigations have been carried out on the band spectra of the diatomic halides (Jevons, 1932), particularly the chlorides (Asundi, 1935; Parker, 1934, 1935) of the elements of the left sub-group II of the Periodic Table and it is fairly well established that these molecules give rise to band systems in the visible and in the ultra-violet regions, involving electronic transitions between a higher  $^2\Pi$  or  $^2\Sigma$  and a lower  $^2\Sigma$  or  $^2\Pi$ . That the ground state of the molecules is a  $^2\Sigma$  is also shown in a few cases by More & Cornell (1938), Morgan (1936), Jenkins and Grinfeld (1934), and Frederickson and Hogan (1934) by the study of the absorption spectrum and of the rotational structure of the bands. The spectra of the halides of the elements of the right sub-group II—Zn, Cd, and Hg—do not appear to have been investigated. The most important work on the halide spectra is that due to Wieland (1929). Later, Cornell (1938) investigated the band spectra of the chlorides of Zn, Cd, and Hg and Subbaraya and others (1937) studied the visible emission bands of Cd and Hg. The fluorides of these elements are not known to have any characteristic bands at all; the system attributed to CdF by Asundi and others (1935) has been shown to be due to CaF by Pearse and Gaydon (1938).

Our knowledge of the spectra, both in emission and in absorption, is still very meagre and it is felt desirable to investigate these further and more extensively before any definite correlation of the various systems and the interpretation of the electronic states of the molecule can be discussed. In

two recent papers the author (1941) described the analysis of the emission bands of  $\text{HgCl}$  and  $\text{HgBr}$  in the ultra-violet and the present paper deals with the results obtained in the case of Mercury Iodide.

Mulliken (1925) mentioned the excitation of the characteristic bands of Mercury Iodide in the nitrogen after glow but there is no published record of any measurements or analysis of the bands. Between  $\lambda 5000$  and  $\lambda 2500$  Wieland photographed the bands in emission by sending a high frequency discharge through the vapour of Mercury Iodide contained in a quartz tube with a low dispersion instrument (a maximum of about 10A per mm.). As in  $\text{HgCl}$ ,  $\text{HgBr}$ , and in the halides of the other elements Zn and Cd, the bands due to  $\text{HgI}$  fall into a number of classes thus:—

Class III	..	..	From $\lambda 4500$ to $\lambda 3400$	diffuse
„ II	..	..	From 3100 to 2800	sharp
„ I	..	..	From 2800 to 2650 ?	sharp
	..	..	2700 ? 2530	sharp

The visible bands forming Class III were also studied by him later in fluorescence. Subbaraya and others measured these bands in emission in the first order of a 10 ft. Concave Grating and suggested a vibrational analysis indicating that the bands are probably due to the electronic transition between  $^2II$  and  $^2\Sigma$  but neither of these levels is common to Wieland's systems.

Little work was done on the Class II and Class I systems lying in the ultra-violet, the latter having not even been measured. The Class II system was ascribed by Wieland to the triatomic molecule  $\text{HgI}_2$  and the Class I to the diatomic molecule  $\text{HgI}$  but no analysis was reported. The present work considers these two ultra-violet systems and an additional system (henceforth styled as Class A) newly obtained by the author in the region  $\lambda 2540$ . The analysis of the Class I and Class A systems will be described here and that of Class II in a succeeding communication.

#### EXPERIMENTAL.

The experimental arrangement and the method of excitation of the bands were the same as those adopted in the case of  $\text{HgCl}$  and  $\text{HgBr}$  and described previously. The discharge in Mercury Iodide was intense violet and found to run easily. After an initial gentle heating, the tube worked very smoothly. The spectra were taken with a Hilger medium and a large Littrow Quartz spectrograph. The dispersion of the latter at  $\lambda 2600$  was about 3A per mm. The time of exposure extended from half an hour to three hours.

Plate IV is a reproduction of the bands. Fig. (a) between  $\lambda 2650$  and  $\lambda 2550$  shows the Class I system. There is a short region in which this system is found to overlap with Class II. Fig. (b) is the newly obtained Class A system, more enlarged.

To ascertain experimentally the probable origin of the bands, spectra of various other compounds containing Hg and I are also taken and by comparison

it is found that all the above bands appeared only in discharges through HgI. Water vapour was invariably present as an impurity and could not be eliminated by the usual simple devices of introducing an absorbing agent in a side tube. But it gave no difficulty as the OH bands do not overlap with the systems of HgI considered at present.

## RESULTS AND DISCUSSION.

On the analogy of the band systems of HgCl and HgBr, the Class II and Class I systems of HgI have both been ascribed by the author to the diatomic molecule. All these occur under identical conditions of excitation, in powerful electrical discharges in which bands due to polyatomic molecules are not expected to appear so intensely. On this basis, a vibrational analysis of the bands has been attempted. Tables I(a) and I(b) give the wave-lengths, wave numbers, and the visual estimates of the intensities of all the measured band heads belonging to the two systems. The measurements are the averages of two different plates but the accuracy is reduced on account of the errors of setting due to the diffuseness of the bands, although the dispersion of the instrument used is fairly large.

TABLE 1: Catalogue and classification of the band heads of the Class I system of HgI.

(a) $\alpha_1$ system				(b) $\beta_1$ system			
Wave-length	Wave number	Int.	Classification ( $v'$ , $v''$ )	Wave-length	Wave number	Int.	$\delta\nu$
			(8,0)	2805.98	38361.7	2	
			(9,1)	07.36	341.5	2	
2556.68	39101.5	4	(10,2)	08.09	330.8	3	770.7
57.36	091.1	3	(11,3)	08.69	322.0	2	769.1
57.95	082.1	2	(7,0)	08.95	318.2	2	763.9
58.56	072.8	3	(8,1)	09.71	307.0	2	765.8
59.17	063.4	4	(9,2)	10.58	294.2	2	769.2
59.94	051.7	2	(10,3)	11.10	286.6	2	765.1
60.65	040.8	1	(6,0)	11.81	276.3	1	764.5
61.27	031.4	2	(7,1)	12.84	261.1	2	770.3
62.00	020.3	3	(8,2)	13.28	254.6	3	765.7
62.64	010.6	3	(9,3)	14.14	242.1	3	768.5
63.49	38997.6	1	(5,0)	14.94	230.0	2	767.6
63.77	993.3	3					
64.29	985.4	3	(6,1)	15.68	219.5	2	765.9
64.63	980.3	3	(7,2)	16.07	213.9	6	766.4
				16.74	204.0	6	
65.96	960.1	4	(4,0)	18.00	185.7	5	774.4 ?
			(5,1)	18.46	179.2	3	
67.54	936.1	3	(6,2)	18.88	172.7	2	763.4
68.14	927.0	3	(7,3)	19.40	165.3	2	761.7
68.98	914.3	4	(3,0)	20.89	143.6	3	770.7
			(4,1)	21.40	136.1	3	

TABLE 1—continued.

(a) $\alpha_1$ system				(b) $\beta_1$ system			
Wave-length	Wave number	Int.	Classification ( $v', v''$ )	Wave-length	Wave-number	Int.	$\delta\nu$
2570.17	38896.2	4	(5,2)	2621.76	38130.9	6	765.3
70.95	884.4	4	(6,3)	22.03	127.1	6	757.3
71.98	868.9	5	(2,0)	23.72	102.5	6	766.4
72.46	861.7	4	(3,1)	24.23	095.1	6	766.6
			(5,3)	25.00	083.8	3	
74.65	827.2	4	Hg?				
74.97	823.7	4	(1,0)	26.78	058.1	3	765.6
75.26	819.4	1	(2,1)	27.26	051.1	2	768.3
75.85	810.5	2	(3,2)	27.68	045.0	1	765.6
76.30	803.7	2	(4,3)	28.17	038.0	1	765.7
77.23	789.7	1	(5,4)	28.76	028.0	1	761.7
77.70	782.7	5	(0,0)	29.63	016.8	6	765.9
			(1,1)	30.02	011.1	6	
79.26	759.2	5	(3,3)	31.21	37994.0	1	765.2
80.18	745.4	4	(4,4)	31.97	983.0	1	762.4
81.28	728.9	2	(0,1)	33.20	965.4	5	763.5
			(1,2)	33.39	962.4	5	
82.20	715.1	4	(2,3)	34.12	952.0	3	763.1
82.76	706.7	4	(3,4)	34.71	943.6	3	763.1
			(4,5)	35.75	928.6	3	
83.61	693.9	1	(5,6)				
84.49	680.7	2	(0,2)	36.36	919.8	3	
85.16	670.8	3	(1,3)	36.67	915.3	2	765.4
				37.31	906.1	3	764.7
85.57	664.6	3	(2,4)	37.66	901.1	3	
85.89	659.8	2		37.80	899.2	3	765.4
86.14	656.1	2	(3,5)	38.54	888.4	2	767.7
86.65	648.4	2	(4,6)	38.96	882.4	2	766.0
87.30	638.8	1	(5,7)	39.71	871.7	3	767.1
				40.08	866.3	3	
87.80	629.9	2	(0,3)	40.39	861.9	3	768.0
88.64	618.8	3	(1,4)	40.91	854.5	3	764.3
				41.44	846.8	3	
88.96	614.0	2					
89.20	610.4	3	(2,5)	41.84	841.1	5	769.3
89.85	600.7	2	(3,6)	42.16	836.5	4	764.2
90.33	593.5	2	(4,7)	42.60	830.4	2	763.1
				43.15	822.4	2	
91.06	582.7	2	(5,8)	43.59	816.0	2	766.7
91.52	575.9	2	(0,4)	44.13	808.4	2	767.5
92.18	566.0	2	(1,5)	44.60	801.0	2	765.0
92.47	558.4	2	(2,6)	45.18	793.3	2	765.1
93.42	547.6	2	(3,7)	45.84	783.9	3	763.7
				46.21	778.7	2	
93.56	545.5	1					
93.93	540.0	1	(4,8)	46.40	775.9	2	764.1
94.34	530.9	1	(5,9)	46.97	767.8	3	763.1
94.91	525.5	1	(6,10)	47.47	760.7	3	764.8
95.41	518.0	2	(1,6)	48.06	752.2	2	765.8
				48.45	746.7	2	
96.85	496.6	1	(3,8)	49.59	730.4	2	765.2

TABLE 1—concluded.

(a) $\alpha_1$ system				(b) $\beta_1$ system			
Wave length	Wave number	Int.	Classification ( $v'$ , $v''$ )	Wave-length	Wave-number	Int.	$\delta\nu$
2597.84	38482.0	1	(0,6)	2650.53	37712.2	2	769.8
98.60	470.8	1	(1,7)	51.43	704.3	1	766.5
99.31	456.2	1	(2,8)	52.69	686.4	2	769.8
99.77	453.5	1					
2600.42	443.8	1	(3,9)	53.13	680.2	2	763.6
00.97	435.8	1	(4,10)	53.99	667.8	2	768.0
01.36	430.1	1	(0,7)	54.42	661.8	2	768.3
			(0,8)	57.98	611.3	2	

However, the tables give data obtained for the first time as Wieland, who reported these bands, could not measure them probably on account of the very small dispersion used by him.

A starting point in the analysis was afforded by the detection of a common wave number interval of about  $766\text{ cm}^{-1}$  among the band heads of the Class I system. An examination of the plate (see Fig. (a)) indicated that what was reported by Wieland as the Class I system consisted of two widely separated systems here designated as  $\alpha_1$  and  $\beta_1$  with a common level, the other levels having the characteristic interval mentioned above. A similar doublet characteristic is found in the bands of CaI, SrI and BaI by Mesnage (1939) and also in the Class III bands of HgI (Subbaraya and others, 1937). The vibrational assignment of each head is shown in the fourth column of Table 1. The system origin is nearly at the centre, the sequences  $\Delta v = -1, -2$  being better developed than the other sequences  $\Delta v = +1, +2$ . The intensities of the band heads of the  $\alpha_1$  and  $\beta_1$  systems are shown in diagonal array in Tables (2) and (3). A very peculiar feature is the absence of the (1,1) and (2,2) heads in the  $\Delta v = 0$  sequence of the  $\alpha_1$  system. It cannot perhaps be ascribed to perturbation of any of these vibrational levels for other heads involving  $v'$  or  $v'' = 1$  or 2 are present. It might be suggestive here to note a similar abrupt absence of the (1,1) head in the bands of HgCl (Class I) system observed both by Wieland (1929) and by Cornell (1938) although the (1,0) and (0,1) heads of the same system are observed to be fairly intense.

The analysis does not show any level in common with the visible bands and all attempts at an alternative classification on the assumption of a common level were unsuccessful. It is only with the present arrangement that nearly all the band heads have entered into the scheme. The  $\Delta G(v)$  intervals are

not quite consistent throughout the array but are considered to be due to the uncertainties of measurement on account of the diffuseness of the heads. The estimated means of these intervals have led to the following formula for the heads assigned to the  $\alpha_1$  system:—

$$\nu = 38786.7 + [47.7(v' + \frac{1}{2}) - 0.8(v' + \frac{1}{2})^2] \\ - [55.2(v'' + \frac{1}{2}) - 0.8(v'' + \frac{1}{2})^2]$$

TABLE 2: Intensity distribution in the  $\alpha_1$  system.

$\begin{smallmatrix} v'' \\ \backslash \\ v' \end{smallmatrix}$	0	1	2	3	4	5	6	7	8	9	10	11
0	5	2	2	2	2	..	1	1				
1	4	..	..	3	3	2	2	1				
2	5	1	..	4	3	3	2	..	1			
3	4	4	2	5	4	2	2	2	1	1		
4	4	..	..	2	4	..	2	2	1	..	1	
5	1	..	4	..	1	..	1	1	2	1		
6	1	3	3	4								
7	2	2	3	3								
8		3	3									
9			4	3								
10			4	2								
11				3								

TABLE 3: Intensity distribution in the  $\beta_1$  system.

$\begin{smallmatrix} v'' \\ \backslash \\ v' \end{smallmatrix}$	0	1	2	3	4	5	6	7	8	9	10	11
0	6	5	2	3	2	..	2	2	2			
1	3	6	5	3	3	2	2	1				
2	6	2	..	3	3	5	2	..	2			
3	3	6	1	1	3	2	4	3	2	2		
4	5	3	..	1	1	3	2	2	2	..	2	
5	2	3	6	3	1	..	..	3	2	3		
6	1	2	2	6							3	
7	2	2	6	2								
8		2	3									
9		2	2	3								
10			3	2								
11				2								

For the  $\beta_1$  system the formula is

$$\nu = 38022.1 + [44.2(v' + \frac{1}{2}) - 0.4(v' + \frac{1}{2})^2] \\ - [55.5(v'' + \frac{1}{2}) - 0.8(v'' + \frac{1}{2})^2]$$

The constants show that the final level is common to the two systems and is probably a  $^2\Sigma$  state of the molecule.

A confirmation of the vibrational assignments by the study of the isotope effect has not been possible. Iodine is not known to have isotopes. The Hg isotope effect has no doubt been detected in the Class I system of HgBr by Wieland—the component heads due to Hg<sup>198</sup> and Hg<sup>202</sup> with Br<sup>79</sup> and Br<sup>81</sup> having been identified. But in the HgI bands, when the classified heads are assumed to be due to Hg<sup>202</sup>I<sup>127</sup> and the isotopic displacement is calculated, the shift for Hg<sup>198</sup>I<sup>127</sup> even for the heads (11,3) of the  $\alpha_1$  and  $\beta_1$  systems are obtained as 0.76 and 1.2 cm<sup>-1</sup> respectively—a difference which is not observable on account of the diffuseness of the bands. The diffuseness itself may be partly due to this unresolved isotope effect.

*Class A system.*

Table 4 gives the wave-length and other data of this newly obtained system. The analysis is simple, the band heads forming obviously narrow sequences. The system, in its general arrangement, resembles the Class II system of HgCl in the region  $\lambda 2800$ , with the difference that the component *P* heads of the (0,0) sequence are also developed. The number of the heads suggests that the transition involved is  $^2\Pi-^2\Sigma$ , with the electronic separation of about 126 cm<sup>-1</sup>. For the *Q*<sub>1</sub> heads, which are the strongest, the vibrational formula

$$\begin{aligned} \nu = & 39231.1 + [98.1(v' + \tfrac{1}{2}) - 2.4(v' + \tfrac{1}{2})^2] \\ & - [92.7(v'' + \tfrac{1}{2}) - 2.0(v'' + \tfrac{1}{2})^2] \end{aligned}$$

has been obtained.

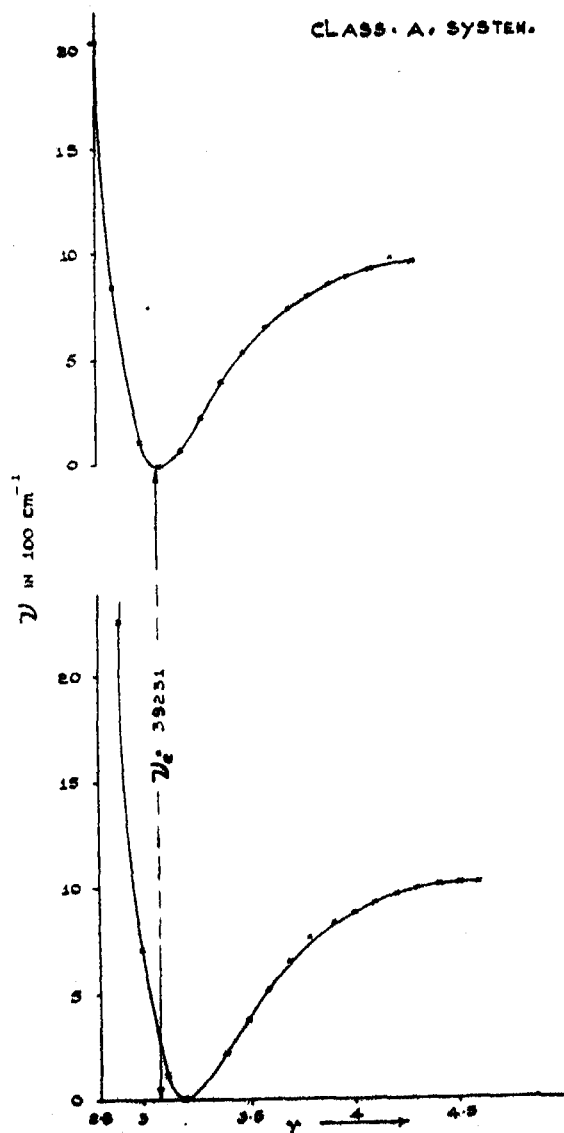


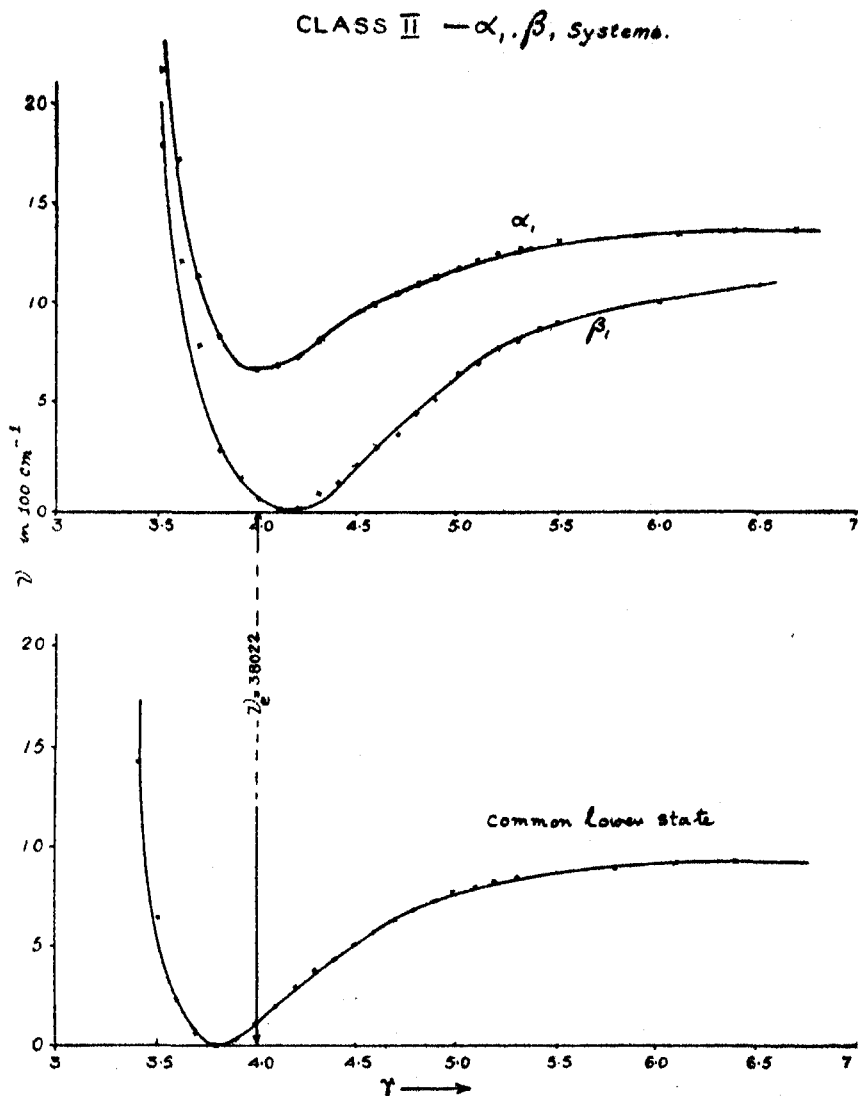
TABLE 4: Catalogue and classification of the band heads of the Class A system of HgI.

Wave-length	Wave number	Int.	Classification ( $v'$ , $v''$ )
2588.40	39383.1	1	(5,5)
38.71	378.2	1	(4,4)
39.02	373.5	1	(3,3)
39.29	369.3	2	(2,2)
39.57	364.9	2	(1,1)
39.84	360.8	2	(0,0)
40.18	355.5	4	(4,4)
40.86	345.0	1	(3,3)
41.24	339.1	1	(2,2)
41.65	332.7	1	(1,1)
42.06	326.4	1	(0,0)
42.33	322.2	1	(8,9)
42.64	317.4	1	(7,8)
42.95	312.6	1	(6,7)
43.47	304.6	1	(5,6)
43.89	298.1	2	(4,5)
44.29	291.9	2	(3,4)
44.68	285.9	3	(2,3)
45.05	280.1	3	(1,2)
45.62	275.4	3	(0,1)
46.14	263.4	1	(5,6)
46.58	256.6	2	(4,4)
47.30	245.5	2	(3,3)
47.44	243.3	2	(2,2)
47.73	238.8	3	(1,1)
48.04	234.1	3	(0,0)
48.77	222.8	2	(4,4)
49.04	218.7	2	(3,3)
49.29	214.7	1	(2,2)
49.49	211.7	1	(1,1)
49.84	206.6	1	(0,0)
50.63	194.4	2	(8,9)
50.89	190.2	2	(7,8)
51.13	186.5	2	(6,7)
51.39	182.5	2	(5,6)
51.84	175.7	3	(4,5)
52.23	169.6	3	(3,4)
52.78	161.4	3	(2,3)
53.28	153.6	4	(1,2)
53.76	146.2	5	(0,1)

The following table gives the values of the energy (in volts) of dissociation and the figures show the potential energy curves for the three systems of bands dealt with in the present paper :—

System	$D'$	$D''$	$\nu$ (atom)
$\alpha_1$ ..	0.09	0.12	4.75
$\beta_1$ ..	0.15	0.12	4.72
A ..	0.14	0.13	4.85





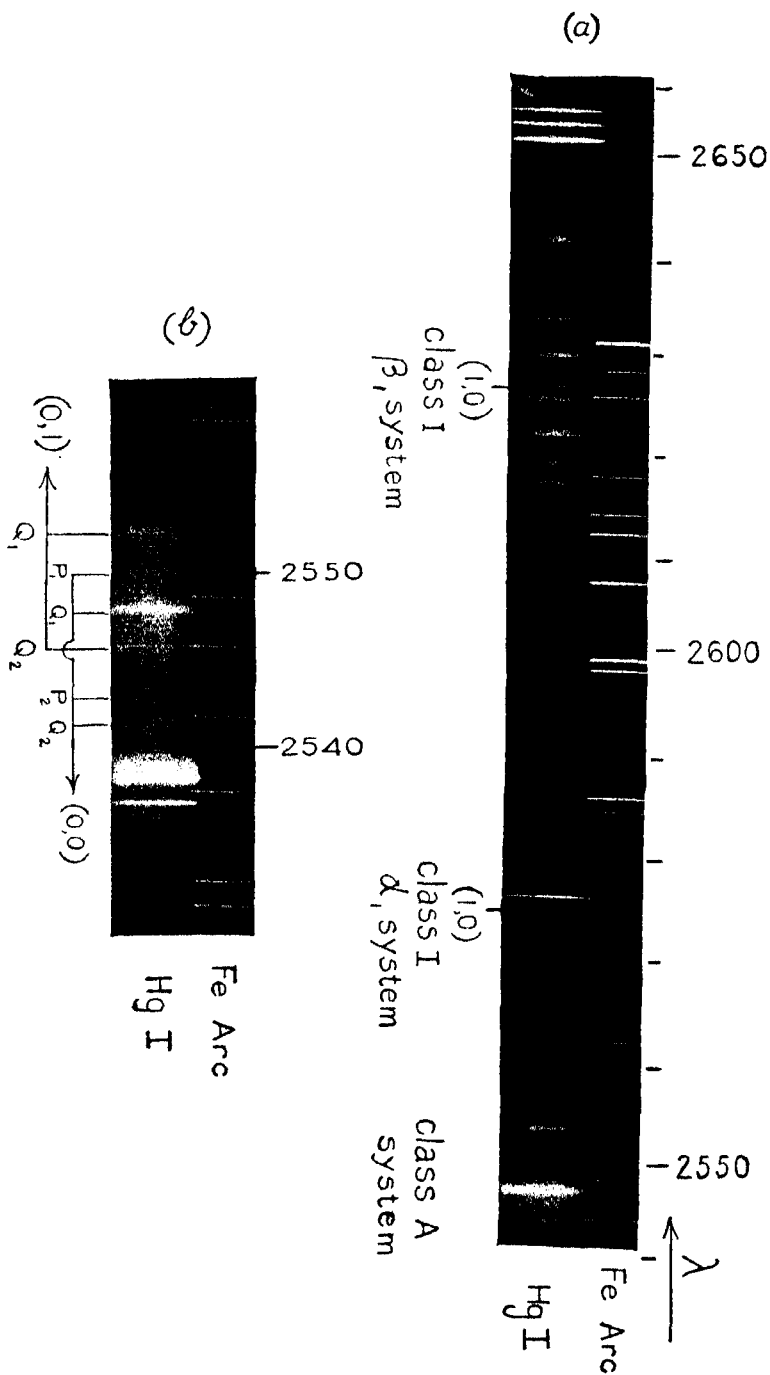
The last column suggests that the dissociation products for the respective electronic states involved in the emission of all these systems are probably the same. This value of  $\nu$  (atom) agrees closely with the atomic excitation energy of 4.9 volts corresponding to the transition  $\text{Hg } ({}^1S)$  to  $\text{Hg } ({}^8P)$  so that these atomic states constitute presumably the respective products of dissociation of the lower and upper electronic states concerned.

The author is indebted to Prof. M. N. Saha, F.R.S., and to Dr. K. R. Rao for their kind interest in the work and to the Andhra University for the award of a Fellowship.

## REFERENCES.

- Asundi, R. K. 1935. Band systems and structure of CaCl. *Proc. Ind. Acad. Sci.*, **1A**, 830.
- Asundi, R. K., Samuel, R., and Zakiuddin, M. 1935. The band systems of cadmium fluoride. *Proc. Phys. Soc. (Lond.)*, **47**, 235.
- Cornell, S. D. 1938. Ultra-violet band spectra of HgCl, CdCl, and ZnCl. *Phys. Rev.*, **54**, 341.
- Frederickson, W. R. and Hogan, Martin E. 1934. The ultra-violet bands of Beryllium chloride. *Phys. Rev.*, **46**, 454.
- Jenkins, F. A. and Grinfeld, Rafael. 1934. The spectrum of MgF. *Phys. Rev.*, **45**, 229.
- Jevons. Report on band spectra of diatomic molecules (1932).
- Mesnage, P. 1939. Iodures alcalino-terreux. *Annales de Physique*, **12**, 69.
- More, K. R. and Cornell, S. D. 1938. The band spectra of SrCl, and SrH. *Phys. Rev.*, **53**, 806.
- Morgan, Frank. 1936. Band spectra of MgCl, MgBr, and MgI in absorption. *Phys. Rev.*, **50**, 603.
- Mulliken, R. S. 1925. Bands of copper iodide. *Phys. Rev.*, **26**, 28.
- Parker, A. E. 1934. Vibrational analysis of BaCl and BeCl bands. *Phys. Rev.*, **45**, 752.
- 1934. Band systems of BaCl. *Phys. Rev.*, **46**, 301.
- 1935. Band systems of MgCl, CaCl, and SrCl. *Phys. Rev.*, **47**, 349.
- Pearse, R. W. and Gaydon, A. G. 1938. A note on the spectrum of Cadmium Fluoride CdF. *Proc. Phys. Soc. (Lond.)*, **50**, 711.
- Sastry, M. G. 1941. The ultra-violet band spectrum of mercuric chloride and mercury bromide. *Proc. Nat. Inst. Sci. Ind.*, **7**, 351, 359.
- Subbaraya, T. S., Nagesha Rao, B., and Narayana Rao, N. A. 1937. On the band spectrum of mercurous iodide. *Proc. Ind. Acad. Sci.*, **5A**, 365.
- Wieland, K. 1929. Band spectra of Mercury, Cadmium, and Zinc halides. *Helv. Phys. Acta*, **2**, 46, 77.





The ultra-violet band spectrum of Mercury Iodide.



# ON INTEGRATION OF STELLAR EQUATIONS FOR BETHE'S LAW OF ENERGY GENERATION.

By U. R. BURMAN.

(Communicated by Prof. N. R. Sen.)

(Received January 27, 1942.)

## ABSTRACT.

The application of Bethe's law of energy generation in the internal constitution of Stellar bodies on the assumption of the radiative transfer of energy, is discussed. Three numerical integrations of the stellar equations have been performed for a central temperature  $2.10^7 K$  and central densities 80, 40, and 1 gm./cm.<sup>3</sup> The configurations all appear to be infinite, behaving ultimately as isothermal gas spheres.

## 1. Introduction.

Bethe<sup>1</sup> has recently suggested a mechanism for the generation of energy in stellar interiors, where the temperature is high enough to produce transmutations of the light atomic nuclei. By this process, the hydrogen content, which is quite in excess in the main sequence stars, takes part in a reaction producing composite nuclei (He) in presence of carbon and nitrogen, which merely behave as catalysts. The binding energy of these composite nuclei is set free and this furnishes the energy necessary to maintain the radiation from stars. The object of the present paper is to study some consequences of this theory when applied to the internal structure of stellar bodies.

We have carried out some numerical integrations of the stellar equations of equilibrium taking as luminosity function the one given by Bethe's theory of energy generation in stellar interiors in its accurate form. Several numerical integrations of the stellar equations<sup>2</sup> are found in the literature on the subject, of which the one which bears some likeness to the present case, is that corresponding to the point-source of energy. The plan followed here has been to start with Strömberg's model of a star like the Sun, having a central temperature of the order of 20 million degrees. Assuming this central temperature, integrations have been performed from the centre, for central densities 80, 40 and 1 gm./cm.<sup>3</sup>, all for a hydrogen concentration of 35 p.c. (by weight), and an opacity formula given by Kramers' law with a continuously varying guillotine factor (except in the last case where it is treated as a constant). The ratio of radiation to gas pressure in the neighbourhood of the centre in the three cases is respectively .003, .006, .25. The radiative transfer of energy has been assumed throughout after an examination of the limit where the radiative gradient is to be replaced by an adiabatic one. It is expected



that a comparison of these models with the standard model or the point-source models will be of considerable interest and help us to explore the possibilities in this line.

The results of integrations have been given in three tables. It is found that none of the three cases really give a stellar body configuration, and all these gas spheres attain isothermal conditions after varying distances from the centre.

According to Bethe's<sup>1</sup> law of energy generation, the energy generated per gm. per sec. may be put in the form

$$\epsilon = \epsilon_0 \rho T^{-\frac{1}{2}} e^{-\frac{B}{T^{\frac{1}{2}}}} \quad \dots \quad (1.1)$$

with

$$\epsilon = \frac{4}{3^{\frac{1}{2}}} \cdot \frac{X_1 X_2 h \Gamma_0^2 Q}{m_1 m_2 m e^2 Z_1 Z_2} \cdot B^2. \quad \dots \quad (1.2)$$

Here  $\rho$  is the density of the gas,  $X_1, X_2$ , the concentrations (by weight) of the two reacting types of nuclei,  $m_1, m_2$ , their masses,  $Z_1 e, Z_2 e$ , their charges,  $m = \frac{m_1 m_2}{m_1 + m_2}$ , the reduced mass,  $r_0$ , the combined radius,  $Q$ , the energy evolved per nuclear reaction,  $\Gamma/h$ , the probability of the nuclear reaction per sec. after penetration, and

$$B = 3 \left( \frac{\pi^2 m e^4 Z_1^2 Z_2^2}{2 h k} \right)^{\frac{1}{2}}, \quad \dots \quad (1.3)$$

$k$  being the Boltzmann constant, and  $h = h/2\pi$ .

For the reaction  $N^{14} + H$ , the following numerical results given by Bethe<sup>1</sup> are used in this paper.

$$\begin{aligned} r_0 &= 3.9 \times 10^{-13} \text{ cm.}, \\ \Gamma &= 5 \text{ volts} = 7.95 \times 10^{-12} \text{ ergs. (at } T = 2.10^7 K), \\ Q &= 7.8 \times 10^{-8} \text{ M.U.} = 7.8 \times 10^{-8} \times 1.49 \times 10^{-8} \text{ ergs.}, \\ m_1(N^{14}) &= 14 \times 1.66 \times 10^{-24} \text{ gm.}, \\ m_2(H^1) &= 1.66 \times 10^{-24} \text{ gm.}, \\ X_1(N) &= 0.1, \\ X_2(H) &= 0.35, \\ Z_1(N) &= 7, \\ Z_2(H) &= 1. \quad \dots \quad (1.4) \end{aligned}$$

## 2. Stellar equations for steady state of equilibrium.

The fundamental equations for steady state equilibrium of stellar bodies are

$$\frac{dP}{dr} = -G \frac{M(r)}{r^2} \rho \quad \dots \quad (2.1)$$

$$\frac{dp_r}{dr} = -\frac{\chi L(r)}{4\pi c r^2} \cdot \rho \quad \dots \quad (2.2)$$

$$dL(r) = 4\pi r^2 \epsilon dr \quad \dots \quad (2.3)$$

$$dM(r) = 4\pi r^2 \rho dr \quad \dots \quad (2.4)$$

where  $P = p_g$  (gas pressure) +  $p_r$  (radiation pressure),

$\rho$  = density,

$M(r)$  = mass within a sphere of radius  $r$ ,

$L(r)$  = luminosity at distance  $r$ , i.e. energyflux across a spherical surface of radius  $r$ ,

$c$  = velocity of light,

$G$  = constant of gravitation,

$\epsilon$  = energy evolved per sec. per gm. as determined by Bethe's formula,

$\chi$  (opacity coefficient)

$$= \chi_0 \frac{\rho}{t T^{\frac{1}{2}}} \text{ (Kramers' law), } \dots \quad (2.5)$$

with  $\chi_0 = 3.9 \times 10^{25} (1 - X_2^2)$ .

In the opacity formula, the guillotine factor  $t$  can according to Bethe, be represented by the form<sup>1</sup>,

$$t = A \rho^{\frac{1}{2}} T^{-\frac{1}{2}} \quad \dots \quad (2.6)$$

for densities between 10 and 100, and for temperatures between  $10^7 K$  and  $3.10^7 K$ ,  $A$  being a constant.

Bethe does not give the value of this constant  $A$ . We have constructed tables connecting  $t$  and  $\rho$  for different values of  $T$  whence in conjunction with (2.6) we obtain  $A = 2.5 \times 10^5$ .

We may, therefore, take the dependence of opacity on density and temperature to be given by

$$\chi = \chi'_0 \rho^{\frac{1}{2}} T^{-\frac{1}{2}} \quad \dots \quad (2.5a)$$

and

$$\chi'_0 = \frac{\chi_0}{A}.$$

Let us introduce a change of variables in the stellar equations, by the following substitutions,

$$\left. \begin{aligned} r &= r_0 x, \quad \rho = \rho_0 \sigma, \quad T = T_0 \tau, \quad M = M_0 m \\ L &= L_0 l, \quad p_r = (p_r)_0 q, \quad p_g = (p_g)_0 p \end{aligned} \right\} \quad \dots \quad (2.7)$$

Here  $r_0^*$ ,  $M_0$ ,  $L_0$  are constants of the dimensions of distance, mass, and luminosity respectively, and further

$\rho_0$  = central density,

$T_0$  = „ temperature,

$(p_r)_0$  = „ radiation pressure,

$(p_g)_0$  = „ gas pressure.

---

\* This  $r_0$  should not be confused with the  $r_0$  in equation (1.2).

Writing the pressure equations as

$$p_g = \frac{k}{\mu H} \rho T, \quad p_r = \frac{1}{3} a T^4 \quad \dots \quad (2.8, 2.9)$$

where  $\mu$  = molecular weight,  $H$  = mass of the proton,  $a$  = Stefan's constant, we get on account of the above definitions

$$q = \tau^4, \quad p = \sigma \tau \dots \dots \dots (2.10, 2.11)$$

We now introduce the substitutions (2.7) in the equations (2.1)–(2.4) and putting

$$\begin{aligned} \alpha &= \frac{(p_r)_0}{(p_g)_0}, \quad \beta' = \frac{GM_0 \rho_0}{r_0 (p_g)_0}, \\ (p_r)_0 &= \frac{\chi_0' \rho_0^{\frac{2}{3}} T_0^{-\frac{1}{3}} L_0}{4\pi c r_0} = \frac{1}{3} a T_0^4, \\ L_0 &= 4\pi \rho_0^2 \epsilon_0 T_0^{-\frac{2}{3}} r_0^3, \\ b &= B/T_0^{\frac{1}{3}}, \quad \dots \quad \dots \quad \dots \quad \dots \quad (2.12) \end{aligned}$$

obtain the following equivalent set of equations

$$\frac{dp}{dx} + \alpha \frac{dq}{dx} = -\beta' \frac{m\sigma}{x^2}, \quad \dots \quad \dots \quad (2.13)$$

$$\frac{dq}{dx} = -\frac{\sigma^{\frac{1}{4}} \tau^{-\frac{1}{4}} l}{x^2}, \quad \dots \quad \dots \quad (2.14)$$

$$\frac{dl}{dx} = \sigma^{\frac{2}{3}} \tau^{-\frac{1}{3}} e^{-\frac{b}{\tau^{\frac{1}{3}}}} x^2, \quad \dots \quad \dots \quad (2.15)$$

$$\frac{dm}{dx} = \sigma x^2. \quad \dots \quad \dots \quad \dots \quad (2.16)$$

Now the constants  $r_0$ ,  $M_0$ ,  $L_0$ ,  $\alpha$ ,  $\beta'$ , may be expressed in terms of the chemical composition, the central density and temperature, as follows

$$r_0^2 = \frac{\frac{1}{3}ac}{\epsilon_0 \chi_0} \cdot \frac{T_0^{\frac{2}{3}}}{\rho_0^{\frac{2}{3}}},$$

$$M_0 = 4\pi \left( \frac{\frac{1}{3}ac}{\epsilon_0 \chi_0} \right)^{\frac{3}{2}} \cdot \frac{T_0^{\frac{5}{6}}}{\rho_0^{\frac{1}{2}}},$$

$$L_0 = 4\pi \epsilon_0 \left( \frac{\frac{1}{3}ac}{\epsilon_0 \chi_0} \right)^{\frac{3}{2}} \cdot \frac{T_0^{\frac{5}{6}}}{\rho_0^{\frac{1}{2}}},$$

$$\alpha = \frac{\frac{1}{2}a}{k/\mu H} \cdot \frac{T_0^3}{\rho_0},$$

$$\beta' = \frac{4\pi G}{k/\mu H} \cdot \frac{\frac{1}{2}ac}{\epsilon_0 \chi_0} \cdot \frac{T_0^{\frac{77}{13}}}{\rho_0^{\frac{5}{2}}}. \quad \dots \quad (2.17)$$

Hence for specified  $\mu$ ,  $\rho_0$  and  $T_0$  all the above constants are known. We put in addition  $\mu = 1$ , which is very nearly true for a star in which the  $H_2$ -content is in abundance. The above constants all then depend on  $\rho_0$  and  $T_0$  only.

Those solutions of the equations (2.13)–(2.16) will correspond to a stellar body, for which  $\sigma$ ,  $\tau$  vanish simultaneously for a finite value of the radius. The boundary conditions at the centre are  $\sigma = 1$ ,  $\tau = 1$ ,  $l = 0$ ,  $m = 0$ .

### 3. Density and temperature gradients.

We shall start our solutions at the centre with given central values of the density and temperature, the energy generation being strictly governed by Bethe's formula. Before proceeding with the numerical work we shall investigate the conditions under which the radiative density gradient in the neighbourhood of the centre remains (i) negative, and (ii) stable, for the energy generation law assumed.

The density gradient  $\frac{\partial \sigma}{\partial x}$  will be positive at start from the centre if  $\left(\frac{\partial^2 \sigma}{\partial x^2}\right)_0 > 0$  (the second derivative not vanishing).

From  $p = \sigma \tau$  we get

$$\left(\frac{\partial^2 \sigma}{\partial x^2}\right)_0 = \left(\frac{\partial^2 p}{\partial x^2}\right)_0 - \left(\frac{\partial^2 \tau}{\partial x^2}\right)_0$$

for  $\sigma$  and  $\tau$  both have the value unity at the centre, and the first derivatives of all the three variables vanish there. Equation (2.13) gives on differentiation

$$\begin{aligned} \left(\frac{\partial^2 p}{\partial x^2}\right)_0 + \alpha \left(\frac{\partial^2 q}{\partial x^2}\right)_0 &= 2\beta' \left(\frac{m\sigma}{x^3}\right)_0 - \beta' \left(\frac{\sigma}{x^2} \cdot \frac{\partial m}{\partial x}\right)_0 \\ &= 2\beta' \left(\frac{m}{x^3}\right)_0 - \beta' \cdot \left(\frac{1}{x^2} \cdot \frac{\partial m}{\partial x}\right)_0. \end{aligned}$$

By expanding  $m$  in a Taylor's series about the origin, we obtain

$$\left(\frac{m}{x^3}\right)_0 = \frac{1}{3},$$

so that

$$\left(\frac{\partial^2 p}{\partial x^2}\right)_0 + \alpha \left(\frac{\partial^2 q}{\partial x^2}\right)_0 = -\frac{1}{3}\beta'.$$

It may also be seen without difficulty that

$$\left(\frac{\partial^2 q}{\partial x^2}\right)_0 = -\frac{1}{2}e^{-b},$$

whence

$$\left(\frac{\partial^2 p}{\partial x^2}\right)_0 = -\alpha \cdot \frac{1}{3}e^{-b} - \frac{1}{3}\beta'.$$

Since

$$\left(\frac{\partial^2 \tau}{\partial x^2}\right)_0 = \frac{1}{4}\left(\frac{\partial^2 q}{\partial x^2}\right)_0$$

the condition for the density gradient to be positive at start from the centre becomes

$$\frac{1}{3}\alpha e^{-b} - \frac{1}{3}\beta' + \frac{1}{12}e^{-b} > 0$$

or

$$e^{-b}\left(\frac{\alpha}{\beta'} + \frac{1}{4\beta'}\right) > 1. \quad \dots \quad (3.1)$$

The constants  $\alpha$ ,  $\beta'$  involve the central density  $\rho_0$  and the central temperature  $T_0$  while  $b$  involves  $T_0$  only. For an assigned  $T_0$ , the above inequality will give a limiting value of the central density, which when exceeded will cause the density gradient near the centre to be positive  $\left(\frac{\partial \sigma}{\partial x} > 0\right)$ . Taking  $T_0 = 2.10^7 K$ , and using Bethe's value of  $b$ , viz.  $b = 56$  for this temperature, this limiting value of  $\rho_0$  comes out to be 75 gm./cm.<sup>3</sup> Hence for  $\rho_0 > 75$ ,  $\frac{\partial \sigma}{\partial x} > 0$  from the start, and for  $\rho_0 < 75$  the gradient is negative.

We now discuss the stability of the radiative gradient. The radiative gradient  $\gamma_R$  is given by

$$\frac{dT}{T} = \gamma_R \frac{dP}{P}, \quad \dots \quad (3.2)$$

while the adiabatic gradient is defined by<sup>3</sup>

$$\frac{dT}{T} = \frac{\Gamma_2 - 1}{\Gamma_2} \cdot \frac{dP}{P}, \quad \dots \quad (3.3)$$

where

$$\Gamma_2 = 1 + \frac{(4 - 3\beta)(\gamma - 1)}{\beta^2 + 3(\gamma - 1)(1 - \beta)(4 + \beta)}, \quad \dots \quad (3.4)$$

in which

$$\beta = \frac{p_g}{P} = \frac{\text{gas pressure}}{\text{total pressure}}$$

and  $\gamma$  = ratio of the two specific heats.

The radiative gradient is stable, if<sup>4</sup>

$$\gamma_R < \frac{\Gamma_2 - 1}{\Gamma_2}, \quad \dots \quad \dots \quad \dots \quad (3.5)$$

otherwise the equilibrium will be convective (adiabatic).

We calculate  $\gamma_R$  at the centre thus:—

Since

$$\frac{dT}{T} = \frac{d\tau}{\tau} = \frac{1}{4} \frac{dq}{q} = -\frac{1}{4} \frac{\sigma^{\frac{1}{2}} \tau^{-\frac{3}{2}} l}{x^2} dx$$

and

$$\frac{dP}{P} = \frac{dp + \alpha dq}{p + \alpha q} = -\beta' \frac{\frac{m\sigma}{x^2} dx}{p + \alpha q},$$

hence

$$\frac{dT}{T} \bigg/ \frac{dP}{P} = \frac{1}{4} \frac{\sigma^{\frac{1}{2}}}{\tau^{\frac{3}{2}}} \cdot \frac{p + \alpha q}{\beta'} \cdot \frac{l}{m}.$$

At the centre,

$$\begin{aligned} \left( \frac{dT}{T} \bigg/ \frac{dP}{P} \right)_0 &= \frac{1 + \alpha}{4\beta'} \left( \frac{dl}{dm} \right)_0 \\ &= \frac{1 + \alpha}{4\beta'} \cdot e^{-b}. \end{aligned}$$

Hence radiative equilibrium is stable if

$$\frac{1 + \alpha}{\beta'} e^{-b} < 4 \left( \frac{\Gamma_2 - 1}{\Gamma_2} \right)_0. \quad \dots \quad \dots \quad \dots \quad (3.6)$$

To obtain the value of  $\rho_0$  for which the condition (3.6) is satisfied, we calculate the function  $\frac{1 + \alpha}{\beta'} e^{-b}$  for different values of  $\rho_0$ , arbitrarily assigned. Further

$$\begin{aligned} 1 - \beta &= 1 - \frac{p_g}{P} \\ &= 1 - \frac{p}{p + \alpha q}. \end{aligned}$$

Hence, at the centre,

$$1 - \beta = \frac{\alpha}{1 + \alpha}.$$

We then plot the central value of  $\frac{1+\alpha}{\beta'} e^{-b}$  against the central value of  $(1-\beta)$  on a logarithmic scale as follows:

$\rho_0$	$\log_{10}(1-\beta)$	$\log_{10}\left(\frac{1+\alpha}{\beta'} \cdot e^{-b}\right)$
5	-1.33	-2.40
10	-1.62	-1.57
25	-2.01	-0.57
50	-2.31	0.18
100	-2.60	0.92

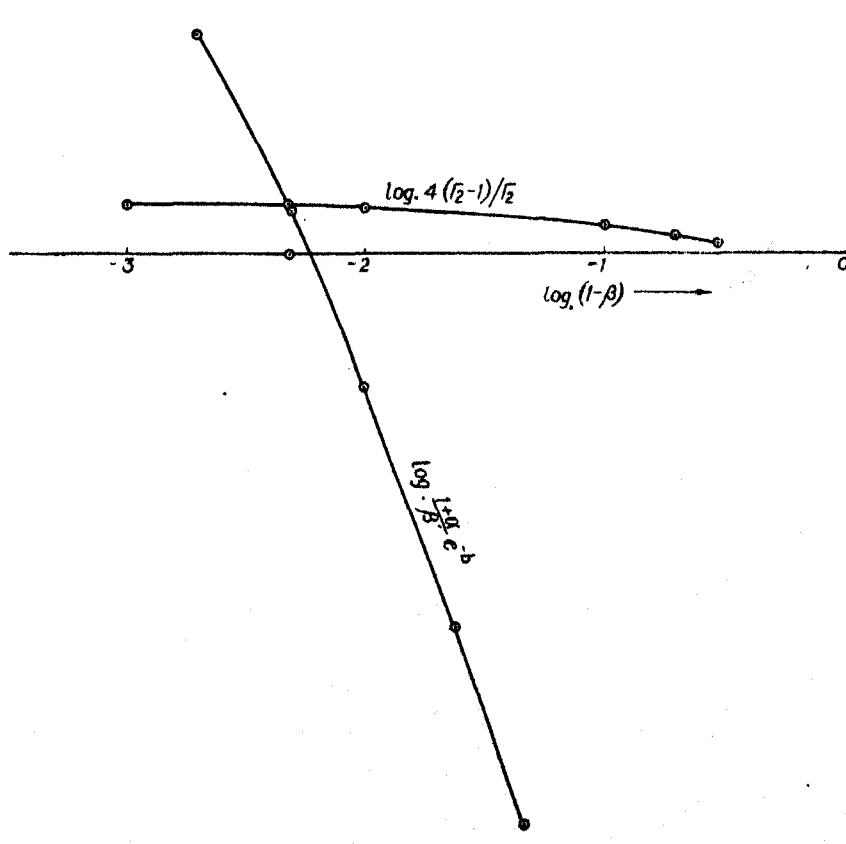


FIG. 1.

In a similar manner the following table gives  $4 \frac{\Gamma_2-1}{\Gamma_2}$  against  $(1-\beta)$ , the figures being taken from Chandrasekhar's 'Stellar Structure'.

$1-\beta$	$4 \frac{\Gamma_2-1}{\Gamma_2}$	$\log_{10}(1-\beta)$	$\log_{10}\left(4 \frac{\Gamma_2-1}{\Gamma_2}\right)$
0	1.6	$-\infty$	0.204
0.1	1.304	-1.0	0.115
0.2	1.177	-0.70	0.071
0.3	1.108	-0.52	0.045

Corresponding to the values  $10^{-3}$ ,  $10^{-2}$  for  $1-\beta$ , we calculate  $4(\Gamma_2-1)/\Gamma_2$  from (3.4) taking  $\gamma = 5/3$ , and obtain two further results as follows:

$\log_{10}(1-\beta)$	$\log_{10}\left(4 \frac{\Gamma_2-1}{\Gamma_2}\right)$
-3.0	0.203
-2.0	0.192

Next we plot  $\log 4 \frac{\Gamma_2-1}{\Gamma_2}$  against  $\log(1-\beta)$  on the paper of our previous graph.

The two curves of  $\log \frac{1+\alpha}{\beta} e^{-\beta}$  and  $\log 4 \frac{\Gamma_2-1}{\Gamma_2}$  intersect at a point for which  $\log(1-\beta) = -2.32$ . This determines  $\alpha$ , and hence the upper limit to  $\rho_0$  satisfying (3.6). This value of  $\rho_0$  comes out to be 52 gm./cm.<sup>3</sup>. Thus, for central densities less than 52 gm./cm.<sup>3</sup>, the equilibrium is radiative; for higher central densities a stable configuration would require a convective gradient.

4. In this section we propose to give the results of our numerical integrations. It has been shown in the previous section, that, if we take a central temperature  $2.10^7 K$  for the Sun, then for central densities greater than 75 gm./cm.<sup>3</sup> the solutions of the equations start with a positive density gradient  $\left(\frac{\partial \sigma}{\partial x} > 0\right)$  just leaving the centre. Further, if the central density be less than 52 gm./cm.<sup>3</sup>, the stable temperature gradient at the centre will be radiative, which will, however, have to be replaced by an adiabatic gradient (non-turbulent convection) when this limit is exceeded. It has been shown by N. R. Son<sup>5</sup> that for an energy generation law with a high power of the temperature as that of Bethe, the temperature gradient, if radiative at the centre, will continue to remain radiative outwards all along. With Bethe's energy generation law in the accurate form, we have performed three integrations. The first is for  $\rho_0 = 80$  gm./cm.<sup>3</sup>  $T_0 = 2.10^7 K$ . This should approximately represent the central condition of the Sun according to Strömgen's suggestion. The solution naturally starts with a positive density gradient. Two other cases worked out both have stable radiative gradients, viz.  $\rho_0 = 40$  gm./cm.<sup>3</sup>,  $\rho_0 = 1$  gm./cm.<sup>3</sup> and  $T_0 = 2.10^7 K$  in both cases. The results are given below.

The process of integration has been extremely slow to begin with. A start has always been made by Adam's method, and after a certain stage, the work has been continued by the method of successive approximations. This is very convenient, when the steps are to be made larger and larger as the integration proceeds. In fact, in the first case of integration, the original



small step of  $x' = 10^{-4}$  has been increased 256 times towards the end of the work. Whenever a step has been doubled, care has been taken to ensure that the check formulae provided by the method are strictly verified within their limitations. Only towards the end, these verifications have been made up to one unit in the last decimal figure, as further accuracy was not possible under the circumstances.

(i)  $\rho_0 = 80 \text{ gm./cm.}^3$ , (radiative gradient not stable).

Here

$$\begin{aligned} r_0 &= 2 \cdot 10^{-3} \\ M_0 &= 4 \cdot 10^{-6} \\ L_0 &= 3 \cdot 10^{20} \\ \alpha &= 3 \cdot 10^{-3} \\ \beta' &= 10^{-25} \end{aligned} \quad \dots \quad (4.1)$$

For the sun, the boundary values are given by

$$\begin{aligned} r &= r_0 x = 7 \cdot 10^{10} \text{ cm.} \\ M &= M_0 m = 2 \cdot 10^{33} \text{ gm.} \\ L &= L_0 l = 4 \cdot 10^{33} \text{ ergs./sec.} \end{aligned}$$

If we introduce another set of variables in place of  $x$ ,  $m$ , and  $l$  defined by

$$\begin{aligned} x &= \frac{7}{2} \cdot 10^{13} \cdot x' \\ m &= 5 \cdot 10^{33} \cdot m' \\ l &= 10^{13} \cdot l', \end{aligned}$$

it may be seen that these new variables are all expressed in terms of the respective solar units except  $l'$  which is  $4/3$  times the solar unit.

With these changes equations (2.13)–(2.16) become

$$\begin{aligned} \frac{dp}{dx'} + \alpha \frac{dq}{dx'} &= -\frac{10}{7} \cdot \frac{m'\sigma}{x'^2} \\ \frac{dq}{dx'} &= -\frac{2}{7} \cdot \frac{\sigma^{\frac{3}{2}} \tau^{-\frac{1}{2}} l'}{x'^2} \\ \frac{dl'}{dx'} &= 5 \cdot 10^{25} \cdot \sigma \tau^{-\frac{2}{3}} e^{-\frac{b}{\tau^{1/3}}} \cdot \frac{dm'}{dx'} \\ \frac{dm'}{dx'} &= 86 \sigma x'^2 \end{aligned} \quad \dots \quad (4.2)$$

At the origin the boundary conditions are  $p = 1$ ,  $q = 1$ ,  $\sigma = 1$ ,  $m' = 0$ ,  $l' = 0$ .

This case has been worked out in nearly 150 steps of which we insert only 24 in table I, and these will show the general character of the solution. We start with an interval  $x' = 10^{-4}$ , the choice of this interval depending on the values of the higher derivatives of the variables at the origin. The interval must be such that we may not have to pass out of the circle of convergence of the Taylor's series which we have to construct in the first few steps of Adam's method.

TABLE I.

$x'$	$\tau$	$\sigma$	$q$	$p$	$m'$	$l'$
0	1	1	1	1	0	0
$1 \times 10^{-4}$	1	1	0.999999	1	$0.3 \times 10^{-10}$	$0.7 \times 10^{-9}$
46	0.99948	1.0001	0.99794	0.99958	$2.8 \times 10^{-6}$	$6.7 \times 10^{-5}$
446	0.95590	1.0035	0.83494	0.95926	$2.6 \times 10^{-3}$	$3.8 \times 10^{-2}$
510	0.94404	1.0028	0.79427	0.94672	$3.8 \times 10^{-3}$	$5.0 \times 10^{-2}$
590	0.92807	1.0000	0.74186	0.92832	$5.9 \times 10^{-3}$	$6.5 \times 10^{-2}$
990	0.84167	0.9530	0.50184	0.8021	$2.7 \times 10^{-2}$	$1.2 \times 10^{-1}$
1374	0.76589	0.8373	0.34408	0.6413	$6.9 \times 10^{-2}$	$1.3 \times 10^{-1}$
1726	0.71104	0.6882	0.25560	0.4893	$1.3 \times 10^{-1}$	$1.4 \times 10^{-1}$
2110	0.671	0.514	0.203	0.345	$2.0 \times 10^{-1}$	$1.4 \times 10^{-1}$
2622	0.639	0.328	0.167	0.210	$3.0 \times 10^{-1}$	"
3134	0.628	0.207	0.155	0.130	$4.0 \times 10^{-1}$	"
3646	0.624	0.135	0.151	0.084	$4.8 \times 10^{-1}$	"
4158	0.619	0.094	0.147	0.058	$5.5 \times 10^{-1}$	"
4670	0.618	0.070	0.147	0.043	$6.2 \times 10^{-1}$	"
5438	0.617	0.044	0.145	0.027	$7.1 \times 10^{-1}$	"
6462	0.617	0.026	0.145	0.016	$8.2 \times 10^{-1}$	"
7486	"	0.018	"	0.011	$9.1 \times 10^{-1}$	"
9534	"	0.009	"	0.005	$10.6 \times 10^{-1}$	"
12094	"	0.005	"	0.003	$12.2 \times 10^{-1}$	"
16178	"	0.002	"	0.001	$14.5 \times 10^{-1}$	"
23346	"	$1.0 \times 10^{-3}$	"	$6.2 \times 10^{-4}$	$18.1 \times 10^{-1}$	"
43826	"	$2.3 \times 10^{-4}$	"	$1.4 \times 10^{-4}$	$26.8 \times 10^{-1}$	"
60210	"	$9.7 \times 10^{-5}$	"	$0.6 \times 10^{-4}$	$31.9 \times 10^{-1}$	"

In tables I, II and III,  $x'$ ,  $\tau$ ,  $\sigma$ ,  $q$ ,  $p$ ,  $m'$ ,  $l'$  represent respectively the central distance, temperature, density, radiation pressure, gas pressure, mass and luminosity in suitable units.

The integration in every case at start is given up to five decimal places, but when the steps of integration become large, the method of integration followed cannot generally give more than three places of correct decimal figures.

We have carried out the integration as far as six times the solar radius. The luminosity  $l'$  attains the constant value 0.1 (in solar unit) at a distance of about 0.2 solar radius, which means that the energy sources extend practically up to this distance. The temperature  $\tau$  takes up the constant value 0.62, the density  $\sigma$  and the gas pressure  $p$  gradually diminishing, but the mass  $m'$  gradually increasing. The whole thing now behaves as an isothermal gas sphere, which is known to have an infinite radius. There is one point to be noticed here; when  $\tau$  becomes 0.62,  $\sigma$  is of the order of 0.1, i.e. the density  $\rho$  is of the order of  $\frac{1}{10}$  of the central density  $\rho_0$  ( $= 80$ ), so that towards the end

of the table we have somewhat overstepped the density limit for the validity of Bethe's representation of the guillotine factor  $l$ . This will not, however, affect the qualitative character of our results, as we have subsequently shown (in the case  $\rho_0 = 1$ ), that taking the proper representation of  $l$  for low densities,

we arrive at a similar result, i.e. an isothermal atmosphere in the end. We give below some values of the polytropic index  $n$  at different distances from the centre.  $n$  starts with a negative value but tends to become infinitely large towards the end, which corresponds to the case of an isothermal atmosphere. We calculate  $n$  from the formula

$$\frac{dP}{P} = \left(1 + \frac{1}{n}\right) \frac{d\rho}{\rho}$$

or

$$\frac{dp + \alpha dq}{p + \alpha q} = \left(1 + \frac{1}{n}\right) \frac{d\rho}{\rho}$$

or

$$\frac{dp}{dx'} + \alpha \frac{dq}{dx'} = \left(1 + \frac{1}{n}\right) \cdot \frac{p + \alpha q}{\sigma} \frac{d\sigma}{dx'}. \quad \dots \quad (4.3)$$

Here the values of  $p$ ,  $q$ ,  $\sigma$  and the derivatives are taken from the integrated results (the derivatives are not shown in the table).

$x'$	$n$
$0 \times 10^{-4}$	$-\frac{3}{5}$
10	$-\frac{1}{6}$
206	$-\frac{1}{8}$
398	$-\frac{1}{58}$
446	$+\frac{1}{62}$
590	$\frac{1}{7}$
2110	5
5438	54
...	$\rightarrow \infty$

(ii)  $\rho_0 = 40 \text{ gm./cm.}^3$ , (radiative gradient stable).

In this case the constants  $\alpha$ ,  $\beta'$ , etc. are given as follows:

$$\alpha = 6 \cdot 10^{-3}, \quad \beta' = 6 \cdot 10^{-25}, \quad r_0 = 5 \cdot 10^{-3}$$

$$L_0 = 25 \cdot 10^{20}, \quad M_0 = 7 \cdot 10^{-5}. \quad \dots \quad (4.4)$$

Expressing the variables  $x, m, l$  in terms of solar units by the transformations

$$x = 1.4 \times 10^{18} x'$$

$$m = \frac{2}{7} \cdot 10^{38} m'$$

$$l = \frac{4}{25} \cdot 10^{13} l'$$

the equations become

$$\begin{aligned} \frac{dp}{dx'} + \alpha \frac{dq}{dx'} &= -\frac{60}{49} \cdot \frac{m'\sigma}{x'^2} \\ \frac{dq}{dx'} &= -\frac{4}{35} \cdot \frac{\sigma^{\frac{3}{2}} \tau^{-\frac{11}{4}} l'}{x'^2} \\ \frac{dl'}{dx'} &= \frac{25}{24} \cdot 10^{25} \cdot \sigma \tau^{-\frac{2}{3}} e^{-\frac{b}{\tau^{1/3}}} \frac{dm'}{dx'} \\ \frac{dm'}{dx'} &= 96 \sigma x'^2. \quad \dots \quad \dots \quad \dots \quad (4.5) \end{aligned}$$

The starting interval is  $x' = 10^{-8}$ , and the total number of steps worked out is thirty-six of which we give only eleven.

TABLE II.

$x'$	$\tau$	$\sigma$	$q$	$p$	$m'$	$l'$
0	1	1	1	1	0	0
$1 \times 10^{-8}$	1	0.99998	0.99999	0.99998	$0.3 \times 10^{-7}$	$0.3 \times 10^{-6}$
10	0.99962	0.99842	0.99846	0.99804	$3.2 \times 10^{-5}$	$2.7 \times 10^{-4}$
52	0.99016	0.95820	0.96121	0.94877	$4.4 \times 10^{-3}$	$3.4 \times 10^{-2}$
100	0.97008	0.85320	0.88553	0.82765	$2.9 \times 10^{-2}$	$1.7 \times 10^{-1}$
196	0.93656	0.55110	0.76937	0.51613	$1.7 \times 10^{-1}$	$5.0 \times 10^{-1}$
260	0.92665	0.37943	0.73732	0.35160	$3.2 \times 10^{-1}$	$6.5 \times 10^{-1}$
388	0.92007	0.17750	0.71662	0.16328	$6.5 \times 10^{-1}$	$8.2 \times 10^{-1}$
548	0.918	0.079	0.712	0.073	1.0	$8.9 \times 10^{-1}$
676	0.918	0.049	0.711	0.045	1.3	$9.3 \times 10^{-1}$
740	0.918	0.032	0.711	0.030	1.4	$9.4 \times 10^{-1}$
..	..	..	..	..	..	$9.4 \times 10^{-1}$

Here also we arrive at an isothermal condition as in the previous case, but there is one point of difference; here the constancy of temperature sets in somewhat before the constancy of the luminosity. This difference will be more marked when we pass on to still lower central densities, and in fact for the case  $\rho_0 = 1$  gm./cm.<sup>3</sup>, the isothermal condition sets in right from the beginning.

(iii)  $\rho_0 = 1$  gm./cm.<sup>3</sup>, (radiative gradient stable).

Here we take the opacity law in the form

$$\kappa = \kappa_0 \frac{\rho}{T^{\frac{1}{2}}}$$

The density being low, Bethe's representation of  $t$  as a function of  $\rho$  and  $T$  is not valid. From the study of our tables connecting  $t$  and  $\rho$  at different temperatures, we find that in the present case  $t$  may be regarded practically as a constant quantity with a value 2.6.

The constants  $\alpha$ ,  $\beta'$ , etc. have the values

$$\begin{aligned}\alpha &= 2.5 \cdot 10^{-1} \\ \beta' &= 2 \cdot 10^{-20} \\ r_0 &= 6.0 \\ M_0 &= 2 \cdot 10^3 \\ L_0 &= 2 \cdot 10^{27}. \quad \dots \quad \dots \quad \dots \quad \dots \quad (4.6)\end{aligned}$$

With

$$\begin{aligned}x &= 6 \cdot 10^{10} x' \\ m &= 10^{30} m' \\ l &= 2 \cdot 10^6 l'\end{aligned}$$

the equations become

$$\begin{aligned}\frac{dp}{dx'} + \alpha \frac{dq}{dx'} &= -\frac{1}{3} \frac{m' \sigma}{x'^2} \\ \frac{dq}{dx'} &= -\frac{1}{3} \cdot 10^{-4} \cdot \frac{\sigma^2 \tau^{-1/2} l'}{x'^2} \\ \frac{dl'}{dx'} &= \frac{1}{2} \cdot 10^{24} \sigma \tau^{-1/2} e^{-\frac{b}{\tau^{1/2}}} \frac{dm'}{dx'} \\ \frac{dm'}{dx'} &= 216 \sigma x'^2. \quad \dots \quad \dots \quad \dots \quad (4.7)\end{aligned}$$

Here  $m'$ ,  $l'$  are values of the respective quantities in solar units, and  $x'$  the value measured in five times the solar unit.

Table III gives the character of the solution.

TABLE III.

$x'$	$\tau$	$\sigma$	$q$	$p$	$m'$	$l'$
0	1	1	1	1	0	0
$1 \times 10^{-3}$	1	0.99998	1	0.99998	$7.0 \times 10^{-8}$	$2.0 \times 10^{-8}$
50	1	0.9706	1	0.9706	$8.7 \times 10^{-2}$	$2.1 \times 10^{-2}$
98	1	0.8967	1	0.8967	$6.2 \times 10^{-2}$	$1.5 \times 10^{-2}$
194	1	0.672	1	0.672	$4.1 \times 10^{-1}$	$7.9 \times 10^{-2}$
290	1	0.451	0.99997	0.451	1.1	$1.5 \times 10^{-1}$
386	1	0.297	0.99996	0.297	2.0	$2.2 \times 10^{-1}$
482	1	0.197	0.99996	0.197	2.9	$2.6 \times 10^{-1}$

5. The setting in of an isothermal condition at some distance from the centre is due to the fact that the derivative  $\frac{dq}{dx}$  determining the temperature gradient is very small, which is a consequence of the energy generation formula. This may be seen from the following analysis.

Expanding  $\frac{dq}{dx}$  in a Taylor's series about the origin we may write

$$\begin{aligned}\frac{dq}{dx} &= \left(\frac{dq}{dx}\right)_0 + x\left(\frac{d^2q}{dx^2}\right)_0 + \frac{x^2}{2!}\left(\frac{d^3q}{dx^3}\right)_0 + \dots \\ &= x\left(\frac{d^2q}{dx^2}\right)_0 + \frac{x^3}{3!}\left(\frac{d^4q}{dx^4}\right)_0 + \dots\end{aligned}$$

The odd derivatives vanish at the origin, as may be seen by differentiating the expression for  $\frac{dq}{dx}$ .

The fourth derivative being of much smaller order of magnitude than the second, the latter is the predominant term in determining the value of  $\frac{dq}{dx}$ .

We have

$$\begin{aligned}\left(\frac{d^2q}{dx^2}\right)_0 &= -\frac{1}{3}e^{-b} \\ &\sim 10^{-25}.\end{aligned}$$

The exponential factor (which is a consequence of the energy generation law) is responsible for the small value of the temperature gradient. This must be connected with the ultimate setting in of isothermal conditions.

### Conclusion.

We have found that when a central temperature of 20 million degrees and a hydrogen concentration of 35% (by weight) are assumed, the integrations of the stellar equations in radiative equilibrium for central densities (i) 80, (ii) 40, and (iii) 1 gm./cm.<sup>3</sup> lead respectively to—

- (i) an approximate isothermal state at a temperature of over 12 million degrees at a central distance of about 0.6 times the solar radius, where the density is about 3% of the central value, and mass 82% of the solar mass. A constant luminosity of about 14% of the solar value is attained in this case at about  $\frac{1}{3}$  of the above central distance;
- (ii) an approximate isothermal state at temperature and density about 92% and 8% respectively of their central values, at a central distance of about 55% of the solar radius, the mass there being about 1 solar unit. A constant luminosity of about 94% of the solar value is attained immediately after this stage;
- (iii) an isothermal state right from the centre.

None of the three cases considered here correspond to a stellar body solution and our expectation is that for the assumptions made regarding energy generation and opacity it will not be possible to find a central density which will give a stellar body solution with finite mass and radius, with a purely

radiative gradient throughout. The theoretical investigations on the nature of the solution near the boundary by N. R. Sen<sup>6</sup> also explain this standpoint. It is of interest to note that our solutions are of the type in which the  $\tau$ - $\sigma$  curve (temperature-density variation within stellar bodies) has a very steep, almost a vertically descending downward gradient as  $\sigma$  decreases to zero for a finite  $\tau = \tau_0$ , as described by Chandrasekhar<sup>7</sup> in his work on the stellar

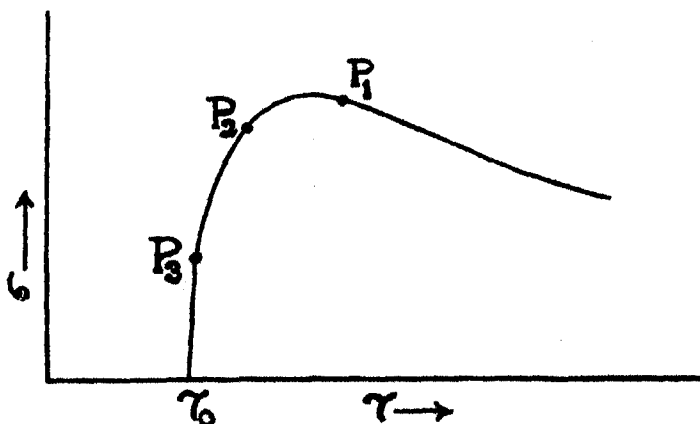


FIG. 2.

structure with a simplified form of energy generation law. This is shown in Fig. 2. The three cases integrated correspond to central conditions represented by  $P_1$ ,  $P_2$ , and  $P_3$  respectively in Fig. 2 on different curves.

The author takes this opportunity of expressing his gratitude to Prof. N. R. Sen for his constant help and advice, and to Dr. R. C. Majumdar for the benefit of frequent discussions with him.

## REFERENCES.

- <sup>1</sup> Bethe, H. (1939). Energy Production in Stars. *Phys. Rev.*, **55**, 434.
- <sup>2</sup> Eddington, A. S. Internal Constitution of Stars, 114.  
Biermann, L. (1931). Numerische Integrationen zur Theorie des Sternaufbaus. *Zs. f. Ap.*, **3**, 116.
- Strömberg, B. (1931). The point-source Model with Coefficient of Opacity  $k = k_1 \rho T^{-3.5}$ . *Zs. f. Ap.*, **2**, 345.
- <sup>3</sup> Chandrasekhar, S. Introduction to the Study of Stellar Structure, 223.
- <sup>4</sup> Chandrasekhar, S. Introduction to the Study of Stellar Structure, 224.
- <sup>5</sup> Sen, N. R. (1941). On the Inversion of Density Gradient and Convection in Stellar Bodies. *Proc. Nat. Inst. Sci. India*, **7**, 183.
- <sup>6</sup> Sen, N. R. (1942). On Stellar Models based on Bethe's Law of Energy Generation. *Proc. Nat. Inst. Sci. India*, **8**, 317.
- <sup>7</sup> Chandrasekhar, S. (1936). The Occurrence of Negative Density Gradients in Stars and Allied Problems (First Paper). *M.N.R.A.S.*, **97**, 132.

Department of Applied Mathematics,  
University of Calcutta.

# ON STELLAR MODELS BASED ON BETHE'S LAW OF ENERGY GENERATION.

By N. R. SEN.

(Received January 27, 1942.)

## ABSTRACT.

Stellar models for a core source of energy, and opacity law of the type  $\kappa \propto \rho^a T^{-b}$ , and radiative energy transfer have been discussed. It is shown, finite stellar configurations may be possible only when  $b < 4a$ . Generally for all positive values of  $a$  and  $b$  there are solutions which ultimately correspond to isothermal gas spheres of infinite mass and radius and non-zero limiting temperature.

## Introduction.

1. U. R. Burman has recently completed some numerical integrations of the equations of stellar equilibrium on the basis of Bethe's law of energy generation<sup>1</sup> in its accurate form, and radiative transfer of energy. His cases show a uniform behaviour of the integrated result. For the central densities he has assumed for integration, almost the entire energy generation is confined towards the central region, and very soon a stage is reached from where outwards the luminosity remains practically constant. Numerical integration reveals in each case a nearly isothermal condition at fairly high temperature sooner or later, suggesting the configurations are infinite.

It is not *a priori* clear why for a fairly large range of central densities assumed by Burman in his integrations he has not found anything to suggest that there exists some finite configuration which may represent a stellar body with a radiative gradient.

The object of this paper is to examine analytically what circumstances lead to isothermal conditions and generally infinite configurations as found by Burman. The problem is posed as follows. There is an energy generating core of a stellar body surrounded by a radiative envelope within which the luminosity is constant. A general opacity law depending on some powers of density and temperature, e.g.  $\kappa = \kappa_0 \rho^a T^{-b}$  ( $a, b$ , positive) is assumed for the envelope. We enquire under what conditions we should obtain a solution with finite mass and radius, and what conditions should lead to solutions corresponding to isothermal spheres. We may also note what other types of solutions with physical significance may be expected. As we shall confine our attention here only to the radiative envelope, the conditions will all refer to the outer boundary only and be only necessary ones. Permissibility of a

---

<sup>1</sup> H. Bethe, Energy Production in stars. *Phys. Rev.*, **55**, 434, (1939).



solution in the central region is for the present outside the scope of our investigation. Nevertheless our investigation will not only throw light on Burman's result but also give us some understanding about some of the implications of a core source of energy and a general opacity law of the type assumed here.

*The equations.*

2. We start with the equations of stellar equilibrium

$$\frac{dP}{dr} = -G \frac{M(r)}{r^2} \rho \quad \dots \quad (1)$$

$$\frac{dp_r}{dr} = -\frac{\kappa \rho}{c} \cdot \frac{L}{4\pi r^2} \quad \dots \quad (2)$$

$$\frac{dM(r)}{dr} = 4\pi r^2 \rho \quad \dots \quad (3)$$

$$P = p_g + p_r, \quad p_g = \frac{k}{\mu H} \cdot \rho T, \quad p_r = \frac{1}{3} a T^4 \quad \dots \quad (4)$$

An opacity formula of the form

$$\kappa = \kappa_0 \rho^a T^{-b} \quad \dots \quad (5)$$

is assumed. We shall assume  $a$  and  $b$  to be positive, which is suggested by the known opacity laws. As we confine ourselves to the region outside the core source of energy,  $L$  is considered to be constant. Making the following substitutions<sup>1</sup>

$$p_g = (p_g)_0 p, \quad p_r = (p_r)_0 q, \quad \rho = \rho_0 \sigma, \quad T = T_0 \tau, \quad r = r_0 x, \quad M = M_0 m. \quad \dots \quad (6)$$

where  $p, q, \sigma, \tau, x$  and  $m$  are pure numbers, we can put the stellar equations (1)–(3), and (4) in the form

$$d(p + \alpha q) = -\beta \cdot m \sigma / x^2 \cdot dx \quad \dots \quad (1a)$$

$$dq = -\sigma^{a+1} \tau^{-b} \cdot dx / x^2 \quad \dots \quad (2a)$$

$$dm = \sigma x^2 dx \quad \dots \quad (3a)$$

and

$$p = \sigma \tau, \quad q = \tau^4 \quad \dots \quad (4a)$$

when the following six equations are satisfied:

$$(p_g)_0 = (k/\mu H) \rho_0 T_0, \quad (p_r)_0 = \frac{1}{3} a T_0^4, \quad (p_r)_0 / (p_g)_0 = \alpha, \quad G M_0 \rho_0 / r_0^2 (p_g)_0 = \beta$$

$$(\kappa_0 L \rho_0^{a+1}) / 4\pi c r_0 (p_r)_0 T_0^b = 1, \quad 4\pi \rho_0 r_0^3 / M_0 = 1. \quad \dots \quad (7)$$

For given  $\mu$  and  $\kappa_0 L$ , equations (7) express any four of  $\alpha, \beta, \rho_0, T_0, r_0, M_0$  in terms of the other two, say  $\alpha$  and  $\beta$ . These two constants are the parameters of the set of our equations. Alternatively, we may consider  $\rho_0, T_0$ , calling them central density and temperature of the configuration, as the two independent parameters in terms of which the remaining four constants are determined by (7). The distance  $r$  and mass  $M$  are then expressed in terms of the new units.

<sup>1</sup> These substitutions are first used by Rosseland. *Zeits. f. Astrophysik*, 4, 255, 1922.

Eliminating  $\sigma$  from (1a), (2a), and (3a) by means of (4a) we obtain

$$dp + \alpha dq = -\beta p q^{-1} \cdot m \cdot dx/x^2 \quad \dots \quad (1b)$$

$$dq = -p^{a+1} \cdot q^{-\frac{a+b+1}{4}} \cdot dx/x^2 \quad \dots \quad (2b)$$

$$dm = p q^{-1} \cdot dx/x^2 \quad \dots \quad (3b)$$

Dividing (1b) by (2b) we obtain  $m$  as follows

$$m = \beta^{-1} \cdot p^a q^{-d} (dp/dq + \alpha) \quad \dots \quad (1c)$$

where

$$4d = a + b \quad \dots \quad (8)$$

Dividing (3b) by (3a) we obtain  $dm/dq$ , and then substituting the above value of  $m$  we obtain

$$\frac{d}{dq} \left[ p^a q^{-d} \left( \frac{dp}{dq} + \alpha \right) \right] = -\beta p^{-a} q^d \cdot x^4 \dots \quad (2c)$$

Introduce the variable

$$\xi = \frac{1}{x}$$

then (2b) gives

$$\frac{d\xi}{dq} = p^{-(a+1)} q^{d+1} \quad \dots \quad (3c)$$

Let us introduce a new variable  $t$  defined by

$$\frac{dq}{dt} = p^a q^{-d} \quad \dots \quad (9)$$

so that

$$p^a q^{-d} \frac{d}{dq} = \frac{d}{dt}.$$

Then (2c), (3c) and (9) are equivalent to the set

$$\frac{d^2 \pi}{dt^2} = -\beta \xi^{-4} \quad \dots \quad (10)$$

$$\frac{d\xi}{dt} = \frac{q^1}{p} \quad \dots \quad (11)$$

$$\frac{dq}{dt} = \frac{p^a}{q^d} \quad \dots \quad (12)$$

where  $\pi = p + \alpha q$ . (10) may be replaced according to (3b) and (1b) by

$$\frac{dm}{dt} = -\xi^{-4}, \quad \frac{d\pi}{dt} = \beta m \quad \dots \quad (10a, b)$$

which are sometimes useful.

We shall discuss the nature of the solutions of (10), (11), and (12) near the boundary. As we confine ourselves strictly to the stellar problem, we note that  $p$ ,  $q$ , and  $\pi$  represent the gas pressure, radiation pressure, and total pressure respectively, and  $\xi$  is proportional to the reciprocal of the central distance.

Moreover from (11) it is apparent that  $\xi'$  (a dash will denote differentiation with regard to  $t$ ) is proportional to  $\rho^{-1}$ , the reciprocal of density. Hence if we define the stellar boundary by the conditions  $p = 0$ ,  $\rho = 0$ , then  $\xi'$  at the boundary is infinite.

Again from

$$q' = \frac{dq}{dx} \cdot \left( -\frac{1}{\xi^2} \right) \cdot \frac{d\xi}{dt} = -\frac{x^2}{\sigma} \frac{dq}{dx}, \quad p' = -\frac{x^2}{\sigma} \frac{dp}{dx} \quad \dots (12a)$$

$$\pi' = p' + \alpha q' = -\frac{x^2}{\sigma} \frac{d}{dx} (p + \alpha q) \propto -\frac{x^2}{\rho} \frac{dP}{dr}$$

we conclude that  $\pi'$  is proportional to the total mass within the sphere passing through the point concerned (equation (1)), and to confine ourselves strictly to astrophysical cases we shall assume  $\pi'$  to be positive. We may also look upon  $p'$  as representing mass in a certain sense; in fact it may be considered to be proportional to the mass which produces that part of the acceleration of gravity which is necessary to balance the gradient of  $p$  at the point concerned. At regions of inverted density gradients  $p'$  may be negative when this interpretation fails. A similar interpretation may be given to  $q'$  which cannot be negative. We are interested in solutions such that at the boundary,  $\pi' = p' + \alpha q'$  must tend to a positive limit, finite or infinite; and if one of  $p'$  and  $q'$  be small compared to the other, this latter must represent practically the whole mass.

Equations (10)–(12) do not contain  $t$  on the right hand side. Hence for integration, given the initial values of  $\xi$ ,  $q$ ,  $\pi$  and  $\pi'$ , the initial value of  $t$  is immaterial. We shall always take  $t = 0$  to correspond to the boundary surface.

### The Solutions.

3. We now proceed to discuss the nature of those solutions of (10)–(12) which may be of astrophysical interest, in the neighbourhood of  $t = 0$ . We are interested only in the region where

$$(\pi, p, q, \xi) > 0,$$

and in solutions for which

$$0 < q_0 < \infty, \quad p_0 = 0, \quad \xi_0' = \infty, \quad \text{and } \pi_0' > 0.$$

Equation (11) shows  $t$  increases with  $\xi$ , and as by (12) immediately below the boundary surface  $t$  will be positive and increasing, we shall be interested in small positive values of  $t$  only. Physical considerations indeed require that all the above quantities should be continuous in this region.

We note the following properties of the solutions we are seeking.

I.  $\xi$  and  $q$  both tend to finite limits  $\xi_0 > 0$ , and  $q_0 > 0$ , as  $t \rightarrow 0$ ; and  $\pi' \rightarrow \pi_0'$ ,  $0 < \pi_0' < \infty$ . This follows from (11) and (12) which show  $\xi$  and  $q$  are monotone increasing functions of  $t$ ; hence as  $t$  decreases to zero,  $\xi$  and  $q$  must decrease monotonically, and each has as limit either zero, or a positive quantity.

The second part is equivalent to the assumption already made that  $\pi'$  must be positive coupled with the property that  $\pi'$  increases monotone as  $t \rightarrow 0$  which follows from (10).

II. When  $\xi_0 \neq 0$ ,  $\pi_0'$  is finite, and so also is  $\pi_0$ .

This follows from (10) since the right hand side is bounded. Hence if  $\xi_0 \neq 0$ , as  $t \rightarrow 0$ ,  $\pi'$  increases to the finite value  $\pi_0'$ , and so  $\pi$  tends to the finite value  $\pi_0$ .

III. As  $\pi_0'$  is positive, finite or infinite,  $\pi'$  is positive as  $t \rightarrow 0$ , hence  $\pi$  decreases to the finite limit  $\pi_0$  as  $t \rightarrow 0$ .

We now consider four possible cases as follows:

Case 1. Let  $\xi_0 = 0$ ,  $q_0 \neq 0$ ; then  $\pi_0 = \alpha q_0 \neq 0$ .

By (12)  $q_0' = 0$ ; we first prove that  $\pi_0' = p_0'$  must not be finite.

For if  $p_0'$  be finite and  $\neq 0$ .

$$p \sim p_0' t \quad (t \rightarrow 0) \quad \dots \quad (14)$$

Then by (11)

$$\xi' \sim \frac{q_0^{\frac{1}{2}}}{p_0' t} \quad (t \rightarrow 0) \quad \dots \quad (14a)$$

and integrating

$$\xi \sim \frac{q_0^{\frac{1}{2}}}{p_0'} \log t \quad (t \rightarrow 0) \quad \dots \quad (14b)$$

which contradicts the assumption  $\xi_0 = 0$ ; hence  $p_0'$  cannot have a finite non-zero value.

Let us take the other alternative  $p_0' = 0$  (in addition to  $\xi_0 = 0$ ,  $q_0 \neq 0$ ).

We note by differentiating (12)

$$q'' = \frac{ap^{a-1}}{q^d} p' - \frac{dp^a}{q^{d+1}} q' \quad \dots \quad (14c)$$

that since  $p_0'$  and  $q_0'$  vanish  $q_0''$  must be zero. Hence by (10),  $p_0''$  must be negative (infinite). Now as also  $p_0 = 0$ ,  $p_0' = 0$ ,  $p$  must be negative as  $t \rightarrow 0$ . Hence the possibility  $p_0' = 0$  is also excluded.

With  $p_0'$  infinite we find by trial the solution has the following structure

$$\xi \sim At^m, \quad 0 < m < 1 \quad (t \rightarrow 0) \quad \dots \quad (15)$$

$$q \sim q_0 + Bt^n, \quad n > 1 \quad (t \rightarrow 0) \quad \dots \quad (16)$$

Firstly, this satisfies  $\xi_0' = \infty$ , and  $q_0' = 0$ . Further we have

$$\pi'' \sim -\frac{\beta}{A^{\frac{1}{2}}} t^{-4m} \quad (t \rightarrow 0) \quad \dots \quad (17)$$

integrating

$$\pi' \sim -\frac{\beta}{A^{\frac{1}{2}}(1-4m)} t^{-4m+1} \quad (t \rightarrow 0) \quad \dots \quad (17a)$$

and

$$\pi \sim \pi_0 - \frac{\beta}{A^{\frac{1}{2}}(1-4m)(2-4m)} t^{-4m+2} \quad (t \rightarrow 0) \quad \dots \quad (17b)$$

where  $\pi_0$  is constant. Since  $\pi_0$  is finite and  $\pi_0' = \infty$ ,  $\frac{1}{4} < m < \frac{1}{2}$ ;  $\pi - \pi_0$  is thus of the order of a power of  $t$  which lies between 0 and 1, and hence less than  $n$ .

Hence also

$$p \sim -\frac{\beta}{A^4(1-4m)(2-4m)} \cdot t^{-4m+2} (t \rightarrow 0) \quad \dots \quad (17c)$$

Equation (11) gives

$$A m t^{n-1} \sim -\frac{q_0^{\frac{1}{2}} A^4(1-4m)(2-4m)}{\beta} t^{4m-2}.$$

Thus

$$n-1 = 4m-2, \text{ i.e. } m = \frac{1}{3},$$

and

$$A = \left(\frac{3\beta}{2q_0^{\frac{1}{2}}}\right)^{\frac{1}{2}}.$$

Equation (12) gives

$$B n t^{n-1} \sim \left(\frac{9\beta}{2A^4}\right)^a \frac{1}{q_0^a} t^{2a/3}$$

which gives

$$n = 1 + \frac{2}{3}a, \quad B = \left(\frac{18}{\beta}\right)^{\frac{a}{3}} q_0^{\frac{a}{3}-a}.$$

Hence for  $\xi_0 = 0$ ,  $q_0 \neq 0$ , we get a solution of the type

$$\xi \sim \left(\frac{3\beta}{2q_0^{\frac{1}{2}}}\right)^{\frac{1}{2}} t^{\frac{1}{2}} (t \rightarrow 0) \quad \dots \quad (15a)$$

$$q \sim q_0 + \left(\frac{18}{\beta}\right)^{\frac{a}{3}} q_0^{\frac{a}{3}-a} t^{1+\frac{2}{3}a} (t \rightarrow 0) \quad \dots \quad (16a)$$

$$p \sim \left(\frac{9q_0}{4\beta^4}\right)^{\frac{1}{2}} t^{\frac{1}{2}} (t \rightarrow 0) \quad \dots \quad (16b)$$

As  $p \propto t^{\frac{1}{2}}$ , and  $\rho \propto \frac{1}{\xi^2} \propto t^{-\frac{1}{2}}$ ,  $P \propto \rho \propto \frac{1}{t^{\frac{1}{2}}}$  (since  $a > 0$ ) as  $t \rightarrow 0$ .

The sphere corresponding to this solution has infinite radius and ultimately behaves as an isothermal gas sphere with a limiting temperature different from zero. Since  $\pi_0'$  is infinite, the mass of the sphere is also infinite.

Case 2. Let  $\xi_0 \neq 0$ ,  $q_0 = 0$ .

Since  $\xi_0 \neq 0$ ,  $\pi_0'$  is finite; also here  $\pi_0 = 0$ .

(i) Let  $q_0' = 0$ . Then by II,  $\pi_0' = p_0'$  is also finite.  $p_0' = 0$  is excluded as that would make  $\pi_0' = 0$ . Since  $p_0 = 0$ ,  $p_0' \neq 0$

$$p \sim p_0' t. \quad (t \rightarrow 0) \quad \dots \quad (18)$$

Substituting in (12) we obtain

$$q^d q' = p^a \sim p_0'^a \cdot t^a$$

and integrating

$$q \sim A^{\frac{a+1}{d+1}} t^{\frac{a+1}{d+1}} \quad (t \rightarrow 0) \quad \dots \quad (19)$$

where

$$A^{\frac{1}{d}} = \left( \frac{d+1}{a+1} p_0'^a \right)^{\frac{1}{d+1}}.$$

This substituted in (11) gives

$$\xi' \sim \frac{A}{p_0'} \cdot t^{\frac{a+1}{d(d+1)}-1} \quad (t \rightarrow 0) \quad \dots \quad (20)$$

whence integrating

$$\xi \sim \xi_0 + \frac{4A}{p_0'} \cdot \frac{d+1}{a+1} t^{\frac{a+1}{d(d+1)}} \quad (t \rightarrow 0) \quad \dots \quad (21)$$

(18), (19), and (21) constitute a solution in the neighbourhood of the boundary surface. Since  $q_0' = 0$ , we must have from (19)

$$a > d, \text{ i.e. } 3a > b. \quad (22)$$

Equation (10) is satisfied up to the highest order in  $t$ . We may note that

$$m \sim m_0 - \xi_0^{-4} t, \text{ and } \pi \sim \beta m_0 t \quad (t \rightarrow 0)$$

and the other conditions, e.g.  $q_0 = 0$ ,  $\xi_0' = \infty$  ( $b$  is positive) are automatically satisfied. Further we have as  $t \rightarrow 0$ ,  $P \propto \rho^{1+\frac{a+1}{b+3}}$ . Near the boundary the sphere behaves (as regards compressibility) as polytrope of index  $n = (b+3)/(a+1)$ , which is less than 3.

(ii) Let  $q_0'$  be finite and  $> 0$ . Then

$$q \sim q_0' t \quad (t \rightarrow 0) \quad \dots \quad (23)$$

Again  $\pi_0 = 0$ ; also since  $\pi_0' = p_0' + a q_0'$  is finite and so also is  $q_0'$ , hence  $p_0'$  must also be finite. Let  $p_0' \neq 0$ , then

$$p \sim p_0' t. \quad (t \rightarrow 0)$$

Equation (11) on integration now gives

$$\xi \sim \xi_0 + \frac{4q_0'}{p_0'} t t. \quad (t \rightarrow 0) \quad \dots \quad (24)$$

By substitution in (12) we obtain

$$q' \sim \frac{p_0'^a}{q_0'^d} t^{a-d}.$$

Hence as  $q_0'$  is finite and  $\neq 0$ , this type of solution exists only when

$$a = d \text{ i.e. } 3a = b \quad (25)$$

and

$$p_0' = q_0' \frac{d+1}{a}.$$

Thus for  $b = 3a$  we have the solution

$$\begin{aligned} q &\sim q_0' t, \quad \pi \sim \pi_0' t \\ \xi &\sim \xi_0 + 4q_0' - \left(\frac{1}{a} + \frac{3}{2}\right) t^2 \quad \dots \quad (26) \end{aligned}$$

Equation (10) is again satisfied up to the highest order in  $t$ .

Thus for  $3a = b$  we obtain finite spheres with  $\rho = 0$ ,  $T = 0$  at the boundary. Also near the boundary  $P \propto \rho^{\frac{1}{2}}$ , so that the spheres behaves there as Emden polytropes  $n = 3$ .

Let now  $p_0' = 0$  in addition to  $q_0'$  being finite and different from zero.

Thus

$$q \sim q_0' t. \quad (t \rightarrow 0) \quad \dots \quad (23)$$

Equation (12) then gives

$$p \sim q_0' \frac{d+1}{a} t^{\frac{d}{a}}, \quad (t \rightarrow 0)$$

so that

$$p' \sim \frac{d}{a} q_0' t^{\frac{d+1}{a} - 1}. \quad (t \rightarrow 0)$$

From equation (11) we have

$$\xi' \sim q_0' \frac{1}{4} - \frac{d+1}{a} t^{\frac{1}{4} - \frac{d}{a}} \quad (t \rightarrow 0) \quad \dots \quad (24a)$$

whence integrating

$$\xi \sim \xi_0 + \frac{q_0'}{\frac{5}{4} - \frac{d}{a}} t^{\frac{5}{4} - \frac{d}{a}} \quad (t \rightarrow 0) \quad \dots \quad (24b)$$

Since  $p_0' = 0$ , and  $\xi$  is finite we have

$$1 < d/a < 5/4,$$

in other words

$$3a < b < 4a. \quad \dots \quad (25a)$$

We note that this also satisfies the condition  $\xi_0' = \infty$ . In this case we easily find near the boundary  $P \propto \rho^{\frac{1}{2}a/(4d-a)}$ , so that the compressibility relation near the boundary is that of a polytrope of index  $n = b/(4a-b)$ , which may lie between 3 and  $\infty$ .

Hence we find that *solutions (which may be of astrophysical interest) satisfying the boundary conditions at a finite boundary may exist when  $b < 4a$ .*

(iii) Let  $q_0' = \infty$ . Since by (12a)  $p_0'$  cannot be negative as  $(dp/dx)_0$  is negative or zero,  $\pi_0'$  is infinite. But as a sphere of finite radius ( $\xi_0$  finite) cannot have infinite mass, this case is of no physical importance.

Case 3. Let  $\xi_0 = 0$ ,  $q_0 = 0$ .

(i) Suppose  $q_0' = 0$ . Then  $\pi_0 = 0$ , and  $\pi_0' = p_0'$ . First suppose  $p_0'$  is finite; its value must be greater than zero since  $\pi_0' > 0$ .

Then

$$p \sim p_0' t. \quad (t \rightarrow 0) \quad \dots \quad (27)$$

From this by following exactly the steps of Case 2(i) we obtain

$$q \sim A t^{\frac{a+1}{d+1}}. \quad (t \rightarrow 0).$$

Since  $q_0' = 0$  we must have  $a > d$ . Again integrating (11) and proceeding as in Case 2(i) we obtain

$$\xi \sim \text{const. } t^{\frac{a+1}{d+1}}. \quad (t \rightarrow 0) \quad \dots \quad (28)$$

Substituting in (10) and integrating we have

$$\pi' \sim \pi_0' + \text{const. } t^{\frac{d-a}{d+1}}. \quad (t \rightarrow 0) \quad \dots \quad (29)$$

Hence  $d > a$ , which contradicts the previous inequality  $a > d$ . Hence  $p_0'$  cannot be finite. We have then to seek a solution satisfying the following boundary conditions

$$\begin{aligned} q_0 = 0, \quad \pi_0 = 0, \quad \xi_0 = 0 \\ q_0' = 0, \quad \pi_0' = \infty, \quad \xi_0' = \infty \end{aligned} \quad \dots \quad (30)$$

We shall prove such solution cannot exist if  $d > a$ , i.e.  $b > 3a$ .

Let  $a < t < t_1$ . Then  $p_0'$  being infinite, and  $p_0 = 0$ , if  $t_1$  be sufficiently small,

$$p > p't > p_1't. \quad (t < t_1) \quad \dots \quad (31)$$

Similarly, since  $q_0 = 0$ , and  $q_0' = 0$

$$q < q't < q_1't. \quad (t < t_1) \quad \dots \quad (32)$$

Now

$$\xi' = \frac{q^t}{p} < \frac{q^t}{p_1't} < \frac{q_1'^t}{p_1'} t^{-t} \quad \dots \quad (33)$$

whence integrating from 0 to  $t$  we have

$$\xi < 4 \left( \frac{q_1'}{p_1'} \right)^{\frac{1}{4}}. \quad t^t = c t^t \quad (t < t_1) \quad \dots \quad (33a)$$

Substituting in (10) we obtain

$$-\pi'' = \beta \xi^{-4} > c't^{-1} \quad \dots \quad (34)$$

whence integrating

$$\pi' - \pi_1' > c' \log(t_1/t). \quad (t < t_1) \quad \dots \quad (35)$$



But we have also  $(\pi_0 = 0, \pi_0' = \infty)$  just like (31)

$$\pi > \pi' t. \quad \dots \dots \dots (31a)$$

Hence

$$\pi > \pi_1' t + c' t \log(t_1/t); \quad (t < t_1) \quad \dots \dots \dots (36)$$

(36) with (32) gives

$$p > p_1' t + c' t \log(t_1/t). \quad (t < t_1) \quad \dots \dots \dots (36a)$$

From equations (12), (32) we have

$$p^a = q^d q' < q'^{d+1} t^d < q_1'^{d+1} t^d$$

so that

$$p < q_1' \frac{d+1}{a} t^{\frac{d}{a}}. \quad (t < t_1) \quad \dots \dots \dots (37)$$

Comparing (37) with (36a) we find these two relations are inconsistent as  $t \rightarrow 0$  if  $d > a$ .

We have succeeded neither in obtaining the form of the solution satisfying (30) as  $t \rightarrow 0$ , for  $d < a$ , i.e.  $b < 3a$ , nor in proving that such a solution does not exist. However, if this solution should exist and have astrophysical significance we note the corresponding sphere should have infinite mass and radius, and the temperature should vanish at infinity, in fact it should diminish to insignificance long before that.

(ii) Suppose  $q_0'$  is finite and  $\neq 0$ . Then since  $q_0 = 0$

$$q \sim q_0' t. \quad (t \rightarrow 0) \quad \dots \dots \dots (38)$$

Substituting in (12) we obtain

$$p \sim q_0' \frac{d+1}{a} t^{\frac{d}{a}}. \quad (t \rightarrow 0) \quad \dots \dots \dots (39)$$

Equation (11) gives

$$\xi' \sim \frac{1}{q_0' \left( \frac{d+1}{a} - \frac{1}{4} \right)} \cdot t^{\frac{1}{4} - \frac{d}{a}} = c_1 t^{\frac{1}{4} - \frac{d}{a}} \quad \dots \quad (t \rightarrow 0) \quad \dots \quad (40)$$

which shows  $\frac{d}{a} > \frac{1}{4}$ . Integration of equation (40) gives

$$\xi \sim c_2 t^{\frac{5}{4} - \frac{d}{a}} \quad (t \rightarrow 0) \quad \dots \dots \dots (41)$$

where  $c_2$  is a positive constant, and

$$\frac{1}{4} < \frac{d}{a} < \frac{5}{4}.$$

Let us use this time equations (10a, b) instead of (10). Substituting (41) in (10a) and integrating we obtain

$$m \sim m_0 - \frac{1}{4c_2 \left( \frac{d}{a} - 1 \right)} t^{\left( \frac{d}{a} - 1 \right)} \quad (t \rightarrow 0) \quad \dots \dots \dots (42)$$

Let us first assume the total mass  $m_0$  to be finite. This requires by (42)

$$\frac{d}{a} > 1 \quad \dots \dots \dots (43)$$

Then integration of (10b) gives

$$\pi \sim q_0' t \quad (t \rightarrow 0) \quad \dots \dots (44)$$

since from (38) we have

$$\beta m_0 = q_0' \quad \dots \dots \dots (45)$$

There exists thus for  $q_0 = 0$ ,  $q_0' =$  finite quantity  $\neq 0$ , a solution with finite mass and infinite radius when

$$1 < \frac{d}{a} < \frac{5}{4}$$

i.e.

$$3a < b < 4a \quad \dots \dots \dots (46)$$

This is really the same solution as under the condition (25a), Case 2 (ii), which is now shown to exist continuously for all  $\xi_0$  up to the limit  $\xi_0 = 0$ .

Next suppose the total mass  $m$  to be infinite ( $\pi_0'$  infinite).

Then

$$m \sim \frac{1}{4c_2^4 \left(1 - \frac{d}{a}\right)} t^{\frac{4}{a} - 1} \quad (t \rightarrow 0) \quad \dots \dots (47)$$

so that

$$\frac{d}{a} < 1.$$

Substituting in (10b) and integrating we have

$$\pi \sim \frac{\beta}{c_2^4 \left(1 - \frac{d}{a}\right) \left(\frac{4d}{a} - 3\right)} t^{\frac{4d}{a} - 3} \quad (t \rightarrow 0) \quad \dots \dots (48)$$

Since  $\pi_0 = 0$ , we must have  $d > 3/4$ , so that

$$\frac{3}{4} < \frac{d}{a} < 1 \quad \dots \dots \dots (49)$$

But since  $4d/a - 3 < 1$  we have comparing (38) and (48)

$$p \sim \frac{\beta}{c_2^4 \left(1 - \frac{d}{a}\right) \left(\frac{4d}{a} - 3\right)} t^{\frac{4d}{a} - 3} \quad (t \rightarrow 0) \quad \dots \dots (50)$$

This is consistent with (39) only when  $d/a = 1$  which contradicts (49). Hence  $q_0' =$  finite  $\neq 0$ , and  $m$  infinite furnishes no solution of interest.

(iii) We now take the third alternative  $q_0' = \infty$ . With this we consider the three possibilities  $\pi_0' = \infty$ , while  $p_0' = 0$ , or a finite quantity  $\neq 0$ , or  $\infty$ .

Let us first take  $p_0' =$  a finite quantity. Since  $p_0 = 0$  we have

$$p \sim p_0' t \quad (t \rightarrow 0) \quad \dots \quad (51)$$

Substituting in (12) and integrating we obtain

$$q \sim \text{const. } t^{\frac{a+1}{d+1}}. \quad (t \rightarrow 0) \quad \dots \quad (52)$$

Since  $q_0' = \infty$ , we must have  $d > a$ . Substituting (51) and (52) in (11) and integrating we have

$$\xi \sim \text{const. } t^{\frac{a+1}{d(d+1)}}. \quad (t \rightarrow 0) \quad \dots \quad (53)$$

Using (53) in (10) we obtain

$$-\pi'' \sim \text{const. } t^{-\frac{a+1}{d+1}}. \quad (t \rightarrow 0) \quad \dots \quad (54)$$

whence

$$\pi' \sim \text{const. } t^{\frac{d-a}{d+1}}. \quad (t \rightarrow 0) \quad \dots \quad (55)$$

Since  $\pi_0' = \infty$ , we should have  $d < a$ , which contradicts our previous inequality  $d > a$ . Hence there is no solution with  $p_0 = a$  non-zero finite quantity.

Let  $p_0' = 0$ . We can easily show that this is incompatible with  $a > d$ .

Since  $p_0 = p_0' = 0$ ,  $q_0 = 0$ ,  $q_0' = \infty$ , then as  $t \rightarrow 0$ ,  $p$  is a small quantity of higher order than  $q$ . Hence as  $t \rightarrow 0$

$$q' = \frac{p''}{q^d} < \frac{q''}{q^d} = q^{a-d}.$$

This relation is incompatible with  $a > d$ . For  $a < d$  an explicit form of the solution has not been obtained.

Let us take the case  $q_0' = \infty$ , and  $p_0' = \infty$ . The following solution has been found by trial. Let

$$\xi \sim A t^m, \quad 0 < m < 1 \quad (t \rightarrow 0) \quad \dots \quad (56)$$

$$q \sim B t^n, \quad 0 < n < 1. \quad (t \rightarrow 0) \quad \dots \quad (57)$$

Substitution in (10) gives

$$\pi'' \sim -\beta A^{-4} t^{-4m}$$

whence integrating we obtain

$$\pi' \sim \frac{\beta}{A^4(4m-1)} t^{1-4m}. \quad (t \rightarrow 0) \quad \dots \quad (58)$$

Hence  $m > \frac{1}{4}$ . A further integration gives

$$\pi \sim \frac{\beta}{A^4(4m-1)(2-4m)} t^{2-4m}. \quad (t \rightarrow 0) \quad \dots \quad (59)$$

Since  $\pi_0 = 0$ , we have  $m < \frac{1}{2}$ , so that  $\frac{1}{4} < m < \frac{1}{2}$ . We write (59) as

$$p + \alpha B t^n \sim \frac{\beta}{A^4(4m-1)(2-4m)} t^{2-4m}; \quad \dots \quad (60)$$

then a solution of the desired form is obtained by taking  $p$  to be a small quantity of much higher order than  $q$ , so that in (60) we put

$$n = 2-4m \quad \dots \quad (61)$$

and

$$\alpha B = \frac{\beta}{A^4(4m-1)(2-4m)} \quad \dots \quad (61a)$$

We note that (61) is compatible with  $n < 1$  while  $\frac{1}{4} < m < \frac{1}{2}$ . The order of  $p$  we determine by substituting in (11)

$$A m t^{n-1} \sim \frac{B^{\frac{1}{4}} t^{\frac{n}{4}}}{p}$$

whence

$$p \sim \frac{B^{\frac{1}{4}}}{A m} \cdot t^{\frac{n}{4}-m+1} \cdot (t \rightarrow 0) \quad \dots \quad (62)$$

We note  $n/4-m+1 > n$  is satisfied. Next substituting in (12) we obtain

$$B^d \cdot t^{nd} \cdot n B t^{n-1} \sim \left( \frac{B^{\frac{1}{4}}}{A m} \right)^a \cdot t^{a(\frac{n}{4}-m+1)}$$

whence

$$nd+n-1 = a\left(\frac{n}{4}-m+1\right)$$

giving

$$m = \frac{2d+1-3a/2}{4d+4-2a} = \frac{b-2a+2}{2b-2a+8} \quad \dots \quad (63)$$

and

$$n B^{d+1} = \left( \frac{B^{\frac{1}{4}}}{A m} \right)^a \quad \dots \quad (64)$$

(61) and (63) give  $m$  and  $n$ , and then (61a) and (64)  $A$  and  $B$ . The solution we can put as

$$\xi \sim \text{const. } t^m, \quad q \sim \text{const. } t^{2-2m} \quad p \sim \text{const. } t^{\frac{3}{2}-2m}, \quad \rho \propto t^{1-m} \cdot (t \rightarrow 0) \quad \dots \quad (65)$$

where  $m$  is given by (63). The condition  $\frac{1}{4} < m < \frac{1}{2}$  imposes the condition  $d > a$ , i.e.  $b > 3a$  for validity of the solution (65). This follows from (63). The permissible models belonging to Case 3 are all infinite with infinite masses.

Case 4. Let  $\xi_0 \neq 0$ ,  $q_0 \neq 0$ . Then  $\pi_0'$  is finite. But as  $q_0' = 0$  by (12),  $\pi_0' = p_0'$ , while  $\pi_0 \neq 0$ . We first take  $p_0' \neq 0$  but finite. Then

$$p \sim p_0' t \cdot (t \rightarrow 0).$$

Equation (11) we can write as

$$\xi' \sim \frac{q_0^{\frac{1}{2}}}{p} = \frac{q_0^{\frac{1}{2}}}{p_0} \cdot \frac{1}{t} \quad (t \rightarrow 0).$$

so that

$$\xi \sim \frac{q_0^{\frac{1}{2}}}{p_0} \log t, \quad (t \rightarrow 0)$$

but this is incompatible with  $\xi_0$  finite. The possibility  $p_0' = 0$  is excluded otherwise we should have  $\pi_0' = 0$ . Hence there can be no solution of interest under Case 4.

#### Conclusion.

4. Our results we summarise as follows. If the energy generation is entirely confined to a region near the centre, outside which the luminosity is constant, and the opacity is given by  $\kappa = \kappa_0 \rho^a T^{-b}$  ( $a, b > 0$ ), then the only case in which *finite* stellar configurations with density and temperature both vanishing at the boundary may be possible occurs when  $b < 4a$  (Case 2). Generally, for all positive values of  $b$  and  $a$  there are solutions which correspond to infinite configurations behaving ultimately as isothermal gas spheres (Case 1). Solutions which correspond to finite stellar configurations with non-zero temperature but zero density at the boundary do not exist under the present scheme.

The first two cases integrated by Burman correspond to  $b > 4a$ , and hence only infinite configurations are to be expected. It is further evident (as is also verified from Burman's Tables) that the solutions obtained all belong to our Case 1, and are of the type described by the equations (15a), (16a) and (16b), which give ultimately isothermal spheres with generally non-zero limiting temperatures.

# ACCURATE CALCULATIONS ON THE CASCADE THEORY OF ELECTRONIC SHOWERS WITHOUT COLLISION LOSS.

By S. K. CHAKRABARTY, *Department of Applied Mathematics, University of Calcutta.*

(Communicated by Dr. H. J. Bhabha, F.R.S., F.N.I.)

(Received May 5, 1942.)

## ABSTRACT.

A rigorous solution of the equations of the Cascade theory, taking the radiation and pair creation cross-sections to be those for complete screening and neglecting collision loss entirely is given. The solution is expressed in the form of an integral, from which the nature of the energy spectra of the shower particles as well as the total number of particles at any depth produced in a particle excited shower and also in a quantum excited shower for various energies of the primary have been obtained. The differences occurring between a particle excited shower and a quantum excited shower has been interpreted physically. The results of the present paper have been compared with similar results of the previous authors.

Following the physical ideas put forward by Bhabha and Heitler (1937) and Carlson and Oppenheimer (1937), the theory of the cascade process in cosmic rays has been worked out by several authors with a view to making a more rigorous treatment of the problem both from the standpoint of physical assumptions and mathematical treatments. Landau and Rumer (1938) tried to work out the problem, neglecting ionisation or collision loss. Starting in a rigorous way, they ultimately made such approximations that instead of giving more accurate figures than those of the preceding authors, their results are often in error by as much as a factor thirty. Later on Serber (1938) tried to work out the same problem and extended the calculations of Snyder (1938). But their analysis is defective for various reasons\*.

In a paper by Bhabha and the present author† a complete theory of the cascade production of cosmic ray showers together with the effect of the collision loss on it has been given. In the present paper we give the results obtained

\* The function  $k(y, s)$ , used by Serber, is easily seen to be given by

$$k_{\mu}(y, s) = \prod_{r=1}^s \frac{r^{\mu}}{(\mu_y - \mu_{y+r})(\mu_y - \nu_{y+r})}; \quad k_{\nu}(y, s) = \prod_{r=1}^s \frac{r^{\nu}}{(\nu_y - \mu_{y+r})(\nu_y - \nu_{y+r})}.$$

With these values of  $k(y, s)$ , the expression for  $Z$ , as given by eq. (6) is an infinite series which obviously *diverges for all values of  $E$* . Consequently,  $Z$  cannot be a proper solution of the problem. Their series does not satisfy the correct boundary conditions at  $t = 0$ , and due to the divergence of the series it is impossible to say that the boundary conditions are satisfied even approximately. The expression given for  $N$  without the term  $k_{\mu}(y, -y)$  will, however, give the total number of particles having energies greater than  $\beta$ , if collision loss is neglected, as will be evident from the present paper.

† In course of publication, referred to in this paper as (A).

when one neglects the collision loss completely. A comparison with similar results obtained by the previous authors has also been made at the end.

In making such calculations the exact cross-sections for radiation loss and pair creation, for the case of complete screening as given by Bethe and Heitler (1934) have been taken. The variation of these cross-sections due to incompleteness of screening and also the effect of collision loss have been neglected. Denoting by  $t$  all lengths measured in terms of a characteristic length such that a length of 1 c.m. in a material corresponds to

$$t = \frac{4NZ^2}{137} \cdot \left( \frac{e^2}{mc^2} \right)^2 \log(183Z^{-1}), \dots \dots \dots (1)$$

let  $P(E, t)dE$  and  $Q(E, t)dE$  be the number of particles and quanta respectively at any depth  $t$  and having energies lying between  $E$  and  $E+dE$ . Also let  $N(E, t)$  be the total number of particles at the depth  $t$  and having energies greater than  $E$ . Following the work of Landau and Rumer, Bhabha and the present author have shown that neglecting collision loss, the total number of particles of energy greater than  $E$ , produced by a primary particle of energy  $E_0$ , is given exactly by,

$$N(E, t) = \frac{1}{2\pi i} \int_{\sigma-i\infty}^{\sigma+i\infty} \left( \frac{E_0}{E} \right)^{S-1} \cdot \frac{1}{S-1} \cdot \left\{ \frac{D-\lambda}{\mu-\lambda} e^{-\lambda t} + \frac{\mu-D}{\mu-\lambda} e^{-\mu t} \right\} dS \quad (2)$$

and also the energy spectrum for particles and quanta are given by

$$P(E, t) = \frac{1}{2\pi i E_0} \int_{\sigma-i\infty}^{\sigma+i\infty} \left( \frac{E_0}{E} \right)^S \cdot \left\{ \frac{D-\lambda}{\mu-\lambda} e^{-\lambda t} + \frac{\mu-D}{\mu-\lambda} e^{-\mu t} \right\} dS \quad \dots \quad (3a)$$

$$Q(E, t) = \frac{1}{2\pi i E_0} \int_{\sigma-i\infty}^{\sigma+i\infty} \left( \frac{E_0}{E} \right)^S \cdot \frac{C}{\mu-\lambda} \cdot \left\{ e^{-\lambda t} - e^{-\mu t} \right\} dS \quad \dots \quad (3b)$$

$$\text{where} \quad A_S = \left( \frac{4}{3} + \alpha \right) \left\{ \frac{d}{dS} \log \Gamma(S) + \gamma - 1 + \frac{1}{S} \right\} + \frac{1}{2} - \frac{1}{S(S+1)}, \dots \quad (4a)$$

$$B_S = 2 \left[ \frac{1}{S} - \left( \frac{4}{3} + \alpha \right) \frac{1}{(S+1)(S+2)} \right], \quad \dots \quad (4b)$$

$$C_S = \left[ \frac{1}{S+1} + \left( \frac{4}{3} + \alpha \right) \frac{1}{S(S-1)} \right], \quad \dots \quad (4c)$$

$$D = \frac{7}{9} - \frac{1}{6} \alpha, \quad \dots \quad (4d)$$

and  $\alpha = 1/9 \log(183Z^{-1})$ ,  $\gamma$  the Euler-Mascheroni constant.

$\lambda, \mu$  are the roots of the equation

$$x^2 - (A_S + D)x + (A_S D - B_S C_S) = 0. \quad \dots \quad (5)$$

$\sigma$  is some real number greater than 1.

We, therefore, have

$$N(E, t) = N_\lambda(E, t) + N_\mu(E, t) \quad \dots \quad (6)$$

$$\text{where} \quad N_\lambda(E, t) = \frac{1}{2\pi i} \int_{\sigma-i\infty}^{\sigma+i\infty} \exp\{y(S-1) - \lambda t\} \cdot \frac{1}{S-1} \cdot \frac{D-\lambda}{\mu-\lambda} dS. \quad (7a)$$

$$N_\mu(E, t) = \frac{1}{2\pi i} \int_{\sigma-i\infty}^{\sigma+i\infty} \exp\{y(S-1) - \mu t\} \cdot \frac{1}{S-1} \cdot \frac{\mu-D}{\mu-\lambda} dS. \quad (7b)$$

$$\text{where} \quad y = \log_e \left( \frac{E_0}{E} \right).$$

The integral (7a) can be evaluated by the saddle point method, with an error which is less than 2 per cent, and is given by

$$N_\lambda(E, t) = \frac{\exp \psi(S_0)}{\sqrt{2\pi\psi''(S_0)}}, \quad \dots \quad (8)$$

$$\text{where} \quad \psi(S) = y(S-1) - \lambda t + \log \left( \frac{1}{S-1} \cdot \frac{D-\lambda}{\mu-\lambda} \right) \quad \dots \quad (9)$$

and  $S_0$  is the saddle point, such that  $\psi'(S_0) = 0$ . A dash represents differentiation with respect to  $S$ .

The values of  $\lambda$ ,  $\mu$ ,  $\frac{d\lambda}{dS}$ ,  $\frac{d\mu}{dS}$ ,  $\frac{d^2\lambda}{dS^2}$  and  $\frac{d^2\mu}{dS^2}$  can be calculated from equations (4) and (5) for all real values of  $S$ . A complete table of such values has been given in (A). From this table the values of  $\psi(S)$ ,  $\psi'(S)$  and  $\psi''(S)$  can be obtained for all real values of  $S$  at intervals of 0.1. For any other value of  $S$  lying between any two tabulated values, the values of  $\psi(S)$  and  $\psi''(S)$  are to be obtained by using Newton's formula for forward interpolation, viz.

$$\phi(S) = \phi(S_1) + \frac{S-S_1}{h} \cdot \Delta \phi(S_1) + \frac{(S-S_1)(S-S_2)}{2! h^2} \Delta^2 \phi(S_1) + \dots \quad (10)$$

where  $S$  lies between  $S_1$  and  $S_2$  which are the tabulated points and  $S_2 - S_1 = h$  and  $\Delta \phi(S_1)$ ,  $\Delta^2 \phi(S_1)$ , etc. are the successive differences. Putting  $\frac{S-S_1}{h} = x$ , we have

$$\phi(S_1 + xh) = \phi(S_1) + x \Delta \phi(S_1) + \frac{x(x-1)}{2!} \Delta^2 \phi(S_1) + \dots \quad (11)$$

Equation (11) has been used for the determinations of  $\psi(S_0)$  and  $\psi''(S_0)$ .

To get the value of  $S_0$  we use (11) taking  $\psi'(S)$  instead of  $\phi(S)$  and putting  $S_0 = S_1 + xh$ , we make  $\psi'(S_1 + xh) = 0$ , so that we have

$$0 = \psi'(S_1) + x \Delta \psi'(S_1) + \frac{x(x-1)}{2!} \Delta^2 \psi'(S_1) + \dots$$

So that,

$$x = - \frac{\psi'(S_1)}{\Delta \psi'(S_1) - \frac{1}{2} \Delta^2 \psi'(S_1)} - \frac{x^2}{2} \cdot \frac{\Delta^2 \psi'(S_1)}{\{\Delta \psi'(S_1) - \frac{1}{2} \Delta^2 \psi'(S_1)\}},$$

and consequently to a second approximation,

$$x = - \frac{\psi'(S_1)}{\Delta \psi'(S_1) - \frac{1}{2} \Delta^2 \psi'(S_1)} - \frac{1}{2} \cdot \frac{\Delta^2 \psi'(S_1) \cdot \{\psi'(S_1)\}^2}{\{\Delta \psi'(S_1) - \frac{1}{2} \Delta^2 \psi'(S_1)\}^2} \quad \dots \quad (12)$$



The value of  $S_1$  for given values of  $y$  and  $t$  can be easily obtained by noting the change in sign of the tabulated values of  $\psi'(S)$ . Since the values of  $S_1$  and  $S_2$  are known to the first place of decimal and to the order of accuracy we require, one more place in the value of  $S_0$  is sufficient, it is enough to consider up to a second approximation. The value of  $x$  given by (12) can thus be considered as sufficiently accurate. Thus knowing  $x$  we get  $S_0$  immediately.

The values of  $N_\lambda$  thus obtained from (8) are given in Table I. It can also be shown as in (A) that

$$N_\mu(E, t) = \exp \left[ \left\{ \frac{1}{2} - \alpha'(\gamma - 1) \right\} t \right] \cdot \left( \frac{2y}{3\alpha't} \right)^{\alpha'/2} \cdot J_{\alpha't}(\sqrt{6\alpha'ty}) \quad \dots (13)$$

where

$$\alpha' = \left( \frac{1}{2} + \alpha \right).$$

The values of  $N_\mu$  are also given in Table I, from which it will be clear that for  $t > 3$ ,  $N_\mu$  is negligible.

TABLE I.  
Values of  $N_\lambda$  and  $N_\mu$  as functions of  $y$  and  $t$  for a particle excited shower.

$y \backslash t$		1.0	2.0	3.0	4.0	6.0	8.0	10.0	15.0	25.0
2	$N_\lambda$	1.14	0.723	0.445	0.247					
	$N_\mu$	0.12	0.02							
3	$N_\lambda$	1.59	2.05	1.73	1.19	0.453	0.168	0.0548		
	$N_\mu$	-0.30	-0.22							
4	$N_\lambda$	2.32	4.07	4.58	4.06	2.13	0.889	0.328	0.0223	
	$N_\mu$	-0.54	-0.34							
5	$N_\lambda$	3.19	7.20	9.91	10.6	7.81	4.07	1.77	0.148	$5.48 \times 10^{-3}$
	$N_\mu$	-0.53	-0.22							
6	$N_\lambda$	4.20	11.64	19.26	24.56	23.52	15.45	7.99	0.909	$4.84 \times 10^{-3}$
	$N_\mu$	-0.38	0.18	0.20						
7	$N_\lambda$	5.70	17.96	34.05	50.70	63.21	50.45	31.34	4.870	$3.39 \times 10^{-3}$
	$N_\mu$	-0.10	0.56	0.30						
8	$N_\lambda$	6.81	25.82	57.51	98.14	157.0	149.6	108.4	22.82	0.230
	$N_\mu$	0.28	0.72	0.22						
9	$N_\lambda$	7.65	36.83	93.64	174.4	340.8	401.9	330.2	98.09	1.43
	$N_\mu$	0.56	0.30	-0.17						
10	$N_\lambda$	9.40	48.37	142.9	305.4	720.2	1000	981.5	371.1	8.24

If the primary be a quantum of energy  $E_0$  instead of a particle, we have for the boundary conditions,

$$P(E, 0) = 0 \text{ and } Q(E, 0) = \delta(E_0 - E). \quad \dots \quad (14)$$

In this case we have

$$P(E, t) = \frac{1}{2\pi i E_0} \int_{\sigma-i\infty}^{\sigma+i\infty} \left(\frac{E_0}{E}\right)^S \cdot \frac{B}{\mu-\lambda} \left\{ e^{-\lambda t} - e^{-\mu t} \right\} dS \quad \dots \quad (15a)$$

$$Q(E, t) = \frac{1}{2\pi i E_0} \int_{\sigma-i\infty}^{\sigma+i\infty} \left(\frac{E_0}{E}\right)^S \cdot \left\{ \frac{\mu-D}{\mu-\lambda} e^{-\lambda t} + \frac{D-\lambda}{\mu-\lambda} e^{-\mu t} \right\} dS. \quad \dots \quad (15b)$$

Consequently, the total number of particles  $N_Q(E, t)$  produced in a quantum excited shower is given by

$$N_Q(E, t) = \frac{1}{2\pi i} \int_{\sigma-i\infty}^{\sigma+i\infty} \left(\frac{E_0}{E}\right)^{S-1} \cdot \frac{B}{\mu-\lambda} \cdot \frac{1}{S-1} \cdot \left( e^{-\lambda t} - e^{-\mu t} \right) dS, \\ \approx \frac{1}{2\pi i} \int_{\sigma-i\infty}^{\sigma+i\infty} \left(\frac{E_0}{E}\right)^{S-1} \cdot \frac{B}{\mu-\lambda} \cdot \frac{1}{S-1} \cdot e^{-\lambda t} dS, \quad \dots \quad (16)$$

except for very small  $t$ .

The values of  $P(E, t)$ ,  $Q(E, t)$  and  $N_Q(E, t)$  can similarly be calculated by the saddle-point method. The values of  $N_Q(E, t)$  for different values of  $y$  and  $t$  are given in Table II.

TABLE II.

Values of  $N_Q(E, t)$  as functions of  $t$  for a quantum excited shower.

$y \backslash t$	1.0	2.0	3.0	4.0	6.0	8.0	10.0	15.0	25.0
2	0.784	0.854	0.662	0.430					
3	1.07	1.70	1.75	1.47	0.735	0.293			
4	1.39	2.04	3.90	4.02	2.76	1.38	0.575		
5	1.81	4.78	7.73	9.36	8.67	5.41	2.68	0.287	
6	2.20	7.12	13.7	19.6	21.9	18.0	10.7	1.55	
7	2.66	10.0	23.2	37.9	58.2	54.1	38.3	7.58	0.0687
8	2.95	14.3	37.1	68.6	131	149	123	32.6	0.441
9	3.54	18.4	57.9	119	279	374	362	130	22.4
10	4.38	25.9	86.5	201	563	901	993	473	13.8

It will be evident from Tables I and II that the curves giving  $N$  as a function of  $t$  are almost the same for a shower produced by a particle or a quantum of the same initial energy, with the difference that the latter curve is shifted to a greater thickness by nearly one unit of length over the whole of its range. It has been shown in (A) that for a given  $y$  the maximum of  $N$

and  $P$  will occur at such a value of  $t$  that the corresponding value of  $S_0$  is 2. From this it can be deduced that for a given  $y$  the maximum of  $N$  for a particle excited shower will occur at a thickness, 0.82 in characteristic units less than that for a quantum excited shower. The value of  $N_{\max}$  for the former, however, will be greater than that of the latter, although the relative difference decreases as  $y$  increases. This will be clear from Fig. 1 where the  $N-t$  curve for two different values of  $y$ , viz. 4 and 10, have been given both for the particle excited shower ( $P$ ) and quantum excited shower ( $Q$ ). This is exactly what is to be expected from the physical nature of the problem. A high energy quanta, on entering the material, creates a pair within a very short distance in which one particle either has an energy *nearly* equal to that of the quanta, which then produces the cascade, or two particles, each with about half the energy, both of which produce smaller cascades.

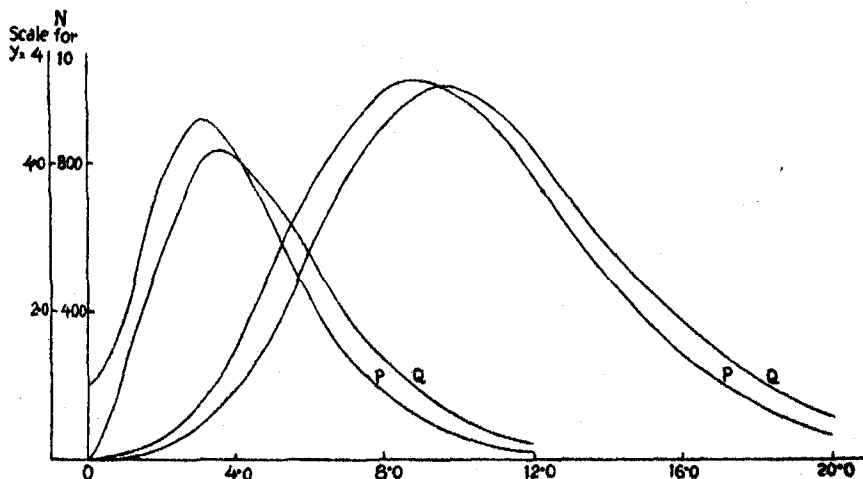


FIG. 1.

A comparison of the values of  $N$  obtained from (7) with similar figures obtained from the work of the previous authors has been made in Table III. It is clear from Table III that the results obtained by Bhabha and Heitler are correct to within thirty per cent at the position of the maximum and also to the left of it in the transition curve. For a particular value of  $y$ , the values of  $N$  as obtained by Bhabha and Heitler are less than that of the present paper before the maximum of the transition curve is attained, after which the values of Bhabha and Heitler are higher than those of the present paper. The values of Carlson and Oppenheimer are very much higher than those of the present paper. This is due to the approximate forms of the expressions assumed for the cross-sections of the different processes.

TABLE III.

Comparison of the values of  $N$  for a particle excited shower.

B. &amp; H. = Bhabha and Heitler.

C. &amp; O. = Carlson and Oppenheimer.

C. = Present author.

$y \backslash t$		2	4	6	8	10	12
3	B. & H.	1.50	1.64	0.60	0.22	0.06	
	C. & O.	3.30	3.00	1.30	0.80	0.20	
	C.	1.83	1.13	0.45	0.17	0.055	
5	B. & H.	6.40	12.00	10.60	6.80	3.20	1.40
	C.	6.98	10.61	7.81	4.07	1.77	0.689
10	B. & H.	40.0	250	640	1130	1360	1040
	C.	48.37	305.4	720.2	1000	981.5	752.0

In conclusion, I wish to express my thanks to Dr. H. J. Bhabha, for his various suggestions during the preparation of this paper and also wish to thank Professors N. R. Sen, M. N. Saha, and D. M. Bose, for their kind interest and encouragement.

A portion of this work was carried out at the Indian Institute of Science, Bangalore. I am much indebted to the Director Dr. J. C. Ghosh for giving me every facility while working at the Institute.

## REFERENCES.

- Bethe, H. and Heitler, W. (1934). On the Stopping of Fast Particles and Creation of Positive Electrons. *Proc. Roy. Soc., A*, **146**, 83-112.
- Bhabha, H. J. and Heitler, W. (1937). The Passage of Fast Electrons and the Theory of Cosmic Showers. *Proc. Roy. Soc., A*, **159**, 432-458.
- Carlson, J. F. and Oppenheimer, J. R. (1937). On Multiplicative Showers. *Phys. Rev.*, **51**, 220-231.
- Landau, L. and Rumar, G. (1938). The Cascade Theory of Electronic Showers. *Proc. Roy. Soc., A*, **166**, 213-228.
- Serber, R. (1938). Transition Effects of Cosmic Rays in the Atmosphere. *Phys. Rev.*, **54**, 317-320.
- Snyder, H. (1938). Transition Effects of Cosmic Rays in the Atmosphere. *Phys. Rev.*, **53**, 960-965.



# CONTRIBUTION TO THE THEORY OF STELLAR MODELS.

By N. R. SEN.

(Received May 20, 1942.)

## ABSTRACT.

Stellar models for the energy generation law  $\eta \propto \rho^\alpha T^\delta$  studied by Chandrasekhar have been examined as regards their dimensions and convective stability. It is found only the standard solutions represent finite configurations. Further, Chandrasekhar's  $\gamma$ -models are all radiatively unstable for  $\gamma > \frac{1}{2}$ . The stability condition for  $(\alpha, \delta)$ -model has also been studied.

## 1. INTRODUCTION.

Stellar models in which the average energy generation per unit mass of enclosed matter denoted by  $\eta$  is given by

$$\eta = \eta_0 \rho^\alpha T^\delta \quad \dots \quad (1)$$

$\rho$  and  $T$  being density and temperature respectively at the point concerned, have been considered by Chandrasekhar (1936, 1937). Taking the opacity to be given by a formula analogous to that of Kramers, Chandrasekhar has studied the relation between  $\rho$  and  $T$  within such stellar bodies, and also the conditions for the inversion of density gradient. The case  $\alpha = 0$ , called by him  $\gamma$ -model, has been considered in detail, and as regards the general character of density-temperature relationship proves to be typical of the more general case  $\alpha > 0$ . Denoting temperature and density measured in suitable units by  $\tau$  and  $\sigma$  respectively, three types of  $\tau$ - $\sigma$  solution curves have been shown to exist. Of these there are two which may correspond to stellar conditions even up to the boundary. The first type of solution, called standard solution by Chandrasekhar (denoted here by  $S$ ), can be represented by a curve starting from the origin ( $\tau = 0, \sigma = 0$ ) at a definite slope rising gradually, in some cases going to infinity, and in others turning back at a certain stage and asymptotically approaching the  $\tau$ -axis. A second type of solution curves starts from the  $\tau$ -axis with a steep gradient, rises upwards to a maximum, and then bends back and quickly assumes an asymptotic form approaching the  $\tau$ -axis. These may correspond to stellar bodies with finite surface temperatures (called in this paper  $I$  solutions). A third type of solution curves in which  $\sigma \rightarrow \text{const. or } \infty$ , as  $\tau \rightarrow 0$  will not be considered here.

Beyond isolating these solutions and studying their density gradients which bring to light the density temperature relationship within the models, further characteristics of these solutions have not been studied by Chandrasekhar. In the present paper we shall consider two other aspects of these solutions. Firstly, we shall study if  $S$  and  $I$  solutions give finite configurations

and masses. Such solutions are of interest in the way that they *may* directly represent stellar body configurations. Secondly, there is the more important question of radiative stability. The above solutions have all been obtained on the assumption that the energy transfer within the models is mainly by radiation. But there are certain conditions which must be satisfied in order that this may be true. We shall test the *S* and *I* solutions of Chandrasekhar from this point of view.

Our examination of these solutions shows that whereas the *S* solutions give finite configurations,\* *I* solutions, as one can easily understand, ultimately correspond to isothermal gas spheres with infinite radii and masses. Further, many of the *S* solutions are radiatively unstable, those for fairly high values of  $\delta$  all along the solution curve, while others for lower values of  $\delta$  for temperatures ( $\tau$  values) higher than certain limiting ones. Values of  $\alpha$  higher than 2 are inconsistent with stability except under some rather unimportant special conditions. The *I* solutions have portions starting somewhat below their maxima and extending up to the  $\tau$ -axis (which they meet for finite values of  $\tau$ ) which are radiatively stable.

## PART I.

### 2. THE EQUATIONS.

For the energy generation defined by (1) and for a law of opacity given by

$$\kappa = \kappa_0 \frac{\rho^b}{T^{3+s}}, \quad \dots \dots \dots (2)$$

we have from the equations

$$\frac{dP}{dr} = - \frac{GM(r)}{r^2} \rho \quad \dots \dots \dots (3)$$

$$\frac{dp_r}{dr} = - \frac{\kappa \rho}{c} \frac{L(r)}{4\pi r^2} \quad \dots \dots \dots (4)$$

by following a well-known analysis of Chandrasekhar (1936)

$$\gamma xy^{\alpha+b} \frac{dy}{dx} = y^{\alpha+b} (1+y) - x \quad \dots \dots \dots (5)$$

where  $y = p_g/p_r = (\text{gas pressure})/(\text{radiation pressure})$ ,  $x = KT^{-4\gamma}$ ,

$$4\gamma = \delta + 3\alpha + 3b - s - 3, \quad K = 4\pi cGM/\kappa_0\eta_0L \cdot \left(\frac{k}{\mu H} \cdot \frac{3}{a}\right)^{\alpha+b} \dots \dots (6)$$

Using Chandrasekhar's variables

$$y = zq, \quad x = q^\gamma, \quad \nu = \alpha + b$$

we can write equation (5) as follows:

$$\frac{dz}{dq} = \frac{1}{q^2} \left(1 - \frac{q^{\gamma-\nu}}{z^\nu}\right). \quad \dots \dots \dots (7)$$

---

\* Chandrasekhar has indeed numerically worked out the *S* solutions for certain values of  $\gamma$ . They give finite configurations.

We want an equation to determine  $r$ . For this purpose we rewrite the equation

$$\frac{1}{r^2} \frac{d}{dr} \left[ \frac{r^2}{\rho} \frac{d}{dr} (p_r + p_q) \right] = -4\pi G \cdot \rho \quad \dots \quad (8)$$

in terms of  $z$  and  $q$ , and replacing  $r$  by the variable  $\xi$ , where

$$r = \left[ \frac{1}{4\pi G} \left( \frac{k}{\mu H} \right)^2 \cdot \frac{3}{a} \cdot K^{-4\gamma} \right]^{\frac{1}{2}} \xi$$

and using (7) to replace the derivative  $dz/dq$ , we have after some calculation the following equation between  $z$  and  $\xi$

$$\frac{1}{\xi^2} \frac{d}{d\xi} \left[ \frac{\xi^2}{zq^{\frac{1}{2}}(1-z^\gamma q^\gamma - \gamma)} \cdot \frac{dz}{d\xi} \right] = -zq^{\frac{1}{2}}. \quad \dots \quad (9)$$

Further from (3) we obtain

$$M(r) \propto - \frac{r^2}{\rho} \frac{dP}{dr} \propto \frac{\xi^2}{zq^{\frac{1}{2}}(1-z^\gamma q^\gamma - \gamma)} \cdot \frac{dz}{d\xi}. \quad \dots \quad (10)$$

Equations (7) and (9) will enable us to find the dimensions of the stellar models.

Chandrasekhar transforms equation (5) in  $\tau$ - $\sigma$  plane by putting

$$\rho = \rho_0 \sigma, \quad T = T_0 \tau \quad \dots \quad (11)$$

the constants  $\rho_0$ ,  $T_0$  being defined by

$$KT_0^{-4\gamma} = \frac{k}{\mu H} \cdot \frac{3}{a} \left( \rho_0 T_0 / K^\gamma \right)^{\frac{1}{2}} = 1. \quad \dots \quad (11a)$$

We have then the following connections between the variables

$$z = \sigma \tau, \quad q = \tau^{-4}, \quad x = \tau^{-4\gamma} = q^\gamma, \quad y = z/\tau^4 = \sigma/\tau^3. \quad \dots \quad (11b)$$

We may note  $\sigma \propto$  density,  $\tau \propto$  temperature,  $q^{-1} \propto$  (radiation pressure),  $z \propto$  gas pressure, and  $\xi \propto$  radial distance.

### 3. THE $\gamma$ -MODEL. $\gamma = 1$ .

The class of stellar models discussed in detail by Chandrasekhar corresponds to  $\alpha = 0$ ,  $b = 1$ ,  $4\gamma = (\delta - s)$ , and has been called by him  $\gamma$ -model. The nature of the integral curves of (5) on  $(\tau, \sigma)$ -plane has been described. The case  $\gamma = 1$  is specially interesting in consideration of the fact that the  $(\tau, \sigma)$  differential equation can then be integrated in closed form, and as regards the behaviour of the solution curves is typical of the cases  $\frac{1}{2} < \gamma < \frac{3}{2}$ . We shall first discuss the case  $\gamma = 1$ , and later proceed to deal with the more general case rather briefly. Rigorous proofs will be given in the Appendix.

Case  $\gamma = 1$ ,  $b = 1$ . We shall seek solutions of the equations

$$\frac{dz}{dq} = \frac{1}{q^2} \left( 1 - \frac{1}{z} \right) \quad \dots \quad (7a)$$

$$\frac{1}{\xi^2} \frac{d}{d\xi} \left[ \frac{\xi^2}{zq^{\frac{1}{2}}(1-z)} \cdot \frac{dz}{d\xi} \right] = -zq^{\frac{1}{2}} \quad \dots \quad (9a)$$



such that as  $\sigma \rightarrow 0$ ,  $\tau \rightarrow 0$ ; these solutions are known to exist ( $S$  solutions). We shall be interested in the region where  $\tau$  is small, and hence also  $z$ . The solution of (7a) in question is

$$\frac{1}{q} = -z - \log(1-z). \quad \dots \dots \dots (12)$$

For small  $z$  we have

$$zq^{\frac{1}{2}} \sim 2^{\frac{1}{2}} z^{\frac{1}{2}} \left(1 - \frac{1}{6} z\right).$$

Substituting in (9a) and putting

$$z^{\frac{1}{2}} = u, \quad 2^{\frac{1}{2}} \xi = \xi_1$$

we obtain for small  $u$

$$\frac{1}{\xi_1^2} \frac{d}{d\xi_1} \left[ \xi_1^2 \left\{ 1 + \frac{7}{6} u^2 + O(u^4) \right\} \frac{du}{d\xi_1} \right] = - \left\{ 1 - \frac{1}{6} u^2 + O(u^4) \right\} u. \quad (13)$$

This has solution such that as  $u \rightarrow 0$ ,  $\xi_1 \rightarrow \xi_0 < \infty$ . In fact it has solution of the type

$$u \sim (\xi_0 - \xi_1)^\alpha [A + B(\xi_0 - \xi_1) + C(\xi_0 - \xi_1)^2 + \dots] \quad (\xi_1 \rightarrow \xi_0)$$

with  $\alpha > 0$ . Substituting and keeping only relevant initial terms we have

$$\begin{aligned} & \left[ 1 + \frac{7}{6} (\xi_0 - \xi_1)^{2\alpha} A^2 \right] [A\alpha(\alpha-1)(\xi_0 - \xi_1)^{\alpha-2} + B\alpha(\alpha+1)(\xi_0 - \xi_1)^{\alpha-1} \\ & + C(\alpha+1)(\alpha+2)(\xi_0 - \xi_1)^\alpha] + \frac{7}{3} A(\xi_0 - \xi_1)^\alpha \cdot A^2 \alpha^2 (\xi_0 - \xi_1)^{2\alpha-2} \\ & + \frac{2}{\xi_0} \left( 1 + \frac{\xi_0 - \xi_1}{\xi_0} \right) [-A\alpha(\xi_0 - \xi_1)^{\alpha-1} - B(\alpha+1)(\xi_0 - \xi_1)^\alpha] = -A(\xi_0 - \xi_1)^\alpha. \end{aligned}$$

From this the initial coefficients can be calculated

$$\alpha = 1$$

$$2B - \frac{2}{\xi_0} A = 0, \quad 6C + \frac{7}{3} A^2 - \frac{4B}{\xi_0} - \frac{2A}{\xi_0^2} = -A$$

whence the asymptotic form (14) is found except for an arbitrary constant  $A$ .  $A$  determines the slope of the  $u$  curve at its zero  $\xi_0$ .

The form of (13) also shows that for every small  $u$  the solution of (13) will behave as the solution of

$$\frac{1}{\xi_1^2} \frac{d}{d\xi_1} \left( \xi_1^2 \frac{du}{d\xi_1} \right) = -u \quad \dots \dots \dots (13a)$$

which represents a polytrope of index 1. The solution of (13a) is of the form  $A(\sin \xi_1/\xi_1) + B(\cos \xi_1/\xi_1)$ , which is oscillatory in character. The amplitude of the oscillation is of the order of  $\frac{1}{\xi_1}$ , while the difference in the solutions of (13) and (13a) in a sufficiently small interval round the zero of the solution (13a) can be shown to be at least of the order of  $\frac{1}{\xi_1^2}$ . So the solution in question of (13) will vanish just like that of (13a).

As regards *I* solutions we can show that (7a) and (9a) admit of solutions such that as  $\sigma \rightarrow 0$ ,  $\tau \rightarrow \tau_0 > 0$ , while  $\xi_1 \rightarrow \infty$ .

Let, as  $\tau \rightarrow \tau_0$ ,  $q \rightarrow q_0$ . Now since

$$\frac{dz}{dq} = \frac{d(\sigma\tau)}{d(\tau-t)} = -\frac{\tau^5}{4} \left( \tau \frac{d\sigma}{d\tau} + \sigma \right) \dots \dots \dots (14)$$

and as in *I* solutions  $d\sigma/d\tau \rightarrow \infty$  as  $\tau \rightarrow \tau_0$ , we note that  $dz/dq \rightarrow -\infty$  as  $q \rightarrow q_0$ , and  $z \rightarrow 0$ . By trial we get the following asymptotic solution

$$\left. \begin{aligned} z &\sim \frac{A}{\xi^\alpha}, \quad \alpha > 0. \quad (\xi \rightarrow \infty) \\ q &\sim q_0 - \frac{B}{\xi^{\alpha+c}}, \quad c > 0 \quad (\xi \rightarrow \infty) \end{aligned} \right\} \dots \dots \dots (15)$$

The condition  $c > 0$  makes  $dz/dq \rightarrow -\infty$  as  $\xi \rightarrow \infty$ . Substituting in (7a) we obtain

$$-\frac{A}{B} \frac{\alpha}{\alpha+c} \xi^c \sim -\frac{1}{Aq_0^2} \xi^\alpha$$

whence

$$c = \alpha, B = \frac{q_0^2 A^2}{2}.$$

Further substitution in (9a) gives

$$\frac{1}{\xi^2} \frac{d}{d\xi} \left( \frac{\alpha}{q_0^4} \xi \right) \sim A \xi^{-\alpha} q_0^4 \quad (\xi \rightarrow \infty)$$

whence

$$\alpha = 2, \text{ and } A = \frac{2}{q_0^4}.$$

Hence there is a solution of the type:

$$z \sim \frac{2}{q_0^4} \frac{1}{\xi^2}, \quad q \sim q_0 - \frac{2q_0}{\xi^4}. \quad (\xi \rightarrow \infty) \quad \dots \dots \dots (15a)$$

Substitution in (10) gives

$$M \sim \frac{\xi^2}{zq^4(z-1)} \frac{dz}{dq} \propto \xi \rightarrow \infty \text{ as } \tau \rightarrow \tau_0.$$

(15a) represents the asymptotic behaviour of *I* solutions for large  $\xi$ , and corresponds to configurations of infinite radii and masses.

On the other hand, it is not possible to construct a regular solution such that  $z \rightarrow 0$ ,  $q \rightarrow q_0$ , while  $\xi \rightarrow \xi_0 < \infty$ . For instance, let us suppose

$$\left. \begin{aligned} z &\sim A(\xi_0 - \xi)^\alpha, \quad \alpha > 1 \\ q &\sim q_0 - B(\xi_0 - \xi)^\beta, \quad \beta > 0 \end{aligned} \right\} \quad (\xi \rightarrow \xi_0) \quad \dots \dots \dots (16)$$

and

Then

$$\frac{dz}{dq} \sim -\frac{A\alpha}{B\beta} (\xi_0 - \xi)^{\alpha-\beta}.$$

Hence  $B > 0$  ( $A$  being positive), and  $\beta > \alpha$ .

(17a)

Substituting in (7a) and comparing both sides of equality we obtain

$$\beta = 2\alpha, B = \frac{A^2 \alpha q_0^2}{\beta} = \frac{A^2 q_0^2}{2} \quad \dots \quad (17b)$$

If now we substitute in (9a), then among the leading terms we have the equivalence

$$\frac{\alpha}{q_0^{\frac{1}{2}}} (\xi_0 - \xi)^{-2} \sim A (\xi_0 - \xi)^{\alpha} q_0^{\frac{1}{2}} \quad \dots \quad (17c)$$

which is impossible as  $\alpha > 1$ .

An idea of the behaviour of the  $I$  solution as  $z \rightarrow 0$  can be formed thus. We know that as  $z \rightarrow 0$

$$\left. \begin{aligned} q &\sim q_0 - \frac{1}{2} q_0^2 z^2 \\ zq^{\frac{1}{2}} &\sim q_0^{\frac{1}{2}} z \left( 1 - \frac{q_0}{8} z^2 \right) \end{aligned} \right\} (z \rightarrow 0) \quad \dots \quad (18)$$

and equation (9a) has the form

$$\frac{1}{\xi^2} \frac{d}{d\xi} \left[ \frac{\xi^2}{zq_0^{\frac{1}{2}}} (1 + z + O(z^2)) \frac{dz}{d\xi} \right] = -zq_0^{\frac{1}{2}} \left[ 1 - \frac{q_0}{8} z^2 + O(z^2) \right] \dots \quad (19)$$

Putting  $\log z = -y$ ,  $q_0^{\frac{1}{2}} \xi = \xi_1$

we find as  $y \rightarrow \infty$  the behaviour of the solution of (19) is the same as that of

$$\frac{1}{\xi_1^2} \frac{d}{d\xi_1} \left( \xi_1^2 \frac{dy}{d\xi_1} \right) = e^{-y} \left[ 1 + \left( \frac{dy}{d\xi_1} \right)^2 \right] \quad \dots \quad (19a)$$

We can convince ourselves that for  $y \rightarrow \infty$  this again has solution behaving as that corresponding to an isothermal gas sphere given by the equation

$$\frac{1}{\xi_1^2} \frac{d}{d\xi_1} \left( \xi_1^2 \frac{dy}{d\xi_1} \right) = e^{-y} \quad \dots \quad (19b)$$

It is known that every solution of (19b) as  $y \rightarrow \infty$  approaches its singular solution  $e^{-y} = 2/\xi_1^2$ , so that on every such solution as  $y \rightarrow \infty$  and  $\xi_1 \rightarrow \infty$ ,  $(dy/d\xi_1)^2 \rightarrow 4/\xi_1^2$ , which will ultimately be negligible compared to 1 on the right-hand side of (19a). Thus as  $y \rightarrow \infty$  (19a) has solutions behaving as those of (19b). These are  $I$  solutions which ultimately correspond to isothermal gas spheres.

The asymptotic behaviour of the solution  $e^{-y} = 2/\xi_1^2$  also throws light on our previous result (15a) where we found  $z \propto 1/\xi^2$ . We know in equation (19b) for isothermal spheres the term  $e^{-y}$  represents density, and in the present case where  $\tau$  is ultimately constant (and  $d\sigma/d\tau \rightarrow \infty$ ),  $z = \sigma\tau$  ultimately will represent density and be expected to behave as  $e^{-y}$ .

#### 4. THE GENERAL CASE ( $\gamma \neq 1$ ).

We have discussed the case  $\gamma = 1$  in detail. The conclusions for this case apply to the more general cases also, but many of the simple arguments

of the above section are not applicable in the more general cases. An analytical proof of the property of the  $S$  solution, constructed by a method followed by the author in a previous paper (Sen, 1942), has been given in the Appendix. As regards the  $I$  solutions we now consider the typical cases treated by Chandrasekhar, suppressing full arguments and details on every occasion.

Take the general  $\gamma$ -model. We put  $\alpha = 0$ ,  $b = 1$ ,  $\nu = 1$  in (9) and (7), and have to satisfy the equations

$$\frac{1}{\xi^2} \frac{d}{d\xi} \left[ \frac{\xi^2}{zq^4} \cdot \frac{1}{(1-zq^{1-\gamma})} \cdot \frac{dz}{d\xi} \right] = -zq^4 \quad \dots \quad (9b)$$

$$\text{and} \quad \frac{dz}{dq} = \frac{1}{q^2} \left( 1 - \frac{q^{\gamma-1}}{z} \right) \quad \dots \quad (7b)$$

For  $I$  solutions we seek the asymptotic forms of those solutions for which as  $\tau \rightarrow \tau_0$ , i.e.  $q \rightarrow q_0$ ,  $z \rightarrow 0$ , and  $dz/dq \rightarrow -\infty$ .

We try the following solution

$$\left. \begin{aligned} z &\sim \frac{A}{\xi^\alpha}, \quad \alpha > 0 \\ q &\sim q_0 - \frac{B}{\xi^{\alpha+c}}, \quad c > 0 \end{aligned} \right\} (\xi \rightarrow \infty) \quad \dots \quad (20)$$

$A$  and  $B$  being positive. This gives

$$\frac{dz}{dq} \sim -\frac{A}{B} \cdot \frac{\alpha}{\alpha+c} \xi^c. \quad (\xi \rightarrow \infty)$$

Substituting in (7b) and using expansions valid for small  $z$ , we obtain by comparing the terms of highest order

$$c = \alpha, \quad B = \frac{A^2}{2q_0^{\gamma-3}}. \quad \dots \quad (21a)$$

Again, the substitution of the asymptotic values (20) in (9b) shows that this latter equation can be satisfied by putting

$$\alpha = 2, \quad Aq_0^{\frac{1}{2}}/\alpha = 1. \quad \dots \quad (21b)$$

(21a) and (21b) determine the four constants in (20) which can be written as

$$\left. \begin{aligned} z &\sim \frac{2}{q_0^{\frac{1}{2}}} \cdot \frac{1}{\xi^2}, \quad q \sim q_0 - 2q_0^{2-\gamma} \frac{1}{\xi^4} \end{aligned} \right\} \xi \rightarrow \infty \quad \dots \quad (22)$$

so that

$$\sigma \sim zq^4 \sim \frac{2}{q_0^{\frac{1}{2}}} \frac{1}{\xi^2}.$$

The more general case ( $(\alpha, \delta)$ -model) may be treated similarly. In fact making the substitution (20) in the original equation (7) we obtain the relations

$$c = \nu\alpha, \quad B = \frac{A^{\nu+1}}{\nu+1} q_0^{2+\nu-\gamma}$$

and further substitution in (9) gives the same relation as (21b). The asymptotic form of the  $I$  solution in this general case is

$$z \sim \frac{2}{q_0^{\frac{1}{2}}} \cdot \frac{1}{\xi^2}, \quad q \sim q_0 - \frac{2^{\gamma+1}}{\gamma+1} \cdot q_0^{\frac{3+\gamma-2\gamma}{2}} \cdot \frac{1}{\xi^4} \quad (\xi \rightarrow \infty) \quad \dots (23)$$

The  $I$  solutions thus all correspond to infinite configurations which ultimately behave as isothermal gas spheres.

The case of the  $S$  solutions is treated rigorously in the Appendix. We can, however, get a physical insight into the nature of the solution near the boundary by an analysis similar to that followed for  $\gamma = 1$ . It has been shown by Chandrasekhar (1937) that for  $\gamma > 2$ , the behaviour of the  $S$  solution is given by

$$z \sim \tau^{4-2\gamma} \left( A - \frac{2}{4-\gamma} \tau^{2\gamma} \right) \quad (\tau \rightarrow 0) \quad \dots \dots (24)$$

$$A = \sqrt{\frac{2}{2-\gamma}}$$

whence we calculate

$$\left. \begin{aligned} zq^{\frac{1}{2}} &\sim \sigma \sim A\tau^{3-2\gamma} - \frac{2}{4-\gamma} \tau^3 \\ zq^{1-\gamma} &\sim A\tau^{2\gamma} - \frac{2}{4-\gamma} \tau^{4\gamma} \end{aligned} \right\} \quad (\tau \rightarrow 0) \quad \dots \dots (25)$$

$$\dots \dots (26)$$

Substituting these in (9b), and using expansions valid near  $\tau = 0$  it can be shown that as  $\tau \rightarrow 0$ , the standard solution (at least for  $1 < \gamma < \frac{5}{2}$ ) behaves as the solution of the polytrope equation of index  $3-2\gamma$ .

## PART II.

### CONVECTIVE STABILITY OF THE MODELS.

#### 5. THE STABILITY CONDITIONS.

We shall now examine how far the  $S$  and  $I$  solutions of Chandrasekhar conform to the stability conditions of the radiative gradient. Generally it will be useful to confine ourselves to those cases for which  $(\tau, \sigma)$  curves have been obtained by Chandrasekhar. It will be necessary to introduce a new variable and connect it with the old ones.

(i) For  $\gamma$ -models defined by

$$\frac{L(r)}{M(r)} \cdot \frac{M}{L} = \eta = \eta_0 T^3 \quad \dots \dots (31)$$

let us put

$$4\pi c G \theta = \frac{\kappa L(r)}{M(r)} \quad \dots \dots (32)$$

Then for Kramers' law

$$\kappa = \kappa_0 \frac{\rho}{T^{3+s}} \quad \dots \quad (2a)$$

we obtain from the three above equations

$$\theta = \left( \frac{a}{3} \frac{\mu H}{k} \cdot K \right)^{-1} \rho T^{4\gamma-3}$$

where  $\gamma$  is defined by  $4\gamma = (\delta - s)$ , and  $K$  has the same value as in (6), except that we now put  $\alpha = 0$ ,  $b = 1$  in that formula. Further as

$$y = \beta/(1-\beta) = \frac{3}{a} \cdot \frac{k}{\mu H} \frac{\rho}{T^3}$$

we may write (32) as (introducing our previous variable  $x$ )

$$\theta = \frac{1}{K} y T^{4\gamma} = \frac{y}{x} \quad \dots \quad (33)$$

Transforming to  $(\tau, \sigma)$  variables we may also write

$$\theta = \frac{y}{x} = \sigma \tau^{4\gamma-3}, \quad y = \frac{\sigma}{\tau^3} \quad \dots \quad (33')$$

(ii) For the more general  $(\alpha, \delta)$ -model of Chandrasekhar defined by (1) and (2), using variables

$$\rho = \rho_0 \sigma, \quad T = T_0 \tau \quad \dots \quad (34)$$

where

$$\begin{aligned} \rho_0 &= \left[ \left( \frac{a}{3} \cdot \frac{\mu H}{k} \right)^{3+s+\delta} \left( \frac{\kappa_0 \eta_0 L}{4\pi c G M} \right)^s \right]^{\frac{1}{3(1-\alpha-\delta)+s-\delta}} \\ T_0 &= \left[ \left( \frac{a}{3} \cdot \frac{\mu H}{k} \right)^{\alpha+b} \left( \frac{\kappa_0 \eta_0 L}{4\pi c G M} \right) \right]^{\frac{1}{3(1-\alpha-\delta)+s-\delta}} \quad \dots \quad (35) \end{aligned}$$

we obtain after some calculation

$$\theta = \sigma^{\alpha+b} \tau^{\delta-s-3}.$$

In our subsequent calculations we shall put  $b = 1$  (corresponding to cases integrated by Chandrasekhar). We then obtain (for  $b = 1$ )

$$\theta = \sigma^{\alpha+1} \tau^{\delta-s-3} = \frac{y^\nu}{x}, \quad y = \frac{\sigma}{\tau^3}, \quad x = \tau^{-4\gamma} \quad \dots \quad (36)$$

where now

$$\alpha+1 = \nu, \quad 4\gamma = \delta-s+3\alpha.$$

It has been shown elsewhere (Sen, 1941) that the radiative gradient is stable, or unstable and is to be replaced by an adiabatic gradient according as the expression

$$f(y, \theta) = \frac{\left(1 + \frac{1}{4}y\right)\theta}{1 - \left(1 + \frac{1}{4}y\right)\theta} - \frac{2}{3} \cdot \frac{(4+y)^2}{y(8+y)}$$

is negative or positive. Or simplifying, we conclude the gradient is radiative or adiabatic, according as

$$\theta \leq \frac{8(4+y)}{5y^2+40y+3} \quad \dots \quad (37)$$

We shall make use of the conditions (33), (36) and (37) to examine if the density temperature curves of Chandrasekhar's stellar models conform to the above condition of stable radiative gradient. Chandrasekhar's curves, it should be noted, have all been drawn on the assumption that the temperature gradient is radiative.

$$6 \text{ } (\gamma\text{-MODEL, } \alpha = 0).$$

From (37) and (33') it is evident that for all members of the  $\gamma$ -model if we put

$$F = \frac{y}{x} - \frac{8(4+y)}{5y^2+40y+32} \quad \dots \quad (38)$$

the gradient is radiative when  $F < 0$  and adiabatic if  $F > 0$ . We shall henceforth always consider the curve  $F = 0$  both in  $(x, y)$  and  $(\tau, \sigma)$ -planes. We are interested only in the first quadrants of these planes.  $F(x, y) = 0$  passes through the origin, and has  $y = x$  as its tangent there. We further note that as  $x \rightarrow \infty$ ,  $F(x, y) = 0$  asymptotically approaches the parabola

$$y^2 = \frac{8}{5}x. \quad (x \rightarrow \infty) \quad \dots \quad (39)$$

Again on  $F(x, y) = 0$  we have from (38)

$$\frac{1}{x} = \left( \frac{1}{y} + \frac{5y^2+40y+128}{5y^2+40y+32} \right) \frac{dy}{dx}, \quad \dots \quad (40)$$

so that  $y$  is monotone increasing. For points in the area lying between  $F(x, y) = 0$  and  $x$ -axis,  $F < 0$ , and the stable gradient there must be radiative, whereas at every point above the curve  $F = 0$  the stable gradient should be adiabatic. These results in  $(x, y)$ -plane are true for all members of the  $\gamma$ -model, but as soon as we go to the  $(\tau, \sigma)$ -plane it becomes necessary to differentiate between cases for different values of  $\gamma$ . Let us first take the special case  $\gamma = 1$ . For this value of  $\gamma$

$$\frac{dy}{dx} = \frac{3y}{4x} - \frac{1}{4} \frac{1}{x^2} \frac{d\sigma}{d\tau}.$$

For  $x \neq 0$  and at the point where  $d\sigma/d\tau = 0$ ,

$$\frac{dy}{dx} = \frac{3y}{4x}. \quad \dots \quad (41)$$

Hence, if there be an extremum value of  $\sigma$  on  $F = 0$  in  $(\tau, \sigma)$ -plane (we shall presently show it is a maximum), the slope at the corresponding point of  $F(x, y) = 0$  in the  $(x, y)$ -plane is given by (41).

Substituting (41) in (40), we note that  $x(\neq 0)$  goes out of the equation altogether, and hence at the extremum on  $F(\tau, \sigma) = 0$  the value of the ratio of the pressures is given by the equation

$$5y^3 + 30y + 96y - 64 = 0. \quad \dots \quad (42)$$

This equation has only one positive root, namely  $y_0 = 0.599$ . There is thus *only one* extremum value of  $\sigma$  on  $F(\tau, \sigma) = 0$ . Now  $x = 0$ ,  $y = 0$  corresponds to  $\sigma = 0$ ,  $\tau = \infty$ , and the tangent  $y = x$  to  $\sigma\tau = 1$ . Thus in the  $(\tau, \sigma)$ -plane  $F = 0$  is asymptotic to  $\sigma\tau = 1$  for  $\tau \rightarrow \infty$  (which is also true of all solution curves in the  $(\tau, \sigma)$ -plane).

Further, the asymptotic parabola (39) corresponds to

$$\sigma^2 = \frac{8}{5}\tau^2, \quad \text{i.e.} \quad \sigma = \sqrt{\frac{8}{5}}\tau \quad \dots \quad (39a)$$

on  $(\tau, \sigma)$ -plane (in the first quadrant). Hence the slope of  $F(\tau, \sigma) = 0$  at origin is given by (39a). It is thus evident that  $F(\tau, \sigma) = 0$  has only one maximum in  $(\tau, \sigma)$ -plane.

Substituting  $y_0$  in  $F = 0$  in (38) we find the corresponding value of  $x$ , namely  $x_0 = 0.858$ . Then by substituting in  $x = \tau^{-4}$ , and  $y = \sigma/\tau^2$ , we find  $\sigma_{\max} = 0.628$ , and the corresponding  $\tau(\sigma_{\max}) = 1.039$ .

The curve  $F(\tau, \sigma) = 0$  divides the  $(\tau, \sigma)$ -plane (first quadrant) into two parts such that at all  $(\tau, \sigma)$  points lying between the curve  $F = 0$  and the  $\tau$ -axis, the radiative gradient is stable, and at all points lying above this curve the radiative gradient is unstable and under suitable conditions can be replaced by a stable adiabatic gradient. Hence, our above analysis shows that for the  $\gamma$ -model with  $\gamma = 1$ , any configuration with a density value making  $\sigma > 0.628$  will be radiatively unstable. If we take the integral curves (for  $\gamma = 1$ ) of Chandrasekhar in  $(\tau, \sigma)$ -plane, and plot also the curve  $F(\tau, \sigma) = 0$  in the same plane, then only those integral curves or parts of curves which lie below  $F = 0$  will represent radiatively stable configurations. For instance we find the standard solution of Chandrasekhar (for  $\gamma = 1$ ) as entirely radiatively unstable. Of the  $I$  solutions only the lower parts of the steep branch are radiatively stable. The case of the standard solution for  $\gamma = 1$  can be roughly seen as follows. The standard solution  $\sigma \sim \sqrt{2}\tau(\tau \rightarrow 0)$  leaves the origin at a slope  $\sqrt{2}$ , while  $F(\tau, \sigma) = 0$  has the slope  $\sqrt{\frac{8}{5}}$  at the origin. As  $\sqrt{2} > \sqrt{\frac{8}{5}}$ , near the origin the standard solution lies above  $F = 0$ . The maximum of the standard solution occurs at  $\sigma = 0.843$  which is greater than  $\sigma_{\max} = 0.628$  calculated above. We shall show presently that for all  $\gamma > 0$  the standard solution curves lie above  $F = 0$  as  $\tau \rightarrow \infty$ . This suggests that the standard solution for  $\gamma = 1$ , is probably wholly radiatively unstable. In fact the result of actual plotting is shown in fig. 2. *The standard solution for  $\gamma = 1$  is thus entirely radiatively unstable.* We can now consider the general case of the  $\gamma$ -model. We first recapitulate the following results obtained from Chandrasekhar's integration of the  $(\tau, \sigma)$  differential equation:—



(i) For  $\gamma < 2$ , as  $\tau \rightarrow 0$ , the solution curve has the form (Chandrasekhar, 1936)

$$\sigma \sim \sqrt{\frac{2}{2-\gamma}} \tau^{3-2\gamma}. \quad \dots \quad (43a)$$

Hence as  $x = \tau^{-4\gamma}$ , and  $y = \sigma/\tau^3$  for  $0 < \gamma < \frac{3}{2}$ ,  $(x, y) \rightarrow \infty$  corresponds to  $(\tau, \sigma) \rightarrow 0$ , and further for  $\frac{3}{2} < \gamma < 2$ ,  $(x, y) \rightarrow \infty$  corresponds to  $\tau \rightarrow 0$ ,  $\sigma \rightarrow \infty$ .

(ii) For every value of  $\gamma$ , as  $\tau \rightarrow \infty$  the solution curve has the form

$$\sigma \sim \tau^{3-4\gamma} \left[ 1 + \frac{\gamma-1}{\tau^{4\gamma}} + \dots \right] \quad \dots \quad (43b)$$

so that for

$0 < \gamma < \frac{3}{4}$ ,	$\sigma \rightarrow \infty$ ,	as	$\tau \rightarrow \infty$
$\gamma > \frac{3}{4}$ ,	$\sigma \rightarrow 0$ ,	as	$\tau \rightarrow \infty$
$\gamma = \frac{3}{4}$ ,	$\sigma \rightarrow 1$ ,	as	$\tau \rightarrow \infty$ .

We can now calculate the position of the curve  $F(\tau, \sigma) = 0$  in  $(\tau, \sigma)$ -plane. We first note that at the maximum  $\sigma$  we must have

$$\frac{dy}{dx} = \frac{3}{4\gamma} \cdot \frac{y}{x} \quad \dots \quad (41a)$$

whence, by substituting in (40) and after subsequent simplification, we obtain the following equation for the value of the pressure ratio at the maximum  $\sigma$  of  $F(\tau, \sigma)$ -curve in  $(\tau, \sigma)$ -plane

$$5(2\gamma-3)y^3 + 30(4\gamma-5)y^2 + 96(4\gamma-5)y + 64(4\gamma-3) = 0. \quad \dots \quad (44)$$

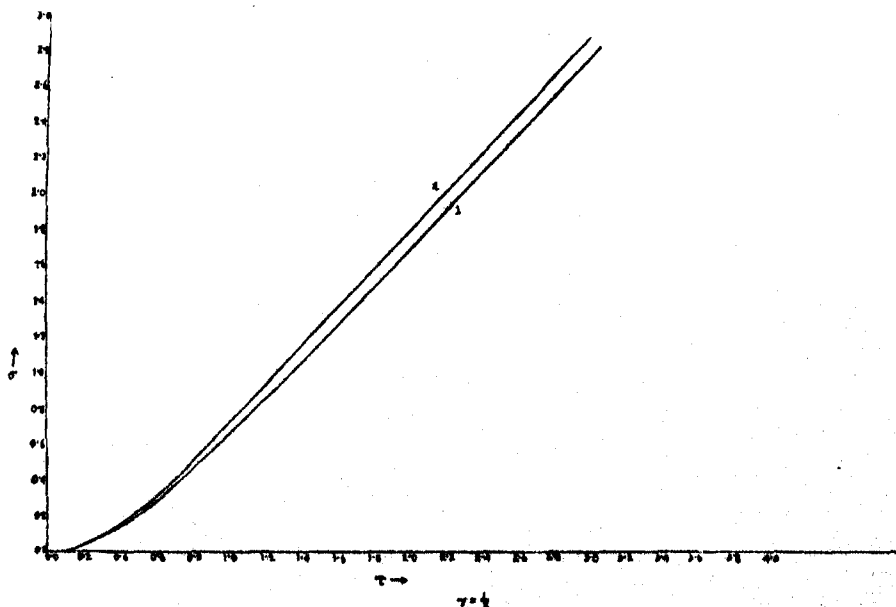


FIG. 1(a).—(2) is the standard solution curve for  $\gamma = \frac{1}{2}$ , and (1) is the curve  $F = 0$  separating the regions of stable and unstable radiative gradients. The lower part has been magnified in fig. 1(b).

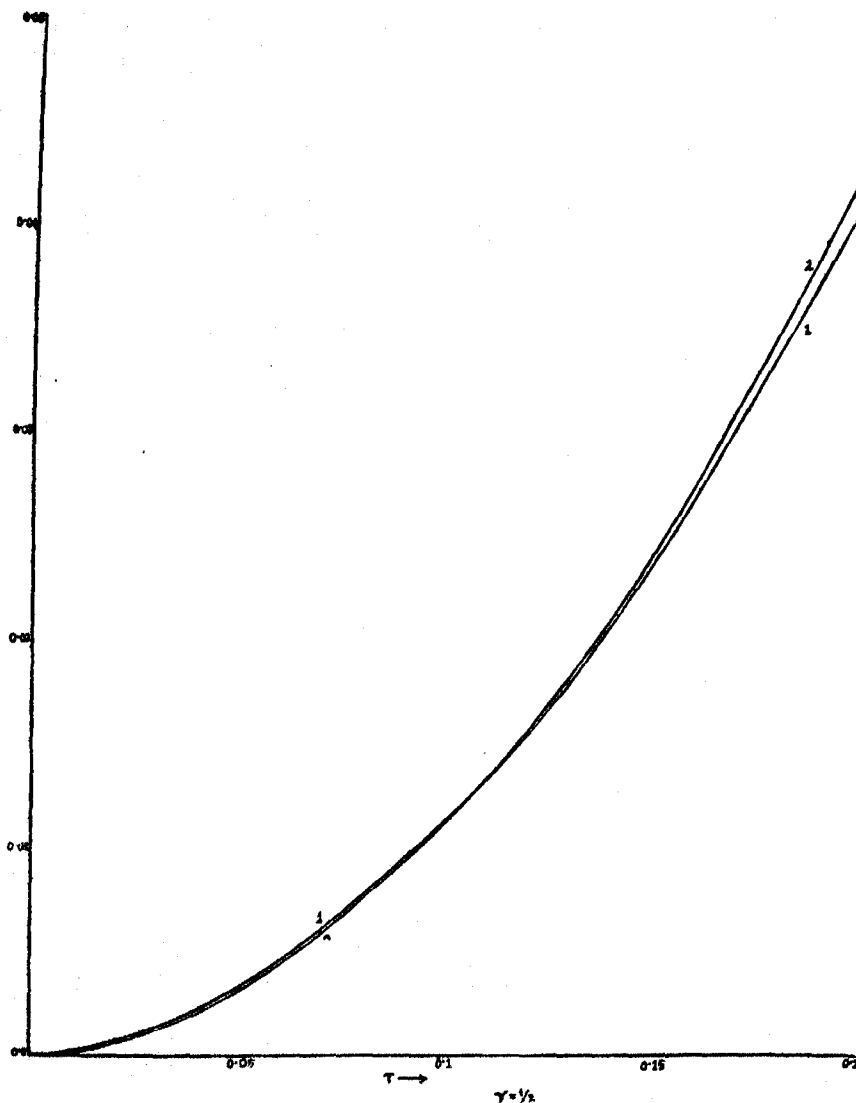


FIG. 1(b).—(2) is the standard solution curve for  $\gamma = \frac{1}{2}$ , and (1) is the curve  $F = 0$  separating the region of unstable from that of stable radiative gradient which latter lies between this curve and  $\tau$ -axis. The standard solution for  $\gamma = \frac{1}{2}$  is radiatively stable only for  $\tau$  values lying between 0 and 0.11 and  $\sigma$  values between 0 and 0.0137.

From a discussion of the roots of this cubic equation we obtain the following results:

For  $\gamma > \frac{1}{2}$ , or  $\gamma < \frac{1}{2}$ , there are no positive roots; for  $\frac{1}{2} < \gamma < \frac{3}{2}$  there is only one positive root.

Hence for every value of  $\gamma$  satisfying  $\frac{3}{4} < \gamma < \frac{5}{4}$  there exists a maximum value of  $\sigma$ , say  $\sigma_{\max}(\gamma)$ , such that a gas configuration in equilibrium with a density-value which makes the corresponding  $\sigma > \sigma_{\max}(\gamma)$  cannot have a stable radiative gradient there.

We can now roughly locate the curve  $F(\tau, \sigma) = 0$  among the integral curves thus.

For all  $\gamma$ -models, such that  $0 < \gamma < \frac{3}{4}$ , the behaviour of the  $S$  solution curves as  $\tau \rightarrow 0$ ,  $\sigma \rightarrow 0$  is given by (43a); whereas (39) shows as  $\tau \rightarrow 0$ ,  $\sigma \rightarrow 0$  the  $F$  curve in  $(\tau, \sigma)$ -plane has the form

$$\sigma \sim \sqrt{\frac{8}{5}} \tau^{3-2\gamma}. \quad (\tau \rightarrow 0)$$

Hence as  $\sigma \rightarrow 0$ ,  $\tau \rightarrow 0$  (close to the boundary), the  $S$  solution curve is steeper than the  $F$  curve if  $2/(2-\gamma) > \frac{3}{2}$ , i.e. if  $\gamma > \frac{3}{4}$ , so that  $F = 0$  lies below the  $S$  solution. Hence for  $\gamma > \frac{3}{4}$  the radiative gradient is unstable near the boundary; for  $\gamma < \frac{3}{4}$  it is stable.

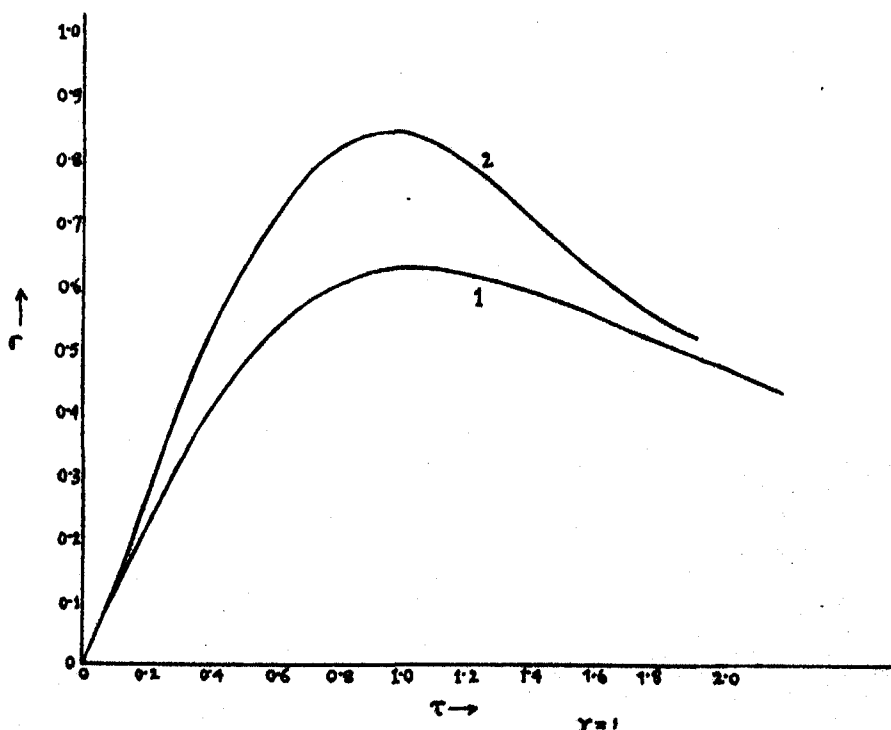


FIG. 2.—(2) is the standard solution curve for  $\gamma = 1$ , and (1) is the curve  $F = 0$  dividing the region of unstable radiative gradient from that of stable radiative gradient which latter lies between this curve and  $\sigma$ -axis. The figure shows the standard solution for  $\gamma = 1$  is radiatively unstable all throughout.

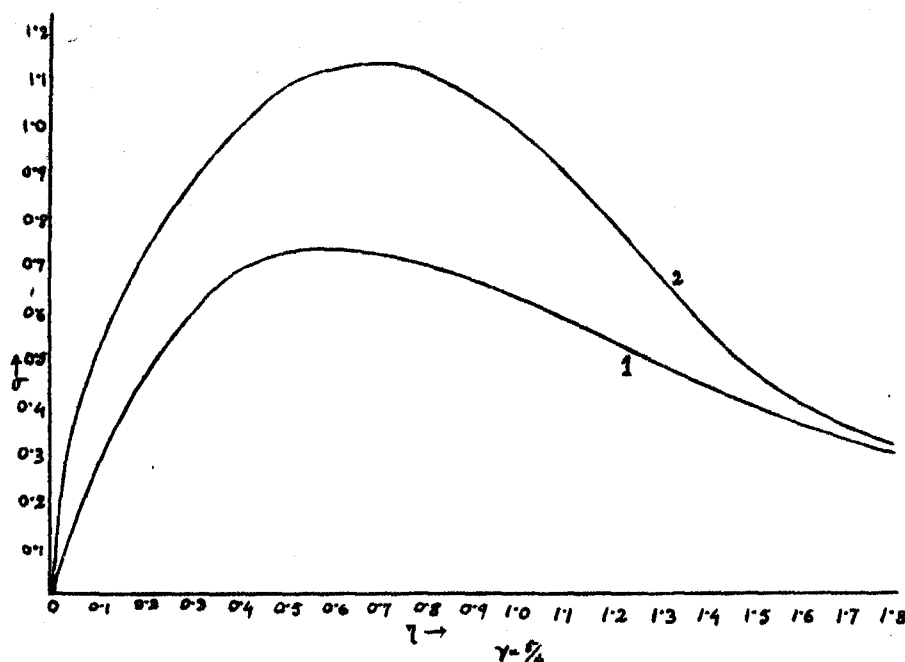


FIG. 3.—(2) is the standard solution curve for  $\gamma = \frac{5}{4}$ , and (1) is the curve  $F = 0$ . The standard solution for  $\gamma = \frac{3}{2}$  is radiatively unstable all throughout.

For  $\frac{3}{4} < \gamma < \frac{3}{2}$  we find that as  $\tau \rightarrow \infty$ , both the  $S$  solution curve and the  $F$  curve (which approaches  $y = x$ ) are asymptotic to

$$\sigma = \tau^{3-4\gamma}.$$

To find the relative positions of the  $S$  and  $F$  curves as  $\tau \rightarrow \infty$  we proceed to the next higher approximation. We find

$$\left. \begin{array}{l} \text{for } F \text{ curve } \sigma \sim \tau^{3-4\gamma}(1 - \tau^{-4\gamma}) \\ \text{for } S \text{ curve } \sigma \sim \tau^{3-4\gamma}[1 - (\gamma - 1)\tau^{-4\gamma}] \end{array} \right\} (\tau \rightarrow \infty) \quad \dots (46)$$

Hence so long as  $\gamma > 0$ ,  $F(\tau, \sigma) = 0$  lies below the  $S$  solution curve as  $\tau \rightarrow \infty$ , so that ultimately the  $S$  solutions all lie in the region of unstable radiative gradient.

Summing up, for  $\frac{3}{4} < \gamma < \frac{3}{2}$  the  $S$  solutions, as  $\tau \rightarrow 0$ ,  $\sigma \rightarrow 0$ , all run in the region of unstable radiative gradient and also lie in the same region as  $\tau \rightarrow \infty$ . For  $0 < \gamma < \frac{3}{4}$ , the  $S$  solutions start at  $\tau = 0$ ,  $\sigma = 0$  with stable radiative gradients, but ultimately as  $\tau \rightarrow \infty$  run into the region of unstable radiative gradient. As the figures 1(a) and 1(b) show then, the  $S$  and  $F$  curves in the  $(\tau, \sigma)$ -plane cross only once, so that only a part of the solution starting from the boundary  $\tau = 0$  to a maximum  $\tau$  is radiatively stable. Hence, if  $0 < \gamma < \frac{3}{4}$ , there is for a given  $\gamma$ , a  $\tau_{\max}(\gamma)$ , such that at all temperatures for which the corresponding  $\tau > \tau_{\max}(\gamma)$ , the standard solution is radiatively unstable. Similarly, there is a minimum  $\gamma_{\min}(\gamma)$ , such that whenever the ratio of the

pressures  $y < y_{\min}(\gamma)$ , the standard solution is radiatively unstable. In the case of  $\gamma = \frac{3}{2}$  equation (44) reduces to (leaving out the root  $y = 0$ )

$$15y^2 + 120y + 384 = 0$$

which has no real positive root. Hence  $F(\tau, \sigma) = 0$  in  $(\tau, \sigma)$  plane has no maximum.

On the standard solution  $\bar{S}$  for  $\gamma = \frac{3}{2}$ , we find  $\sigma$  behaves as

$$\sigma_S \sim \tau^{\frac{1}{2}} \left[ \sqrt{\frac{8}{5}} - \frac{8}{13} \tau^{\frac{1}{2}} \right] \quad (\tau \rightarrow 0) \quad \dots \quad (47a)$$

while on  $F(\tau, \sigma) = 0$  we find after some calculation the behaviour of  $\sigma$  to be given by

$$\sigma_F \sim \tau^{\frac{1}{2}} \left[ \sqrt{\frac{8}{5}} - 4\tau^{\frac{1}{2}} \right]. \quad (\tau \rightarrow 0) \quad \dots \quad (47b)$$

Further, as  $\tau \rightarrow \infty$

$$\sigma_F \sim 1 - \tau^{-2}, \quad \sigma_S \sim 1 - \frac{1}{4} \tau^{-2}. \quad \dots \quad (47c)$$

Thus at both ends  $\sigma_S > \sigma_F$ . The  $S$  solution curve for  $\gamma = \frac{3}{2}$  (as is found by actual plotting of curves) lies indeed entirely above  $F(\tau, \sigma) = 0$ , and so the radiative gradient must be unstable all throughout for  $\gamma = \frac{3}{2}$ .

The  $F$  and  $S$  curves have been actually plotted and three cases are shown in figs. 1(a), 2 and 3 for  $\gamma = \frac{1}{2}$ ,  $\gamma = 1$  and  $\gamma = \frac{3}{2}$  respectively. The crossing of the two curves for  $\gamma = \frac{1}{2}$  is shown in fig. 1(b) drawn in a magnified scale. 1(a) and 2 are typical of the cases  $0 < \gamma < \frac{3}{2}$  and  $\frac{3}{2} < \gamma < \frac{5}{2}$  respectively.

Our result for the  $\gamma$ -model can be summarised thus. For  $0 < \gamma < \frac{3}{2}$  only a part of the standard solution from the boundary up to a definite minimum value of the ratio of gas to radiation pressure (to a maximum value of  $\tau$ ) depending on  $\gamma$  is radiatively stable; hence such a configuration is wholly radiatively stable only if this pressure ratio at the centre does not fall below a minimum critical value (and the central  $\tau$  value does not exceed a critical maximum value); in the contrary case the configuration is radiatively unstable, the unstable region being an internal one involving the centre. For  $\frac{3}{2} < \gamma < \frac{5}{2}$ , the standard solution is entirely radiatively unstable.

By examining the position of the  $F$  curve among  $I$  solutions it becomes apparent that the lower portions of  $I$  solutions which fall steeply must be all radiatively stable. There exists a critical minimum pressure ratio in this case also.

This result clearly points to the necessity of sometimes including a central convection zone (with adiabatic gradient) in the construction of stellar models.

## 7. $(\alpha, \delta)$ -MODELS.

The analysis of the two previous sections discusses the stability of radiative equilibrium of a typical stellar model ( $\gamma$ -model) discussed by Chandrasekhar. We shall now very briefly describe the general characteristics of the

more general  $(\alpha, \delta)$ -model in respect of the stability of the radiative transfer of energy.

We define in this connection a function  $F_1$

$$F_1 = x - \frac{y^\nu (5y^2 + 40y + 32)}{8(4+y)} \quad \dots \quad (48)$$

where  $x, y$  and  $\nu$  are given by (36) ( $\nu$  may be taken positive). We can show that for given  $(x, y)$  values the stable gradient is radiative or adiabatic according as

$$F_1 \gtrless 0. \quad \dots \quad (49)$$

The curve  $F_1(x, y) = 0$  divides the (first quadrant of)  $(x, y)$ -plane into two regions of which the lower one between  $F_1 = 0$  and  $x$ -axis represents the region of stable radiative gradient, while the upper one corresponds to the region of stable adiabatic gradient.

The gradient of  $F_1(x, y) = 0$  is given by

$$\frac{dy}{dx} \left\{ \frac{\nu}{y} + \frac{5y^2 + 40y + 128}{(4+y)(5y^2 + 40y + 32)} \right\} = \frac{1}{x} \quad \dots \quad (50)$$

so that ( $\nu$  being positive)  $y$  is monotone increasing with  $x$ . From (36) we obtain when  $d\sigma/d\tau = 0$

$$\frac{dy}{dx} = \frac{3}{4\gamma} \cdot \frac{y}{x}.$$

Substituting this value of  $dy/dx$  in (50), we obtain the value of  $y$  at that point of  $F_1(\tau, \sigma) = 0$  where  $\sigma$  has an extreme value. Proceeding as before, we find this value of  $y$  to be given by

$$5(d-3)y^3 + 60(d-2)y^2 + 192(d-2)y + 128d = 0 \quad \dots \quad (51)$$

where

$$d = 4\gamma - 3\nu,$$

$\gamma$  and  $\nu$  being now given by (36).

A simple discussion shows that when  $0 < d < 3$  equation (51) has only one positive root, and for  $d > 3$  or  $d < 0$ , (51) has no positive root. Hence for  $0 < 4\gamma - 3\nu < 3$ , i.e. when  $3 + s < \delta < 6 + s$ , the equation  $F_1(\tau, \sigma) = 0$  on  $(\tau, \sigma)$  plane has only one maximum, say  $\sigma_{\max}$ , and for any  $\sigma > \sigma_{\max}$ , the corresponding radiative gradient cannot be stable. When  $x \rightarrow 0$ ,  $F_1 = 0$  has the asymptotic form

$$x = y^\nu, \quad \dots \quad (52a)$$

and for  $y$  large,  $F_1 = 0$  has the form

$$x = \frac{5}{8} y^{\nu+1}$$

or

$$y = \left( \frac{8}{5} x \right)^{\frac{1}{\nu+1}} \quad \dots \quad (52b)$$

Near the origin of  $(\tau, \sigma)$ -plane, we have the following approximate forms of  $F_1 = 0$ , and of the standard solution  $S$

$$F_1: \quad \sigma \sim \left(\frac{8}{5}\right)^{\frac{1}{\nu+1}} \tau^{3-\frac{4\gamma}{\nu+1}} \quad \dots \quad (52c)$$

$$S: \quad \sigma \sim \left(\frac{\nu+1}{\nu+1-\gamma}\right)^{\frac{1}{\nu+1}} \tau^{3-\frac{4\gamma}{\nu+1}} \quad \dots \quad (52d)$$

Hence the standard solution  $S$  lies below  $F_1$  curve if

$$\frac{\nu+1}{\nu+1-\gamma} < \frac{8}{5}$$

i.e.

$$\gamma < \frac{3}{8}(\nu+1)$$

which by (36) is equivalent to

$$\delta < 3+s-\frac{3}{2}\alpha. \quad \dots \quad (53)$$

Thus, when (53) is satisfied the standard solution  $S$  runs in the region of stable radiative gradient near  $\tau = 0$ ; for the opposite inequality it is in the region of unstable radiative gradient. In every case the  $F_1(\tau, \sigma)$  curve has a maximum, the standard solution has unstable radiative gradient near the boundary.

We shall now find the position of  $F_1 = 0$  as  $\tau \rightarrow \infty$ , i.e.  $x \rightarrow 0$  while  $(\gamma > 0)$ . In this region we find the following asymptotic forms for  $F_1$  and  $S$ :

$$F_1: \quad \sigma \sim \tau^{3-\frac{4\gamma}{3}} \left\{ 1 - \frac{1}{\nu} \tau^{-\frac{4\gamma}{\nu}} \right\} \quad \dots \quad (54a)$$

$$S: \quad \sigma \sim \tau^{3-\frac{4\gamma}{3}} \left\{ 1 - \frac{1}{\nu} \frac{\left(1 - \frac{\gamma}{\nu}\right)}{\tau^{4\gamma/\nu}} \right\} \quad \dots \quad (54b)$$

Hence for  $4\gamma = \delta - s + 3\alpha > 0$  ( $\nu$  being supposed positive) the standard solution is ultimately (i.e. as  $\tau \rightarrow \infty$ ) in the region of unstable radiative gradient.

For  $\delta - s + \frac{3\alpha}{2} > 3$ , the configuration given by the standard solution is radiatively unstable; for  $-\frac{3\alpha}{2} < \delta - s + \frac{3\alpha}{2} < 3$ , the configuration given by the standard solution has stable radiative gradient up to a minimum value of the ratio of gas to radiation pressure. It is evident that for  $\alpha > 2$  radiative stability is not possible if only  $\delta > s$ , which will be satisfied for energy generation law with even quite small power of temperature.

The  $I$  solutions, as before, will be all radiatively stable along lower parts of their vertical downward course, there being a critical minimum pressure ratio in this case also.

## APPENDIX.

To bring the analysis in a line with our previous work (Sen, 1942) on the behaviour of the solutions of stellar equations near the boundary of the configurations, we introduce the notations used elsewhere, which are different from those used in the present paper. The Appendix forms a section by itself, and its equations, unless expressly stated, should not be compared with those of this paper.

We take a more general case, and suppose the opacity and energy generation to be given by the following laws:

$$\kappa = \kappa_0 \rho^a T^{-b} \quad \dots \quad (a)$$

$$\eta = \frac{L(r)}{M(r)} = \eta_0 \rho^\alpha T^\delta \quad \dots \quad (b)$$

Consider equations (3), (4) of section 2, and

$$\frac{dM(r)}{dr} = 4\pi r^2 \rho$$

$$p_g = \frac{k}{\mu H} \rho T, \quad p_r = \frac{1}{3} a T^4$$

and substitute in these equations

$$p_g = (p_g)_0 p, \quad p_r = (p_r)_0 q, \quad T = T_0 \tau, \quad \rho = \rho_0 \sigma, \quad r = r_0 x, \quad M = M_0 m,$$

where  $\rho_0, T_0$  are respectively the central density and temperature. Then we can replace the above equations by the following set of equations among dimensionless quantities,

$$dp + \alpha' dq = -\beta \frac{\sigma m}{x^2} dx \quad \dots \quad (c)$$

$$dq = -\sigma^{a+\alpha+1} \tau^{\delta-b} \frac{m}{x^2} dx \quad \dots \quad (d)$$

$$dm = \sigma x^3 dx \quad \dots \quad (e)$$

where the scale constants are connected by the equations

$$M_0 = 4\pi r_0^3 \rho_0, \quad \frac{\kappa_0 \eta_0}{4\pi c r_0} \cdot \frac{\rho_0^{a+\alpha+1}}{(p_r)_0} T_0^{\delta-b} \cdot M_0 = 1$$

and

$$(p_g)_0 = \frac{k}{\mu H} \rho_0 T_0, \quad (p_r)_0 = \frac{1}{3} a T_0^4, \quad \alpha' = (p_r)_0 / (p_g)_0, \quad \beta = -\frac{GM_0 \rho_0}{r_0 (p_g)_0}.$$

Now put

$$\xi = \frac{1}{x}, \quad \pi = p + \alpha' q, \quad a + \alpha = d, \quad \delta - b - \alpha - a = 4f$$

and

$$pq^{-1} d\xi = dt. \quad \dots \quad (g)$$

\*  $a$  in this formula need not be confused with  $a$  in the expression for  $\kappa$  in (a).



Then we replace (c), (d), (e) by

$$\frac{d\pi}{dt} = \beta m \quad \dots \dots \dots (i)$$

$$\frac{dq}{dt} = mp^d q' \quad \dots \dots \dots (ii)$$

$$\frac{dm}{dt} = -\xi^{-4} \quad \dots \dots \dots (iii)$$

to which we add (g) as

$$\frac{d\xi}{dt} = \frac{q^{\frac{1}{2}}}{p} \quad \dots \dots \dots (iv)$$

Equations (i)–(iv) show that as  $t$  decreases  $\xi$  also decreases, and if as  $t \rightarrow 0$ ,  $\xi$  also tends to a finite limit  $\xi_0 > 0$ , then  $m$  also tends to a finite limit  $m_0$  (which in astrophysically significant solutions we take to be greater than zero), and then  $\pi$  also decreases to a finite limit  $\pi_0$ .

Since the right-hand sides of (i), (ii), (iii) and (iv) do not involve  $t$ , the solutions of the equations will not depend on the initial value of  $t$ . We shall take  $t = 0$  to correspond to the boundary surface. Let us investigate the behaviour of a solution for which  $m \rightarrow m_0 > 0$ , as  $t \rightarrow 0$ . At the boundary of the configuration we take  $\tau = 0$  and  $\sigma = 0$ , so that  $\pi = 0$ . Hence by (i)

$$\pi \sim \beta m_0 t. \quad (t \rightarrow 0) \quad \dots \dots \dots (h)$$

Let us try the solution

$$q = At^n. \quad (n > 0) \quad (t \rightarrow 0) \quad \dots \dots (i)$$

Then (ii) gives

$$Ant^{n-1} \sim m_0(\beta m_0 t - \alpha At^n)^d. A' t^{n'}.$$

This will be generally satisfied if  $q$  be a small quantity of higher order than  $p$ , and hence

$$n-1 = d+nf, \quad An = \beta^d m_0^{d+1} A'$$

which give

$$n = \frac{d+1}{1-f}, \quad A = \left( \frac{d+1}{1-f} \cdot \frac{1}{\beta^d m_0^{d+1}} \right)^{\frac{1}{1-f}}. \quad \dots \dots (j)$$

Since  $n > 0$ , we must have

$$1 > f. \quad \dots \dots \dots (v)$$

Equation (iv) gives

$$\frac{d\xi}{dt} \sim \frac{At^{\frac{1}{2}}}{\beta m_0} \cdot t^{\frac{1}{2} \left( \frac{d+1}{1-f} \right) - 1} \quad (t \rightarrow 0)$$

whence integrating

$$\xi \sim \xi_0 + \frac{At^{\frac{1}{2}}}{\beta m_0} \cdot \frac{4(1-f)}{d+1} t^{\frac{1}{2} \left( \frac{d+1}{1-f} \right)}. \quad \dots \dots \dots (k)$$

Since the right-hand side of (iv) is  $\sigma^{-1}$ ,  $d\xi/dt \rightarrow \infty$  as  $t \rightarrow 0$ . Hence

$$\frac{1}{4} \left( \frac{d+1}{1-f} \right) < 1, \quad \text{i.e. } d+4f < 3. \quad \dots \dots (vi)$$

Now the assumption that  $q$  is of higher order than  $p$  implies  $n > 1$ , i.e.

$$\frac{d+1}{1-f} > 1, \quad \text{i.e. } d+f > 0. \quad \dots \quad \dots \quad \dots \quad \text{(vii)}$$

Now suppose, if possible,  $\xi_0 = 0$ . Then we get from (iii)

$$\frac{dm}{dt} \sim \text{const. } t^{-\frac{d+1}{1-f}} \quad (t \rightarrow 0)$$

so that

$$m \sim m_0 - \text{const. } t^{-\left(\frac{t+d}{1-f}\right)}. \quad (t \rightarrow 0) \quad \dots \quad \dots \quad \dots \quad \text{(l)}$$

But on account of (v) and (vii), (l) contradicts the assumption  $m \rightarrow m_0$  as  $t \rightarrow 0$ . Hence  $\xi_0 \neq 0$ . We have then the solution

$$m \sim m_0 - \xi_0^{-4} t \quad (t \rightarrow 0)$$

and

$$p = \beta m_0 t, \quad q \sim A t^{\frac{d+1}{1-f}}, \quad \xi \sim \xi_0 + \frac{A t}{\beta m_0} \cdot \frac{4(1-f)}{d+1} t^{\left(\frac{d+1}{1-f}\right)}$$

with the value of  $A$  in (j). Hence

$$p \sim \frac{\beta m_0}{A^{\frac{1-f}{d+1}}} \cdot \tau^{\frac{4(1-f)}{d+1}}$$

so that

$$\sigma \sim \frac{\beta m_0}{A^{(1-f)(d+1)}} \cdot \tau^{\frac{4(1-f)}{d+1}-1}. \quad (\tau \rightarrow 0) \quad \dots \quad \dots \quad \text{(m)}$$

These solutions are valid when

$$f < 1, \quad d+f > 0, \quad \text{and } d+4f < 3$$

of which the second and the third relations together imply the first. The form (m) shows that it is Chandrasekhar's  $S$  solution. Replacing  $d, f$  by  $\alpha, \delta$ , etc., we conclude that the  $S$  solutions correspond to finite configurations provided

$$3(a+\alpha) > b-\delta, \quad \text{and } \delta-b < 3. \quad \dots \quad \dots \quad \text{(vi, vii)}$$

In case of  $\gamma$ -models, we put  $\alpha = 0, a = 1, 4\gamma = \delta - b + 3$ . The above conditions show that for  $\gamma$ -models the  $S$  configuration is finite when  $\gamma$  lies between 0 and  $\frac{3}{4}$ . In case of  $\gamma = 0$ , it can be easily shown that  $p$  and  $q$  are both of the first order in  $t$ ; then an  $S$  solution corresponding to finite configuration can be constructed. Hence for  $\gamma$ -models all  $S$  solutions give finite configurations so long as  $0 < \gamma < \frac{3}{4}$ .

It can be shown that the behaviour of  $I$  solutions as  $\sigma \rightarrow 0, \tau \rightarrow \tau_0$  is given by

$$p \sim A t^{\frac{1}{2}}, \quad q \sim q_0 + B t^{\frac{1}{2}(1+d)}, \quad \xi \sim D t^{\frac{1}{2}}, \quad m \sim C t^{-\frac{1}{2}} \quad (t \rightarrow 0) \quad \text{(n)}$$

where  $A, B, C, D$  are the constants

$$A = \left(\frac{18q_0}{\beta}\right)^{\frac{1}{2}}, \quad B = \frac{3q_0'}{2(1+d)} \left(\frac{16q_0^{d+1}}{3\beta^{4+d}} \cdot 18^d\right)^{\frac{1}{2}}, \quad C = \left(\frac{16q_0}{3\beta^4}\right)^{\frac{1}{2}}, \quad D = \left(\frac{3\beta}{2q_0^{\frac{1}{2}}}\right)^{\frac{1}{2}}.$$

It should be noted that  $\xi$  now represents the reciprocal of the radial distance.

We can further show easily that there are no solutions which correspond to finite configurations with non-zero temperature at the boundary. Further calculations here are suppressed.

REFERENCES.

- Chandrasekhar, S. (1936). *M.N.R.A.S.*, 97, 132. (1937). *Zeits. f. Astrophysik*, 14, 164.  
There is also an account of the whole work in Chandrasekhar's *Introduction to the Study of Stellar Structure*. Chap. IX.
- Sen, N. R. (1941). On the Inversion of Density Gradient and Convection in Stellar Bodies. *Proc. Nat. Inst. Sc. India*, 7, 183. (1942). On Stellar Models based on Bethe's law of Energy generation. *Proc. Nat. Inst. Sc. India*, 8, 317.

# FERMI-DIRAC AND BOSE-EINSTEIN GAS IN A GRAVITATIONAL FIELD.

By BRIJ NATH and P. L. BHATNAGAR, *University of Delhi.*

(Communicated by Dr. D. S. Kothari.)

(Received June 15, 1942 ; Read October 5, 1942.)

## ABSTRACT.

The distribution with height of pressure and concentration for a Fermi-Dirac and a Bose-Einstein gas subject to a uniform gravitational field is considered. The non-relativistic non-degenerate and degenerate, and the relativistic non-degenerate and degenerate cases are discussed. Because of its connection with radiation, the relativistic case of Bose-Einstein statistics is particularly interesting.

§1. In a recent paper (Kothari and Auluck, 1942) the problem of density distribution for a Fermi-Dirac and a Bose-Einstein gas, both for the relativistic and non-relativistic cases, in the presence of a uniform field of force has been discussed. The force on a particle of the gas due to the field is assumed to be independent of the energy of the particle. This assumption, however, is in general untenable when the field of force is due to gravitation, for in this case the force on a particle is proportional to its mass and this depends upon the energy of the particle in accordance with relativity. If  $\epsilon$  be the kinetic energy of a particle whose rest mass is  $m$ , then the force on the particle due to a gravitational field of intensity  $g$  will be  $(\epsilon + mc^2) \frac{g}{c^2}$  (where  $c$  is the velocity of light), and this in the relativistic case, when the kinetic energy is very large compared to the rest mass energy, becomes  $\frac{g\epsilon}{c^2}$ . In the present paper we shall treat the problem of the distribution of pressure and concentration for a Fermi-Dirac and a Bose-Einstein gas subject to a gravitational field, taking into account the effect of relativistic mechanics. As usual, we shall consider four limiting cases, viz. non-relativistic non-degeneracy and degeneracy, and relativistic non-degeneracy and degeneracy.

§2. Let us consider an ideal Fermi-Dirac or Bose-Einstein gas placed in a uniform gravitational field which we assume to be directed along the negative direction of the  $x$ -axis and extending from  $x = 0$  to  $x = \infty$ . Then the equation of hydrostatic equilibrium is

$$dp = -n(E + mc^2) \frac{g}{c^2} dx, \quad \dots \dots \dots (1)$$

where  $p$  is the pressure,  $E$  the average kinetic energy per particle and  $n$  the number of particles per unit volume, all at height  $x$ .

The pressure and  $\zeta$ , the Gibb's free energy per particle, are connected by the thermodynamic relation

$$\left(\frac{\partial p}{\partial \zeta}\right)_T = n,$$

where  $T$  is the temperature. This relation is well known, but for the sake of completeness the proof for the relevant special case is indicated below.

The pressure is given by\*

$$p = \frac{4\pi q}{3c^3 h^3} \int_0^\infty \frac{(\epsilon^2 + 2mc^2\epsilon)^{\frac{1}{2}}}{e^{\frac{\epsilon - \zeta}{kT}} + \beta} d\epsilon, \quad \dots \quad (2)$$

and hence

$$\left(\frac{\partial p}{\partial \zeta}\right)_T = \frac{4\pi q}{3c^3 h^3} \int_0^\infty \frac{d\epsilon}{kT} \frac{(\epsilon^2 + 2mc^2\epsilon)^{\frac{1}{2}} e^{\frac{\epsilon - \zeta}{kT}}}{\left[e^{\frac{\epsilon - \zeta}{kT}} + \beta\right]^2}, \quad \dots \quad (3)$$

where  $q$  is the weight factor of the particle and  $k$  and  $h$  have their usual meanings. For classical statistics we have  $\beta = 0$ , for Bose-Einstein statistics  $\beta = -1$  and for Fermi-Dirac statistics  $\beta = +1$ . Integrating (3) by parts we obtain

$$\left(\frac{\partial p}{\partial \zeta}\right)_T = \frac{4\pi q}{c^3 h^3} \int_0^\infty \frac{(\epsilon^2 + 2mc^2\epsilon)^{\frac{1}{2}} (\epsilon + mc^2) d\epsilon}{e^{\frac{\epsilon - \zeta}{kT}} + \beta},$$

or

$$\left(\frac{\partial p}{\partial \zeta}\right)_T = n. \quad \dots \quad (4)$$

Substituting (4) in (1) we have

$$\left(\frac{d\zeta}{dx}\right)_T = -\left(E + mc^2\right) \frac{g}{c^2}. \quad \dots \quad (5)$$

We shall now proceed to discuss separately the non-relativistic  $\left(\frac{E}{mc^2} \rightarrow 0\right)$  and relativistic  $\left(\frac{E}{mc^2} \rightarrow \infty\right)$  cases. Consider first the non-relativistic case. We have from (5)

$$\zeta - \bar{\zeta} = -mgx, \quad \dots \quad (6)$$

where a bar over a quantity denotes its value at the level  $x = 0$ .

---

\* The expressions for  $p$ ,  $\zeta$ , etc., quoted here will be found collected in a paper by Kothari and Singh (1941).

Substituting for  $\zeta$  the expression

$$\zeta = kT [\log A_0 + 2\beta b_2 A_0 - \frac{3}{2} b_3 A_0^3 + \dots],$$

where \*

$$A_0 = \frac{nh^3}{q(2\pi mkT)^{\frac{3}{2}}}$$

$$b_2 = \frac{1}{2^{\frac{5}{2}}} = 0.1768$$

$$b_3 = \frac{2}{3^{\frac{7}{2}}} - \frac{1}{4^{\frac{3}{2}}} = 0.00330,$$

we have [retaining terms up to the first order in  $A_0$ ]

$$(\log A_0 + 2\beta b_2 A_0) - (\log \bar{A}_0 + 2\beta b_2 \bar{A}_0) = -\frac{mgx}{kT}, \quad \dots \quad (7)$$

and hence

$$\log \frac{A_0}{\bar{A}_0} = \log \frac{n}{\bar{n}} = -\frac{x}{x_0} + 2\beta b_2 \bar{A}_0 \left(1 - e^{-\frac{x}{x_0}}\right),$$

or

$$n = \bar{n} \left\{1 + 2\beta b_2 \bar{A}_0 \left(1 - e^{-\frac{x}{x_0}}\right)\right\} e^{-\frac{x}{x_0}}, \quad \dots \quad (8)$$

where  $x_0$  is a quantity of the dimension of length defined by

$$x_0 = \frac{kT}{mg}.$$

Equation (8) shows that for a given  $\bar{n}$ , the decrease of concentration with height is *smaller* for a Fermi-Dirac gas than what it would be for a classical gas ( $\beta = 0$ ). In the Bose-Einstein case the decrease is greater than the classical value. These results are what would be expected from the physical properties of the Fermi-Dirac and Bose-Einstein statistics.

Let  $N$  denote the total number of particles in a cylinder of unit cross-section and extending from  $x = 0$  to  $x = \infty$ , then we have

$$N = \int_0^{\infty} n dx = \bar{n} x_0 + \bar{n} x_0 \beta b_2 \bar{A}_0,$$

or

$$\bar{n} = \frac{N}{x_0} (1 - \beta b_2 \bar{A}_0). \quad \dots \quad (9)$$

Substituting (9) in (8) we obtain

$$n = \frac{N}{x_0} \left\{1 + \beta b_2 \bar{A}_0 \left(1 - 2e^{-\frac{x}{x_0}}\right)\right\} e^{-\frac{x}{x_0}}. \quad \dots \quad (10)$$

---

\*  $A_0 < 1$  for non-degeneracy.

Thus we see that for a given  $N$ , the total number of particles, and for any height  $x < x_0 \log 2$ , the concentration  $n$  in the Fermi-Dirac case is less than, and in the Bose-Einstein case more than, what it would be for the classical case ( $\beta = 0$ ). At the height  $x = x_0 \log 2$  the difference between the classical, Fermi-Dirac, and Bose-Einstein cases vanishes. For  $x > x_0 \log 2$  the concentration for the Fermi-Dirac statistics is greater and for Bose-Einstein statistics less than what it would be for the classical statistics.

Let us define a quantity  $D$ , called for brevity the 'statistical variation' by the relation

$$D = \frac{n - n^*}{n^*},$$

where  $n^*$  is the concentration in the classical case ( $\beta = 0$ ),  $n$ ,  $n^*$  both referring to the same height  $x$ . From (8) and (10) we have

$$(a) \quad D = 2\beta b_2 A_0 \left(1 - e^{-\frac{x}{x_0}}\right) \text{ for fixed } \bar{n},$$

and

$$(b) \quad D = \beta b_2 A_0 \left(1 - 2e^{-\frac{x}{x_0}}\right) \text{ for fixed } N.$$

In the case of fixed  $\bar{n}$  (the concentration at  $x = 0$ ),  $D$  is practically zero for  $x < < x_0$ , and increases to a value  $2\beta b_2 A_0$  when  $x > > x_0$ . On the other hand in the case of a fixed  $N$  (total number of particles),  $D$  is practically equal to  $-\beta b_2 A_0$  for  $x < < x_0$ , vanishes for  $x = x_0 \log 2$ , and for  $x > > x_0$  approaches the value  $\beta b_2 A_0$ .

§3. We shall now consider the *relativistic* non-degenerate case.

In the relativistic case the rest-mass energy of a particle is negligible compared to its kinetic energy. Equation (1) therefore becomes

$$dp = -\frac{ngE}{c^2} dx,$$

and as

$$p = \frac{1}{3} nE$$

we have

$$p = \bar{p} e^{-\frac{x}{x_0}}, \quad \dots \dots \dots (11)$$

where for the relativistic case  $x_0$  is defined by

$$x_0 = \frac{c^2}{3g}. \quad \dots \dots \dots (12)$$

Substituting for  $p$  the expression

$$p = nkT [1 + \beta b_2 A_0 - b_2 A_0^2 + \dots],$$

where \*

$$A_0 = \frac{n}{8\pi q} \left( \frac{ch}{kT} \right)^3$$

$$b_2 = \frac{1}{2^4} = 0.06250$$

$$b_3 = \frac{2}{3^4} - \frac{1}{4^3} = 0.009066,$$

we obtain [up to first powers in  $A_0$ ]

$$n = \bar{n} \left[ 1 + \beta b_2 A_0 \left( 1 - e^{-\frac{x}{x_0}} \right) \right] e^{-\frac{x}{x_0}}. \quad \dots \quad (13)$$

Denoting as before by  $N$  the total number of particles in a column of unit cross-section we have

$$N = \bar{n} x_0 \left\{ 1 + \beta b_2 \frac{A_0}{2} \right\},$$

and hence

$$n = \frac{N}{x_0} \left\{ 1 + \frac{\beta b_2 A_0}{2} \left( 1 - 2e^{-\frac{x}{x_0}} \right) \right\} e^{-\frac{x}{x_0}}. \quad \dots \quad (14)$$

Equations (13) and (14), except for numerical coefficients, are similar to the corresponding non-relativistic equations (8) and (10), and, therefore, their discussion need not be repeated here. We may note that in this case  $D$  will be given by

$$(a) \quad D = \beta b_2 A_0 \left( 1 - e^{-\frac{x}{x_0}} \right) \text{ for fixed } \bar{n},$$

and

$$(b) \quad D = \frac{\beta b_2 A_0}{2} \left( 1 - 2e^{-\frac{x}{x_0}} \right) \text{ for fixed } N.$$

It should be particularly noticed that in the relativistic case equation (11) for pressure distribution is independent of the statistics obeyed by the gas and also of temperature. However, the dependence on statistics (shown by the appearance of terms containing  $\beta$  as a factor) comes in when we consider the distribution of concentration instead of pressure. In fact equation (11) being merely an expression of hydrostatic equilibrium holds not only for the non-degenerate case that we are considering but also for degeneracy. In the relativistic case, *whatever statistics a gas may follow, and both for degeneracy and non-degeneracy, the pressure distribution is given by equation (11)*. In the non-relativistic case, however, the expressions are different for the different cases.

---

\*  $A_0 < 1$  for non-degeneracy.



§4. We shall now consider the degenerate case. In the non-relativistic case, for a particle in a uniform gravitational field the force acting on it, being independent of the kinetic energy, becomes constant, and thus the problem is identical with that treated by Kothari and Auluck (*loc. cit.*). We shall, therefore, here consider only the case of relativistic degeneracy. Taking first the Fermi-Dirac case, and substituting in (11) the expression for pressure

$$p = \frac{1}{4} n \zeta_0 \left[ 1 + \frac{2\pi^2}{3} \left( \frac{kT}{\zeta_0} \right)^2 \right], \quad \dots \quad (15)$$

where

$$\zeta_0 = ch \left( \frac{3n}{4\pi g} \right)^{\frac{1}{3}},$$

we have

$$n = \bar{n} \left[ 1 - \frac{\pi^2}{2} \left( \frac{kT}{\zeta_0} \right)^2 \left\{ e^{\frac{2x}{\zeta_0}} - 1 \right\} \right] e^{-\frac{3x}{4\zeta_0}}, \quad \dots \quad (16)$$

or for  $T = 0$ ,

$$n = \bar{n} e^{-\frac{3x}{4\zeta_0}}. \quad \dots \quad (17)$$

Equation (17) may be compared with the relativistic non-degenerate equation (13) which for  $\bar{A}_0 \rightarrow 0$  is

$$n = \bar{n} e^{-\frac{x}{\zeta_0}}. \quad \dots \quad (17')$$

The two expressions (17) and (17') differ only by a numerical factor in the power of the exponential\*. While, therefore, there is no great difference between the expressions for concentration distribution for the relativistic degeneracy and non-degeneracy, there is a fundamental difference between relativistic degeneracy and non-relativistic degeneracy. In non-relativistic degeneracy, as is well known (see Kothari and Auluck, *loc. cit.*), the distribution effectively extends from  $x = 0$  to a certain height  $x = l$ . Above  $x = l$  the number of particles is negligibly small and it vanishes altogether when the degeneracy is complete (i.e.  $T = 0$ ). For complete degeneracy ( $T = 0$ )  $n$  is exactly proportional to  $(l-x)^{\frac{1}{3}}$  within the interval  $x = 0$  to  $x = l$ , where the length  $l$  is given by

$$l = \frac{h^2}{2m^2 g} \left( \frac{3n}{4\pi^2} \right)^{\frac{1}{3}}. \quad \dots \quad (18)$$

In the relativistic case even for complete degeneracy the distribution is not confined within any finite interval but continues to vary exponentially with height.

So far we have considered the relativistic degenerate case of Fermi-Dirac statistics. We shall now discuss the Bose-Einstein case. For a Bose-

---

\* The definitions of  $\zeta_0$  in (17) and (17') are different.

Einstein gas, the Gibb's free energy is always less than zero for non-degeneracy, and equal to zero in degeneracy. According to the fundamental equation (5)  $\zeta$  decreases with increasing  $x$ , its maximum value occurring at  $x = 0$ . Hence it follows that for a *Bose-Einstein gas the degeneracy can occur only at the level  $x = 0$  and above this level the gas must necessarily be non-degenerate.*

For a degenerate Bose-Einstein gas the pressure is independent of concentration and for the relativistic case that we are considering  $p$  is given by

$$p = \frac{8}{45} \frac{\pi^5}{(ch)^3} (kT)^4. \quad \dots \dots \dots (19)$$

As in a degenerate Bose-Einstein gas placed in a field of force degeneracy occurs only at the ground level, we have by combining (19) with (11)

$$p = \frac{8\pi^5}{45(ch)^3} (kT)^4 e^{-\frac{x}{x_0}}, \quad \dots \dots \dots (20)$$

where 
$$x_0 = \frac{c^2}{3g}.$$

Since black-body radiation constitutes a relativistic degenerate Bose-Einstein gas, equation (20) shows the possibility of the occurrence of non-degenerate radiation (at  $x \neq 0$ ) when the gravitational field is extremely large. The astrophysical implications of this result will be considered elsewhere.

It is a great pleasure to record our grateful thanks to Dr. D. S. Kothari for his kind interest in the work.

#### REFERENCES.

- Kothari, D. S. and Auluck, F. C., (1942). Fermi-Dirac and Bose-Einstein Gas in a Uniform Field of Force. *Proc. Nat. Inst. Sci. India*, 8, 165-171.  
 Kothari, D. S. and Singh, B. N., (1941). Bose-Einstein statistics and degeneracy. *Proc. Roy. Soc. A*, 178, 135.



## ON THE ELASTIC SCATTERING OF THE FAST MESONS.

By S. GUPTA, *Department of Applied Mathematics, University of Calcutta.*

(Communicated by Prof. N. R. Sen, D.Sc., Ph.D., F.N.I.)

(Received July 2, 1942 ; Read October 5, 1942.)

### ABSTRACT.

The differential cross-sections of the elastic scattering of mesons with spin one and zero are calculated from Duffin-Kemmer's  $\beta$ -formalism by a method which is analogous to the elegant method of Sauter as applied to Dirac's electron.

### INTRODUCTION.

The problem of the elastic scattering of meson with spin one was discussed by various authors (Laporte, 1938; Massey and Corben, 1939; Majumdar and Gupta, 1941) assuming the field theory of meson obeying Proca's equation. Recently Duffin (1938) and Kemmer (1939) derived the equations of particles with spin one and zero in a form which is analogous to Dirac's equation. This formulation of Duffin-Kemmer, as shown by various authors (Booth and Wilson, 1940; Wilson, 1940; Christy and Kusaka, 1941) on performing the calculations by a method which is somewhat similar to that as applied to Dirac's electron, can be used with more advantage in the problems of the interaction between meson and the electromagnetic field than the usual field theory. The relativistic theory of the elastic scattering of charged particle with spin half was first worked out by Mott (1929) from the Dirac's theory of electron and the calculation was later on much simplified by an elegant method by Sauter (1933). In the latter method a Born's approximation was used and the scalar force field through which the colliding particle interacts with the nucleus was left as completely general. As this general field was not specialised to Coulomb field, until the final stage, it was possible to avoid all convergence difficulties. The purpose of this note is to calculate the differential cross-section of the elastic scattering of meson from the Duffin-Kemmer's formalism by a method which is analogous to the method of Sauter. By this procedure we can avoid the use of the method of second quantisation which is usually utilised in a similar problem of meson when using the field theory of Proca. Laporte, of course, applied to Proca's equation a treatment which is somewhat similar to Sauter's one; but his calculations were not so simple. The advantage of using the Duffin-Kemmer's formalism is that the cross-sections for particles with spin one and zero are obtained from a single scheme.

## CALCULATIONS.

The meson is defined in the presence of the electromagnetic field by Kemmer by the equation

$$\left(\frac{\partial}{\partial x_\mu} - \frac{ie}{\hbar c} \phi_\mu\right) \beta_\mu \psi + \kappa \psi = 0, \quad \dots \quad (1)$$

where  $\kappa = \frac{mc}{\hbar}$ ,  $x_4 = ict$ , together with the following commutation rules for the Duffin's  $\beta$ -matrices

$$\beta_\mu \beta_\nu \beta_\rho + \beta_\rho \beta_\nu \beta_\mu = \beta_\mu \delta_{\nu\rho} + \beta_\rho \delta_{\nu\mu} \dots \quad (2)$$

The wave function  $\psi$  satisfies the initial condition

$$\left(\frac{\partial}{\partial x_k} - \frac{ie}{\hbar c} \phi_k\right) \beta_k \beta_4^2 \psi + \kappa (1 - \beta_4^2) \psi = 0, \quad (k = 1, 2, 3). \quad (3)$$

The second order wave equation, which is satisfied by each component of  $\psi$ , is given by

$$\begin{aligned} \left(\frac{\partial}{\partial x_\mu} - \frac{ie}{\hbar c} \phi_\mu\right) \left(\frac{\partial}{\partial x_\mu} - \frac{ie}{\hbar c} \phi_\mu\right) \psi &= \kappa^2 \psi + \frac{ie}{2\hbar c} F_{\mu\nu} (\beta_\mu \beta_\nu - \beta_\nu \beta_\mu) \psi \\ &+ \frac{ie}{2mc^2} \left(\frac{\partial}{\partial x_\mu} - \frac{ie}{\hbar c} \phi_\mu\right) F_{\nu\rho} (\beta_\rho \beta_\mu \beta_\nu - \beta_\nu \delta_{\mu\rho}) \psi. \end{aligned} \quad (4)$$

To be definite we shall consider in our subsequent discussion the case of positive meson, but our final result will also be valid for negative meson. In the absence of the magnetic field and for any arbitrary scalar potential function  $V$ , the equation (4) assumes the form

$$\begin{aligned} \left\{ \nabla^2 + \left(\frac{V-E}{\hbar c}\right)^2 - \frac{m^2 c^2}{\hbar^2} \right\} \psi &= -\frac{1}{\hbar c} \frac{\partial V}{\partial x_k} (\beta_k \beta_4 - \beta_4 \beta_k) \psi \\ &+ \frac{1}{mc^2} \left(\frac{V-E}{\hbar c}\right) \frac{\partial V}{\partial x_k} \beta_k \beta_4^2 \psi - \frac{1}{mc^2} \frac{\partial}{\partial x_l} \left(\frac{\partial V}{\partial x_k} \beta_k \beta_l \beta_k \psi\right), \quad (k, l = 1, 2, 3), \end{aligned}$$

or

$$\begin{aligned} \left(\nabla^2 + \frac{V^2}{\hbar^2 c^2}\right) \psi &= \frac{1}{\hbar c} \left\{ \frac{2EV}{\hbar c} - \frac{\partial V}{\partial x_k} (\beta_k \beta_4 - \beta_4 \beta_k) - \frac{E}{mc^2} \frac{\partial V}{\partial x_k} \beta_k \beta_4^2 \right\} \psi \\ &- \frac{1}{mc^2} \frac{\partial}{\partial x_l} \left(\frac{\partial V}{\partial x_k} \beta_k \beta_l \beta_k \psi\right) + \frac{1}{\hbar c} \left\{ -\frac{V^2}{\hbar c} + \frac{1}{mc^2} V \frac{\partial V}{\partial x_k} \beta_k \beta_4^2 \right\} \psi \dots \quad (5) \end{aligned}$$

In this equation we regard  $V$  as a perturbing potential and assume  $\psi$  to be of the form

$$\psi = \psi_0 + \psi_1 + \psi_2 + \dots, \quad \dots \quad (6)$$

where  $\psi_0$  represents the wave function of the free meson and has the form

$$\psi_0 = u^+(\mathbf{p}) e^{\frac{i}{\hbar} (\mathbf{p}\mathbf{r})}, \quad \dots \quad (7)$$

and further from (1) and (3) we have

$$\{-E\beta_4 + ic(\mathbf{p}\beta) + mc^2\} u^+(\mathbf{p}) = 0, \quad \dots \quad (8)$$

with the equation of condition

$$u^+(\mathbf{p}) = \left\{ 1 - \frac{i}{mc} (\mathbf{p}\beta) \right\} \beta_4^2 u^+(\mathbf{p}). \quad \dots \quad (9)$$

From (5) and (6) one then obtains the recurrence formula for  $\psi_n$  as

$$\begin{aligned} \left( \nabla^2 + \frac{p^2}{\hbar^2} \right) \psi_n = & \frac{1}{\hbar c} \left\{ \frac{2EV}{\hbar c} - \frac{\partial V}{\partial x_k} (\beta_k \beta_4 - \beta_4 \beta_k) - \frac{E}{mc^2} \frac{\partial V}{\partial x_k} \beta_k \beta_4^2 \right\} \psi_{n-1} \\ & - \frac{1}{mc^2} \frac{\partial}{\partial x_l} \left( \frac{\partial V}{\partial x_k} \beta_4 \beta_l \beta_k \psi_{n-1} \right) + \frac{1}{\hbar c} \left( -\frac{V^2}{\hbar c} + \frac{1}{mc^2} V \frac{\partial V}{\partial x_k} \beta_k \beta_4^2 \right) \psi_{n-2}. \quad \dots \quad (10) \end{aligned}$$

In this note, as we are interested only on the first order approximation, the last term on the right hand side of (5) may be neglected at large distances  $R$  from the scattering centre, and the equation for  $\psi_1$  then becomes

$$\begin{aligned} \left( \nabla^2 + \frac{p^2}{\hbar^2} \right) \psi_1 = & \frac{1}{\hbar c} \left\{ \frac{2EV}{\hbar c} - \frac{\partial V}{\partial x_k} (\beta_k \beta_4 - \beta_4 \beta_k) - \frac{E}{mc^2} \frac{\partial V}{\partial x_k} \beta_k \beta_4^2 \right\} \psi_0 \\ & - \frac{1}{mc^2} \frac{\partial}{\partial x_l} \left( \frac{\partial V}{\partial x_k} \beta_4 \beta_l \beta_k \psi_0 \right). \quad \dots \quad (11) \end{aligned}$$

The solution of this equation is well known and has the form

$$\begin{aligned} \psi_1 = & \frac{1}{4\pi\hbar c} \int e^{\frac{ip}{\hbar} |\mathbf{R}-\mathbf{r}|} \left[ \left\{ -\frac{2EV}{\hbar c} + \frac{\partial V}{\partial x_k} (\beta_k \beta_4 - \beta_4 \beta_k) + \frac{E}{mc^2} \frac{\partial V}{\partial x_k} \beta_k \beta_4^2 \right\} \psi_0 \right. \\ & \left. + \frac{\hbar}{mc} \frac{\partial}{\partial x_l} \left( \frac{\partial V}{\partial x_k} \beta_4 \beta_l \beta_k \psi_0 \right) \right] d\tau, \quad \dots \quad (12) \end{aligned}$$

where  $\mathbf{R} (= \xi_1, \xi_2, \xi_3)$  is the space-vector of the reference point at which  $\psi_1$  is to be calculated, and  $\mathbf{r} (= x_1, x_2, x_3)$  is the integration point. The sign of the power of  $e$  is so chosen that (12) represents an outgoing spherical wave at a great distance from the scattering centre.

We integrate (12) by parts and neglect the surface integrals, and since

$$\frac{\partial}{\partial x_k} f(\mathbf{R}-\mathbf{r}) = -\frac{\partial}{\partial \xi_k} f(\mathbf{R}-\mathbf{r}),$$

and  $\psi_0$  is a function of  $\mathbf{r}$  only, we have

$$\begin{aligned} \psi_1 = & \frac{1}{4\pi\hbar c} \int \left[ -\frac{2EV}{\hbar c} + \frac{\partial V}{\partial x_k} \left\{ (\beta_k \beta_4 - \beta_4 \beta_k) + \frac{E}{mc^2} \beta_k \beta_4^2 \right. \right. \\ & \left. \left. + \frac{\hbar}{mc} \beta_4 \beta_l \beta_k \frac{\partial}{\partial \xi_l} \right\} \right] \psi_0 \frac{e^{\frac{ip}{\hbar} |\mathbf{R}-\mathbf{r}|}}{|\mathbf{R}-\mathbf{r}|} d\tau \quad \dots \quad (13) \end{aligned}$$

To determine the scattering probability we are mainly concerned with the behaviour of this function at great distances from the scattering centre. We then have

$$|\mathbf{R}-\mathbf{r}| = R \left\{ 1 + \frac{r^2}{R^2} - \frac{2}{R} (\mathbf{n}\mathbf{r}) \right\}^{\frac{1}{2}} = R - (\mathbf{n}\mathbf{r}), \text{ approximately,}$$

where  $\mathbf{n}$  denotes the unit vector in the direction of  $\mathbf{R}$ , that is in the direction of observation; further we introduce the unit vector  $\mathbf{e} = \frac{\mathbf{p}}{|\mathbf{p}|}$  in the primary direction of the meson. Hence for large  $R$  we have approximately by (7)

$$\begin{aligned} \int f(r) \psi_0 \cdot e^{\frac{ip}{\hbar} |\mathbf{R}-\mathbf{r}|} \frac{1}{|\mathbf{R}-\mathbf{r}|} d\tau &= u^+(\mathbf{p}) \int f(r) \cdot e^{\frac{ip}{\hbar} \{ |\mathbf{R}-\mathbf{r}| + (\mathbf{e}\mathbf{r}) \}} \frac{1}{|\mathbf{R}-\mathbf{r}|} d\tau \\ &\rightarrow u^+(\mathbf{p}) \frac{e^{\frac{ip}{\hbar} R}}{R} \cdot \int f(r) e^{\frac{ip}{\hbar} (\mathbf{e}-\mathbf{n}, \mathbf{r})} d\tau, \quad \dots \quad (14) \end{aligned}$$

and

$$\begin{aligned} \psi_1 &= \frac{1}{4\pi\hbar c} \cdot e^{\frac{ip}{\hbar} R} \cdot \int \left[ -\frac{2EV}{\hbar c} + \frac{\partial V}{\partial x_k} \{ (\beta_k \beta_4 - \beta_4 \beta_k) + \frac{E}{mc^2} \beta_k \beta_4^2 \right. \\ &\quad \left. + \frac{ip}{mc} \beta_4 (\beta \mathbf{n}) \beta_k \} \right] \cdot u^+(\mathbf{p}) e^{\frac{ip}{\hbar} (\mathbf{e}-\mathbf{n}, \mathbf{r})} d\tau. \quad \dots \quad (15) \end{aligned}$$

Again integrating by parts and neglecting the surface integrals, we get

$$\begin{aligned} \psi_1 &= \frac{1}{4\pi\hbar^2 c^2} \cdot e^{\frac{ip}{\hbar} R} \cdot \left[ -2E + icp (\beta \beta_4 - \beta_4 \beta, \mathbf{n}-\mathbf{e}) + \frac{iEp}{mc} (\beta, \mathbf{n}-\mathbf{e}) \beta_4^2 \right. \\ &\quad \left. - \frac{p^2}{m} \beta_4 (\beta \mathbf{n}) (\beta, \mathbf{n}-\mathbf{e}) \right] \cdot u^+(\mathbf{p}) \int V e^{\frac{ip}{\hbar} (\mathbf{e}-\mathbf{n}, \mathbf{r})} d\tau. \quad \dots \quad (16) \end{aligned}$$

On the application of the equation of condition (9), (16) then assumes the form

$$\begin{aligned} \psi_1 &= \frac{1}{4\pi\hbar^2 c^2} \cdot e^{\frac{ip}{\hbar} R} \cdot \left[ -2E\beta_4^2 + \frac{2iEp}{mc} (\beta \mathbf{e}) \beta_4^2 + icp (\beta, \mathbf{n}-\mathbf{e}) \beta_4 \right. \\ &\quad \left. - \frac{p^2}{m} \beta_4 (\beta, \mathbf{n}-\mathbf{e}) (\beta \mathbf{e}) \beta_4^2 + \frac{iEp}{mc} (\beta, \mathbf{n}-\mathbf{e}) \beta_4^2 - \frac{p^2}{m} \beta_4 (\beta \mathbf{n}) (\beta, \mathbf{n}-\mathbf{e}) \beta_4^2 \right] \\ &\quad \times u^+(\mathbf{p}) \int V e^{\frac{ip}{\hbar} (\mathbf{e}-\mathbf{n}, \mathbf{r})} d\tau. \quad \dots \quad (17) \end{aligned}$$

The complex conjugate expression is

$$\begin{aligned} \psi_1^* = & \frac{1}{4\pi\hbar^2 c^2} \cdot \frac{e}{R} \cdot \frac{-\frac{ip}{\hbar} R}{R} \cdot u^+(\mathbf{p})^* \left[ -2E\beta_4^2 - \frac{2iEp}{mc}\beta_4^2(\beta\mathbf{e}) - icp\beta_4(\beta, \mathbf{n}-\mathbf{e}) \right. \\ & \left. - \frac{p^2}{m}\beta_4^2(\beta\mathbf{e})(\beta, \mathbf{n}-\mathbf{e})\beta_4 - \frac{iEp}{mc}\beta_4^2(\beta, \mathbf{n}-\mathbf{e}) - \frac{p^2}{m}\beta_4^2(\beta, \mathbf{n}-\mathbf{e})(\beta\mathbf{n})\beta_4 \right] \\ & \times \left( \int V e^{\frac{ip}{\hbar}(\mathbf{e}-\mathbf{n}, \mathbf{r})} d\tau \right)^* \quad \dots \quad (17') \end{aligned}$$

The intensity of the scattered meson, that is, the number of secondary meson that crosses in the direction  $\mathbf{n}$  per unit area at a distance  $R$  from the scattering centre, is given by the relation

$$I = c\psi_1^+(\beta\mathbf{n})\psi_1 \rightarrow v\psi_1^*\beta_4\psi_1, \quad \dots \quad (18)$$

and by (17) and (17') we get

$$\begin{aligned} I = & \frac{v}{R^2} \cdot \frac{1}{(4\pi\hbar^2 c^2)^2} \cdot u^+(\mathbf{p})^* \beta_4^2 \left[ 4E^2\beta_4 + \frac{4Ep^2}{m} \{ (\beta\mathbf{n})^2 - (\beta\mathbf{e})^2 \} \right. \\ & \left. - \frac{p^4}{m^2} \{ (\beta\mathbf{e})^2\beta_4(\beta\mathbf{n})(\beta, \mathbf{n}-\mathbf{e}) + (\beta, \mathbf{n}-\mathbf{e})(\beta\mathbf{n})\beta_4(\beta\mathbf{e})^2 \} \right] \beta_4^2 u^+(\mathbf{p}) \\ & \times \left| \int V e^{\frac{ip}{\hbar}(\mathbf{e}-\mathbf{n}, \mathbf{r})} d\tau \right|^2 \quad \dots \quad (19) \end{aligned}$$

When  $\beta$ 's are 10-rowed matrices the meson has spin one and for a given  $\mathbf{p}$  it has three polarisation states. Hence we shall have to average over the three directions of polarisation in the unperturbed state. To perform this we sum over the three directions of polarisation and divide by 3. The detail method of this calculation and of subsequent evaluation of spurs are given by Booth and Wilson. After performing the above operations we get for meson of spin one

$$\begin{aligned} I = & \frac{v}{R^2} \cdot \frac{1}{(4\pi\hbar^2 c^2)^2} \cdot \frac{1}{6E} \text{spur } \beta_4 \left[ 4E^2\beta_4 + \frac{4Ep^2}{m} \{ (\beta\mathbf{n})^2 - (\beta\mathbf{e})^2 \} \right. \\ & \left. - \frac{p^4}{m^2} \{ (\beta\mathbf{e})^2\beta_4(\beta\mathbf{n})(\beta, \mathbf{n}-\mathbf{e}) + (\beta, \mathbf{n}-\mathbf{e})(\beta\mathbf{n})\beta_4(\beta\mathbf{e})^2 \} \right] \\ & \times \beta_4 \left\{ mc^2 + \frac{p^2}{m} (\beta\mathbf{e})^2 + E\beta_4 \right\} \left| \int V e^{\frac{ip}{\hbar}(\mathbf{e}-\mathbf{n}, \mathbf{r})} d\tau \right|^2 \quad \dots \quad (20) \end{aligned}$$

When  $\beta$ 's are 5-rowed matrices the meson has spin zero and it has only one polarisation, viz. in the direction of motion. The equation (20) is valid even in this case with the omission of the factor  $\frac{1}{3}$  which arises because of the averaging over the three polarisations.



After evaluating the spurs, we have, for meson of spin one

$$I = \frac{v}{R^2} \cdot \frac{E^2}{(2\pi\hbar^2 c^2)^2} \cdot \left[ 1 + \frac{p^4}{6m^2 E^2} \{ 1 - (\mathbf{e}\mathbf{n})^2 \} \right] \left| \int V e^{\frac{ip}{\hbar} (\mathbf{e} - \mathbf{n}, \mathbf{r})} d\tau \right|^2, \quad \dots (21a)$$

and for meson of spin zero

$$I = \frac{v}{R^2} \cdot \frac{E^2}{(2\pi\hbar^2 c^2)^2} \cdot \left| \int V e^{\frac{ip}{\hbar} (\mathbf{e} - \mathbf{n}, \mathbf{r})} d\tau \right|^2. \quad \dots (21b)$$

Let us now denote the angle between  $\mathbf{n}$  and  $\mathbf{e}$  by  $\theta$  and since

$$E = \gamma mc^2, \quad p = \gamma mv, \quad \gamma = \left( 1 - \frac{v^2}{c^2} \right)^{-\frac{1}{2}},$$

the differential cross-section  $d\phi$  of our scattering process within a solid angle  $d\Omega$  is given for meson of spin one by

$$d\phi = \frac{R^2 I}{v} d\Omega = \frac{m^2 \gamma^2}{(2\pi\hbar^2)^2} \left\{ 1 + \frac{(\gamma^2 - 1)^2}{6\gamma^2} \sin^2 \theta \right\} \left| \int V e^{\frac{ip}{\hbar} (\mathbf{e} - \mathbf{n}, \mathbf{r})} d\tau \right|^2 d\Omega \quad \dots (22a)$$

and for meson of spin zero by

$$d\phi = \frac{m^2 \gamma^2}{(2\pi\hbar^2)^2} \left| \int V e^{\frac{ip}{\hbar} (\mathbf{e} - \mathbf{n}, \mathbf{r})} d\tau \right|^2 d\Omega. \quad \dots (22b)$$

For a pure Coulomb field,  $V = \frac{ze^2}{r}$ , and we have

$$\int V e^{\frac{ip}{\hbar} (\mathbf{e} - \mathbf{n}, \mathbf{r})} d\tau = \frac{4\pi ze^2 \hbar^2}{p^2 |\mathbf{e} - \mathbf{n}|^2} = \frac{\pi ze^2 \hbar^2}{\gamma^2 m^2 v^2 \sin^2 \frac{\theta}{2}}.$$

Then (22a) reduces to

$$d\phi = \left( \frac{ze^2}{2mv^2} \right)^2 \cdot \frac{1}{\gamma^2 \sin^4 \frac{\theta}{2}} \cdot \left\{ 1 + \frac{(\gamma^2 - 1)^2}{6\gamma^2} \sin^2 \theta \right\} d\Omega, \quad \dots (23a)$$

and (22b) to

$$d\phi = \left( \frac{ze^2}{2mv^2} \right)^2 \cdot \frac{1}{\gamma^2 \sin^4 \frac{\theta}{2}} \cdot d\Omega. \quad \dots (23b)$$

The result (23a) agrees with the expressions obtained by Laporte, Massey and Corben, and Majumdar and Gupta; and (23b) is the well-known result as obtained from Klein-Gordon equation.

## REFERENCES.

- Booth, F. and Wilson, A. H. (1940).—Radiative Processes involving Fast Mesons. *Proc. Roy. Soc. (A)*, **175**, 483.
- Christy, R. F. and Kusaka, S. (1941).—The Interaction of  $\gamma$ -rays with Mesotrons. *Phys. Rev.*, **59**, 414.
- Duffin, R. J. (1938).—On the Characteristic Matrices of Covariant Systems. *Phys. Rev.*, **54**, 1114.
- Kemmer, N. (1939).—The Particle Aspects of Meson. *Proc. Roy. Soc. (A)*, **173**, 91.
- Laporte, O. (1938).—Elastic Scattering of Yukawa Particles. *Phys. Rev.*, **54**, 905.
- Majumdar, R. C. and Gupta, S. (1939–41).—On the Elastic scattering of Meson by a Coulomb Field. *Trans. Bose Research Inst.*, **14**, 183.
- Massey, S. W. and Corben, H. C. (1939).—Elastic Collisions of Mesons with Electrons and Protons. *Proc. Camb. Phil. Soc.*, **35**, 463.
- Mott, N. F. (1929).—The Scattering of Fast Electrons by Atomic Nuclei. *Proc. Roy. Soc. (A)*, **124**, 425.
- Sauter, F. (1933).—Zur Stationären Behandlung der elastischen Streuung sehr schneller Elektronen. *Zs. f. Phys.*, **86**, 818.
- Wilson, A. H. (1940).—The Calculations of Processes involving Mesons by Matrix Methods. *Proc. Camb. Phil. Soc.*, **36**, 363.



# PRESSURE IONISATION AND MAXIMUM RADIUS FOR A COLD BODY.

By P. L. BHATNAGAR and D. S. KOTHARI, *University of Delhi.*

(Received June 3, 1942 ; Read October 5, 1942.)

## ABSTRACT.

The degree of ionisation in degenerate matter depends essentially on the pressure or density of the material. The results on ionisation of heavy ions (produced in Uranium fission) can be readily utilised to determine the degree of ionisation in degenerate matter. This is done in §1 of the present paper. The results of §1 are applied in §2 to determine the mass-radius relation for cold stellar bodies.

§ 1. In the case of cold \* matter the pressure of the degenerate electron gas is given by the relation

$$\left. \begin{aligned} p &= K \frac{\rho^{\frac{4}{3}}}{\mu^{\frac{4}{3}}}, \\ K &= \frac{8\pi h^2}{15m} \left( \frac{3}{8\pi m_H} \right)^{\frac{1}{3}}, \end{aligned} \right\} \quad \dots \dots \dots (1)$$

where  $k$  is called the degenerate gas constant,  $\rho$  is the density of the material, and  $\mu$  the mean molecular weight per free electron.  $m$  represents the mass of electron and  $m_H$  that of proton, and  $h$  is the Planck's constant.

The mean molecular weight per free electron is the measure of the degree of ionisation of the material: the free electron concentration  $n$  being given by

$$n = \frac{\rho}{\mu m_H} \quad \dots \dots \dots (2)$$

If the cold body be supposed to consist of material of atomic weight  $A$  and atomic number  $Z$ , then, for complete ionisation of the material into free electrons and bare nuclei,  $\mu$  will be equal to  $\frac{A}{Z} \simeq 2$  (except for hydrogen when it is equal to 1). If the ionisation be incomplete so that there are only  $r$  free electrons per atom, then

$$\mu = \frac{A}{r}.$$

The dependence of  $\mu$  on the density of the material has been worked out previously (Kothari, 1936, 1938) though the theory is admittedly crude being based on several simplifying assumptions.

---

\* Matter will be referred to as cold when any free electrons present in it constitute a degenerate gas.

Following the recent discovery of Uranium fission, the problem of the energy loss of heavy ions and their degree of ionisation has (following Bohr, 1941) received considerable attention. The degree of ionisation or the average charge of a heavy ion depends primarily on its velocity  $V$ ; in fact the velocity  $V_e$  of the outermost electron in the ion is (almost) equal to the velocity  $V$  of the ion. The results on the ionisation of heavy ions can be readily applied to estimate the degree of ionisation in degenerate matter. In the case of ions produced by fission the velocity of the ion is very high compared to the thermal velocity of the molecules of the atmosphere surrounding the ion. It is just the reverse in the case of degenerate matter where, because of its larger mass, the ionic velocity is negligible compared to the velocity of the surrounding free electrons, and the maximum relative velocity of the ion with respect to the free electrons will be the maximum electron-velocity for Fermi-distribution,

$$V = \frac{h}{m} \left( \frac{3n}{8\pi} \right)^{\frac{1}{3}},$$

or 
$$V = \frac{h}{m} \left( \frac{3\rho}{8\pi\mu m_H} \right)^{\frac{1}{3}} \quad \dots \quad (3)$$

The degree of ionisation of the material will be such that the velocity  $V$  given by (3) equals the velocity  $V_e$  of the outermost bound-electron in the ion.

Knipp and Teller (1941) have calculated on the Thomas-Fermi model the velocity of the most loosely bound electron for different values of the ionic charge.\* The first column in the following table gives  $\frac{r}{Z}$ , and the corresponding values of  $\left( \frac{hV_e}{2\pi e^2 Z^{\frac{1}{2}}} \right)$ , taken from Knipp and Teller, are given in the second column. The other columns in the table give  $\mu = \frac{A}{r}$ , density and pressure of the material. The density is determined as follows:—

Assuming  $V = V_e$ , we have from (3)

$$\rho = \alpha \frac{\left( \frac{hV_e}{2\pi e^2 Z^{\frac{1}{2}}} \right)^3}{\left( \frac{r}{Z} \right)}, \quad \dots \quad (4)$$

where

$$\alpha = \frac{64}{3} A Z m_H \pi^4 \left( \frac{e}{h} \right)^6 m^3,$$

and hence  $\rho$  is found by using the values given in columns (1) and (2) of the table. The relation between pressure, density, and  $\mu$  is expressed by (1).

---

\* The expression for pressure-ionisation given by Kothari (Kothari, 1936, 1938) is based on the assumption of a uniform electron-distribution within the atomic cell.

The values of  $\mu$ , density, and pressure given in the table refer to the case of iron ( $Z = 26$ ).

TABLE I.

$\frac{r}{Z}$	$\frac{hV_e}{2\pi e^2 Z^{\frac{1}{2}}}$	$A = 55.8; Z = 26$		
		$\mu$	$\rho$ (gm./cm. <sup>3</sup> )	$p$ (dyne/cm. <sup>2</sup> )
0.01	0.11	215	73.3	$1.65 \times 10^{12}$
0.02	0.15	107	92.9	$7.78 \times 10^{12}$
0.05	0.21	42.9	102	$4.18 \times 10^{13}$
0.10	0.28	21.5	121	$1.77 \times 10^{14}$
0.121	0.295	17.7	117	$5.56 \times 10^{14}$
0.223	0.411	9.63	171	$1.20 \times 10^{15}$
0.522	0.75	4.11	445	$2.43 \times 10^{16}$
0.761	1.19	2.82	$1.22 \times 10^8$	$2.44 \times 10^{17}$
0.949	2.29	2.26	$6.97 \times 10^8$	$6.45 \times 10^{18}$

When the ionisation has proceeded to the stage  $r = Z - 1$ , then the orbital velocity of the last bound electron will be

$$V_e = \frac{2\pi e^2 Z}{h},$$

and hence if the ionic velocity exceeds the above value the atom will be completely ionised. It follows, therefore, that for *complete ionisation* of the material

$$V = \frac{h}{m} \left( \frac{3n}{8\pi} \right)^{\frac{1}{2}} \geq \frac{2\pi e^2 Z}{h}$$

or

$$\rho \geq \frac{64 \pi^4 e^6 Z^3 m^3 \mu m_H}{3 h^6}.$$

Substituting numerical values and taking the case of iron ( $\mu = \frac{A}{Z} = 2.147$ ), for complete ionisation the density must exceed

$$1.43 \times 10^4 \text{ gm./cm.}^3$$

In fig. 1 the continuous curve represents  $\log_{10} p$  against  $\log_{10} \rho$  and the ladder marked on the curve denotes the corresponding values of  $\mu$ . The dotted curve depicts the results previously obtained by Kothari (1938) and are

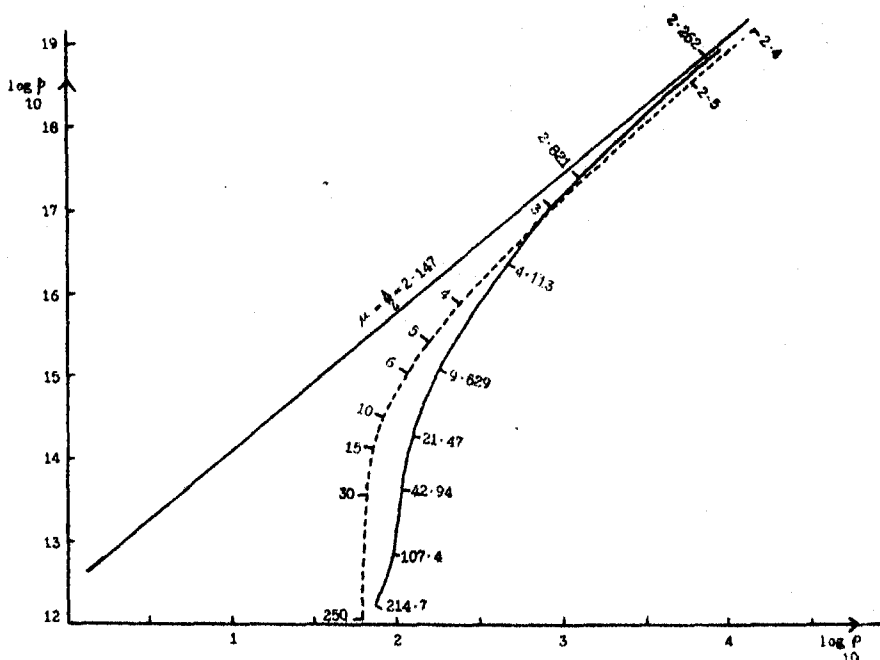


FIG. 1. The figure shows the relation between pressure and density of the material which for numerical evaluation is assumed to be iron. The continuous curve exhibits the results of the present paper. The dotted curve, based on Kothari's earlier calculations, is inserted for comparison. A ladder of  $\mu$  values has been marked along the curves.

The straight line in the figure would represent the pressure-density relation if the ionisation did not vary with density but was complete ( $\mu = \frac{A}{Z}$ ) at all densities.

based, as already remarked, on a uniform electronic distribution within the atomic cell. According to Kothari  $\mu$  is given by

$$\mu = \frac{\frac{A}{Z}}{\left[1 - \left(\frac{\Delta Z A}{\rho}\right)^{\frac{1}{2}}\right]^{\frac{1}{2}}}, \quad \dots \dots (5)$$

where

$$\Delta = \left[3^{\frac{1}{2}} \cdot 2\pi^{\frac{1}{2}} \frac{me^2}{\hbar^2} m_H^{\frac{1}{2}}\right]^3.$$

The values of  $\mu$ ,  $\rho$ , and  $p$  given in Table II and the dotted curve in fig. 1 are obtained by using this expression for  $\mu$  in (1). As is to be expected the continuous and the dotted curves are in reasonable agreement.

The straight line in figure 1 represents  $\log_{10} p$  against  $\log_{10} \rho$  when  $\mu$  is assumed to be constant and equal to  $\frac{A}{Z}$ . The straight line, therefore, represents the relation between  $p$  and  $\rho$  when we ignore the phenomenon of pressure-ionisation whereas the curves take account of it.

TABLE II.

$$Z = 26$$

$\mu$	$\rho$ (gm./cm. <sup>3</sup> )	$p$ (dyne/cm. <sup>2</sup> )
250	63.0	$9.96 \times 10^{11}$
40	64.2	$3.52 \times 10^{13}$
30	65.1	$3.60 \times 10^{13}$
20	67.5	$7.53 \times 10^{13}$
15	70.7	$1.31 \times 10^{14}$
10	79.8	$3.15 \times 10^{14}$
6	114	$1.06 \times 10^{15}$
5	146	$2.73 \times 10^{15}$
3	805	$1.11 \times 10^{17}$
2.147	$\infty$	$\infty$

§ 2. We shall now apply the above results to determine the maximum radius for a cold body.

In case of a stellar body composed of degenerate matter we have to deal with two opposing tendencies: (i) the mutual gravitational forces tending to diminish the radius, and (ii) the pressure of the degenerate electron gas (varying roughly as the square of the concentration) tending to inflate the configuration. For a spherical aggregate composed of degenerate matter the mass  $M$  and the radius  $R$  are connected by the well-known relation due to Milne (1932),

$$R = \frac{l}{\mu^{\frac{1}{2}}} \left( \frac{\oplus}{M} \right)^{\frac{1}{2}}, \quad \dots \dots \dots (6)$$

where

$$l = \frac{5(\omega_0^0)^{\frac{1}{2}} K}{2^{\frac{1}{2}} \pi^{\frac{1}{2}} G \oplus^{\frac{1}{2}}} = 1.932 \times 10^{11} \text{ cm.},$$

$\omega_0^0$  ( $= 132.39$ ) is a constant characteristic of the Emden-solution of Emden's equation of index  $3/2$ ,  $G$  is the constant of gravitation, and  $\oplus$  is the mass of the earth.  $\mu$  is assumed to be constant throughout the configuration but its dependence on  $M$  can be determined as follows:—

The mean density  $\rho_m$  of the configuration is

$$\rho_m = \frac{M}{\frac{4}{3} \pi R^3} = \frac{3\mu^5 M^2}{4\pi \oplus l^3}. \quad \dots \dots \dots (7)$$

For a given value of the density we can find from Table I the corresponding value of  $\mu$ , and hence the value of  $M$  is obtained from (7). Using this value of  $M$  in (6) we find the corresponding value of  $R$ .



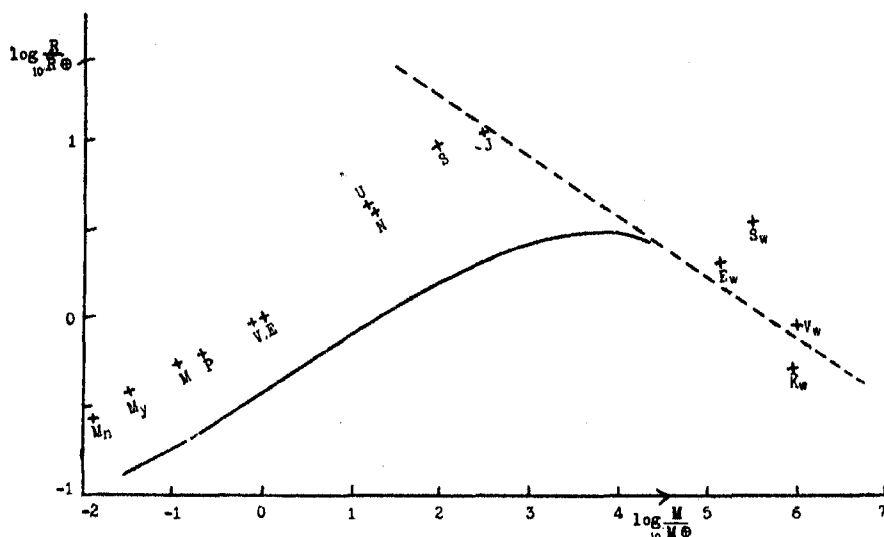


FIG. 2. The figure shows the theoretical mass-radius relation for a cold body. The material is assumed to be iron. The straight line depicts ( $M$ - $R$ ) relation on the erroneous assumption that the material is always completely ionised. The curve takes account of the dependence of ionisation on density (or mass) in accordance with the theory of pressure ionisation discussed in the text.

$M_n$ = Moon	$J$ = Jupiter	$E_w$ = $O_3$ Eridani B.
$M_y$ = Mercury	$S$ = Saturn	$S_w$ = Sirius B.
$V$ = Venus	$U$ = Uranus	$K_w$ = A.C. 70°8247.
$E$ = Earth	$N$ = Neptune	$V_w$ = Van Maanen's Star.
$M$ = Mars	$P$ = Pluto	

Fig. 2 exhibits the results of our calculations (the material is assumed to be iron). The observed ( $M$ ,  $R$ ) values for planets and white dwarf stars are shown in the figure and, as has been noticed before (Kothari (1938)), the run of the theoretical curve follows the trend of the observed values:—the maximum radius predicted by the theory is about one-third that of Jupiter.\*

#### REFERENCES.

- Bohr, N. (1941). Velocity-range relation for fission fragments. *Phys. Rev.*, **59**, 270-75.  
 Knipp, J. and Teller, E. (1941). On the energy loss of heavy ions. *Phys. Rev.*, **59**, 659-69.  
 Kothari, D. S. (1936). Internal constitution of the planets. *Mon. Not. R. Astro. Soc.*, **96**, 833-43.  
 Kothari, D. S. (1938). Theory of pressure ionisation and its applications. *Proc. Roy. Soc.*, **165**, 486-500.  
 Milne, E. A. (1932). The problem of Stellar Structure. *Mon. Not. R. Astro. Soc.*, **92**, 611-43.

\* In the calculations given here the material has been assumed to be iron. On the hypothesis of hydrogen abundance the predicted maximum value for the radius of a cold body comes out to be somewhat larger than Jupiter (Kothari 1938).

## PHOTOCHEMICAL ANALYSIS.

By G. GOPALA RAO and P. T. RAMACHARLU, *Physico-Chemical Laboratories, Andhra University, Waltair.*

(Communicated by Dr. N. R. Dhar, F.N.I., I.E.S.)

(Received April 24, 1942; Read October 5, 1942.)

It is well known that many chemical reactions are prompted by exposure to light of suitable wavelength. It therefore appeared to the authors that some of these photochemical reactions could be used as the basis of some interesting quantitative estimations, while still others might be used for qualitative detection.

The reaction which we have selected for experimental study is the photochemical reaction between mercuric chloride and sodium oxalate. It is our desire to make this reaction the basis for the volumetric estimation of mercuric chloride. Mercuric chloride cannot be titrated with standard thiocyanate solution by the Volhard's method. This method is very convenient for the estimation of mercuric nitrate solutions, but even here chlorides and bromides interfere. The estimation of mercuric chloride is of importance especially in connection with pharmaceutical preparations. Many analysts have applied themselves to this problem. Rupp (1906) and Rupp and Müller (1925) reduced mercuric chloride by formaldehyde in alkaline medium and determined the liberated mercury by the iodine thiosulphate titration. This method was employed by these workers for the estimation of corrosive sublimate in pharmaceutical preparations. This method has not been found altogether satisfactory and recourse was made to other reducing agents. Hillebrand and Lundell (1929) recommended reduction with phosphorous acid in hydrochloric acid solution and gravimetric estimation of the precipitated mercurous chloride after filtration and washing through Gooch crucible and drying at 100–105°C. This method has two drawbacks: (1) the reduction is slow and hence the solution must be allowed to stand for twelve hours or more before filtering; (2) mercurous chloride is appreciably soluble in water, especially in water containing chloride ions, giving too low results. Winkler (1924) and Moser and Niessner (1928) have investigated a method involving the reduction of mercuric salts to mercury by hypophosphorous acid in acid solution. Robinson (1929) studied the same method for the estimation of smaller quantities of mercury. We do not propose to discuss the numerous publications on the subject for the sake of brevity. It may, however, be said here that the several methods proposed till now are not satisfactory either on account of (1) lack

of sufficient accuracy, or (2) cumbrousness involving considerable time, filtration, etc., or (3) involving costly reagents.

Mercuric chloride and sodium oxalate do not interact in the dark at the ordinary temperatures. According to Dhar (1917) the dark reaction even at 80° is extremely slow. The light sensitiveness of this reaction was discovered by Planche (1815) and was utilised by Becquerel and Fremy (1868) and Eder (1879) for measuring the intensity of light. The photochemical reaction is represented by the equation:

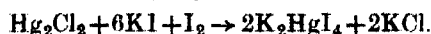


If this reaction were to be utilized for quantitative estimation it must be stoichiometric without interference by side reactions. We have, therefore, investigated this reaction carefully in order to establish conditions under which the mercurous chloride formed corresponds quantitatively to the mercuric chloride originally taken. Under these conditions, by estimating the mercurous chloride formed by the iodine thiosulphate titration, we can determine the amount of mercuric chloride originally taken.

#### *Experimental.*

The mercuric chloride and the sodium oxalate employed in our investigation are the Merck's analytical reagents.

Working with Monax or Pyrex glass conical flasks in sunlight, we found that the reaction is very slow. Hence, we used uranyl nitrate as a photo-sensitiser. After exposure to light for the requisite time the mixture is treated without filtration, with a known excess of a standard solution of iodine in potassium iodide. The M/20 solution of iodine must contain at least 50 grams of potassium iodide per litre. The precipitated mercurous chloride dissolves readily according to the following equation:—



After the addition of the iodine solution, the flask is stoppered and allowed to stand for a few minutes with occasional agitation, until complete solution has taken place. The residual iodine is titrated with standard sodium thio-sulphate solution with starch as the indicator. From the volume of the standard iodine solution consumed in the oxidation of mercurous to mercuric ion, we can calculate the amount of mercurous chloride formed in the photochemical reaction and hence that of the mercuric chloride originally taken. The uranyl nitrate does not interfere with the reaction or with the iodometric estimation in any other manner under the conditions described.

We made a large number of experiments varying the concentration of uranyl nitrate. Working with 5 ml. of M/20 mercuric chloride, the amount of uranyl nitrate solution (M/50) can be varied from 1 ml. to 6 ml. when quantitative reduction is obtained in about thirty minutes' exposure. With lower amounts of uranyl nitrate than 1 ml. the speed of the reaction is slower, necessitating unduly long exposures. With amounts of uranyl nitrate larger

than 6 ml. darkening of the precipitated mercurous chloride was observed due to the formation of mercury.

In another set of experiments the concentration of sodium oxalate was varied within wide limits (2 ml. to 20 ml. of N/5 oxalate for 5 ml. of M/20 mercuric chloride), without any noticeable difference in the results.

TABLE 1.

5 ml. of M/20  $\text{HgCl}_2$  + 5 ml. of N/2  $\text{Na}_2\text{C}_2\text{O}_4$  + 1 ml. of M/50 uranyl nitrate exposed to sunlight in 100 ml. Monax conical flasks (12 noon to 3 p.m.).

Mercury taken in each exposure = 50.15 mg.

Time of exposure in minutes.	Mercury found in mg.	Remarks.
5	46.03	
10	48.74	
20	49.72	
30	50.03	
40	50.03	
50	50.03	
60	50.03	
90	50.03	
120	50.47	Slightly darkens.
180	51.34	..

From the above table it will be noted that it is possible to reduce mercuric chloride to mercurous chloride easily and quantitatively; hence this photochemical reaction can be made the basis of a process for the estimation of mercuric chloride. We have made numerous estimations and we give below a few typical results to indicate the accuracy of our procedure.

TABLE 2.

*Variation of Mercury taken.*

X ml. of M/20  $\text{HgCl}_2$  + X ml. of N/5  $\text{Na}_2\text{C}_2\text{O}_4$  + X/5 ml. of M/50 uranyl nitrate exposed to sunlight for 45 minutes in 100 ml. Monax conical flasks.

X	Mercury taken in mg.	Mercury found in mg.	Error %.
1	10.03	9.99	0.40
2	20.06	19.95	0.55
5	50.15	50.03	0.24
10	100.30	100.00	0.30
15	150.45	150.14	0.20
20	200.60	200.06	0.27

*Estimation of micro amounts of mercuric chloride.*

We made experiments with varying volumes of M/200 mercuric chloride. We found that the concentration of oxalate has to be kept low if accurate

results are to be obtained. If the concentration of the oxalate is high there is a tendency for the mercurous chloride to undergo further reduction to metallic mercury. Moreover, a high concentration of oxalate will interfere in the subsequent iodometric estimation of mercurous chloride due to a slight reaction between the oxalate and iodine. The iodometric treatment was made with N/200 solution of iodine and the hypo solution employed was also N/200. Otherwise the details of the procedure are the same as those employed for the estimation of the more concentrated solution. The results given in the following table will show that the method is quite accurate even with solutions containing 1 mg. of mercury.

TABLE 3.

*Variation of Mercury taken.*

X ml. of M/200  $\text{HgCl}_2$  + X ml. of N/50  $\text{Na}_2\text{C}_2\text{O}_4$  + 0.2 X ml. of uranyl nitrate exposed to sunlight for 45 minutes in 100 ml. Monax conical flasks.

X	Mercury taken in mg.	Mercury found in mg.	Error %.
1	1.003	1.010	0.7
2	2.006	2.000	0.3
5	5.015	5.000	0.3
10	10.03	10.09	0.6
15	15.045	14.950	0.62

*Experiments in artificial light.*

As bright sunlight may not be available at all places, we thought it desirable to employ an artificial source of light in order to make this method one of common utility. The source of light employed by us was a Heraeus Quartz Mercury vapour lamp worked on 220 D.C. mains at 4 amps. The arc was cooled by means of a fan.

Different types of exposure were tried. If the ultra-violet light from the quartz mercury vapour lamp was allowed to fall horizontally on the reaction mixture contained in a rectangular quartz stoppered cell, the mercurous chloride formed easily underwent further reduction to metallic mercury. It was found that the most satisfactory procedure was to expose the solution in an open glass conical flask directly under the arc. Under these conditions even long exposures did not produce metallic mercury, and mercurous chloride formed corresponded quantitatively to mercuric chloride taken, provided the time of exposure was at least thirty minutes. Exposure in conical flasks is convenient for another reason as well; the subsequent treatment with iodine and titration with thiosulphate could be done in the same vessel without transferring into another. Flat dishes for exposure are not convenient for this reason. The following table contains results of some of the experiments conducted in artificial light.

TABLE 4.

Mercury taken in mg.	Mercury found in mg.	Error %.
100.30	99.81	0.49
50.15	50.04	0.22
20.06	20.11	0.25
7.021	6.998	0.30
5.015	5.013	0.04
3.009	3.001	0.26
1.003	1.011	0.80

The concentration of oxalate and uranyl nitrate are the same as in the experiments with sunlight.

We also made experiments with 1,000 watt tungsten filament lamp under otherwise identical conditions, but the time required for complete reaction is unduly long.

From the results in Table 4 we find that even minute amounts of mercury can be estimated by our procedure with a considerable degree of accuracy.

When one compares the details of our procedure with those recommended by others, one finds that our method is more suitable. Simple laboratory ware and common reagents are sufficient for the work.

#### SUMMARY.

1. A new technique has now been introduced by us into analytical chemistry. We are the first to employ the photochemical action of light as an aid to quantitative chemical analysis.

2. Applying this technique we have shown that mercuric chloride can be estimated with a considerable degree of accuracy and rapidity. Our method is more rapid and suitable than the methods now in use.

3. A detailed study has been made of the conditions under which our photochemical method can be applied to the estimation of mercuric chloride under natural and artificial sources of illumination.

4. From our experience, we lay down the following criteria which must be satisfied if a photochemical reaction can be used for quantitative estimation : (1) the reaction must be sensitive to the action of the light employed, or must be capable of being made sensitive by the addition of a suitable photosensitiser; (2) the reaction selected must be capable of reaching completion without involving undesirable side reactions; and (3) the selected reaction must be fairly rapid, obviating unduly long exposures.

In conclusion we desire to place on record our deep debt of gratitude to Prof. N. R. Dhar, D.Sc. (Lond.), Dr.és Science (Paris), of Allahabad for his kind interest in this investigation. One of us (P. T. R.) desires to thank the authorities of the Andhra University, Waltair, for permitting him to join in this work.

# REFERENCES.

- Becquerel, E. and Fremy, L. (1868). *La lumière ses causes et ses effets*. Tome 2, 69.
- Dhar, N. R. (1917). Catalysis. Part IV. Temperature coefficients of catalysed reactions. *J. Chem. Soc.*, **3**, 707.
- Eder, J. M. (1879). *Wien. Akad. Ber.*, **2**, 80.
- Hillebrand, W. F. and Lundell, G. E. F. (1929). *Applied Inorganic Analysis*. 172. John Wiley & Son.
- Moser, L. and Niessner, J. (1928). Determination of mercuric salts. *Z. anal. chem.*, **74**, 200.
- Planché (1815). *J. de Pharm.*, 49.
- Robinson, R. (1929). Determination of small quantities of mercury in the presence of organic and inorganic compounds. *Analyst*, **54**, 145.
- Rupp, E. (1906). Volumetric estimation of mercury. *Ber.*, **39**, 3702.
- Rupp, E. and Muller, K. (1925). Determination of mercury in cinnabar and similar substances. *Z. anal. chem.*, **67**, 20.
- Winkler, L. W. (1924). Determination of mercury as mercurous chloride and as metal. *Z. anal. chem.*, **64**, 262.

# ON THE EXTRA SPOTS IN LAUE PHOTOGRAPHS OF META-DINITROBENZENE.

By M. GANGULY, *M.Sc., Dacca University.*

(Communicated by Dr. K. Banerjee, D.Sc., F.N.I.)

(Received July 11, 1942; Read October 5 1942.)

## ABSTRACT.

Extra spots in the Laue photographs of metadinitrobenzene have been studied. The directions of the maxima in the spots make approximately an angle with the incident ray which is double the Bragg angle for the plane that produces the extra spot for the characteristic radiation. The direction of this maximum lies also in the plane of incidence. The peak intensities have been measured by the photographic photometer method. The intensities have been found to fall off rapidly with increase of  $\Delta$ , the difference between the angle of incidence and the Bragg angle. The spots are definitely diffuse and their half intensity widths as measured by the photographic photometer method in the radial and the transverse directions differ from each other. The widths change slowly with  $\Delta$  and for some spots they are practically independent of  $\Delta$ .

## INTRODUCTION.

The presence of extra spots or streaks is familiar to any one having experience of taking Laue photographs. In fact radial streaks in Laue photographs of sylvine were observed by Friedrich as early as 1913. Ten years after Friedrich's photograph was published Faxen (1923) suggested that these streaks were due to the disturbance of the geometrical atomic pattern by thermal agitation of the atoms. He showed that maxima should exist in the diffuse scattering of monochromatic radiation by a crystal set nearly, but not exactly, at the Bragg angle corresponding to any reflecting plane. The direction of the maximum is given by the relation

$$\sin \theta + \cos \theta \tan \phi = 2 \sin \theta_B$$

where  $\theta_B$  is the Bragg angle,  $\theta$  the glancing angle of incidence, and  $\phi$  the glancing angle of reflection.

Extra spots in the Laue photographs have been first noted by Preston (1938) and this observation has created a great interest in the subject and the effect is being studied in several laboratories. Preston (1939) explained these spots as due to diffraction of X-rays more or less independently from very small groups into which he supposes the crystal to be broken up by the thermal vibration of the lattice. The cell dimensions in these small groups should according to him differ from the extended lattice and so the directions of the maxima should be different from the Bragg directions. W. H. Bragg (1941),



however, showed that the postulate of the change of cell dimension is not necessary; diffraction by a small group of points will show maxima in monochromatic light for any orientation of the group.

Zachariasen (1940), on the other hand, ascribed the effect to thermal vibrations of the lattice and obtained an expression for the intensity of diffuse scattering in different directions which could be directly evaluated. The value of the intensity of this diffusely scattered X-ray thus obtained leads to maxima in certain specified directions giving rise to new diffraction spots.

The extra reflections have been explained by Raman (1940) from quite a different point of view. According to him the regular geometrical array of atoms in the crystal is set into vibration as a result of absorption of energy from the incident beam. The vibration of the lattice thus excited create dynamic stratifications of the electron density and these give rise to regular reflection of X-rays with a change of frequency. The absorption of energy, in his more recent publications, have been regarded as due to excitation of infra-red oscillations in the crystal.

The equation relating to the relative position of the modified spot and the corresponding Laue spot on this theory is

$$2d \sin \psi \sin (\vartheta \pm \epsilon) = n\lambda \sin \vartheta$$

where  $d$  = planar spacing.

$2\psi$  = the angle between the incident and reflected X-rays.

$\vartheta$  = inclination of plane of constant phase of the lattice oscillations to the static crystal planes.

In the earlier papers these spots have generally been described as diffuse. According to Faxen and Zachariasen theories, these reflections should be very diffuse and according to Raman's theory they should be quite sharp. Experimental results obtained so far, however, show that though in the majority of cases the reflections are diffuse, cases occur in which the reflections are sharp. The object of the present investigations have been to collect such data as will be necessary for the proper understanding of the origin of these reflections. In the present paper is described the results of a study of the falling off of the intensity of the diffuse reflection in different directions as well as with increase of  $\Delta$  and also to determine the variation of  $\phi$  with  $\Delta$  in the case of metadinitrobenzene.

### *Experimental Methods.*

For our photographs small crystals were chosen and were mounted with the help of a goniometer so that the X-ray beam could be made to pass through the crystal accurately in any desired direction. The X-ray tube used was one of the Hadding-Siegbahn type with copper anticathode running at a voltage of about 50 kV with nearly 15 milliamperes.

For taking the Laue photographs there was a deviation from the orthodox method in that a cylindrical camera was used for the following advantages:

(i) the angular range of observation was considerably extended, and (ii) the falling off of intensity with angle of diffraction was minimised. For calculating the diameter of the film and comparing the intensities of the extra spots in the different photographs, a very fine aluminium wire was mounted vertically just in contact with the crystal. Time of exposure varied from 7 to 8 hours, and photographs were taken with the crystal rotated to different orientations. Plate V shows some typical photographs.

Small perfect crystals of metadinitrobenzene were obtained from alcoholic solution. The substance crystallises in the orthorhombic system having a unit cell with sides  $a = 13.3$  A.U.,  $b = 14.2$  A.U., and  $c = 3.82$  A.U. The space-group is  $C_{2v}^0$  Pbn with 4 molecules in the unit cell.

As the Laue photographs have been taken with a cylindrical camera, the usual method of obtaining the gnomonic projection and thence to identify the planes is not applicable here and hence the following method has been used for identifying the spots. The angular co-ordinates  $\psi$  and  $\mu$  of the Laue spots were determined from the relations,

$$\psi = \frac{x}{R}$$

$$\mu = \tan^{-1} \frac{y}{R}$$

where  $x$  = horizontal distance on the film from a vertical line through the centre of the undeviated beam,

$y$  = vertical distance from the equatorial layer line,

and  $R$  = radius of the film (determined from the powder lines of Al).

Now, we know from the Laue equations that if  $\alpha, \beta, \gamma$  be the direction cosines of the diffracted beam in the Laue direction and  $\alpha_0, \beta_0, \gamma_0$  be the direction cosines of the incident beam, then,

$$\left. \begin{aligned} \frac{a(\alpha - \alpha_0)}{b(\beta - \beta_0)} &= \frac{h}{k} \\ \frac{b(\beta - \beta_0)}{c(\gamma - \gamma_0)} &= \frac{k}{l} \end{aligned} \right\} \dots \dots \dots (1)$$

where  $a, b, c$  are the three axial lengths and  $h, k, l$  the millerian indices of the reflecting plane.

From the known setting of the crystal it was possible to find  $\alpha, \beta, \gamma$  and  $\alpha_0, \beta_0, \gamma_0$  and thus determine the indices of the spots from the ratios  $\frac{h}{k}$  and  $\frac{k}{l}$ .

In the case of metadinitrobenzene the beam of X-rays was incident on the crystal along the  $a$ -axis in the first photograph while the  $c$ -axis was vertical. Hence because the crystal belongs to the orthorhombic system  $\beta_0$  and  $\gamma_0$  were zero while  $\alpha_0$  was equal to one. Similarly,  $\alpha = \cos 2\theta$ ,  $\gamma = \sin \mu$  and  $\beta =$

$\cos \mu \sin \psi$  where  $2\theta$  = angle of diffraction of the spot and was given by  $\cos 2\theta = \cos \psi \cos \mu$ . Thus the equations (1) reduce to

$$\frac{a(\cos 2\theta - 1)}{b \cos \mu \sin \psi} = \frac{h}{k},$$

$$\frac{b \cos \mu \sin \psi}{c \sin \mu} = \frac{k}{l}.$$

From the measurements of the positions of the maxima in the extra spots, their angular co-ordinates  $\psi_s$  and  $\mu_s$  were obtained. In the 2nd column of Table I are given the indices of the planes which produce these reflections, in the 4th column are given the values of  $(\theta + \phi)$  where  $\theta$  is the glancing angle of incidence and  $\phi$  is the glancing angle of scattering. They are obtained from  $\psi_s$  and  $\mu_s$  by the relation  $\cos(\theta + \phi) = \cos \psi_s \cos \mu_s$ . The value of  $\theta$  is obtained from the position of the Laue spot by the relation  $\cos 2\theta = \cos \psi \cos \mu$  where  $\psi$  and  $\mu$  are the angular co-ordinates of the Laue spots and are determined in the same way. Then  $\theta_B$ , the corresponding Bragg angle was calculated from the relation  $2d \sin \theta_B = n\lambda$  where  $d$  is the spacing of the reflecting plane.

For determining the half-intensity widths of the extra spots the photographs containing the spots were placed on the object carriage of the Zeiss recording microphotometer and the scanning spot of light was made to traverse each diffuse spot twice, (i) in a direction joining the centres of the diffuse spot and the direct beam, (ii) in a direction perpendicular to the former. Due to non-uniformity of intensity distribution over the spots, the length of the scanning spot of light was so reduced that the region covered by the light spot was practically of uniform blackening, care being taken to see that in both the traversals the spot of light passed across the maximum inside the spot. Since the intensity of X-ray incident at any point cannot be taken to be proportional to the deflection of the electrometer fibre when the scanning spot of light traverses that point, the intensity was obtained by comparing the photometer curve of the spot with that of a standard wedge obtained by Robinson's method (1933).

In order to compute the intensities corresponding to the ordinates of the photometer curves of the spots the ordinates of these curves were matched with the ordinates of the photometer curve of the standard wedge and the corresponding readings of the abscissae of the latter curve gave the desired intensities. The maximum intensity thus computed was the peak intensity of the spots. The half-intensity width was obtained from half of the difference between the abscissae corresponding to half of the maximum intensity on either side of the maximum.

#### *Discussion of results.*

It has been tried to test the following points:—

- (i) Whether the glancing angle of incidence  $\theta$  has any influence on the deviation  $(\theta + \phi)$  and if so, how does it depend on  $\Delta$ , the

difference between the glancing angle of incidence and the Bragg angle.

- (ii) Whether the direction of the maximum intensity remains in the plane of incidence or not.
- (iii) The nature of variation of the peak intensity with  $\Delta$ .
- (iv) Radial diffuseness of the spots as measured by the half-intensity widths along the radial direction.
- (v) Transverse diffuseness of the spots as measured by the half-intensity widths along a direction normal to the radial direction.

*Comparison of  $(\theta + \phi)$  with  $2\theta_B$ :* The values of  $(\theta + \phi)$  for the extra spots have been tabulated in Table I. In the first column is given the indices of the planes which produce these reflections. The 2nd, 3rd and 4th columns give the values of  $\Delta$ ,  $(\theta + \phi)$  and  $2\theta_B$  respectively. The extra spots of this substance are diffuse and hence very accurate measurements of  $(\theta + \phi)$  are not possible. *Within the limits of experimental error* it is found that  $(\theta + \phi)$  does not differ appreciably from  $2\theta_B$ .

TABLE I.

Indices of planes giving rise to the extra spots.	$\Delta = \theta - \theta_B$	$\theta + \phi$	$2\theta_B$	
140	3°15'	26°6'	25°56'	
"	1°11'	26°15'	"	
"	-1°39'	26°6'	"	
121	-1°4'	27°25'	27°20'	
"	-1°32'	27°28'	"	
"	-3°11'	27°31'	"	
131	2°24'	30°52'	30°48'	
"	1°22'	30°55'	"	
"	0°1'	30°34'	"	
131	0°48'	28°	..	27°36'
"	0°14'	27°38'	..	"
"	-1°36'	27°44'	..	"
241	-0°30'	36°55'	37°6'	
"	-0°58'	37°25'	"	
"	-3°1'	36°54'	"	

For testing whether the direction of the maximum in the extra reflection lies in the plane of incidence, we have to see whether the extra spot lies in the plane passing through the incident ray and the Laue spot, since the incident ray and the Laue spot fixes the plane of incidence. It can easily be shown that directions, for which  $\frac{\sin \psi}{\tan \mu}$  is constant, will lie in a plane containing the direction of the incident beam. So the most convenient way of testing the

above point is to compare the values of  $\frac{\sin \psi}{\tan \mu}$  of the extra spots with those of the corresponding Laue spots. The results are given in Table II.

The half-intensity widths of the extra spots measured in the plane of incidence and normal to it are given in Table IV, and the results show definitely that the extra spots are diffuse.

TABLE II.

Indices of planes giving rise to the extra spots.		$\frac{\sin \psi}{\tan \mu}$	
		For Laue spot.	For extra spot.
121	1°4'	·544	·539
"	1°32'	·506	·544
"	3°11'	·548	·536
131	-2°24'	·798	·825
"	-1°22'	·794	·821
"	-0°1'	·763	·821
241	0°30'	1·16	1·09
"	0°58'	1·12	1·10
"	3°1'	1·09	1·08

From a comparison of  $\frac{\sin \psi}{\tan \mu}$  for Laue and extra spots it is found that within the limits of experimental error, the extra spot (131) indicates a deviation from plane of incidence.

Table III shows the variation of the peak intensities of the diffuse spots for different values of  $\Delta$ . The results show that peak intensities fall off rapidly with increase of  $\Delta$ . The nature of the variation has been found to be similar for all the spots that have been studied. The number of different values of  $\Delta$  for which the peak intensities could be measured accurately are, however, not sufficient for making any general conclusions, and hence further investigations on this point are in progress.

TABLE III.

Indices of planes giving rise to the extra spots.	$\Delta$	Relative peak intensity.
140	4°28'	Very very weak. 4·1 5·4
"	1°39'	
"	1°11'	
131	1°22'	10
"	2°24'	6·3
"	4°36'	3·1
"	5°54'	Very very weak.

The half-intensity widths of the extra spots measured in the plane of incidence and normal to it are given in Table IV and the results show definitely that the extra spots are diffuse.

TABLE IV.

Indices of planes giving rise to the extra spots.	$\Delta$	Angular half-intensity width.	
		In the plane of incidence.	Normal to the plane of incidence.
131	4°36'	1°36'	0°53'
"	2°24'	1°27'	0°51'
"	1°22'	1°3'	0°53'
140	1°11'	54'	0°58'
"	1°39'	31'	0°53'

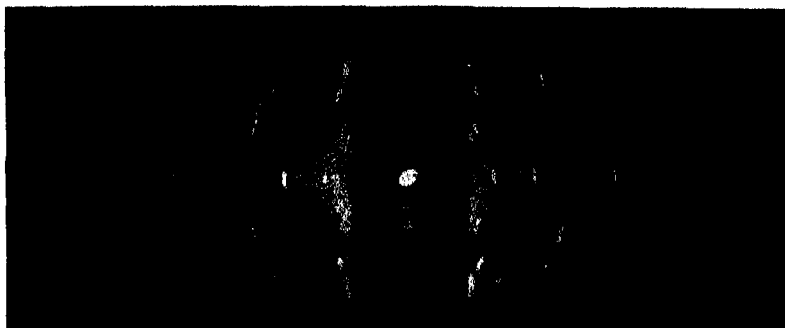
The half-intensity widths in the radial and the transverse directions for the same spot are not equal. For the spot due to (140) plane of metadinitrobenzene the radial half-intensity widths are smaller than the transverse, while for the extra spot from the (131) plane of metadinitrobenzene the radial half-intensity width is greater than the transverse. The variation of the half-intensity widths with  $\Delta$  is, however, small and for most of the planes it is within the limits of experimental accuracy practically constant.

The author expresses his hearty thanks to Dr. K. Banerjee for kindly suggesting the problem and constant guidance during the progress of the work.

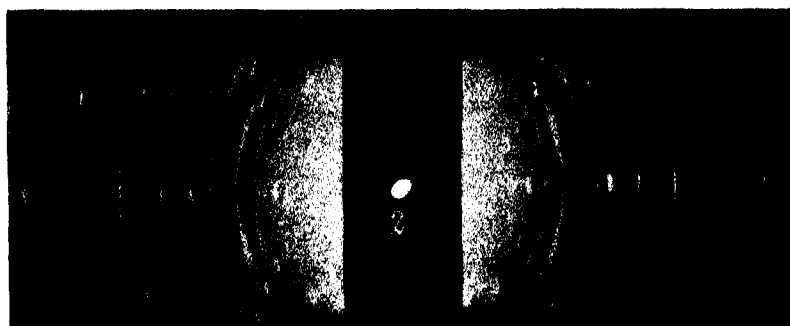
## REFERENCES.

- Bragg, W. H. (1941). The Diffuse Spots in X-ray Photographs. *Nature*, **50**, 146.  
 Faxen, H. (1923). Die bei Interferenz Von Rontgenstrahlen infolge der Warmebewegung entstehende Streustrahlung. *Zeits. f. Phys.*, **17**, 266.  
 Friedrich, W. (1913). Rontgonstrahlinterferenzen. *Phys. Zeits.*, **14**, 1079.  
 Preston, G. D. (1938). The diffraction of X-rays by Age-hardening of Aluminium Copper Alloys. *Proc. Roy. Soc.*, **167A**, 526.  
 Preston, G. D. (1939). Diffraction of X-rays by Crystals at Elevated Temperature. *Proc. Roy. Soc.*, **172A**, 116.  
 Raman, C. V. (1940). 'The Quantum Theory of X-ray Reflection: Basic Ideas' and 'Quantum Theory of X-ray Reflection: Mathematical Formulation'. *Proc. Ind. Acad. Sci.*, **14**, 317 and 332.  
 Robinson, B. W. (1933). An Integrating Photometer for X-ray Crystal Analysis. *Jour. Sci. Instr.*, **10**, 233.  
 Zachariasen, W. H. (1940). A Theoretical Study of the Diffuse Scattering of X-rays by Crystals. *Phys. Rev.*, **57**, 795.

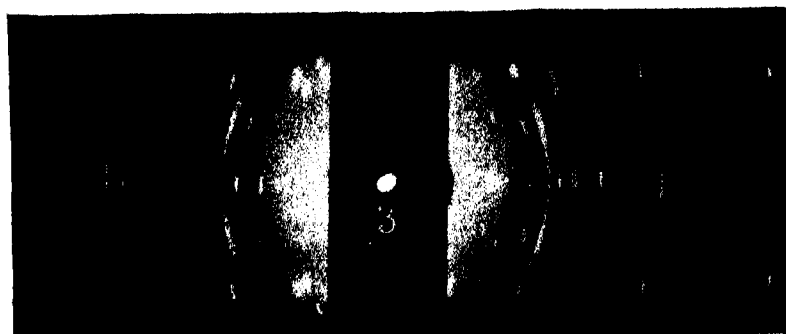




X-ray normal  
to  $a$ -face.



X-ray making  
 $1^{\circ}11'$  with  
 $a$ -axis.



X-ray making  
 $1^{\circ}39'$  with  
 $a$ -axis.



X-ray making  
 $3^{\circ}15'$  with  
 $a$ -axis.





## OBITUARY NOTICE.

RAI BAHADUR GOURIPATI CHATTERJEE, M.Sc., F.N.I.

Rai Bahadur Gouripati Chatterjee, M.Sc., F.N.I., was the fourth son of the late Ashutosh Chatterjee, the premier stevedore of Calcutta. He was a descendant of an ancient Brahmin family of Mahesh (District Hooghly) with great Sanskrit culture and tradition. He was born at Calcutta on the 4th March, 1892. With continuous ill-health from his infancy he received his early education in the Bangabasi Collegiate School from where he passed the Entrance Examination in the year 1909, securing a Second Grade Scholarship. On account of serious meningitis and acute myopia he was seriously handicapped in his studies, but he passed the Intermediate Examination in Science from the Presidency College in the First Division in the year 1911. His health broke down almost completely and he could not sit for his B.Sc. Examination for three years successively and the doctors advised him to discontinue further studies. For the sake of his health his brothers suggested that he should join their stevedoring business, but on account of his indomitable will to carry on with scientific studies he could not persuade himself to take up a business career with bright financial prospects. He sat for his B.Sc. Examination against doctors' advice and passed it with distinction in the year 1916. His health further deteriorated and he could not appear at the M.Sc. Examination until 1919 when he got a First Class First in Physics and was awarded the University of Calcutta Gold Medal and Matilal Mullick Gold Medal. After getting his M.Sc. degree he worked as a research scholar in the Presidency College where he repaired many delicate scientific instruments for the college laboratory. This mechanical and scientific talent of his was highly appreciated by his various professors and he was selected for the post of a scientific assistant in the Indian Meteorological Department and joined the Upper Air Observatory at Agra on the 15th April, 1921. He was appointed Meteorologist from the 28th February, 1922 and became the Meteorologist-in-Charge from the 1st April, 1928 with a special allowance. In 1929 he went as the head of an upper air expedition to Jhinkargachia, District Jessore. In this expedition he did a lot of upper air investigations by letting off special balloons for the exploration of upper air. He contributed a paper on 'Some Upper Air Instruments for investigating the Lower Layers of the Earth's Atmosphere' for publication in the festival number in honour of Prof. Koppen's 85th birthday in 'Gerlands Beiträge Zur Geophysik', and on receipt of this paper Prof. Dr. Conrad expressed the opinion that his methods for sounding the lower layers of the earth's atmosphere will no doubt be used also in Europe in future, before all at the Air Mail Service. In 1930 the Agra University started a Meteorology course in M.Sc. and he was selected as its Professor of

Meteorology. He was awarded the Silver Jubilee Medal in 1935 and the Coronation Medal in 1937. He became the Superintending Meteorologist from the 1st October, 1938 and was made a Rai Bahadur on the 1st January, 1939. He was a highly resourceful, practical and experimental meteorologist and a creator of some of the most ingenious, delicate and yet serviceable and accurate instruments for upper air research. He took charge of the small observatory workshop and office at Agra from Mr. Field (the then Director-General of Observatories) in 1924 and later of the large headquarters in New Delhi with over 40 upper air observatories providing all the data that war conditions demand of them. His achievement during the last 18 years of his life is a proof of his ability in skilful and thorough planning and direction, and of his unfailing care, enthusiasm, determination and devotion.

In his school days his recreation was painting and his portrait painting was recognised by many a connoisseur to be of a very high order. Always straight-forward and generous in his behaviour he led a very simple life. He sacrificed his personal comforts and even necessities in order to help the poor. He was widely read and his knowledge of Economics and Horticulture was remarkable. Although a born scientist, he believed that agriculture must eventually play a vital part in the Indian national life. He had a creative urge in him and, being a bachelor with no encumbrances, he decided to give his best to develop a farm and nursery on the most up-to-date scientific lines. With this purpose he acquired extensive lands in the village Rohta in the district of Agra and laid the foundation of what was to become a unique institution, where he wanted to educate the children of the soil so that they may take to scientific farming which he believed would bring about the economic salvation of India for the coming generations. But God willed it otherwise. On the 1st June, 1942 he underwent an operation on account of an abscess on his foot and it was discovered that he was a victim of diabetes in an advanced stage. In spite of the best efforts of the doctors he expired on the 10th July, 1942.

N. K. S.

## **Eighteenth Ordinary General Meeting.**

An Ordinary General Meeting of the National Institute of Sciences of India was held at 3 p.m. on Monday, the 5th October, 1942, in the rooms of the Royal Asiatic Society of Bengal, 1 Park Street, Calcutta.

### **Present :—**

Prof. M. N. Saha, in the Chair.  
Rai Bahadur Dr. K. N. Bagchi.  
Rai Bahadur Dr. S. L. Hora.  
Dr. D. N. Majumdar.  
Prof. S. K. Mitra.  
Mr. V. P. Sondhi.  
Prof. S. P. Agharkar, *Honorary Secretary.*

1. The minutes of the Seventh Annual General Meeting, held on the 1st January, 1942, were confirmed.
2. Dr. D. N. Majumdar and Mr. V. P. Sondhi signed the duplicate obligation and were admitted as Fellows as per Rule 13.
3. The following papers were read :—
  - (1) Photochemical Analysis. By G. Gopala Rao and P. T. Ramacharlu. (Communicated by Dr. N. R. Dhar.)
  - (2) Accurate Calculations on the Cascade Theory of Electronic Showers without Collision Loss. By S. K. Chakrabarty. (Communicated by Dr. H. J. Bhabha.)
  - (3) Contribution to the Theory of Stellar Models. By N. R. Sen.
  - (4) Pressure Ionisation and Maximum Radius for a Cold Body. By P. L. Bhatnagar and D. S. Kothari.
  - (5) Fermi-Dirac and Bose-Einstein Gas in a Gravitational Field. By Brij Nath and P. L. Bhatnagar. (Communicated by Dr. D. S. Kothari.)
  - (6) An Account of the Chondrocranium of *Rana Afghana* and *Megophrys*, with a description of the masticatory musculature of some tadpoles. By L. S. Ramaswami. (Communicated by Dr. B. Prashad.)
  - (7) On the Extra Spots in Laue Photographs of Metadinitrobenzene. By M. Ganguly. (Communicated by Dr. K. Banerjee.)
  - (8) On the Elastic Scattering of the Fast Mesons. By S. Gupta. (Communicated by Prof. N. R. Sen.)
  - (9) The Pliocene and Pleistocene Boundary in North-Western India. By D. N. Wadia.
  - (10) On the Electromagnetic Field and the Self-energy of Meson. By S. Gupta. (Communicated by Prof. N. R. Sen.)

- (11) Gametogenesis and Embryogeny of *Eulophea Epidendraea* Fischer.  
By B. G. L. Swami. (Communicated by Dr. P. Maheshwari.)

4. The Council's proposal that owing to the difficulty of holding meetings under the prevailing abnormal conditions a committee consisting of the Secretaries, Treasurer, and Dr. S. L. Hora, in consultation with the President, be authorised to act on its behalf, actions taken being subsequently reported to the Council, was approved.

# INDEX

	PAGE		PAGE
Accurate calculations on the cascade theory of electronic showers without collision loss (Chakrabarty) ..	331	Calcutta, Fine structure in the directional intensity of cosmic rays at (Bhattacharya) ..	273
Address, Annual (Prashad) ..	27	Calcutta and Darjeeling, East-west asymmetry of cosmic rays at (Bhattacharya) ..	263
Analysis, Photochemical (Gopala Rao and Ramacharlu) ..	383	Cascade theory of electronic showers without collision loss, Accurate calculations on the (Chakrabarty) ..	331
Annual Address (Prashad) ..	27	Chakrabarty, S. K.—Accurate calculations on the cascade theory of electronic showers without collision loss ..	331
Annual General Meeting, Seventh ..	5	Charanjit—See Sarma, H. R., Kapur, P. L. and Charanjit ..	277
Annual Report ..	9	Chowdri, A. G.—See Singh, B. N. and Chowdri, A. G. ..	89
Ascorbic acid as inductor, Induced reactions with (Gopala Rao and Subba Rao) ..	137	Cobalt, Co <sup>57</sup> , On the existence of an isotope of (Sen-Chowdhury) ..	55
Auluck, F. C.—White dwarf and harmonic oscillator ..	147	Cold body, Pressure ionisation and maximum radius for a (Bhatnagar and Kothari) ..	377
Auluck, F. C.—See Kothari, D. S. and Auluck, F. C. ..	157, 165	Collision between meson and electron, On the (Gupta and Majumdar) ..	199
Band spectrum of mercury iodide, The ultra-violet (Sastri) ..	289	Confluent hyper-geometric function, Properties of a (Mohan) ..	93
Banerji, A. C.—The instability of radial oscillations of a variable star and the origin of the solar system ..	173	Contribution to the theory of stellar models (Sen) ..	339
Bethe's law of energy generation, On integration of stellar equations for (Burman) ..	301	Cosmic rays, On the production of mesons by non-ionising agents in (Sirkar and Ghosh) ..	233
Bethe's law of energy generation, On stellar models based on (Sen) ..	317	Cosmic rays at Calcutta, Fine structure in the directional intensity of (Bhattacharya) ..	273
Bhatnagar, P. L.—See Nath, Brij and Bhatnagar, P. L. ..	361	Cosmic rays at Calcutta and Darjeeling, East-west asymmetry of (Bhattacharya) ..	263
Bhatnagar, P. L. and Kothari, D. S.—Pressure ionisation and maximum radius for a cold body ..	377	Darjeeling, East-west asymmetry of cosmic rays at Calcutta and (Bhattacharya) ..	263
Bhattacharya, P. C.—East-west asymmetry of cosmic rays at Calcutta and Darjeeling ..	263	Degenerate gas and the motion of a particle in a uniform field (Kothari and Auluck) ..	157
Bhattacharya, P. C.—Fine structure in the directional intensity of cosmic rays at Calcutta ( $\lambda = 12^\circ \text{ N.}, h = 80 \text{ ft.}$ ) ..	273	Development of embryo-sac and endosperm-haustoria in <i>Tetranema mexicana</i> Benth. and <i>Verbascum thapsus</i> Linn. (Krishna Iyengar) ..	59
Bishui, B. M.—See Sirkar, S. C. and Bishui, B. M. ..	217	Development of seed and its nutritional mechanism in Scrophulariaceae (Krishna Iyengar) ..	249
Bose-Einstein gas, The relation of gas pressure to radiation pressure in a (Singh and Chowdri) ..	89	Dhar, J. and Niyogi, B. B.—X-ray studies in Indian coals. Part I ..	127
Bose-Einstein gas in a gravitational field, Fermi-Dirac and (Nath and Bhatnagar) ..	361	Directional intensity of cosmic rays at Calcutta, Fine structure in the (Bhattacharya) ..	273
Bose-Einstein gas in a uniform field of force, Fermi-Dirac and (Kothari and Auluck) ..	165	East-west asymmetry of cosmic rays at Calcutta and Darjeeling (Bhattacharya) ..	263
Burman, U. R.—On integration of stellar equations for Bethe's law of energy generation ..	301		
Calculations on the cascade theory of electronic showers without collision loss, Accurate (Chakrabarty) ..	331		

# INDEX

	PAGE		PAGE
Eighteenth Ordinary General Meeting ..	309	General Meeting, Seventh Annual ..	5
Elastic scattering of the fast mesons, On the (Gupta) ..	369	Ghosh, S. K.—See Sirkar, S. C. and Ghosh, S. K. ..	233
Electron, On the collision between meson and (Gupta and Majumdar) ..	199	Gopala Rao, G. and Ramachariu, P. T.—Photochemical Analysis ..	383
Electronic showers without collision loss, Accurate calculations on the cascade theory of (Chakrabarty) ..	331	Gopala Rao, G. and Subba Rao, T. V.—Induced reactions with ascorbic acid as inductor ..	137
Embryo-sac and endosperm-haustoria in <i>Tetranema mexicana</i> Benth. and <i>Verbascum thapsus</i> Linn., Development of (Krishna Iyengar) ..	59	Gravitational field, Fermi-Dirac and Bose-Einstein gas in a (Nath and Bhatnagar) ..	361
Endosperm haustoria in <i>Tetranema mexicana</i> Benth. and <i>Verbascum thapsus</i> Linn., Development of embryo-sac and (Krishna Iyengar) ..	59	Gupta, S.—On the elastic scattering of the fast mesons ..	369
Existence of an isotope of cobalt, Co <sup>57</sup> , On the (Sen-Chowdhury) ..	55	Gupta, S. and Majumdar, R. C.—On the collision between meson and electron ..	199
Extra spots in Laue photographs, On the origin of (Sirkar and Bishui) ..	217	Gynaeceum constitution, Floral anatomy of the Moringaceae with special reference to (Puri) ..	71
Extra spots in Laue photographs of metadinitrobenzene, On the (Ganguly) ..	389	Harmonic oscillator, White dwarf and (Auluck) ..	147
Fast mesons, On the elastic scattering of the (Gupta) ..	369	Helium-filled Geiger-Müller counters, Studies on (Sarna, Kapur and Charanjit) ..	277
Fermi-Dirac and Bose-Einstein gas in a gravitational field (Nath and Bhatnagar) ..	361	Hyper-geometric function, Properties of a confluent (Mohan) ..	93
Fermi-Dirac and Bose-Einstein gas in a uniform field of force (Kothari and Auluck) ..	165	Indian coals. Part I. X-ray studies in (Dhar and Niyogi) ..	127
Field, Degenerate gas and the motion of a particle in a uniform (Kothari and Auluck) ..	157	Induced reactions with ascorbic acid as inductor (Gopala Rao and Subba Rao) ..	137
Field of force, Fermi-Dirac and Bose-Einstein gas in a uniform (Kothari and Auluck) ..	165	Inductor, Induced reactions with ascorbic acid as (Gopala Rao and Subba Rao) ..	137
Fine structure in the directional intensity of cosmic rays at Calcutta ( $\lambda = 12^\circ \text{N.}$ , $h = 80 \text{ ft.}$ ) (Bhattacharya) ..	273	Instability of radial oscillations of a variable star and the origin of the solar system, The (Banerji) ..	173
Floral Anatomy. II. Floral anatomy of the Moringaceae with special reference to gynaeceum constitution, Studies on (Puri) ..	71	Integration of stellar equations for Bethe's law of energy generation, On (Burman) ..	301
Force, Fermi-Dirac and Bose-Einstein gas in a uniform field of (Kothari and Auluck) ..	165	Isotope of cobalt, Co <sup>57</sup> , On the existence of an (Sen-Chowdhury) ..	55
Ganguly, M.—On the extra spots in Laue photographs of metadinitrobenzene ..	389	Kapur, P. L.—See Sarna, H. R., Kapur, P. L. and Charanjit ..	277
Gas pressure to radiation pressure in a Bose-Einstein gas, the relation of (Singh and Chowdri) ..	89	Kothari, D. S.—See Bhatnagar, P. L. and Kothari, D. S. ..	377
Geiger-Müller counters, Studies on helium-filled (Sarna, Kapur and Charanjit) ..	277	Kothari, D. S. and Auluck, F. C.—Degenerate gas and the motion of a particle in a uniform field ..	157
General Meeting, Eighteenth Ordinary ..	399	Kothari, D. S. and Auluck, F. C.—Fermi-Dirac and Bose-Einstein gas in a uniform field of force ..	165
General Meeting, Seventeenth Ordinary ..	1	Krishna Iyengar, C. V.—Development of embryo-sac and endosperm-haustoria in <i>Tetranema mexicana</i> Benth. and <i>Verbascum thapsus</i> Linn. ..	59
		Krishna Iyengar, C. V.—Development of seed and its nutritional mechanism in Scrophulariaceae ..	249
		Laue photographs, On the origin of extra spots in (Sirkar and Bishui) ..	217

# INDEX

PAGE	PAGE
Laue photographs of metadinitrobenzene, On the extra spots in (Ganguly) .. 389	Photochemical Analysis (Gopala Rao and Ramacharlu) .. 383
Law of energy generation, On integration of stellar equations for Bethe's (Burman) .. 301	Physical theory of the solar corona, On a (Saha) .. 99
Law of energy generation, On stellar models based on Bethe's (Sen) .. 317	Prashad, Dr. Beini—Annual Address .. 27
Majumdar, R. C.—See Gupta, S. and Majumdar, R. C. .. 199	Pressure ionisation and maximum radius for a cold body (Bhatnagar and Kothari) .. 377
Maximum radius for a cold body, Pressure ionisation and (Bhatnagar and Kothari) .. 377	Production of mesons by non-ionising agents in cosmic rays, On the (Sirkar and Ghosh) .. 233
Meeting, Eighteenth Ordinary General .. 399	Properties of a confluent hypergeometric function (Mohan) .. 93
Meeting, Seventeenth Ordinary General .. 1	Puri, V.—Studies in floral anatomy, II. Floral anatomy of the Moringaceae with special reference to gynaeceum constitution .. 71
Meeting, Seventh Annual General .. 5	Radial oscillations of a variable star and the origin of the solar system, The instability of (Banerji) .. 173
Mercury iodide, The ultra-violet band spectrum of (Sastry) .. 289	Radiation pressure in a Bose-Einstein gas, The relation of gas pressure to (Singh and Chowdri) .. 89
Mesons, On the elastic scattering of the fast (Gupta) .. 369	Radio-activity of rubidium (Sen-Chowdhury) .. 45
Meson and electron, On the collision between (Gupta and Majumdar) .. 199	Radius for a cold body, Pressure ionisation and maximum (Bhatnagar and Kothari) .. 377
Mesons by non-ionising agents in cosmic rays, On the production of (Sirkar and Ghosh) .. 233	Rai Bahadur Gouripati Chatterjee, Obituary Notice .. 397
Metadinitrobenzene, On the extra spots in Laue photographs of (Ganguly) .. 389	Ramacharlu, P. T.—See Gopala Rao, G. and Ramacharlu, P. T. .. 383
Mohan, B.—Properties of a confluent hypergeometric function .. 93	Reactions with ascorbic acid as inductor, Induced (Gopala Rao and Subba Rao) .. 137
Moringaceae with special reference to gynaeceum constitution, Floral anatomy of the (Puri) .. 71	Relation of gas pressure to radiation pressure in a Bose-Einstein gas, The (Singh and Chowdri) .. 89
Motion of a particle in a uniform field, Degenerate gas and the (Kothari and Auluck) .. 157	Report, Annual .. 9
Nath, Brij, and Bhatnagar, P. L.—Fermi-Dirac and Bose-Einstein gas in a gravitational field .. 361	Rubidium, Radio-activity of (Sen-Chowdhury) .. 45
Niyogi, B. B.—See Dhar, J. and Niyogi, B. B. .. 127	Saha, M. N.—On a physical theory of the solar corona .. 99
Non-ionising agents in cosmic rays, On the production of mesons by (Sirkar and Ghosh) .. 233	Sarna, H. R., Kapur, P. L. and Charanjit—Studies on helium-filled Geiger-Müller counters .. 277
Nutritional mechanism in Scrophulariaceae, Development of seed and its (Krishna Iyengar) .. 249	Sastry, M. G.—The ultra-violet band spectrum of mercury iodide .. 289
Obituary Notice: Rai Bahadur Gouripati Chatterjee .. 397	Scrophulariaceae, Development of seed and its nutritional mechanism in (Krishna Iyengar) .. 249
Ordinary General Meeting, Eighteenth .. 399	Seed and its nutritional mechanism in Scrophulariaceae, Development of (Krishna Iyengar) .. 249
Ordinary General Meeting, Seventeenth .. 1	Sen, N. R.—Contribution to the theory of stellar models .. 339
Origin of extra spots in Laue photographs, On the (Sirkar and Bishui) .. 217	Sen, N. R.—On stellar models based on Bethe's law of energy generation .. 317
Origin of the solar system, The instability of radial oscillations of a variable star and the (Banerji) .. 173	Sen-Chowdhury, P. K.—On the existence of an isotope of cobalt, Co <sup>57</sup> .. 55
Particle in a uniform field, Degenerate gas and the motion of a (Kothari and Auluck) .. 157	Sen-Chowdhury, P. K.—Radio-activity of rubidium .. 45



# INDEX

	PAGE
Seventeenth Ordinary General Meeting ..	1
Seventh Annual General Meeting ..	5
Singh, B. N. and Chowdri, A. G.— The relation of gas pressure to radiation pressure in a Bose- Einstein gas ..	89
Sirka, S. C. and Biahui, B. M.— On the origin of extra spots in Laue photographs ..	217
Sirka, S. C. and Ghosh, S. K.—On the production of mesons by non- ionising agents in cosmic rays ..	233
Solar corona, On a physical theory of the (Saha) ..	99
Solar system, The instability of radial oscillations of a variable star and the origin of the (Banerji) ..	173
Stellar equations for Bethe's law of energy generation, On integration of (Burman) ..	301
Stellar models, Contribution to the theory of (Sen) ..	339
Stellar models based on Bethe's law of energy generation, On (Sen) ..	317
Structure in the directional intensity of cosmic rays at Calcutta, Fine (Bhattacharya) ..	273

	PAGE
Subba Rao, T. V.—See Gopala Rao, G. and Subba Rao, T. V. ..	137
<i>Tetranema mexicana</i> Benth. and <i>Verbascum thapsus</i> Linn., Deve- lopment of embryo-sac and endosperm-haustoria in (Krishna Iyengar) ..	59
Theory of stellar models, Contribu- tion to the (Sen) ..	339
Ultra-violet band spectrum of mer- cury iodide, The (Sastri) ..	289
Uniform field, Degenerate gas and the motion of a particle in a (Kothari and Auluck) ..	157
Uniform field of force, Fermi- Dirac and Bose-Einstein gas in a (Kothari and Auluck) ..	165
Variable star and the origin of the solar system, The instability of radial oscillations of a (Banerji) ..	173
<i>Verbascum thapsus</i> Linn., Develop- ment of embryo-sac and endo- sperm-haustoria in <i>Tetranema</i> <i>mexicana</i> Benth. and (Krishna Iyengar) ..	59
White dwarf and harmonic oscillator (Auluck) ..	147
X-ray studies in Indian coals. Part I (Dhar and Niyogi) ..	127





